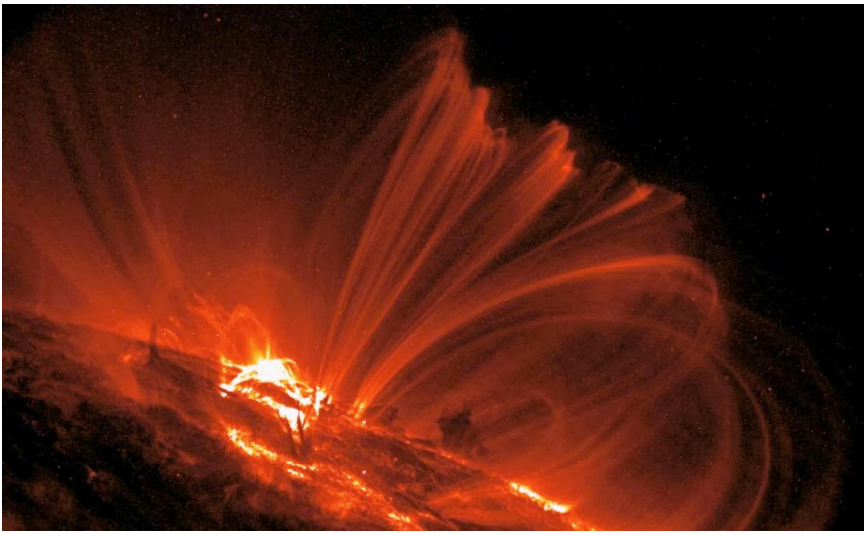

Graduate courses in Physics

Electrodynamics

Electricity, Magnetism and Radiation

Ph.W. Courteille
Universidade de São Paulo
Instituto de Física de São Carlos
30/10/2023

.

Preface

The script was developed for the course *Electromagnetism A* (SFI5708) offered by the Institute of Physics of São Carlos (IFSC) of the University of São Paulo (USP). The course is divided into two parts. Part I of the script gives an introduction to electromagnetism at the level of an undergraduate course. From electrical and magnetic phenomena observed in experiments we derive the fundamental laws of Gauss, Faraday, Ampère, and Maxwell allowing a complete description of electromagnetism, which culminates in Maxwell's equations. The procedure in part II of the script is inverse. From Maxwell's equations we deduce electromagnetic phenomena, such as the radiation of accelerated charges or the role of electromagnetic forces in atoms. Also, we derive fundamental conservation laws and the relationship of electromagnetism with the theory of special relativity. This part is a postgraduate course in classical electrodynamics.

The course is intended for masters and PhD students in physics. The script is a preliminary version continually being subject to corrections and modifications. Error notifications and suggestions for improvement are always welcome. The script incorporates exercises the solutions of which can be obtained from the author.

Information and announcements regarding the course will be published on the website:
http://www.ifsc.usp.br/ strontium/ − > Teaching − > Semester

The student's assessment will be based on written tests and a seminar on a special topic chosen by the student. In the seminar the student will present the chosen topic in 15 minutes. He will also deliver a 4-page scientific paper in digital form. Possible topics are:
- Existence of magnetic monopoles and the quantization of charge,
- The Goos-Hänchen and the Imbert-Fedorov shift,
- The Abraham-Minkowski dilemma,
- The Aharonov-Bohm effect,
- Superconductivity and the Meissner effect,
- Cerenkov radiation,
- Bremsstrahlung,
- The Lorentz model of the radiation of an atom (Sec. 7.2.3),
- The Drude model for light-metals interaction (Sec. 7.2.5),
- The Kramers-Kronig relations (Sec. 7.2.6),
- The optical theorem,
- Analytical signal,
- Quantization of the electromagnetic field,
- Optical fibers,
- Diffraction through apertures,
- Laguerre-Gaussian light modes,
- Bessel beams and laser swords,
- Free-electron laser,
- The ionosphere as a resonant cavity: Schumann resonances,
- Excitation of surface plasmon polaritons,
- The Faraday effect,

- Birefringent crystals and wave plates,
- Forbidden photonic bands and photonic crystals,
- The Ewald-Oseen theorem,
- The Thomas precession,
- Anderson localization,
- Mie scattering and Mie resonances,
- The of coupled dipoles model,
- Gaussian optics,
- Negative refraction and the perfect lens,
- The Kerr effect,
- The quantum Hall effect,
- Anti-reflective and reflective dielectric coatings,
- Hyperbolic metamaterials,
- Comparison between electromagnetic waves and matter waves,
- Bragg Scattering,
- Schlieren photography,
- The Fresnel-Fizeau effect,
- The Sagnac effect.

The following literature is recommended for preparation and further reading:

Ph.W. Courteille, script on *Optical spectroscopy: A practical course* (2020)

Ph.W. Courteille, script on *Electrodynamics: Electricity, magnetism, and radiation* (2020)

Ph.W. Courteille, script on *Quantum mechanics applied to atomic and molecular physics* (2020)

J.B. Marion, *Classical Eletromagnetic Radiation*, Dover (2012)

W.K.H. Panofsky and M. Phillips, *Classical Electricity and Magnetism*, Dover (2012)

J.J. Jackson, *Classical electrodynamics*, John Wiley & Sons (1999)

D.J. Griffiths, *Introduction to Electrodynamics*, Cambridge University Press (2017)

J.R. Reitz, F.J. Milford, R.W. Christy, *Foundation of electromagnetic theory*

M. Born, *Principles of Optics*, 6^{th}ed. Pergamon Press New York (1980)

P. Horowitz and W. Hill, *The Art of Electronics*, Cambridge University Press (2001)

U. Tietze & Ch. Schenk, *Halbleiterschaltungstechnik*, Springer-Verlag (1978)

Content

Chapter 1

Foundations and mathematical tools

The electrodynamic force is one of the four fundamental forces, together with gravitation, the strong nuclear force, and the weak nuclear force. It is a long-range force ($F \propto r^{-2}$) in the same way as gravitation, but unlike nuclear forces, which are short-ranged. Unlike gravitation, it can be attractive or repulsive. The experimentally

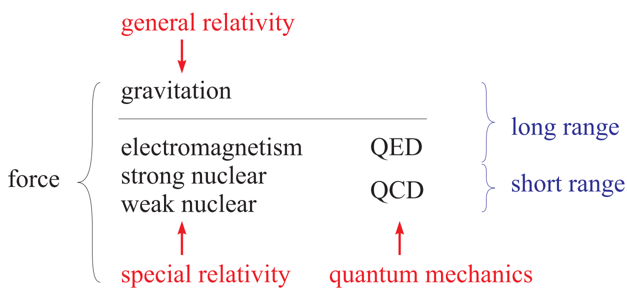

Figure 1.1: The four known fundamental forces.

observed fact, that two spatially separated bodies can exert mutual forces (beyond gravitation), is not explained within classical mechanics. It is necessary to introduce a new degree of freedom called *electric charge* which, to take account of the existence of attractive and repulsive forces, must exist in two different types called positive or negative charges. *Identical charges repel each other, different charges attract each other.* Other observations suggest that the charge is a *conserved and quantized* quantity.

Electrodynamics is an *field theory*, that is, it can describe all electric or magnetic phenomena observed in the following way: Every charge gives rise to a force field, called field electric $\vec{\mathcal{E}}$, which accelerates other charges. But other experimental observations suggest the existence of another force field, called the magnetic field $\vec{\mathcal{B}}$, whose existence is necessary to understand forces only acting on moving charges. That is, the electric and magnetic fields are introduced to explain the forces named after Coulomb and Lorentz,

$$\mathbf{F} = q\vec{\mathcal{E}} + \mathbf{v} \times \vec{\mathcal{B}} \ . \tag{1.1}$$

Thus, fields are quantities distributed in space, which in addition can vary in time,

$$\mathbf{F} = \mathbf{F}(\mathbf{r}, t) \ . \tag{1.2}$$

The concept of a field represents a powerful mathematical tool for describing forces, which are the only observable magnitudes of electromagnetism. That is, we have no sense to *see* the electricity. We can only infer their existence from the observation of forces. On the other hand, the formulation of electrodynamics via vectorial force fields, can be replaced by a description via potentials, which are either scalar or vectorial fields. In many circumstances, potentials facilitate the resolution of electrodynamic problems, but it is important to keep in mind, that potentials are not directly observable.

Maxwell's electrodynamics has a very deep relationship to Einstein's theory of special relativity, such that each theory is conditioned to the validity of the other. The relativistic formulation allows to distill the symmetry inherent to electrodynamics in a highly aesthetic way.

In view of the fundamental role played by scalar and vector fields in electrodynamics, we will start this course the basic mathematical notions of field theory, that is, differential and integral calculus with fields in Cartesian or curvilinear coordinates. We will also have to review basic notions of complex numbers and the Dirac distribution.

1.1 Differential calculus

1.1.1 Scalar and vector fields

The most basic application of vectors is the designation of positions in space, $\mathbf{r} = x\hat{\mathbf{e}}_x + y\hat{\mathbf{e}}_y + z\hat{\mathbf{e}}_z$. But other physical quantities may also depend on the position where they are measured. In case the quantity varying with position is a scalar, $\Phi = \Phi(\mathbf{r})$, we speak of *scalar field*. An example for a scalar field is the temperature distribution across a room. In the case the quantity is a vector, $\mathbf{A} = \mathbf{A}(\mathbf{r})$, we speak of *vector field*. Light propagating through space is an example for a vector field.

A position is generally defined with respect to the center of the coordinate system, called the origin, such that the distance from the center is given by,

$$r \equiv \sqrt{\mathbf{r}\cdot\mathbf{r}} = \sqrt{x^2 + y^2 + z^2} \ , \tag{1.3}$$

with $\hat{\mathbf{e}}_r$ being a unit vector pointing in the direction of $\mathbf{r}$. In electrodynamics we will often deal with quantities (fields) that depend on the distance between a source located at a position $\mathbf{r}'$ and a detector placed at a position $\mathbf{r}$, such as $\Phi(R) = \Phi(\mathbf{r}-\mathbf{r}')$,

$$\hat{\mathbf{e}}_R = \frac{(x-x')\hat{\mathbf{e}}_x + (y-y')\hat{\mathbf{e}}_y + (z-z')\hat{\mathbf{e}}_z}{\sqrt{(x-x')^2 + (y-y')^2 + (z-z')^2}} \ . \tag{1.4}$$

1.1.2 The gradient

The derivative of a one-dimensional function $\Phi(x)$ measures, how fast the function changes when we move the position x. That is, when we change x by an amount dx, Φ changes by an amount $d\Phi$ given by,

$$d\Phi = \left(\frac{d\Phi}{dx}\right) dx \ . \tag{1.5}$$

Of course it gets trickier, when Φ is a field depending on three coordinates, because we need to specify in which direction we are changing the position. We have,

$$d\Phi = \left(\frac{\partial\Phi}{\partial x}\right) dx + \left(\frac{\partial\Phi}{\partial y}\right) dy + \left(\frac{\partial\Phi}{\partial z}\right) dz \ . \tag{1.6}$$

This equation resembles the scalar product because,

$$d\Phi = \left(\hat{\mathbf{e}}_x \frac{\partial\Phi}{\partial x} + \hat{\mathbf{e}}_y \frac{\partial\Phi}{\partial y} + \hat{\mathbf{e}}_z \frac{\partial\Phi}{\partial z}\right) \cdot (dx\hat{\mathbf{e}}_x + dy\hat{\mathbf{e}}_y + dz\hat{\mathbf{e}}_z) \equiv \nabla\Phi \cdot d\mathbf{r} \ , \tag{1.7}$$

where we defined a new operator called *nabla*,

$$\nabla \equiv \begin{pmatrix} \partial/\partial x \\ \partial/\partial y \\ \partial/\partial z \end{pmatrix} \ . \tag{1.8}$$

The three-dimensional derivative $\nabla\Phi$ is called the *gradient* of the scalar field Φ,

$$\nabla\Phi(\mathbf{r}) = \hat{\mathbf{e}}_x \frac{\partial\Phi}{\partial x} + \hat{\mathbf{e}}_y \frac{\partial\Phi}{\partial y} + \hat{\mathbf{e}}_z \frac{\partial\Phi}{\partial z} \ , \tag{1.9}$$

and it measures the variation of the value of the field from Φ to $\Phi + d\Phi$, when we move the vector by an infinitesimal amount between two points $\mathbf{r}$ and $\mathbf{r} + d\mathbf{r}$.

We understand the geometric interpretation of the gradient through its formulation as a scalar product:

$$d\Phi = \nabla\Phi \cdot d\mathbf{r} = |\nabla\Phi| \cdot |d\mathbf{r}| \cos\theta \ , \tag{1.10}$$

where θ is the angle between the gradient and the infinitesimal displacement. Now, we fix a *magnitude* of the displacement $|d\mathbf{r}|$ and look for the direction θ in which the variation $d\Phi$ is maximum. Obviously, we find the direction $\theta = 0$, that is, when the gradient points in the same direction as the predefined displacement.

> *The gradient of a scalar field $\Phi(\mathbf{r})$ calculated at a point $\mathbf{r}$ indicates the direction of the greatest field variation from this point, and its absolute value is a measure for the variation.*

The concept of the gradient is easy to understand in a two-dimensional landscape: Imagine being on the slope of a mountain. Depending on the direction in which you are heading and the duration of the journey $d\mathbf{r}$, you will gain or lose a certain amount of potential energy $d\Phi$, which you can calculate by the scalar product $\nabla\Phi \cdot d\mathbf{r}$. If the direction chosen is that indicated by the gradient, you will lose (or gain) a maximum of potential energy. If you choose to go in a direction perpendicular to the gradient, that is, along an equipotential line, the potential energy remains unchanged. This is illustrated in Fig. 1.2.

Let us consider the example of a parabolic field, $\Phi(\mathbf{r}) = -r^2$:

$$\nabla(-r^2) = \begin{pmatrix} -2x \\ -2y \\ -2z \end{pmatrix} = -2\mathbf{r} \ . \tag{1.11}$$

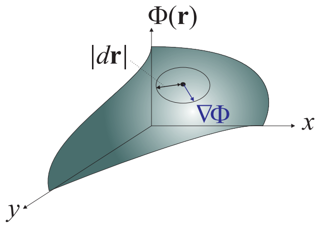

Figure 1.2: The gradient indicates the direction of the largest field variation Φ.

We find that at all points of space the variation is faster in radial direction.

Although the operator ∇ has the shape of a vector, it has no meaning by itself. In fact, it is a *vector operator*, that is, a mathematical *prescription* telling us what to do with the scalar field on which it acts. Nevertheless, it assimilates all the properties of a vector. (We will see in quantum mechanics, that this is more than a coincidence.) Thus, in a way similar as done for the gradient of scalar fields, we can try to apply the ∇ operator on vector fields using the definitions of the scalar and vector products,

$$\text{grad } \Phi(\mathbf{r}) \equiv \nabla\Phi(\mathbf{r}) \quad \text{and} \quad \text{div } \mathbf{A}(\mathbf{r}) \equiv \nabla \cdot \mathbf{A}(\mathbf{r}) \quad \text{and} \quad \text{rot } \mathbf{A}(\mathbf{r}) \equiv \nabla \times \mathbf{A}(\mathbf{r}) \ . \tag{1.12}$$

We practice the calculation with the ∇ operator in the Excs. 1.1.7.1 to 1.1.7.3.

1.1.3 The divergence

Let us now analyze the possible meaning of the expression $\nabla \cdot \mathbf{A}$ called *divergence*. It is easy to show,

$$\nabla \cdot \mathbf{A}(\mathbf{r}) = \frac{\partial A_x}{\partial x} + \frac{\partial A_y}{\partial y} + \frac{\partial A_z}{\partial z} \ . \tag{1.13}$$

Obviously the divergence is a scalar field calculated from a vector field.

> *The divergence measures how much a vector field* $\mathbf{A}(\mathbf{r})$ *spreads out starting from a point* $\mathbf{r}$*. For a given infinitesimal volume it measures the difference between the number of incoming and outgoing field lines.*

Exposed to a field with divergence, an extended distribution of masses will start to concentrate (spread out) in case of a drain (source). The field lines trace the masses trajectories.

Example 1 (*Divergence of a radial field*): We consider the example of the radial field, $\mathbf{A}(\mathbf{r}) = \mathbf{r}$:

$$\nabla \cdot \mathbf{r} = \frac{\partial x}{\partial x} + \frac{\partial y}{\partial y} + \frac{\partial z}{\partial z} = 3 \ . \tag{1.14}$$

1.1.4 The rotation

Let us now examine the possible meaning of the expression $\nabla \times \mathbf{A}$ called *rotation*. It is easy to show,

$$\nabla\times\mathbf{A}(\mathbf{r}) = \begin{vmatrix} \hat{\mathbf{e}}_x & \hat{\mathbf{e}}_y & \hat{\mathbf{e}}_z \\ \partial_x & \partial_y & \partial_z \\ A_x & A_y & A_z \end{vmatrix} = \hat{\mathbf{e}}_x \left(\frac{\partial A_z}{\partial y} - \frac{\partial A_y}{\partial z}\right) + \hat{\mathbf{e}}_y \left(\frac{\partial A_x}{\partial z} - \frac{\partial A_z}{\partial x}\right) + \hat{\mathbf{e}}_z \left(\frac{\partial A_y}{\partial x} - \frac{\partial A_x}{\partial y}\right) . \tag{1.15}$$

Obviously the rotation is a vector field calculated from another vector field.

> *The rotation measures how many of the field lines of a vector field* $\mathbf{A}(\mathbf{r})$ *passing through an infinitesimal volume, return into it.*

Exposed to a field with rotation, an extended distribution of masses will start spinning in closed orbits.

We consider the examples shown in Fig. 1.3. The properties of divergence and rotation are complementary. There are fields exhibiting only one of the properties, or both, or none of them. In cases where there is rotation, it is problematic to specify equipotential lines: Either, the field lines are not orthogonal to the equipotential lines, or they come back.

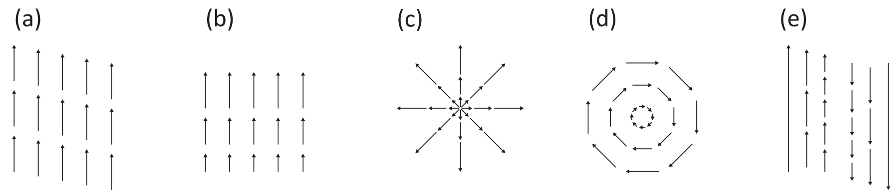

Figure 1.3: (a) Field without divergence, (b) with constant divergence, (c) with radial divergence, (d) with rotation, and (e) with rotation.

Example 2 (*Rotation of a radial field*): We consider the example of a radial field, $\mathbf{A}(\mathbf{r}) = -y\hat{\mathbf{e}}_x + x\hat{\mathbf{e}}_y$:

$$\nabla \times \mathbf{A} = \begin{pmatrix} 0 - \partial_z x \\ \partial_z(-y) - 0 \\ \partial_x x - \partial_y(-y) \end{pmatrix} = 2\hat{\mathbf{e}}_z \ . \tag{1.16}$$

We practice the calculation with divergence and rotation in the Excs. 1.1.7.4 to 1.1.7.7.

1.1.5 Taylor expansion of scalar and vector fields

We know well the Taylor expansion of functions of one variable:

$$\Phi(x+h) = \exp(h\tfrac{d}{dx})\Phi(x) = \sum_{\nu=0}^{\infty} \tfrac{1}{\nu!}(h\tfrac{d}{dx})^\nu \Phi(x) = \Phi(x) + h\Phi'(x) + \tfrac{h}{2}\Phi''(x) + \dots \ . \tag{1.17}$$

The generalization of the expansion to a scalar field, which depends on a vector, is,

$$\Phi(\mathbf{r}+\mathbf{h}) = \exp(\mathbf{h}\cdot\nabla_{\mathbf{r}})\Phi(\mathbf{r}) = \sum_{\nu=0}^{\infty}\frac{1}{\nu!}(\mathbf{h}\cdot\nabla_{\mathbf{r}})^{\nu}\Phi(\mathbf{r}) \tag{1.18}$$
$$= \Phi(\mathbf{r}) + (\mathbf{h}\cdot\nabla_{\mathbf{r}})\Phi(\mathbf{r}) + \tfrac{1}{2}(\mathbf{h}\cdot\nabla_{\mathbf{r}})(\mathbf{h}\cdot\nabla_{\mathbf{r}})\Phi(\mathbf{r}) + \ldots\ .$$

We see that the operator $\nabla_{\mathbf{r}}$ generates a translation. We study the Taylor expansion of scalar fields in Exc. 1.1.7.8.

The generalization of the gradient of a vector field is the Jacobian,

$$\mathbf{A} = \begin{pmatrix} A_1 \\ \vdots \\ A_n \end{pmatrix} \qquad \Longrightarrow \qquad J[\mathbf{A}] = \begin{pmatrix} \frac{\partial A_1}{\partial x_1} & \cdots & \frac{\partial A_1}{\partial x_n} \\ \vdots & \ddots & \vdots \\ \frac{\partial A_n}{\partial x_1} & \cdots & \frac{\partial A_n}{\partial x_n} \end{pmatrix}\ . \tag{1.19}$$

Therefore, the generalization of the expansion to a vector field is,

$$\mathbf{A}(\mathbf{r}+\mathbf{h}) = \exp(\mathbf{h}\cdot\nabla_{\mathbf{r}})\mathbf{A}(\mathbf{r}) = \mathbf{A}(\mathbf{r}) + \begin{pmatrix} (\mathbf{h}\cdot\nabla_{\mathbf{r}})A_1 \\ \vdots \\ (\mathbf{h}\cdot\nabla_{\mathbf{r}})A_n \end{pmatrix} + \ldots \tag{1.20}$$
$$= \mathbf{A}(\mathbf{r}) + \begin{pmatrix} h_1\frac{\partial F_1}{\partial x_1} + \ldots + h_n\frac{\partial F_1}{\partial x_n} \\ \vdots \\ h_1\frac{\partial F_n}{\partial x_1} + \ldots + h_n\frac{\partial F_n}{\partial x_n} \end{pmatrix} + \ldots = \mathbf{A}(\mathbf{r}) + J[\mathbf{A}]\mathbf{h} + \ldots\ .$$

1.1.6 Rules for calculation with derivatives

In total there are four possible ways of defining products involving scalar and vector fields, $\Phi\Psi$, $\Phi\mathbf{A}$, $\mathbf{A}\cdot\mathbf{B}$, and $\mathbf{A}\times\mathbf{B}$, and six product rules to calculate the following expressions,

$$\nabla(\Phi\Psi)\quad,\quad\nabla(\mathbf{A}\cdot\mathbf{B})\quad,\quad\nabla\cdot(\Phi\mathbf{A})\quad,\quad\nabla\cdot(\mathbf{A}\times\mathbf{B})\quad,\quad\nabla\times(\Phi\mathbf{A})\quad,\quad\nabla\times(\mathbf{A}\times\mathbf{B})\ . \tag{1.21}$$

Second derivatives can also be defined in six different combinations,

$$\nabla\cdot(\nabla\phi)\quad,\quad\nabla\times(\nabla\phi)\quad,\quad\nabla(\nabla\cdot\mathbf{A})\quad,\quad\nabla\cdot(\nabla\times\mathbf{A})\quad,\quad\nabla\times(\nabla\times\mathbf{A})\ . \tag{1.22}$$

As these rules are used frequently, we summarized them in Secs. 10.6.1 and 10.6.2.

The rules can be derived componentwise from scalar product rules. Very useful tools for this are the *Kronecker symbol* and the *Levi-Civita tensor*. Let us consider a Cartesian coordinate system $i = 1, 2, 3$. The coordinates in this system are x_i and the derivatives $\partial_i \equiv \frac{\partial}{\partial x_i}$. The Kronecker symbol is defined by,

$$\delta_{mn} = \begin{cases} 1 & \text{for } m = n \\ 0 & \text{else} \end{cases}\ . \tag{1.23}$$

The Levi-Civita tensor is defined by,

$$\epsilon_{kmn} = \begin{cases} 1 & \text{when } (kmn) \text{ is an even permutation of } (123) \\ -1 & \text{when } (kmn) \text{ is an odd permutation of } (123) \\ 0 & \text{when at least two indices are identical} \end{cases}\ . \tag{1.24}$$

Adopting Einstein's summing convention, we automatically take the sum of an expression over all indexes appearing twice. For example, the scalar product can be written,

$$\mathbf{A}\cdot\mathbf{B} = \sum_i A_i B_i \equiv A_i B_i \ . \tag{1.25}$$

For the vector product we obtain,

$$(\mathbf{A}\times\mathbf{B})_k \equiv \epsilon_{kmn} A_m B_n \ . \tag{1.26}$$

Other examples will be discussed in the Excs. 1.1.7.9 to 1.1.7.11.

1.1.7 Exercises

1.1.7.1 Ex: Differential operators

Find the gradients of the following scalar fields:
a. $\Phi(\mathbf{r}) = x^2 + y^3 + z^4$,
b. $\Phi(\mathbf{r}) = x^2 y^3 z^4$,
c. $\Phi(\mathbf{r}) = e^x \sin y \ln z$.

1.1.7.2 Ex: 2D landscape

A 2D landscape is parametrized by $h(x,y) = 10(2xy - 3x^2 - 4y^2 - 18x + 28y + 12)$.
a. Where is mountain top?
b. What is its height?

1.1.7.3 Ex: Differential operators

Calculate $\nabla_{\mathbf{r}'}|\mathbf{r}-\mathbf{r}'|^n$.

1.1.7.4 Ex: Differential operators

Calculate the divergence and the rotation of the vector field $\mathbf{A} = e^{-x^2 y}\hat{\mathbf{e}}_x + \frac{z}{1+y^2}\hat{\mathbf{e}}_y + x\hat{\mathbf{e}}_z$ at the position $(0,1,1)$.

1.1.7.5 Ex: Sources and vertices

a. Determine the divergence and the rotation of the vector field $\mathbf{A} = A_x\hat{\mathbf{e}}_x + A_y\hat{\mathbf{e}}_y + A_z\hat{\mathbf{e}}_z$.
b. Calculate for the following fields the sources and vortices:

$$\mathbf{A}_1 = -y\hat{\mathbf{e}}_x + x\hat{\mathbf{e}}_y \quad , \quad \mathbf{A}_2 = +y\hat{\mathbf{e}}_x + x\hat{\mathbf{e}}_y \ ,$$
$$\mathbf{A}_3 = +x\hat{\mathbf{e}}_x + y\hat{\mathbf{e}}_y \quad , \quad \mathbf{A}_4 = +x\hat{\mathbf{e}}_x + x\hat{\mathbf{e}}_y \ .$$

c. Make a graphic illustration of the fields and give a geometric interpretation of div and rot.

1.1.7.6 Ex: Sources and vertices

Calculate the divergence $\nabla\cdot\frac{\mathbf{r}}{r^3}$.

1.1.7.7 Ex: Chain rule for functions of vector field

Apply the chain rule to the gradient of a scalar function of a vector field: $\nabla\phi(\mathbf{E}(\mathbf{r}))$. Use the rule to calculate $\nabla\sqrt{a\mathbf{r}^2}$.

1.1.7.8 Ex: Taylor expansion in 3D

Consider the function,

$$f(\mathbf{x}) = \frac{1}{|\mathbf{d}-\mathbf{x}|} \ .$$

Calculate the Taylor expansion in x of this function in Cartesian coordinates at the position $x = 0$ (in all three spatial coordinates) up to second-order.

1.1.7.9 Ex: Levi-Civita tensor

Prove the following relationships for the Kronecker symbol and the Levi-Civita tensor by distinguishing the cases in the indices,
a. $\epsilon_{ijk}\delta_{ij} = 0$,
b. $\epsilon_{ijk}\epsilon_{ijk} = 6$,
d. $\epsilon_{ijk}\epsilon_{imn} = \delta_{jm}\delta_{kn} - \delta_{jn}\delta_{km}$,
c. $\epsilon_{ijk}\epsilon_{ijn} = 2\delta_{kn}$.

1.1.7.10 Ex: Levi-Civita tensor

Let the vectors $\mathbf{A}$, $\mathbf{B}$, $\mathbf{C}$, and $\mathbf{D} \in \mathbb{R}^3$ be given. Using the Kronecker Symbol and the Levi-Civita Tensor
a. show $\{\mathbf{A}\times\mathbf{B}\}_i = \epsilon_{ijk}A_jB_k$;
b. prove the relationship, $(\mathbf{A}\times\mathbf{B})\cdot\mathbf{C} = (\mathbf{B}\times\mathbf{C})\cdot\mathbf{A} = (\mathbf{C}\times\mathbf{A})\cdot\mathbf{B}$; c. Using the formulas of (b) derive the following rules of calculation:

i. $(\mathbf{A}\times\mathbf{B})^2 = \mathbf{A}^2\mathbf{B}^2 - (\mathbf{A}\cdot\mathbf{B})^2$
ii. $(\mathbf{A}\times\mathbf{B})\cdot(\mathbf{C}\times\mathbf{D}) = (\mathbf{A}\cdot\mathbf{C})(\mathbf{B}\cdot\mathbf{D}) - (\mathbf{A}\cdot\mathbf{D})(\mathbf{B}\cdot\mathbf{C})$;

d. prove that:

i. $(\mathbf{A}\times\mathbf{B})\cdot[(\mathbf{B}\times\mathbf{C})\times(\mathbf{C}\times\mathbf{A})] = [\mathbf{A}\cdot(\mathbf{B}\times\mathbf{C})]^2$
ii. $\mathbf{A}\times(\mathbf{B}\times\mathbf{C}) + \mathbf{B}\times(\mathbf{C}\times\mathbf{A}) + \mathbf{C}\times(\mathbf{A}\times\mathbf{B}) = 0$.

1.1.7.11 Ex: Levi-Civita tensor and vector tautologies

Be Ψ and Φ scalar fields and $\mathbf{A}$, $\mathbf{B}$, $\mathbf{C}$, and $\mathbf{D}$ vector fields. Show the following identities with the help of the Kronecker symbol.:
a. $\mathbf{A}\cdot(\mathbf{B}\times\mathbf{C}) = \mathbf{B}\cdot(\mathbf{C}\times\mathbf{A})$,
b. $(\mathbf{A}\times\mathbf{B})\cdot(\mathbf{C}\times\mathbf{D}) = (\mathbf{A}\cdot\mathbf{C})(\mathbf{B}\cdot\mathbf{D}) - (\mathbf{B}\cdot\mathbf{C})(\mathbf{A}\cdot\mathbf{D})$,
c. $(\mathbf{A}\times\mathbf{B})\times(\mathbf{C}\times\mathbf{D}) = ((\mathbf{A}\times\mathbf{B})\cdot\mathbf{D})\mathbf{C} - ((\mathbf{A}\times\mathbf{B})\cdot\mathbf{C})\mathbf{D}$,
d. $\nabla(\Phi\Psi) = \Phi\nabla\Psi + \Psi\nabla\Phi$,

e. $\nabla \times (\Phi \mathbf{A}) = (\nabla\Phi) \times \mathbf{A} + \Phi\nabla \times \mathbf{A}$,
f. $\nabla \times (\mathbf{A} \times \mathbf{B}) = (\mathbf{B} \cdot \nabla)\mathbf{A} - (\mathbf{A} \cdot \nabla)\mathbf{B} + \mathbf{A}(\nabla \cdot \mathbf{B}) - \mathbf{B}(\nabla \cdot \mathbf{A})$,
g. $\nabla(\mathbf{A} \cdot \mathbf{B}) = \mathbf{A} \times (\nabla \times \mathbf{B}) + \mathbf{B} \times (\nabla \times \mathbf{A}) + (\mathbf{A} \cdot \nabla)\mathbf{B} + (\mathbf{B} \cdot \nabla)\mathbf{A}$,
h. $\nabla \cdot (\nabla\Phi) = \Delta\Phi$,
i. $\mathbf{A} \cdot (\nabla\Phi) = (\mathbf{A} \cdot \nabla)\Phi$,
j. $\mathbf{A} \times (\nabla\Phi) = (\mathbf{A} \times \nabla)\Phi$.
k. $\nabla \cdot (\mathbf{A} \times \mathbf{B}) = \mathbf{B} \cdot (\nabla \times \mathbf{A}) - \mathbf{A} \cdot (\nabla \times \mathbf{B})$,
l. $\nabla\,(\Psi\mathbf{A}) = \mathbf{A} \cdot \nabla\Psi + \Psi\nabla \cdot \mathbf{A}$,
m. $\nabla \cdot (\Psi\nabla\Psi) = \Psi\Delta\Psi + (\nabla\Psi)^2$
n. $\nabla \cdot (\mathbf{A} \times \mathbf{B}) = \mathbf{B} \cdot (\nabla \times \mathbf{A}) - \mathbf{A} \cdot (\nabla \times \mathbf{B})$,
o. $\nabla \cdot (\nabla \times \mathbf{A}) = 0$,
p. $\nabla \times (\nabla\Phi) = 0$,
q. $\nabla \times (\nabla \times \mathbf{A}) = \nabla(\nabla \cdot \mathbf{A}) - \nabla^2\mathbf{A}$.

1.2 Integral calculus

Three types of integrals are often used in electrodynamics, the *path integral*, the *surface integral*, and the *volume integral*.

1.2.1 Path integral

The path integral is defined on a trajectory $\mathcal{C}(\mathbf{a}, \mathbf{b})$ through a (scalar or vector) field linking a start point $\mathbf{a}$ to an end point $\mathbf{b}$. While following the path point by point, incrementing the infinitesimal displacement vector $d\mathbf{l}$ (see Fig. 1.4), we evaluate the local value and the direction of the field, multiply it with $d\mathbf{l}$, and sum it up,

$$\int_{\mathcal{C}(\mathbf{a},\mathbf{b})} \Phi d\mathbf{l} \quad , \quad \int_{\mathcal{C}(\mathbf{a},\mathbf{b})} \mathbf{A} \cdot d\mathbf{l} \ . \tag{1.27}$$

Note that in case of a vector field, the integral is taken over the scalar product between the local field vector and the path element. The work exerted by a force field, $W \equiv \int \mathbf{F} \cdot \mathbf{l}$ is an example. For a path through a field crossing all force lines under right angle, the path integral zeroes, meaning that no work is accumulated.

Depending on the properties of the field, the integral may only depend on the points $\mathbf{a}$ and $\mathbf{b}$ and not on the path $\mathcal{C}$ chosen to go from one to the other. In this case, we say that the vector field is *conservative*, but this is not always the case. Choosing $\mathbf{a} = \mathbf{b}$ we get a closed path, which can be thought of as delimiting a surface in 3D space. We use the notation,

$$\oint_{\partial S} \mathbf{A} \cdot d\mathbf{l} \ , \tag{1.28}$$

where the symbol ∂S suggests, that the path goes along the edge of the surface S.

In practice, it is often useful to find a parametrization $\mathbf{l}(t)$ for the path with a parameter (e.g. time) defined over $t \in [0, 1]$. It allows us to calculate explicitly,

$$\int_{\mathcal{C}(\mathbf{a},\mathbf{b})} \nabla\Phi \cdot d\mathbf{l} = \int_0^1 \nabla\Phi(\mathbf{r}) \cdot \frac{d\mathbf{l}(t)}{dt} dt \ . \tag{1.29}$$

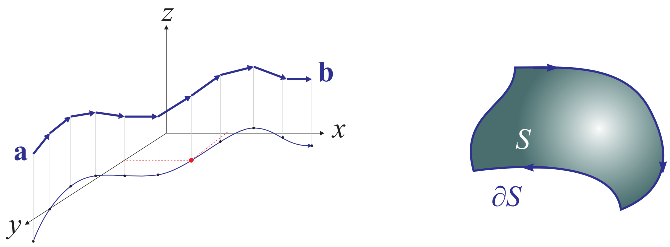

Figure 1.4: Integrating along a path in three-dimensional space.

Example 3 (*Path integral*): As an example, we will calculate the integral along the path parametrized by $\mathbf{l}(t) = \hat{\mathbf{e}}_x \cos t + \hat{\mathbf{e}}_y \sin t$, which is a unit circle around the origin, inside the field $\mathbf{A}(\mathbf{r}) = -y\hat{\mathbf{e}}_x + x\hat{\mathbf{e}}_y$:

$$\oint \mathbf{A}\cdot d\mathbf{l} = \int_0^{2\pi} (-y\hat{\mathbf{e}}_x + x\hat{\mathbf{e}}_y)\cdot \frac{dl}{dt}dt \tag{1.30}$$
$$= \int_0^{2\pi} (-\hat{\mathbf{e}}_x \sin t + \hat{\mathbf{e}}_y \cos t)\left(\hat{\mathbf{e}}_x \frac{d\cos t}{dt} + \hat{\mathbf{e}}_y \frac{d\sin t}{dt}\right) dt = \int_0^{2\pi} (\sin^2 t + \cos^2 t)dt = 2\pi \ .$$

We calculate other examples of path integrals in the Excs. 1.2.7.1 to 1.2.7.4.

1.2.2 Surface integral

The surface integral is defined on a surface $\mathcal{S}$, which can be folded in three-dimensional space. The surface is parceled into infinitesimal areas $d\mathbf{S}$, the local value and the direction of the field are evaluated, multiplied with $d\mathbf{S}$, and summed up,

$$\int_{\mathcal{S}} \Phi d\mathbf{S} \quad , \quad \int_{\mathcal{S}} \mathbf{A}\cdot d\mathbf{S} \ . \tag{1.31}$$

The vector of the area $d\mathbf{S}$ is the local normal vector. In case of the vector field, the integral is taken over the scalar product between the field and the local area. The flux, that is the field lines crossing a surface, $\Psi \equiv \int \mathbf{E}\cdot d\mathbf{S}$ it is an example. The normal vector of the surface of a volume is usually taken as pointing *out of the volume*. For example, a surface element of the x-y plane can be written $d\mathbf{S} = \hat{\mathbf{e}}_z dxdy$ in Cartesian coordinates. For curved surfaces or in curvilinear coordinates the expression will be more complicated.

Often we consider closed surfaces, which can be considered as delimiting a volume in 3D space. We use the notation,

$$\oint_{\partial\mathcal{V}} \mathbf{A}\cdot d\mathbf{S} \ , \tag{1.32}$$

where the symbol $\partial\mathcal{V}$ suggests that the surface encloses the volume $\mathcal{V}$.

Example 4 (*Flow of a field*): As an example, we calculate the field flux

$\mathbf{A} = -y\hat{\mathbf{e}}_x + x^2 y\hat{\mathbf{e}}_y$ through the unit cube:

$$\begin{aligned}\oint_{cubo} \mathbf{A}\cdot dS = &\int_{-1}^{1}\int_{-1}^{1} \mathbf{A}|_{z=1}\hat{\mathbf{e}}_z dxdy + \int_{-1}^{1}\int_{-1}^{1} \mathbf{A}|_{z=-1}(-\hat{\mathbf{e}}_z)dxdy + \int_{-1}^{1}\int_{-1}^{1} \mathbf{A}|_{x=1}\hat{\mathbf{e}}_x dydz \\ &+ \int_{-1}^{1}\int_{-1}^{1} \mathbf{A}|_{x=-1} dydz + \int_{-1}^{1}\int_{-1}^{1} \mathbf{A}|_{y=1}\hat{\mathbf{e}}_y dzdx + \int_{-1}^{1}\int_{-1}^{1} \mathbf{A}|_{y=-1}(-\hat{\mathbf{e}}_y)dzdx \\ &= 0 + 0 + \int_{-1}^{1}\int_{-1}^{1} (-y)dydz + \int_{-1}^{1}\int_{-1}^{1} ydydz + \int_{-1}^{1}\int_{-1}^{1} x^2 dzdx + \int_{-1}^{1}\int_{-1}^{1} x^2 dzdx \\ &= \frac{8}{3} \ . \end{aligned} \tag{1.33}$$

We calculate other examples of surface integrals in Excs. 1.2.7.5 to 1.2.7.8.

1.2.3 Volume integral

The volume integral defined by,

$$\int_{\mathcal{V}} \Phi dV \quad , \quad \int_{\mathcal{V}} \mathbf{A} dV \ . \tag{1.34}$$

In the case of a vector field, we simply write: $\hat{\mathbf{e}}_x \int A_x dV + \hat{\mathbf{e}}_y \int A_y dV + \hat{\mathbf{e}}_z \int A_z dV$.

Example 5 (*Integral de volume*): As an example, we calculate the mass of a cube with homogeneous density ρ_0:

$$m = \int_{-a/2}^{a/2}\int_{-a/2}^{a/2}\int_{-a/2}^{a/2} \rho_0 dxdydz = a^3\rho_0 \ . \tag{1.35}$$

We calculate another example of a volume integral in Exc. 1.2.7.9.

1.2.4 Fundamental theorem for gradients

The fundamental theorem of infinitesimal calculus says,

$$\int_{f_a}^{f_b} df = \int_a^b F(x)dx = f(b) - f(a) \qquad \text{or} \qquad df = F(x)dx \ , \tag{1.36}$$

for $F(x) = \frac{df}{dx}$. That is, derivation and integration are inverse operations.

Now in vector analysis, as explained above, we know three different types of derivatives. For each one we need to formulate the fundamental theorem in a specific way. For gradients,

$$\boxed{\int_{\mathcal{C}(\mathbf{a},\mathbf{b})} \nabla\Phi\cdot d\mathbf{l} = \Phi(\mathbf{b}) - \Phi(\mathbf{a})} \qquad \text{or} \qquad d\Phi = \nabla\Phi\cdot d\mathbf{l} \ . \tag{1.37}$$

Since the right-hand side does not depend on the path $\mathcal{C}$, the integral of the gradient can not either. As a consequence,

$$\boxed{\oint_{\mathcal{C}} \nabla\Phi\cdot d\mathbf{l} = 0} \ . \tag{1.38}$$

The geometric interpretation of the fundamental theorem for gradients is simple: Climbing a mountain following a path step by step and gaining at each step the potential energy $d\Phi = \nabla\Phi dx$, we accumulate between the end and the start point of the path the energy $\Phi(\mathbf{b}) - \Phi(\mathbf{a})$. Path independence is an inherent property of gradients.

Example 6 (*Fundamental theorem for gradients*): Let us consider the following example. To travel inside the potential $\Phi(\mathbf{r}) = xy^2$ between the points $\mathbf{r}_1 = (0,0,0)$ and $\mathbf{r}_2 = (2,1,0)$, we can choose between several paths, f.ex. $\mathbf{l}_1(t) = \hat{\mathbf{e}}_x 2t + \hat{\mathbf{e}}_y t$ or $\mathbf{l}_2(t) = \hat{\mathbf{e}}_x 2t + \hat{\mathbf{e}}_y t^2$ with $t \in [0,1]$. In both cases we gain the same potential energy $\Phi(\mathbf{r}_2) - \Phi(\mathbf{r}_1) = 2$:

$$\int_{\mathcal{C}(\mathbf{r}_1,\mathbf{r}_2)} \nabla\Phi \cdot d\mathbf{l}_1 = \int_0^1 (\hat{\mathbf{e}}_x y^2 + \hat{\mathbf{e}}_y 2xy) \cdot (\hat{\mathbf{e}}_x 2 + \hat{\mathbf{e}}_y) dt = \int_0^1 (2t^2 + 4t^2) dt = 2 \tag{1.39}$$

$$\int_{\mathcal{C}(\mathbf{r}_1,\mathbf{r}_2)} \nabla\Phi \cdot d\mathbf{l}_2 = \int_0^1 (\hat{\mathbf{e}}_x y^2 + \hat{\mathbf{e}}_y 2xy) \cdot (\hat{\mathbf{e}}_x 2 + \hat{\mathbf{e}}_y 2t) dt = \int_0^1 (2t^4 + 8t^4) dt = 2 \ .$$

An example for the application of the fundamental theorem for gradients is discussed in Exc. 1.2.7.10.

1.2.5 Stokes' theorem

Stokes' theorem allows us *to convert a surface integral into a path integral* provided the field to be integrated can be expressed as a rotation,

$$\boxed{\int_{\mathcal{S}} (\nabla \times \mathbf{A}) \cdot d\mathbf{S} = \oint_{\partial\mathcal{S}} \mathbf{A} \cdot d\mathbf{l}} \ . \tag{1.40}$$

To find a geometric interpretation we remember that the rotation measures the *twist* of a field $\mathbf{A}$. The integral over the rotation within a given surface (or, more precisely, the flux of the rotation through this surface) measures the total amount of vorticity. A rotating region is like a *kitchen beater* stirring the surface of an incompressible liquid: The more beaters are in the area, the more the liquid will be moved along the edges of the area. Instead of measuring the number of beaters (left-hand side of the theorem (1.40)), we can also walk along the edge of the area and measure the flux along the rim (right-hand side of the theorem (1.40)).

An interesting consequence of Stokes' theorem is that the path integral is independent of the shape of the surface. That is, if the field to be integrated can be expressed bin terms of a rotation, we can deform the surface (without touching the edge) without changing the twist of the field,

$$\boxed{\oint_{\mathcal{S}} (\nabla \times \mathbf{A}) \cdot d\mathbf{S} = 0} \ . \tag{1.41}$$

This is analogous to the corollary obtained for gradients (1.38).

Example 7 (*Teorema de Stokes*): Consider the following example. A field be given by, $\mathbf{A} = -y\hat{\mathbf{e}}_x + x\hat{\mathbf{e}}_y$, such that $\nabla \times \mathbf{A} = 2\hat{\mathbf{e}}_z$. The surface be a disk of radius R enclosed by a circular path parametrized by, $\mathbf{l} = \begin{pmatrix} R\cos\omega t \\ R\sin\omega t \\ 0 \end{pmatrix}$. Then,

$$\oint_{circle} \mathbf{A} \cdot dl = \int_0^{2\pi} \mathbf{A} \cdot \dot{l} dt = \int_0^{2\pi/\omega} \begin{pmatrix} -y \\ x \\ 0 \end{pmatrix} \cdot \begin{pmatrix} -R\omega\sin\omega t \\ R\omega\cos\omega t \\ 0 \end{pmatrix} dt = 2\pi R^2$$

$$\int_{disk} (\nabla \times \mathbf{A}) \cdot dS = \int_{disk} \begin{pmatrix} 0 \\ 0 \\ 2 \end{pmatrix} \hat{\mathbf{e}}_z d\mathbf{A} = 2 \int_{disk} dA = 2\pi R^2 \ .$$

In the Excs. 1.2.7.11 and 1.2.7.12 we show applications of Stokes' theorem.

1.2.6 Gauß' theorem

Gauß theorem allows us *to convert a volume integral into a surface integral* provided the field to be integrated can be expressed by a divergence,

$$\boxed{\int_{\mathcal{V}} (\nabla \cdot \mathbf{A}) \cdot dV = \oint_{\partial\mathcal{V}} \mathbf{A} \cdot d\mathbf{S}} \ . \tag{1.42}$$

To find a geometric interpretation we remember that the divergence measures the *expansion* force of the field $\mathbf{A}$. The integral over the divergence within a given volume measures the total amount of expansion. A divergent region with is like a tap releasing an incompressible liquid: The more taps are in the volume, the more liquid will be expelled by the edges of the volume. Instead of measuring the number of taps (left-hand side of the theorem (1.42)), we can also bypass the volume by measuring the flux through the surface (right-hand side of the theorem (1.42)).

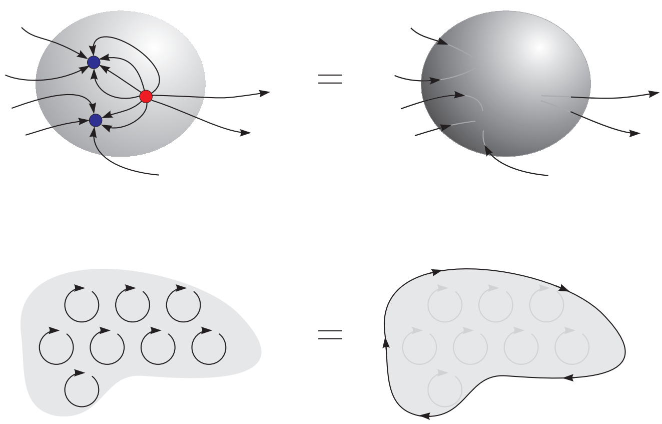

Figure 1.5: Illustration of the theorems of Gauß (above) and Stokes (below).

Example 8 (*Gauß theorem*): Consider the following example. A field be given by, $\mathbf{A} = \mathbf{r}$, such that $\nabla \cdot \mathbf{A} = 3$. The volume be a sphere of radius R

enclosed by a surface. So:

$$\oint_{sphericalsurface} \mathbf{A} \cdot d\mathbf{S} = \int_{sphericalsurface} \mathbf{r} \cdot \hat{\mathbf{e}}_r dS = rr^2 \int_0^{2\pi} \int_0^{\pi} \sin\theta d\theta d\phi = 4\pi R^3$$

$$\int_{sphere} (\nabla \cdot A) dV = \int_{sphere} 3dV = 3\frac{4\pi}{3} R^3 = 4\pi R^3 \ .$$

In the Excs. 1.2.7.13 to 1.2.7.16 we show applications of Gauß' theorem.

The theorems of Stokes and Gauß are often used in the context of cylindrical or spherical coordinates. Therefore, we will postpone the presentation of further examples, until we have discussed curvilinear coordinates.

1.2.7 Exercises

1.2.7.1 Ex: Path integral and work

Be the field electric $\mathbf{A}(\mathbf{r}) = E_0 z \hat{\mathbf{e}}_z$ be given. A charge $+q$ be shifted on a straight line from the point $(0, 0, 0)$ to the point $(1, 1, 1)$.
a. Write down parametrization for the trajectory.
b. Calculate the work spent on this charge explicitly along the path integral $W = q \int \mathbf{E}(\mathbf{r}) \cdot d\mathbf{r}$.
c. Calculate the work via the potential ϕ.

1.2.7.2 Ex: Path integral and work

Consider a field $\mathbf{E}$ depending on z in the following way $\mathbf{E} = E_0 z \hat{\mathbf{e}}_z$. A charge q is moved on a spiral-shaped trajectory $\mathbf{r}(t)$ with radius R,

$$\mathbf{r}(t) = \begin{pmatrix} R\cos t \\ R\sin t \\ \frac{h}{6\pi} t \end{pmatrix}$$

between $z = 0$ until $z = h$. Make a scheme of $\mathbf{r}(t)$. Calculate work made on the charge explicitly via a path integral $W = q \int \mathbf{E} \cdot d\mathbf{r}$. How can we calculate work more easily?

1.2.7.3 Ex: Path integral and work

Calculate the path integral in the field $\Phi = x^2 \hat{\mathbf{e}}_x + 2yz \hat{\mathbf{e}}_y + y^2 \hat{\mathbf{e}}_z$ from the origin to the point $(1, 1, 1)$ on three different paths:
a. For the path $(0, 0, 0) \longrightarrow (1, 0, 0) \longrightarrow (1, 1, 0) \longrightarrow (1, 1, 1)$;
b. for the path $(0, 0, 0) \longrightarrow (0, 0, 1) \longrightarrow (0, 1, 1) \longrightarrow (1, 1, 1)$;
c. and on a straight line.

1.2.7.4 Ex: Curve parametrization

The movement of a mass point is given in Cartesian coordinates by the vector $\mathbf{r}(t) = (\rho\cos\phi(t), \rho\sin\phi(t), z_0)$ with $\rho = vt$ and $\phi = \omega t + \phi_0$. What is the geometric figure dashed by the movement? Express the speed $\dot{\mathbf{r}}(t)$ and the acceleration $\ddot{\mathbf{r}}(t)$ in Cartesian coordinates. Calculate $|\mathbf{r}(t)|^2$, $|\dot{\mathbf{r}}(t)|^2$,$\mathbf{r}(t) \cdot \ddot{\mathbf{r}}(t)$ and $\mathbf{r}(t) \times \dot{\mathbf{r}}(t)$.

1.2.7.5 Ex: Surface integrals

Given be the vector field $\mathbf{A} = zy\hat{\mathbf{e}}_x + y^3 \sin^2 x\hat{\mathbf{e}}_y + xy^2 e^z \hat{\mathbf{e}}_z$. Calculate the integrals $\int \mathbf{A} \cdot d\mathbf{F}$ over the triangle $(0,0,0) \to (0,3,0) \to (0,0,3) \to (0,0,0)$, and over the rectangle $(2,2,0) \to (2,4,0) \to (4,4,0) \to (4,2,0) \to (2,2,0)$.

1.2.7.6 Ex: Surface integrals

Calculate the integral over a closed surface
a. of the field $\mathbf{A} = \mathbf{r}$ over the cube $0 \le x \le 1$, $0 \le y \le 1$, $0 \le z \le 1$ e
b. of the field $\mathbf{A} = \rho\mathbf{E}_\rho$ over the radial surface of the cylinder $0 \le z \le 1$, $0 \le \rho \le 1$.

1.2.7.7 Ex: Surface integrals

Calculate for the vector field $\mathbf{A}(\mathbf{r}) = c\mathbf{r}$ with c =constant the surface integral

$$I = \int_F \mathbf{A}(\mathbf{r}) \times d\mathbf{S}$$

a. over the surface of a sphere (radius R, center in the origin of coordinates)
b. over the surface of a cylinder (radius R, length L).

1.2.7.8 Ex: Surface integrals

Prove the relationship:

$$t_{ij} \equiv \int_{O(a)} d\mathbf{f} x_i x_j = \frac{4\pi}{3} a^4 \delta_{ij} \ ,$$

where $i, j = 1, 2, 3$, $x_1 = x$, $x_2 = y$, $x_3 = z$, and the integral has to be calculated on the surface of a sphere with radius a.

1.2.7.9 Ex: Volume integrals

Calculate the volume integral of the function $\Phi = z^2$ over the tetrahedron with the corners in $(0,0,0)$, $(1,0,0)$, $(0,1,0)$, and $(0,0,1)$.

1.2.7.10 Ex: Fundamental theorem for gradients

What is the energy gain within the potential $\Phi(\mathbf{r}) = \Phi_0 \frac{\sin kr}{kr}$ along a path keeping a constant distance from the origin.

1.2.7.11 Ex: Stokes integral theorem

Calculate for following field,

$$\mathbf{A}(\mathbf{r}) = \begin{pmatrix} yz \\ azx \\ xy \end{pmatrix}$$

using Stokes' law the path integral $\oint \mathbf{A} \cdot \mathbf{r}$ for an integration along a circle with radius R around the z-axis at the position $z = h$.

1.2.7.12 Ex: Stokes integral theorem

Calculate the integral $\oint_{\mathcal{C}} x(\hat{\mathbf{e}}_x + \hat{\mathbf{e}}_y)\, d\mathbf{r}$, where $\mathcal{C}$ be the unit circle in the x-y-plane.

1.2.7.13 Ex: Gauß integral theorem

Calculate the flux of the vector field $\mathbf{A}(\mathbf{r}) = \mathbf{r}$ through a sphere with radius R
a. by the surface integral and
b. with the help of Gauß's theorem for the volume integral over the divergence.

1.2.7.14 Ex: Gauß integral theorem

Let F be the surface of an arbitrary volume V. Determine for $\mathbf{A}(x_1, x_2, x_3) = (ax_1, bx_2, cx_3)$ the validity of the relationship,

$$\oint_F d\mathbf{F} \cdot \mathbf{A} = (a+b+c)V \ .$$

1.2.7.15 Ex: Gauß integral theorem

Be a a scalar field and $\mathbf{B}$ a vector field. Show,

$$\int_V d^3\mathbf{r}\ \mathbf{B} \cdot \nabla a = \int_{O(V)} a\mathbf{B} \ \cdot \ d\mathbf{F} - \int_V d^3\mathbf{r}\ a\nabla \cdot \mathbf{B} \ .$$

1.2.7.16 Ex: Gauß integral theorem

Calculate the integral $\oint_{\mathcal{C}} x(\hat{\mathbf{e}}_x + \hat{\mathbf{e}}_y) \cdot d\mathbf{r}$ about a unitary circular path $\mathcal{C}$ along the equator and the integral $\oint_{\mathcal{F}} x(\hat{\mathbf{e}}_x + \hat{\mathbf{e}}_y) \cdot d\mathbf{F}$, where $\mathcal{F}$ be the surface of a unit sphere.

1.3 Curvilinear coordinates

The most commonly used coordinate systems are Cartesian, cylindrical and spherical. Cylindrical coordinates are expressed in terms of Cartesian coordinates by,

$$\begin{pmatrix} x \\ y \\ z \end{pmatrix} = \begin{pmatrix} \rho\cos\phi \\ \rho\sin\phi \\ z \end{pmatrix} \ . \tag{1.43}$$

And spherical coordinates are expressed in terms of Cartesian coordinates by,

$$\begin{pmatrix} x \\ y \\ z \end{pmatrix} = \begin{pmatrix} r\sin\theta\cos\phi \\ r\sin\theta\sin\phi \\ r\cos\theta \end{pmatrix} \ . \tag{1.44}$$

The task now is to express the differential elements (that is, line, surface and volume elements), as well as differential operators (that is, the gradient, divergent and rotation) and the Laplacian in term of curvilinear coordinates.

Let us first consider the general case. The transformation from a Cartesian coordinate system (x, y, z) into a general, curvilinear system (u, v, w) is given by,

$$\mathbf{r} \equiv \begin{pmatrix} x(u,v,w) \\ y(u,v,w) \\ z(u,v,w) \end{pmatrix} . \tag{1.45}$$

The change $d_u\mathbf{r}$ resulting from a small variation du is then $d_u\mathbf{r} = \frac{\partial \mathbf{r}}{\partial u}du$ and occurs in the direction of the new unit vector $\hat{\mathbf{e}}_u$. The unit vectors of the new system, therefore, can be written as,

$$\hat{\mathbf{e}}_u = U(u,v,w)\frac{\partial \mathbf{r}}{\partial u} \quad , \quad \hat{\mathbf{e}}_v = V(u,v,w)\frac{\partial \mathbf{r}}{\partial v} \quad , \quad \hat{\mathbf{e}}_w = W(u,v,w)\frac{\partial \mathbf{r}}{\partial w} \; , \tag{1.46}$$

where

$$U = \left|\frac{\partial \mathbf{r}}{\partial u}\right|^{-1} \quad , \quad V = \left|\frac{\partial \mathbf{r}}{\partial v}\right|^{-1} \quad , \quad W = \left|\frac{\partial \mathbf{r}}{\partial w}\right|^{-1} . \tag{1.47}$$

In the Excs. 1.3.8.1 we study transformations into cylindrical and spherical coordinates.

1.3.1 Differential elements in curvilinear coordinates

In the following we restrict ourselves to orthogonal coordinates, where the unit vectors are perpendicular. In this case, the total differential $d\mathbf{r}$ has the form,

$$d\mathbf{r} = \frac{\partial \mathbf{r}}{\partial u}du + \frac{\partial \mathbf{r}}{\partial v}dv + \frac{\partial \mathbf{r}}{\partial w}dw = \hat{\mathbf{e}}_u\frac{du}{U} + \hat{\mathbf{e}}_v\frac{dv}{V} + \hat{\mathbf{e}}_w\frac{dw}{W} \; , \tag{1.48}$$

and has the length,

$$|d\mathbf{r}|^2 = \left(\frac{du}{U}\right)^2 + \left(\frac{dv}{V}\right)^2 + \left(\frac{dw}{W}\right)^2 . \tag{1.49}$$

The volume element is,

$$d\tau = ds_u ds_v ds_w \; . \tag{1.50}$$

1.3.2 Gradient in curvilinear coordinates

We can now express the gradient of a scalar field Φ in orthogonal curvilinear coordinates,

$$\text{grad}\;\Phi = \nabla\Phi = f_u\hat{\mathbf{e}}_u + f_v\hat{\mathbf{e}}_v + f_w\hat{\mathbf{e}}_w \; , \tag{1.51}$$

where the f_i are functions which have yet to be determined. To this end we compare the coefficients of the expressions,

$$d\Phi = \frac{\partial \Phi}{\partial u}du + \frac{\partial \Phi}{\partial v}dv + \frac{\partial \Phi}{\partial w}dw \; , \tag{1.52}$$

and, inserting (1.48) and (1.51),

$$d\Phi = d\mathbf{r} \cdot \nabla\Phi = \frac{f_u}{U}du + \frac{f_v}{V}dv + \frac{f_w}{W}dw \ . \tag{1.53}$$

We obtain,

$$\nabla\Phi = \left(U\frac{\partial\Phi}{\partial u}\right)\hat{\mathbf{e}}_u + \left(V\frac{\partial\Phi}{\partial v}\right)\hat{\mathbf{e}}_v + \left(W\frac{\partial\Phi}{\partial w}\right)\hat{\mathbf{e}}_w \ . \tag{1.54}$$

1.3.3 Divergence in curvilinear coordinates

Now we will show how to express the divergence of a vector field $\mathbf{A}$ in orthogonal curvilinear coordinates,

$$\text{div } \mathbf{A} = \nabla \cdot \mathbf{A} \ . \tag{1.55}$$

The derivation is a bit complicated. We begin by expressing the unit vectors $\hat{\mathbf{e}}_u$, $\hat{\mathbf{e}}_v$, and $\hat{\mathbf{e}}_w$ by the gradients ∇u, ∇v, and ∇w, using the expression for the gradient (1.54),

$$\nabla u = U\hat{\mathbf{e}}_u \quad , \quad \nabla v = V\hat{\mathbf{e}}_v \quad , \quad \nabla w = W\hat{\mathbf{e}}_w \ . \tag{1.56}$$

We now express each unit vector as the vector product of two of these gradients,

$$\begin{aligned}\nabla u \times \nabla v &= UV\ \hat{\mathbf{e}}_u \times \hat{\mathbf{e}}_v = UV\hat{\mathbf{e}}_w \\ \nabla v \times \nabla w &= VW\ \hat{\mathbf{e}}_v \times \hat{\mathbf{e}}_w = VW\hat{\mathbf{e}}_u \\ \nabla w \times \nabla u &= WU\ \hat{\mathbf{e}}_w \times \hat{\mathbf{e}}_u = WU\hat{\mathbf{e}}_v \ .\end{aligned} \tag{1.57}$$

After that we write $\mathbf{A} = a_u\hat{\mathbf{e}}_u + a_v\hat{\mathbf{e}}_v + a_w\hat{\mathbf{e}}_w$ and start considering the first term of the divergence:

$$\begin{aligned}&\nabla \cdot (a_u\hat{\mathbf{e}}_u) = \nabla \cdot \left(\frac{a_u}{VW}\nabla v \times \nabla w\right) \\ &= (\nabla v \times \nabla w) \cdot \nabla\left(\frac{a_u}{VW}\right) + \frac{a_u}{VW}\nabla \cdot (\nabla v \times \nabla w) \quad \text{using} \quad \nabla \cdot (\alpha\mathbf{A}) = \mathbf{A} \cdot (\nabla\alpha) + \alpha(\nabla \cdot \mathbf{A}) \\ &= VW\hat{\mathbf{e}}_u \cdot \left[\hat{\mathbf{e}}_u U\frac{\partial}{\partial u}\left(\frac{a_u}{VW}\right) + \hat{\mathbf{e}}_v V\frac{\partial}{\partial v}\left(\frac{a_v}{VW}\right) + \hat{\mathbf{e}}_w W\frac{\partial}{\partial w}\left(\frac{a_w}{VW}\right)\right] \\ &\quad + \frac{a_u}{VW}\left[\nabla w \cdot (\nabla \times \nabla v) - \nabla v \cdot (\nabla \times \nabla w)\right] \quad \text{using} \quad \nabla \cdot (\mathbf{A} \times \mathbf{B}) = \mathbf{B} \cdot (\nabla \times \mathbf{A}) - \mathbf{A} \cdot (\nabla \times \mathbf{B}) \\ &= UVW\frac{\partial}{\partial u}\left(\frac{a_u}{VW}\right) \quad \text{using} \quad \nabla \times (\nabla\alpha) = 0 \ .\end{aligned} \tag{1.58}$$

Similarly we can show,

$$\nabla \cdot (a_v\hat{\mathbf{e}}_v) = UVW\frac{\partial}{\partial v}\left(\frac{a_v}{UW}\right) \quad \text{and} \quad \nabla \cdot (a_w\hat{\mathbf{e}}_w) = UVW\frac{\partial}{\partial w}\left(\frac{a_w}{UV}\right) \ . \tag{1.59}$$

With this we finally get,

$$\nabla \cdot \mathbf{A} = UVW\left[\frac{\partial}{\partial u}\left(\frac{a_u}{VW}\right) + \frac{\partial}{\partial v}\left(\frac{a_v}{UW}\right) + \frac{\partial}{\partial w}\left(\frac{a_w}{UV}\right)\right] \ . \tag{1.60}$$

1.3.4 Rotation in curvilinear coordinates

Now we will show how to express the rotation of a vector field $\mathbf{A}$ in orthogonal curvilinear coordinates,

$$\text{rot } \mathbf{A} = \nabla \times \mathbf{A} \ . \tag{1.61}$$

We write again, $\mathbf{A} = a_u\hat{\mathbf{e}}_u + a_v\hat{\mathbf{e}}_v + a_w\hat{\mathbf{e}}_w$ and start considering the first term of the rotation:

$$\begin{aligned}
\nabla \times (a_u\hat{\mathbf{e}}_u) &= \nabla \times \left(\frac{a_u}{U}\nabla u\right) \quad \text{using} \quad (1.56) \\
&= \left(\nabla\frac{a_u}{U}\right) \times \nabla u + \frac{a_u}{U}(\nabla \times \nabla u) \quad \text{using} \quad \nabla \times (\alpha\mathbf{A}) = (\nabla\alpha) \times \mathbf{A} + \alpha(\nabla \times \mathbf{A}) \\
&= U\left(\nabla\frac{a_u}{U}\right) \times \hat{\mathbf{e}}_u \quad \text{and} \quad \nabla \times (\nabla\alpha) = 0 \quad \text{using} \quad (1.56) \\
&= U\left[\hat{\mathbf{e}}_u U\frac{\partial}{\partial u}\left(\frac{a_u}{U}\right) + \hat{\mathbf{e}}_v V\frac{\partial}{\partial v}\left(\frac{a_u}{U}\right) + \hat{\mathbf{e}}_w W\frac{\partial}{\partial w}\left(\frac{a_u}{U}\right)\right] \times \hat{\mathbf{e}}_u \\
&= U\left[\hat{\mathbf{e}}_v W\frac{\partial}{\partial w}\left(\frac{a_u}{U}\right) - \hat{\mathbf{e}}_w V\frac{\partial}{\partial v}\left(\frac{a_u}{U}\right)\right] \\
&= UVW\left[\hat{\mathbf{e}}_v \frac{1}{V}\frac{\partial}{\partial w}\left(\frac{a_u}{U}\right) - \hat{\mathbf{e}}_w \frac{1}{W}\frac{\partial}{\partial v}\left(\frac{a_u}{U}\right)\right] \ .
\end{aligned} \tag{1.62}$$

Similarly we can show,

$$\begin{aligned}
\nabla \times (a_v\hat{\mathbf{e}}_v) &= UVW\left[\hat{\mathbf{e}}_w \frac{1}{W}\frac{\partial}{\partial u}\left(\frac{a_v}{V}\right) - \hat{\mathbf{e}}_u \frac{1}{U}\frac{\partial}{\partial w}\left(\frac{a_v}{V}\right)\right] \\
\nabla \times (a_w\hat{\mathbf{e}}_w) &= UVW\left[\hat{\mathbf{e}}_u \frac{1}{U}\frac{\partial}{\partial v}\left(\frac{a_w}{W}\right) - \hat{\mathbf{e}}_v \frac{1}{V}\frac{\partial}{\partial u}\left(\frac{a_w}{W}\right)\right] \ .
\end{aligned} \tag{1.63}$$

With this we finally obtain,

$$\begin{aligned}
\nabla \times \mathbf{A} = \hat{\mathbf{e}}_u VW\left[\frac{\partial}{\partial v}\left(\frac{a_w}{W}\right) - \frac{\partial}{\partial w}\left(\frac{a_v}{V}\right)\right] &+ \hat{\mathbf{e}}_v UW\left[\frac{\partial}{\partial w}\left(\frac{a_u}{U}\right) - \frac{\partial}{\partial u}\left(\frac{a_w}{w}\right)\right] \\
&+ \hat{\mathbf{e}}_w UV\left[\frac{\partial}{\partial u}\left(\frac{a_v}{V}\right) - \frac{\partial}{\partial v}\left(\frac{a_u}{U}\right)\right] \ ,
\end{aligned} \tag{1.64}$$

or, written as a determinant,

$$\nabla \times \mathbf{A} = UVW \ \det\begin{pmatrix} \frac{\hat{\mathbf{e}}_u}{U} & \frac{\hat{\mathbf{e}}_v}{V} & \frac{\hat{\mathbf{e}}_w}{W} \\ \frac{\partial}{\partial u} & \frac{\partial}{\partial v} & \frac{\partial}{\partial w} \\ \frac{a_u}{U} & \frac{a_v}{V} & \frac{a_w}{W} \end{pmatrix} \ . \tag{1.65}$$

1.3.5 Cylindrical coordinates

Let us now identify the general coordinates u, v, and w with the cylindrical coordinates ρ, θ, and ϕ defined in Eq. (1.43). In Exc. 1.3.8.2 we calculate for the line element,

$$d\mathbf{r} = d\rho\hat{\mathbf{e}}_\rho + \rho d\phi e_\phi + dz\hat{\mathbf{e}}_z \ , \tag{1.66}$$

the distance element,

$$|d\mathbf{r}|^2 = (d\rho)^2 + (\rho d\phi)^2 + (dz)^2 \ , \tag{1.67}$$

the surface element given by $z = z(\rho, \phi)$,

$$d\mathbf{s} = \left(-\frac{\partial z}{\partial \rho}\hat{\mathbf{e}}_\rho - \frac{1}{\rho}\frac{\partial z}{\partial \phi}\hat{\mathbf{e}}_\phi + \hat{\mathbf{e}}_z \right) \rho d\rho d\phi \ , \tag{1.68}$$

and the volume element,

$$d\tau = rdz\phi dr \ . \tag{1.69}$$

In the Excs. 1.3.8.3 to 1.3.8.5 we calculate, respectively, the gradient,

$$\nabla\Phi = \hat{\mathbf{e}}_\rho \, \frac{\partial \Phi}{\partial \rho} + \hat{\mathbf{e}}_\phi \, \frac{1}{\rho} \, \frac{\partial \Phi}{\partial \phi} + \hat{\mathbf{e}}_z \, \frac{\partial \Phi}{\partial z} \ , \tag{1.70}$$

the divergence,

$$\nabla \cdot \mathbf{A} = \frac{1}{\rho}\frac{\partial}{\partial \rho}[\rho \ a_\rho] + \frac{1}{\rho}\frac{\partial}{\partial \phi}[a_\phi] + \frac{\partial}{\partial z}[a_z] \ , \tag{1.71}$$

the rotation,

$$\nabla \times \mathbf{A} \ = \hat{\mathbf{e}}_\rho \ \frac{1}{\rho} \left[\frac{\partial a_z}{\partial \phi} - \rho \frac{\partial a_\phi}{\partial z} \right] + \hat{\mathbf{e}}_\phi \ \left[\frac{\partial a_\rho}{\partial z} - \frac{\partial a_z}{\partial \rho} \right] + \hat{\mathbf{e}}_z \ \frac{1}{\rho} \left[\frac{\partial}{\partial \rho}(\rho a_\phi) - \frac{\partial a_\rho}{\partial \phi} \right] \tag{1.72}$$

and the Laplace operator,

$$\Delta\Phi \equiv \nabla \cdot (\nabla\Phi) = \frac{1}{\rho}\frac{\partial}{\partial \rho}\left(\rho \frac{\partial \Phi}{\partial \rho} \right) + \frac{1}{\rho^2}\frac{\partial^2 \Phi}{\partial \phi^2} + \frac{\partial^2 \Phi}{\partial z^2} \ . \tag{1.73}$$

in cylindrical coordinates.

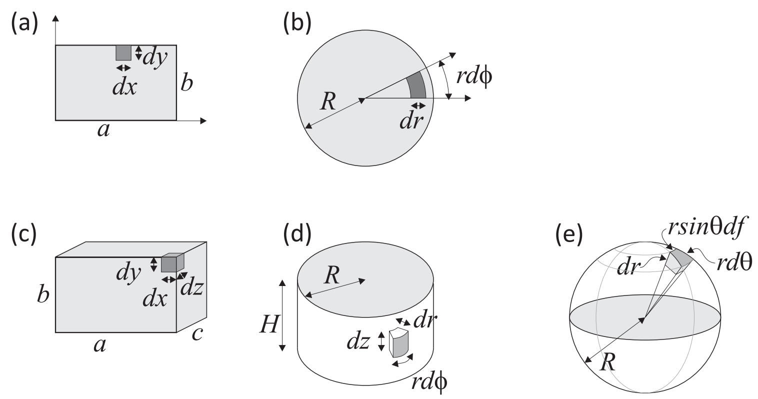

Figure 1.6: Illustration of Cartesian, polar, cylindrical and spherical coordinates.

1.3.6 Spherical coordinates

Let us now identify the general coordinates u, v, and w with the spherical coordinates r, θ, and ϕ defined in Eq. (1.44). In Exc. 1.3.8.2 we calculate for the line element,

$$d\mathbf{r} = dr\hat{\mathbf{e}}_r + rd\theta e_\theta + r\sin\theta d\phi\hat{\mathbf{e}}_\phi \ , \tag{1.74}$$

the distance element,

$$|d\mathbf{r}|^2 = (dr)^2 + (rd\theta)^2 + (r\sin\theta d\phi)^2 \ , \tag{1.75}$$

the surface element given by $r = r(\theta, \phi)$,

$$d\mathbf{s} = \left(\hat{\mathbf{e}}_r - \frac{1}{r}\frac{\partial r}{\partial\theta}\hat{\mathbf{e}}_\theta - \frac{1}{r}\frac{1}{\sin\theta}\frac{\partial r}{\partial\phi}\hat{\mathbf{e}}_\phi\right) r^2\sin\theta d\theta d\phi \ , \tag{1.76}$$

and the volume element,

$$d\tau = ds_u ds_v ds_w = r^2\sin\theta d\theta d\phi dr \ . \tag{1.77}$$

In the Excs. 1.3.8.3 to 1.3.8.5 we calculate, respectively, the gradient,

$$\nabla\Phi = \hat{\mathbf{e}}_r \ \frac{\partial\Phi}{\partial r} + \hat{\mathbf{e}}_\theta \ \frac{1}{r} \ \frac{\partial\Phi}{\partial\theta} + \hat{\mathbf{e}}_\phi \ \frac{1}{r\sin\phi} \ \frac{\partial\Phi}{\partial\phi} \ , \tag{1.78}$$

the divergence,

$$\nabla\cdot\mathbf{A} = \frac{1}{r^2}\frac{\partial}{\partial r}[r^2 a_r] + \frac{1}{r\sin\theta}\frac{\partial}{\partial\theta}[\sin\theta \ a_\theta] + \frac{1}{r\sin\theta}\frac{\partial}{\partial\phi}[a_\phi] \ , \tag{1.79}$$

the rotation,

$$\begin{aligned}\nabla\times\mathbf{A} = \hat{\mathbf{e}}_r \ \frac{1}{r\sin\theta}\left[\frac{\partial}{\partial\theta}(\sin\theta a_\phi) - \frac{\partial}{\partial\phi}(a_\theta)\right] + \hat{\mathbf{e}}_\theta \ \frac{1}{r\sin\theta}\left[\frac{\partial}{\partial\phi}(a_r) - \sin\theta\frac{\partial}{\partial r}(ra_\phi)\right] \\ + \hat{\mathbf{e}}_\phi \ \frac{1}{r}\left[\frac{\partial}{\partial r}(ra_\theta) - \frac{\partial}{\partial\theta}(a_r)\right]\end{aligned} \tag{1.80}$$

and the Laplace operator,

$$\Delta\Phi \equiv \nabla\cdot(\nabla\Phi) = \frac{1}{r^2}\frac{\partial}{\partial r}\left(r^2\frac{\partial\Phi}{\partial r}\right) + \frac{1}{r^2\sin\theta}\frac{\partial}{\partial\theta}\left(\sin\theta\frac{\partial\Phi}{\partial\theta}\right) + \frac{1}{r^2\sin^2\theta}\frac{\partial^2\Phi}{\partial\phi^2} \ , \tag{1.81}$$

in spherical coordinates. We note that the radial part of the Laplace operator can also be written,

$$\frac{1}{r}\frac{\partial^2}{\partial r^2}(r\Phi) \ . \tag{1.82}$$

1.3.7 Differential operators for tensor fields

Until now, we restricted to scalar and vector fields, that is spatially dependent physical quantities such as the temperature or the magnetic field distribution in a room. Some quantities, however, need to be given as matrices or even higher-dimensional objects, for example, gravity gradients or the susceptibility of a crystal. These objects are called tensors. With the definition,

$$\hat{\mathbf{e}}_k \otimes \hat{\mathbf{e}}_l = \hat{\mathbf{e}}_k\hat{\mathbf{e}}_l^\intercal \tag{1.83}$$

we can express a scalar, vector, and second-order tensor as,

$$\Phi \quad , \quad \mathbf{A} = A_k\hat{\mathbf{e}}_k \quad , \quad \mathcal{G} = G_{kl}\hat{\mathbf{e}}_k\otimes\hat{\mathbf{e}}_l \ . \tag{1.84}$$

For instance, in Cartesian coordinates a second-order tensor reads,

$$\mathcal{G} = G_{xx}\hat{\mathbf{e}}_x\hat{\mathbf{e}}_x^\intercal + G_{xy}\hat{\mathbf{e}}_x\hat{\mathbf{e}}_y^\intercal + G_{yx}\hat{\mathbf{e}}_y\hat{\mathbf{e}}_x^\intercal + G_{yy}\hat{\mathbf{e}}_y\hat{\mathbf{e}}_y^\intercal = \begin{pmatrix} G_{xx} & G_{xy} \\ G_{xy} & G_{yy} \end{pmatrix} . \tag{1.85}$$

If a tensor $\mathcal{T} = \Phi(\mathbf{r}), \mathbf{A}(\mathbf{r}), \mathcal{G}(\mathbf{r})$ varies in space, we can apply differential operators to it. The gradient $\nabla\mathcal{T}(\mathbf{r})$ of a tensor field in the direction of an arbitrary constant vector $\mathbf{x}$ is defined as,

$$\boxed{\mathbf{x} \cdot \nabla\mathcal{T} = \lim_{\alpha\to 0} \frac{d}{d\alpha}\mathcal{T}(\mathbf{r} + \alpha\mathbf{x})} . \tag{1.86}$$

The gradient of a tensor field of order n is a tensor field of order $n+1$. In Cartesian coordinates, $\mathbf{x} = x\hat{\mathbf{e}}_x + y\hat{\mathbf{e}}_y + z\hat{\mathbf{e}}_z$,

$$\begin{aligned} \nabla\Phi &= \hat{\mathbf{e}}_k \frac{\partial}{\partial x_k}\Phi \equiv \Phi_{,k}\hat{\mathbf{e}}_k = \begin{pmatrix} \partial_x\Phi \\ \partial_y\Phi \end{pmatrix} \\ \nabla\mathbf{A} &= \hat{\mathbf{e}}_k \frac{\partial}{\partial x_k} \otimes A_l\hat{\mathbf{e}}_l \equiv A_{,kl}\hat{\mathbf{e}}_k \otimes \hat{\mathbf{e}}_l = \begin{pmatrix} \partial_x A_x & \partial_y A_x \\ \partial_x A_y & \partial_y A_y \end{pmatrix} \\ \nabla\mathcal{G} &= \hat{\mathbf{e}}_k \frac{\partial}{\partial x_k} \otimes G_{lm}\hat{\mathbf{e}}_l \otimes \hat{\mathbf{e}}_m \equiv G_{,klm}\hat{\mathbf{e}}_k \otimes \hat{\mathbf{e}}_l \otimes \hat{\mathbf{e}}_m = \begin{pmatrix} \partial_x \\ \partial_y \end{pmatrix} \begin{pmatrix} G_{xx} & G_{xy} \\ G_{xy} & G_{yy} \end{pmatrix} . \end{aligned} \tag{1.87}$$

The divergence of a tensor field $\mathcal{T}(\mathbf{r})$ is defined using the recursive relation,

$$\begin{aligned} (\nabla \cdot \mathbf{A}) \cdot \mathbf{x} &= \text{Tr } (\nabla\mathbf{A}) \\ (\nabla \cdot \mathcal{G}) \cdot \mathbf{x} &= \nabla \cdot (\mathbf{x} \cdot \mathcal{G}^\intercal) . \end{aligned} \tag{1.88}$$

In Cartesian coordinates the divergence is,

$$\begin{aligned} \nabla \cdot \mathbf{A} &= \hat{\mathbf{e}}_k \frac{\partial}{\partial x_k} \cdot A_l\hat{\mathbf{e}}_l = \frac{\partial A_k}{\partial x_k} \equiv A_{k,k} \\ \nabla \cdot \mathcal{G} &= \hat{\mathbf{e}}_k \frac{\partial}{\partial x_k} \cdot G_{lm}\hat{\mathbf{e}}_l \otimes \hat{\mathbf{e}}_m = \frac{\partial G_{lk}}{\partial x_k} \otimes \hat{\mathbf{e}}_l \equiv G_{lk,k}\hat{\mathbf{e}}_l . \end{aligned} \tag{1.89}$$

The curl of an order $n > 1$ tensor field $\mathcal{T}(\mathbf{r})$ is also defined using the recursive relation,

$$\begin{aligned} (\nabla \times \mathbf{A}) \cdot \mathbf{x} &= \nabla \cdot (\mathbf{A} \times \mathbf{c}) \\ (\nabla \times \mathcal{G}) \cdot \mathbf{x} &= \nabla \times (\mathbf{x} \cdot \mathcal{G}^\intercal) , \end{aligned} \tag{1.90}$$

where c is an arbitrary constant vector. In Cartesian coordinates the divergence the rotation is,

$$\begin{aligned} \nabla \times \mathbf{A} &= \epsilon_{klm}\hat{\mathbf{e}}_k\partial_l A_m \\ \nabla \times \mathcal{G} &= \epsilon_{klm}\hat{\mathbf{e}}_m \otimes \hat{\mathbf{e}}_n\partial_k G_{nl} . \end{aligned} \tag{1.91}$$

1.3.8 Exercises

1.3.8.1 Ex: Spherical and cylindrical coordinates

a. Express the cylindrical coordinates ρ, φ, z in terms of the Cartesian ones x, y, z.
b. Express the spherical coordinates r, θ, φ in terms of the Cartesian ones x, y, z.

1.3.8.2 Ex: Differential elements in curvilinear coordinates

We have seen in class that the transformation from a Cartesian coordinate system (x, y, z) to another curvilinear and orthogonal system (u, v, w) is given by $\mathbf{r} \equiv (x(u, v, w), y(u, v, w), z(u, v, w))$. Now consider the spherical polar coordinates $\mathbf{r} \equiv (x(r, \theta, \phi), y(r, \theta, \phi), z(r, \theta, \phi)$ defined in class.
a. Calculate the functions U_r, V_θ, W_ϕ defined by,

$$U_r = \left|\frac{\partial \mathbf{r}}{\partial r}\right|^{-1} \quad , \quad V_\theta = \left|\frac{\partial \mathbf{r}}{\partial \theta}\right|^{-1} \quad , \quad W_\phi = \left|\frac{\partial \mathbf{r}}{\partial \phi}\right|^{-1} .$$

b. Determine the Cartesian coordinates of the new unit vectors $\hat{\mathbf{e}}_r,\ \hat{\mathbf{e}}_\theta,\ \hat{\mathbf{e}}_\phi$, draw the position of these vectors at a point $\mathbf{r}_0$, and check the orthogonality of the unit vectors. Express the Cartesian unit vectors by the spherical ones.
c. Determine the total differential $d\mathbf{r}$, the line element $(ds)^2 = |d\mathbf{r}|^2$, and the volume element $d\tau = ds_u ds_v ds_w$ in terms of the new coordinates.
d. Repeat steps (a)-(c) for planar polar coordinates.

1.3.8.3 Ex: Spherical and cylindrical coordinates

Calculate $\nabla\Phi,\ \ \nabla \cdot \mathbf{A},\ \ \nabla \times \mathbf{A}$ and $\ \Delta\Phi = \nabla \cdot (\nabla\Phi)$
a. in spherical coordinates $(r,\ \theta,\ \phi)$.
b. in cylindrical coordinates $(\rho,\ \phi,\ z)$.

1.3.8.4 Ex: Divergence in curvilinear coordinates

Calculate the divergence of the force field $\mathbf{F}(\mathbf{r}) = \begin{pmatrix} x^2y \\ 2yz \\ x+z \end{pmatrix}$ (a) in Cartesian and (b) cylindrical coordinates and compare the results.

1.3.8.5 Ex: Differential operators in curvilinear coordinates

In Cartesian coordinates the differential line element has the form $d\mathbf{r} = \hat{\mathbf{e}}_x dx + \hat{\mathbf{e}}_y dy + \hat{\mathbf{e}}_z dz$ and in arbitrary orthogonal coordinates $d\mathbf{r} = \hat{\mathbf{e}}_1 h_1 dq_1 + \hat{\mathbf{e}}_2 h_2 dq_2 + \hat{\mathbf{e}}_3 h_3 dq_3$ with $\hat{\mathbf{e}}_i = \frac{\partial \mathbf{r}}{\partial q_i} \cdot \left|\frac{\partial \mathbf{r}}{\partial q_i}\right|^{-1}$ and $h_i = \left|\frac{\partial \mathbf{r}}{\partial q_i}\right|$. For spherical coordinates (r, ϕ, θ) we find $h_r = 1, h_\phi = r\sin\theta, h_\theta = r$; for cylindrical coordinates (ρ, ϕ, z) we find $h_\rho = 1, h_\phi = \rho, h_z = 1$.
a. The gradient has the general form,

$$\nabla_i \Phi(\mathbf{r}) = \frac{1}{h_i}\frac{\partial}{\partial q_i}\Phi(\mathbf{r}) .$$

Determine the gradient in spherical and cylindrical coordinates.
b. The divergence of a vector field $\mathbf{A}$ has the general form,

$$\nabla \cdot \mathbf{A}(\mathbf{r}) = \frac{1}{h_1 h_2 h_3}\left[\frac{\partial}{\partial q_1}(A_1 h_2 h_3) + \frac{\partial}{\partial q_2}(A_2 h_1 h_3) + \frac{\partial}{\partial q_3}(A_3 h_1 h_2)\right] .$$

Determine $\nabla \cdot \mathbf{A}$ in spherical and cylindrical coordinates.
c. Use the results of (a) and (b) to determine the Laplace operator

$$\Delta = \nabla \cdot \nabla$$

in spherical coordinates.

1.3.8.6 Ex: Acceleration in spherical coordinates

In spherical coordinates the velocity vector has the following form,

$$\mathbf{v} = \frac{d\mathbf{r}}{dt} = \dot{r}\hat{\mathbf{e}}_r + r\dot{\theta}\hat{\mathbf{e}}_\theta + \dot{\phi}r\sin\theta\hat{\mathbf{e}}_\phi \ .$$

Calculate the acceleration vector in spherical coordinates. Respect the fact that the basis vectors must also be derived by time.

1.3.8.7 Ex: Volume element in curvilinear coordinates

a. Calculate the surface of a rectangle with width a and height b in Cartesian coordinates.
b. Calculate the surface of a disk of radius R in polar coordinates.
c. Calculate the volume of a cuboid with dimensions a, b, c in Cartesian coordinates.
d. Calculate the volume of a cylinder with the radius R and height H in cylindrical coordinates.
e. Calculate the volume a sphere with the radius R in spherical coordinates.

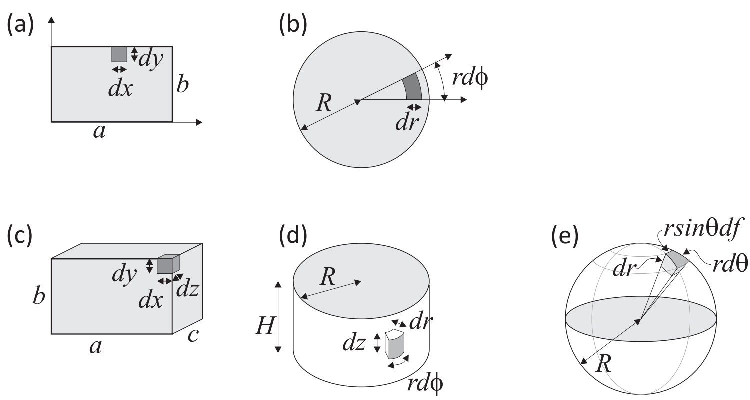

Figure 1.7: Curvilinear coordinates.

1.3.8.8 Ex: Spherical volume

The volume of a body is given by the following formula:

$$V = \int_V 1 \ dV \ .$$

a. Calculate the volume of a 3D-sphere in spherical coordinates.
By the Gauß integral law we can establish a relationship between the volume of the sphere and its surface. (**Help:** For which vector field $\mathbf{A}$ holds: $\nabla \cdot \mathbf{A} = 1$?)
b. Now calculate the volume of the sphere in this sense. You may assume that the surface of the sphere is known.
c. Similarly to the above formula, derive a general relationship between the volume of an n-dimensional hypersphere and its $(n-1)$-dimensional hypersurface. **Help:** Gauß's law holds in arbitrary dimensions with the n-dimensional operator nabla-operator defined by, $\nabla = (\partial/\partial x_1, \ldots, \partial/\partial x_n)$.

1.3.8.9 Ex: Spherical volume

The density distribution of a gas be given by $n(\mathbf{r}) = C^2 - \frac{x^2}{r_0^2} - \frac{y^2}{r_0^2} - \frac{z^2}{r_0^2}$. Determine the constant C in such a way that the density $n(\mathbf{r})$ is normalized to the number of atoms in the gas, i.e., $\int_{\mathcal{V}} n(\mathbf{r}) d^3\mathbf{r} = N$, where $\mathcal{V}$ is the volume within which the density is positive, $n(\mathbf{r}) \geq 0$.

1.3.8.10 Ex: Spherical and cylindrical volume

a. Integrate a circular surface with radius R in Cartesian coordinates and then in polar coordinates.
b. The density distribution of a trapped atomic gas is described by $n(\mathbf{r}) = n_0 e^{-r^2/\bar{r}^2}$, where $n_0 = 10^{13}\,\text{cm}^{-1}$ is the maximum density and $\bar{r} = 100\,\mu\text{m}$ a measure for the extent of the distribution. Calculate the number of atoms $N = \int_{\mathbb{R}^3} n(\mathbf{r}) d^3\mathbf{r}$, integrating over Cartesian coordinates and then over polar coordinates.
c. Calculate the density of a homogeneous cylinder of mass 10 kg and length 20 cm by integrating over its volume..
d. The density distribution of a trapped atomic gas is described by
$n(\rho, z) = \max\left\{0, n_0 \cdot \left(1 - \frac{\rho^2}{\rho_m^2} - \frac{z^2}{z_m^2}\right)\right\}$, where $n_0 = 10^{13}\,\text{cm}^{-3}$ is the maximum density and $z_m = 2\rho_m = 100\,\mu\text{m}$ a measure for the extent of the distribution. Calculate the number of atoms by integrating over cylindrical coordinates.

1.3.8.11 Ex: Cylindrical volume

Consider a material (gas or liquid) whose mass density $\rho(\mathbf{r})$ depends on the z-coordinate as follows: $\rho(\mathbf{r}) = \rho_0(1 - \alpha z)$. This material is filled into a cylinder (radius R and height c) until the total mass in the cylinder is M. The cylinder stands in a circular area above the xy in $z = 0$.
a. Calculate the density parameter ρ_0.
b. Calculate vector of center of mass $\mathbf{r}_s$ of the material in the cylinder.
c. Now fill the same material inside a sphere of radius R instead of the cylinder. What are the results in this case if $\alpha = 0.1$ /m, $R = 1$ m, and $M = 10$ kg.
d. A cake of mass M, height h and radius R be cut into fourth equal pieces. Calculate the center of mass of a piece. Calculate the center of mass of the rest of the cake when a piece is taken.

1.3.8.12 Ex: Vector potential in curvilinear coordinates

Be given a constant field $\mathbf{B}$ oriented in z-direction. What is the vector potential $\mathbf{A}$ in (a) spherical coordinates, (b) cylindrical coordinates, and (c) Cartesian coordinates? For case (c) also consider the gauge transformation $\mathbf{A}' = \mathbf{A} + \nabla\lambda$ with $\lambda = \pm Bxy/2$.

1.3.8.13 Ex: Gauß' theorem in curvilinear coordinates

a. Check Gauß' theorem for function $\mathbf{A} = r^2\hat{\mathbf{e}}_r$ using the volume of a sphere of radius R.
b. Do the same for the function $\mathbf{B} = r^{-2}\hat{\mathbf{e}}_r$ and discuss the result.

1.3.8.14 Ex: Gauß' theorem in curvilinear coordinates

Calculate the divergence of the function,

$$\mathbf{A} = r\hat{\mathbf{e}}_r\cos\theta + r\hat{\mathbf{e}}_\theta\sin\theta + r\hat{\mathbf{e}}_\varphi\sin\theta\cos\varphi \ .$$

Verify Gauß's theorem for this function using the volume of an inverted semisphere of radius R lying in the x-y-plane.

1.3.8.15 Ex: Gauß' theorem in curvilinear coordinates

Calculate the gradient and Laplacian of the function $T = r(\cos\theta + \sin\theta\cos\varphi)$. Check the Laplacian by converting T into Cartesian coordinates. Verify Gauß's theorem using the path $l_1(t) = 2\hat{\mathbf{e}}_x\cos\pi t + 2\hat{\mathbf{e}}_y\sin\pi t$ for $t \in [0, 0.5]$ followed by $l_2(t) = 2\hat{\mathbf{e}}_y\sin\pi t - 2\hat{\mathbf{e}}_z\cos\pi t$ para $t \in [0.5, 1]$.

1.3.8.16 Ex: Gauß' theorem in curvilinear coordinates

a. Find the divergence of the function,

$$\mathbf{A} = \rho\hat{\mathbf{e}}_\rho(2 + \sin^2\varphi) + \rho\hat{\mathbf{e}}_\varphi\sin\varphi\cos\varphi + 3z\hat{\mathbf{e}}_z \ .$$

b. Verify Gauß' theorem for this function using a quadrant of cylinder with radius $R = 2$ and height $h = 5$.
c. Find the rotation of $\mathbf{A}$.

1.4 Differential geometry in curved space

In previous sections we mainly concentrated on orthogonal coordinate systems, such as Cartesian, cylindrical, or spherical. In cases one has to use non-orthogonal systems the formalism needs to be generalized. For this purpose it is necessary to introduce some new concepts and notations.

Repeat expressions in index formalism *Einstein's sum rule*, $a^n a_n = \sum_a^n a_n$,

$$\boxed{ds^2 = g_{mn}dx^m dx^n} \ . \tag{1.92}$$

1.4.1 Co- and contravariant tensors

A *contravariant* vector or tangent vector (often abbreviated simply as vector, such as a direction vector or velocity vector) has components that contra-vary with a change of basis to compensate. That is, the matrix that transforms the vector components must be the inverse of the matrix that transforms the basis vectors. Examples of contravariant vectors include the position of an object relative to an observer, or any derivative of position with respect to time, including velocity and acceleration. Contravariant components are denoted with upper indices as in,

$$\mathbf{v} = v^i \mathbf{e}_i \ . \tag{1.93}$$

A *covariant* vector or cotangent vector has components that co-vary with a change of basis. That is, the components must be transformed by the same matrix as the change of basis matrix. Examples of covariant vectors generally appear when taking a gradient of a function. Covariant components are denoted with lower indices as in,

$$\mathbf{w} = w_i \mathbf{e}^i \ . \tag{1.94}$$

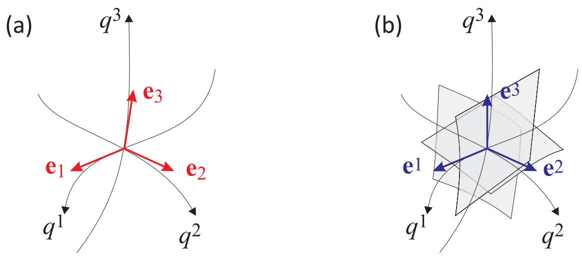

Figure 1.8: (a) Covariant and (b) contravariant basis.

1.4.2 Jacobian for coordinate transformations

The *Jacobian* of a vector field **F** is a matrix defined by,

$$\mathbf{J} \equiv \frac{\partial(F_1, .., F_m)}{\partial(x_1, .., x_n)} \equiv \left(\frac{\partial F_m}{\partial x_n}\right) \equiv (J^m_{\ n}) \ . \tag{1.95}$$

We may understand a curvilinear coordinate system $\{x^\mu\}$ as a vector field in Cartesian space $\{x'^\nu\}$,

$$x^\mu = x^\mu(x'^1, .., x'^\nu, .., x'^m) \tag{1.96}$$

for $\mu = 1, .., m$. The Jacobian of this field represents a tool used to transform between the coordinate systems by taking the rate of change of each component of an old basis with respect to each component of a new basis and expressing them as coefficients that make up an old basis. Do the Excs. 1.4.4.2 and 1.4.4.3,

$$\boxed{J^i_{\ j} \equiv \frac{\partial^i x}{\partial x'^j}} \ . \tag{1.97}$$

Example 9 (*Jacobian for polar coordinates*): For example, the Jacobian matrix that transforms polar coordinates to Cartesian coordinates in 2 dimensions is given by,

$$J^i{}_j = \begin{pmatrix} \partial_r x & \partial_\theta x \\ \partial_r y & \partial_\theta y \end{pmatrix} = \begin{pmatrix} \cos\theta & r\sin\theta \\ \sin\theta & r\cos\theta \end{pmatrix} . \tag{1.98}$$

The components of Cartesian basis vectors can now be written as a linear combination of these coefficients and their corresponding polar bases,

$$\begin{aligned} \hat{\mathbf{e}}_x &= \frac{\partial x}{\partial r}\hat{\mathbf{e}}_r + \frac{\partial x}{\partial \theta}\hat{\mathbf{e}}_\theta = \hat{\mathbf{e}}_r \cos\theta - \hat{\mathbf{e}}_\theta r \sin\theta \\ \hat{\mathbf{e}}_y &= \frac{\partial y}{\partial r}\hat{\mathbf{e}}_r + \frac{\partial y}{\partial \theta}\hat{\mathbf{e}}_\theta = \hat{\mathbf{e}}_r \sin\theta + \hat{\mathbf{e}}_\theta r \cos\theta . \end{aligned} \tag{1.99}$$

In the case of relating the Jacobian to the *metric* tensor, the Jacobian can be used to transform the components of one metric to another via the following method,

$$g'_{ij} = \frac{\partial}{\partial x'^i}\frac{\partial}{\partial x'^j} = \left(\frac{\partial x^a}{\partial x'^i}\frac{\partial}{\partial x^a}\right)\left(\frac{\partial x^b}{\partial x'^i}\frac{\partial}{\partial x^b}\right) = \frac{\partial x^a}{\partial x'^i}\frac{\partial x^b}{\partial x'^i}\left(\frac{\partial}{\partial x^a}\frac{\partial}{\partial x^b}\right) = J^a{}_i J^b{}_j g_{ab} . \tag{1.100}$$

Knowing this, taking the determinant of the metric g_{ij} requires taking the determinant of the Jacobian matrices and g_{ab} as well,

$$\det g'_{ij} = (\det J^a{}_i)(\det J^b{}_j)(\det g_{ab}) . \tag{1.101}$$

Since both Jacobian terms are part of the same matrix and are just written using different indices to differentiate between the components of the old basis,

$$(\det J^a{}_i)(\det J^b{}_j) = (\det J)^2 . \tag{1.102}$$

In the case of our old basis being written in Cartesian coordinates,

$$\det g_{ab} = \det \mathbb{I} = 1 . \tag{1.103}$$

Therefore the equation of our new transformed metric g_{ij}, simplifies to,

$$\det g_{ij} = (\det J)^2 \quad \Longrightarrow \quad \det J = \sqrt{\det g_{ij}} . \tag{1.104}$$

It can be shown that,

$$\frac{d}{dt}\frac{\partial(u,v)}{\partial(x,y)} \equiv \frac{\partial(\frac{d}{dt}u, v)}{\partial(x,y)} + \frac{\partial(u, \frac{d}{dt}v)}{\partial(x,y)} . \tag{1.105}$$

The *Hessian* is a square matrix of second-order partial derivatives of a scalar field.

1.4.3 Metric and geodesic equation in Euclidean space

For an arbitrary curvilinear coordinate system u^i we define tangent vectors forming a basis,

$$\mathbf{e}_i = \frac{\partial}{\partial u^i} = \partial_i , \tag{1.106}$$

the metric tensor is,

$$g_{ij} \equiv \mathbf{e}_i \cdot \mathbf{e}_j . \tag{1.107}$$

See also Secs. ?? and 9.5.

1.4.3.1 Metric in spherical coordinates

For spherical coordinates,

$$\mathbf{r} = \begin{pmatrix} x \\ y \\ z \end{pmatrix} = \begin{pmatrix} r\sin\theta\cos\phi \\ r\sin\theta\sin\phi \\ r\cos\theta \end{pmatrix} \quad , \quad \begin{pmatrix} r \\ \theta \\ \phi \end{pmatrix} = \begin{pmatrix} \sqrt{x^2+y^2+z^2} \\ \arccos\frac{z}{\sqrt{x^2+y^2+z^2}} \\ \arctan\frac{y}{x} \end{pmatrix} \quad , \tag{1.108}$$

the tangent vectors are,

$$\begin{aligned} \mathbf{e}_r &= \frac{\partial\mathbf{r}}{\partial r} = \hat{\mathbf{e}}_x\sin\theta\cos\phi + \hat{\mathbf{e}}_y\sin\theta\sin\phi + \hat{\mathbf{e}}_z\cos\theta = \hat{\mathbf{e}}_r \\ \mathbf{e}_\theta &= \frac{\partial\mathbf{r}}{\partial\theta} = r\hat{\mathbf{e}}_x\cos\theta\cos\phi + r\hat{\mathbf{e}}_y\cos\theta\sin\phi - r\hat{\mathbf{e}}_z\sin\theta = r\hat{\mathbf{e}}_\theta \\ \mathbf{e}_\phi &= \frac{\partial\mathbf{r}}{\partial\phi} = -r\sin\theta\hat{\mathbf{e}}_x\sin\phi + r\sin\theta\hat{\mathbf{e}}_y\cos\phi = r\sin\theta\hat{\mathbf{e}}_\phi\ . \end{aligned} \tag{1.109}$$

Note that, in contrast to the basis vectors $\hat{\mathbf{e}}_i$ the tangent vectors $\mathbf{e}_i$ are not normalized. The spherical metric is,

$$g_{ij} = \frac{\partial x_a}{\partial u^i}\frac{\partial x^a}{\partial u^j} = \begin{pmatrix} \mathbf{e}_r\cdot\mathbf{e}_r & \mathbf{e}_r\cdot\mathbf{e}_\theta & \mathbf{e}_r\cdot\mathbf{e}_\phi \\ \mathbf{e}_\theta\cdot\mathbf{e}_r & \mathbf{e}_\theta\cdot\mathbf{e}_\theta & \mathbf{e}_\theta\cdot\mathbf{e}_\phi \\ \mathbf{e}_\phi\cdot\mathbf{e}_r & \mathbf{e}_\phi\cdot\mathbf{e}_\theta & \mathbf{e}_\phi\cdot\mathbf{e}_\phi \end{pmatrix} = \begin{pmatrix} 1 & 0 & 0 \\ 0 & r^2 & 0 \\ 0 & 0 & r^2\sin^2\theta \end{pmatrix} ,$$

with $x_a = x, y, z$, $u^i = r, \theta, \phi$, and the contra-variant spherical metric being,

$$g^{ij} = \frac{\partial u^i}{\partial x_a}\frac{\partial u^j}{\partial x^a} = \begin{pmatrix} 1 & 0 & 0 \\ 0 & r^{-2} & 0 \\ 0 & 0 & r^{-2}\sin^{-2}\theta \end{pmatrix} . \tag{1.110}$$

we obtain the contra-variant tangent vectors,

$$\begin{aligned} \mathbf{e}^r &= g^{rr}\mathbf{e}_r = \hat{\mathbf{e}}_x\sin\theta\cos\phi + \hat{\mathbf{e}}_y\sin\theta\sin\phi + \hat{\mathbf{e}}_z\cos\theta = \hat{\mathbf{e}}_r \\ \mathbf{e}^\theta &= g^{\theta\theta}\mathbf{e}_\theta = \frac{1}{r}\hat{\mathbf{e}}_x\cos\theta\cos\phi + \frac{1}{r}\hat{\mathbf{e}}_y\cos\theta\sin\phi - \frac{1}{r}\hat{\mathbf{e}}_z\sin\theta = \frac{1}{r}\hat{\mathbf{e}}_\theta \\ \mathbf{e}^\phi &= g^{\phi\phi}\mathbf{e}_\phi = -\frac{1}{r\sin\theta}\hat{\mathbf{e}}_x\sin\phi + \frac{1}{r\sin\theta}\hat{\mathbf{e}}_y\cos\phi = \frac{1}{r\sin\theta}\hat{\mathbf{e}}_\phi\ . \end{aligned} \tag{1.111}$$

The diagonal shape of the metrics are comes from the fact that spherical coordinates are orthogonal. In the example 10 we discuss the metric of an non-orthogonal coordinate system.

Example 10 (*Metric in elliptical coordinates*): In contrast to polar, cylindrical, or spherical coordinates, elliptical coordinates given by,

$$\mathbf{r} = \begin{pmatrix} x \\ y \end{pmatrix} = \begin{pmatrix} ar\cos\phi \\ br\sin\phi \end{pmatrix} \quad , \quad \begin{pmatrix} r \\ \phi \end{pmatrix} = \begin{pmatrix} \sqrt{(\frac{x}{a})^2+(\frac{y}{b})^2} \\ \arctan\frac{ay}{bx} \end{pmatrix} \quad , \tag{1.112}$$

are not orthogonal. The tangent vectors are,

$$\begin{aligned} \mathbf{e}_r &= \frac{\partial\mathbf{r}}{\partial r} = \hat{\mathbf{e}}_x a\cos\phi + \hat{\mathbf{e}}_y b\sin\phi \\ \mathbf{e}_\phi &= \frac{\partial\mathbf{r}}{\partial\phi} = -\hat{\mathbf{e}}_x ar\sin\phi + \hat{\mathbf{e}}_y br\cos\phi\ . \end{aligned} \tag{1.113}$$

Note that, in contrast to the basis vectors $\hat{\mathbf{e}}_i$ the tangent vectors $\mathbf{e}_i$ are not normalized. The elliptical metric is,

$$g_{ij} = \frac{\partial x_a}{\partial u^i}\frac{\partial x^a}{\partial u^j} = \begin{pmatrix} \mathbf{e}_r\cdot\mathbf{e}_r & \mathbf{e}_r\cdot\mathbf{e}_\phi \\ \mathbf{e}_\phi\cdot\mathbf{e}_r & \mathbf{e}_\phi\cdot\mathbf{e}_\phi \end{pmatrix} = \begin{pmatrix} a^2\cos^2\phi + b^2\sin^2\phi & (b^2-a^2)r\sin\phi\cos\phi \\ (b^2-a^2)r\sin\phi\cos\phi & (a^2\sin^2\phi + b^2\cos^2\phi)r^2 \end{pmatrix} ,$$

with $x_a = x, y$, $u^i = r, \phi$, and the contra-variant elliptical metric being,

$$g^{ij} = \frac{\partial u^i}{\partial x_a}\frac{\partial u^j}{\partial x^a} = \frac{1}{a^2b^2r^2}\begin{pmatrix} a^2r^2\sin^2\phi + b^2r^2\cos^2\phi & (a^2-b^2)r\sin\phi\cos\phi \\ (a^2-b^2)r\sin\phi\cos\phi & a^2\cos^2\phi + b^2\sin^2\phi) \end{pmatrix} . \tag{1.114}$$

we obtain the cotangent vectors,

$$\mathbf{e}^r = g^{ri}\mathbf{e}_i = g^{rr}\mathbf{e}_r + g^{r\phi}\mathbf{e}_\phi = \hat{\mathbf{e}}_x a^{-1}\cos\phi + \hat{\mathbf{e}}_y b^{-1}\sin\phi \tag{1.115}$$
$$\mathbf{e}^\phi = g^{\phi i}\mathbf{e}_i = g^{\phi r}\mathbf{e}_r + g^{\phi\phi}\mathbf{e}_\phi = -\hat{\mathbf{e}}_x a^{-1}r^{-1}\sin\phi + \hat{\mathbf{e}}_y b^{-1}r^{-1}\cos\phi .$$

The fact that the metric is not diagonal is due to the elliptical coordinates not being orthogonal. One verifies,

$$\mathbf{e}^r\cdot\mathbf{e}_\phi = 0 = \mathbf{e}_r\cdot\mathbf{e}^\phi \quad , \quad \mathbf{e}^r\cdot\mathbf{e}_r = 1 = \mathbf{e}_\phi\cdot\mathbf{e}^\phi . \tag{1.116}$$

Interestingly, while neither the tangent nor the cotangent vectors are orthogonal, they are mutually orthogonal.

1.4.3.2 Christoffel symbols

The Christoffel symbols are defined by,

$$\Gamma^k{}_{ij} \equiv \frac{\partial \mathbf{e}_i}{\partial x^j}\cdot\mathbf{e}^k . \tag{1.117}$$

They yields for spherical coordinates with $j = r, \theta, \phi$,

$$\Gamma^a{}_{ir} = \begin{pmatrix} 0 & 0 & 0 \\ 0 & r^{-1} & 0 \\ 0 & 0 & r^{-1} \end{pmatrix} \quad , \quad \Gamma^a{}_{i\theta} = \begin{pmatrix} 0 & -r & 0 \\ r^{-1} & 0 & 0 \\ 0 & 0 & -\tan\theta \end{pmatrix} \tag{1.118}$$
$$\Gamma^a{}_{i\phi} = \begin{pmatrix} 0 & 0 & -r\cos^2\theta \\ 0 & r^{-1} & \sin\theta\cos\theta \\ r^{-1} & -\tan\theta & 0 \end{pmatrix} .$$

Do the Exc. 1.4.4.4.

1.4.3.3 Geodesic equation

In differential geometry the *geodesic equation* is a curve representing in some sense the shortest path between two points in a surface, or more generally in a Riemannian manifold. It is a generalization of the notion of a 'straight line'. The geodesic line is obtained by solving the differential equation,

$$\frac{d^2x^k}{ds^2} + \Gamma^k{}_{ab}\frac{dx^a}{ds}\frac{dx^b}{ds} = 0 . \tag{1.119}$$

1.4.4 Exercises

1.4.4.1 Ex: Tensors of rank n

Be given $\mathbf{F} = \mathbf{E} + \imath\mathbf{B}$ and $\mathbf{F}^* = \mathbf{E} - \imath\mathbf{B}$. Identify (in this order) the scalar $\mathbf{F}^* \cdot \mathbf{F}/(8\pi)$, teh vector $\mathbf{F}^* \times \mathbf{F}/(8\pi\imath)$, and the dyade (tensor) $(\mathbf{F}^* \cdot \mathbf{F} + \mathbf{F} \cdot \mathbf{F}^*)/(8\pi)$. What happens to these quantities if we exchange $\mathbf{F}$ for $e^{-\imath\phi}\mathbf{F}$, where ϕ is supposed constant?

1.4.4.2 Ex: Jacobian for transformation into curvilinear coordinates

a. Calculate the Jacobian of the transformation from cylindrical coordinates (ρ, z, φ) to Cartesian coordinates (x, y, z).
b. Calculate the Jacobian of the transformation from spherical coordinates (r, θ, φ) to Cartesian coordinates (x, y, z).

1.4.4.3 Ex: Jacobian for Galilei and Lorentz transform

Determine the Jacobean of the Galilei transformation,

$$ct' = ct \quad \text{and} \quad x' = x \quad \text{and} \quad y' = y \quad \text{and} \quad z' = z - \tfrac{u}{c}ct \ ,$$

and the Lorentz transformation,

$$ct' = \gamma(ct - \tfrac{u}{c}x) \quad \text{and} \quad x' = x \quad \text{and} \quad y' = y \quad \text{and} \quad z' = \gamma(z - \tfrac{u}{c}z) \ .$$

1.4.4.4 Ex: Christoffel symbols for two-dimensional polar coordinates

Derive the Christoffel symbols for two-dimensional polar coordinates.

1.4.4.5 Ex: Distorted polar coordinates

a. Study the coordinate system,

$$\mathbf{r} = \begin{pmatrix} x \\ y \end{pmatrix} = \begin{pmatrix} f(r)\cos\phi \\ g(r)\sin\phi \end{pmatrix}$$

for arbitrary radial functions $f(r)$ and $g(r)$.
b. Consider the particular cases (i) $f = g$ and (ii) $f = ar$ and $g = br$.

1.4.4.6 Ex: Metric for ellipsoidal coordinates

Generalize the metric for ellipsoidal coordinates.

1.5 Dirac's δ-function

Calculating the divergence of the vector field $\mathbf{A} = \mathbf{r}/r^3$ in spherical coordinates [1],

$$\nabla \cdot \mathbf{A} = \frac{1}{r^2}\frac{\partial}{\partial r}\left(r^2 \frac{1}{r^2}\right) = 0 \ , \tag{1.120}$$

[1] Or in Cartesian coordinates: $\nabla \cdot \mathbf{A} = \frac{\partial}{\partial r^3}\frac{x}{r^3} + \frac{\partial}{\partial r^3}\frac{y}{r^3} + \frac{\partial}{\partial r^3}\frac{z}{r^3} = \frac{3r^3 - 3x^2 r}{r^6} + ... = 0$.

we expect,

$$\int_{sphere} \nabla \cdot \mathbf{A} dV = 0 \ . \tag{1.121}$$

This is surprising, because intuition tells us to expect a huge divergence near the origin. The problem is that the field **A** diverges at the origin, which calls for a modification of the expression for the gradient. Gauß' law gives us an indication since, according to this law, the result (1.121) should be equal to the surface integral,

$$\oint_{\partial\ sphere} \mathbf{A} \cdot d\mathbf{S} = \int_0^{2\pi} \int_0^{\pi} \frac{\hat{\mathbf{e}}_r}{R^2} \cdot (R^2 \sin\theta d\theta d\phi \hat{\mathbf{e}}_r) = 4\pi \ . \tag{1.122}$$

As the integral (1.121) contains a divergence within the volume of integration, we conclude that the integral (1.122), which has no divergence within the integration surface is more reliable. Therefore, we look for a function δ satisfying,

$$\int_{sphere} \nabla \cdot \mathbf{A}(\mathbf{r}) dV = \int_{sphere} 4\pi\delta(\mathbf{r}) dV = 4\pi \ , \tag{1.123}$$

that is, a function having the property of killing integrals.

1.5.1 The Dirac function in 1 dimension

In one dimension the *Dirac function* is defined by,

$$\boxed{\delta(x) \equiv \begin{cases} 0 & \text{for} \quad x \neq 0 \\ \infty & \text{for} \quad x = 0 \end{cases}} \ , \tag{1.124}$$

such that,

$$\int_{-\infty}^{\infty} \delta(x) dx = 1 \ . \tag{1.125}$$

The Dirac function can be expressed as the limit of a series of continuous functions,

$$\begin{aligned} \delta(x) &= \lim_{n\to\infty} \frac{n}{\pi} \frac{1}{1+n^2x^2} \\ \delta(x) &= \lim_{n\to\infty} \frac{n}{\pi} \left(\frac{\sin nx}{nx}\right)^2 \\ \delta(x) &= \lim_{n\to\infty} \frac{1}{\pi} \frac{\sin nx}{x} = \lim_{n\to\infty} \frac{1}{2\pi} \int_{-n}^{+n} e^{\imath kx} dk \ . \end{aligned} \tag{1.126}$$

We also note that the Dirac function is even, $\delta(-x) = \delta(x)$, non-linear, $\delta(ax) = \delta(x)/|a|$, and can be interpreted as the derivative of the *Heavyside function*,

$$\int_{-\infty}^{x} \delta(x')dx' = \Theta(x) \qquad \text{or} \qquad \frac{d\Theta}{dx} = \delta(x) \ . \tag{1.127}$$

We will train the calculus with the Dirac function in Excs. 1.5.4.1 to 1.5.4.3.

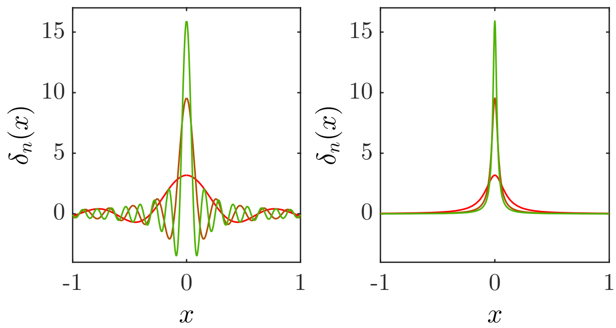

Figure 1.9: (code) Illustration of the function $\frac{1}{\pi}\frac{\sin nx}{x}$ (left) and of the function $\frac{1}{\pi}\frac{n}{1+n^2x^2}$ (right) for various $n \to \infty$.

When the argument of a Dirac function is itself a function $f(x)$, the Dirac is evaluated at each zero-passage of f,

$$\boxed{\int_a^b dx\ g(x)\delta(f(x)) = \int_a^b dx\ g(x)\sum_i \frac{\delta(x-x_i)}{|f'(x_i)|}}\ , \tag{1.128}$$

where $f'(x_i) \neq 0$. We will apply this theorem in Exc. 1.5.4.4.

1.5.2 The Dirac function in 2 and 3 dimensions

In more dimensions the δ-function is often used to parametrize points, paths, or surfaces within a volume. For example, a point charge Q at the position $\mathbf{a}$ can be described by the three-dimensional density distribution,

$$\rho(\mathbf{r}) = Q\delta^3(\mathbf{r}-\mathbf{a}) = Q\delta(x-a_x)\delta(y-a_y)\delta(z-a_z)\ , \tag{1.129}$$

a current I in a circular loop with radius R within the $z=0$ plane generates a current density,

$$\mathbf{j} = I\delta(r-R)\delta(z)\hat{\mathbf{e}}_\phi\ , \tag{1.130}$$

called a *current yarn*. Similarly, a two-dimensional arrangement of charges σ homogeneously distributed over the surface of a sphere with radius R can be described by the three-dimensional density distribution,

$$\rho(\mathbf{r}) = \sigma\delta(r-R)\ . \tag{1.131}$$

Such parametrizations are useful, because they can be applied in fundamental laws of electromagnetism (see Exc. 1.5.4.5).

Example 11 (*Parametrization of a current distribution*): As an example we calculate the current I produced by the distribution (1.130) crossing a rectangular area around the point $\mathbf{r} = R\hat{\mathbf{e}}_x$,

$$\int_{area}\mathbf{j}\cdot d\mathbf{A} = I\int_{R-\Delta x}^{R+\Delta x}\int_{-\Delta z}^{\Delta z}\delta(r-R)\delta(z)\hat{\mathbf{e}}_y d\mathbf{A} = I\int_{r-\Delta x}^{r+\Delta x}\delta(x-R)dx = I\ .$$

Example 12 (*Parametrization of a charge distribution*): In another example we calculate the total charge Q produced by the distribution (1.131),

$$\int_{volume} \rho(\mathbf{r})dV = \sigma \int_0^{2\pi} \int_0^{\pi} \int_0^{\infty} \delta(r-R)r^2 \sin\theta d\theta d\phi dr = \sigma 4\pi R^2 = Q \ .$$

Example 13 (*Dirac function in Coulomb's Law*): In a third example we show that the field of a point charge, $\varrho(\mathbf{r}) = Q\delta(x)\delta(y)\delta(z)$, can be obtained from Coulomb's law,

$$\vec{\mathcal{E}} = \int \frac{\varrho(\mathbf{r}')}{4\pi\varepsilon_0} \frac{\mathbf{r}-\mathbf{r}'}{|\mathbf{r}-\mathbf{r}'|^3} dV' = \frac{Q}{4\pi\varepsilon_0} \frac{\mathbf{r}}{r^3} \ .$$

1.5.3 Analytical signals

In signal processing theory, an *analytic signal* is a complex-valued function without negative frequency components. The real and imaginary parts of an analytic signal are mutually related by a *Hilbert transform*. Conversely, the analytic representation of a real-valued function is an analytic signal, which comprises the original function and its Hilbert transform. This representation facilitates many mathematical manipulations. The basic idea is that the negative frequency components of the Fourier transform (or spectrum) of a real function are superfluous due to the Hermitian symmetry of such a spectrum. These negative-frequency components can be discarded without loss of information, as long as we are willing to deal with a complex function. This makes certain attributes of the function more accessible, particularly for application in radiofrequency manipulation techniques.

While the manipulated function has no negative frequency components (that is, it is still analytic), the inverse conversion from complex to real is just a matter of discarding the imaginary part. The analytical representation is a generalization of the *phasor* concept: while the phasor is restricted to time-invariant amplitudes, phases and frequencies, the analytic signal allows for temporally variable parameters.

1.5.3.1 Transfer function generating an analytical signal

We consider a real function $s(t)$ with its Fourier transform $S(f)$. Then the transformed function exhibits a Hermitian symmetry about the point $f = 0$, since,

$$S(-f) = S(f)^* \ , \tag{1.132}$$

The function,

$$S_a(f) \equiv \begin{cases} 2S(f) & \text{for } f > 0 \\ S(f) & \text{for } f = 0 \\ 0 & \text{for } f < 0 \end{cases} = S(f) + \text{sgn}(f)S(f) \ , \tag{1.133}$$

where sgn(f) calculates the sign of f, only contains the non-negative components of $S(f)$. This operation is reversible due to the Hermitian symmetry of $S(f)$:

$$S(f) = \begin{cases} \frac{1}{2}S_a(f) & \text{para } f > 0 \\ S_a(f) & \text{para } f = 0 \\ \frac{1}{2}S_a(-f)^* & \text{para } f < 0 \end{cases} = \tfrac{1}{2}[S_a(f) + S_a(-f)^*] \ . \tag{1.134}$$

The analytical signal of $s(t)$ is the inverse Fourier transform of $S_a(f)$,

$$\begin{aligned} s_a(t) &\equiv \mathcal{F}^{-1}[S_a(f)] = \mathcal{F}^{-1}[S(f) + \text{sgn}(f) \cdot S(f)] \\ &= \mathcal{F}^{-1}[S(f)] + \mathcal{F}^{-1}[\text{sgn}(f)] \star \mathcal{F}^{-1}[S(f)] = s(t) + \imath \left[\tfrac{1}{\pi t} \star s(t)\right] = s(t) + \imath\hat{s}(t) \ , \end{aligned} \tag{1.135}$$

where $\star$ denotes the convolution.

$$\boxed{\hat{s}(t) \equiv \mathcal{H}[s(t)] \equiv \tfrac{1}{\pi t} \star s(t) = \tfrac{1}{\pi}\mathcal{P}\int_{-\infty}^{\infty} \frac{s(\tau)}{t-\tau} d\tau} \ , \tag{1.136}$$

with $\mathcal{P}$ denoting Cauchy's principal value, is the definition of the *Hilbert transform* of $s(t)$ [2].

Example 14 (*Analytical signal of the cosine function*): We consider the signal $s(t) = \cos\omega t$, where $\omega > 0$. Now

$$\begin{aligned} \hat{s}(t) &= \cos(\omega t - \tfrac{\pi}{2}) = \sin\omega t \ , \\ s_a(t) &= s(t) + \imath\hat{s}(t) = \cos\omega t + \imath \sin\omega t = e^{\imath\omega t} \ . \end{aligned}$$

In general, the analytical representation of a simple sinusoidal function is obtained by expressing it in terms of complex exponentials, discarding the negative frequency components, and doubling the positive frequency components, as in the example $s(t) = \cos(\omega t + \theta) = \frac{1}{2}(e^{\imath(\omega t+\theta)} + e^{-\imath(\omega t+\theta)})$. Here, we get directly from Euler's formula,

$$s_a(t) = \begin{cases} e^{\imath(\omega t+\theta)} &= e^{\imath|\omega|t}e^{\imath\theta} & \text{if } \omega > 0 \\ e^{-\imath(\omega t+\theta)} &= e^{\imath|\omega|t}e^{-\imath\theta} & \text{if } \omega < 0 \end{cases} .$$

The analytical representation of a sum of sinusoidal functions is the sum of the analytical representations of the individual sinuses.

We note that it is not forbidden to compute $s_a(t)$ for a complex $s(t)$. But this representation may be irreversible, since the original spectrum is usually not symmetric. Therefore, with the exception of the case $s(t) = e^{-\imath\omega t}$ with $\omega > 0$, where,

$$\begin{aligned} \hat{s}(t) &= \imath e^{-\imath\omega t} \\ s_a(t) &= e^{-\imath\omega t} + \imath^2 e^{-\imath\omega t} = e^{-\imath\omega t} - e^{-\imath\omega t} = 0 \ , \end{aligned} \tag{1.137}$$

[2] Also holds,

$$\begin{aligned} \hat{s}(t) &= -\tfrac{1}{\pi} \lim_{\epsilon\to 0} \int_{\epsilon}^{\infty} \frac{s(t+\tau) - s(t-\tau)}{\tau} d\tau \\ \mathcal{H}(\mathcal{H}(s))(t) &= -s(t) \ . \end{aligned}$$

we assume real $s(t)$.

We also note that, since $s(t) = \mathfrak{Re}\,[s_a(t)]$, we can retrieve the negative-frequency components simply by discarding $\mathfrak{Im}\,[s_a(t)]$, which may seem counterintuitive. On the other hand, the conjugate complex part $s_a^*(t)$ contains only the negative-frequency components. Therefore, $s(t) = \mathfrak{Re}\,[s_a^*(t)]$ retrieves the suppressed positive frequency components. In Exc. 1.5.4.7 we calculate the intensity of an electromagnetic wave.

1.5.3.2 Envelope and instantaneous phase

An analytical signal can also be expressed in polar coordinates,

$$s_a(t) = |s_a(t)|e^{\imath\phi(t)} \ , \tag{1.138}$$

in terms of an instantaneous amplitude or *envelope* $|s_a(t)|$ varying with time and an instantaneous phase angle $\phi(t) \equiv \arg[s_a(t)]$. In Fig. 1.10 the blue curve shows $s(t)$ and the red curve shows $|s_a(t)|$.

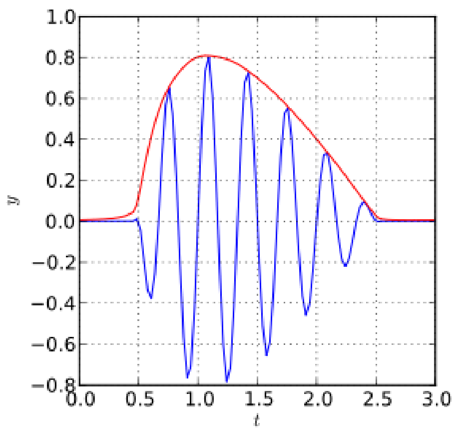

Figure 1.10: Illustration of a function (blue) and the magnitude of its analytical representation (red).

The time derivative of the unwrapped instantaneous phase is the instantaneous angular frequency,

$$\omega(t) \equiv \frac{d\phi(t)}{dt} \ . \tag{1.139}$$

The instantaneous amplitude and the instantaneous phase and frequency are used in some applications to measure and detect local characteristics of the signal or to describe the demodulation of a modulated signal. Polar coordinates conveniently separate amplitude and phase modulation effects.

Analytical signals are often frequency-shifted (down-converted) to 0 Hz, which can create negative (non-symmetric) frequency components:

$$s'_a(t) \equiv s_a(t)e^{-\imath\omega_0 t} = s_m(t)e^{\imath(\phi(t)-\omega_0 t)} \ , \tag{1.140}$$

where ω_0 is an arbitrary reference angular frequency. The function $s'_a(t)$ is called *complex envelope* or 'baseband'. The complex envelope is not unique, but determined by the choice of ω_0. This concept is often used to deal with band-pass signals. When $s(t)$ is a modulated signal, ω_0 is conveniently chosen as the carrier frequency.

1.5.4 Exercises

1.5.4.1 Ex: Dirac's δ function

a. Calculate $\int_0^\pi d\theta\ \sin^3\theta\ \delta(\cos\theta - \cos\frac{\pi}{3})$.
b. Now, be $\mathbf{r}_0$ a fixed three-dimensional vector with Cartesian coordinates x_0, y_0, and z_0. For the three-dimensional δ-function holds,

$$\int_V f(\mathbf{r})\delta(\mathbf{r}-\mathbf{r}_0)d^3r = \begin{cases} f(\mathbf{r}_0) & \text{if } \mathbf{r}_0 \text{ is within the volume } V \\ 0 & \text{else} \end{cases} .$$

In Cartesian coordinates, $\delta^{(3)}(\mathbf{r}-\mathbf{r}_0) \equiv \delta(x-x_0)\delta(y-y_0)\delta(z-z_0)$. Express $\delta^{(3)}(\mathbf{r}-\mathbf{r}_0)$ in cylindrical coordinates (ρ,φ,z) as a product of three one-dimensional functions δ in $\rho-\rho_0$, $\varphi-\varphi_0$, and $z-z_0$.

1.5.4.2 Ex: Dirac's δ function

Calculate the following expressions:
a. $\int_{-1}^{+1}\delta(x)[f(x)-f(0)]\ dx$,
b. $\int_{-1}^{3}(x^3-x)\sin\left(\frac{\pi}{4}x\right)\delta(x-2)\ dx$,
c. $\int_0^{2\pi}\sin x\ \delta(\cos x)dx$,
d. $\int_{\mathbb{R}^3}\delta(r-R)d^3\mathbf{r}$,
e. $\int_{\mathbb{R}^3}\delta(r-R)\delta(z)d^3\mathbf{r}$,
f. $\int_{-\infty}^{\infty}\left(\frac{d}{dx}\delta(x)\right)f(x)dx$ por integration parcial,
g. $\int_{-\infty}^{\infty}\left(\frac{d^n}{dx^n}\delta(x)\right)f(x)dx$.

1.5.4.3 Ex: Dirac's δ function

Show,

$$\int_{-\infty}^{\infty} 1\cdot\hat{f}(k)dk = \int_{-\infty}^{\infty}\hat{1}(x)f(x)dx = 2\pi f(0)\ ,$$

where $\hat{f}(k) \equiv \int_{-\infty}^{\infty} e^{-\imath kx}dx$ is the Fourier transform and $f(x) \equiv \int_{-\infty}^{\infty} e^{\imath kx}dk$ the inverse transform. Also show,

$$\hat{1} = 2\pi\delta(x)\ .$$

Help: $1 = e^{\imath k0}$.

1.5.4.4 Ex: Dirac's δ function

The following properties are, among others, characteristics for Dirac's δ-function,

$$\int_a^b f(x)\delta(x-c)\ dx = \begin{cases} f(c) & \text{if } c\in[a,b] \\ 0 & \text{else} \end{cases} .$$

Being $g(x)$ a function with simple zero passages x_n, that is, $g(x_n) = 0$ and $g'(x_n) \neq 0$, we have

$$\delta(g(x)) = \sum_n \frac{1}{|g'(x_n)|}\delta(x - x_n) \ .$$

Use these relationships to solve the following integrals,
a. $\int_{-2}^{5} \ dx \ (x^2 - 5x + 6) \ \delta(x - 3)$.
b. $\int_{-\infty}^{\infty} \ dx \ x^2 \ \delta(x^2 - 3x + 2)$.

1.5.4.5 Ex: Dirac's δ function

Demonstrate the following property of the δ-function:

$$\delta(\omega_1 - \omega)\delta(\omega_2 - \omega) = \frac{\delta(\omega_1 - \omega) + \delta(\omega_2 - \omega)}{|\omega_1 - \omega_2|} \ .$$

1.5.4.6 Ex: Parametrization of currents

Parametrize the current density $\mathbf{j}(\mathbf{r}')$ of a current loop
a. in Cartesian coordinates and
b. in spherical coordinates.

1.5.4.7 Ex: Intensity of an electromagnetic wave

Calculate the intensity of the electromagnetic wave given by (a) $\vec{\mathcal{E}}(\mathbf{r}, t) = \vec{\mathcal{E}}_0 \cos(kz - \omega t)$ and (b) $\vec{\mathcal{E}}(\mathbf{r}, t) = \vec{\mathcal{E}}_0 e^{\imath kz - \imath\omega t}$. Discuss!

1.6 Further reading

J.D. Jackson, *Classical Electrodynamics* [ISBN]

D.J. Griffiths, *Introduction to Electrodynamics* [ISBN]

D. Halliday, R. Resnick, and J. Walker, *Fundamentals of Physics* [ISBN]

H.M. Nussenzveig, *Curso de Física Básica: Eletromagnetismo (Volume 3)* [ISBN]

Chapter 2

Electrostatics

We have already seen that all electromagnetic phenomena are due to charges, that these charges are quantized and conserved, and that the superposition principle holds for electromagnetic forces. In principle, it should be possible to explain all electromagnetic phenomena by calculation the forces exerted by every charge on every other charge for arbitrary charge distributions. In reality however, the situation is much more complex, because the forces not only depend on the position of the charges, but also on their speed and acceleration. In addition, any information on the actual state of a charge is only transmitted at the finite speed of light, which gives rise to retardation effects.

To simplify the problem we will initially only consider immobile charges. The theory dealing with immobile electric charges is named *electrostatics*. Its fundamental task of electrostatics resides in calculating the force exerted by spatial distributions of charges.

2.1 The electric charge and the Coulomb force

2.1.1 Quantization and conservation of the charge

We know that ordinary matter consists of electrically neutral atoms. An atom, consists of a heavy nucleus and a shell of very light-weighted electrons. The nucleus, in turn, is made up of a number of protons and neutrons. Each proton carries a positive elementary charge $Q = +e$, that is, the charge is quantized in units of e. For an atom to be neutral, the number of electrons (with negative charge $-e$) in the shell must be equal to the number of atoms.

Macroscopic bodies are usually neutral, but that does not mean that positive and negative charges are annihilated. What they can do, is to bunch by equal numbers within restricted regions of space. Then, the forces exerted by the positive and negative charges of a specific region on other far-away charges compensate each other. This effect is called shielding.

Nevertheless, it is possible, exerting work, to separate positive and negative charges, to generate polarizations in dielectric materials or currents in conducting metals, and to perform experiments with electrically charged macroscopic objects.

2.1.2 Coulomb's law

To begin with, we consider a single point charge Q at the position $\mathbf{r}'$ exerting a force on another charge located in $\mathbf{r}$. The so-called *Coulomb force* is,

$$\mathbf{F}_C = \frac{Qq}{4\pi\varepsilon_0}\frac{\mathbf{r}-\mathbf{r}'}{|\mathbf{r}-\mathbf{r}'|^3} \ , \tag{2.1}$$

where ε_0 is a constant called the permittivity of free space. The Coulomb force decreases quadratically with the distance and is directed along the straight line connecting the two charges. Note that the force can be attractive (for $Qq < 0$) or repulsive (for $Qq > 0$). See the Excs. 2.1.3.1 to 2.1.3.22.

According to the *superposition principle* the force acting on the charge is not influenced by the possible existence of other forces, for example, exerted by other charges Q_k located in other positions $\mathbf{r}_k$,

$$\mathbf{F} = \mathbf{F}_1 + \mathbf{F}_2 + ... = \sum_k \frac{Q_k q}{4\pi\varepsilon_0}\frac{\mathbf{r}-\mathbf{r}_k}{|\mathbf{r}-\mathbf{r}_k|^3} \ . \tag{2.2}$$

Introducing an abbreviation,

$$\vec{\mathcal{E}} = \sum_k \frac{Q_k}{4\pi\varepsilon_0}\frac{\mathbf{r}-\mathbf{r}_k}{|\mathbf{r}-\mathbf{r}_k|^3} \ , \tag{2.3}$$

called the *electric field*, we can express the Coulomb force as,

$$\boxed{\mathbf{F}_C = q\vec{\mathcal{E}}} \ . \tag{2.4}$$

Using the Dirac function we can parametrize the distribution of charges by,

$$\varrho(\mathbf{r}) = \sum_k Q_k\delta^3(\mathbf{r}-\mathbf{r}_k) \ . \tag{2.5}$$

The charge of a single electron is small, and often many charges are involved in electrical phenomena. Thus, the discrete character of the charge does not appear, and the charge distribution appears as a smooth distribution of *charge density*, such that,

$$\int_{\mathbb{R}} \varrho(\mathbf{r}')dV' = \int_{\mathbb{R}} \sum_k Q_k\delta^3(\mathbf{r}'-\mathbf{r}_k)dV' = \sum_k Q_k \ . \tag{2.6}$$

With this (fluid model) approximation,

$$\sum_k Q_k ... \longrightarrow \int dV'\varrho(\mathbf{r}')... \ , \tag{2.7}$$

the *Coulomb law* can be written,

$$\boxed{\vec{\mathcal{E}} = \int \frac{\varrho(\mathbf{r}')}{4\pi\varepsilon_0}\frac{\mathbf{r}-\mathbf{r}'}{|\mathbf{r}-\mathbf{r}'|^3}dV'} \ , \tag{2.8}$$

since by inserting the discrete distribution (2.5) we recover Coulomb's law (2.3).

It is also possible to define from ϱ a two-dimensional *surface charge density* σ or a one-dimensional *linear charge density* λ using the Dirac function. For example, the surface charge density on a spherical shell,

$$\varrho(\mathbf{r}) = \sigma(\theta, \phi)\delta(r - R) \ , \tag{2.9}$$

or the linear charge density on a ring,

$$\varrho(\mathbf{r}) = \lambda(\phi)\delta(r - R)\delta(z) \ . \tag{2.10}$$

Substituting ϱ of the Coulomb law with these expressions, we reduce the dimensionality of the integral. We will study problems related to charge distributions in the Excs. 2.2.4.1 to 2.2.4.12.

2.1.3 Exercises

2.1.3.1 Ex: • Coulomb force

A point charge of $-2.0\,\mu$C and a point charge of $4.0\,\mu$C are separated by a distance L. Where should a third point charge be placed in order for the electrostatic force on this third charge to be zero?

2.1.3.2 Ex: • Coulomb force

A point particle with a charge of $-1.0\,\mu$C is located at the origin; a second point particle with a charge of $2.0\,\mu$C is located at $x = 0$, $y = 0.1\,$m; and a third point particle with a charge of $4.0\,\mu$C is located at $x = 0.2\,$m, $y = 0$. Determine the electrostatic force on each of the three particles.

2.1.3.3 Ex: • Coulomb force

A point charge of $-5.0\,\mu$C is located at $x = 4.0\,$m, $y = -2.0\,$m, and a second point charge of $12.0\,\mu$C is located at $x = 1.0\,$m, $y = 2.0\,$m.
a. Determine the absolute value, the direction and the orientation of the electric field in $x = -1.0\,$m, $y = 0$.
b. Calculate the absolute value, the direction and the orientation of the electric force acting on an electron placed in the electric field at $x = -1.0\,$m, $y = 0$.

2.1.3.4 Ex: Coulomb force

Imagine an electron near the Earth's surface. At what point should we place a second electron in order for the electrostatic force between the electrons to compensate the gravitational force acting on the first electron?

2.1.3.5 Ex: Coulomb force

Three positive point charges Q_1, Q_2, and Q_3 are placed at the corners of an equilateral triangle with the edge length $L = 10\,$cm. Calculate the value and direction of the force acting on an electron located in the center of the triangle.

2.1.3.6 Ex: • Coulomb force

Two particles carrying equal charges q are placed at a mutual distance of $r = 3\,\text{mm}$ and then released. The acceleration of the first particle after having been released is $a_1 = 7\,\text{m/s}^2$, and the acceleration of the second particle is $a_2 = 2\,\text{m/s}^2$. The mass of the first particle is $m_1 = 6 \cdot 10^{-7}\,\text{kg}$.
a. What is the mass of the second particle?
b. What is the charge of the particles?

2.1.3.7 Ex: • Coulomb force

A small ball of graphite (mass $m = 1\,\text{kg}$) suspended on a wire is touched by an electrically charged plastic stick and picks up 1% of its charge. The result is that the ball is displaced by an angle of 30°, while the stick is held in place at the former position of the ball. The distance between the center of the ball and the end of the stick is 10 cm.
a. Calculate the force exerted by the wire on the ball?
b. Assume that the charge on the stick is fully concentrated at its end. What are the charges on the ball and on the stick?

2.1.3.8 Ex: • Acceleration of charges

An electron has an initial velocity of $v_0 = 2 \cdot 10^6\,\text{m/s}$ in $+x$-direction. It enters a region of uniform electric field $\vec{\mathcal{E}} = (300\,\text{N/C})\ \hat{\mathbf{e}}_x$.
a. Determine the acceleration of the electron.
b. How long does it take for the electron to travel a distance of $s = 10.0\,\text{cm}$ along the x-axis towards $+x$ in the region that has field.
c. At what angle and in what direction does the motion of the electron deflect as it travels 10.0 cm in x-direction?

2.1.3.9 Ex: • Acceleration of charges

A charged particle of 2.0 g is released from rest in a region that has a uniform electric field, $\vec{\mathcal{E}} = (300\,\text{kN/C})\hat{\mathbf{e}}_x$. After traveling a distance of 0.5 m in this region, the particle has a kinetic energy of 0.12 J. Determine the particle's charge.

2.1.3.10 Ex: Charged copper coins

The positive proton charge and the negative electron charge have the same absolute value. Assume that the absolute values would have a relative difference of only 0.0001%. Consider copper coins with $3 \cdot 10^{22}$ atoms. What would be the repulsive force of two coins 1 m apart?
Help: A neutral copper atom contains 29 protons and the same amount of electrons.

2.1.3.11 Ex: • Weight of the electron

A metal sphere is charged with $Q = +1\,\mu\text{C}$. Determine whether the mass of the sphere increases or decreases due to the charging and calculate the value?

2.1.3.12 Ex: The hydrogen atom

In the hydrogen atom the typical distance between the positively charged proton and the negatively charged electron is $d \sim 5 \cdot 10^{-11}$ m.
a. Calculate the Coulomb force.
b. Compare this force with the gravitational force between the two particles.
c. What should be the speed of the electron around the nucleus to compensate for the gravitational attraction by the centrifugal force?

2.1.3.13 Ex: Exercise of understanding

Two metallic spheres are placed at a distance d from each other and respectively charged with $+Q$ and $-2Q$.
a. Do spheres attract or repel each other?
b. What happens if we let the spheres contact each other and then put them at the same distance d. How much does the force change?

2.1.3.14 Ex: • Charged sphere on a spring

A ball with the m is suspended on a spring with the spring constant f.
a. What will be the displacement of the ball due to its weight? What will be the frequency of oscillation?
b. Now the ball is loaded with the charge Q and a second ball with the same charge is approached from below the first ball. Derive the relationship between the position of the first ball z_1 and the position of the second z_2. The position $z_1 = 0$ is the resting position of the spring, that is, the position that the spring would have without suspended mass. CAUTION: you'll get a third order equation in z_1, don't try to solve it!
c. For which position z_2 of the second ball does the first ball stay at the resting position of the spring, that is, for which z_2 do we find $z_1 = 0$ to be solution? Are there any other solutions? What are your interpretations?
d. What is the frequency of oscillation under these conditions, when ball 1 is only slightly displaced around $z_1 = 0$? Use the approximation $\frac{1}{(a-x)^2} \approx \frac{1}{a^2} + \frac{2}{a^3}x$, which holds for $x \ll a$.

2.1.3.15 Ex: Stability of a charge distribution

The charge distributions shown in the figure are given. All positive and negative charges have the same absolute value.
a. Determine whether one of these distributions is stable? What happens in different cases?
b. Is it possible to choose the absolute values of the charges in such a way as to make the configurations stable?

2.1.3.16 Ex: Stability of a charge distribution

Three balls with mass m and each charged with the charge Q are placed in a parabolic bowl. This can be described as a surface in space, where the coordinate z of the surface is given by $z = z(x, y) = A(x^2 + y^2)$. Gravitation shows into $-\hat{\mathbf{e}}_z$ direction. What is

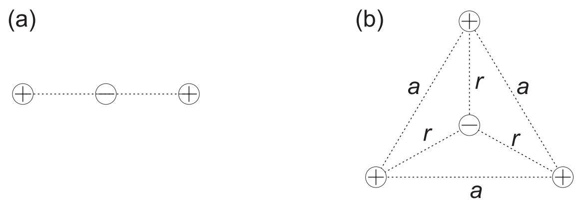

Figure 2.1: Geometry of charge distribution.

the distance the balls adopt, when we set as an additional condition, that all charges are at the same height?

2.1.3.17 Ex: Ions in a harmonic potential

Two ions with the positive charge $+e$ are confined to an isotropic harmonic potential. Each ion has the potential energy $U = \frac{1}{2}m\omega^2 r^2$, where r is the distance from the center of the potential. The ions are at rest, only consider two dimensions.
a. What is the distance of the two ions from the center?
b. Calculate the distance for three identical ions.

2.1.3.18 Ex: Spheres on a wire

Two identical spheres with mass $m = 0.1\,\text{kg}$ are suspended at the same point of a ceiling by a 1 m long wire and have the same charge. What is the value of the charge if the two centers of the spheres are 4 cm apart. Use the approximation $\sin\alpha \approx \tan\alpha \approx \alpha$ for small angles α.

2.1.3.19 Ex: Oscilloscope

We consider a simple model of an oscilloscope. Inside the device is a Braun tube, inside which electrons are accelerated by a voltage U to a speed v. Then, the electrons fly through the plates of a capacitor and are deflected by the electric field E of the capacitor. (In a real oscilloscope there are two capacitors: one for horizontal deviation and one for vertical.) Behind the capacitor, the electrons fly to a screen, where they produce a bright spot.
a. Calculate the electron velocity v for an accelerating voltage of $U = 1\,\text{kV}$. (Do not consider relativistic effects!)
b. The capacitor has a length of $l = 5$ cm and a distance from the plates of $d = 2\,\text{cm}$. What is the maximum allowable voltage U_{max} at the capacitor to prevent electrons from hitting one of the capacitor plates? (Electrons enter the capacitor in the center between the plates.)
c. What should be the distance between the plates and the screen (which is 10 cm wide), so that with maximum voltage U_{max} the entire area of the screen is used?
Comment: Disregard capacitor edge effects!

2.1.3.20 Ex: • Electron between charged plates

Between two parallel horizontal plates there is a homogeneous electric field $|\vec{\mathcal{E}}| = 2 \cdot 10^3\,\text{N/C}$. The lower plate is charged with a positive charge, the upper plate with a negative, such that the field is oriented upwards. The length of the plates is $L = 10\,\text{cm}$, their distance $d = 2\,\text{cm}$. From the left edge of the bottom plate an electron is shot at an initial velocity $|v_0| = 6 \cdot 10^6\,\text{m/s}$ under an angle $45°$ into the space between the plates.
a. When will the electron hit one of the plates?
b. Which plate is eventually hit and at what horizontal distance from the firing point?

2.1.3.21 Ex: • The Coulomb-Kepler problem

We consider two particles charged with charges Q_1 and Q_2 and masses $m = m_1 = m_2$ which, for simplicity, can only move along the $\hat{\mathbf{e}}_z$-axis and are subject to mutual Coulomb forces.
a. Derive the differential equations for the positions z_1 and z_2 of the two particles. Reduce the number of variables of the problem by introducing the difference variable $z = z_2 - z_1$ and establish the differential equation for z.
b. The differential equation obtained has the same shape as that of the Kepler problem in mechanics, which, however, is not defined along an axis but on a plane. What are the solutions to Kepler's problem? What important physical quantity does not appear to constrain the freedom of movement to one axis? What would be the impact of this constraint on the solutions to Kepler's problem? What is the additional degree of freedom in the Coulomb-Kepler problem as compared to the Kepler problem?
c. Kepler's differential equation is not easy to solve. Even so, we can learn something by looking at the phase space diagram. For this, we consider two identical particles $Q = Q_1 = Q_2$ and $m = m_1 = m_2$, placed at a distance z_0. What is going to happen? How will the velocities v_1 and v_2 of the two particles behave with respect to each other? Derive a relationship between the distance z and the velocity v of one of the particles (energy conservation). What is the value of the velocity for $z \to \infty$? Prepare a phase space diagram in (z, v) for three different distances z_0.

2.1.3.22 Ex: Particle spinning around a charged wire

An infinitely long line uniformly charged with negative charge, has a charge density of λ and is located on the z-axis. A small positively charged particle has mass m and a charge q and is on circular orbit of radius R in the xy-plane centered on the charge line.
a. Deduce an expression for the velocity of the particle.
b. Obtain an expression for the period of the particle's orbit.

2.2 Properties of the electric field

In principle the fundamental problem of electrostatics is solved by Coulomb's law. In practice however, the calculation of the electric field generated by a charge distribution can be complicated. On the other hand, electrostatic problems often exhibit symmetries, which allow for their resolution by other techniques avoiding the integrals of Coulomb's law.

2.2.1 Field lines and the electric flux

When we calculate the electric vector field for a charge distribution on a matrix of points in space, we get diagrams like the one shown in Fig. 2.2. The arrows represent, through the lengths of the vectors, the value of the field and, through the orientation of the vector, the direction of the force exerted by the field. The diagram suggests to connect the arrows thus forming lines called *field lines*. These lines are nothing more than the trajectories taken by test charges placed inside the field [1]. Field lines can never intersect (otherwise the direction of force acting on a test charge would be ambiguous) and can never begin or end in free space. They always start from a positive charge and end up in a negative charge.

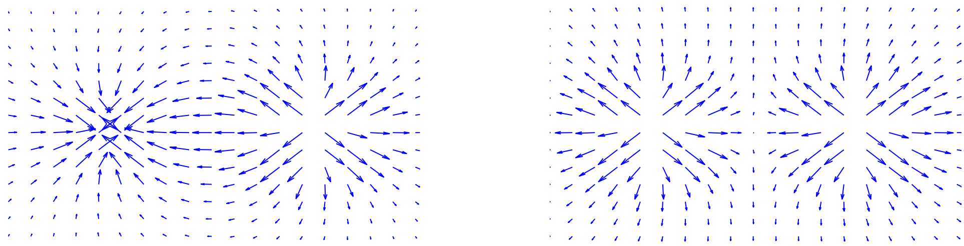

Figure 2.2: Field lines of two equal charges (right) and two opposed charges (left).

The *electric flux* is a measure for the density of field lines crossing a surface. As we have already said, the field line density corresponds to the amplitude of the electric field $\vec{\mathcal{E}}$. The normal vector of the surface $\mathbf{S}$ being locally perpendicular to the plane, we must calculate the flux by taking the integral of the scalar product,

$$\boxed{\Psi_E \equiv \int_{\mathcal{S}} \vec{\mathcal{E}} \cdot d\mathbf{S}} \ . \tag{2.11}$$

Then, instead of illustrating the amplitude of a field through the length of the arrows representing the force exerted on a charge, $\vec{\mathcal{E}} \propto \mathbf{F}$, we can illustrate the amplitude through the local density of lines field, $\vec{\mathcal{E}} \propto \Psi_E$.

The concept of the flux allows us to quantitatively formulate the statement, that field lines can not start or end in free space, but always come out (or penetrate) into charges. For this, we calculate the flux through a sphere around an electric charge q located at the origin using Coulomb's law:

$$\oint_{spherical\ surface} \vec{\mathcal{E}} \cdot d\mathbf{S} = \oint_{spherical\ surface} \frac{1}{4\pi\varepsilon_0} \frac{q}{|\mathbf{r}|^2} \hat{\mathbf{e}}_\mathbf{r} \cdot r^2 \sin\theta d\theta d\phi \hat{\mathbf{e}}_\mathbf{r} = \frac{q}{\varepsilon_0} \ . \tag{2.12}$$

[1]Note, that the representation by lines (instead of vectors) misses the information about the local field strength. However, this information is still encoded in the local density of the field lines.

With the superposition principle we can generalize this result to arbitrary distributions of charges Q. The so-called *Gauß' law*, or Maxwell's third equation,

$$\boxed{\oint_{\partial\mathcal{V}} \vec{\mathcal{E}} \cdot d\mathbf{S} = \frac{Q}{\varepsilon_0}} \ , \tag{2.13}$$

states, that the number of field lines entering a charge-free volume $\mathcal{V}$ through a closed surface $\partial\mathcal{V}$ must equal the number of lines leaving it. The law also states that *there exist electric charges* acting as sources or drains of field lines. We will resolve flux problems in the Excs. 2.2.4.13 to 2.2.4.29.

2.2.2 Divergence of the electric field and Gauß' law

Gauß' integral theorem (1.42) allows us to rewrite Gauß' law (2.13). On the one hand, we have,

$$\oint_{\partial\mathcal{V}} \vec{\mathcal{E}} \cdot d\mathbf{S} = \int_{\mathcal{V}} \nabla \cdot \vec{\mathcal{E}} dV \ , \tag{2.14}$$

on the other hand, we can express the total charge inside the volume $\mathcal{V}$ as a sum over the charge distribution,

$$Q = \int_{\mathcal{V}} \varrho(\mathbf{r}) dV \ . \tag{2.15}$$

comparing the integrands, we obtain the differential form of Gauß' law or Maxwell's third equation:

$$\boxed{\nabla \cdot \vec{\mathcal{E}} = \frac{\varrho}{\varepsilon_0}} \ . \tag{2.16}$$

The Gauß law can also be derived directly from the general Coulomb law: We calculate the divergence of the field of formula (2.8),

$$\begin{aligned} \nabla \cdot \vec{\mathcal{E}} &= \nabla_{\mathbf{r}} \cdot \int \frac{\varrho(\mathbf{r}')}{4\pi\varepsilon_0} \frac{\mathbf{r} - \mathbf{r}'}{|\mathbf{r} - \mathbf{r}'|^3} dV' = \frac{1}{4\pi\varepsilon_0} \int \varrho(\mathbf{r}') \nabla_{\mathbf{r}} \cdot \frac{\mathbf{r} - \mathbf{r}'}{|\mathbf{r} - \mathbf{r}'|^3} dV' \\ &= \frac{1}{4\pi\varepsilon_0} \int \varrho(\mathbf{r}') 4\pi \delta^3(\mathbf{r} - \mathbf{r}') dV' = \frac{\varrho(\mathbf{r})}{\varepsilon_0} \ . \end{aligned} \tag{2.17}$$

In the integral form, Gauß' law is very useful for calculating electric fields particularly in situations with a high degree of symmetry. Let us discuss some examples in the following.

Example 15 (*Electric field outside a charged sphere*): We consider a sphere with radius R carrying the total charge Q. Gauß' law says,

$$\oint_{\partial\mathcal{V}} \vec{\mathcal{E}} \cdot d\mathbf{S} = \frac{Q}{\varepsilon_0} \ ,$$

where we choose as volume a sphere with radius $r > R$. At first glance, this does not seem to help much because the field, in which we are interested, is under the integral. But we can explore the symmetry of the system to simplify the integral, since $\vec{\mathcal{E}} = \mathcal{E}\hat{\mathbf{e}}_r$ and $\mathrm{d}\mathbf{S} = dS\hat{\mathbf{e}}_r$, such that we can write the integral,

$$\int_0^{\pi} \int_0^{2\pi} \mathcal{E} r^2 \sin\theta d\theta d\phi = 4\pi r^2 \mathcal{E} = \frac{Q}{\varepsilon_0} \ .$$

Hence,

$$\vec{\mathcal{E}} = \frac{Q}{4\pi\varepsilon_0 r^2}\hat{\mathbf{e}}_r \ .$$

This is precisely Coulomb's law. It is interesting to note that the field does not depend on the distribution ϱ of the charge within the volume. Of course, to take advantage of the symmetry of the system, it is important to choose the adequate volume.

Example 16 (*Box containing an interface*): Let us now give another example of the utility of Gauß' law. We are interested in the electric field generated by an infinitely extended plane carrying a homogeneous surface charge density σ. By symmetry, the $\vec{\mathcal{E}}$-field must cross the plane perpendicularly and have opposite directions above and below the plane. We now imagine a rectangular pill box enclosing a small area of the plane, so that two surfaces of the box (with area S) are parallel to the plane. Inside the box we find the charge,

$$Q = \varepsilon_0 \oint_{\mathcal{S}_{box}} \vec{\mathcal{E}} \cdot d\mathbf{S} = \varepsilon_0 \int_{\mathcal{S}_{upper}} \mathcal{E} dS + \varepsilon_0 \int_{\mathcal{S}_{lower}} \mathcal{E} dS = 2S\mathcal{E} \ .$$

On the other hand, $Q = \int_{\mathcal{V}_{box}} \varrho dV = \sigma S$. Hence,

$$\vec{\mathcal{E}} = \frac{\sigma}{2\varepsilon_0}\hat{\mathbf{n}} \ .$$

It may seem strange that the electric field does not depend on the distance from the plane, but this is due to the fact that the plane is supposed infinite, which is an unrealistic concept. For a limited surface we expect field components not being perpendicular to the interface, which come from the edges of the surface.

2.2.3 Rotation of the electric field and Stokes' law

Stokes' integral theorem (1.40) allows us to rewrite Maxwell's fourth equation(2.23). From

$$\boxed{\oint_{\partial\mathcal{S}} \vec{\mathcal{E}} \cdot d\mathbf{r} = 0} = \int_{\mathcal{S}} (\nabla \times \vec{\mathcal{E}}) \cdot d\mathbf{S} \ , \tag{2.18}$$

we obtain the differential form of Maxwell's second equation:

$$\boxed{\nabla \times \vec{\mathcal{E}} = 0} \ . \tag{2.19}$$

The second Maxwell equation (applied to electrostatics) can also be derived directly from the general Coulomb law: We calculate the rotation of the field of formula (2.3),

$$\nabla \times \vec{\mathcal{E}} = \nabla_{\mathbf{r}} \times \int \frac{\varrho(\mathbf{r}')}{4\pi\varepsilon_0} \frac{\mathbf{r}-\mathbf{r}'}{|\mathbf{r}-\mathbf{r}'|^3} dV' = \frac{1}{4\pi\varepsilon_0} \int \varrho(\mathbf{r}') \nabla_{\mathbf{r}} \times \frac{\mathbf{r}-\mathbf{r}'}{|\mathbf{r}-\mathbf{r}'|^3} dV' = 0 \ . \tag{2.20}$$

The fact that the rotation of any electrostatic field must vanish is a severe constraint. For example, there is no charge distribution leading to a field of the form $\vec{\mathcal{E}} = y\hat{\mathbf{e}}_x$.

A direct consequence of this law is that we can introduce the concept of the potential. This is fundamental, because electrodynamics can be fully formulated in terms of scalar potentials. We will devote the whole next section to electric potentials.

2.2.4 Exercises

2.2.4.1 Ex: Use of Dirac's function in Coulomb's law

Show how the following Coulomb law formulas for one-, two- and three-dimensional density distributions,

$$\vec{\mathcal{E}}(\mathbf{r}) = \frac{1}{4\pi\varepsilon_0}\int_V \frac{\mathbf{r}-\mathbf{r}'}{|\mathbf{r}-\mathbf{r}'|^3}\rho(\mathbf{r}')dV'$$
$$\vec{\mathcal{E}}(\mathbf{r}) = \frac{1}{4\pi\varepsilon_0}\int_A \frac{\mathbf{r}-\mathbf{r}'}{|\mathbf{r}-\mathbf{r}'|^3}\sigma(\mathbf{r}')dA'$$
$$\vec{\mathcal{E}}(\mathbf{r}) = \frac{1}{4\pi\varepsilon_0}\int_C \frac{\mathbf{r}-\mathbf{r}'}{|\mathbf{r}-\mathbf{r}'|^3}\lambda(\mathbf{r}')dC'$$

are linked using Dirac's δ-function, defined by,

$$\delta(x) = \left\{ \begin{array}{cc} \infty \text{ for } & x = 0 \\ 0 \text{ for } & x \neq 0 \end{array} \right\} \qquad \text{such that} \qquad \int f(x)\delta(x-a)dx = f(a)\infty\frac{1}{\infty} = f(a) \ .$$

Use the examples of a. A linear charge distribution along the x-axis, given by $\rho(\mathbf{r}') = \lambda(x')\delta(y')\delta(z')$, and b. a surface charge distribution in the $z = 0$ plane, given by$\rho(\mathbf{r}') = \sigma(x', y')\delta(z')$.

2.2.4.2 Ex: Electric field generated by a linear charge distribution

Calculate the electric field generated by a linear charge distribution. Analyze the field in a remote region.

2.2.4.3 Ex: Electric field produced by a charged disc

a. Calculate the electric field along the symmetry axis generated by a thin disk of radius R evenly charged with the charge Q.
b. Discuss the limit $R \to \infty$ assuming that the surface charge density is kept constant.

2.2.4.4 Ex: Electric field produced by a spherical layer

A charge q is deposited on a solid conducting sphere of radius R.
a. Parametrize the charge distribution $\rho(\mathbf{r})$.
b. Determine the surface charge density σ on the sphere's surface.
c. Using the Gauß law, $\oint_{\partial V} \vec{\mathcal{E}}(\mathbf{r})\cdot d\mathbf{a} = \frac{Q}{\varepsilon_0}$, calculate the electric field inside and outside the sphere.
d. Using the Coulomb law, $\vec{\mathcal{E}}(\mathbf{r}) = \frac{1}{4\pi\varepsilon_0}\int_A \frac{\mathbf{r}-\mathbf{r}'}{|\mathbf{r}-\mathbf{r}'|^3}\sigma(\mathbf{r}')dA'$ in spherical coordinates,

$$\mathbf{r}' = \begin{pmatrix} R\sin\theta'\cos\phi' \\ R\sin\theta'\sin\phi' \\ R\sin\theta' \end{pmatrix} \qquad \text{and} \qquad dA' = R^2\sin\theta' d\theta d\phi' \ ,$$

calculate the electric field $E_z(z)$ along the z-axis in- and outside the sphere. Help:

$$\int_{-R}^{R} \frac{z-z'}{\sqrt{z^2-2zz'+R^2}^3} dz' = \begin{cases} \frac{-2R}{z^2} & z<-R \\ 0 \quad \text{for} & -R<z<R \\ \frac{2R}{z^2} & R<z \end{cases} .$$

2.2.4.5 Ex: Field of a homogeneously charged sphere

Calculate with the Gauß law the electric field of a homogeneously charged sphere (charge Q, radius R)
a. for $r<R$ and
b. for $r \geq R$.

2.2.4.6 Ex: Field of a charge distribution with spherical symmetry

The electric field generated by a spherically symmetric charge distribution $\rho(r)$ can be given in the form,

$$\vec{\mathcal{E}}(\mathbf{r}) = \frac{\mathbf{r}}{r^3}\, 4\pi \int_0^r dr'\, r'^{\,2}\, \rho(r') ,$$

where the origin is in the center of the sphere and $r=|\mathbf{r}|$.
a. Show that $\text{div}\vec{\mathcal{E}} = 4\pi\,\rho$ and $\text{rot}\vec{\mathcal{E}} = 0$.
b. Calculate the field for a sphere of radius R, which is homogeneously charged in the entire volume with the total charge Q.
c. Resolve (b) for a homogeneously charged hollow concentric sphere with inner radius R_i, outer radius R_a and full load Q.
d. Resolve (c) for the case, that the center of the hollow spherical part is displaced by a vector $\mathbf{d}$ with respect to the center of the spherical surface.
Help: The electric field is an additive quantity.

2.2.4.7 Ex: Field of a charge distribution with spherical symmetry

A sphere of radius R is in a vacuum. It is made of a material with a constant permittivity ε and carries the charge q in its center.
a. Calculate the field the electrostatic field $\vec{\mathcal{E}}$ inside and outside the sphere.
b. Calculate the electrostatic potential Φ in the entire space.

2.2.4.8 Ex: Charge distribution

We consider the charge density $\rho(\mathbf{r}) = cr\int_0^R dr'\delta(r'-r)$, where $r=|\mathbf{r}|$, $R>0$ and $c=const$. The total charge be Q.
a. Make a scheme of the function $\rho(\mathbf{r})$. What is the relationship between the constant c and the total charge Q?
b. Start by showing that the electric field created by a spherically symmetric charge distribution ρ can be written as $\vec{\mathcal{E}}(\mathbf{r}) = \frac{\mathbf{r}}{r^3}\int_0^r dr' r'^2 \frac{1}{\varepsilon_0}\rho(r')$. Here, $\mathbf{r}$ is the vector starting from the origin at the center of symmetry and reaching the surface. Determine the absolute value and direction of the electric field $\vec{\mathcal{E}}(\mathbf{r})$ for $|\mathbf{r}|<R$ and $|\mathbf{r}|>R$ for the given charge distribution. Make a scheme of the profile $|\vec{\mathcal{E}}(\mathbf{r})|$.

2.2.4.9 Ex: Charge distribution

A thin, square and conductive sheet has $d = 5.0$ m long edges and a charge of $Q = 80\,\mu\text{C}$. Assume that the load is evenly distributed on the faces of the sheet.
a. Determine the charge density on each face of the sheet and the electric field in the vicinity of one face.
b. The sheet is placed to the right of an infinite, non-conductive plane charged with the charge density $\sigma_{inf} = 2.0\ \mu\text{C/m}^2$, with the faces of the sheet parallel to the plane. Determine the electric field on each face of the sheet and determine the charge density on each face.

2.2.4.10 Ex: Charge distribution

A large, flat, non-conductive and non-uniformly charged surface is placed along the $x = 0$ plane. At the origin, the charge density is $\sigma = 3.1\,\mu\text{C/m}^2$. At a short distance from the surface in the positive direction of the x-axis, the x-component of the electric field is $\mathcal{E}_{dir} = 4.65 \cdot 10^5$ N/C. What is the value of $\mathcal{E}_x$ a short distance from the surface in the negative direction of the axis x.

2.2.4.11 Ex: Charge distribution

An infinite flat non-conductive blade with surface charge density $\sigma_1 = +3.0\,\mu\text{C/m}^2$ is located in the $y_0 = -0.6$ m plane. A second infinite flat blade with surface charge density of $\sigma_2 = -2.0\,\mu\text{C/m}^2$ is located in the $x_0 = 1.0$ m plane. Finally, a thin non-conductive spherical shell with radius $R = 1.0$ m and its center in the $z_0 = 0$ plane at the intersection of the two charged blades, has a surface charge density of $\sigma_3 = -3.0\,\mu\text{C/m}^2$. Determine the magnitude, direction, and orientation of the electric field along the x-axis and
a. $x_1 = 0.4$ m and
b. $x_2 = 2.5$ m.

2.2.4.12 Ex: Charged sphere

A solid non-conducting sphere with radius $R = 1.0$ cm carries a uniform volumetric charge density. The magnitude of the electric field at a distance $r = 2.0$ cm from the center of the sphere is $\mathcal{E}_r = 1.88 \cdot 10^3$ N/C.
a. What is the volumetric charge density of the sphere?
b. Determine the magnitude of the electric field at a distance $d = 5.0$ cm from the center of the sphere.

2.2.4.13 Ex: Electrical flow

A point charge Q is placed in the center of a hypothetical ball with radius R, which on one side is cut at a height h. What is the flow of electric field $\vec{\mathcal{E}}$ through the plane of the cut A illustrated in the figure?

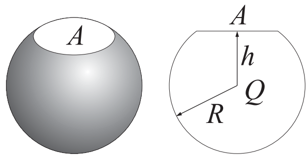

Figure 2.3: Scheme.

2.2.4.14 Ex: Electrical flow

The cube shown in the figure has an edge length of $d = 1.4\,\mathrm{m}$ and is located inside an electric field.
a. Calculate the electrical flux through the right surface of the cube for an electric field given by $\vec{\mathcal{E}} = -3\,\mathrm{V/m}\cdot\hat{\mathbf{e}}_x + 4\,\mathrm{V/m}\cdot\hat{\mathbf{e}}_z$. What is the total flux across the entire surface of the cube?
b. Calculate the total flux across the entire surface of the cube for the electric field $\vec{\mathcal{E}} = -4\,\mathrm{V/m}^2\cdot\hat{\mathbf{e}}_x + (6\,\mathrm{V/m} + 3\,\mathrm{V/m}^2\cdot y)\hat{\mathbf{e}}_y$. What charge is contained in the cube?

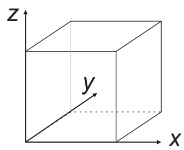

Figure 2.4: Scheme.

2.2.4.15 Ex: Electrical flow

Calculate the electric field flux $\vec{\mathcal{E}}(\mathbf{r}) = \mathcal{E}_0\hat{\mathbf{e}}_z$ through the semi-sphere with radius R shown in the figure.

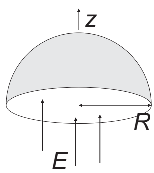

Figure 2.5: Scheme.

2.2.4.16 Ex: Electrical flow

Calculate the flow of the vector field with cylindrical symmetry $\vec{\mathcal{E}}(\mathbf{r}) = \mathcal{E}_0\hat{\mathbf{e}}_\rho$ through the half cylindrical surface shown in the figure with radius R and length L.

2.2.4.17 Ex: Electric field of a charged sheet

An infinitely extended non-conductive sheet carries a charge with a surface density of $0.1\,\mu\mathrm{C/m}^2$ on either side. What is the distance of the equipotential surfaces for a

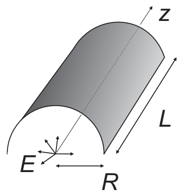

Figure 2.6: Scheme.

potential difference of 50 V?

2.2.4.18 Ex: Electric field between charged planes

Consider two thin, non-conductive planes with infinite length perpendicular to the x-axis and crossing this axis at the positions x_1 and x_2 with $x_1 < x_2$. The planes are uniformly charged with charge densities σ_2. Calculate the electric fields in the three regions $x < x_1$ and $x_1 < x < x_2$ and $x_2 < x$. Discuss the particular cases $\sigma_2 = \sigma_1$ and $\sigma_2 = -\sigma_1$.

2.2.4.19 Ex: Electric field of a photocopier

The electric field just above the surface of the electrically charged drum of a photocopier has the absolute value $2.3 \cdot 10^5$ N/C. The drum has a length of 42 cm and a diameter of 12 cm.
a. What is the charge density on the surface supposed conductive?
b. What is the total charge on the drum?
c. Decreasing the drum to 8 cm in order to build a more compact photocopier, the field on the surface must remain the same. What should the charge be in this case?

2.2.4.20 Ex: Geiger counter

A Geiger-Müller meter consists essentially of a metal tube filled with gas (inner radius r_a) with a thin wire inside (radius r_i). A high voltage is applied between the two. The meter serves, for example, to detect charged particles, which produce pairs of electrons and ions from the gas, which are then extracted by an applied voltage and detected as an electrical signal.
a. Calculate the potential $\phi(r)$, where $\phi(r_a) = 0$ and $\phi(r_i) = U = 1000$ V.
b. Be $r_i = 15$ µm, $r_a = 1$ cm. Calculate the strength of the field at the tube's surface.
c. The average free path in the gas is $L = 3$ µm. At what distance R_I from the wire does an avalanche form, that is, an electron stopped due to a collision is accelerated over a distance L up to the ionization energy $E_I = 5$ eV and, thus, can generate another electron-ion pair in the subsequent collision?

2.2.4.21 Ex: Electrical flow

A thin, non-conductive uniformly charged spherical shell with radius R, has a total positive charge equal to Q. A small piece is removed from the surface.
a. What are the absolute value, the direction and the orientation of the electric field

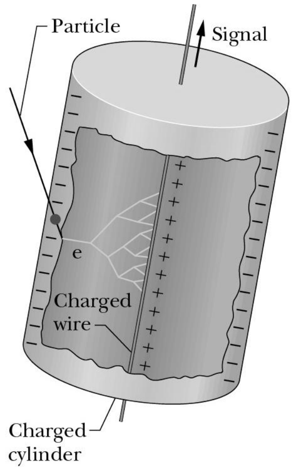

Figure 2.7: Geiger counter.

at the center of the void?
b. The piece is placed back into the void. Determine the electrical force exerted on the piece.
c. Using the strength of the force, calculate the electrostatic pressure that tends to expand the sphere.

2.2.4.22 Ex: Flow through a cone

An imaginary straight circular cone with base angle θ and base radius R is in a charge-free region exposed to a uniform electric field $\vec{\mathcal{E}}$ (the field lines are vertical to the cone axis). What is the ratio between the number of field lines per unit area entering the base and the number of lines per unit area entering the cone's conical surface. Use Gauß's law in your answer.

2.2.4.23 Ex: Flow of a field

Consider the rectangle with the corners,

$$\begin{pmatrix} x_i \\ y_i \\ z_i \end{pmatrix} = \begin{pmatrix} b \\ \frac{a}{\sqrt{2}} \\ 0 \end{pmatrix} , \begin{pmatrix} 0 \\ \frac{a}{\sqrt{2}} \\ 0 \end{pmatrix} , \begin{pmatrix} 0 \\ 0 \\ \frac{a}{\sqrt{2}} \end{pmatrix} , \begin{pmatrix} b \\ 0 \\ \frac{a}{\sqrt{2}} \end{pmatrix}$$

and calculate the flux integral of the field $\mathbf{A}(\mathbf{r})$ through the area $\mathbf{F}$ of the rectangle,

$$\mathbf{A}(\mathbf{r}) = \begin{pmatrix} y^2 \\ 2xy \\ 3z^2 - x^2 \end{pmatrix} .$$

2.2.4.24 Ex: Flow of a vector field

Calculate the flux of the vector field $\mathbf{A}(\mathbf{r})$ across the surface of a sphere of radius R around the origin of the coordinate system for
a.

$$\mathbf{A}(\mathbf{r}) = 3\frac{\mathbf{r}}{\mathbf{r}^2} \ .$$

b.

$$\mathbf{A}(\mathbf{r}) = \begin{pmatrix} 3z - 2y \\ x + 5z \\ y + x \end{pmatrix} \ .$$

2.2.4.25 Ex: Van de Graaff generator

The spherical shell (radius R) of a Van de Graaf generator must be charged until a potential difference of 10^6 V. What should be the minimum diameter of the sphere to avoid lightning discharge?
Help: The field for disruptive discharge in air is $3 \cdot 10^6$ V/m.

2.2.4.26 Ex: Van de Graaff accelerator

Protons are released from rest in a Van de Graaff accelerator system. The protons are initially located at a position where the electrical potential has a value of 5.0 MV, and then, they travel through vacuum to a region where the potential is zero.
a. Determine the final velocity of these electrons.
b. Determine the magnitude of the accelerating electric field if the potential changes uniformly over a distance of 2 m.

2.2.4.27 Ex: Faraday cage

Show that in a space confined by a grounded surface the electric field must disappear.

2.2.4.28 Ex: Waveguide

The figure shows a portion of the cross section of an infinitely long concentric cable. The inner conductor has a linear charge density of 6 nC/m and the outer conductor has no net charge.
a. Determine the electric field for all values of R, where R is the distance perpendicular to the common axis in the cylindrical system.
b. What are the surface charge densities on the surfaces inside and outside the outer conductor?

2.2.4.29 Ex: Fundamental equations of electrostatics

a. Gives the fundamental electrostatic equations in integral and differential form.
b. Gives the fundamental equation in terms of the electrostatic potential.

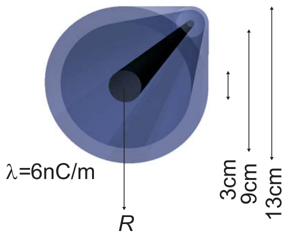

Figure 2.8: Waveguide.

2.3 The scalar electrical potential

We already noted that the electric field generates a force that can accelerate a charge Q along a field line. Therefore, the electric field contains a potential energy which it can convert into kinetic energy by exerting work, $W = \int \mathbf{F} \cdot \mathbf{r} = Q \int \vec{\mathcal{E}} \cdot \mathbf{r}$. The quantity [2],

$$\boxed{\Phi_{\mathbf{a},\mathbf{b}} \equiv \int_{\mathcal{C}_{\mathbf{a},\mathbf{b}}} \vec{\mathcal{E}} \cdot d\mathbf{r}} \tag{2.21}$$

is called the difference of *electric potential* between the points **a** and **b** connected by a path $\mathcal{C}_{\mathbf{a},\mathbf{b}}$.

Stokes' law (2.18) allows us to state, that the potential difference (2.21) does not depend on the path chosen, because for two different paths $\mathcal{C}$ and $\mathcal{C}'$ between the points **a** and **b** we have,

$$\int_{\mathcal{C}(\mathbf{a},\mathbf{b})} \vec{\mathcal{E}} \cdot d\mathbf{r} - \int_{\mathcal{C}'(\mathbf{a},\mathbf{b})} \vec{\mathcal{E}} \cdot d\mathbf{r} = 0 \; . \tag{2.22}$$

Consequently, the potential defined between a reference point $\mathcal{O}$ and any observation point **r** is unambiguous,

$$\Phi(\mathbf{r}) = -\int_{\mathcal{O}}^{\mathbf{r}} \vec{\mathcal{E}} \cdot d\mathbf{r} \; , \tag{2.23}$$

and the potential difference between two points **a** and **b** is well defined,

$$\Phi(\mathbf{b}) - \Phi(\mathbf{a}) = -\int_{\mathbf{a}}^{\mathbf{b}} \vec{\mathcal{E}} \cdot d\mathbf{r} \; . \tag{2.24}$$

The fundamental theorem for gradients, on the other hand, says that,

$$\Phi(\mathbf{b}) - \Phi(\mathbf{a}) = \int_{\mathbf{a}}^{\mathbf{b}} (\nabla\Phi) \cdot d\mathbf{r} \; . \tag{2.25}$$

These results being valid for any choice of points **a** and **b**, we conclude by comparing these two equations,

$$\boxed{\vec{\mathcal{E}} = -\nabla\Phi} \; . \tag{2.26}$$

[2] We note that the electric potential is linked to potential energy, but is not the same.

Example 17 (*Potential of a point charge*): For an electric field generated by an electric charge e located at the origin we can easily calculate the integral along a path $\mathcal{C}$ between two points a and b using Coulomb's law:

$$\int_{\mathcal{C}} \vec{\mathcal{E}} \cdot d\mathbf{r} = \int_{\mathbf{a}}^{\mathbf{b}} \frac{1}{4\pi\varepsilon_0} \frac{e}{|\mathbf{r}|^2} \hat{\mathbf{e}}_{\mathbf{r}} \cdot (\hat{\mathbf{e}}_{\mathbf{r}} dr + \hat{\mathbf{e}}_{\theta} r d\theta + \hat{\mathbf{e}}_{\phi} r \sin\theta d\phi)$$
$$= \frac{1}{4\pi\varepsilon_0} \int_{\mathbf{a}}^{\mathbf{b}} \frac{e}{r^2} dr = \frac{1}{4\pi\varepsilon_0} \left(\frac{e}{r_a} - \frac{e}{r_b} \right) .$$

With the superposition principle we can generalize this result for distributions of arbitrary charges Q.

Some comments are appropriate at this point:

- The formulation by the potential (a scalar field) instead of the vector electric field is more compact. It summarized the Coulomb (2.8) law along with the constraint (2.19).

- The reference point $\mathcal{O}$ is arbitrary. Exchanging this reference point by another $\mathcal{O}'$ only adds a global constant to the potential,

$$\Phi'(\mathbf{r}) = -\int_{\mathcal{O}'}^{\mathbf{r}} \vec{\mathcal{E}} \cdot d\mathbf{r} = -\int_{\mathcal{O}'}^{\mathcal{O}} \vec{\mathcal{E}} \cdot d\mathbf{r} - \int_{\mathcal{O}}^{\mathbf{r}} \vec{\mathcal{E}} \cdot d\mathbf{r} = K + \Phi(\mathbf{r}) , \tag{2.27}$$

  but does not affect neither the difference of two potentials,

$$\Phi'(\mathbf{b}) - \Phi'(\mathbf{a}) = \Phi(\mathbf{b}) - \Phi(\mathbf{a}) , \tag{2.28}$$

  nor the electric field,

$$\nabla\Phi' = \nabla\Phi . \tag{2.29}$$

  We conclude that the potential is not a real quantity, but a mathematical trick to simplify our life [3]. Generally, the reference point is placed at infinity, $\mathcal{O} = \infty$, fixing the free choice of the global constant by,

$$\Phi(\infty) \equiv 0 . \tag{2.30}$$

- In the same way as the electric field, the electric potential also obeys the superposition principle.

2.3.1 The equations of Laplace and Poisson

We already learned the two equations defining the electrostatic field (2.19) and (2.16), that is, $\nabla \times \vec{\mathcal{E}} = 0$ and $\nabla \cdot \vec{\mathcal{E}} = \varrho/\varepsilon_0$. Let us now rewrite these equations for the electric potential,

$$\nabla \times (\nabla\Phi) = 0 \quad , \quad \nabla \cdot \nabla\Phi = \Delta\Phi = -\varrho/\varepsilon_0 . \tag{2.31}$$

Thus, the formulation by the potential (2.21) automatically satisfies the requirement (2.22), that the rotation must disappear.

On the other side, we have a second-order differential equation called the *Poisson equation*. In regions with no charge, this equation turns into a *Laplace equation*,

$$\Delta\Phi = 0 . \tag{2.32}$$

[3] We shall see later that this conclusion must be reviewed in quantum mechanics in the context of the Aharonov-Bohm effect.

2.3.2 Potential generated by localized charge distributions

The Poisson equation allows us to reconstruct a charge distribution once its potential is known. However, we usually want to do the opposite. Let us start with a point charge, located at the origin, the potential of which is,

$$\Phi(\mathbf{r}) = -\int \vec{\mathcal{E}} \cdot d\mathbf{r}' = \frac{-1}{4\pi\varepsilon_0} \int \frac{Q}{r'^2} dr' = \frac{1}{4\pi\varepsilon_0} \frac{Q}{r'}\bigg|_\infty^{\mathbf{r}} = \frac{1}{4\pi\varepsilon_0} \frac{Q}{r} \ . \tag{2.33}$$

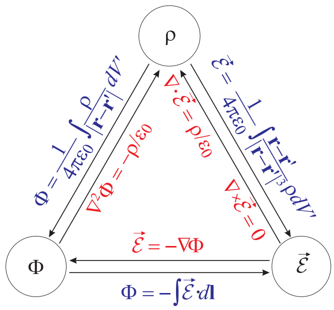

Figure 2.9: The fundamental laws of electrostatics relate the three fundamental quantities, the charge distribution ϱ, the electric field $\vec{\mathcal{E}}$, and the electric potential Φ.

According to the superposition principle, for a discrete distribution of charges Q_k located at the positions $\mathbf{r}_k$,

$$\Phi(\mathbf{r}) = \frac{1}{4\pi\varepsilon_0} \sum_k \frac{Q_k}{|\mathbf{r} - \mathbf{r}_k|} \ . \tag{2.34}$$

Finally, for a continuous distribution $\varrho(\mathbf{r}')$, we obtain the fundamental solution of the electrostatic problem,

$$\boxed{\Phi(\mathbf{r}) = \frac{1}{4\pi\varepsilon_0} \int \frac{dQ'}{|\mathbf{r} - \mathbf{r}'|} = \frac{1}{4\pi\varepsilon_0} \int \frac{\varrho(\mathbf{r}')}{|\mathbf{r} - \mathbf{r}'|} d^3r'} \ . \tag{2.35}$$

From this equation we can derive the Coulomb law (2.8).

Low-dimensional distributions can be treated by suitable parametrization, as in the examples (2.9) and (2.10).

2.3.3 Electrostatic boundary conditions

We have already noticed that the electric field always suffers a discontinuity when passing through a surface charge distribution. To study this, we consider a charged interface traversed by an external electric field $\vec{\mathcal{E}}_{ext}$. Now, we make two thought experiments: (1) We envision a rectangular pill box enclosing a small part of the interface, as shown in Fig. 2.10. The height ϵ of the box is so small that the flux through the sides of the box can be neglected. With this,

$$\oint \vec{\mathcal{E}} \cdot d\mathbf{S} = \tfrac{1}{\varepsilon_0} Q = \tfrac{1}{\varepsilon_0} \sigma S \ , \tag{2.36}$$

where $\vec{\mathcal{E}}$ is the total electric field (that is, the sum of the field generated by the surface charge and field $\vec{\mathcal{E}}_{ext}$). A is the surface of the box. This gives,

$$\mathcal{E}^{\perp}_{top} - \mathcal{E}^{\perp}_{bottom} = \frac{1}{\varepsilon_0}\sigma \; . \tag{2.37}$$

(2) We imagine a rectangular surface perpendicular to the interface and cutting through the interface. As shown in Fig. 2.10, the height ϵ of the surface is so small that the potential difference along the vertical branches can be neglected. With this,

$$\oint \vec{\mathcal{E}} \cdot d\mathbf{l} = \int \vec{\mathcal{E}}_{top} \cdot d\mathbf{l} + \int \vec{\mathcal{E}}_{bottom} \cdot d\mathbf{l} = (\vec{\mathcal{E}}_{top} - \vec{\mathcal{E}}_{bottom}) \cdot \mathbf{l} = 0 \; , \tag{2.38}$$

where l is the length of the surface. This gives,

$$\vec{\mathcal{E}}^{\parallel}_{top} = \vec{\mathcal{E}}^{\parallel}_{bottom} \; . \tag{2.39}$$

That is, when traversing a charged interface, only the part of the electric field which is perpendicular to the interface suffers a discontinuity. This simply reflects the fact that the charge generates its own electric field, which is perpendicular to the interface and superposes to the external field.

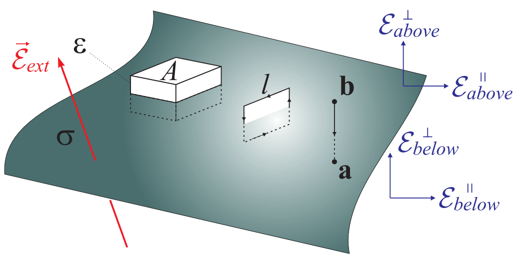

Figure 2.10: Surface S around a box-shaped volume enclosing a small part of the interface, path l around a small area cutting through the interface, and potential difference between two points **a** and **b**.

The potential, on the other hand, is continuous, since the integral between a point **a** above the interface and a point **b** below is,

$$\int_{\mathbf{b}}^{\mathbf{a}} \vec{\mathcal{E}} \cdot d\mathbf{l} = \Phi(\mathbf{b}) - \Phi(\mathbf{a}) \overset{\mathbf{a}\to\mathbf{b}}{\longrightarrow} 0 \; . \tag{2.40}$$

We study the electrostatic boundary conditions in Exc. 2.3.4.18.

2.3.4 Exercises

2.3.4.1 Ex: Earnshaw theorem

Show that the electrostatic potential in free space does not exhibit a maximum. **Comment:** This is why it is not possible to confine charged particles in electrostatic fields.

2.3.4.2 Ex: Electrical potential between point charges

A point particle with a charge equal to $+2\,\mu C$ is fixed at the origin.
a. hat is the electrical potential V at a point $4\,m$ from the origin, considering that $V = 0$ at infinity?
b. How much work must be done to bring a second point charge with a charge of $+3\,\mu C$ from infinity to a distance of $4.0\,m$ from the first charge?

2.3.4.3 Ex: Electrical potential between point charges

Three identical point particles with charge q are located at the corners of an equilateral triangle that is circumscribed in a circle of radius a contained in the plane $z = 0$ and centered at the origin. The values of q and a are $+3.0\,\mu C$ and $60\,cm$, respectively. (Consider that, far from all charges, the potential is zero.)
a. What is the electrical potential at the origin?
b. What is the electrical potential at the point of the z-axis being at $z = a$?
c. How would your responses to the parts (a) and (b) change if the charges q were larger? Explain your answer.

2.3.4.4 Ex: Electrical potential between point charges

Two identical positively charged point particles are fixed to the x-axis at $x = +a$ and $x = -a$.
a. Write down an expression for the electrical potential $V(x)$ as a function of x for all points on the x-axis.
b. Draw $V(x)$ versus x for all points on the x-axis.

2.3.4.5 Ex: Electrical potential between point charges

The electric field on the x-axis due to a fixed point charge at the origin is given by $\vec{\mathcal{E}} = (b/x^2)\hat{\mathbf{e}}_x$, where $b = 6.0\,kV \cdot m$ and $x \neq 0$.
a. Determine the amplitude and sign of the point charge.
b. Determine the potential difference between the points on the x-axis at $x = 1\,m$ and $x = 2\,m$. Which of these points is at a higher potential?

2.3.4.6 Ex: Dielectric disruption of air

Determine the maximum surface charge density σ_{max} that can exist on the surface of any conductor before dielectric discharge in the air occurs.

2.3.4.7 Ex: Potential energy of a charged sphere

a. How much charge is on the surface of an isolated spherical conductor that has a radius of $R = 10.0\,cm$ and is charged with $2.0\,kV$?
b. What is the electrostatic potential energy of this conductor? (Consider that the potential is zero far from the sphere.)

2.3.4.8 Ex: Energy of a particle in a potential

Four point charges are attached to the vertices of a square centered on the origin. The length of each side of the square is $2a$. The charges are located as follows: $+q$ is in $(-a, +a)$, $+2q$ is in $(+a, +a)$, $-3q$ is in $(+a, -a)$, and $+6q$ is in $(-a, -a)$. A fifth particle with mass m and charge $+q$ is placed at the origin and released from rest. Determine its velocity when it is far from the origin.

2.3.4.9 Ex: Energy of a particle in a potential

Two metallic spheres have radii of 10 cm each. The centers of the two spheres are separated by 50 cm. The spheres are initially neutral, but a charge Q is transferred from one sphere to another, creating a potential difference between them of 100 V. A proton is released from rest at the surface of the positively charged sphere and travels to the negatively charged sphere.
a. What is the kinetic energy once it reaches the negatively charged sphere?
b. At what velocity does it collide with the sphere?

2.3.4.10 Ex: Potential of connected spheres

A spherical conductor of radius R_1 is charged with $V_i = 20\,\text{kV}$. When it is connected through a very thin and long conductive wire to a second very distant spherical conductor, its potential drops to $V_f = 12\,\text{kV}$. What is the radius of the second sphere?

2.3.4.11 Ex: Potential of a charged disk

Along the central axis of a uniformly loaded disc, at a point 0.6 m away from the center of the disc, the potential is 80 V and the field intensity is 80 V/m. At a distance of 1.5 m, the potential is 40 V and the electric field strength is 23.5 V/m. (Consider that the potential is very far from the disk). Determine the total charge of the disk.

2.3.4.12 Ex: Potential of spherical shells

Two conductive concentric spherical shells have equal charges with opposite signs. The inner shell has an external radius a and the charge $+q$; the outer shell has an internal radius b and the charge $-q$. Determine the potential difference $V_a - V_b$ between the shells.

2.3.4.13 Ex: Electrical potential of a disk

A disk of radius R has a surface charge distribution given by $\sigma = \sigma_0 r^2/R^2$, where σ_0 is a constant and R is the distance from the center of the disk.
a. Determine the total charge on the disk.
b. Find the expression for the electrical potential at a distance z from the center of the disk along the axis that passes through the center of the disk and is perpendicular to its plane.

2.3.4.14 Ex: Electrical potential of a rod

A stick of length L has a total charge Q evenly distributed along its length. The stick is placed along the x-axis with its center at the origin.
a. What is the electrical potential as a function of the position along the x-axis for $x > L/2$?
b. Show that for $x \gg L/2$, your result reduces to that due to a point charge Q.

2.3.4.15 Ex: Potential of a thin disk

Calculate the electrical potential of a thin disc homogeneously charged with the charge Q along the symmetry axis.

2.3.4.16 Ex: Electrical potential of four wires

Consider four wires oriented parallel to the z-direction, as shown in the figure. The wires are charged with the charge per unit length q/L.
a. Calculate the electrical potential as a function of x and y.
b. Expand the potential around $x = 0$ and $y = 0$ ($|x|, |y| \ll a$) up to second order. What is the shape of the potential at this point?

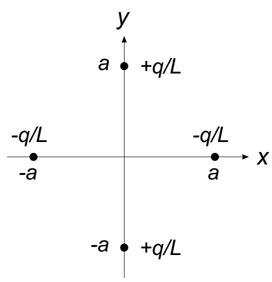

Figure 2.11: Four wires.

2.3.4.17 Ex: Stokes law

Consider a thin straight wire of infinite length uniformly charged with linear charge density λ.
a. Parametrize the linear load density using the δ-function.
b. Using Gauss' law, calculate the electric field.
c. Calculate the path integral $\int \vec{\mathcal{E}} \cdot d\mathbf{s}$ for the path parametrized by $\mathbf{s}(t) = \rho(\hat{\mathbf{e}}_x \cos t + \hat{\mathbf{e}}_y \sin t)$ with $t \in [0, 2\pi]$.
d. From the electric field obtained in (b) calculate $\nabla \times \vec{\mathcal{E}}$ in Cartesian or cylindrical coordinates.
Help: $\nabla \times \mathbf{S} = \hat{\mathbf{e}}_\rho \, \frac{1}{\rho} \left[\frac{\partial S_z}{\partial \phi} - \rho \frac{\partial S_\phi}{\partial z} \right] + \hat{\mathbf{e}}_\phi \, \left[\frac{\partial S_\rho}{\partial z} - \frac{\partial S_z}{\partial \rho} \right] + \hat{\mathbf{e}}_z \, \frac{1}{\rho} \left[\frac{\partial}{\partial \rho}(\rho S_\phi) - \frac{\partial S_\rho}{\partial \phi} \right]$.

2.3.4.18 Ex: Surface of a conductor

Consider an arbitrary macroscopic conductor whose surface is closed and smooth. Starting from Gauss's law and the electrostatic rotation of the electric field:
a. calculate the electric field inside the conductor;
b. obtain the normal component of the electric field on the outer surface of the conductor in terms of the surface charge density;
c. obtain the tangential component of the electric field on the outer surface of the conductor.

2.4 Electrostatic energy

We calculate the work required to move a test charge q between two points $\mathbf{a}$ and $\mathbf{b}$ within the potential created by a charge distribution,

$$W = -\int_{\mathbf{a}}^{\mathbf{b}} \mathbf{F} \cdot d\mathbf{r} = -q \int_{\mathbf{a}}^{\mathbf{b}} \vec{\mathcal{E}} \cdot d\mathbf{r} = q[\Phi(\mathbf{b}) - \Phi(\mathbf{a})] \ . \tag{2.41}$$

Since the work does not depend on the path, we call the potential *conservative*. Taking the test charge from the reference point to infinity,

$$W = q[\Phi(\mathbf{b}) - \Phi(\infty)] = q\Phi(\mathbf{b}) \ . \tag{2.42}$$

In this sense, the potential is nothing more than the energy per unit of charge q required to take a particle from infinity to a point $\mathbf{r}$.

2.4.1 Energy of a charge distribution

The next question is, what energy is needed to put together a distribution of charges taking them one by one from infinity to predefined points. Every charge Q_k uses an amount of work W_k, only the first charge does not, $W_1 = 0$. Using the abbreviation,

$$W_{k,m} \equiv \frac{1}{4\pi\varepsilon_0} \frac{Q_k Q_m}{|\mathbf{r}_k - \mathbf{r}_m|} \ , \tag{2.43}$$

the work is easily calculated for the second charge, $W_2 = W_{1,2}$. For the third and fourth charge we need *additionally* the amounts of work,

$$W_3 = W_{1,3} + W_{2,3} \qquad \text{and} \qquad W_4 = W_{1,4} + W_{2,4} + W_{3,4} \ . \tag{2.44}$$

The general rule is obvious: For N charges we need in *total* to provide the work,

$$W = \sum_{k=1}^{N} W_k = \sum_{k=1}^{N} \sum_{\substack{m=1 \\ m<k}}^{N} W_{k,m} = \frac{1}{2} \sum_{k=1}^{N} \sum_{\substack{m=1 \\ m\neq k}}^{N} W_{k,m} \ . \tag{2.45}$$

Explicitly, calling Φ the potential created by all charges minus the charge Q_k,

$$\Phi(\mathbf{r}_k) \equiv \sum_{\substack{m=1 \\ m\neq k}}^{N} \frac{1}{4\pi\varepsilon_0} \frac{Q_m}{|\mathbf{r}_k - \mathbf{r}_m|} \ , \tag{2.46}$$

we can write the energy as,

$$W = \tfrac{1}{2}\sum_k Q_k\Phi(\mathbf{r}_k) \ . \tag{2.47}$$

For continuous distributions, this equation turns into,

$$W = \tfrac{1}{2}\int \Phi dQ = \tfrac{1}{2}\int \varrho\Phi dV \ . \tag{2.48}$$

2.4.2 Energy density of an electrostatic field

The energy of a continuous charge distribution can be rewritten using Gauß' law,

$$W = \tfrac{\varepsilon_0}{2}\int (\nabla\cdot\vec{\mathcal{E}})\Phi dV \ . \tag{2.49}$$

Integration by parts allows transferring the derivative of $\vec{\mathcal{E}}$ to Φ,

$$W = \tfrac{\varepsilon_0}{2}\left[\oint_{\partial\mathcal{V}} \Phi\vec{\mathcal{E}}\cdot d\mathbf{S} - \int_{\mathcal{V}} \vec{\mathcal{E}}\cdot(\nabla\Phi)dV\right] \ . \tag{2.50}$$

The surface integral can be neglected, because we can choose the integration volume arbitrarily large $\mathcal{V}$. Expressing the gradient by the field,

$$W = \tfrac{\varepsilon_0}{2}\int_{\mathcal{V}} \vec{\mathcal{E}}^2 dV = \tfrac{\varepsilon_0}{2}\int_{\mathcal{V}} u dV \ , \tag{2.51}$$

introducing the *energy density*,

$$\boxed{u \equiv \tfrac{\varepsilon_0}{2}\vec{\mathcal{E}}^2} \ . \tag{2.52}$$

Example 18 (*Electrostatic energy of a charged spherical layer*): As an example we calculate the electrostatic energy of a spherical shell of radius R uniformly charged with the total charge Q. Using the formula (2.48) we obtain,

$$W = \frac{1}{2}\int \varrho\Phi dV = \frac{1}{2}\int \frac{Q}{4\pi R^2}\delta(r-R)\Phi R^2\sin\theta d\theta d\phi dr = \frac{Q}{2}\Phi(R) = \frac{Q}{2}\frac{1}{4\pi\varepsilon_0}\frac{Q}{R} = \frac{Q^2}{8\pi\varepsilon_0}\frac{1}{R} \ .$$

Alternatively, we calculate by the formula (2.51),

$$W = \frac{\varepsilon_0}{2}\int_{\mathbb{R}^3}\vec{\mathcal{E}}^2 dV = \frac{\varepsilon_0}{2}\int_{r\geq R}\left(\frac{1}{4\pi\varepsilon_0}\frac{Q}{R^2}\right)^2 R^2\sin\theta d\theta d\phi dr = \frac{Q^2}{8\pi\varepsilon_0}\int_R^\infty \frac{1}{R^2}dr = \frac{Q^2}{8\pi\varepsilon_0}\frac{1}{R} \ .$$

1. Comparing the expressions for the electrostatic energy (2.47) and (2.51) [4] we perceive an inconsistency, since the second only allows positive energies, while the former allows positive and negative energies, for example, in the case of two charges with opposed signs aiming to attract each other.

   In fact, both equations are correct, but they describe slightly different situations. Equation (2.47) does not take into account of the work necessary to create these

[4] Or equivalently (2.48), which also can not be negative.

elementary point charges in the first place. In fact, equation (2.51) indicates that the energy of a point charge diverges,

$$W = \frac{\varepsilon_0}{2}\frac{1}{(4\pi\varepsilon_0)^2}\int_{\mathbb{R}^3}\left(\frac{e}{r^2}\right)^2 r^2\sin\theta drd\theta d\phi = \frac{e^2}{8\pi\varepsilon_0}\int_0^\infty \frac{1}{r^2}r^2\sin\theta drd\theta d\phi \to \infty \ .$$

The equation (2.51) is more complete in the sense that it gives the total energy stored in the charge configuration, but the (2.47) is more appropriate when working with point charges, because we then prefer to ignore the part needed for the construction of the electrons. Anyway, we do not know how to create or dismount electrons.

The inconsistency enters the derivation, when we make the transition between the Eqs. (2.47) and (2.48). In the first equation, $\Phi(\mathbf{r}_i)$ represents the potential due to all the other charges except q_i, while in the second $\Phi(\mathbf{r})$ is the total potential. For continuous distributions there is no difference, since the amount of charge at any mathematical point $\mathbf{r}$ is negligible, and its contribution to the potential is zero.

In practice, the divergence does not appear because, when we use Eq. (2.51), generally we consider smooth distributions of charges and not point-like charges.

2. The energy is stored in the entire electrostatic field, that is, we need to integrate over the entire space $\mathbb{R}^3$.

3. The superposition principle is not valid for electrostatic energy, since it is quadratic in the fields, $\int(\vec{\mathcal{E}}_1+\vec{\mathcal{E}}_2)^2dV \neq \int(\vec{\mathcal{E}}_1^2+\vec{\mathcal{E}}_2^2)dV$.

2.4.3 Dielectrics and conductors

In an *insulating* material, such as rubber or glass, all electrons are attached to individual atoms. They can be displaced inside the atom by an external electric field, which creates a polarization of the atom. But they do not move away from the atom. In contrast, in a *conducting* material, such that a metal, one or more electrons per atom can move freely.

What are the characteristics of an ideal conductor?

1. $\vec{\mathcal{E}} = 0$ **inside a conductor.** The electric field inside a conductor must vanish, otherwise there would be forces on the charges working to rearrange them until the forces (and the motion of charges) compensate. In the presence of an external electric field, the charges arrange themselves in such a way as to generate their own field designed to compensate the external field.

2. $\varrho = 0$ **inside a conductor.** Since there is no electric field, Gauß' law prevents residual charges in the interior, since $\varrho = \nabla\cdot\vec{\mathcal{E}}/\varepsilon_0$.

3. **All residual charge is on the surface,** simply because it can not be inside.

4. **Conductor as an equipotential.** As there is no electric field, Stokes' law prevents different potentials because $\Phi(\mathbf{b})-\Phi(\mathbf{a}) = -\int_{\mathbf{a}}^{\mathbf{b}}\vec{\mathcal{E}}\cdot d\mathbf{r} = 0$.

5. $\vec{\mathcal{E}}$ **is perpendicular to the surface near the surface.** Otherwise, the electric field components parallel to the surface would create forces to rearrange the residual charges until the parallel components disappear. Consequently, electric field lines always meet a conductor orthogonally to the surface $\vec{\mathcal{E}} \perp \partial V$.

2.4.4 Induction of charges (influence)

When we place a charge in front of a neutral conductor we measure an attraction force. The reason is that free charges of the conductor with opposite sign are attracted, while charges with the same sign are repelled [5]. Now, since the charges with opposite sign are closer to the charge in front than those with the same sign, the attractive force will dominate the repulsive force (see Fig. 2.12 left).

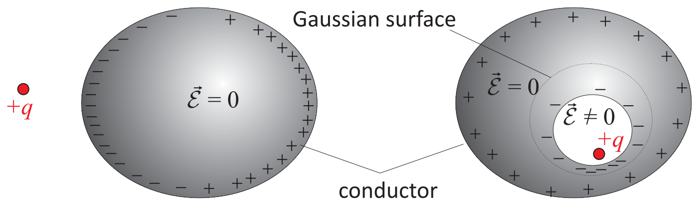

Figure 2.12: Electrostatic induction.

The electric field inside a conductor must vanish, but this only holds for the conductor's bulk material and not necessarily for dielectric impurities or cavities enclosed by the conductor. For example, in the case where there is a charge $+q$ inside a enclosed cavity [see Fig. 2.12(right)], the electric field inside the cavity is clearly nonzero. However, since it must vanish within the conductor, Gauß' law requires that within a volume enclosed by a Gaussian surface, the total charge must be zero. Choosing this Gaussian surface very close to the cavity, we find that a surface charge must have formed at the edges of the cavity, compensating for the charge $+q$ inside the cavity. This charge can only come from the outer surface, which is now charged with the opposite charge, as well. In this way *the charge $+q$ becomes visible from the outside of the conductor.*

The electric field inside a cavity without charges enclosed by a conductor must be zero, because without charges, the field lines could only traverse the cavity. However, the entrance and exit points between the cavity and the conductor are on the same potential, and have no surface charge. This is the principle of *Faraday's cage*, where people inside a conductive cage are shielded and thus protected from electrical phenomena like lightning discharges.

The migration of free excess charges in conductors to the surface is also called *skin effect*: The potential inside the metal the same everywhere, and the electric field disappears $\vec{\mathcal{E}} = 0$.

Example 19 (*Conductors with enclosed cavities*): Two cavities with radii a and b are excavated from a neutral conducting sphere of radius R. In the center of each cavity there be charges, q_a and q_b, respectively.

[5] That is, the charges in the conductor rearrange to compensate for the electric field created by the charge in front until the total field inside the conductor has vanished.

- The charges on the surfaces of the cavities σ_a and σ_b must be organized such as to shield the charges $q_{a,b}$ in order to prevent the formation of an electric field inside the conductor. If the charges are at the centers of the spheres we simply obtain, $\sigma_a = \frac{q_a}{4\pi a^2}$ and $\sigma_b = \frac{q_b}{4\pi b^2}$. The charges used for shielding are missing from the conductor and must be compensated for by charges of opposite sign. The only place where these opposite charges can accumulate is the outer surface of the conductor. Thus, we have the surface charge $\sigma_R = \frac{-q_a - q_b}{4\pi R^2}$.
- The field outside the driver is consequently, $\vec{\mathcal{E}} = \frac{q_a+q_b}{4\pi\varepsilon_0}\frac{\mathbf{r}}{r^3}$, where $\mathbf{r}$ is the point of observation with respect to the center of the conductor.
- Inside each cavity the electric field is determined by Gauß' law, $\vec{\mathcal{E}} = \frac{q_{a,b}}{4\pi\varepsilon_0}\frac{r}{r^3}$, where $\mathbf{r}$ is the observation point respect to the center of the cavity. Note that the surface charge $\sigma_{a,b}$ does not influence the field.
- Since the charges $q_{a,b}$ do not feel external fields, they are not subject to forces.
- Putting a third charge q_c near the conductor, the charge distribution σ_R would change in order to compensate the field within the conductor. Thus, the other quantities determined in (a)-(d) would not change. *The conductor effectively decouples all processes occurring on disconnected surfaces.*

2.4.5 Electrostatic pressure

What is the force exerted by an applied electric field $\vec{\mathcal{E}}_{ext}$ on a charged conductive surface? We know that the surface charge causes a discontinuity of the electric field, so that we need to calculate the force on a surface element dS as the average of the forces acting from above and from below,

$$d\mathbf{F} = dS\frac{\sigma}{2}(\vec{\mathcal{E}}_{top} + \vec{\mathcal{E}}_{bottom}) = \vec{\mathcal{P}}dS \ , \tag{2.53}$$

where $\vec{\mathcal{P}}$ is the *electrostatic pressure* (see Fig. 2.13).

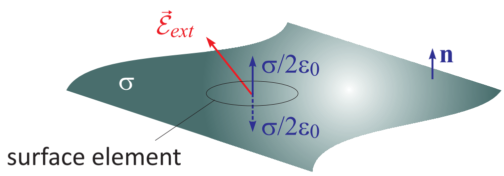

Figure 2.13: Electrostatic pressure exerted by a field $\vec{\mathcal{E}}_{ext}$ on a charged surface element.

In the case of a thin surface, we have,

$$\vec{\mathcal{E}}_{top} = \vec{\mathcal{E}}_{ext} + \frac{\sigma}{2\varepsilon_0}\hat{\mathbf{n}} \quad , \quad \vec{\mathcal{E}}_{bottom} = \vec{\mathcal{E}}_{ext} - \frac{\sigma}{2\varepsilon_0}\hat{\mathbf{n}} \ , \tag{2.54}$$

such that the pressure is,

$$\vec{\mathcal{P}} = \sigma\vec{\mathcal{E}}_{ext} \ . \tag{2.55}$$

In the case of a charged surface of a massive conductor without external field,

$$\vec{\mathcal{E}}_{outside} = \frac{\sigma}{\varepsilon_0}\hat{\mathbf{n}} \quad , \quad \vec{\mathcal{E}}_{inside} = 0 \ , \tag{2.56}$$

such that the pressure is,

$$\vec{\mathcal{P}} = \frac{\sigma}{2}\frac{\sigma}{2\varepsilon_0}\hat{\mathbf{n}} = \frac{\varepsilon_0}{2}\mathcal{E}^2_{outside}\hat{\mathbf{n}} \ . \tag{2.57}$$

That is, even without external field a charged conductor suffers a force trying to push it into the field created by itself, regardless of the sign of the charge. It is interesting to note that this force goes with the square of σ and of $\vec{\mathcal{E}}_{outside}$.

2.4.6 Exercises

2.4.6.1 Ex: Motion of two charges

Two particles with masses m_1 and m_2 and charges $Q_1 > 0$ and $Q_2 > 0$ are placed at a mutual distance d_0 and can move freely in space.
a. What will happen to the particles qualitatively? Which relation holds at all times for the velocities v_1 and v_2 of the two particles?
b. Calculate the velocities of the two particles as a function of their distance and plot the functions $v_1(d)$, respectively $v_2(d)$ (phase space diagrams). What are the velocities reached in the limit $d \to \infty$?

2.4.6.2 Ex: Paul trap

We consider four parallel wires oriented along the z-direction and forming a quadrupolar configuration in the xy-plane, as shown in the figure. The wires are charged with $\pm q$ per unit of length l. Calculate the electrical potential as a function of x and y in the center between the wires and expand around $x = 0$ and $y = 0$ ($|x|, |y| \ll a$) up to second order. What is the shape of the potential at this position? Do you think it is possible to trap a charged particle in this potential?

2.4.6.3 Ex: Energy of the electron

Supposing that the charge is homogeneously distributed over a sphere, calculate the *classical electron radius*.

2.4.6.4 Ex: Radius of the electron

a. Try to calculate the electrostatic energy of the field of an electron via,

$$E_F = \int_{\mathbb{R}^3} \frac{\varepsilon_0}{2}\vec{\mathcal{E}}^2(\mathbf{r})\ d^3r$$

What problem appears in the calculation of the radial part of the integral $\int dr$, if the lower limit of integration goes to $r_0 \to 0$?
b. This problem is known as *self-energy divergence*. It is possible to work around this problem, leaving the limits out and choosing the classic electron radius r_0 as the integration limit. The energy E_F of the electric field is then identified with half the energy $E = \frac{1}{2}m_ec^2$ of the electron rest mass m_e. Calculate the classic electron radius!

2.4.6.5 Ex: Electrostatic energy

a. Write the potential energy of a charge q in an external field $\vec{\mathcal{E}} = -\vec{\nabla}\Phi$?
b. What is the value of the electrostatic energy of N point charges?
c. What is the value of the energy of a charge distribution in the electric field $\vec{\mathcal{E}}(\mathbf{r})$?
d. What are the boundary conditions for the $\vec{\mathcal{E}}$-field on a conductor's surface?
e. Draw the electric field of a point charge q located in front of a metallic plane. What is the induced charge? What is the value of the force on the charge q?

2.4.6.6 Ex: Electrostatic energy

What is the electrostatic energy of
a. four equal charges Q located at the corners of a tetrahedron with the edge length d?
b. a dielectric sphere with radius R homogeneously charged with the charge Q? To do this, calculate the electric field inside and outside the sphere using Gauß' law.

2.4.6.7 Ex: Electrostatic energy

a. Eight point charges q are placed in the corners of a cube with the edge length l. Calculate the electrostatic energy of this configuration.
b. A balloon with radius R is charged homogeneously with the charge Q. What is the value of electrostatic energy? What is the force required to inflate the balloon even more, neglecting the elastic force of the balloon?

2.4.6.8 Ex: Charge separation

Two conducting neutral spheres are in contact and attached to insulating rods on a large wooden table. A positively charged stick is brought close to the surface of one of the spheres on the side opposite the point of contact with the other sphere.
a. Describe the charges induced in the two conductive spheres and discuss the charge distribution in both.
b. The two spheres are separated and then the charged stick is taken away. Then, the spheres are separated by a great distance. Discuss the charge distributions on the spheres after they are separated.

2.5 Treatment of boundary conditions and the uniqueness theorem

In practice, the solution of an electrostatic problem, that is, the resolution of the Poisson equation, can be hampered by boundary conditions. For example, charges in front of conducting surfaces induce a redistribution of charges in the conductor which modifies the electric field. The field is unequivocally determined by the charge and the boundary conditions. In this section we will discuss the method of image charges, which is a heuristic model, and the mathematical treatment of boundary conditions.

2.5.1 The method of images charges

One way to simulate boundary conditions is to 'invent' imaginary charges and distribute them in a way that the total field automatically satisfies these boundary conditions. This is usually only helpful when the boundary conditions exhibit a high degree of symmetry. This is the method of the so-called *image charges*.

The simplest case is that of the point charge Q at a distance d in front of a conductive and grounded plane. By induction the charge will cause a redistribution of charges on the surface of the conductor in such a way, that the field lines cross the surface of the conductor at right angles. But the same boundary conditions can be satisfied by replacing the conductive plane with a second imaginary charge with opposite sign at the position of the image of the first charge regarding the plane as a mirror. From the point of view of the electric field the two configurations are equivalent, but the field is much easier to calculate for a charge and its image using Coulomb's law. See Excs. 2.5.6.1, 2.5.6.2, 2.5.6.3, 2.5.6.4, and 2.5.6.5.

Example 20 (*Induced surface charge*): In the case of the point charge in front of a conducting plane, which is the simplest case imaginable, the boundary conditions are,

$$\Phi(x,y,0) = 0 \quad , \quad \Phi(|\mathbf{r}| \gg d) = 0 \ ,$$

the potential is,

$$\Phi(\mathbf{r}) = \frac{1}{4\pi\varepsilon_0}\left(\frac{Q}{\sqrt{x^2+y^2+(z-d)^2}} + \frac{-Q}{\sqrt{x^2+y^2+(z+d)^2}}\right) \ ,$$

and the field is,

$$\vec{\mathcal{E}} = -\nabla\Phi = \frac{-Q}{4\pi\varepsilon_0}\left(\frac{-1}{\sqrt{x^2+y^2+(z-d)^2}^3}(\hat{\mathbf{e}}_z - \mathbf{r}) + \frac{1}{\sqrt{x^2+y^2+(z+d)^2}^3}(\hat{\mathbf{e}}_z + \mathbf{r})\right) \ .$$

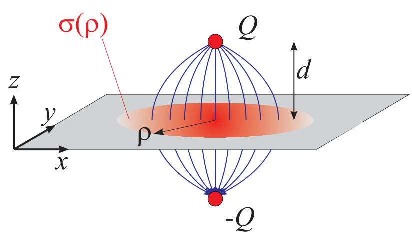

Figure 2.14: Point charge in front of a conductive plane.

We can now calculate the charge distribution on the surface. Gauß' law says,

$$\int_{box} \vec{\mathcal{E}} \cdot d\mathbf{S} = \frac{Q}{\varepsilon_0} = \frac{1}{\varepsilon_0}\int \varrho(\mathbf{r})dV = \frac{1}{\varepsilon_0}\int \sigma(x,y)\delta(z)dV = \frac{1}{\varepsilon_0}\int \sigma(x,y)dA \ .$$

Therefore, on the surface,

$$\hat{\mathbf{e}}_z \cdot \vec{\mathcal{E}}(x,y,z=0) = \frac{\sigma(x,y)}{\varepsilon_0} \ .$$

Resolving by the charge density,

$$\sigma(x,y) = \varepsilon_0 \hat{\mathbf{e}}_z \cdot \vec{\mathcal{E}}(x,y,z=0) = \frac{-Q}{4\pi} \frac{2}{\sqrt{x^2+y^2+d^2}^3} .$$

Also, we can verify that the total surface charge is, $Q_s = -Q$.

2.5.2 Formal solution of the electrostatic problem

The solution of the Laplace equation will, in general, depend on boundary conditions imposed by the geometry of the system. For example, a charge in free space will generate another field than a charge above a conductive surface. The two most common boundary conditions are named after *Dirichlet* and *von Neumann*. The Dirichlet condition fixes the value of the potential on a geometry of surfaces enclosing a volume, $\Phi|_{\partial\mathcal{V}} = \Phi_0$, while the von Neumann condition fixes the value of the potential gradient, $\nabla\Phi|_{\partial\mathcal{V}} = \vec{\mathcal{E}}_0$. Let us discuss these conditions in the following.

Using the following four relationships,

$$\begin{aligned} &\text{(i)} \quad \nabla^2 \tfrac{1}{4\pi|\mathbf{r}-\mathbf{r}'|} = -\delta(\mathbf{r}-\mathbf{r}') \\ &\text{(ii)} \quad \nabla\cdot(\phi\mathbf{F}) = \phi(\nabla\cdot\mathbf{F}) + (\nabla\phi)\cdot\mathbf{F} \\ &\text{(iii)} \quad \int_{\mathcal{V}} \nabla\cdot\mathbf{F}dV' = \int_{\partial V} \mathbf{F}\cdot d\mathbf{S}' \\ &\text{(iv)} \quad \nabla^2\Phi = -\tfrac{\varrho}{\varepsilon_0} , \end{aligned} \tag{2.58}$$

we now solve the Poisson equation,

$$\Phi(\mathbf{r}) = \int_{\mathcal{V}} \Phi(\mathbf{r}')\delta(\mathbf{r}-\mathbf{r}')dV' = \tfrac{-1}{4\pi}\int_{\mathcal{V}} \underbrace{\Phi(\mathbf{r}')}_{\phi}\nabla\cdot\underbrace{\left(\nabla\tfrac{1}{|\mathbf{r}-\mathbf{r}'|}\right)}_{\mathbf{F}}dV' \qquad \text{with (i)} \tag{2.59}$$

$$= \tfrac{1}{4\pi}\int_{\mathcal{V}} \underbrace{\nabla\Phi(\mathbf{r}')}_{\mathbf{F}}\cdot\underbrace{\nabla\tfrac{1}{|\mathbf{r}-\mathbf{r}'|}}_{\phi}dV' - \tfrac{1}{4\pi}\int_{\mathcal{V}} \nabla\cdot\left(\Phi(\mathbf{r}')\nabla\tfrac{1}{|\mathbf{r}-\mathbf{r}'|}\right)dV' \qquad \text{with (ii)}$$

$$= -\tfrac{1}{4\pi}\int_{\mathcal{V}} \tfrac{1}{|\mathbf{r}-\mathbf{r}'|}\nabla\cdot\nabla\Phi(\mathbf{r}')dV' + \tfrac{1}{4\pi}\int_{\mathcal{V}} \nabla\cdot\left(\tfrac{1}{|\mathbf{r}-\mathbf{r}'|}\nabla\Phi(\mathbf{r}')\right)dV' - \tfrac{1}{4\pi}\int_{\mathcal{V}} \nabla\cdot\left(\Phi(\mathbf{r}')\nabla\tfrac{1}{|\mathbf{r}-\mathbf{r}'|}\right)dV' .$$

Finally, using relations (iii and iv), we obtain the final result,

$$\boxed{\Phi(\mathbf{r}) = \tfrac{1}{4\pi\varepsilon_0}\int_{\mathcal{V}} \tfrac{\varrho(\mathbf{r}')}{|\mathbf{r}-\mathbf{r}'|}dV' + \tfrac{1}{4\pi}\oint_{\partial\mathcal{V}} \left(\Phi(\mathbf{r}')\nabla'\tfrac{1}{|\mathbf{r}-\mathbf{r}'|} - \tfrac{1}{|\mathbf{r}-\mathbf{r}'|}\nabla'\Phi(\mathbf{r}')\right)\cdot d\mathbf{S}'} , \tag{2.60}$$

which is an integral version of the Poisson equation. For volumes going to infinity, where the potential disappears, the surface integrals can be neglected, and we get the familiar form of Coulomb's law. For finite volumes, boundary conditions on surfaces can dramatically influence the potential.

Example 21 (*Consistency of Green's relationship*): Obviously, by imposing boundary conditions that coincide with equipotential surfaces of the field created by the charge distribution, the surface terms vanish. Choosing as an example a point charge placed at the origin, $\varrho(\mathbf{r}') = Q\delta^3(\mathbf{r}')$, and inserting its potential,

$$\Phi(\mathbf{r} = R\hat{\mathbf{e}}_r) = \frac{Q}{4\pi\varepsilon_0}\frac{1}{R} = \frac{Q}{4\pi\varepsilon_0}\left.\frac{1}{|\mathbf{r} - \mathbf{r}'|}\right|_{\mathbf{r}\in\partial\mathcal{V}} . \tag{2.61}$$

in the relationship (2.60), we find that the surface integrals cancel out.

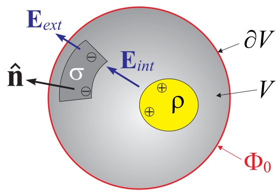

Figure 2.15: Illustration of boundary conditions.

The surface term can be interpreted in terms of a surface charge density, because we know that the normal electric field is discontinuous when crossing a charged surface [6]:

$$\frac{\sigma(\mathbf{r}')}{\varepsilon_0} = -\nabla'\Phi(\mathbf{r}')\cdot\hat{\mathbf{n}} . \tag{2.62}$$

We consider the example of a charge distribution, $\varrho(\mathbf{r}')$, surrounded by a surface on which the potential is zero, $\Phi(\mathbf{r}')|_{\partial\mathcal{V}'} = 0$, such that the first surface term of the relation (2.60) fades away. Inserting the expression (2.62) in the second surface term, the relation becomes,

$$\Phi(\mathbf{r}) = \frac{1}{4\pi\varepsilon_0}\int_{\mathcal{V}}\frac{\varrho(\mathbf{r}')}{|\mathbf{r} - \mathbf{a}|} + \frac{1}{4\pi\varepsilon_0}\oint_{\partial\mathcal{V}}\frac{\sigma(\mathbf{r}')}{|\mathbf{r} - \mathbf{r}'|}dS' . \tag{2.63}$$

The interpretation of this modified Coulomb law is, that the charge induces a density distribution of surface charges σ within the conducting plane which modifies the electric potential, such that the boundary condition is satisfied.

2.5.3 Green's Function

The function $\frac{1}{4\pi|\mathbf{r}-\mathbf{r}'|}$ not the only one to satisfy the condition (2.58)(i). In fact, there is an entire class of functions called Green functions defined by,

$$\nabla^2 G(\mathbf{r}, \mathbf{r}') \equiv -\delta(\mathbf{r} - \mathbf{r}') . \tag{2.64}$$

[6] We can derive this considering a thin disk located within the x-y plane and homogeneously charged with the charge density σ_0,

$$\Phi(z\hat{\mathbf{e}}_z) = \frac{1}{4\pi\varepsilon_0}\int_{disco}\frac{\sigma(\mathbf{r}')}{|z\hat{\mathbf{e}}_z - \mathbf{r}'|}dA' = \frac{\sigma_0}{2\varepsilon_0}\int_0^R\frac{1}{\sqrt{r'^2 + z^2}}r'dr' = \frac{\sigma_0}{2\varepsilon_0}[\sqrt{R^2 + z^2} - z] ,$$

and therefore,

$$E_z = -\frac{d\Phi(z\hat{\mathbf{e}}_z)}{dz} = -\frac{\sigma_0}{2\varepsilon_0}\left(\frac{z}{\sqrt{R^2 + z^2}} - 1\right) \stackrel{z\ll R}{\longrightarrow} \frac{\sigma_0}{2\varepsilon_0} .$$

Obviously, for these functions the formula derived in (2.59) will be generalized,

$$\boxed{\Phi(\mathbf{r}) = \frac{1}{\varepsilon_0}\int_{\mathcal{V}} \varrho(\mathbf{r}')G(\mathbf{r},\mathbf{r}')dV' + \oint_{\partial\mathcal{V}} (\Phi(\mathbf{r}')\nabla G(\mathbf{r},\mathbf{r}') - G(\mathbf{r},\mathbf{r}')\nabla\Phi(\mathbf{r}')) \cdot d\mathbf{S}'} \; . \tag{2.65}$$

The advantage of the Green function is, that we have the freedom to add any function F,

$$G(\mathbf{r},\mathbf{r}') = \frac{1}{4\pi|\mathbf{r}-\mathbf{r}'|} + F(\mathbf{r},\mathbf{r}') \tag{2.66}$$

satisfying the Laplace equation,

$$\nabla^2 F(\mathbf{r},\mathbf{r}') = 0 \; , \tag{2.67}$$

and the Green function (2.66) will still satisfy the definition (2.64). In particular, we can choose the function F in a way to eliminate one of the two surface integrals in Eq. (2.65) and to obtain an expression only involving Dirichlet's or von Neumann's boundary conditions.

2.5.4 Poisson equation with Dirichlet's boundary conditions

The first *uniqueness theorem* proclaims,

> *The solution of the Poisson (or Laplace) equation in a volume $\mathcal{V}$ is uniquely determined, if Φ is specified on the surface of the volume $\partial\mathcal{V}$.*

To prove this theorem, let us specify that the potential adopts the (not necessarily constant) value Φ_0 on the surface and consider two possible solutions of the Laplace equation, Φ_1 and Φ_2. The difference $\Phi_3 \equiv \Phi_1 - \Phi_2$ disappears on the surface, $\Phi_3|_{\partial\mathcal{V}} = 0$, and must also satisfy the Laplace equation: $\nabla^2\Phi_3 = 0$. Now, since the Laplace equation does not allow local maxima or minima [7], Φ_3 must be zero throughout space (see Fig. 2.16 left).

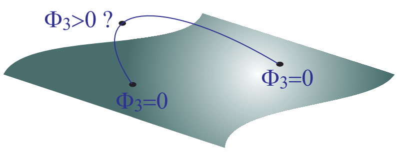

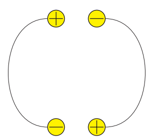

Figure 2.16: Illustration of the uniqueness theorems.

We consider as an example a finite volume V without charges, $\varrho = 0$, surrounded by a conducting border ∂V maintained at a fixed potential, $\Phi(\mathbf{r} \in \partial\mathcal{V}) = \Phi_0 = const.$ This is a typical situation realized, for example, in conductive materials such as metals. Therefore, $\Delta\Phi = 0$ within the volume. A possible trivial solution of the Laplace equation is, $\Phi(\mathbf{r}) = \Phi_0$. The uniqueness theorem now tells us that this is the *unique* solution.

To implement this theorem we choose the following boundary conditions,

$$G_D(\mathbf{r},\mathbf{r}'_{\in\partial\mathcal{V}}) = 0 \; , \tag{2.68}$$

[7] For in a hypothetical maximum (minimum) we would have $\nabla^2\Phi_3 < 0$ (> 0).

such that the relationship (2.64) becomes,

$$\boxed{\Phi(\mathbf{r}) = \frac{1}{\varepsilon_0}\int_{\mathcal{V}} \varrho(\mathbf{r}')G_D(\mathbf{r},\mathbf{r}')dV' + \oint_{\partial\mathcal{V}} \Phi(\mathbf{r}')\nabla' G_D(\mathbf{r},\mathbf{r}')\cdot d\mathbf{S}'} \ . \tag{2.69}$$

Do the Excs. 2.5.6.7, 2.5.6.8, 2.5.6.9, and 2.5.6.10.

2.5.5 Poisson equation with von Neumann's boundary conditions

The second uniqueness theorem proclaims,

> *In a volume $\mathcal{V}$ surrounded by conductors and containing a specified charge density ϱ, the electric field is uniquely determined by the total charge of each conductor.*

To prove this theorem, we will consider a sample of conductors i each one carrying the charge Q_i. Assuming that there are two solutions for the electric field between the conductors, $\vec{\mathcal{E}}_1$ and $\vec{\mathcal{E}}_2$, each of these fields must satisfy, $\nabla\cdot\vec{\mathcal{E}}_1 = \nabla\cdot\vec{\mathcal{E}}_2 = Q_i$. The difference $\vec{\mathcal{E}}_3 \equiv \vec{\mathcal{E}}_1 - \vec{\mathcal{E}}_2$ must also satisfy Gauss' law $\nabla\cdot\vec{\mathcal{E}}_3 = 0$. Hence, $\vec{\mathcal{E}}_3$ must be vanish throughout the space (see Fig. 2.16 right) [8].

In the case of von Neumann boundary conditions we choose,

$$\nabla' G_N(\mathbf{r},\mathbf{r}'_{\in\partial\mathcal{V}}) = -\frac{\hat{\mathbf{n}}}{S} \ , \tag{2.70}$$

because we must satisfy the definition (2.60),

$$-1 = \int_{\mathcal{V}} \nabla'^2 G_N(\mathbf{r},\mathbf{r}')dV' = \oint_{\partial\mathcal{V}} \nabla' G_N(\mathbf{r},\mathbf{r}')\cdot d\mathbf{S} = \oint_{\partial\mathcal{V}} \frac{-\hat{\mathbf{n}}}{S}\cdot d\mathbf{S} \tag{2.71}$$

such that,

$$\boxed{\Phi(\mathbf{r}) = \frac{1}{\varepsilon_0}\int_{\mathcal{V}} \varrho(\mathbf{r}')G_N(\mathbf{r},\mathbf{r}')dV' - \frac{1}{A}\oint_{\partial\mathcal{V}} \Phi(\mathbf{r}')dA' - \oint_{\partial\mathcal{V}} G_N(\mathbf{r},\mathbf{r}')\nabla'\Phi(\mathbf{r}')\cdot d\mathbf{S}'} \ . \tag{2.72}$$

The first surface term is simply the average of the potential over the area of the surface.

2.5.6 Exercises

2.5.6.1 Ex: Mirror charge

A long, thin wire is suspended along the y-direction at a distance $z = d$ parallel to a grounded metal plate located in the $z = 0$-plane. The surface of the wire carries the charge Q/l per unit length.
a. Draw a scheme of the electric field in the semi-space $z > 0$. **Help:** Use the principle of image charges!
b. Calculate the profile of the electric field near the surface of the plate.

[8] We present here a slightly simplified argumentation. See [42] for a more complete proof.

c. What is the surface density $\sigma(x, y)$ of charges on the plate surface.
d. What is the charge induced in the plate per unit length in y-direction?
Comment: A similar problem occurs for conductors on printed circuits. The metal plate corresponds to the copper coating on the backside of the circuit board.

2.5.6.2 Ex: Mirror charge

Consider the scheme, illustrated in the figure, of a point charge $+q$ in front of a corner of a grounded wall.
a. Determine the positions and values of the image charges.
b. Calculate the electrostatic potential $\Phi(\mathbf{r})$ in the upper right quadrant.

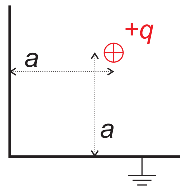

Figure 2.17: Mirror charge.

2.5.6.3 Ex: Mirror charge

Inside a grounded hollow metallic sphere with the inner radius a be a charge $+Q$ at the position $\mathbf{r}_1 = (0, 0, z_1)$. Determine the charge Q' and the position $\mathbf{r}_2$ of an image charge with which it is possible to describe the potential $\Phi(\mathbf{r})$ of the original charge distribution using only the system consisting of the charge and the image charge. Determine $\Phi(\mathbf{r})$.
Help: The position $\mathbf{r}_2$ and the charge Q' are not unambiguously determined. Choose $\mathbf{r}_1 = (0, 0, z_1)$ and $z_2/a = a/z_1$.

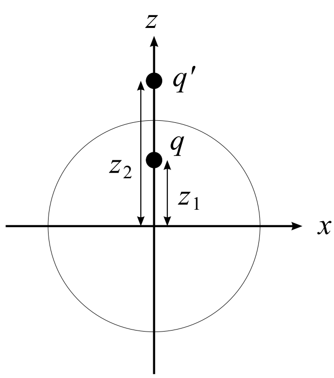

Figure 2.18: Mirror charge.

2.5.6.4 Ex: Mirror charge

A conductive surface in the (x, y)-plane has a protrusion in the form of a semi-sphere with radius R. The center of the sphere is in the plane and at the origin of the coordinates. On the symmetry axis $\hat{\mathbf{e}}_z$ at a distance $d > R$ from the plane there is a point charge Q. Determine with the image charge method the potential $\Phi(\mathbf{r})$ and the force $\mathbf{F}$ on the charge Q.
a. To make the surface of the semisphere an equipotential surface ($\Phi \equiv 0$) we need a mirror charge Q_1 on the z-axis at a distance z_1 from the origin. Determine Q_1 and z_1.
b. For the (x, y)-plane to become an equipotential surface as well, we need two more image charges Q_2 and Q_3. Determine the value and position of these charges.
c. With the values and positions of the charges determine: The electrostatic potential $\Phi(\mathbf{r})$ at an arbitrary point $\mathbf{r}$ above the conductive surface, the force $\mathbf{F}$ on the charge Q and its direction (repulsive or attractive).

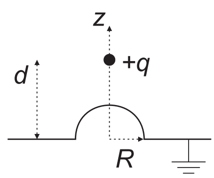

Figure 2.19: Mirror charge.

2.5.6.5 Ex: Mirror charge

Consider a hollow conducting sphere with radius R whose center is at the origin. At the position with the vector $\mathbf{a}$ ($|\mathbf{a}| > R$) be a point charge q.
a. The sphere is grounded (that is, $\Phi = 0$ at the edge of the hollow sphere). Calculate the potential outside the sphere using the image charge method.
b. Calculate the charge induced on the surface of the sphere.
c. What changes when the sphere is not grounded, but neutral?

2.5.6.6 Ex: Point charges in front of a conductor

Consider a point charge Q located at a distance d in front of an infinitely extended conductive plane.
a. Find the parametrization $\varrho(\mathbf{r})$ of the volume charge distribution for the charge and its image.
b. Calculate the potential from the distribution $\varrho(\mathbf{r})$.
c. Calculate the electric field from the distribution $\varrho(\mathbf{r})$.
d. Calculate the surface charge distribution $\sigma(\rho)$ induced in the conductor using Gauss' law.
e. Calculate the potential $\Phi(z)$ along the z-axis from Coulomb's law using the surface charge distribution $\sigma(\rho)$.
f. Compare the result obtained in (e) with the potential produced by the image charge

calculated in (b).

Help:: $\int \frac{1}{\sqrt{u^2+a^2}^3} \frac{1}{\sqrt{u^2+b^2}} u du = \frac{1}{a^2-b^2} \sqrt{\frac{u^2+b^2}{u^2+a^2}}$

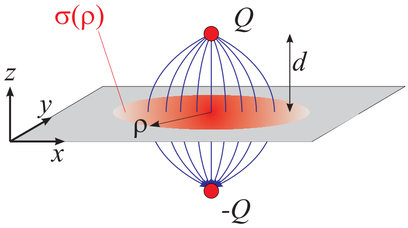

Figure 2.20: Mirror charge.

2.5.6.7 Ex: Dirichlet boundary conditions by the Green method

Here we want to analyze the problem of a potential in the semi-space defined by $z \geq 0$ with Dirichlet boundary conditions in the $z = 0$-plane and at infinity.
a. Determine the corresponding Greens function.
b. The potential has in the $z = 0$-plane within a circle of radius a the fixed value Φ_0. Outside this circle and on the same plane the potential is $\Phi = 0$. Derive the integral expression for the potential at a point in the upper semi-space with the cylindrical coordinates (ρ, ϕ, z).
c. Now show that the potential along an axis perpendicularly traversing the center of the circle is given by $\Phi(z) = \Phi_0(1 - z/\sqrt{a^2 + z^2})$.

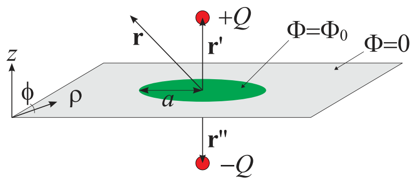

Figure 2.21: Green's function.

2.5.6.8 Ex: Conductor plates with mirror charges by the Green method

We consider two flat conductive plates (infinitely extended) with the mutual distance L. Exactly in the middle between the plates there is a point charge $+q$. Use the method of an infinite series of mirror images to calculate the potential between the plates and the force on a plate.

2.5.6.9 Ex: Hollow sphere by the Green method

We consider an infinitely thin conductive hollow sphere with radius a. In spherical coordinates, the potential on the surface of the sphere is given by $\Phi(a, \theta, \phi) = \Phi_0 \cos\theta$.
a. Calculate, using the Green function for the sphere, the potential and the field inside

the sphere on the z-axis.
b. Show that $\Phi(r,\theta,\phi) = \Phi_0(r/a)\cos\theta$ is the solution for the interior of the sphere and that $\vec{\mathcal{E}}(\mathbf{r}) = -(\Phi_0/a)\hat{\mathbf{e}}_z$.

2.5.6.10 Ex: Unambiguity of the solution of the contour problem

Show that with the Dirichlet boundary condition $\Phi(\mathbf{r}) = \Phi_0(\mathbf{r})|_{\in\partial V}$ or the von Neumann boundary condition $\frac{\partial\Phi}{\partial n}\big|_{\partial V} = -\frac{\sigma}{\varepsilon_0}$ within the region of the volume V the potential Φ is unambiguously determined by the Poisson equation $\Delta\Phi = -\frac{1}{\varepsilon_0}\rho(\mathbf{r})$and a constant.

2.6 Solution of the Laplace equation in situations of high symmetry

The Poisson (or Laplace) equation is a second order partial differential equation, which depends on three spatial coordinates. Many situations are characterized by symmetries, which allow us to disregard some spatial dimensions and dramatically simplify the mathematical problem. In the following, we will discuss situations of Cartesian, cylindrical and spherical symmetry.

2.6.1 Variable separation in Cartesian coordinates

In situations where the symmetry of the problem suggests a separation of the Cartesian variables, we can make the ansatz,

$$\Phi(\mathbf{r}) = X(x)Y(y)Z(z)\ . \tag{2.73}$$

In Cartesian coordinates the Laplace equation is written,

$$\left[\frac{\partial^2}{\partial x^2} + \frac{\partial^2}{\partial y^2} + \frac{\partial^2}{\partial z^2}\right]\Phi = 0\ . \tag{2.74}$$

Inserting the ansatz into the Laplace equation and dividing by Φ,

$$\frac{1}{X}\frac{\partial^2 X}{\partial x^2} + \frac{1}{Y}\frac{\partial^2 Y}{\partial y^2} + \frac{1}{Z}\frac{\partial^2 Z}{\partial z^2} = 0\ . \tag{2.75}$$

The three terms are functions of different variables and must therefore be constant independently and separately,

$$\frac{1}{X}\frac{\partial^2 X}{\partial x^2} = C_1 \quad , \quad \frac{1}{Y}\frac{\partial^2 Y}{\partial y^2} = C_2 \quad , \quad \frac{1}{Z}\frac{\partial^2 Z}{\partial z^2} = C_3 = -C_1 - C_2\ . \tag{2.76}$$

The advantage of this procedure is that, the differential equations for the three spatial coordinates being decoupled, we can be solve them separately. In the best case, the field is homogeneous in one of the coordinates, which reduces the dimensionality of the problem.

Example 22 (*Field of a grounded board*): For example, to calculate the field of a plate held at a fixed potential Φ_0 and being infinitely extended in the x-y-plane, we can let $X'(x) = Y'(y) = 0$ and solve the equation,

$$\frac{\partial^2 Z}{\partial z^2} = 0 \; , \tag{2.77}$$

which gives, $\Phi(\mathbf{r}) = Z(z) = Cz + \Phi_0$ and $\vec{\mathcal{E}} = C\hat{\mathbf{e}}_z$. The constants C and Φ_0 must be specified by additional boundary conditions. See Exc. 2.6.4.1.

2.6.2 Variable separation in cylindrical coordinates

In situations where the symmetry of the problem suggests a possible separation of cylindrical variables, we can try the ansatz,

$$\Phi(\mathbf{r}) = R(r)F(\phi)Z(z) \; . \tag{2.78}$$

In cylindrical coordinates the Laplace equation is written,

$$\left[\frac{1}{\rho}\frac{\partial}{\partial\rho}\left(\rho\frac{\partial}{\partial\rho}\right) + \frac{1}{\rho^2}\frac{\partial^2}{\partial\phi^2} + \frac{\partial^2}{\partial z^2}\right]\Phi = 0 \; . \tag{2.79}$$

Inserting the ansatz into the Laplace equation and dividing by Φ,

$$\frac{1}{R\rho}\frac{\partial}{\partial\rho}\left(\rho\frac{\partial R}{\partial\rho}\right) + \frac{1}{F}\frac{\partial^2 F}{\partial\phi^2} + \frac{1}{Z}\frac{\partial^2 Z}{\partial z^2} = 0 \; . \tag{2.80}$$

The three terms are functions of different variables and must therefore be constant separately,

$$\frac{1}{R\rho}\frac{\partial}{\partial\rho}\left(\rho\frac{\partial R}{\partial\rho}\right) = C_1 \quad , \quad \frac{1}{F}\frac{\partial^2 F}{\partial\phi^2} = C_2 \quad , \quad \frac{1}{Z}\frac{\partial^2 Z}{\partial z^2} = C_3 = -C_1 - C_2 \; . \tag{2.81}$$

Example 23 (*Field of a straight wire*): Many geometries have cylindrical symmetry, such that the equations in θ and z become trivial. For example, to calculate the field of a straight and infinite wire maintained at a fixed potential, it is enough to solve a radial differential equation,

$$\frac{\partial}{\partial\rho}\left(\rho\frac{\partial R}{\partial\rho}\right) = 0 \; ,$$

which gives, $\Phi(\mathbf{r}) = R(\rho) = C\ln\rho + \Phi_0$ and $\vec{\mathcal{E}} = C\hat{\mathbf{e}}_\rho/\rho$. The constants C and Φ_0 must be specified by additional boundary conditions.

2.6.3 Variable separation in spherical coordinates

In situations where the symmetry of the problem suggests a possible separation of the spherical variables, we can try the make ansatz,

$$\Phi(\mathbf{r}) = R(r)T(\theta)F(\phi) \; . \tag{2.82}$$

In spherical coordinates the Laplace equation is written,

$$\left[\frac{1}{r^2}\frac{\partial}{\partial r}\left(r^2\frac{\partial}{\partial r}\right)+\frac{1}{r^2\sin\theta}\frac{\partial}{\partial\theta}\left(\sin\theta\frac{\partial}{\partial\theta}\right)+\frac{1}{r^2\sin^2\theta}\frac{\partial^2}{\partial\phi^2}\right]\Phi=0\ . \tag{2.83}$$

Inserting the ansatz into the Laplace equation and dividing by Φ,

$$\frac{1}{R}\frac{\partial}{\partial r}\left(r^2\frac{\partial R}{\partial r}\right)+\frac{1}{T\sin\theta}\frac{\partial}{\partial\theta}\left(\sin\theta\frac{\partial T}{\partial\theta}\right)+\frac{1}{Fr^2\sin^2\theta}\frac{\partial^2 F}{\partial\phi^2}=0\ . \tag{2.84}$$

The three terms are functions of different variables and must therefore be constant separately,

$$\frac{1}{R}\frac{\partial}{\partial r}\left(r^2\frac{\partial R}{\partial r}\right)=C_1\quad,\quad\frac{1}{T\sin\theta}\frac{\partial}{\partial\theta}\left(\sin\theta\frac{\partial T}{\partial\theta}\right)=\ell(\ell+1) \tag{2.85}$$
$$\frac{1}{Fr^2\sin^2\theta}\frac{\partial^2 F}{\partial\phi^2}=m=-C_1-\ell(\ell+1)\ .$$

Example 24 (*Sphere with fixed potential*): Many geometries have spherical symmetry, such that the equations in θ and ϕ become trivial. For example, to calculate the field of a sphere held at a fixed potential, we only have to solve a radial differential equation,

$$\frac{1}{R}\frac{\partial}{\partial r}\left(r^2\frac{\partial R}{\partial r}\right)=0\ ,$$

which gives, $\Phi(\mathbf{r})=R(r)=-C/r+\Phi_0$ and $\vec{\mathcal{E}}=C\hat{\mathbf{e}}_r/r^2$. The constants C and Φ_0 must be specified by additional boundary conditions.

In case of *only azimuthal* symmetry, we have $m=0$ and $C_1=-\ell(\ell+1)$. The solutions of the radial equation are simple,

$$R(r)=A_\ell r^\ell+\frac{B_\ell}{r^{\ell+1}}\ . \tag{2.86}$$

The solutions of the angular equation are called *Legendre polynomials*,

$$T(\theta)=P_\ell(\cos\theta)\ . \tag{2.87}$$

They can be derived from the *Rodrigues formula*,

$$P_\ell(z)=\frac{1}{2^\ell\ell!}\left(\frac{d}{dz}\right)^\ell(z^2-1)^\ell\ . \tag{2.88}$$

The first polynomials are,

$$P_0(z)=1\quad,\quad P_1(z)=z\quad,\quad P_2(z)=\tfrac{1}{2}(3z^2-1)\quad,\quad P_3(z)=\tfrac{1}{2}(5z^3-3z)\ . \tag{2.89}$$

All in all we get,

$$\boxed{\Phi(\mathbf{r})=\sum_{\ell=0}^{\infty}\left(A_\ell r^\ell+\frac{B_\ell}{r^{\ell+1}}\right)P_\ell(\cos\theta)}\ . \tag{2.90}$$

Example 25 (*Charged spherical layer*): In this example we consider a spherical shell carrying a surface charge described by $\sigma(\theta)$. The regions $r \leq R$ and $r \geq R$ are treated separately. The ansatz (2.90) can not diverge, neither within the sphere where we must let $B_\ell = 0$, nor outside the sphere where we have to let $A_\ell = 0$. On the surface even the potential has to be continuous, such that

$$0 = [\Phi_\geq - \Phi_\leq]_{r=R} = \sum_{\ell=0}^{\infty} \frac{B_l}{R^{\ell+1}} P_\ell(\cos\theta) - \sum_{\ell=0}^{\infty} A_\ell R^\ell P_\ell(\cos\theta) \ ,$$

resulting in $B_\ell = A_\ell R^{2\ell+1}$. On the other hand, the electric field is discontinuous,

$$-\frac{\sigma(\theta)}{\varepsilon_0} = \left[\frac{\partial\Phi_\geq}{\partial r} - \frac{\partial\Phi_\leq}{\partial r}\right]_{r=R} = \sum_{\ell=0}^{\infty}(2\ell+1)A_\ell R^{\ell-1} P_\ell(\cos\theta) \ .$$

The coefficients are,

$$A_\ell = \frac{1}{2\varepsilon_0 R^{\ell-1}} \int_0^\pi \sigma(\theta) P_\ell(\cos\theta)\sin\theta d\theta \ ,$$

which can be verified from the orthogonality relation,

$$\int_{-1}^{1} P_\ell(z) P_{\ell'}(z) dz = \frac{2\delta_{\ell,\ell'}}{2\ell+1} \ .$$

Particularly for the case $\sigma(\theta) = \sigma_0\cos\theta = \sigma_0 P_1(\cos\theta)$ we obtain,

$$A_\ell = \frac{\sigma_0}{2\varepsilon_0 R^{\ell-1}} \int_0^\pi P_1(z) P_l(z) dz = \frac{\sigma_0}{2\varepsilon_0 R^{\ell-1}} \frac{2}{2\ell+1}\delta_{\ell,1} = \frac{\sigma_0}{3\varepsilon_0}\delta_{\ell,1} \ .$$

Finally,

$$\Phi(\mathbf{r}) = \begin{cases} \frac{\sigma_0}{3\varepsilon_0} r\cos\theta = \frac{\sigma_0}{3\varepsilon_0}\mathbf{r}\cdot\hat{\mathbf{e}}_z & \text{for} \quad r \leq R \\ \frac{\sigma_0 R^3}{3\varepsilon_0}\frac{1}{r^2}\cos\theta = \frac{\sigma_0 R^3}{3\varepsilon_0}\frac{\mathbf{r}\cdot\hat{\mathbf{e}}_z}{r^3} & \text{for} \quad r \geq R \end{cases} .$$

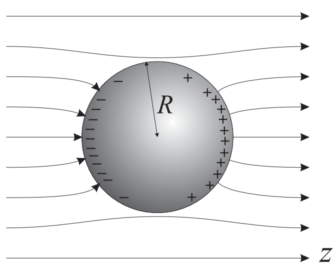

Figure 2.22: Distortion of a homogeneous field by a metallic sphere.

2.6.4 Exercises

2.6.4.1 Ex: Variable separation

Calculate the potential within an infinite rectangular waveguide in the z-direction by solving the Laplace equation using the variable separation method.

2.6.4.2 Ex: Field of a sphere with a hole

On the surface of a hollow sphere of radius R, from which a cap defined by the opening angle $\theta = \alpha$ was cut out at the north pole, there is a homogeneously distributed surface charge density $Q/4\pi R^2$.
a. Show that the potential within the volume of the sphere can be written in the form,

$$\Phi(r,\theta,\phi) = \frac{Q}{2}\sum_{\ell=0}^{\infty}\frac{1}{2\ell+1}\left[P_{\ell+1}(\cos\alpha) - P_{\ell-1}(\cos\alpha)\right]\frac{r^\ell}{R^{\ell+1}}P_\ell(\cos\theta)$$

where for $\ell = 0$ we have to let $P_{\ell-1}(\cos\alpha) = -1$. What is the shape of the potential outside the hollow sphere?
b. Determine the absolute value and the direction of the electric field at the origin.
c. What potential do we get for $\alpha \to 0$?
Help: Use the following relation for the surface charge density:

$$-\frac{\sigma}{\varepsilon_0} = \left[\frac{\partial\Phi_>}{\partial r} - \frac{\partial\Phi_<}{\partial r}\right]_{r=R} ,$$

where the indices $<$ resp. $>$ hold for regions inside resp. outside the sphere. For the integration, the following recursion relation is useful,

$$P_l(x) = \frac{1}{2\ell+1}\left(\frac{dP_{\ell+1}(x)}{dx} - \frac{dP_{\ell-1}(x)}{dx}\right)$$

that holds for $\ell > 0$.

2.7 Multipolar expansion

The basic idea of *multipolar expansion* is the approximate description of the potential generated by an arbitrary distribution of charges localized within a volume $\mathcal{V}$. The larger the distance between the observation point and the charge distribution in comparison to the extent of the volume $\mathcal{V}$, the more the potential looks like that of a point charge. The smaller the distance, the more terms (multipole moments) must be taken into account, $\Phi(\mathbf{r}) = \sum_k \Phi_k(\mathbf{r})$. High multipolar orders decay faster (like r^{-k}) with the distance between the observation point and the volume where the charge is concentrated.

We have already seen how to do the Taylor expansion of scalar fields in the formula (1.17) [9]. Here, we want to expand in terms of r^{-1}. We start by expanding the function,

$$\frac{1}{|\mathbf{r}-\mathbf{r}'|} = \frac{1}{r}\sum_{\ell=0}^{\infty}\left(\frac{r'}{r}\right)^\ell P_\ell(\cos\theta') , \tag{2.91}$$

[9] Using the following property of the Legendre polynomials,

$$\frac{1}{\sqrt{1+\eta(\eta-2z)}} = \sum_\ell \eta^\ell P_\ell(z) ,$$

where the left side is called the generating function of the polynomials.

where θ' is the angle between $\mathbf{r}$ and $\mathbf{r}'$. Inserting the expansion into Coulomb's law (2.35),

$$\Phi(\mathbf{r}) = \frac{1}{4\pi\varepsilon_0}\int \frac{\varrho(\mathbf{r}')}{|\mathbf{r}-\mathbf{r}'|}d^3r' = \frac{1}{4\pi\varepsilon_0}\sum_{\ell=0}^{\infty}\frac{1}{r^{\ell+1}}\int \varrho(\mathbf{r}')r'^{\ell}P_\ell(\cos\theta')d^3r' \ . \tag{2.92}$$

Example 26 (*Multipolar expansion by Legendre polynomials*): To discuss the multipolar expansion of the function $\frac{1}{|\mathbf{r}-\mathbf{r}'|}$ we chose the axis $\hat{\mathbf{r}}$ as the symmetry axis, as shown in Fig. 2.23, because in this coordinate system the function has azimuthal symmetry in the variable $\mathbf{r}'$. Therefore, we can apply the solution of the Laplace equation in spherical coordinates derived above,

$$\Phi(\mathbf{r}') = \sum_{\ell=0}^{\infty}\left(A_\ell r'^{\ell} + \frac{B_\ell}{r'^{\ell+1}}\right)P_\ell(\cos\theta') \ .$$

We consider two cases: In a first case in which $r' < r$, for the solution $\Phi(\mathbf{r}')$ to converge, we need to guarantee $B_\ell = 0$ such that,

$$\frac{1}{|\mathbf{r}-\mathbf{r}'|} = \sum_{\ell=0}^{\infty}A_\ell(r)r'^{\ell}P_\ell(\cos\theta') \ .$$

In the second case in which case $r' > r$, we need to ensure $A_\ell = 0$, such that,

$$\frac{1}{|\mathbf{r}-\mathbf{r}'|} = \sum_{\ell=0}^{\infty}\frac{B_\ell(r)}{r'^{\ell+1}}P_\ell(\cos\theta') \ ,$$

The coefficients $A_\ell(\mathbf{r})$ and $B_\ell(\mathbf{r})$ can not depend on $\mathbf{r}'$. Let us now have a closer look at this second case and rename the variables $\mathbf{r} \leftrightarrow \mathbf{r}'$:

$$\frac{1}{|\mathbf{r}'-\mathbf{r}|} = \sum_{\ell=0}^{\infty}\frac{B_\ell(r')}{r^{\ell+1}}P_\ell(\cos\theta) \ .$$

Comparing this to the first case and using $\theta = -\theta'$ we find,

$$A_\ell(r)r^{\ell+1} = \frac{B_\ell(r')}{r'^{\ell}} = const = C \ .$$

Hence,

$$\frac{1}{|\mathbf{r}-\mathbf{r}'|} = \sum_{\ell=0}^{\infty}C\frac{r'^{\ell}}{r^{\ell+1}}P_\ell(\cos\theta') \ .$$

The constant C can be calibrated considering a particular case, for example $\mathbf{r} \parallel \mathbf{r}'$ and $r \gg r'$. In this case, since $P_\ell(1) = 1$, the multipolar expansion,

$$\frac{1}{|\mathbf{r}-\mathbf{r}'|} = \frac{1}{|r-r'|} = \sum_{\ell=0}^{\infty}C\frac{r'^{\ell}}{r^{\ell+1}} \ ,$$

is nothing more than a Taylor expansion around the point $r - r' \simeq r$.

2.7.1 The monopole

For $n = 0$ the contribution of the *monopole moment* Q to the potential is,

$$\boxed{\Phi_0(\mathbf{r}) = \frac{Q}{4\pi\varepsilon_0}\frac{1}{r}} \quad \text{where} \quad \boxed{Q = \int_{\mathcal{V}} d^3r' \ \varrho(\mathbf{r}')} \tag{2.93}$$

is just the electric charge.

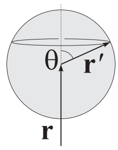

Figure 2.23: In the coordinate system $\hat{\mathbf{r}} = \hat{\mathbf{e}}_z$ the function $|\mathbf{r}-\mathbf{r}'|^{-1}$ has azimuthal symmetry.

2.7.2 The dipole

For $n = 1$ the contribution of the *electric dipole moment* $\mathbf{d}$ to the potential follows immediately from formula (2.91),

$$\Phi_1(r) = \tfrac{1}{4\pi\varepsilon_0}\tfrac{1}{r^2}\int \varrho(\mathbf{r}')r'P_1(\cos\theta')d^3r'$$
$$= \tfrac{1}{4\pi\varepsilon_0}\tfrac{1}{r^3}\int \varrho(\mathbf{r}')rr'\cos\theta' d^3r' = \tfrac{1}{4\pi\varepsilon_0}\tfrac{\mathbf{r}}{r^3}\cdot\int \varrho(\mathbf{r}')\mathbf{r}'d^3r' \ .$$

We obtain,

$$\boxed{\Phi_1(\mathbf{r}) = \frac{1}{4\pi\varepsilon_0}\sum_k d_k\frac{x_k}{r^3}} \quad \text{where} \quad \boxed{\mathbf{d} = \int_{\mathcal{V}} d^3r'\ \mathbf{r}'\varrho(\mathbf{r}')} \ . \tag{2.94}$$

2.7.3 The quadrupole

For $n = 2$ the contribution of the *electric quadrupole moment* $q_{i,j}$ to the potential follows immediately from the formula(2.91),

$$\Phi_2(r) = \tfrac{1}{4\pi\varepsilon_0}\tfrac{1}{r^3}\int \varrho(\mathbf{r}')r'^2P_2(\cos\theta')d^3r' = \tfrac{1}{4\pi\varepsilon_0}\tfrac{1}{r^3}\int \varrho(\mathbf{r}')r'^2\tfrac{3\cos^2\theta'-1}{2}d^3r'$$
$$= \tfrac{1}{4\pi\varepsilon_0}\tfrac{1}{2r^5}\int \varrho(\mathbf{r}')(3(\mathbf{r}\cdot\mathbf{r}')^2 - r^2r'^2)d^3r'$$
$$= \tfrac{1}{4\pi\varepsilon_0}\tfrac{1}{2r^5}\sum_{k,m}\int \varrho(\mathbf{r}')(3x_kx'_kx_mx'_m - x_kx_mr'^2\delta_{k,m})d^3r' \ .$$

We obtain,

$$\boxed{\Phi_2(\mathbf{r}) = \frac{1}{4\pi\varepsilon_0}\frac{1}{2}\sum_{k,m} q_{k,m}\frac{x_kx_m}{r^5}} \quad \text{where} \quad \boxed{q_{k,m} = \int_{\mathcal{V}} d^3r'\ (3x'_kx'_m - r'^2\delta_{k,m})\varrho(\mathbf{r}')} \ . \tag{2.95}$$

Example 27 (*Multipole moments of a dipole*): As an example, we consider the simplest dipole, which consists of two charges e and $-e$ separated by a fixed distance a, which we choose parallel to the z-axis. The monopolar moment is,

$$Q = \int d^3r'\ [e\delta(\tfrac{a}{2}\hat{\mathbf{e}}_z - \mathbf{r}') - e\delta(\tfrac{a}{2}\hat{\mathbf{e}}_z + \mathbf{r}')] = 0 \ ,$$

as expected. The dipole moment is,

$$\mathbf{d} = \int d^3r'\ \mathbf{r}'[e\delta(\tfrac{a}{2}\hat{\mathbf{e}}_z - \mathbf{r}') - e\delta(\tfrac{a}{2}\hat{\mathbf{e}}_z + \mathbf{r}')] = ea\begin{pmatrix}0\\0\\1\end{pmatrix} \ ,$$

and the quadrupolar moment is,

$$\begin{aligned} q_{k,m} &= \int d^3r'\ (3x'_k x'_m - r'^2\delta_{km})[e\delta(\tfrac{a}{2}\hat{\mathbf{e}}_z - \mathbf{r}') - e\delta(\tfrac{a}{2}\hat{\mathbf{e}}_z + \mathbf{r}')] \\ &= \frac{ea^2}{4}\begin{pmatrix}-1&0&0\\0&-1&0\\0&0&2\end{pmatrix} - \frac{ea^2}{4}\begin{pmatrix}-1&0&0\\0&-1&0\\0&0&2\end{pmatrix} = 0 \ . \end{aligned}$$

See the Excs. 2.7.5.1 to 2.7.5.10.

Example 28 (*The electric dipole*): The gradient of the potential of a dipole is,

$$\begin{aligned} \vec{\mathcal{E}}_1 &= -\nabla\frac{\mathbf{r}\cdot\mathbf{d}}{4\pi\varepsilon_0 r^3} = \frac{-1}{4\pi\varepsilon_0}\hat{\mathbf{e}}_x\frac{\partial}{\partial x}\frac{xd_x + yd_y + zd_z}{(x^2+y^2+z^2)^{3/2}} + \ldots \\ &= \frac{-1}{4\pi\varepsilon_0}\hat{\mathbf{e}}_x\frac{d_x(x^2+y^2+z^2)^{3/2} - (xd_x + yd_y + zd_z)3x(x^2+y^2+z^2)^{1/2}}{(x^2+y^2+z^2)^3} + \ldots \\ &= \frac{-1}{4\pi\varepsilon_0}\hat{\mathbf{e}}_x\frac{d_x r^2 - \mathbf{r}\cdot\mathbf{d}3x}{r^5} + \ldots = \frac{1}{4\pi\varepsilon_0}\frac{3(\hat{\mathbf{e}}_r\cdot\mathbf{d})\hat{\mathbf{e}}_r - \mathbf{d}}{r^3} \ . \end{aligned}$$

2.7.4 Expansion into Cartesian coordinates

The multipolar expansion can also be done in Cartesian coordinates by a Taylor series of the Green function [10]. To take this into account, we evaluate the function $G(\mathbf{r},\mathbf{r}') = G(\mathbf{r}-\mathbf{r}')$ around the distance $\mathbf{r}-\mathbf{r}' \simeq \mathbf{r}$,

$$G(\mathbf{r}-\mathbf{r}') = \sum_k \frac{1}{k!}(\mathbf{r}'\cdot\nabla)^k G(\mathbf{r}) = G(\mathbf{r}) + \sum_{k=1} x'_k\frac{\partial}{\partial x_k}G(\mathbf{r}) + \frac{1}{2!}\left(\sum_{k=1}^3 x'_k\frac{\partial}{\partial x_k}\right)^2 G(\mathbf{r}) + \ldots \tag{2.96}$$

$$\begin{aligned} &= G(\mathbf{r}) + \sum_{k=1} x'_k\frac{\partial}{\partial x_k}G(\mathbf{r}) + \frac{1}{2!}\sum_{k,m=1}^3 x'_k x'_m\frac{\partial^2}{\partial x_k\partial x_m}G(\mathbf{r}) + \ldots \\ &= G(\mathbf{r}) + \sum_{k=1} x'_k\frac{\partial}{\partial x_k}G(\mathbf{r}) + \frac{1}{6}\sum_{k,m=1}^3 (3x'_k x'_m - r'^2\delta_{k,m})\frac{\partial^2}{\partial x_k\partial x_m}G(\mathbf{r}) + \ldots \end{aligned}$$

The last transformation is valid if the function G satisfies the Laplace equation, $\nabla^2 G = 0$.

[10] We can imagine the Green function as the potential created by a point-charge distribution, $\varrho(\mathbf{r}') = Q\delta(\mathbf{r}-\mathbf{a})$, since $\Phi(\mathbf{r}) = \int G(\mathbf{r}-\mathbf{r}')\varrho(\mathbf{r}')dV' = QG(\mathbf{r}'-\mathbf{a})$. That is, the multipolar terms come into play due to a small stretching of the charge distribution around the point $\mathbf{r}' = \mathbf{a}$

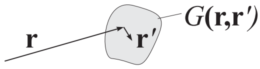

Figure 2.24: Taylor expansion of the Green function around the point $\mathbf{r}-\mathbf{r}'\simeq\mathbf{r}$.

Example 29 (*Cartesian multipolar expansion*): As an example, we expand the Coulomb potential, $G(\mathbf{r}-\mathbf{r}')=\frac{1}{|\mathbf{r}-\mathbf{r}'|}$. The first derivatives,

$$\frac{\partial}{\partial x_k}\frac{1}{|\mathbf{r}-\mathbf{r}'|}=\frac{x_k-x_k'}{|\mathbf{r}-\mathbf{r}'|^3}\ ,$$

and the second derivatives,

$$\frac{\partial^2}{\partial x_k\partial x_m}\frac{1}{|\mathbf{r}-\mathbf{r}'|}=\frac{3(x_k-x_k')^2-(\mathbf{r}-\mathbf{r}')^2\delta_{k,m}}{|\mathbf{r}-\mathbf{r}'|^5}\ ,$$

allow us to calculate,

$$\frac{1}{|\mathbf{r}-\mathbf{r}'|}=\frac{1}{r}+\frac{\mathbf{r}\cdot\mathbf{r}'}{r^3}+\frac{1}{6}\sum_{k,m=1}^{3}\frac{3x_kx_m-r^2\delta_{k,m}}{r^5}(3x_k'x_m'-r'^2\delta_{k,m})\ .$$

The octupolar term of the multipole expansion of the Coulomb potential is,

$$\frac{1}{3!}(\mathbf{r}'\cdot\nabla)^3\frac{1}{r'}=\frac{1}{6}\sum_{k,m,n=1}^{3}x_k'x_m'x_n'\frac{-15x_kx_mx_n+3r''(x_k\delta_{mn}+x_m\delta_{kn}+x_n\delta_{mk})}{r^7}\ .$$

Inserting this into Coulomb's Law,

$$\Phi(\mathbf{r})=\frac{1}{4\pi\varepsilon_0}\int\frac{\varrho(\mathbf{r}')}{|\mathbf{r}-\mathbf{r}'|}dV'=\frac{1}{4\pi\varepsilon_0}\left(\frac{1}{r}Q+\frac{\mathbf{r}}{r^3}\cdot\mathbf{d}+\frac{1}{6}\sum_{k,m=1}^{3}\frac{3x_kx_m-r^2\delta_{k,m}}{r^5}q_{k,m}+...\right)\ ,$$

with the definitions of the multipole moments.

2.7.5 Exercises

2.7.5.1 Ex: Multipoles

A point charge $+2Q$ is at the position $(0,0,a)$ and another charge $+1Q$ at the position $(0,0,-a)$. Calculate a. The monopolar, b. the dipolar, and c. the quadrupolar contribution of the multipolar expansion.

2.7.5.2 Ex: Di- and quadrupolar momenta of spherical charge distributions

Do spherically symmetrical load distributions have dipole or quadrupolar moments? Justify!

2.7.5.3 Ex: Electric dipole

An electrical dipole consists of two charges of the value $q=1.5\,\text{nC}$ distant by $a=6\,\mu\text{m}$.
a. What is the dipole moment?
b. Calculate the dipole potential along the $\hat{\mathbf{e}}_z$ axis of symmetry and in the xy-plane.
c. The dipole is in an $1100\,\text{N/C}$ electric field. What is the difference in potential energies comparing parallel and antiparallel orientations of the dipole.

2.7.5.4 Ex: Electric dipole

An electric dipole with the moment $\mathbf{d}$ is at the position $\mathbf{r}$. At the origin of the coordinate system there is a point charge e.
a. Calculate the potential energy of the dipole.
b. Calculate the force acting on the dipole.
c. Calculate the force acting on the charge. Is Newton's axiom of mechanics valid: 'actio = reactio'?

2.7.5.5 Ex: Electric dipole in a field

What is the force acting on an electric dipole $\mathbf{d} = ea \cdot \hat{\mathbf{e}}_r$ at a point $\mathbf{r}$ being aligned along the field lines of an external field produced by a sphere with radius R homogeneously charged with a charge Q?

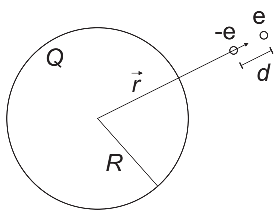

Figure 2.25: Electric dipole in a field.

2.7.5.6 Ex: Electric dipole in a field

Consider a molecule that consists of two rigidly bound masses $m_1 = m_2 = 10^{-25}$ kg at a distance of $a = 10^{-12}$ m and with charges $+e$ resp. $-e$.
a. Calculate the electric dipole moment $\mathbf{d} = d \cdot \hat{\mathbf{e}}_x$ of this charge distribution.
b. Now the molecule is put into rotation by a homogeneous electric field $\vec{\mathcal{E}} = \hat{\mathbf{e}}_z \cdot 100\,\text{V/m}$. Calculate the rotation speed of the molecule as a function of the angle between the dipole moment and the electric field.
Help: The sum of the kinetic and electrostatic energies is conserved during the rotation.

2.7.5.7 Ex: Dipolar field in two dimensions

Consider two infinitely long parallel conductors with distance d carrying the linear charge density $+\lambda$ resp. $-\lambda$ (charge $\pm Q$ per length l of the conductor). Using the Gauß theorem, first calculate the electric field and the electric potential of one conductor. Then calculate the potential of both conductors by overlapping the individual potentials as a function of the distance r and the angle α (see Fig. 2.26). **Note:** Choose as integration volume a cylinder with length l and radius r along the symmetry axis around the wire. Determine the asymptotic behavior for $r \gg d/2$ and for $r \ll d/2$. To do this, do a Taylor expansion of the expression using: $\ln \frac{1+\epsilon}{1-\epsilon} \approx -2\epsilon + O(\epsilon^3)$. Write the result as a function of the dipole moment $\mathbf{p}$, where $p = |\mathbf{p}| = \lambda d$ is positive and indicates the direction of the dipole moment vector showing from the positive conductor to the negative.

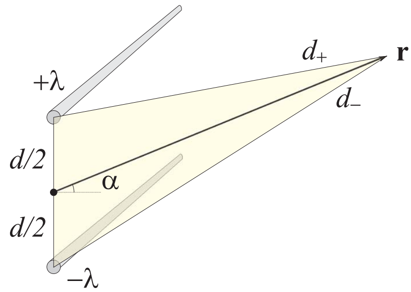

Figure 2.26: Dipolar field.

2.7.5.8 Ex: Dipolar and quadrupolar fields

Let us consider a system of three point charges aligned to the z-axis. At the positions $z = \pm a$ we have charges $+Q$, at the position $z = 0$ the charge $-2Q$.
a. Determine the charge distribution in terms of the δ-function in Cartesian coordinates.
b. Calculate the electrostatic potential $\Phi(\mathbf{r})$ of this charge distribution and approximate for long distances $|\mathbf{r}| \gg a$. (**Help:** Write the denominators that appear as $\frac{1}{|\mathbf{r}\pm\mathbf{a}|} = \frac{1}{r}\frac{1}{\sqrt{1+x}}$ with $x \equiv \frac{a^2 \pm 2\mathbf{a}\cdot\mathbf{r}}{r^2}$ and expand up to second order in a.)
c. Calculate the monopolar moment and the Cartesian components of the dipolar moment and the quadrupolar tensor.
d. Calculate the monopolar, dipolar, and quadrupolar potentials and show that the results coincides with the expansion (b).
e. Now rotate the coordinate system around the x-axis by an angle of 45°. What are the new values for multipolar moments? (**Help:** The quadrupolar tensor is transformed with the rotation matrix λ as $q'_{il} = \lambda_{il} q_{lm} \lambda^\dagger_{mj}$).

2.7.5.9 Ex: Multipoles

The two charge distributions shown in the graph are given.
a. Calculate for both cases first the electrical potential Φ for the distances $r = 2a$, $r = 10a$, and $r = 100a$ for the angles $\alpha = 0°$, $\alpha = 45°$, and $\alpha = 90°$, respectively.
b. The results must now be compared with those of the quadrupolar expansion. What are the monopolar, dipolar and quadrupolar moments for these two geometries? Calculate the monopolar, dipolar and quadrupolar contributions of the electrical potential for the same positions as above. Compare these values with those calculated exactly and identify the dominant contributions.

2.7.5.10 Ex: Multipoles

Four point charges $+e$ and $-e$ are located at the Cartesian coordinates $(x, y, z) = (0, d, 0)$, $(0, -d, 0)$, $(0, 0, d)$, $(0, 0, -d)$ and four other charges $-e$ at the points $(-d, 0, 0)$, $(-\frac{d}{2}, 0, 0)$, and $(d, 0, 0)$. Calculate the monopolar moment and the Cartesian components of the dipolar and quadrupolar moment of this charge distribution.

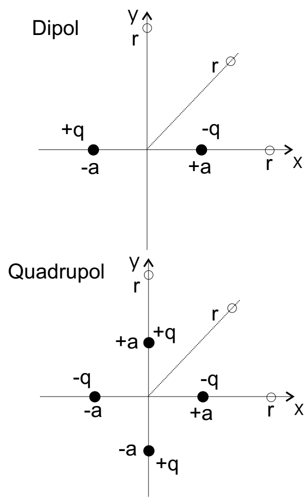

Figure 2.27: Multipoles.

2.7.5.11 Ex: Multipolar moments of a charge distribution

An ideal hollow sphere with radius R_0 has the surface charge density $\sigma(r,\theta,\phi) = \sigma_0 \cos\theta$ with σ_0 =const. Calculate:
a. The multipolar moments of this charge distribution.
b. The electrostatic potential outside the sphere.

2.7.5.12 Ex: Multipolar moment of an atomic nucleus

A simple model of a deformed atomic nucleus is a body homogeneously charged with the full charge Ze and being delimited by the quadrupolar surface $R(\theta) = R_0(a(\beta) + \beta Y_{20}(\theta))$. We now assume that the absolute value of the deformation parameter β is very small with respect to 1. For the average radius it is $R_0 = 1.2\ A^{1/3}$ [fm], where A is the number of nucleons present.
a. Visualize the shape of the nucleus.
b. Determine $a(\beta)$ up to second order in β from the request, that the core volume is always $V = 4\pi R_0^3/3$.
c. Calculate the multipolar moments Q_{lm} up to the octupolar term and up to the linear terms in β. Are there any multipolar moments that zero exactly?
d. Calculate also the electrostatic potential also up to linear terms in β.

2.7.5.13 Ex: Dipole-dipole interaction

a. Consider an electric dipole with dipole moment $\mathbf{d}$. Show that the electric field of the dipole is given by:

$$\vec{\mathcal{E}}(\mathbf{r} = r\hat{\mathbf{e}}_r) = -\frac{1}{4\pi\varepsilon_0}\frac{\mathbf{d} - 3\hat{\mathbf{e}}_r(\hat{\mathbf{e}}_r \cdot \mathbf{d})}{r^3} \ .$$

You may use the expression for a dipole potential.
b. Use this result to calculate the interaction energy U_{12} of two equal dipoles located

at a distance d from one another for the dipole configurations shown in the scheme.
Help: To calculate the interaction energy $U_{12}(\mathbf{a})$ between the two dipoles we con-

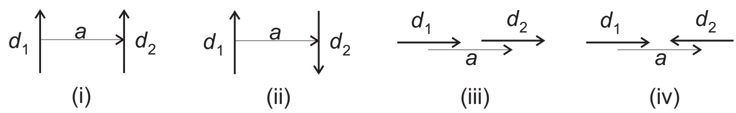

Figure 2.28: Dipole-dipole interaction.

sider the energy of dipole 1 in the electric field of dipole 2. So, $U_{12}(\mathbf{a}) = -\mathbf{d}_1\vec{\mathcal{E}}_2$. In which configurations do the dipoles attract, in which do they repel each other?
c. A current research area deals with cold dipolar molecules, for example, RbLi molecules having a permanent dipole electrical moment of $d_{RbLi} = 4.3$ Debye. What should be the atomic density n, where $n = a^{-3}$, in order to obtain a dipolar interaction U_0 at least as large as the thermal energy of the molecules? Ultra-cold molecular gases typically have a temperature around 10^{-6} K.

2.7.5.14 Ex: Photoelectric effect

During the process described by the photoelectric effect, ultraviolet light can be used to electrically charge a piece of metal.
a. If this light strikes a bar of conductive material electrons, and are ejected with sufficient energy to escape from the surface of the metal, after how much time will the metal have accumulated a charge of $+1.5\,$nC if $1.0 \cdot 10^6$ electrons are ejected per second?
b. If $1.3\,$eV is required to eject an electron from the surface, what is the power of the light beam? (Consider the process to be 100% efficient.)

2.7.5.15 Ex: Polonium and the use of the Green function

The radioactive metal Polonium (Po), discovered by Marie and Pierre Curie in 1898, crystallizes in a simple cubic lattice (each atom has six neighbors on a regular grid). The nucleus contains 84 protons and the diameter of the atom is approximately $3 \cdot 10^{-8}\,$cm. Calculate the distribution of the potential within a primitive cell of a Po crystal traversed by a constant current. Suppose the following model for the crystal: Atomic nuclei (radius $\sim 9 \cdot 10^{-13}\,$cm) are at positions $\mathbf{x}'_{\lambda\mu\nu} = (\lambda a + a/2, \mu a + a/2, \nu a + a/2)$ for $\lambda, \mu\nu = 0, \pm1, \pm2, ...$, and will be treated as point charges. The electronic shell of a Po atom is represented by charges induced in a grounded conducting cube of size a, in the middle of which is located the positively charged nucleus inducing these charges. Proceed as follows:
a. Start showing that,

$$G(\mathbf{r}, \mathbf{r}') = \frac{32}{\pi a} \sum_{l,m,n=1}^{\infty} \frac{1}{l^2+m^2+n^2} \sin\frac{l\pi x}{a} \sin\frac{l\pi x'}{a} \sin\frac{m\pi y}{a} \sin\frac{m\pi y'}{a} \sin\frac{n\pi z}{a} \sin\frac{n\pi z'}{a} ,$$

is the Green function for the Dirichlet contour problem of a cube with edge length a.
b. Calculate the potential in the atom at the position $(a/2, a/2, a/2)$, where we assume

for the interior of the cube a charge $\rho(x', y', z') = q\delta(x' - a/2)\delta(y' - a/2)\delta(z' - a/2)$ and that the potential on the six surfaces of the cube adopts the following values: $\Phi(\mathbf{r}') = 0$ on the surface $x' = 0$, $\Phi(\mathbf{r}') = V_0$ on the surface $x' = a$, and $\Phi(\mathbf{r}') = V_0 x'/a$ on the other 4 surfaces $y' = 0,\ y' = a,\ z' = 0,\ z' = a$.
c. Reformulate the term describing the contribution of the surface to the potential using that for $0 < x < \pi$ holds: $1 = (4/\pi)(\sin x + (1/3)\sin 3x + (1/5)\sin 5x + ...)$ and $x = 2(\sin x - (1/2)\sin 2x + (1/3)\sin 3x - (1/4)\sin 4x + ...)$.

2.7.5.16 Ex: Electrostatic potential of a hollow sphere via Green function

On the surface of a hollow sphere with radius b without charge there be a certain potential $V(\theta, \phi) = V_0[P_2(\cos\theta) + \alpha P_3(\cos\theta)]$. Calculate the electrostatic potential $\Phi(\mathbf{r})$ inside the sphere.
Help: Green's function for the interior space between two concentric spheres with radii a and b ($a < b$) is,

$$G(\mathbf{r}, \mathbf{r}') = \sum_{l=0}^{\infty} \frac{4\pi}{2l+1} \left[1 - \left(\frac{a}{b}\right)^{2l+1}\right] \left[r_<^l - \frac{a^{2l+1}}{r_<^{l+1}}\right] \left[\frac{1}{r_>^{l+1}} - \frac{r_>^l}{b^{2l+1}}\right] \sum_{m=-l}^{+l} Y_{lm}(\Omega) Y_{lm}^*(\Omega') \,.$$

where $r_< \equiv \min(|\mathbf{r}|, |\mathbf{r}'|)$ and $r_> \equiv \max(|\mathbf{r}|, |\mathbf{r}'|)$. We also know, $Y_{l0}(\theta, \phi) = \sqrt{(2l+1)/4\pi} P_l(\cos\theta)$.

2.8 Further reading

D.J. Griffiths, *Introduction to Electrodynamics* [ISBN]

D. Halliday, R. Resnick, and J. Walker, *Fundamentals of Physics* [ISBN]

H.M. Nussenzveig, *Curso de Física Básica: Eletromagnetismo (Volume 3)* [ISBN]

Chapter 3

Electrical properties of matter

There are many types of materials, such as solids, liquids, gases, metals, wood or glass, all of which respond differently to applied electric fields. However, most materials can at least roughly be classified into two categories: In materials called *dielectrics* (or insulators) the electrons are strongly bound to the atoms, while in *metals* there are free electrons. Some materials, such as semiconductors, have particular properties, which do not fit into these categories.

Under the influence of electric (or magnetic) forces the electrons can be displaced within a macroscopic body, thus producing a polarization, when the electrons are bound, or a current, when the electrons are free.

3.1 Polarization of dielectrics

Let us first discuss dielectrics. The elementary blocks (molecules) of dielectric materials can react in various ways to applied electric fields, For example, they can be insensitive to electric fields or behave like *permanent dipoles*. Permanent dipoles exist independently of the application of an external field, but generally (without external field) they have random and disorderly orientations. Under the influence of an external field the dipoles will try to reorient themselves, which is called *orientation polarization*.

It is also possible that a material does not have intrinsic dipole moments, but *develops* dipole moments under the action of an external field. In this case we speak of *induced dipoles*. Induced dipoles are formed in the presence of a field displacing bound positive and negative charges in molecules against each other, thus producing a *translation polarization*.

3.1.1 Energy of permanent dipoles

Polar molecules exhibit permanent electric moments. Water is an example or salt Na^+Cl^-. The reason is that halogens, which have a much higher electro-affinity than alkalines, and try to steal electrons from their partner and monopolize the electronic cloud.

The potential energy of a dipole depends on its orientation with respect to the electric field. Using the parametrization $\varrho(\mathbf{r}') = Q[\delta^3(\mathbf{r}' - \frac{\mathbf{a}}{2}) - \delta^3(\mathbf{r}' + \frac{\mathbf{a}}{2})]$, we find for the interaction energy with a homogeneous field given by $\Phi(\mathbf{r}') = -\mathcal{E}_0 z'$,

$$H_{int} = \int \varrho(\mathbf{r}')\Phi(\mathbf{r}')dV = -Q\mathcal{E}_0 a_z = -\mathbf{d}\cdot\vec{\mathcal{E}} \ . \tag{3.1}$$

Hence [1],

$$\boxed{H_{int} = -\mathbf{d}\cdot\vec{\mathcal{E}}} \ . \tag{3.2}$$

The energy is minimal when $\mathbf{d} \parallel \vec{\mathcal{E}}$.

To calculate the interaction energy between two dipoles $\mathbf{d}_1$ and $\mathbf{d}_2$ we calculate the energy of $\mathbf{d}_1$ within the field created by $\mathbf{d}_2$ (which has been derived in the example 28),

$$H_{int} = -\mathbf{d}_1\cdot\vec{\mathcal{E}}_2 = -\mathbf{d}_1\cdot\frac{1}{4\pi\varepsilon_0}\frac{3(\hat{\mathbf{e}}_r\cdot\mathbf{d}_2)\hat{\mathbf{e}}_r - \mathbf{d}_2}{r^3} = \frac{1}{4\pi\varepsilon_0}\frac{\mathbf{d}_1\cdot\mathbf{d}_2 - 3(\mathbf{d}_1\cdot\hat{\mathbf{e}}_r)(\mathbf{d}_2\cdot\hat{\mathbf{e}}_r)}{r^3} \ . \tag{3.3}$$

3.1.1.1 Alignment of permanent dipoles

In a homogeneous field the force on an (neutral) electric dipole $\mathbf{d} = Q\mathbf{a}$ vanishes, since $\mathbf{F} = Q\vec{\mathcal{E}} + (-Q)\vec{\mathcal{E}} = 0$. However, there will be a torque because,

$$\vec{\tau} = \frac{\mathbf{a}}{2}\times Q\vec{\mathcal{E}} + \frac{-\mathbf{a}}{2}\times(-Q)\vec{\mathcal{E}} = \mathbf{d}\times\vec{\mathcal{E}} \ . \tag{3.4}$$

This means that a freely moving molecule will rotate about its mass center, as illustrated in Fig. 3.1, until (in the presence of dissipation) it finds the orientation with the lowest energy. In this orientation the molecule is aligned to the applied field. See Exc. 3.1.7.1.

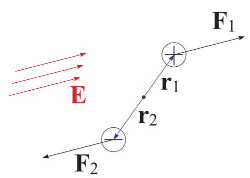

Figure 3.1: Torque on a dipole exerted by an electric field.

In a *non-homogeneous* field, the forces on the charges $\pm Q$ do not compensate [2], $\mathbf{F} = Q\vec{\mathcal{E}}_+ - Q\vec{\mathcal{E}}_- = Q(\mathbf{a}\cdot\nabla)\vec{\mathcal{E}}$. Hence,

$$\boxed{\mathbf{F} = (\mathbf{d}\cdot\nabla)\vec{\mathcal{E}}} \ . \tag{3.5}$$

Placed in front of a conductive surface a dipole feels the forces exerted by the charge of its own image. In Exc. 3.1.7.2 we calculate the torque exerted by a conducting surface on a dipole.

[1] We can also calculate the energy of a dipole in an electric field by the work required to rotate it away from its rest position, $H_{int} = \int \vec{\tau}\cdot d\theta = \int \mathbf{d}\times\vec{\mathcal{E}} d\theta = \int_0^\theta dE\sin\theta d\theta = -dE\cos\theta$.

[2] We note that the force that a field exerts on a dipole can be calculated as a gradient of the interaction energy: $\mathbf{F} = -\nabla H_{int} = \nabla(\mathbf{d}\cdot\vec{\mathcal{E}}) = (\mathbf{d}\cdot\nabla)\vec{\mathcal{E}} + (\vec{\mathcal{E}}\cdot\nabla)\mathbf{d} + (\mathbf{d}\times\nabla)\times\vec{\mathcal{E}} + (\vec{\mathcal{E}}\times\nabla)\times\mathbf{d} = (\mathbf{d}\cdot\nabla)\vec{\mathcal{E}}$.

3.1.2 Induction of dipoles in dielectrics

A priori, neutral non-polar atoms and molecules should not react to applied electric fields. However, the fact that atoms are composed of positive charge distributions (concentrated in a heavy nucleus) and negative ones (concentrated in a light-weighed electron shell), permits a more or less important displacement of these charge distributions with respect to the center-of-mass. Consequently, an electric field *polarizes the atom* and induces an electric dipole moment whose magnitude is approximately proportional to the field,

$$\boxed{\mathbf{d} = \alpha_{pol}\vec{\mathcal{E}}} \ , \tag{3.6}$$

where the constant α_{pol} is called *polarizability*.

Example 30 (*Polarizability of a primitive atom*): In a primitive model we envision an atom as a point-like nucleus carrying the charge $+Q$ surrounded by a uniformly charged electron sphere with radius a carrying the inverse charge $-Q$. In the presence of an external field $\vec{\mathcal{E}}$ the nucleus will be slightly shifted by a distance $\epsilon/2$ to one side and the electron sphere by a distance $-\epsilon/2$ to the opposite side. The polarized atom is in equilibrium, when the field created by the induced dipole $\mathcal{E}_{dp}$ (calculated in Exc. 2.2.4.5) equalizes the external field, i.e.,

$$\mathcal{E}_{dp} = \frac{1}{4\pi\varepsilon_0}\frac{Q\epsilon}{a^3} = \mathcal{E} \ .$$

Hence,

$$\frac{\alpha_{pol}}{4\pi\varepsilon_0} = \frac{d}{4\pi\varepsilon_0\mathcal{E}} = a^3 \approx 0.15\cdot 10^{-30}\,\mathrm{m}^3 \ ,$$

using for $a = a_B$ the Bohr radius. Despite the simplicity of the model, this results represents a good approximation. A slightly better model is discussed in Exc. 3.1.7.3.

The values for the atomic polarizability range from $\alpha_{pol}/4\pi\varepsilon_0 = 0.205\cdot 10^{-30}\,\mathrm{m}^3$ for helium to $59.6\cdot 10^{-30}\,\mathrm{m}^3$ for cesium. This shows that it is far more difficult to polarize atoms with closed electron shells (like noble gases) than atoms with isolated valence electron (such as alkaline atoms). Molecules may react in a more complicated way to the applied fields necessitating an interpretation of the polarizability α_{pol} in terms of a tensor represented by a matrix.

3.1.2.1 Energy of induced dipoles

We now calculate the energy of a polarizable molecule inside an external electric field. We expect two contributions: The first one is the energy W_{ind} stored in the field created by the separation of charges under the action of the external field. The second contribution is the energy H_{int} due to the interaction of the induced dipole with the external field.

W_{ind} is calculated by the work spent on separating the charges. Let e be the valence charge bound to the molecule. The force between this charge and the molecule is described, in first approximation, by a harmonic oscillator with the spring constant k. Inside the electric field, the charge feels the force $e\vec{\mathcal{E}}$, but at the same time the force of the 'molecular spring' goes in the opposite direction. In equilibrium,

$$-k\mathbf{a} + e\vec{\mathcal{E}} = 0 \ . \tag{3.7}$$

To induce this dipole, the electric field must do the work,

$$W_{ind} = \tfrac{1}{2}ka^2 = \tfrac{1}{2}e\mathcal{E}a \ . \tag{3.8}$$

Defining the induced dipole as $\mathbf{d}_{ind} \equiv Ze\mathbf{d}$, we obtain:

$$W_{ind} = \tfrac{1}{2}\mathbf{d}_i \cdot \vec{\mathcal{E}} \ . \tag{3.9}$$

Since the energy of a dipole in an external electric field is, $H_{int} = -\mathbf{d}_i \cdot \vec{\mathcal{E}}$, for the induced dipole we obtain the total energy,

$$H_{tot} = H_{int} + W_{ind} = -\tfrac{1}{2}\mathbf{d}_i \cdot \vec{\mathcal{E}} \ . \tag{3.10}$$

The energy value is less than in the case of a permanent dipole (3.5), since part of the energy had to be spent on creating the dipole in the first place. Expressing the dipole moment by the polarizability (3.6),

$$\boxed{H_{tot} = -\frac{\alpha_{pol}}{2}\vec{\mathcal{E}}^2} \ . \tag{3.11}$$

3.1.3 Macroscopic polarization

With these results we can now describe, what happens to a dielectric material placed in an electric field: If the substance consists of neutral atoms (or non-polar molecules), the field will induce in each particle a small dipole moment pointing in the direction of the field. If the substance consists of polar molecules, each permanent dipole will try to orientate itself along the field [3].

Note that both mechanisms produce the same result: a multitude of small dipoles aligned along the applied field. The sum of the microscopic moments gives rise to a macroscopic *polarization* defined by the sum over all dipole moments,

$$\vec{\mathcal{P}} = \frac{N\mathbf{d}}{V} \ . \tag{3.12}$$

In reality, the two types of polarization are not always well separated, and there are cases where both contribute. Nevertheless, it is usually much easier to rotate a molecule (rotational energy) than to stretch it (vibrational energy). In some (ferro-electric) materials it is possible to freeze the polarization.

3.1.4 Electrostatic field on a polarized or dielectric medium

In this section we will describe the electric field inside a polarized medium forgetting the physical cause of the polarization $\vec{\mathcal{P}}$. The field produced by the polarization (not the external field) can be calculated by the sum of the fields produced by the individual dipoles,

$$\Phi(\mathbf{r}) = \frac{1}{4\pi\varepsilon_0}\sum_k \frac{\mathbf{d}_k \cdot (\mathbf{r} - \mathbf{r}_k)}{|\mathbf{r} - \mathbf{r}_k|^3} \longrightarrow \frac{1}{4\pi\varepsilon_0}\int_{\mathcal{V}} dV' \frac{\vec{\mathcal{P}}(\mathbf{r}') \cdot (\mathbf{r} - \mathbf{r}')}{|\mathbf{r} - \mathbf{r}'|^3} \ , \tag{3.13}$$

[3] Note that thermal motion, particularly at high temperatures, competes with this process, such that the alignment will never be perfect.

introducing the dipole moment distribution $\vec{\mathcal{P}}(\mathbf{r}')$ by $\mathbf{d}_k \to \vec{\mathcal{P}}dV'$. We can rewrite the integral in the form,

$$\Phi(\mathbf{r}) = \frac{1}{4\pi\varepsilon_0}\int_{\mathcal{V}} \vec{\mathcal{P}}(\mathbf{r}') \cdot \nabla' \frac{1}{|\mathbf{r}-\mathbf{r}'|}dV' = \frac{1}{4\pi\varepsilon_0}\left[\int_{\mathcal{V}} \nabla' \cdot \frac{\vec{\mathcal{P}}(\mathbf{r}')}{|\mathbf{r}-\mathbf{r}'|}dV' - \int_{\mathcal{V}} \frac{1}{|\mathbf{r}-\mathbf{r}'|}\nabla'\vec{\mathcal{P}}(\mathbf{r}')dV'\right]$$
$$= \frac{1}{4\pi\varepsilon_0}\oint_{\partial\mathcal{V}} \frac{\vec{\mathcal{P}}(\mathbf{r}')}{|\mathbf{r}-\mathbf{r}'|}dS' - \frac{1}{4\pi\varepsilon_0}\int_{\mathcal{V}} \frac{1}{|\mathbf{r}-\mathbf{r}'|}\nabla' \cdot \vec{\mathcal{P}}(\mathbf{r}')dV' \ . \tag{3.14}$$

Defining,

$$\boxed{\sigma_b \equiv \vec{\mathcal{P}} \cdot \mathbf{n}_S} \qquad \text{and} \qquad \boxed{\varrho_b \equiv -\nabla \cdot \vec{\mathcal{P}}} \ , \tag{3.15}$$

we obtain

$$\Phi(\mathbf{r}) = \frac{1}{4\pi\varepsilon_0}\oint_{\partial\mathcal{V}} \frac{\sigma_b}{|\mathbf{r}-\mathbf{r}'|}dS' - \frac{1}{4\pi\varepsilon_0}\int_{\mathcal{V}} \frac{\varrho_b}{|\mathbf{r}-\mathbf{r}'|}dV' \ . \tag{3.16}$$

The meaning of this result is that the potential (and therefore the field) of a polarized object is the same as the one produced by a volume distribution ϱ_b plus a surface charge distribution σ_b. The index b indicates the fact that we consider here 'bound charges' (i.e. localized charges). Instead of integrating the field contributions of all individual infinitesimal dipoles, as in Eq. (3.13), we can try to find these bound charges, and then calculate the fields they produce, as we already did in the previous chapter.

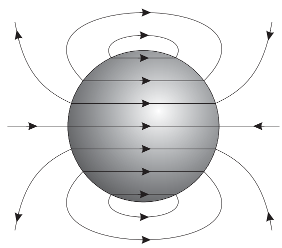

Figure 3.2: Distortion of polarization.

Example 31 (*Microscopic theory of induced dipoles*): As an example we calculate the electric field produced by a homogeneous polarization within a sphere. While the volume charge is zero (otherwise $\vec{\mathcal{P}}$ could not be uniform), the surface charge is $\sigma_b = \vec{\mathcal{P}} \cdot \mathbf{n}_S = \mathcal{P}\cos\theta$. This charge distribution generates a potential which, applying the result derived in example 25, we can write,

$$\Phi(r,\theta) = \begin{cases} \frac{\mathcal{P}}{3\varepsilon_0}r\cos\theta = \frac{1}{4\pi\varepsilon_0}\frac{\mathbf{d}\cdot\mathbf{r}}{R^3} & \text{for } r \leq R \\ \frac{\mathcal{P}}{3\varepsilon_0}\frac{R^3}{r^2}\cos\theta = \frac{1}{4\pi\varepsilon_0}\frac{\mathbf{d}\cdot\mathbf{r}}{r^3} & \text{for } r \geq R \end{cases} ,$$

with $\mathbf{d} = \frac{4\pi}{3}R^3\vec{\mathcal{P}}$. The potential produces a field, which is uniform within the sphere,

$$\vec{\mathcal{E}} = -\nabla\Phi = \begin{cases} -\frac{\mathcal{P}}{3\varepsilon_0}\hat{\mathbf{e}}_z\frac{\partial\Phi}{\partial z} = -\frac{\vec{\mathcal{P}}}{3\varepsilon_0} & \text{for } r \leq R \\ \frac{\mathcal{P}}{3\varepsilon_0}\frac{R^3}{r^2}\cos\theta = \frac{1}{4\pi\varepsilon_0}\frac{3(\hat{\mathbf{e}}_r\cdot\mathbf{d})\hat{\mathbf{e}}_r-\mathbf{d}}{r^3} & \text{for } r \geq R \end{cases} .$$

The physical interpretation of the surface charge produced by a uniform polarization is simply a displacement of all the electrons of the body with respect to the positively charged nuclei. Since the electrons remain attached to the nuclei, the volume charge inside the sphere remains neutral. However, the edges of the body accumulate negative charge on one side and positive charge on the other.

3.1.5 Electric displacement

In the previous section we found that the phenomenon of polarization can be understood as being due to a volume charge $\varrho_b = -\nabla \cdot \vec{\mathcal{P}}$ inside the dielectric and a surface charge on the surface of the body $\sigma_b = \vec{\mathcal{P}} \cdot \mathbf{n}_S$. However, many materials have dielectric characteristics and at the same time conductive characteristics, which do not result from a polarization and which we take into account via a distribution of free charges, ϱ_f, the index f indicating 'free charges'.

3.1.5.1 Gauß' Law in dielectric media

Gauß's law can now be generalized for arbitrary media,

$$\varepsilon_0 \nabla \cdot \vec{\mathcal{E}} = \varrho = \varrho_b + \varrho_f = -\nabla \cdot \vec{\mathcal{P}} + \varrho_f \ , \tag{3.17}$$

where $\vec{\mathcal{E}}$ is the total electric field. Defining a new field called the *electric displacement*,

$$\boxed{\vec{\mathcal{D}} \equiv \varepsilon_0 \vec{\mathcal{E}} + \vec{\mathcal{P}}} \ , \tag{3.18}$$

we can now write,

$$\nabla \cdot \vec{\mathcal{D}} = \varrho_f \ . \tag{3.19}$$

The electric displacement is that part of the electric field, which comes only from free charges (which is the part useful for generating currents). We can also define the *electric susceptibility* χ_ε via,

$$\vec{\mathcal{P}} = \varepsilon_0 \chi_\varepsilon \vec{\mathcal{E}} \ , \tag{3.20}$$

or the *permittivity* ε via,

$$\vec{\mathcal{D}} = \varepsilon \vec{\mathcal{E}} = \varepsilon_0 (1 + \chi_\varepsilon) \vec{\mathcal{E}} \ . \tag{3.21}$$

Note that the rotation of the polarization *does not necessarily vanish*, since the susceptibility may depend on position, $\chi_\varepsilon = \chi_\varepsilon(\mathbf{r})$,

$$\nabla \times \vec{\mathcal{D}} = \varepsilon_0 (\nabla \times \vec{\mathcal{E}}) + \nabla \times \vec{\mathcal{P}} = \nabla \times (\varepsilon_0 \chi_\varepsilon \vec{\mathcal{E}}) \neq 0 \ . \tag{3.22}$$

Therefore, $\vec{\mathcal{D}}$ generally can not be derived from a potential, and Coulomb's law is not valid for $\vec{\mathcal{D}}$.

3.1.5.2 Boundary conditions involving dielectrics

The integral version of Gauß's law, $\oint \vec{\mathcal{D}} \cdot d\mathbf{S} = Q_f$, allows us to determine the behavior of the electric displacement near interfaces,

$$\mathcal{D}^\perp_{top} - \mathcal{D}^\perp_{bottom} = \sigma_f \ . \tag{3.23}$$

On the other hand, Stokes' law $\nabla \times \vec{\mathcal{D}} = \varepsilon_0 \nabla \times \vec{\mathcal{E}} + \nabla \times \vec{\mathcal{P}} = \nabla \times \vec{\mathcal{P}}$ yields,

$$\vec{\mathcal{D}}^{||}_{top} - \vec{\mathcal{D}}^{||}_{bottom} = \vec{\mathcal{P}}^{||}_{top} - \vec{\mathcal{P}}^{||}_{bottom} \ . \tag{3.24}$$

This is in contrast to the behavior of the electric $\vec{\mathcal{E}}$ field at interfaces described by Eqs. (2.37) and (2.39).

3.1.6 Electrical susceptibility and permittivity

3.1.6.1 Linear dielectrics

In many materials, as long as the applied electric field is not too strong, the polarization is proportional to the field, $\vec{\mathcal{P}} \propto \vec{\mathcal{E}}$, that is, the electric susceptibility depends on the material's microscopic properties and external factors such as temperature, but not on the applied field, $\chi_\varepsilon \neq \chi_\varepsilon(\vec{\mathcal{E}})$. Hence, linear media can be characterized by a constant,

$$\varepsilon_r \equiv \frac{\varepsilon}{\varepsilon_0} \ , \tag{3.25}$$

called *relative permittivity*.

In *non-linear* media, in contrast, the susceptibility $\chi_\varepsilon(\vec{\mathcal{E}})$ depend on the strength of the electric field. Often the polarization can be expanded in orders of the electric field,

$$\vec{\mathcal{P}}(\vec{\mathcal{E}}) = \varepsilon^{(1)}\vec{\mathcal{E}} + \varepsilon^{(2)}\vec{\mathcal{E}}^2 + \varepsilon^{(3)}\vec{\mathcal{E}}^3 + \ldots \ . \tag{3.26}$$

In *anisotropic* materials the situation gets more complicated, because the susceptibility and the permittivity must be understood as tensors,

$$\mathcal{P}_k(\vec{\mathcal{E}}) = \sum_m \varepsilon^{(1)}_{km}\mathcal{E}_m + \sum_{ml} \varepsilon^{(2)}_{kml}\mathcal{E}_m\mathcal{E}_l + \sum_{mlj} \varepsilon^{(3)}_{kmlj}\mathcal{E}_m\mathcal{E}_l\mathcal{E}_j + \ldots \ . \tag{3.27}$$

Example 32 (*Microscopic theory of induced dipoles*): We know that an *external electric field* $\vec{\mathcal{E}}_{ext}$ applied to a linear purely dielectric medium generates a *macroscopic polarization* proportional to the field,

$$\vec{\mathcal{P}} = \chi_\varepsilon \varepsilon_0 \vec{\mathcal{E}}_{ext} \ .$$

On the other hand, if the material consists of atoms (or non-polar molecules), the *microscopic dipole moment* induced in each atom is proportional to the *local field*,

$$\mathbf{d}_{ind} = \alpha_{pol}\vec{\mathcal{E}}_{loc} \ .$$

Here, $\vec{\mathcal{E}}_{loc}$ is the *total field* due to the applied field $\vec{\mathcal{E}}_{ext}$ plus the field $\vec{\mathcal{E}}_{self}$ generated by the polarization of the other atoms which are around. The question now is, what is the relationship between the atomic polarizability α_{pol} (characterizing the sample from a microscopic point of view) and the susceptibility χ_e (characterizing the sample from a macroscopic point of view)?
To begin with we consider low densities, in which case it is a good approximation to suppose that the atom does not feel the polarization of its neighbors, that is $\vec{\mathcal{E}}_{loc} \simeq \vec{\mathcal{E}}_{ext}$. We already noticed in Eq. (??) that the polarization is nothing more than the sum over all the dipole moments induced by the local electric field, such that, comparing the last two relations, a first trial would be to affirm,

$$\chi_\varepsilon = \frac{N}{V}\frac{\alpha_{pol}}{\varepsilon_0} \ .$$

But for dense gases, there will be a correction, and the local field will be a superposition of the external field and the field generated by the surrounding dipoles, $\vec{\mathcal{E}}_{loc} = \vec{\mathcal{E}}_{ext} + \vec{\mathcal{E}}_{self}$. To estimate this field, we imagine a single dipole located inside a sphere. The polarization of the surrounding medium is modeled by a surface charge density with the value $\sigma_b \equiv -\mathcal{P}\cos\theta$. The electric field produced by this charge distribution was calculated in example 31: $\vec{\mathcal{E}}_{self} = \vec{\mathcal{P}}/3\varepsilon_0$. With this we calculate,

$$\chi_\varepsilon = \frac{\mathcal{P}}{\varepsilon_0\mathcal{E}_{ext}} = \frac{\mathcal{P}}{\varepsilon_0(\mathcal{E}_{loc} - \mathcal{E}_{self})} = \frac{\mathcal{P}}{\varepsilon_0(\frac{p_{ind}}{\alpha_{pol}} - \frac{\mathcal{P}}{3\varepsilon_0})} = \frac{N\alpha_{pol}/\varepsilon_0 V}{1 - N\alpha_{pol}/3\varepsilon_0 V} \ . \tag{3.28}$$

This equation is known as *Clausius-Mossotti formula*. The difference between the denominator and 1, called *Lorentz-Lorenz shift*, comes from the energy displacements of the atoms due to the dipole-dipole interactions. At low densities we recover the linear relation. In terms of the relative permittivity we can also write,

$$\frac{\alpha_{pol}}{\varepsilon_0} = \frac{3V}{N}\frac{\varepsilon_r - 1}{\varepsilon_r + 2} \ .$$

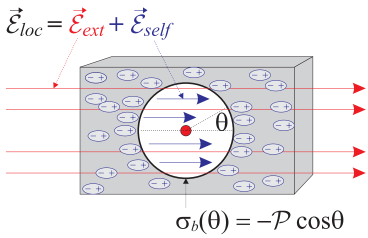

Figure 3.3: The local field $\vec{\mathcal{E}}_{loc}$ is the sum of the external field $\vec{\mathcal{E}}_{ext}$ and the field generated by the polarization $\vec{\mathcal{E}}_{self}$.

3.1.7 Exercises

3.1.7.1 Ex: Torque on dipoles

Calculate the torque on a dipole in front of a conducting surface.

3.1.7.2 Ex: Torque on dipoles

Consider the configuration of two dipoles shown in the figure and calculate the reciprocal torques.

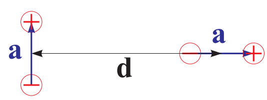

Figure 3.4: Dipoles.

3.1.7.3 Ex: Polarizability of hydrogen

In quantum mechanics we find for the electronic charge distribution in a hydrogen atom,

$$\varrho(r) = \frac{Q}{\pi a_B^3} e^{-2r/a_B} \ .$$

Calculate the polarizability.

3.1.7.4 Ex: Susceptibility

One liter of water is evaporated in $10\,\text{m}^3$ of dry air at room temperature $T = 300\,\text{K}$.
a. Calculate the dipolar density n of the air. Assume that only the dipolar moments of the evaporated molecules contribute.
b. Determine the susceptibility χ_ε of the air. Use the relation $\mathcal{P} = \varepsilon_0 \chi_\varepsilon \mathcal{E}$, as well as Curie's law for the polarization $\mathcal{P}$.

3.2 Influence of charges and capacitance

We now assume that we have two separate conductors, one carrying the charge $+Q$ and the other $-Q$. Since the potential of each conductor is the same at each point of its body, we can specify a potential difference, called *voltage*, between them,

$$U \equiv \Phi_+ - \Phi_- = -\int_{(-)}^{(+)} \vec{\mathcal{E}} \cdot d\mathbf{l} \ , \tag{3.29}$$

which does not depend on the distribution of the charges throughout the conductors. However, we know from Coulomb's law that the electric field is proportional to the charge Q and from the above equation, also the voltage. The proportionality factor is called *capacitance*,

$$C \equiv \frac{Q}{U} \ . \tag{3.30}$$

3.2.1 Capacitors and storage of electric energy

A device capable of storing charges is called *capacitor*.

> **Example 33 (*Plate capacitor*):** The simplest geometry for a capacitor are two parallel conducting plates (area S) maintained at a distance d. The surface charge distribution $\sigma = Q/S$ produces a field $\mathcal{E} = \sigma/\varepsilon_0$ and a potential difference $U = \mathcal{E}d$, such that,
>
> $$C = \varepsilon_0 \frac{S}{d} \ . \tag{3.31}$$

To charge a capacitor we must bring electrons from the positive side to the negative side of the capacitor. For a single electron, this requires the work

$$\Delta W_e = \int_0^d \mathbf{F} \cdot d\mathbf{r} = ed|\vec{\mathcal{E}}| = eU \ .$$

For a small amount of charge dq,

$$\Delta W_e = \int U\ dQ = \int_0^Q \frac{Q}{C} dQ = \frac{Q^2}{2C} = \frac{1}{2} CU^2 \ .$$

Resolve the Excs. 3.2.2.1-3.2.2.10.

3.2.1.1 Capacitors with dielectrics

In the presence of a dielectric the capacitance increases, $C = \varepsilon_r C_{vac}$. Thus, the field energy also increases by a factor of ε_r.

We consider a capacitor filled with a linear dielectric and charged with the free charge ϱ_f, which generates a voltage U between the electrodes. We want to know the work needed to add a little bit more charge $\delta\varrho_f$ to the volume element dV,

$$\delta W = \int U\ \delta\varrho_f dV \ . \tag{3.32}$$

Now, with Eq. (3.19) we write $\varrho_f = \nabla \cdot \vec{\mathcal{D}}$ and $\delta\varrho_f = \nabla \cdot \delta\vec{\mathcal{D}}$, such that,

$$\delta W = \int_{\mathcal{V}} U \nabla \cdot \delta\vec{\mathcal{D}} dV = \int_{\partial\mathcal{V}} U\ \delta\vec{\mathcal{D}} \cdot d\mathbf{S} - \int_{\mathcal{V}} \delta\vec{\mathcal{D}} \cdot \nabla U dV = \int_{\mathcal{V}} \delta\vec{\mathcal{D}} \cdot \vec{\mathcal{E}} dV \ . \tag{3.33}$$

For a linear dielectric, $\vec{\mathcal{D}} = \varepsilon\vec{\mathcal{E}}$, such that, $\vec{\mathcal{E}} \cdot \delta\vec{\mathcal{D}} = \vec{\mathcal{E}}\varepsilon \cdot \delta\vec{\mathcal{E}} = \frac{1}{2}\delta(\varepsilon E^2) = \frac{1}{2}\delta(\vec{\mathcal{D}} \cdot \vec{\mathcal{E}})$, giving,

$$\delta W = \tfrac{1}{2} \int \delta(\vec{\mathcal{D}} \cdot \vec{\mathcal{E}}) dV \ . \tag{3.34}$$

Finally, to charge the capacitor completely,

$$W = \int \delta W = \tfrac{1}{2} \int \vec{\mathcal{D}} \cdot \vec{\mathcal{E}} = \int u dV \ , \tag{3.35}$$

with the energy density,

$$\boxed{u = \frac{1}{2} \vec{\mathcal{E}} \cdot \vec{\mathcal{D}}} \ . \tag{3.36}$$

Do the Excs. 3.2.2.11-3.2.2.18.

Example 34 (*Forces on dielectrics*): Dielectrics in electric fields are subjected to forces due to the polarization induced in the medium. Let us consider the example of a plate capacitor inside which we insert a dielectric. In the scheme shown in Fig. 3.5 the electric field homogeneously traverses the capacitor and also the dielectric body, such that the forces should disappear. On the other hand, on its edges the dielectric distorts the field, such that forces become possible.
The easiest way to calculate these forces is via the potential energy gradient, $\mathbf{F} = -\nabla W$. If the dielectric body is free to move in x-direction, we have,

$$\mathbf{F} = -\frac{dW}{dx} = -\frac{d}{dx} \frac{Q^2}{2C} = -\frac{d}{dx} \frac{CU^2}{2} \ .$$

We use the first expression, in case the charge on the capacitor is kept constant, and the second, when the voltage on the capacitor is kept constant. Gradually inserting the dielectric, a part of the volume of the capacitor will be empty and another part will be filled with the dielectric medium:

$$C = C_{vac}\frac{x}{a} + C_{vac}\varepsilon_r\frac{a-x}{a} \ .$$

Keeping the charge constant, we get,

$$\mathbf{F} = \frac{Q^2}{2C^2}\frac{dC}{dx} = -\frac{d}{dx}\frac{Q^2}{2(C_{vac}\frac{x}{a} + C_{vac}\varepsilon_r\frac{a-x}{a})} = \frac{Q^2}{2C_{vac}}\frac{-a\chi_\varepsilon}{(a-x\chi_\varepsilon)^2} \ .$$

Since the force is negative, the dielectric is drawn into the capacitor.
The situation is different when we keep the voltage constant, for example, by connecting the capacitor to a battery. In this case we need to use the second expression. However, we must take into account the work UdQ that the battery must do to increase the charge on the capacitor in order to maintain the voltage constant while we increase the capacity via $C_{vac} \to C$,

$$dW = -Fdx + UdQ \ .$$

Hence,

$$F = -\frac{dW}{dx} + U\frac{dQ}{dx} = -\frac{U^2}{2}\frac{dC}{dx} + U^2\frac{dC}{dx} = \frac{Q^2}{2C^2}\frac{dC}{dx} \ ,$$

and we get the same result as in the case where we kept the charge constant.

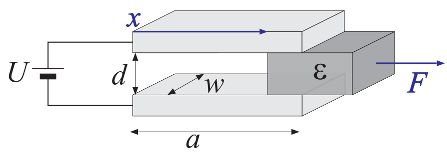

Figure 3.5: Force on the dielectric between the plates of a capacitor.

3.2.1.2 Capacitor circuits

For parallel circuits $C_{tot} = C_1 + C_2$, for circuits in series $C_{tot}^{-1} = C_1^{-1} + C_2^{-1}$. Do the Excs. 3.2.2.19-3.2.2.27.

3.2.2 Exercises

3.2.2.1 Ex: Capacitors

Be given two isolated conductors carrying equal charges but with opposite signs $\pm Q$. The capacity of this configuration is the ratio between the absolute value of the charge of one conductor and the absolute value of the potential difference between the two conductors. Using Gauß' law calculate the capacity of
a. 2 large parallel plates with area A being at a short distance d;
b. 2 concentric cylindrical conductors (without surfaces at the ends of the cylinders) with radii ρ_1 and ρ_2.
c. 2 concentric spherical surfaces with radii r_1 and r_2.
Help: Choose integration volumes that fits the symmetry of your system.

3.2.2.2 Ex: Capacitance of a mercury drop

The capacity of a spherical drop of mercury with radius R is given by $C = 4\pi\varepsilon_0$. Now, two of these drops merge. What is the capacity of this larger drop?

3.2.2.3 Ex: Charged plates

Consider a thin, very extended metal plate, $d^2 \ll A$, with area A and thickness d carrying the charge Q. Calculate the charge distribution (surface charge density) and the electric field on both sides of the plate neglecting edge effects. How do the charge distribution and the electric field change, when we have two plates instead of one with thickness d at a distance l, one being charged with the charge Q and the other with $-Q$.

3.2.2.4 Ex: Plate capacitor

A capacitor is made of two flat metal plates with the surfaces $1\,\text{m}^2$. What should be the distance of the plates to give the capacitor a capacity of $1\,\text{F}$? Is it possible to build such a capacitor?

3.2.2.5 Ex: Cylindrical capacitor

A cylindrical capacitor is made of two infinitesimally thin coaxial cylindrical surfaces with radii R_1 and R_2. For simplicity, assume that the cylinders are infinitely extended in z-direction. The charge per unit length on the inner cylinder is $+Q/l$, on the outer cylinder $-Q/l$. Calculate the electric field $\vec{\mathcal{E}}(r)$ as a function of the distance r from the symmetry axis for $r \leq R_1$, $R_1 < r < R_2$, and $r \geq R_2$.
Help: Use the symmetry of the problem and Gauß' law.

3.2.2.6 Ex: Cylindrical capacitor (T7)

Two concentric infinitely thin hollow conductive cylinders with radii a and b $(a < b)$ and length l are charged with charges $+q$ resp. $-Q$. l is much larger than b, such that border effects are negligible. For symmetry reasons, the electric field can only have one radial component.
a. Write down the charge distribution $\varrho(\mathbf{r})$ in cylindrical coordinates (r, ϕ, z) with the help of the δ-function.
b. Calculate the electric field $\vec{\mathcal{E}}(r, \phi, z)$ in the whole space $(r < a,\ a < r < b,\ b < r)$. Use for this the fundamental equations of electrostatics and $\nabla \cdot \vec{\mathcal{E}} = \frac{1}{r}\frac{d}{dr}(eE_r)$. Alternatively, this part can be resolved using Gauß' law.
c. Calculate the potential difference $|\Phi(r = b) - \Phi(r = a)|$ between the two surface of the cylinders. To do this, calculate the line integral $\int \vec{\mathcal{E}} \cdot d\mathbf{r}$ along a suitable path.
d. The capacity C of the device is defined by the absolute value of the ratio between the charge on one cylinder and the potential difference between the cylinders. Calculate the capacity of this 'cylindrical capacitor'.

3.2.2.7 Ex: Spherical capacitor

Consider a homogeneously charged ball with radius R_1 and an infinitely thin spherical homogeneously charged shell with radius R_2. The ball has the full charge $+Q$, the shell $-Q$. Calculate the electric field $\vec{\mathcal{E}}(r)$ for $r \leq R_1$, $R_1 < r < R_2$ and $r \geq R_2$.
Help: Use the fact that $\vec{\mathcal{E}}$ must be, for symmetry reasons, radially symmetrical, and depends on the charge density via $\nabla \cdot \vec{\mathcal{E}}(r) = \varrho(r)/\varepsilon_0$. Also use Gauß' law.

3.2.2.8 Ex: Thunderstorm

The cloud of a thunderstorm with $17\,\text{km}^2$ of total area floats at a height of 900 m above the Earth's surface and forms with it a plate capacitor.
a. Calculate the capacity of this plate capacitor (the area to be considered on Earth is equal to that of the cloud).
b. What is the maximum charge of the thundercloud before the capacitor discharges? (The discharge electric field in air is $10^4\,\text{V/cm}$).
c. The capacitor is totally discharged by a lightning, once the critical field strength is reached. What is the current flowing to Earth if the lightning's duration is 1 ms?
d. What power does this correspond to? For how long a power station with a power of 2000 MW needs to work to produce the energy released by lightning?

3.2.2.9 Ex: Spherical capacitor

A spherical capacitor consists of two concentric conducting spheres of radii R_1 and R_2, with $R_1 < R_2$. The inner sphere has a charge $+Q$ and the outer sphere has a charge $-Q$.
a. Calculate the absolute value of the electric field and the energy density as a function of r, where r is the radial distance from the center of the spheres for any r.
b. Determine the capacitance C of the capacitor.
c. Calculate the energy associated with the electric field integrated over a spherical shell of radius r, thickness dr, and volume $4\pi r^2 dr$ located between the conductors. Integrate the obtained expression to find the total energy between the conductors. Give your answer in terms of the charge Q and the capacitance C.

3.2.2.10 Ex: Lightning rod

The absorption of lightning by a lightning rod can be described by the following model (outlined in the figure): The (x, y) plane of a Cartesian coordinate system divides a half space with the conductivity κ (the soil of the Earth, $z < 0$) from a space with conductivity 0 (air, $z > 0$). In the center of the coordinates is an extremely conductive semispherical electrode connected with the lightning rod of diameter d. Current I can cross the semisphere and enter the conducting half space. For symmetry reasons, the current density may only depend on the distance r from the origin of the coordinates and must be oriented radially: $\mathbf{j} = j_r(r)\hat{\mathbf{e}}_r$. All of the following questions refer to points in the conductive semi-space outside the electrode.
a. Calculate the current density $\mathbf{j}$ as a function of the current amplitude I and the distance r from the source. **Help:** The current flowing from the electrode to the conducting half space must also exit the semisphere K.

b. Determine the electric field $\vec{\mathcal{E}}(\mathbf{r})$.
c. Determine the electrical voltage $U(x, s)$ between two points on the positive x-axis, having the coordinates x and $x + s$, respectively.
d. Determine the voltage U_{tot} for $x = d/2$ and $s \to \infty$. What ohmic resistance can be attributed to the conducting half space?

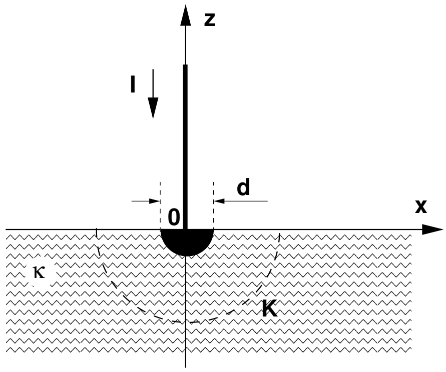

Figure 3.6:

3.2.2.11 Ex: Plate capacitor (H13)

An ideal plate capacitor consists of two parallel plates at a distance d. One of the plates, defined by the corners $(0, 0, 0)$, $(a, 0, 0)$, $(a, b, 0)$, and $(0, b, 0)$), be charged with the charge $-Q$, the other plate, defined by the corners $(0, 0, d)$, $(a, 0, d)$, (a, b, d) and $(0, b, d)$, has the charge $+Q$. A part of the intermediate space (up to the surface between the points $(x, 0, 0)$, $(x, b, 0)$, (x, b, d), and $(x, 0, d)$) be filled with a homogeneous dielectric with the dielectric constant ε; the rest of the space between the plates is empty. We assume that a and b are very large, such that border effects can be neglected.
a. Calculate the electric field $\vec{\mathcal{E}}$ and the dielectric displacement $\vec{\mathcal{D}}$ between the plates.
Help: Use $\nabla \times \vec{\mathcal{E}} = 0$ and $\nabla \cdot \vec{\mathcal{D}} = \varrho$. Use surface charge densities.
b. Calculate the energy of the electrostatic field W of this device.
c. What force $F = -dW/dx$ acts on the dielectric for an infinitesimal displacement dx?

3.2.2.12 Ex: Spherical capacitor with dielectric (H14)

Two concentric conducting spheres with radii a and b ($a < b$) carry the charges $\pm Q$. Half of the space between the spheres is filled by a dielectric $\varepsilon = const$.
a. Determine the electric field at all points between the spheres.
b. Calculate the surface charge distribution on the inner sphere.
c. Calculate the polarization charge density induced on the surface of the dielectric at $r = a$.

3.2.2.13 Ex: Potential of a charged sphere (T10)

A sphere of radius R be in the vacuum. It consists of a material with the dielectricity constant $\varepsilon = const$ and carries in its center the charge q. Calculate the potential in full space.

3.2.2.14 Ex: Plate capacitor with dielectric

We consider two parallel electrodes with area A and distance d (see figure). Calculate the force on the upper electrode in the x-direction, once for constant voltage V_0 and once for constant charge Q for the following two cases:
a. The electrodes are inside a dielectric liquid with permittivity ε;
b. a fixed dielectric with permittivity ε is introduced between capacitor plates. In the residual gap there is no dielectric medium.

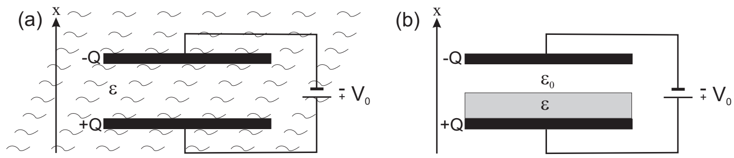

Figure 3.7: Plate capacitor.

3.2.2.15 Ex: Plate capacitor with dielectric

The plate capacitor shown in the figure has a plate surface of $A = 115\,\mathrm{cm}^2$ and a plate distance of $d = 1.24\,\mathrm{cm}$. Between the plates we have the potential difference $U_0 = 85.5\,\mathrm{V}$ produced by a battery. Now, the battery is removed and a dielectric $b = 0.78\,\mathrm{cm}$ thick plate with dielectric constant $\varepsilon = 2.61$ is inserted, as shown in the figure. First calculate
a. capacitance without dielectric and
b. the free charge on the capacitor plates.
c. Now, the dielectric is inserted. Calculate the electric field in the voids and within the dielectric, as well as
d. the potential difference between the plates.
e. What is the capacitance with dielectric?
f. Now assume that the battery remains connected to the capacitor while the dielectric is inserted into the space between the plates. Calculate now the capacitance,
g. the charge on the capacitor plates, and
h. the electric field in the void and inside the dielectric.

3.2.2.16 Ex: Plate capacitor with dielectric

Consider a quadratic plate capacitor with edge length l and plate distance d.
a. What is the capacity of the empty capacitor? What is the electrostatic energy when the plates are charged with the charges kept fixed $+Q$ and $-Q$?
b. A dielectric with thickness d, width $L > l$, and dielectric constant ε is now inserted

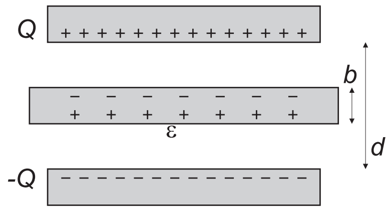

Figure 3.8: Plate capacitor.

from the side. What is the electrostatic energy as a function of penetration depth x for $0 < x < l$?
c. What is the force acting on the dielectric with function of x for $0 < x < l$?

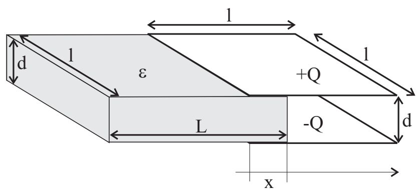

Figure 3.9: Plate capacitor.

3.2.2.17 Ex: Plate capacitor with dielectric

At a plate capacitor consisting of two parallel metal plates of area $0.5\,\text{m}^2$ and distant by $d = 10\,\text{cm}$, there be a voltage of $U_0 = 1000\,\text{V}$.
a. What are the values for the capacitance of the capacity C, the electrical field E between plates, and the charge surface density σ on the plates?
b. A quarter of the capacitor volume is now filled with a dielectric ($\varepsilon = 5$), as shown in the diagram. What is now the capacitance C_g?
Help: We may construct an equivalent circuit diagram by inserting imaginary capacitor plates along equipotential surfaces.

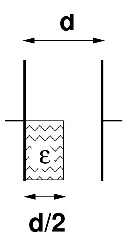

Figure 3.10: Plate capacitor.

3.2.2.18 Ex: Water capacitor

Consider a plate capacitor (plate distance $d = 20\,\text{cm}$, plate surface area $A = 400\,\text{cm}^2$), which can be half filled with water (dielectric constant $\varepsilon_w = 80.3$). We apply a voltage of $U = 240\,\text{V}$.
a. Calculate the capacitance of the capacitor for the following cases:
i. No water.
ii. The water is perpendicular to the plates..
iii. The water is parallel to the plates.
b. Calculate the charges on the plates for these three cases.
c. Compare the electric field energy of the cases (i) and (iii). From what source does the energy difference come from when the capacitor is filled with water?

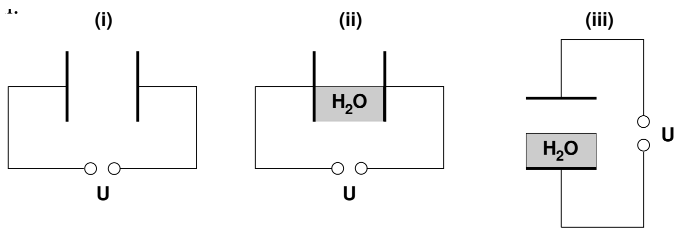

Figure 3.11: Capacitor.

3.2.2.19 Ex: Capacitor circuit

The capacitance of the capacitors in the schematic circuit are $C_1 = 10\,\mu\text{F}$, $C_2 = 5\,\mu\text{F}$ and $C_3 = 4\,\mu\text{F}$. The voltage is $U = 100\,\text{V}$.
a. Calculate the total capacitance.
b. Determine for each capacitor the value of the charge, voltage, and stored energy.

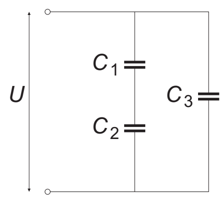

Figure 3.12: Capacitor.

3.2.2.20 Ex: Capacitor circuit

Calculate the total capacitance of the circuits shown in the figure.
a. between the points P1 and P3,
b. between the points P1 and P2.

3.2.2.21 Ex: Capacitor circuit

Calculate the total capacitance of the circuits shown in the figure.

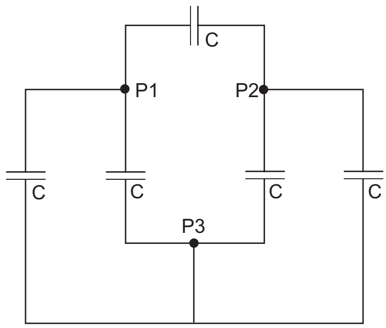

Figure 3.13: Capacitor circuit.

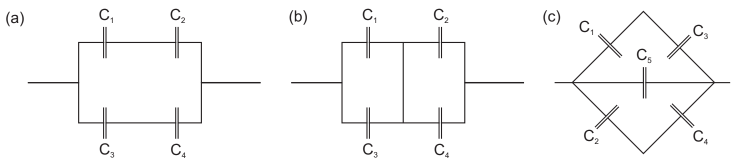

Figure 3.14: Capacitor circuit.

3.2.2.22 Ex: Energy in combinations of capacitors

a. Two identical capacitors are connected in parallel. This combination is then connected to the terminals of a battery. How does the total energy stored in the parallel combination of these two capacitors compare to the total energy stored if only one of the capacitors were connected to the terminals of the same battery?
b. Two identical discharged capacitors are connected in series. This combination is then connected to the terminals of a battery. How does the total energy stored in the in-series combination of these two capacitors compare to the total energy stored if only one of the capacitors were connected to the terminals of the same battery?

3.2.2.23 Ex: Plate capacitor

An air-filled plate capacitor consists of plates of $2.0\,\mathrm{m}^2$ area separated by $1\,\mathrm{mm}$ and is charged with $100\,\mathrm{V}$.
a. What is the electric field between the plates?
b. What is the electrical energy density between the plates?
c. Determine the total energy by multiplying the response to part (b) with the volume between the plates.
d. Determine the capacitance of this arrangement.
e. Calculate the total energy using $U = \frac{1}{2}CV^2$ and compare your answer with the result of part (c).

3.2.2.24 Ex: Combination of capacitors

A 10.0 μF capacitor and a 20.0 μF capacitor are connected in parallel to the terminals of a 6.0 V battery.
a. What is the equivalent capacitance of this combination?
b. What is the potential difference in each capacitor?
c. Determine the charge on each capacitor.
d. Determine the energy stored in each capacitor.

3.2.2.25 Ex: Infinite series of capacitors

What is the equivalent capacitance (in terms of C, which is the capacitance of one of the capacitors) of the infinite chain shown in the figure.

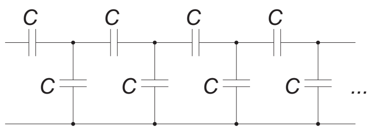

Figure 3.15: Capacitor circuit.

3.2.2.26 Ex: Reconnecting capacitors

A 100 pF capacitor and a 400 pF capacitor are both charged at 2.0 kV. They are then disconnected from the voltage source and connected together, positive plate to positive plate and negative plate to negative plate.
a. Determine the resulting potential difference at each capacitor.
b. Determine the dissipated energy when the connection is made.

3.2.2.27 Ex: Reconnecting capacitors

A 1.2 μF capacitor is charged at 30 V. After charging the capacitor is disconnected from the voltage source and is connected to the terminals of a second capacitor that had previously been discharged. The final voltage on the 1.2 μF capacitor is 10 V.
a. What is the capacitance of the second capacitor?
b. How much energy was dissipated when the connection was made?

3.3 Conduction of current and resistance

To charge a capacitor we need to carry charges to its electrodes. By permitting a displacement of charges we escape, in this section, for the first time from the premises of electrostatics and introduce the concept of a *current* as being due to a movement of charges within a conductor. For now, let us not raise the question, how this current will act on other charges or currents, this subject being discussed in the next chapter.

3.3.1 Motion of charges in dielectrics and conductors

In electrostatics the *electromotive force* accelerating a charge Q is the Coulomb force, $\mathbf{F} = Q\vec{\mathcal{E}}$. Interpreting the current as the sum of the motions v_k of all charges $\sum_k \frac{N_k}{V} Q_k$ within a volume V, we introduce the *current density* in a way analogous to the charge density,

$$\mathbf{j}(\mathbf{r}) = \sum_k \tfrac{N_k Q_k}{V} \mathbf{v}_k \longrightarrow \varrho(\mathbf{r}) \mathbf{v}_{med}(\mathbf{r}) \ , \tag{3.37}$$

where the average is calculated over a small volume. The flow of charges in and out of the volume satisfies the *continuity equation*,

$$\boxed{\nabla \cdot \mathbf{j} + \partial_t \varrho = 0} \ . \tag{3.38}$$

To interpret this equation we consider a volume $\mathcal{V}$ and calculate the flow of charges through the surface of the volume,

$$I \equiv \oint_{\partial \mathcal{V}} \mathbf{j} d\mathbf{S} = \int_{\mathcal{V}} \nabla \cdot \mathbf{j} dV = \int_{\mathcal{V}} \dot{\varrho} dV = \dot{Q} \ . \tag{3.39}$$

That is, the charges passing through the surface must accumulate within the volume. The charge flow I is called *current*.

3.3.2 Ohm's law, stationary currents in continuous media

In the case of free charges inside a conductor, we empirically observe that the electromotive force leads to a stationary current. Obviously, this current depends on the electric field,

$$\mathbf{j} = \mathbf{j}(\vec{\mathcal{E}}) \ , \tag{3.40}$$

despising the magnetic force, which is usually weak. Moreover, we find empirically that the current is often proportional to the field,

$$\boxed{\mathbf{j} = \varsigma \vec{\mathcal{E}}} \ . \tag{3.41}$$

with the *conductivity* ς. This observation is called *Ohm's law*.

We said earlier that $\vec{\mathcal{E}} = 0$ inside a conductor for electrostatic situations, $\mathbf{j} = 0$. This remains valid for perfect conductors, $\vec{\mathcal{E}} = \mathbf{j}/\varsigma = 0$, even when current is flowing.

3.3.2.1 Microscopic view of conduction

Ohm's law may seem surprising, since the current arising from charges accelerated by a potential difference, we would expect that the flow of charges (i.e. the current) should grow in time as the velocity of the charges increases. But in fact, the accelerated electrons often collide with the atoms of the conducting material and are decelerated by the electromotive force $F = m_e a$ or redirected. Moreover, at finite temperature, the thermal velocity of the electrons is very high,

$$v_{term} = \sqrt{\frac{2k_B T}{3m_e}} \approx 6700\,\mathrm{m/s} \ , \tag{3.42}$$

so that the average velocity is constant. The time between two collisions of an electron can be related to its mean free path λ by,

$$t = \frac{\lambda}{v_{term}} \ . \tag{3.43}$$

Now, the average velocity is,

$$v_{med} = \frac{1}{t}\int_0^t v(t')dt' = \frac{at}{2} \ . \tag{3.44}$$

Finally, with n_a molecules per unit volume, each one providing N free electrons, the current density is,

$$\mathbf{j} = n_a NQ\mathbf{v}_{med} = n_a Nq\frac{t}{2m_e}\mathbf{F} = n_a NQ\frac{\lambda}{2m_e v_{term}}\mathbf{F} = \frac{n_a NQ^2\lambda}{2m_e v_{term}}\vec{\mathcal{E}} \ . \tag{3.45}$$

That is, the conductivity can be estimated as,

$$\varsigma = \frac{n_a NQ^2\lambda}{2m_e v_{term}} \ . \tag{3.46}$$

The *resistivity* is

$$\rho \equiv \frac{1}{\varsigma} \ . \tag{3.47}$$

We note that the resistivity depends on the temperature, $\rho \propto T^{1/2}$.

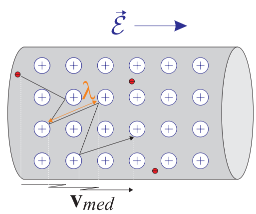

Figure 3.16: Microscopic view of the current.

Example 35 (*Estimation of the average velocity of electrons in a conductor*): Based on Eq. (3.37) we now want to estimate the average propagation velocity of electrons in a copper wire (radius $R = 1\,\text{mm}$) carrying a current of $I = 1\,\text{A}$. With the density of copper of $\rho_m = 8920\,\text{kg/m}^3$, its atomic mass $m_a = 63.5u$ and $N = 1$ valence electron per atom we estimate,

$$v_{med} = \frac{I}{n_a Ne\pi R^2} = \frac{Iu}{m_a e\pi R^2} \simeq 8.5\,\text{cm/h} \ .$$

3.3.2.2 Resistors and energy consumption

Let us consider the conductor with the most common geometry: a metallic wire with the shape of a cylinder with cross section S and length L. Applying an electric field, we get,

$$I = \mathbf{j} \cdot \mathbf{S} = \varsigma \vec{\mathcal{E}} \cdot \mathbf{S} = \frac{\varsigma S}{L} U \ , \tag{3.48}$$

where $R = l/\varsigma A$ is called *resistance*. In this form the Ohm's law adopts the following form,

$$\boxed{U = RI} \ . \tag{3.49}$$

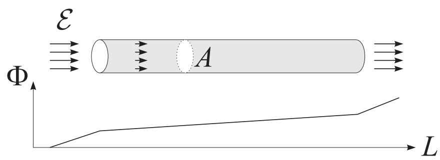

Figure 3.17: Concept of resistance.

A consequence of the frequent collisions of the electrons with the atoms is, that the conductor heats up. The power wasted on a resistance R is,

$$P = VI = RI^2 \ . \tag{3.50}$$

3.3.2.3 Resistor circuits

For parallel circuits $R_{tot}^{-1} = R_1^{-1} + R_2^{-1}$, for circuits in series $R_{tot} = R_1 + R_2$.

3.3.3 Exercises

3.3.3.1 Ex: The α-particle

A beam of α-particles ($q = +2e$), which move with constant kinetic energy $E = 20\,\text{MeV}$, corresponds to a current of $I = 0.25\,\mu\text{A}$. The beam is directed perpendicular to a flat surface.
a. How many α-particles hit the surface in $t = 3\,\text{s}$?
b. How many α-particles are at each instant of time within a $s = 20\,\text{cm}$ long beam segment?
c. What potential difference does an α-particle have to travel to be accelerated from rest to an energy of $20\,\text{MeV}$?

3.3.3.2 Ex: Electric power

A potential difference of $120\,\text{V}$ powers a heater whose resistance is $1\,\Omega$ when it is hot.
a. At what rate does this device transform electricity into heat?
b. What is the electricity consumption bill for $t = 5\,\text{h}$ of operation with a price for electricity of $S = 5\,\text{ct/kWh}$?

3.3.3.3 Ex: Ohm's Law and electric Power

By how many degrees does a copper conductor of 100 m in length and $1.2\,\mathrm{mm}^2$ in diameter heat up, when it is traversed for 1 hour by a current of 6 A? Assume the heat is not dissipated and use the following data: specific resistivity: $\rho = 0.02\,\Omega\mathrm{mm}^2/\mathrm{m}$; density: $\rho_{\mathrm{Cu}} = 8.93\,\mathrm{kg/dm}^3$; specific heat capacity: $c_{\mathrm{Cu}} = 389.4\,\mathrm{J/kg\ K}$.

3.3.3.4 Ex: Continuity equation and conserved quantities

The continuity equation,

$$\dot{\rho} + \nabla \cdot (\vec{v}\rho) = 0 \ ,$$

appears in various areas of physics and describes, for example, the conservation of matter, charge or probability.
a. Explain, based on Gauß' law, the relationship between the continuity equation and charge conservation.
b. Consider a simple mechanical example: A 10 l gas bottle is opened letting gas escape. Determine with the help of the continuity equation after how many minutes half of the gas is gone, if the gas exits at a constant velocity of $v = 1\,\mathrm{m/s}$ and the outlet valve has a cross-sectional area of $A = 10\,\mathrm{mm}^2$?

3.3.3.5 Ex: Drift of electrons in a conducting wire

A gold wire has a circular cross section of 0.1 mm diameter. The ends of this wire are connected to the terminals of a 1.5 V battery. If the wire length is 7.5 cm, how long does it take on average for two electrons leaving the negative terminal of the battery to reach the positive terminal? Consider a resistivity of gold of $2.44 \cdot 10^{-8}\,\Omega\mathrm{m}$.

3.4 The electric circuit

Within a (ideal) conductor potential differences vanish everywhere $\Delta\Phi = 0$, regardless of the conductor's length or shape. In a stationary situations, that is, in the presence of static electric fields, the free electrons of the conductor self-organize their spatial distribution (if necessary by creating local charge imbalances) in order to satisfy this condition. As soon as the condition is satisfied, the movement of charges, necessary for their spatial reorganization, comes to an end.

To sustain a stationary current we need to recycle the electrons, that is, waste the electrons accumulated on the side, where the conductor is connected to the positive potential and provide new electrons on the side, where the conductor is connected to the negative potential. In other words, we need to *close* the circuit by an source-drain device for electrons, called *voltage source* or *current source* depending on the properties of the device.

In addition to the source, there is a wide variety of electronic components capable of manipulating the potential or the current in different ways, such as resistors, capacitors, inductors or transistors. In a circuit, these components are interconnected by conductive wires assumed to be ideal in the sense that they a potential without losses from one component to another.

3.4.1 Kirchhoff's rules

Electrical circuits can be more complicated and consist of several branches. The *mesh rule*,

$$\sum_k U_k = 0 \tag{3.51}$$

and the *node rule*,

$$\sum_k I_k = 0 \ , \tag{3.52}$$

govern the behavior of the potentials and currents in any circuit and serve to analyze its properties.

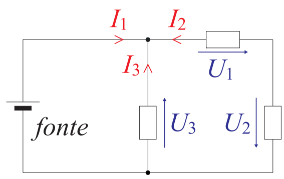

Figure 3.18: Illustration of Kirchhoff mesh and node rules.

Example 36 (*R-C circuit in series*)**:** In addition to the voltage source we got to know two types of elements which can locally influence the voltage or the current: the capacitor and the resistor. The simplest imaginable electrical circuit containing these two components is the R-C circuit shown in Fig. 3.19. This circuit can be treated by Kirchhoff's laws,

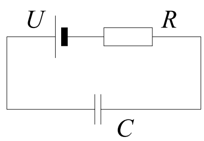

Figure 3.19: Illustration of a R-C-circuit.

$$0 = U_F + U_C + U_R \qquad \text{and} \qquad I_F = I_C = I_R \ . \tag{3.53}$$

Since the current is the same at each point of the circuit, we get the differential equation,

$$0 = U_F + \frac{Q}{C} + RI = U_F + \tfrac{1}{C}\int_0^t I dt' + RI \ , \tag{3.54}$$

which can quickly be solved by imposing the condition that the charge of the capacitor is initially zero,

$$I(t) = I_0(1 - e^{-t/RC}) \ . \tag{3.55}$$

3.4.2 Measuring instruments

Instruments for voltage and current measurement are discussed in the applied undergraduates courses, and we will not repeat this here.

3.4.3 Exercises

3.4.3.1 Ex: Motor starter issues

The starter of a car runs too slow. The mechanic has to decide which part is defective: the motor, the power cord, or the battery. According to the manufacturer's technical instructions, the internal resistance of the $U_0 = 12\,\mathrm{V}$ battery should not exceed $R_{bat} < 0.02\,\Omega$, resistance of the motor must not exceed $R_{mot} < 0.2\,\Omega$, and the resistance of the power cord must not exceed $R_{cab} < 0.04\,\Omega$. Examining the starter motor the mechanic finds a potential difference of 11.4 V at the battery, 3 V in the cable, and a current of 50 A in the starter circuit. Which element of the starter is defective?

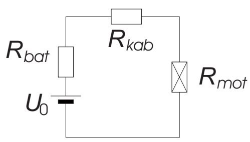

Figure 3.20: Motor starter circuit.

3.4.3.2 Ex: Solar cell

A solar cell generates a voltage of 0.1 V at a resistive load of 500 Ω, but only a voltage of 0.15 V at a resistive load of 1000 Ω. Consider the cell as a *real* voltage source with an internal resistance.
a. What are the internal resistance and unloaded voltage of the cell?
b. Calculate the efficiencies obtained with the two mentioned loads.

3.4.3.3 Ex: Current and voltage measurement

Circuit (a) shows an arrangement with an amperemeter with internal resistance R_A and a voltmeter with internal resistance R_U to measure resistance R. The value of the resistance follows from $R = U_V/I_R$, where U_V is the value indicated by the voltmeter and I_R the current through the resistance. A part of the current I_A measured by the amperemeter, however, flows through the voltmeter, such that the ratio U_V/I_A of the measured values only indicates an apparent resistance, which we will call R'.
a. How are the true resistance R and the apparent resistance R' interconnected through the internal resistance R_V voltmeter? How should the internal resistance of the voltmeter be chosen to guarantee that $R' \to R$?
b. With the circuit (b) it is also possible to measure a resistance with an amperemeter and a voltmeter, and also in this case the ratio between the measured values gives only an apparent resistance. How can we determine the true resistance R in this circuit, and how should the internal resistance R_A of the amperemeter be chosen?

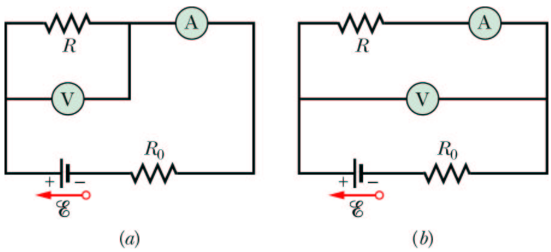

Figure 3.21: Current and voltage measurement.

3.4.3.4 Ex: Real current source

a. How should the internal resistance of a current source R_i be specified in order to obtain a current as independent as possible from the consuming load?
b. You want to run 40 A through an electric coil. The coil has the ohmic resistance of $R = 1\,\Omega$. What should be the internal resistance of the current source in order for a 10% increase in resistance not to change the current by more than 0.1%?

3.4.3.5 Ex: Real voltage source

A battery can be understood as a real voltage source, consisting of an ideal voltage source U_0 and an internal resistance R_i. The voltage supplied by the battery depends on the consuming load. Which current flows through the resistor R and which voltage U_{out} does the battery supply? How must the resistive load be chosen to maximize the power spent at the ohmic resistor?

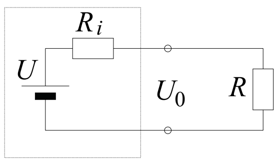

Figure 3.22: Battery.

3.4.3.6 Ex: Battery circuit

Two batteries 1 and 2 (voltages $U_1 = 2\,\text{V}$ and $U_2 = 0.5\,\text{V}$) and three resistors $R_1 = R_2 = R_3 = 1\,\Omega$ are connected as shown in the figure.
a. What currents flow through the resistors R_1, R_2, and R_3?
b. What is the voltage drop between points A and B?

3.4.3.7 Ex: Circuit with battery

Three batteries ($U_1 = 20\,\text{V}$, $U_2 = 5\,\text{V}$, $U_3 = 20\,\text{V}$) each with a finite internal resistance of $0.1\,\Omega$ are connected in parallel. In series with this circuit two resistors are connected ($R_1 = 100\,\Omega$, $R_2 = 200\,\Omega$) (see scheme). What is the electrical voltage at R_1 and R_2?

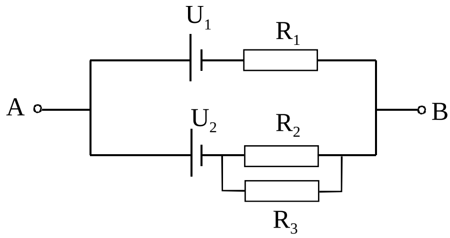

Figure 3.23: Battery circuit.

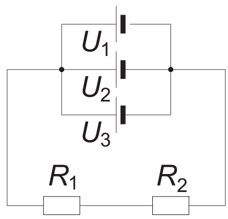

Figure 3.24: Battery circuit.

3.4.3.8 Ex: Kirchhoff's rules

The current circuit shown in the figure consists of voltage sources, $U_1 = 20\,\text{V}$ and $U_2 = 10\,\text{V}$ and resistors, $R_1 = 150\,\Omega$, $R_2 = R_3 = R_5 = 100\,\Omega$, and $R_4 = 50\,\Omega$. What is the current measured by the Ampèremeter A?

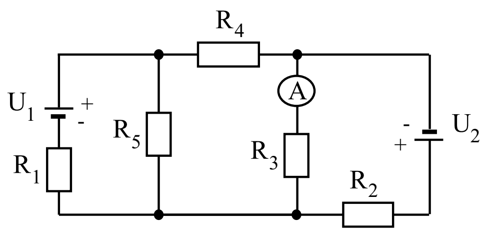

Figure 3.25: Circuits.

3.4.3.9 Ex: Kirchhoff's rules

Be given $R_1 = 1\,\Omega$, $R_2 = 2\,\Omega$, as well as $\varepsilon_1 = 2\,\text{V}$ and $\varepsilon_2 = \varepsilon_3 = 4\,\text{V}$.
a. Show that Kirchhoff's node rule for steady currents is a consequence of the continuity equation $\oint \vec{j} d\vec{A} = \frac{dq}{dt}$.
b. Calculate the currents across the three ideal batteries in the circuit shown in figure.
c. Calculate the potential difference between points a and b.

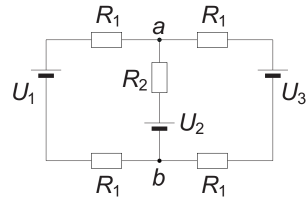

Figure 3.26: Circuits.

3.4.3.10 Ex: Kirchhoff's rules

Consider the following circuit fed by a battery of voltage V. Using Kirchhoff's laws calculate the voltages and currents at the points $P1$ and $P2$. What is the total resistance of this circuit?

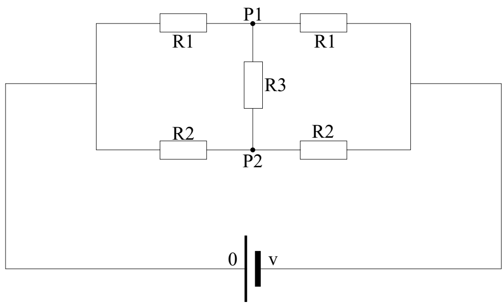

Figure 3.27: Circuits.

3.4.3.11 Ex: Combination of resistors

You have a maximum of 5 resistors of $100\,\Omega$ each. With these try to build circuits having the total resistance of a. $R = 25\,\Omega$, b. $R = 66.\bar{6}\,\Omega$, c. $R = 120\,\Omega$.

3.4.3.12 Ex: Circuit with capacitors and resistors

In the circuit shown in the figure be $R_1 = 600\,\Omega$, $R_2 = 200\,\Omega$, $R_3 = 300\,\Omega$, $C = 20\,\mu\text{F}$, and $U = 12\,\text{V}$.
a. Calculate the voltages measured at the individual resistors and the capacitor as well as the total current I_{ges} when the capacitor is fully charged (stationary case).
b. At time $t = 0$ the switch S is opened. After which time the capacitor voltage drops to $10\,\text{mV}$?

3.4.3.13 Ex: Circuits with resistors and capacitors

Consider the circuit shown in the figure with the following values, $R_1 = R_3 = 100\,\Omega$, $R_2 = R_4 = 200\,\Omega$, $C_1 = C_2 = 10\,\mu\text{F}$, and $U_0 = 20\,\text{V}$.
a. Calculate equivalent resistance and the equivalent capacity of the circuit.
b. At time $t = 0$ the switch S is closed. Find the differential equation for the voltage

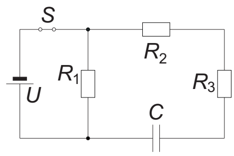

Figure 3.28: Circuits.

$U(t)$ at the capacitor C_1 and solve it. When does the voltage drop to $1/e$ of its maximum value?
c. Determine the evolution of the amplitude of the resistor current R_3.

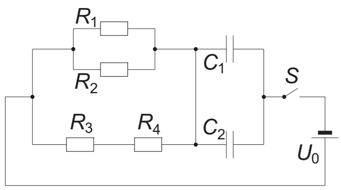

Figure 3.29: Circuits.

3.4.3.14 Ex: Circuits with resistors and capacitors

Calculate the total resistances and capacitances of the following circuits.
Help for (e): Consider the capacitor as a set of capacitors with/without dielectric in series and in parallel.

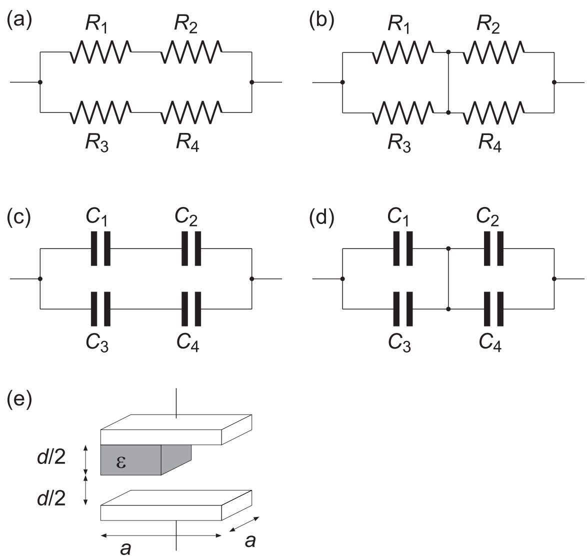

Figure 3.30: Circuits.

3.4.3.15 Ex: Charging a capacitor

The circuit shown in Fig. 3.19 consists of a voltage source U, a resistance R, and a capacity C. Initially be $U = 0$. From the time $t = 0$ on the voltage source shall give the constant value $U = U_0$. Calculate the time evolution of the current I in the circuit as well as the time evolution of the voltages at the capacitor and at the resistance.
Help: Begin by establishing the differential equation for the current I.

3.4.3.16 Ex: R-C circuit

Consider the electrical circuit shown in the figure with the ideal voltage sources U_k, the resistors R_k, and the capacitor C. Initially the switch C_1 is open.
a. Calculate the charge Q_0 on the capacitor after a long time.
b. Now, the switch is closed. Using Kirchhoff's laws, express the charge on the capacitor as a function of the current I_C across the capacitor and the parameters shown in the figure.
c. Based on the result obtained in (b), calculate the time evolution of the capacitor charge.
d. Indicate the values for $t = 0$ and $t \to \infty$.
e. Discuss the cases (i) $U_2 = U_1$ and (ii) $U_2 = -U_1$.

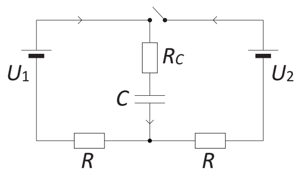

Figure 3.31: Circuits.

3.4.3.17 Ex: Internal resistance of a battery

A 5 V power supply has an internal resistance of 50 Ω. What is the smallest resistor that can be taken in series with the power source so that the potential drop in the resistor is larger than 4.5 V?

3.4.3.18 Ex: Circuit with two batteries

In the circuit shown in the figure, the batteries have negligible internal resistances. Determine
a. the current in each branch of the circuit
b. the potential difference between the points a and b, and
c. the power supplied by each battery.

3.4.3.19 Ex: Circuit with three batteries

For the circuit shown in the figure, determine the potential difference between the points a and b.

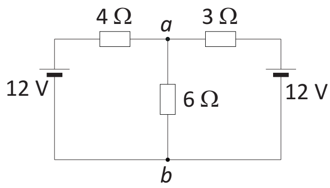

Figure 3.32: Circuits.

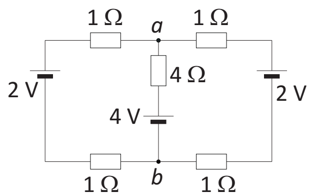

Figure 3.33: Circuits.

3.4.3.20 Ex: Real voltmeter

The voltmeter shown in the figure can be modeled as an *ideal* voltmeter (a voltmeter that has an infinite internal resistance) in parallel with a $10\,\mathrm{M\Omega}$ resistor. Calculate the voltmeter reading when
a. $R = 1.0\,\mathrm{k\Omega}$,
b. $R = 10.0\,\mathrm{k\Omega}$,
c. $R = 1.0\,\mathrm{M\Omega}$,
d. $R = 10.0\,\mathrm{M\Omega}$,
e. $R = 100.0\,\mathrm{M\Omega}$.
f. What is the largest possible value of R if the measured voltage should be within 10% of the *true* voltage (i.e. the voltage drop at R without placing the voltmeter)?

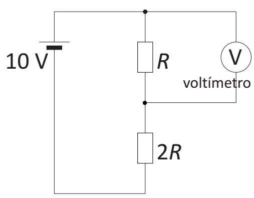

Figure 3.34: Voltmeter.

3.4.3.21 Ex: Circuit with battery and capacitor

The switch shown in the figure is closed after having been open for a long time.
a. What is the initial value of battery current right after the switch S has been closed?
b. What is the battery current a long time after the key has been closed?
c. What are the charges on the capacitor plates a long time after the switch has been closed?

d. Now, the switch S is opened again. What are the charges on the capacitor plates a long time after the switch has been reopened?

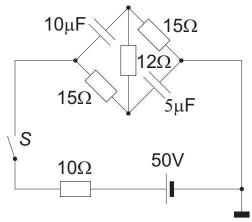

Figure 3.35: Circuits.

3.4.3.22 Ex: Circuit with battery and capacitor

In the circuit shown in the figure, the capacitor has a capacitance of 2.5 μF and the resistor has a resistance of 0.5 M Ω. Before the switch is closed, the potential drop in capacitor is 12 V, as shown in the figure. The switch S is closed at $t = 0$.
a. What is the current immediately after the switch has been closed?
b. At what instant of time t is the voltage on the capacitor 24 V?

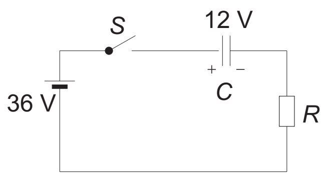

Figure 3.36: Circuits.

3.4.3.23 Ex: Three-phase current

Three-phase current is generated by three potential differences with respect to ground described by,

$$U_n(t) = U_0 \sin(\omega t + n\tfrac{2\pi}{3}) \ ,$$

where $n = 1, 2, 3$ labels the three phases. Assuming $U_0 = 127$ V.
a. What is the period-averaged voltage of each phase with respect to ground?
b. What is the period-averaged voltage difference between two phases?
c. What is the amplitude of the voltage difference between two phases?
d. Derive the time-dependent expressions for all currents labeled in Fig. 3.37(a).

3.5 Further reading

D.J. Griffiths, *Introduction to Electrodynamics* [ISBN]

D. Halliday, R. Resnick, and J. Walker, *Fundamentals of Physics* [ISBN]

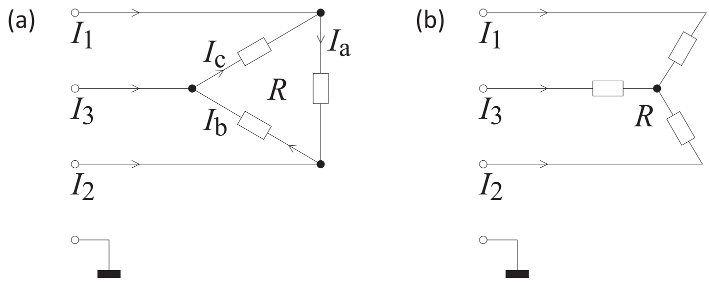

Figure 3.37: (a) Star connection, (b) triangular connection.

H.M. Nussenzveig, *Curso de Física Básica: Eletromagnetismo (Volume 3)* [ISBN]

Chapter 4

Magnetostatics

Magnetostatics is the theory dealing with stationary currents, the fundamental problem being the calculation of the force exerted by spatial current distributions. Since a current is always due to displacement of charges, it is obviously not stationary in the strict sense. On the other hand, if the charge is transported in such a way that every charge leaving a volume element is immediately replaced by another equivalent charge, the integral over the volume element yields a stationary charge distribution.

4.1 Electric current and the Lorentz force

In the previous chapter we have shown that charges can travel through electric conductors, thus producing currents. We observe experimentally that electrically neutral conductors can exert reciprocal forces. For example, passing currents through two parallel, almost infinitely long thin wires, we find that they attract (repel) each other when their directions are (anti-)parallel. We also observe that a compass needle is deflected near a current-carrying conductor in directions describing concentric circles around the conductor. If the compass needle traces the field lines of a yet unknown field, the force attracting (or repelling) two currents DOES NOT point in the direction of the field lines. These observations show the presence of another phenomenon and another force not explained by Coulomb's law (see Fig. 4.1).

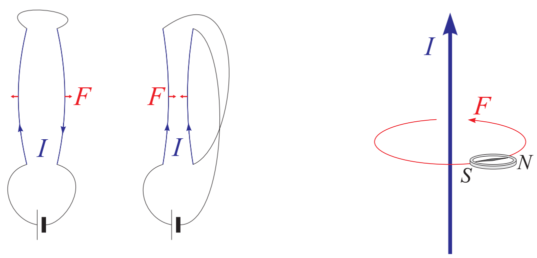

Figure 4.1: Mutual force between two conductors carrying antiparallel and parallel currents. Torque exerted by a current on a compass.

Apparently, the new force is not oriented in the direction of the current I, nor in the direction of the lines described by the compass needle, but perpendicular to the two. To describe this fact, we postulate the existence of a field $\vec{\mathcal{B}}$ called *magnetic* *field*, such that the force is described by the vector product,

$$\mathbf{F}_L = I\mathbf{l} \times \vec{\mathcal{B}} \ , \tag{4.1}$$

where $\mathbf{l}$ is an element of the current path. This force is called *Lorentz force*. Note, that this force behaves like a pseudo-vector.

In order to analyze this phenomenon from the microscopic point of view, we put forward the hypothesis that the observed force has to do with the *motion* of the charges constituting the current within the postulated magnetic field. We have already introduced in the previous chapter the notion of the *current*, and we connected the current density with the propagation velocity of charges in the Eqs. (3.37) and (3.45),

$$\mathbf{j}(\mathbf{r}') = \varrho(\mathbf{r}')\mathbf{v}' \ . \tag{4.2}$$

With this we get,

$$\begin{aligned} \mathbf{F}_L &= I\int_{\mathcal{C}} d\mathbf{l}' \times \vec{\mathcal{B}} = I\int_{\mathcal{C}} \hat{\mathbf{e}}'_j \times \vec{\mathcal{B}} dl' \qquad (4.3)\\ &= \int_{\mathcal{V}} I\delta^2(\mathbf{r}'_\perp - \mathbf{l}_\perp)\hat{\mathbf{e}}'_j \times \vec{\mathcal{B}} dV' = \int_{\mathcal{V}} \mathbf{j}(\mathbf{r}') \times \vec{\mathcal{B}} dV' = \int_{\mathcal{V}} \varrho(\mathbf{r}')\mathbf{v}' \times \vec{\mathcal{B}}(\mathbf{r}') dV' \ , \end{aligned}$$

where we simplified the notation $\mathbf{j}(\mathbf{r}') = I\delta^2(\mathbf{r}'_\perp - \mathbf{l}_\perp)\hat{\mathbf{e}}'_j = I\delta(\hat{\mathbf{e}}_1 \cdot \mathbf{r}' - \hat{\mathbf{e}}_1 \cdot \mathbf{l})\delta(\hat{\mathbf{e}}_2 \cdot \mathbf{r}' - \hat{\mathbf{e}}_2 \cdot \mathbf{l})\hat{\mathbf{e}}'_j$, where $\hat{\mathbf{e}}_{1,2}$ and $\hat{\mathbf{e}}'_j$ are all mutually orthogonal. We conclude,

$$\boxed{\mathbf{F}_L = Q\mathbf{v} \times \vec{\mathcal{B}}} \ . \tag{4.4}$$

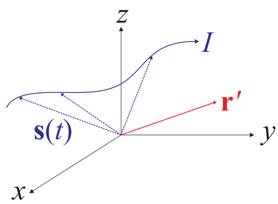

Figure 4.2: Parametrization of a yarn of current using the following recipe: For each point in space $\mathbf{r}' \in \mathbb{R}$ check that this point is also in $\mathbf{r}' \in \mathcal{C}$, that is, whether there exists a t such that $\mathbf{r}' = \mathbf{l}(t)$. At this point determine the direction of the path, $\hat{\mathbf{e}}'_j = d\mathbf{l}/|d\mathbf{l}|$, find two orthogonal unit vectors $\hat{\mathbf{e}}_{1,2}$ and apply the Dirac distribution to these dimensions.

Example 37 (*Cyclotron and synchrotron motion*): A consequence of the fact that, according to (4.4), the force on moving charges is always perpendicular to their velocity is, that their trajectory in a homogeneous magnetic field are *circular*. The centrifugal force compensates for the Lorentz force when,

$$F_L = Qv\mathcal{B} = m\frac{v^2}{R} = F_{cf} \ ,$$

which allows to determine the radius R of the circle [1].

This fact is used in particle accelerators called *cyclotrons*, where beams of

[1]This behavior can be observed by injecting a charged particles into a homogeneous magnetic field. Collimated electron beams can be created by an electrode device called the *Wehnelt's cylinder* used in cathode ray tubes called *Braun's tube*.

charged particles are accelerated in by electric fields and deflected by homogeneous magnetic fields located between the regions of acceleration.

An important consequence of the particular form of the Lorentz force is the fact that *magnetic forces do not work*,

$$W_{mg} = \int_{\mathcal{C}} \mathbf{F} \cdot d\mathbf{l} = 0 \ .$$

The direction of motion of a charge can be changed by magnetic fields, but not the absolute value of its velocity. This may seem surprising, as we know that magnets can exert forces of iron bodies.

Example 38 (*Work exerted by magnetic fields*): We consider a conductive wire loop carrying current and being partially immersed in a homogeneous magnetic field, as shown in Fig. 4.3. The device is in equilibrium, when,

$$F = Ia\mathcal{B} = mg \ .$$

When the current exceeds the value $mg/a\mathcal{B}$, a vertical force lifting the device is observed, such that the device gains potential energy,

$$W = Fh \ ,$$

where h is the acquired height. However, the vertical motion corresponds to a current $I\hat{\mathbf{e}}_z$, which creates a force contrary to the current I, such that the battery feeding the wire loop needs to work to maintain the current. The magnetic field only reorients the force into a direction having a parallel component to the horizontal part of the wire loop, thus allowing the battery to work against this force. We shall discuss this from another point of view in context of the Lenz-Faraday law.

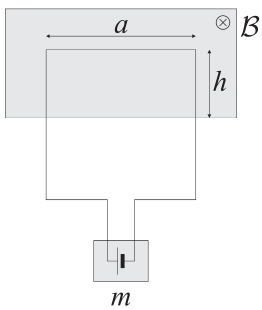

Figure 4.3: Hypothetical device to make the magnetic field work.

4.1.1 The Hall effect

As an example we consider the *Hall effect*: As shown in Fig. 4.4, a current flows to the right through a rectangular rod made of conductive material in the presence of a perpendicular uniform magnetic field $\vec{\mathcal{B}}$. If the mobile charges are positive, they will be deflected by the magnetic field in downward direction. This deflection results in an accumulation of charges on the upper and lower boundaries of the rod which, in turn, generates an electric Coulomb force counteracting the magnetic force. A balance is reached when the two forces compensate:

$$F_C = Q\mathcal{E} = Q\frac{U_H}{w} = Qv_{med}\mathcal{B} = F_L \ . \tag{4.5}$$

The difference of the electric potentials on the upper and lower boundaries is called *Hall voltage*. The average velocity of the charges can be estimated from Eq. (3.45),

$$v_{med} = \frac{j}{n_a NQ} \ , \tag{4.6}$$

where n_a is the volumetric density of molecules of the rod material, each molecule providing N free electrons. Now, using the dimensions of the rod outlined in Fig. 4.4, we calculate the Hall voltage,

$$U_H = v_{med}\mathcal{B}w = \frac{j}{n_a NQ}\mathcal{B}w = \frac{I\mathcal{B}}{d\ n_a NQ} = A_H\frac{I\mathcal{B}}{d} \ , \tag{4.7}$$

where $A_H = 1/n_a NQ$ is a constant which depends on the rod material.

If the mobile charges were negative, the Hall voltage would change its sign. This fact can be used to identify the sign of free charges in unknown current conductors. Resolve the Excs. 4.1.3.1-4.1.3.13.

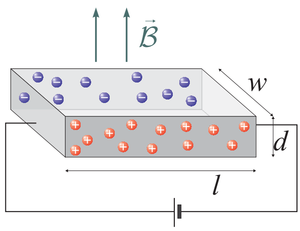

Figure 4.4: Illustration of the Hall Effect.

4.1.2 Biot-Savart's law

In the same way as we parametrize charge distributions (linear, superficial and volumetric) in electrostatics,

$$\sum_k (..)Q_k \longrightarrow \int_{\mathcal{C}} (..)\lambda dl \sim \int_{\mathcal{S}} (..)\sigma dS \sim \int_{\mathcal{V}} (..)\varrho dV \ , \tag{4.8}$$

we can parametrize current distributions (linear, superficial and volumetric) in magnetostatics,

$$\sum_k (..)Q_k\mathbf{v}_k \longrightarrow \int_{\mathcal{C}} (..)\mathbf{I}dl \sim \int_{\mathcal{S}} (..)\vec{\kappa}dS \sim \int_{\mathcal{V}} (..)\mathbf{j}dV \ . \tag{4.9}$$

In electrostatics we had the condition $\dot{\varrho} = 0$, which implies, via the continuity equation (3.38),

$$\nabla \cdot \mathbf{j} = 0 \ . \tag{4.10}$$

In magnetostatics we furthermore demand that $\dot{\mathbf{j}} = 0$.

The equivalent of Coulomb's law in magnetostatics is the Biot-Savart law,

$$\boxed{\vec{\mathcal{B}}(\mathbf{r}) = \frac{\mu_0}{4\pi}\int_{\mathcal{C}} \frac{\mathbf{I}(\mathbf{r}') \times (\mathbf{r}-\mathbf{r}')}{|\mathbf{r}-\mathbf{r}'|^3} dl' = \frac{\mu_0 I}{4\pi}\int_{\mathcal{C}} \frac{d\mathbf{l}' \times (\mathbf{r}-\mathbf{r}')}{|\mathbf{r}-\mathbf{r}'|^3} = \frac{\mu_0}{4\pi}\int_{\mathcal{V}} \mathbf{j}(\mathbf{r}') \times \frac{\mathbf{r}-\mathbf{r}'}{|\mathbf{r}-\mathbf{r}'|^3} dV'} \ . \tag{4.11}$$

Analogously to the way in which we apply Coulomb's law to electrostatics to calculate the electric field produced by charge distributions, we can apply the Biot-Savart's law in magnetostatics to calculate the magnetic field produced by currents.

Example 39 (*Magnetic field of a straight current wire*): We consider an infinitely long and thin wire oriented along the z-axis carrying a current I parametrized by $\mathbf{j}(\mathbf{r}') = \hat{\mathbf{e}}_z I\delta(x')\delta(y')$. Using $\mathbf{r} = \rho\hat{\mathbf{e}}_\rho + z\hat{\mathbf{e}}_z$ and $\mathbf{r}' = z'\hat{\mathbf{e}}_z$ we calculate,

$$\begin{aligned}\vec{\mathcal{B}}(\mathbf{r}) &= \frac{\mu_0 I}{4\pi}\int_{-\infty}^{\infty} dz' \frac{\hat{\mathbf{e}}_z \times (\mathbf{r}-\mathbf{r}')}{|\mathbf{r}-\mathbf{r}'|^3} = \frac{\mu_0 I}{4\pi}\hat{\mathbf{e}}_z \times \rho\hat{\mathbf{e}}_\rho \int_{-\infty}^{\infty} \frac{dz'}{\sqrt{\rho^2+(z-z')^2}^3} \\ &= \frac{\mu_0 I}{4\pi}\hat{\mathbf{e}}_z \times \rho\hat{\mathbf{e}}_\rho \left[\frac{z'}{\rho^2}(\rho^2+z'^2)^{-\frac{1}{2}}\right]_{-\infty}^{\infty} = \frac{\mu_0 I}{4\pi}\hat{\mathbf{e}}_z \times \rho\hat{\mathbf{e}}_\rho \frac{2}{\rho^2} = \frac{\mu_0 I}{2\pi\rho}\hat{\mathbf{e}}_\phi \ .\end{aligned}$$

With this we can now calculate the force exerted by this current on another current I_2 flowing in parallel direction but at a distance ρ:

$$\mathbf{F} = I_2 l\hat{\mathbf{e}}_z \times \vec{\mathcal{B}} = \frac{\mu_0 I I_2 l}{2\pi\rho}(-\hat{\mathbf{e}}_\rho) \ .$$

So the force is attractive.

Example 40 (*Magnetic field of a loop of circular current*): We consider a circular current parametrized by $\mathbf{j}(\mathbf{r}') = \hat{\mathbf{e}}_\phi I\delta(z)\delta(\rho - R)$. Following the Biot-Savart law the generated magnetic field is,

$$\vec{\mathcal{B}}(\mathbf{r}) = \frac{\mu_0}{4\pi}\int_{\mathcal{V}} \frac{\mathbf{j}(\mathbf{r}') \times (\mathbf{r}-\mathbf{r}')}{|\mathbf{r}-\mathbf{r}'|^3} dV' = \frac{\mu_0 I}{4\pi}\oint_{\mathcal{C}} \frac{\hat{\mathbf{e}}_{\phi'} \times (\mathbf{r} - R\hat{\mathbf{e}}_{r'})}{|\mathbf{r} - R\hat{\mathbf{e}}_{r'}|^3} R d\phi' \ .$$

On the symmetry axis $\mathbf{r} = z\hat{\mathbf{e}}_z$ we get,

$$\begin{aligned}\vec{\mathcal{B}}(z\hat{\mathbf{e}}_z) &= \frac{\mu_0 IR}{4\pi}\oint_{\mathcal{C}} \frac{\hat{\mathbf{e}}_{\phi'} \times (z\hat{\mathbf{e}}_z - R\hat{\mathbf{e}}_{r'})}{\sqrt{R^2\cos^2\phi' + R^2\sin^2\phi' + z^2}^3} d\phi' \\ &= \frac{\mu_0 IR}{4\pi}\oint_{\mathcal{C}} \frac{z\hat{\mathbf{e}}_r + R\hat{\mathbf{e}}_z}{\sqrt{R^2+z^2}^3} d\phi' = \frac{\mu_0 IR^2}{2\sqrt{R^2+z^2}^3}\hat{\mathbf{e}}_z \ ,\end{aligned}$$

where the integral containing the term $z\hat{\mathbf{e}}_r$ vanishes by symmetry.

Resolve the Excs. 4.1.3.14-4.1.3.15.

4.1.3 Exercises

4.1.3.1 Ex: Force on a current conductor

A piece wire having the shape of a semicircle (radius R) congruent to the xy-plane at $z = 0$ is immersed in a homogeneous magnetic $\vec{\mathcal{B}}$-field oriented along $\hat{\mathbf{e}}_z$, as shown in the scheme. Through the wire runs a current I. Calculate the force on the loop and compare it to the force on a piece of straight wire oriented along the y-axis with length $2R$. The current in this wire runs along $\hat{\mathbf{e}}_y$.

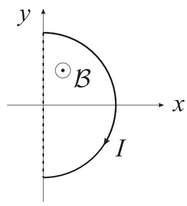

Figure 4.5: Wires.

4.1.3.2 Ex: Lorentz force

In a wooden cylinder of mass $m = 0.25\,\text{kg}$ and length $L = 10\,\text{cm}$ is wound a 10 turns coil of conducting wire such that the axis of the cylinder is within the plane of the coil. The cylinder is (not slipping) on an plane inclined by $\alpha = 30°$ with respect to the horizontal, so that the plane of the coil is parallel to the inclined plane. The whole setup is subject to a homogeneous vertical magnetic field with the absolute value $\mathcal{B} = 0.5\,\text{T}$. What should be the minimum current through the coil to prevent the coil from rotating around its center of mass?

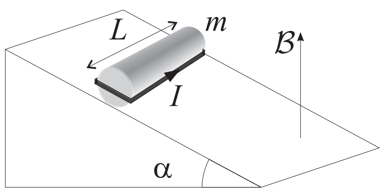

Figure 4.6: Lorentz force.

4.1.3.3 Ex: Magnetic field mass spectrometer

A spectrometer is used to separate doubly ionized uranium ions of mass $3.92 \times 10^{-25}\,\text{kg}$ from other similar isotopes. The ions are first accelerated by a potential difference of $100\,\text{kV}$ and then enter a homogeneous magnetic field, where they are deviated into a circular orbit of radius $1\,\text{m}$. After having covered an angle of $180°$, they enter through a $1\,\text{mm}$ wide and $1\,\text{cm}$ high slit and are accumulated in a collector.
a. Determine the magnetic field of the mass spectrometer from the energy balance of

the (individual) ions.
b. The device should be able to separate 100 mg of the desired ions per hour. What should be the intensity of the ionic flux in the beam?
c. What heat is produced in the collector in one hour?

4.1.3.4 Ex: Mass spectrometer

In a mass spectrometer, a $^{24}Mg^{+}$ ion has a mass of $3.983 \cdot 10^{-26}$ kg and is accelerated by a potential difference of 2.5 kV. It then enters a region, where it is deflected by a magnetic field of 557 G.
Determine the radius of curvature of the orbits of the ion.
b. What is the difference between the radii of the orbits of the ions ^{26}Mg and ^{24}Mg? Consider a ratio between the masses of 26 : 24.

4.1.3.5 Ex: Magnetron

A magnetron consists of a diode tube, an anode shaped like a circular cylinder with radius $R_A =$ cm in the center of which the cathode filament is coaxially located. On the glass tube of this diode is a wound cylindrical coil whose axis coincides with the anode. The coil is long enough that the magnetic field along the cathode can be considered homogeneous. The electrons emitted from the cathode wire simultaneously are subject to the electric field between cathode and anode, $U = 1000$ V and the magnetic field $\mathcal{B} = 0.533 \cdot 10^{-2}$ T. The latter has been adjusted so that the electrons barely do not reach the anode. The whole apparatus is basically a velocity filter for electrons and thus a compact version of J.J. Thomson's e/m experiment (1987). From the equation of motion of an electron in the tube, determine the ratio e/m.

4.1.3.6 Ex: Conductive copper strips

A copper strip of length $l = 2$ cm, width $b = 1$ cm, and thickness $d = 150$ µm lies within a homogeneous magnetic field $\vec{\mathcal{B}}$ of value 0.65 T, oriented perpendicular to the flat side of the strip. The concentration of free charges in copper is 8.47×10^{28} electrons/m^3. What is the potential difference V across the width of the tape, if it is traversed by a current of $I = 23$ A?

4.1.3.7 Ex: Lorentz force

A firm, horizontal, 25 cm long linear wire has a mass of 5 g and is connected to an emf-source via light and flexible wires. A magnetic field of 1.33 T is horizontal and perpendicular to the wire. Determine the current needed for the wire to float, that is, when the wire is released from rest, it remains at rest.

4.1.3.8 Ex: Lorentz force

A current carrying wire is bent in a closed semicircle of radius R in the xy-plane. The wire is inside a uniform magnetic field oriented in $+z$-direction, as shown in the figure. Verify that the force exerted on the ring is zero.

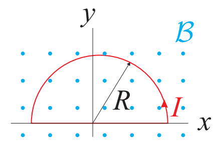

Figure 4.7: Lorentz force.

4.1.3.9 Ex: Coulomb and Lorentz force

Two equal point charges are, at some instant of time, located at $(0, 0, 0)$ and $(0, b, 0)$. Both are moving with velocity v in $+x$-direction (consider $v \ll c$). Determine the ratio between the magnitude of the magnetic force and the magnitude of the electric force at each charge.

4.1.3.10 Ex: Penning trap

In Penning traps, charged particles move under the influence of a homogeneous magnetic field $\vec{\mathcal{B}} = \mathcal{B}_h \hat{\mathbf{e}}_z$ and a quadrupolar electric field $\vec{\mathcal{E}} = \mathcal{E}_q(\rho\hat{\mathbf{e}}_\rho - 2z\hat{\mathbf{e}}_z)$. On which orbits do the particle move?
Help: Consider the axial and radial movements separately. For the radial motion consider two cases:
1. The influence of the electric field is negligible,
2. centripetal force is negligible.

4.1.3.11 Ex: Magnetic trap near a current wire

An infinitely long conducting wire (radius R, axis in z-direction at position $x = y = 0$) carries the current I.
a. Calculate the magnetic field inside and outside the wire.
b. Now a homogeneous magnetic field is added, $\vec{\mathcal{B}}_{apl} = \mathcal{B}_0\hat{\mathbf{e}}_x$. Calculate the absolute value of the total magnetic field $|\vec{\mathcal{B}}_{tot}|$ inside and outside of wire.
c. Where inside and outside the wire do appear points where $|\vec{\mathcal{B}}_{tot}|$ vanishes? What conditions for the parameters I, R, and $\mathcal{B}_0$ must be met for such points to exist?

4.1.3.12 Ex: Charge in homogeneous fields

A charge e moves in vacuum under the influence of homogeneous fields $\vec{\mathcal{E}}$ and $\vec{\mathcal{B}}$. Suppose that $\vec{\mathcal{E}} \cdot \vec{\mathcal{B}} = 0$ and $\mathbf{v} \cdot \vec{\mathcal{B}} = 0$. At what speed does the charge move without acceleration? What is the absolute value of its speed if $|\vec{\mathcal{E}}| = |\vec{\mathcal{B}}|$?

4.1.3.13 Ex: Rain accelerated by the Earth's magnetic field

Analyze the following train propulsion concept. The train shall be propelled by the magnetic force of the vertical component of the Earth's magnetic field acting on the current-carrying axes of the train. The value of the vertical component of the Earth's magnetic field is 10 μT, the axes have a length of 3 m. The current is fed by the rails and flows from one rail through the conducting wheels and axles to the other rail.
a. What must be the amplitude of the current to generate the modest force of 10 kN

on an axis?
b. What is the rate of electric energy loss due to heat production?

4.1.3.14 Ex: Biot-Savart law

We consider an infinitely long and thin wire oriented along the z-axis and concentrically embraced by a hollow conductor with radius R and negligible wall thickness. Through the conductor flows the current I_0 and through the wire the current I_1.
a. Calculate based on the Biot-Savart law the magnetic field produced by the inner wire at a distance d from the z-axis.
b. Calculate the force exerted by the magnetic field of the inner wire on a surface element of the current conductor.
c. What is the resulting pressure with $I_1 = -I_0 = 10$ A, $R = 1$ mm?
Help:

$$\int_a^b (c^2 + x^2)^{-\frac{3}{2}} dx = \left[\frac{x}{c^2} (c^2 + x^2)^{-\frac{1}{2}} \right]_a^b$$

4.1.3.15 Ex: Biot-Savart law

We consider an infinitely long hollow conductor running along the z-axis with finite wall thickness with inner radius $R - \epsilon$ and outer radius $R + \epsilon$. The current density j_0 within the hollow conductor is constant and the total current is I_0.
a. Calculate j_0 from I_0, ϵ, and R.
b. Calculate, based on Ampere's law, the magnetic field produced by the hollow conductor at a distance ρ from the z-axis for $R - \epsilon < \rho < R + \epsilon$.
c. Calculate the resulting force on a volume element of the current-carrying conductor.
d. Integrate the radial force and calculate the limit $\epsilon \to 0$.
e. What is the resulting pressure in $I_0 = 10$ A, $R = 1$ mm? Does the force act inward or outward?

4.1.3.16 Ex: Magnetic field of the Earth

The Earth's magnetic field is approximately 0.6 G at the magnetic poles and points vertically downwards at the magnetic pole of the northern hemisphere. If the magnetic field were due to an electric current circulating on a ring with a radius equal to Earth's inner iron core (approximately 1300 km),
a. what would be the required amplitude of the current?
b. What orientation would the current need to have, the same as Earth's rotational motion or the opposite? Justify.

4.1.3.17 Ex: Biot-Savart law

Consider the following device: A current I runs through two identical infinitely thin rings with radius R. The common center of the two rings is at the origin of the coordinates. One ring lies in the xy-plane and the other on the xz-plane.
a. Parametrize the current density $\mathbf{j}$ in spherical coordinates.

b. Show that the $\vec{\mathcal{B}}$ field resulting from this device at source is given by:

$$\vec{\mathcal{B}}(\mathbf{0}) = -\frac{\mu_0 I}{2}\frac{1}{R}\hat{\mathbf{e}}_z - \frac{\mu_0 I}{2}\frac{1}{R}\hat{\mathbf{e}}_y \ .$$

Help: A δ-function in spherical coordinates for the r variable must be multiplied by $\frac{1}{r}$; a δ-function in spherical coordinates for the ϕ variable must be multiplied by $\frac{\pi}{2}$.

4.2 Properties of the magnetic field

4.2.1 Field lines and magnetic flux

The *magnetic flux* is introduced in the same way as the electric flux,

$$\boxed{\Psi_M \equiv \int_{\mathcal{S}} \vec{\mathcal{B}} \cdot d\mathbf{S}} \ . \tag{4.12}$$

Resolve the Exc. 4.2.4.1.

4.2.2 Divergence of the magnetic field and Gauß's law

Let us compute the divergence of a magnetic field given by Biot-Savart's law [2],

$$\nabla_r \cdot \vec{\mathcal{B}} = \frac{\mu_0}{4\pi}\int_{\mathcal{V}} [\nabla_r \times \mathbf{j}(\mathbf{r}')] \cdot \frac{\mathbf{r}-\mathbf{r}'}{|\mathbf{r}-\mathbf{r}'|^3} dV' - \frac{\mu_0}{4\pi}\int_{\mathcal{V}} \mathbf{j}(\mathbf{r}') \cdot \left[\nabla_r \times \frac{\mathbf{r}-\mathbf{r}'}{|\mathbf{r}-\mathbf{r}'|^3}\right] dV' = 0 \ , \tag{4.13}$$

since, as we have already shown, the rotation of a Coulombian field is zero. Therefore,

$$\boxed{\nabla \cdot \vec{\mathcal{B}} = 0} \ . \tag{4.14}$$

With Gauß' law we can derive the integral version of this statement,

$$\boxed{\oint_{\partial\mathcal{V}} \vec{\mathcal{B}} \cdot d\mathbf{S} = 0} \ . \tag{4.15}$$

Comparing this equation with the corresponding electrostatic equation (2.13), we deduce the following interpretation: The total magnetic flux Ψ_M across a closed surface must vanish and can not be changed by *hypothetical magnetic charges*, i.e. *magnetic charges do not exist*!

A direct consequence of this law is that we can introduce the concept of the vector potential, which is fundamental in the sense that it allows us to formulate electrodynamics completely in terms of potentials. We will dedicate the whole next section to magnetic potentials.

[2] Using the rule $\nabla \cdot (\vec{\mathcal{E}} \times \vec{\mathcal{B}}) = (\nabla \times \vec{\mathcal{E}}) \cdot \vec{\mathcal{B}} - \vec{\mathcal{E}} \cdot (\nabla \times \vec{\mathcal{B}})$.

4.2.3 Rotation of the magnetic field and Ampère's law

Let us now calculate the rotation of the magnetic field given by Biot-Savart's law [3],

$$\nabla_r \times \vec{\mathcal{B}} = \frac{\mu_0}{4\pi}\int_{\mathcal{V}} -[\mathbf{j}(\mathbf{r}')\cdot\nabla_r]\frac{\mathbf{r}-\mathbf{r}'}{|\mathbf{r}-\mathbf{r}'|^3}dV' + \frac{\mu_0}{4\pi}\int_{\mathcal{V}} \mathbf{j}(\mathbf{r}')\left(\nabla_r\cdot\frac{\mathbf{r}-\mathbf{r}'}{|\mathbf{r}-\mathbf{r}'|^3}\right)dV' \tag{4.16}$$

$$= \frac{\mu_0}{4\pi}\int_{\mathcal{V}} [\mathbf{j}(\mathbf{r}')\cdot\nabla_{r'}]\frac{\mathbf{r}-\mathbf{r}'}{|\mathbf{r}-\mathbf{r}'|^3}dV' + \frac{\mu_0}{4\pi}\int_{\mathcal{V}} \mathbf{j}(\mathbf{r}')4\pi\delta(\mathbf{r}-\mathbf{r}')dV'$$

$$= \frac{\mu_0}{4\pi}\int_{\mathcal{V}} [\mathbf{j}(\mathbf{r}')\cdot\nabla_{r'}]\frac{\mathbf{r}-\mathbf{r}'}{|\mathbf{r}-\mathbf{r}'|^3}dV' + \mu_0\mathbf{j}(\mathbf{r}) \ . \tag{4.17}$$

Considering the x-component,

$$(\nabla_r \times \vec{\mathcal{B}})_x = \frac{\mu_0}{4\pi}\int_{\mathcal{V}} \mathbf{j}(\mathbf{r}')\cdot\nabla_{r'}\frac{x-x'}{|\mathbf{r}-\mathbf{r}'|^3} + \mu_0 j_x(\mathbf{r})$$

$$= -\frac{\mu_0}{4\pi}\oint_{\partial\mathcal{V}} \mathbf{j}(\mathbf{r}')\frac{x-x'}{|\mathbf{r}-\mathbf{r}'|^3}d\mathbf{S}' + \frac{\mu_0}{4\pi}\int_{\mathcal{V}}\frac{x-x'}{|\mathbf{r}-\mathbf{r}'|^3}\nabla_{r'}\cdot\mathbf{j}(\mathbf{r}')dV' + \mu_0 j_x(\mathbf{r}) \ .$$

The surface integral vanishes when the volume goes to infinity. On the other hand, $\nabla\cdot\mathbf{j} = -\dot{\varrho} = 0$. With this, we obtain,

$$\boxed{\nabla\times\vec{\mathcal{B}} = \mu_0\mathbf{j}} \ . \tag{4.18}$$

The results (4.14) and (4.18) represent parts of Maxwell's first and fourth equations. The equation (4.18) is also called *Ampère's law*. The integral version can be obtained from Stokes' law,

$$\boxed{\oint_{\mathcal{C}} \vec{\mathcal{B}}\cdot d\mathbf{l} = \mu_0 I} \ . \tag{4.19}$$

The interpretation of Ampere's law is, that *every current produces a rotational magnetic field*, that is, a field with closed field lines. Measuring the magnetic field along an closed path we can evaluate the current passing through the surface delimited by the path.

Ampère's law has many applications. Let's discuss some in the next.

Example 41 (*Magnetic field of a straight current-carrying wire*): Let us re-evaluate the example 39 using Ampere's law,

$$\oint \vec{\mathcal{B}}\cdot d\mathbf{l} = B\int_0^{2\pi}\rho d\phi = \mathcal{B}2\pi\rho = \mu_0 I \ .$$

Hence,

$$\mathcal{B} = \frac{\mu_0 I}{2\pi\rho} \ .$$

Example 42 (*Ampère's law*): We can use Ampère's law to show that a locally uniform magnetic field, such as the one shown in Fig. 4.8, is impossible. Let

[3] Using the rule $\nabla\times(\vec{\mathcal{E}}\times\vec{\mathcal{B}}) = (\vec{\mathcal{B}}\cdot\nabla)\vec{\mathcal{E}} - (\vec{\mathcal{E}}\cdot\nabla)\vec{\mathcal{B}} + \vec{\mathcal{E}}(\nabla\cdot\vec{\mathcal{B}}) - \vec{\mathcal{B}}(\nabla\cdot\vec{\mathcal{E}})$.

us have a look at the rectangular curve shown by the dashed lines. With the chosen geometry, the curve does not include current,

$$\mu_0 I = 0 \ .$$

On the other hand, the magnetic field accumulated along the curve is,

$$\oint_C \vec{\mathcal{B}} \cdot d\mathbf{l} \neq 0 \ .$$

This is a contradiction. Thus, this example shows that, in the absence of cur-

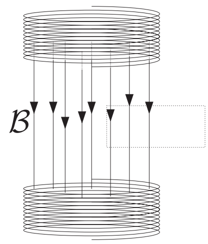

Figure 4.8: Impossibility of a localized homogeneous magnetic field.

rents, any magnetic field is conservative. We could then define a scalar potential whose gradient would be the magnetic field, but this potential must be *simply connected*, i.e. not be traversed by currents, which limits the practical use of such a potential.

Example 43 (*Field of a solenoid*): A solenoid is a very long coil (the distance between two consecutive turns is much smaller than the radius and the total length l of the coil) carrying a current I (see diagram in Fig. 4.9). Ampère's law can be used to easily calculate the magnetic field inside a solenoid composed of N turns,

$$\mathcal{B} dl = \oint_C \vec{\mathcal{B}} \cdot d\mathbf{r} = \mu_0 I \ dN \ .$$

Hence,

$$\mathcal{B} = \mu_0 I \frac{dN}{dl} \ .$$

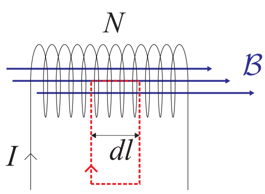

Figure 4.9: Scheme of a solenoid with loop density dN/dl.

Resolve the Excs. 4.2.4.2 to 4.2.4.9. In the Excs. 4.2.4.10 to 4.2.4.12 we apply the Biot-Savart law to *Helmholtz coils* and *anti- Helmholtz coils*.

4.2.4 Exercises

4.2.4.1 Ex: Magnetic flux

A long solenoid has n turns per unit length, radius R_1, and carries a current I. A circular coil with radius R_2 and N turns is coaxial to the solenoid and is equidistant from its ends.
a. Determine the magnetic flux through the coil if $R_2 < R_1$.
b. Determine the magnetic flux through the coil if $R_2 > R_1$.

4.2.4.2 Ex: Magnetic field of a conducting ring and Ampère's law

A ring-shaped conducting loop lies in the yz-plane; the loop's symmetry axis is the x-axis. It is traversed by a current I generating on the axis the field $\mathcal{B}_x = \frac{1}{2}\mu_0 I R^2(x^2+R^2)^{-3/2}$.
a. Calculate the line integral $\int \vec{\mathcal{B}} \cdot d\mathbf{s}$ along the x-axis between $x = -L$ and $x = +L$.
b. Show that for $L \to \infty$ the line integral converges to $\mu_0 I$.
Help: This result can also be obtained with Ampère's law, when we close the integration path through a semicircle with radius L, for which holds $\mathcal{B} \simeq 0$, when L is very large.

4.2.4.3 Ex: Biot-Savart's and Ampère's laws

a. Calculate the magnetic field generated by a constant current I on a straight conductor piece of length L.
b. Show that for an infinitely long conductor the Biot-Savart law becomes Ampere's law.

4.2.4.4 Ex: Solenoid

a. To determine the number of turns of a solenoid with diameter $D = 4\,\text{cm}$ and length $L = 10\,\text{cm}$, an experimenter passes a current $I = 1\,\text{A}$ through the coil. He measures the magnetic field $\mathcal{B} = 10\,\text{mT}$. How many windings are there?
b. To confirm it measures the diameter of the copper wire ($d = 1\,\text{mm}$) and ohmic resistance finding $R = 2\,\Omega$. On the internet he finds the resistivity of copper $\rho = 1.7 \cdot 10^{-8}\,\Omega\text{m}$.

4.2.4.5 Ex: Toroidal coil

A coil with N turns is arranged in a toroidal form with rotational symmetry around z-axis and has its center at the origin of the coordinates. The coil is densely wound and traversed by a current I (see scheme).
a. Calculate the $\hat{\mathbf{e}}_\phi$-component of the $\vec{\mathcal{B}}$-field for $z = 0$ (xy-plane) as a function of distance ρ from the origin.
b. Determine the $\hat{\mathbf{e}}_\phi$-component of the $\vec{\mathcal{B}}$-field in the entire *inner* space outside the toroid. Draw the $\hat{\mathbf{e}}_\phi$ component as a function of ρ.
c. What should be the value of b, so that $\mathcal{B}_\phi$ is constant within the toroid with an accuracy of $\alpha = 1\%$, when $a = 1\,\text{cm}$? [That is: $\mathcal{B}_\phi(b-a) - \mathcal{B}_\phi(b+a) < \alpha \cdot \mathcal{B}_\phi(b)$]

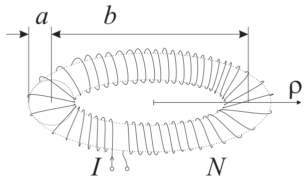

Figure 4.10: Toroidal coil.

4.2.4.6 Ex: Toroidal coil

A toroidal coil tightly wound with 1000 turns has an inner radius of 1.0 cm, an outer radius of 2.0 cm, carries a current of 1.5 A. The torus is centered at the origin with the centers of the individual turns in the $z = 0$ plane. What is the intensity of the magnetic field in the $z = 0$ plane a distance of (a) 1.1 cm and (b) 1.5 cm away from the origin?

4.2.4.7 Ex: Inhomogeneous current density

The current density on a straight wire of infinite length with the radius R grows linearly from the center outward, $\mathbf{j}(r) = j_0 r\hat{\mathbf{e}}_z$, where $\hat{\mathbf{e}}_z$ shows in the direction of the wire and the total current going through the wire is I.
a. Calculate j_0 as a function of I.
b. Calculate, using Ampere's law, the magnetic field inside and outside the wire.
c. Make a graph of the normalized magnetic field, $\mathcal{B}(r)/\mathcal{B}_R$, versus r/R, where $\mathcal{B}_R \equiv \mu_0 I/2\pi R$.

4.2.4.8 Ex: Magnetic field in a coaxial cable

A coaxial cable consists of an inner conductor with radius R_1 and a cylindrical outer conductor with inner radius R_2 and outer radius R_3. In both conductors flows the same current I in opposite directions. The current densities in each conductor are homogeneous.
a. Calculate the current densities in each conductor.
b. Calculate the magnetic field $\mathcal{B}(r)$ for $r \leq R_1$,
c. for $R_1 \leq r \leq R_2$,
d. for $R_2 \leq r \leq R_3$,
e. for $R_3 \leq r$.

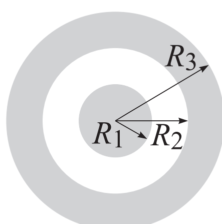

Figure 4.11: Magnetic field in a coaxial cable.

4.2.4.9 Ex: Magnetic field of a current conductor

In a straight, infinitely long conductor with circular cross-sectional area with radius R runs a current I with a uniform current density distribution. How are the magnetic induction field lines $\vec{\mathcal{B}}$?
a. Calculate $\vec{\mathcal{B}}$ inside and outside the conductor.
b. Prepare a scheme of the profile $\mathcal{B}(r) \equiv |\vec{\mathcal{B}}(r)|$, where r be the distance from the symmetry axis of the conductor in a direction perpendicular to it.

4.2.4.10 Ex: Helmholtz and anti-Helmholtz coils

a. Show that the magnetic field of a round current loop conductor with radius R on the symmetry axis is given by,

$$\vec{\mathcal{B}}(z) = -\frac{\mu_0 I}{2}\frac{R^2}{\sqrt{R^2+z^2}^3}\hat{\mathbf{e}}_z \ .$$

b. Now consider two identical parallel loops placed on the symmetry axis with distance $d = R$. The loops are traversed by currents of equal amplitude. What is the behavior of the magnetic field on the symmetry axis for (i) equal directions of currents (ii) opposite directions? Choosing as the origin the center between the two coils, expands the magnetic field to second order in a Taylor series around the origin.

4.2.4.11 Ex: Helmholtz coils

Two identical circular coils of radius R and negligible thickness are mounted with their axes coinciding with the z-axis, as shown in the figure below. Their centers are separated by a distance d, with the midpoint P coinciding with the origin of the z-axis. The coils carry electric currents of the same intensity I, and both counterclockwise.
a. Use the Biot-Savart law to show that the magnetic field $\mathcal{B}(z)$ along the z-axis is,

$$\vec{\mathcal{B}}_{t+}(z) = -\frac{\mu_0 I}{2}\hat{\mathbf{e}}_z\left(\frac{R^2}{\sqrt{R^2+(z-R/2)^2}^3} \pm \frac{R^2}{\sqrt{R^2+(z+R/2)^2}^3}\right) \ .$$

b. Assuming that the spacing d is equal to the radius R of the coils, show that at point P the following equalities are valid: $d\mathcal{B}/dz = 0$ and $d^2\mathcal{B}/dz^2 = 0$.
c. Looking at the graphs below, which curve describes the magnetic field along the z-axis in the configuration of item (b)? Justify!
d. Assuming that the current in the upper coil is reversed, calculate the new value of the magnetic field at point P.

4.2.4.12 Ex: Helmholtz coils

A pair of identical coils, each with a radius of 30 cm, is separated by a distance equal to their radii. Called Helmholtz coils, they are coaxial and carry equal currents oriented such that their axial fields point into the same z-direction. A feature of Helmholtz coils is, that the resulting magnetic field in the region between the coils is quite uniform. Assume that the current in each one is 15 A and that there are 250 turns for each coil. Using a spreadsheet, calculate and plot the magnetic field

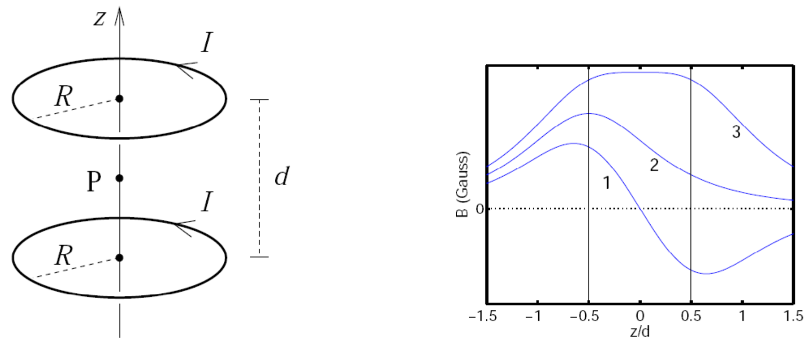

Figure 4.12: (code) Geometry and magnetic field amplitude of a pair of Helmholtz coils.

along the z-axis for $-30\,\text{cm} < z < +30\,\text{cm}$. Within which z-range does the field vary by less than 20%?

4.3 The magnetic vector potential

The fact that the divergence of the magnetic field vanishes, $\nabla \cdot \vec{\mathcal{B}} = 0$, allows us to introduce a vector field $\mathbf{A}$ called *vector potential* of which the magnetic field is the rotation,

$$\boxed{\vec{\mathcal{B}} = \nabla \times \mathbf{A}}\ . \tag{4.20}$$

4.3.1 The Laplace and Poisson equations

Ampère's law says,

$$\mu_0 \mathbf{j} = \nabla \times \vec{\mathcal{B}} = \nabla \times (\nabla \times \mathbf{A}) = \nabla(\nabla \cdot \mathbf{A}) - \nabla^2 \mathbf{A}\ . \tag{4.21}$$

Note that, just as we can add a constant to the electrostatic potential without changing the electric field, we have the freedom to add to the vector potential the *gradient of a scalar field*,

$$\nabla \times \mathbf{A} = \nabla \times (\mathbf{A} + \nabla \chi)\ , \tag{4.22}$$

since the rotation of a gradient always vanishes. This freedom allows us to impose other conditions on this scalar field $\chi(\mathbf{r})$. One of them is called the *Coulomb gauge*,

$$\boxed{\nabla \cdot \mathbf{A} \equiv 0}\ . \tag{4.23}$$

To show that it is always possible to choose a function χ such, that the potential vector $\mathbf{A} + \nabla\chi$ satisfies the condition (4.23) and at the same time produces the same magnetic field (4.22), we just insert this potential into Eq. (4.23) and find a formal solution of the following Poisson equation,

$$\nabla^2 \chi = -\nabla \cdot \mathbf{A}\ . \tag{4.24}$$

is simply the Coulomb potential [see (2.33)],

$$\chi(\mathbf{r}) = \frac{1}{4\pi}\int_{\mathcal{V}} \frac{\nabla_{r'}\cdot\mathbf{A}(\mathbf{r}')}{|\mathbf{r}-\mathbf{r}'|}dV' \ , \tag{4.25}$$

supposing that $\nabla\cdot\mathbf{A} \overset{r\to\infty}{\longrightarrow} 0$.

Within the Coulomb gauge the Eq. (4.21) also adopts the simple form of a Poisson equation,

$$\boxed{\nabla^2\mathbf{A} = -\mu_0\mathbf{j}} \ , \tag{4.26}$$

which we can solve,

$$\boxed{\mathbf{A}(\mathbf{r}) = \frac{\mu_0}{4\pi}\int \frac{\mathbf{j}(\mathbf{r}')}{|\mathbf{r}-\mathbf{r}'|}d^3\mathbf{r}'} \ . \tag{4.27}$$

This relationship is the equivalent of the electrostatic potential (2.35). We verify that we recover Biot-Savart's law (4.8) via,

$$\nabla_r \times \mathbf{A}(\mathbf{r}) = \frac{\mu_0}{4\pi}\int_{\mathcal{V}} \mathbf{j}(\mathbf{r}') \times \frac{|\mathbf{r}-\mathbf{r}'|}{|\mathbf{r}-\mathbf{r}'|^3}dV' \ . \tag{4.28}$$

Example 44 (*Vector potential of a one-dimensional current*): As an example we consider a one-dimensional current, $\mathbf{j}(\mathbf{r}') = I\delta^2(\mathbf{r}'-\mathbf{s}_\perp)\hat{\mathbf{e}}'_j$,

$$\mathbf{A}(\mathbf{r}) = \frac{\mu_0 I}{4\pi}\int_{\mathcal{C}} \frac{d\mathbf{s}'}{|\mathbf{r}-\mathbf{r}'|} \qquad \text{and} \qquad \vec{\mathcal{B}}(\mathbf{r}) = \frac{\mu_0 I}{4\pi}\int_{\mathcal{C}} \frac{d\mathbf{s}'\times|\mathbf{r}-\mathbf{r}'|}{|\mathbf{r}-\mathbf{r}'|^3} \ .$$

For a current element oriented along the z-axis,

$$\mathbf{A}(\mathbf{r}) = \frac{\mu_0 I}{4\pi}\int_0^a \frac{\hat{\mathbf{e}}_z dz'}{\sqrt{\rho^2+(z-z')^2}} = \frac{\mu_0 I}{4\pi}\hat{\mathbf{e}}_z \ln\frac{-(z-a)+\sqrt{r^2+(z-a)^2}}{-z+\sqrt{r^2+z^2}} \ .$$

The scheme 4.13 summarizes the fundamental laws of magnetostatics.

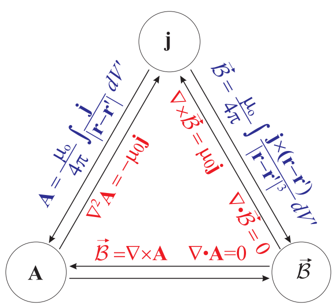

Figure 4.13: Organization chart for the fundamental laws of magnetostatics. Note, that there is no simple expression to calculate $\mathbf{A}$ from $\vec{\mathcal{B}}$.

4.3.2 Magnetostatic boundary conditions

In order to find the magnetostatic boundary conditions imposed by current-carrying interfaces, we proceed in the same way as in the electrostatic case. First, we consider a 'pill box', as schematized in Fig. 4.14. From

$$\oint \vec{\mathcal{B}} \cdot d\mathbf{S} = 0 \ , \tag{4.29}$$

we find for the component of the magnetic field perpendicular to the interface,

$$\mathcal{B}_{top}^{\perp} = \mathcal{B}_{down}^{\perp} \ . \tag{4.30}$$

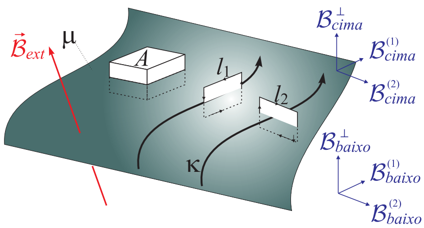

Figure 4.14: Illustration of the pillbox-shaped volume delimited by the surface A cutting through a small part of the interface. Also shown are paths on the interface being perpendicular (l_1) or parallel (l_2) to the surface current κ.

We now consider a closed loop in the plane defined by the magnetic field and perpendicular to the current. From

$$\oint \vec{\mathcal{B}} \cdot d\mathbf{l}_2 = (\mathcal{B}_{top}^{(2)} - \mathcal{B}_{bottom}^{(2)})l_2 = \mu_0 I = \mu_0 \kappa l_2 \ , \tag{4.31}$$

where we defined $\kappa \equiv I/l_2$ as the surface current density, that is, the current dI flowing through a ribbon of width dl_2 sticking to the interface. We find,

$$\mathcal{B}_{top}^{(2)} - \mathcal{B}_{bottom}^{(2)} = \mu_0 \kappa \ . \tag{4.32}$$

Thus, the component of $\vec{\mathcal{B}}$ parallel to the surface but perpendicular to the current is discontinuous by a value $\mu_0 \kappa$.

Similarly, a closed loop in the direction parallel to the current shows that the parallel component of $\vec{\mathcal{B}}$ is continuous,

$$\oint \vec{\mathcal{B}} \cdot d\mathbf{l}_1 = (\mathcal{B}_{top}^{(1)} - \mathcal{B}_{bottom}^{(1)})l_1 = 0 \ . \tag{4.33}$$

In summary,

$$\vec{\mathcal{B}}_{top} - \vec{\mathcal{B}}_{bottom} = \vec{\mathcal{B}}_{top}^{\parallel} - \vec{\mathcal{B}}_{bottom}^{\parallel} = \mu_0 \vec{\kappa} \times \hat{\mathbf{n}} \ . \tag{4.34}$$

In the same way as the scalar potential in electrostatics, the potential vector remains continuous through the interface,

$$\mathbf{A}_{top} = \mathbf{A}_{bottom} \ , \tag{4.35}$$

because $\nabla \cdot \mathbf{A} = 0$ ensures that the normal component is continuous and,

$$\oint \mathbf{A} \cdot d\mathbf{l} = \int \nabla \times \mathbf{A} \cdot d\mathbf{S} = \int \vec{\mathcal{B}} \cdot d\mathbf{S} = \Psi_M \ , \tag{4.36}$$

means that the tangential components are continuous (the flux through an Amperian loop of negligible thickness vanishes). On the other hand, the derivative of $\mathbf{A}$ inherits the discontinuity of $\vec{\mathcal{B}}$:

$$\frac{\partial \mathbf{A}_{top}}{\partial n} - \frac{\partial \mathbf{A}_{bottom}}{\partial n} = -\mu_0 \vec{\kappa} \ , \tag{4.37}$$

where n is the coordinate perpendicular to the surface.

Example 45 (*Proof of the discontinuity of the derivative of the vector potential*): To prove the statement (4.37) we consider a surface current in the direction $\vec{\kappa} = \kappa \hat{\mathbf{e}}_x$ within an interface located in the x-y-plane. So,

$$\vec{\mathcal{B}}_{top} - \vec{\mathcal{B}}_{bottom} = \begin{pmatrix} 0 \\ \mu_0 \kappa \\ 0 \end{pmatrix} = \begin{pmatrix} \partial_y A^{(z)}_{top} - \partial_z A^{(y)}_{top} \\ \partial_z A^{(x)}_{top} - \partial_x A^{(z)}_{top} \\ \partial_x A^{(y)}_{top} - \partial_y A^{(x)}_{top} \end{pmatrix} - \begin{pmatrix} \partial_y A^{(z)}_{bottom} - \partial_z A^{(y)}_{bottom} \\ \partial_z A^{(x)}_{bottom} - \partial_x A^{(z)}_{bottom} \\ \partial_x A^{(y)}_{bottom} - \partial_y A^{(x)}_{bottom} \end{pmatrix} \ .$$

Now,

$$0 = \partial_y A^{(z)}_{top} - \partial_y A^{(z)}_{bottom} = \partial_z A^{(y)}_{top} - \partial_z A^{(y)}_{bottom} = \partial_x A^{(y)}_{top} - \partial_x A^{(y)}_{bottom} = \partial_y A^{(x)}_{top} - \partial_y A^{(x)}_{bottom}$$
$$\mu_0 \kappa_x = \partial_z A^{(x)}_{top} - \partial_z A^{(x)}_{bottom} - \partial_x A^{(z)}_{top} + \partial_x A^{(z)}_{bottom} \ .$$

Assuming a uniform field, only the derivative in z can contribute, such that,

$$\mu_0 \kappa_x = \partial_z A^{(x)}_{top} - \partial_z A^{(x)}_{bottom} \ .$$

4.3.3 Exercises

4.3.3.1 Ex: Vector potential and electric field of a rotating charged sphere

On the surface of a hollow sphere with radius R be evenly distributed the charge Q. The sphere rotates at constant angular velocity $\vec{\omega}$ around one of its diameters.
a. Determine the current density generated by the motion $\mathbf{j}(\mathbf{r})$.
b. Derive the components of the potential vector $\mathbf{A}(\mathbf{r})$ and the magnetic field $\vec{\mathcal{B}}(\mathbf{r})$.

4.3.3.2 Ex: Magnetic field of a rotating spherical layer with spherical harmonics

Calculate the vector potential, magnetic field and magnetization of a charged rotating spherical layer using spherical harmonics.

4.3.3.3 Ex: Conducting thin loops

Consider a circular conducting loop with radius R. The wire of the loop is infinitely thin (δ-function). Through the loop flows a continuous current I.
a. What is the expression for current density $\mathbf{j}(\mathbf{r})$? Express the result in spherical coordinates considering that the integral of the current over a surface perpendicular to the wire must give I.
b. Calculate the magnetic dipolar moment of this current loop,

$$\mathbf{m} = \frac{1}{2}\int [\mathbf{r} \times \mathbf{j}(\mathbf{r})] d^3r \ .$$

c. For large distances from a localized current distribution, the potential vector $\mathbf{A}$ is dominated by the dipolar contribution,

$$\mathbf{A}(\mathbf{r}) = \frac{\mathbf{m} \times \mathbf{r}}{r^3} \ .$$

What are, in this approximation, the values of the potential vector $\mathbf{A}$ and the magnetic field $\vec{\mathcal{B}}$ for the conducting loop?

4.3.3.4 Ex: Conducting thin loops

Consider a system of N different conducting loops (use δ-functions) through which runs a current I_j ($j = 1, \ldots, N$). The magnetic flux through the j-th loop is then given by,

$$\Phi_j = \sum_{m=1}^{N} \int_{F_j} \vec{\mathcal{B}}_m \cdot d\mathbf{S} \ ,$$

where the integral must be taken over the area enclosed by the current loops j and $\vec{\mathcal{B}}_m$ is the part of the magnetic field due to the j-th loop.
a. Show,

$$\Phi_j = c \sum_{m=1}^{N} L_{jm} I_m$$

with the induction coefficient,

$$\frac{L_{jm} = \frac{1}{c^2} \int_j \int_m d\mathbf{r}_j \cdot d\mathbf{r}_m}{|\mathbf{r}_j - \mathbf{r}_m| \ ,}$$

where the integrals are taken over the loops j and m.
b. Also show that the magnetic field energy of the loop system is given by,

$$W = \frac{1}{2} \sum_{j,m} L_{jm} I_j I_m \ .$$

4.3.3.5 Ex: Conducting thin loops

A conducting loop made of two semicircles (see diagram) with radii $r_i = 0.3\,\text{m}$ and $r_a = 0.5\,\text{m}$ carries a current $I = 1.5\,\text{A}$.
a. Calculate the magnetic moment $\vec{\mu}$ of the conducting loop.
b. The conducting loop is now traversed by a $\mathcal{B}$-field of amplitude $\mathcal{B} = 0.3\,\text{T}$. Calculate the resulting torque $\mathbf{m}$ on the loop, when the $\mathcal{B}$-field is directed (i) toward z, (ii) toward x, and (iii) orthogonal to the plane of the scheme.

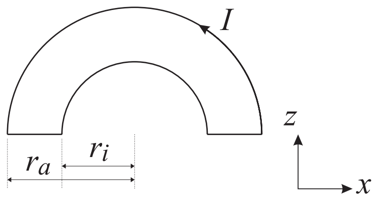

Figure 4.15: Loop.

4.3.3.6 Ex: Gauge transformation

Be given the potential vector,

$$\mathbf{A}(\mathbf{r}) = \frac{1}{y^2+z^2+a^2}\begin{pmatrix} 0 \\ z \\ -y \end{pmatrix} .$$

Discusses the corresponding magnetic field $\vec{\mathcal{B}} = \nabla \times \mathbf{A}$.
a. Show that the potential

$$\mathbf{A}'(\mathbf{r}) = \frac{1}{y^2+z^2+a^2}\begin{pmatrix} 0 \\ y+z \\ z-y \end{pmatrix}$$

gives the same magnetic field as the potential $\mathbf{A}(\mathbf{x})$.
b. Show:

$$\mathbf{A}'(\mathbf{r}) = \mathbf{A}(\mathbf{r}) - \nabla\alpha(\mathbf{r})$$

and determine $\alpha(\mathbf{r})$.

4.3.3.7 Ex: Coulomb gauge

Be given the vector potential,

$$\mathbf{A}(x,y,z) = \frac{(x+y)\hat{\mathbf{e}}_x + (-x+y)\hat{\mathbf{e}}_y}{\sqrt{x^2+y^2}} .$$

Find a gauge transformation $\alpha(x,y,z)$, where $\mathbf{A} \to \mathbf{A}' = \mathbf{A} - \nabla\alpha$, such that transformed vector potential satisfies the Coulomb gauge.

Help: The Laplace operator in cylindrical coordinates has the form,

$$\Delta = \frac{1}{\rho}\frac{\partial}{\partial\rho}\left(\rho\frac{\partial}{\partial\rho}\right) + \frac{\partial^2}{\partial z^2} + \frac{1}{\rho^2}\frac{\partial^2}{\partial\phi^2} \ .$$

where $\rho^2 = x^2 + y^2$.

4.3.3.8 Ex: Vector potential of a homogeneous field

We consider a homogeneous magnetic field in z-direction,

$$\vec{\mathcal{B}} = \mathcal{B}\hat{\mathbf{e}}_z \ .$$

Invent a potential vector $\mathbf{A}$, such that $\vec{\mathcal{B}} = \text{rot } \mathbf{A}$. How does the potential vector look like in the Coulomb gauge (that is, under the condition: div $\mathbf{A} = 0$).

4.4 Multipolar expansion

Using the expansion (2.91) we can expand the vector potential in the same way as we did with the electrostatic potential in formula (2.92),

$$\mathbf{A}(\mathbf{r}) = \frac{\mu_0 I}{4\pi}\oint \frac{1}{|\mathbf{r}-\mathbf{r}'|}d\mathbf{l}' = \frac{\mu_0 I}{4\pi}\sum_{\ell=0}^{\infty}\frac{1}{r^{\ell+1}}\oint r'^{\ell}P_\ell(\cos\theta')d\mathbf{l}' \ . \tag{4.38}$$

Explicitly,

$$\mathbf{A}(\mathbf{r}) = \frac{\mu_0 I}{4\pi}\left[\frac{1}{r}\oint d\mathbf{l}' + \frac{1}{r^2}\oint r'\cos\theta' d\mathbf{l}' + \frac{1}{r^3}\oint r'^2(\tfrac{3}{2}\cos^2\theta' - \tfrac{1}{2})d\mathbf{l}' + ...\right] \ . \tag{4.39}$$

4.4.1 Multipolar magnetic moments

Since there are no magnetic monopoles, the first term of the multipolar expansion will be $\oint d\mathbf{l}' = 0$. The next term is the dipole term,

$$\mathbf{A}_{dip} = \frac{\mu_0 I}{4\pi r^2}\oint \hat{\mathbf{r}}\cdot\mathbf{r}' d\mathbf{l}' \ . \tag{4.40}$$

Doing the calculation,

$$\begin{aligned}\mathbf{c}\cdot\oint \hat{\mathbf{r}}\cdot\mathbf{r}' d\mathbf{l}' &= \oint \mathbf{c}(\hat{\mathbf{r}}\cdot\mathbf{r}')\cdot d\mathbf{l}' = \int \nabla_{r'}\times[\mathbf{c}(\hat{\mathbf{r}}\cdot\mathbf{r}')]\cdot d\mathbf{S}' \qquad (4.41)\\ &= -\int [\mathbf{c}\times\nabla_{r'}(\hat{\mathbf{r}}\cdot\mathbf{r}')]\cdot d\mathbf{S}' = -(\mathbf{c}\times\hat{\mathbf{r}})\cdot\int d\mathbf{S}' = -\mathbf{c}\cdot\left(\hat{\mathbf{r}}\times\int d\mathbf{S}'\right) \ ,\end{aligned}$$

for arbitrary constants $\mathbf{c}$, we find,

$$\boxed{\mathbf{A}_{dip} = -\frac{\mu_0 I}{4\pi r^2}\hat{\mathbf{r}}\times\int d\mathbf{S}' = \frac{\mu_0}{4\pi}\frac{\mathbf{m}\times\hat{\mathbf{r}}}{r^2}} \quad \text{where} \quad \boxed{\mathbf{m} \equiv I\int d\mathbf{S}} \tag{4.42}$$

is the *magnetic dipole moment*.

Example 46 (*Magnetic moment of a current loop*): The magnetic moment of a conductive coil of radius R lying in the x-y-plane and traversed by a current is calculated by,

$$\mathbf{m} = I \int d\mathbf{S} = I\pi R^2 \hat{\mathbf{e}}_z \ .$$

We will show in Exc. 4.4.2.1 how the magnetic dipole moment of a current loop can also be calculated from a suitable parametrization via the definition,

$$\boxed{\mathbf{m} = \tfrac{1}{2} \int \mathbf{r}' \times \mathbf{j}(\mathbf{r}', t) d^3 r'} \ . \tag{4.43}$$

4.4.2 Exercises

4.4.2.1 Ex: Magnetic moment

Calculate the torque on a rectangular coil with N loops placed in a homogeneous magnetic field, as shown in the figure.

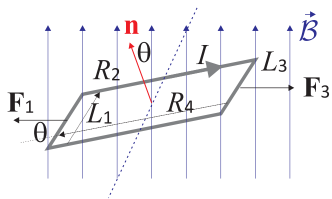

Figure 4.16: Magnetic moment.

4.4.2.2 Ex: Magnetic moment

a. Determine the magnetic moment of a circular conducting loop with radius R carrying a current I_1. The loop is in the xy-plane.
b. Now two outer segments of the circle are deformed at a distance a at right angles to the direction $-\hat{\mathbf{e}}_z$. What is the magnetic moment of the new configuration.
c. Now consider an infinitely long current line I_2 at a distance d from the origin and oriented in z-direction. What is the torque acting on the configurations in (a) and (b).

4.4.2.3 Ex: Magnetic moment of a cube

A conductor carries the current $I = 6\,\text{A}$ along the path shown in the figure, which runs through 8 of the 12 corners of the cube whose length is $L = 10\,\text{cm}$.
a. Calculate dipole magnetic moment along the way.
b. Calculate the magnetic induction $\vec{\mathcal{B}}$ at the points $(x, y, z) = (0, 5\,\text{m}, 0)$ and $(x, y, z) = (5\,\text{m}, 0, 0)$.

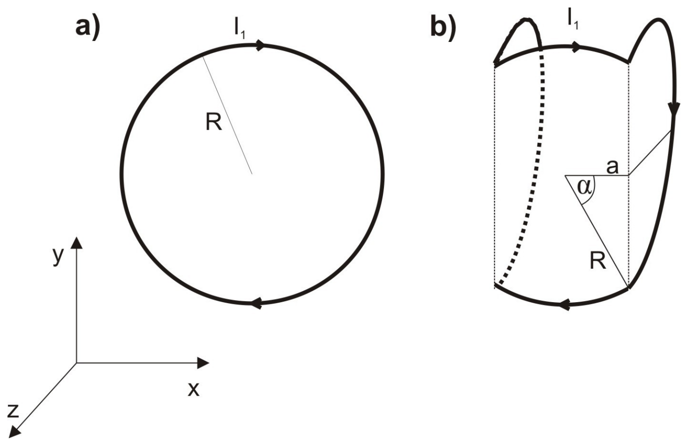

Figure 4.17: Magnetic moment.

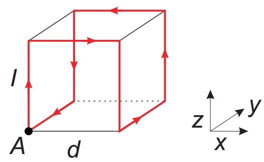

Figure 4.18: Magnetic moment.

4.4.2.4 Ex: Magnetic moment of thin circular disk

Consider a very thin disk with radius R, homogeneously charged with the charge Q, and spinning around the z-axis with angular velocity ω.
a. Parametrize the charge and current distributions.
b. Calculate the magnetic moment.

4.4.2.5 Ex: Magnetic compass

A topographer uses a magnetic compass while standing 6.1 m under a high voltage line on which flows a current of 100 A. The horizontal component of the Earth's magnetic field at this place is 20 μT. How large is the magnetic field due to the current at the position of the compass? Will the magnetic field disturb the compass noticeably?

4.4.2.6 Ex: Torque of a magnetic needle

A magnetic needle has a dipolar magnetic moment $\mu = 10^{-2}\,\text{Am}^2$. Calculate the torque on the needle due to the horizontal component of the Earth's magnetic field at the equator ($\mathcal{B}_H = 4 \cdot 10^{-5}\,\text{T}$), if the magnetic north pole of the needle points in northeastern direction.

4.4.2.7 Ex: Curved conductive circuit

A rectangular conducting loop is deformed in the middle of the edges (length a) to form a right angle. The conducting loop is traversed by a current I. Calculate the dipolar magnetic moment $\mathbf{m}$ of this configuration. Give the absolute value and orientation of $\mathbf{m}$.
Help: Use the overlapping principle and replace the above geometry with an overlap of two conductive loops.

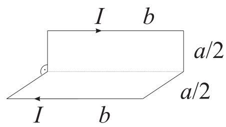

Figure 4.19: Curved conductive circuit.

4.4.2.8 Ex: Magnetic dipole

A magnetic dipole $\vec{\mu} = \mu\hat{\mathbf{e}}_z$ is at origin of the coordinate system and has the value $\mu = 1\,\text{esu}\cdot\text{cm}$. This dipole generates a magnetic field of the form,

$$\vec{\mathcal{B}}(\mathbf{r}) = \frac{3\mathbf{r}(\vec{\mu}\cdot\mathbf{r}) - r^2\vec{\mu}}{r^5} \ .$$

a. At what distance from the origin does the absolute value of $\vec{\mathcal{B}}$ take the value $1\,\text{esu/cm}^2$ going (i) in z-direction, (ii) in x-direction, and (iii) in a diagonal direction with in the xz-plane?
b. Which direction does $\vec{\mathcal{B}}$ point in these three cases?

4.4.2.9 Ex: Fields of electric and magnetic point dipoles

a. Calculate the field of an electric dipole taking care to remove the divergence in the center of origin by calculating the field averaged over a sphere and comparing it with known results.
b. Repeat the procedure of (b) for a magnetic dipole.

4.4.2.10 Ex: Magnetic dipole moment of a rectangular conducting loop

A (ideal) rectangular conducting loop with edge lengths a and b carries a current I.
a. Give the current density distribution $\mathbf{j}$.
b. Calculate the corresponding dipolar magnetic moment $\vec{\mathcal{M}}$.

4.4.2.11 Ex: Dipolar magnetic moment of a rectangular loop

The rectangular conducting loop of Exc. 4.4.2.10 is deformed in the middle of the edges (length a) to form a right angle (see figure). It is traversed by a current I. Calculate the dipolar magnetic moment of this geometry.

4.4.2.12 Ex: Force on the walls of a hollow cylinder

Consider an infinitely long cylindrical shell of radius a in which flows a current. The magnetic force on this hollow cylinder is such that it tries to compress the cylinder. To counteract this force, we can fill the inside of the cylinder with a gas of pressure P. What is the pressure required to balance the magnetic force?

4.4.2.13 Ex: Infinitely dense coil

A coil with N 'infinitely dense' windings carries a current I. It forms with respect to the z-axis a torus with rotational symmetry with an inner radius $b-a$ and an outer radius $b+a$. The figure shows the cross-sectional area of a cut in the plane perpendicular to the xy-plane.
a. Calculate by exploiting the symmetric geometry of this device in cylindrical coordinates (ρ, ϕ, z) a ϕ-component of the magnetic $\vec{\mathcal{B}}$-field in the xy-plane (that is, for $z=0$) as a function of the distance ρ from the origin of the coordinate system. **Help:** Use Stokes' law.
b. What is the value of the ϕ-component of $\vec{\mathcal{B}}$ in the entire space *outside* of the torus (that is, also for $z \neq 0$).
c. Draw the profile of $\mathcal{B}_\phi(\rho)$ in the $z=0$ plane as a function of ρ.
d. Let $a = 1$ cm. What should be the value of b in first approximation, so that $\mathcal{B}_\phi$ in the torus is constant within 1%? **Help:** $(1 \pm \epsilon)^{-1} \approx 1 \mp \epsilon$.

4.4.2.14 Ex: Magnetic field in a cylindrical hollow space

Parallel to the axis of an infinitely long massive conducting cylinder of radius a at a distance d from it, there is a hollow cylindrical space of radius b $(d + b < a)$. The current density within this perforated metal cylinder is homogeneous and oriented parallel to the symmetry axis. Using Ampère's law and the linear superposition principle, determine the absolute value and orientation of the magnetic field inside the hollow space.

4.4.2.15 Ex: Torque of a conducting cylinder

Determine the torque (per unit length) felt by a massive conducting cylinder of radius R that slowly rotates with constant angular velocity ω inside a homogeneous $\vec{\mathcal{B}}$-field around its symmetry axis. $\vec{\mathcal{B}}$ be oriented orthogonal to the axis of the cylinder.

4.4.2.16 Ex: Rotating rings

Consider two 'infinitely thin' concentric rings with radii a and b $(a < b)$. The rings are in the xy-plane and their common center is at the origin. On the inner ring there is a homogeneously distributed charge $+q$ (that is, the linear charge density is constant), and the outer ring carries the homogeneously distributed charge $-q$.
a. Write down the charge density $\rho(\mathbf{r}) = \rho(r, \phi, z)$ in cylindrical coordinates.
b. Now the entire device rotates with constant angular velocity ω around the symmetry axis z. Determine the resulting current density $\mathbf{j}(\mathbf{r}) = \mathbf{j}(r, \phi, z)$ in cylindrical coordinates, as well.

c. What are the Cartesian components of current density $\mathbf{j}$?
d. Calculate the magnetic dipole moment $\mathbf{m}$ of the rotating device.

4.4.2.17 Ex: Magnetic field inside a current tube

A thin hollow conducting tube is traversed by a current along its symmetry axis. The current is homogeneously distributed. Calculate the magnetic field inside and outside
a. from Ampère's law,
b. from the Biot-Savart law.

4.4.2.18 Ex: Magnetic induction in a hollow conductor

A conductor (ideal and infinitely thin) be on the z-axis and carries a current I flowing in $+z$-direction. This conductor is enclosed by a conductive hollow cylinder with radius R, within which a homogeneously distributed total current I runs in the opposite direction $-z$ (coaxial cable). Calculate the magnetic induction inside and outside this device.

4.4.2.19 Ex: Current ring

A (ideal) current ring in the xy-plane with radius a and centered at the origin is traversed by a current I. In spherical coordinates the current density is given by,

$$\mathbf{j}(\mathbf{r}) = \mathbf{j}(r,\theta,\phi) = \frac{I}{a}\delta(\cos\theta)\delta(r-a)\hat{\mathbf{e}}_\phi \ .$$

For $|\mathbf{r}| \gg a$ the corresponding potential then has the form,

$$\mathbf{A}(\mathbf{r}) = \mathbf{A}(r,\theta,\phi) = \frac{I\pi a^2}{cr^2}\sin\theta\hat{\mathbf{e}}_\phi \ .$$

and for magnetic field holds,

$$\vec{\mathcal{B}}(\mathbf{r}) = \vec{\mathcal{B}}(r,\theta,\phi) = \frac{I\pi a^2}{cr^3}\left(2\cos\theta\hat{\mathbf{e}}_r + \sin\theta\hat{\mathbf{e}}_\theta\right) \ .$$

where $\hat{\mathbf{e}}_r$, $\hat{\mathbf{e}}_\theta$, and $\hat{\mathbf{e}}_\phi$ are the unit vectors in r, θ, and ϕ-direction.
a. Calculate the Cartesian components of $\mathbf{j}(\mathbf{r})$.
b. Calculate the Cartesian components of the dipolar magnetic moment $\vec{\mathcal{M}}$ using the formula,

$$\vec{\mathcal{M}} = \frac{1}{2c}\int d^3r'(\mathbf{r}' \times \mathbf{j}(\mathbf{r}')) \ .$$

c. What are the components of $\vec{\mathcal{M}}$ in r, θ, and ϕ-direction.
d. Show with the help of (c) that the magnetic field at a point $\mathbf{r}$ of the arbitrary surface can be written,

$$\vec{\mathcal{B}}(\mathbf{r}) = \frac{3\hat{\mathbf{e}}_r(\vec{\mathcal{M}}\cdot\hat{\mathbf{e}}_r) - \vec{\mathcal{M}}}{r^3} \ .$$

e. Calculate the Cartesian components of magnetic field and check, with the help of (b), that also in Cartesian coordinates holds,

$$\vec{\mathcal{B}}(\mathbf{r}) = \frac{3\mathbf{r}(\vec{\mathcal{M}}\cdot\mathbf{r}) - r^2\vec{\mathcal{M}}}{r^5} \ .$$

4.4.2.20 Ex: Magnetic field of a long coil

Determine the magnetic $\vec{\mathcal{H}}$-field inside a very long current-carrying coil. The number of turns is n, the length of the coil l, its radius a, and the amplitude of the current I. How does the magnetic field change, if the coil has an iron core with the permeability μ?

4.4.2.21 Ex: Shielded dipolar field

The magnetic field of a dipole is shielded by a hollow sphere (inner radius a, outer radius b) made of a material with permeability μ. The dipole $\vec{\mathcal{P}}_M$ is in the center of the sphere and points towards z.
a. Show that the magnetic field $\vec{\mathcal{H}}$ in the entire space can be written as the negative gradient of a potential $\Phi_M(\mathbf{r})$.
b. Show that this magnetic potential satisfies the Laplace equation in whole space, $\triangle\Phi_M(\mathbf{r}) = 0$.
c. To solve this Laplace equation, do the following ansatz of variable separation,

$$\Phi_M^{(i)}(r,\theta\phi) = \sum_{l=0}^{\infty}\sum_{m=-l}^{+l}\frac{4\pi}{2l+1}\left[\beta_{lm}^{(i)}r^l + \gamma_{lm}^{(i)}\frac{1}{r^{l+1}}\right]Y_{lm}(\theta,\phi) \ .$$

where the $\beta_{lm}^{(i)}$ and $\gamma_{lm}^{(i)}$ be constant and $i = I, II, II$ denote the different regions $(I : 0 \leq r < a \ , II : a \leq r \leq b \ , III : b < r)$. What are the consequences for $\beta_{lm}^{(i)}$ and $\gamma_{lm}^{(i)}$ due to the fact that Φ_M
i. is, in the origin, the potential of a pure dipolar field $\vec{\mathcal{P}}_M$?
ii. is cylindrically symmetrical about the z-axis?
iii. disappears at infinity?
d. At the interfaces between the different regions the normal component of the magnetic $\vec{\mathcal{B}}$-field and the tangential component of the $\vec{\mathcal{H}}$-field are discontinuous. Use these conditions to establish a system of equations for the coefficients $\beta_{lm}^{(i)}$ and $\gamma_{lm}^{(i)}$, using $\text{grad}_r\Phi_M = \frac{\partial\Phi_M}{\partial r}$, $\text{grad}_\theta\Phi_M = \frac{1}{r}\frac{\partial\Phi_M}{\partial\theta}$, $\frac{\partial Y_{10}}{\partial\theta} = \sqrt{\frac{2l+1}{4\pi}}P_l^1(\cos\theta)$, as well as the orthogonality relations $\int d\Omega Y_{l0}^*(\Omega)Y_{l'0}(\Omega) = \delta_{ll'}$ and $\int_{-1}^{+1} dx P_l^1(x)P_{l'}^1(x) = \delta_{ll'}\frac{2}{2l+1}\frac{(l+1)!}{(l-1)!}$.
e. Solve the equation system first for the case $l \neq 1$.
f. Solve the system of equations for $l = 1$.
g. What does the magnetic field look like outside the sphere for $\mu \gg 1$?

4.5 Further reading

T. Bergeman et al., *Magnetostatic trapping fields for neutral atoms* [DOI]

Chapter 5

Magnetic properties of matter

The most common manifestations of magnetism are certainly magnets, compass needles, and the Earth's magnetic field, and it is not obvious how they are related to the magnetic fields produced by currents, discussed in the previous chapter. Nevertheless, all magnetic phenomena are ultimately due to currents, even if they are microscopic, for example, electrons orbiting atomic nuclei or spinning around their own axis. From the macroscopic point of view we can treat these circular currents as magnetic dipoles. Generally, the dipoles of a medium have random orientations, such that the generated magnetic fields cancel out. However, when we apply a *external* magnetic field, the dipoles can realign and *magnetize* the medium.

5.1 Magnetization

There are several macroscopic manifestations of microscopic dipole moments known as para-, dia-, and ferromagnetism. We will discuss these in the following sections.

5.1.1 Energy of permanent dipoles and paramagnetism

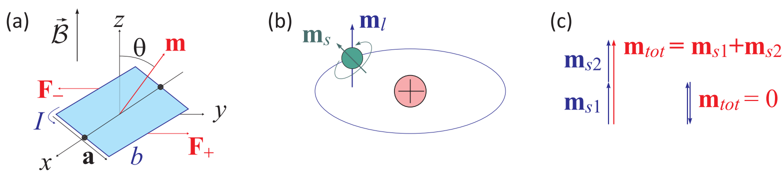

Figure 5.1: (a) Illustration of the torque exerted by a magnetic field on a magnetic dipole. (b) An electron spinning around a nucleus may have orbital and intrinsic angular momentum. (c) Dipole moments are added as vectors.

We consider current loops of rectangular shape [1]. In the case of the geometry shown in Fig. 5.1(a) the Lorentz forces acting on the wire sections a being parallel to the z-y-plane compensate each other, because the forces and the points on which they act are all on a straight line. On the other side, the forces acting on the wire sections b,

$$\mathbf{F}_{\pm} = \pm I\mathbf{b} \times \vec{\mathcal{B}} = \pm Ib\mathcal{B}\hat{\mathbf{e}}_y \ , \tag{5.1}$$

[1] Arbitrary shapes can be constructed by two-dimensional arrays of rectangular loops.

both contribute to create a torque,

$$\vec{\tau} = \frac{\mathbf{a}}{2} \times \mathbf{F}_+ + \frac{-\mathbf{a}}{2} - \times \mathbf{F}_- = I\mathcal{B}b\mathbf{a} \times \hat{\mathbf{e}}_y = Iab\mathcal{B}\hat{\mathbf{e}}_x \sin\theta \ , \tag{5.2}$$

With the definition of the magnetic moment (4.42) we find,

$$\boxed{\vec{\tau} = \mathbf{m} \times \vec{\mathcal{B}}} \ . \tag{5.3}$$

We can also calculate the energy of a dipole in a magnetic field by the work required to rotate it out of its equilibrium position,

$$H_{int} = \int_0^\theta \vec{\tau} \cdot d\theta = \int_0^\theta \mathbf{m} \times \vec{\mathcal{B}} d\theta = \int_0^\theta m\mathcal{B} \sin\theta d\theta = -m\mathcal{B}\cos\theta \ , \tag{5.4}$$

such that,

$$\boxed{H_{int} = -\mathbf{m} \cdot \vec{\mathcal{B}}} \ . \tag{5.5}$$

The formula (5.3) holds for homogeneous magnetic fields or, alternatively, for almost point-like dipoles in inhomogeneous fields. It represents the magnetic equivalent of the torque on electric dipoles (3.4). The torque is oriented so as to align the dipole moment to the direction of the magnetic field. This mechanism is used to explain the phenomenon of paramagnetism [see Fig. 5.3(a)].

In atomic physics we learn that electrons bound to atoms may have, besides an orbital angular momentum due to the planetary motion around the atomic nucleus, an *intrinsic angular momentum* called *spin* as if the electron were a small electrically charged sphere rotating about its own axis [see illustration of Fig. 5.1(b)]. The spins of the various electrons in the electron layer of an atom generally couple to form a total dipole moment, which then interacts with external magnetic fields. This is called *Zeeman effect*. The spins may pair and add up or compensate pairwise such as to zero the magnetic dipole moment of the atom [see illustration of Fig. 5.1(c)]. Note that a strong external magnetic field can break the angular momentum coupling and interact with the electron spins separately. This is called *Paschen-Back effect*.

The phenomenon of *paramagnetism* is observed in materials whose molecules have permanent magnetic dipole moments, that is, in chemical elements with unpaired valence electrons. It is not observed in noble gases, covalent crystals, etc..

Unlike the torque, the *force exerted by a homogeneous field* on a dipole vanishes,

$$\mathbf{F} = I \oint d\mathbf{l} \times \vec{\mathcal{B}} = I \left(\oint d\mathbf{l} \right) \times \vec{\mathcal{B}} = 0 \ . \tag{5.6}$$

For inhomogeneous fields we need to calculate the force from the energy gradient as,

$$\mathbf{F} = -\nabla H_{int} = \nabla(\mathbf{m} \cdot \vec{\mathcal{B}}) = \mathbf{m} \times (\nabla \times \vec{\mathcal{B}}) + (\mathbf{m} \cdot \nabla)\vec{\mathcal{B}} = (\mathbf{m} \cdot \nabla)\vec{\mathcal{B}} \ . \tag{5.7}$$

This formula can be obtained by Taylor expansion of the magnetic field (see Exc. 5.1.7.1).

5.1.2 Impact of magnetic fields on electronic orbits and diamagnetism

A magnetic field can have another effect on the motion of electrons. Let us consider an electron rotating on a circular orbit of radius R. If the motion of the electron is

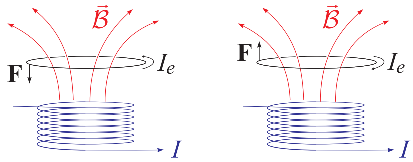

Figure 5.2: Illustration of the force exerted by an inhomogeneous magnetic field on a magnetic dipole: A dipole oriented in the same direction as the magnetic field will be drawn to the field maximum, if it is oriented anti-parallel, it is repelled from the field maximum.

fast, it will generate a current,

$$I = \frac{-e}{T} = \frac{-ev}{2\pi R} , \tag{5.8}$$

creating a dipole moment,

$$\mathbf{m} = I\mathbf{A} = \frac{-e}{T}\pi R^2 \hat{\mathbf{e}}_z = \frac{-e}{2} vR\hat{\mathbf{e}}_z . \tag{5.9}$$

Now, the orbit of the electron can be, for example, an atomic orbital or a trajectory of a free electron in a conductor. The magnetism of a free electron gas in a metal is treated by the theory of *Landau diamagnetism*. This theory considers the trajectories of electrons as being curved by the Lorentz force which, because of the rule of Lenz, generates a field contrary to the applied magnetic field. That is, the magnetic flux is expelled from the material. Hence, in inhomogeneous magnetic fields, diamagnetic materials are repelled from high field regions [2].

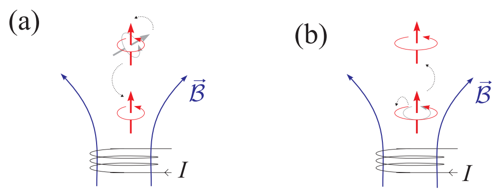

Figure 5.3: Classical interpretation of paramagnetism (a) and diamagnetism (b): In paramagnetic materials the permanent dipoles reorient in the direction of the external field. Exposed to inhomogeneous fields, the dipoles are thus attracted to field maxima. In diamagnetism, currents are forced into circular orbits, and the so-formed dipoles are oriented in a direction opposite the external external. Exposed to inhomogeneous fields, the dipoles are thus repelled from the field maxima.

The case of electronic orbitals in atoms is treated by the theory of *Langevin diamagnetism*. In this theory we consider Bohr orbitals of electrons bound to a nucleus by the Coulomb force. In the presence of an external magnetic field the dipole feels a torque, but in addition, the field has the effect of accelerating or decelerating the electron depending on its orientation. To estimate this effect we consider the equilibrium condition for an electronic orbit,

$$\mathbf{F}_C = \frac{1}{4\pi\varepsilon_0}\frac{e^2}{R^2} = m_e\frac{v^2}{R} = \mathbf{F}_{centrifugal} . \tag{5.10}$$

[2]Note that some metals may be weakly paramagnetic due to an effect called *Pauli paramagnetism*.

Adding a magnetic field oriented along the rotation axis [3],

$$\mathbf{F}_C + \mathbf{F}_L = \frac{1}{4\pi\varepsilon_0}\frac{e^2}{R^2} + ev'\Delta\mathcal{B} = m_e\frac{v'^2}{R} = \mathbf{F}_{centrifugal} \ . \tag{5.11}$$

Subtracting these equations,

$$ev'\Delta\mathcal{B} = \frac{m_e}{R}(v'^2 - v^2) = \frac{m_e}{R}(v' - v)(v' + v) \simeq \frac{2m_e}{R}v'\Delta v \ , \tag{5.12}$$

such that,

$$\Delta v = \frac{eR\Delta\mathcal{B}}{2m_e} \ . \tag{5.13}$$

The acceleration of the electron, when we switch on the magnetic field, increases the value of the dipole moment because, with the formula (5.9),

$$\Delta\mathbf{m} = \frac{-e}{2}\Delta v R\hat{\mathbf{e}}_z = -\frac{e^2R^2}{4m_e}\Delta\vec{\mathcal{B}} \ . \tag{5.14}$$

But the ***variation*** is *always contrary to the direction of the magnetic field*, even if the dipole moment was initially aligned to the field [see Fig. 5.3(b)] [4]. Therefore, the dipole is repelled by an inhomogeneous magnetic field. Note that changing the sign of the charge does not affect $\Delta\mathbf{m}$.

Diamagnetism is a property of all materials, but is often hidden by the presence of permanent magnetic moments. Therefore, to observe diamagnetism, one must choose materials with no permanent magnetic moment, such as atoms with completely filled electron shells. Many amorphous materials (such as wood, glass, rubber, etc.) and many metals as diamagnets.

It is worth mentioning that the magnetic behavior of a macroscopic body is not necessarily the same as the one of its elementary components. For example, metallic sodium is diamagnetic, while gaseous sodium is paramagnetic.

paramagnetism	diamagnetism
atoms with unpaired e^-	atoms with paired e^-
$\mathbf{m}$ robust and independent of $\vec{\mathcal{B}}$	$\mathbf{m}$ weak and $\mathbf{m} \propto \vec{\mathcal{B}}$
$\vec{\mathcal{M}} \parallel \vec{\mathcal{B}} \curvearrowright$ attractive force	$\vec{\mathcal{M}} \parallel -\vec{\mathcal{B}} \curvearrowright$ repulsive force
$\mu > 1 \curvearrowright \chi > 0$	$\mu < 1 \curvearrowright \chi < 0$

It is also important to note that essential aspects of *para- and atomic diamagnetism are quantum*. That is, quantitative theories must be formulated within quantum mechanics. A classical theory can only give an qualitative picture of the effect.

5.1.3 Macroscopic magnetization

In the presence of a magnetic field, matter becomes magnetized, that is, the atomic or molecular dipoles align in a particular direction. We have already discussed two

[3] In Exc. 5.1.7.2 we have shown, that the radius of the electronic orbit does not change under the influence of an external magnetic field.

[4] If the charge distribution is spherically symmetric, we can assume $\langle x^2\rangle = \langle y^2\rangle = \langle z^2\rangle = \frac{1}{3}\langle r^2\rangle$, where $\langle r^2\rangle$ is the average distance between the electron and the nucleus. Therefore, $\langle R^2\rangle = \langle x^2\rangle + \langle y^2\rangle = \frac{2}{3}\langle r^2\rangle$. If N is the number of atoms per unit volume, we have $\chi = \frac{\mu_0 N m}{\mathcal{B}} = -\frac{\mu_0 N Z e^2}{6m}\langle r^2\rangle$.

possible mechanisms causing this reorientation, the para- and the diamagnetism. Regardless of the mechanism we measure the degree of alignment by the vector quantity,

$$\vec{\mathcal{M}} = \frac{N\mathbf{m}}{V} \tag{5.15}$$

called *magnetization*. It plays the same role as the polarization in electrostatics. In the following section we will calculate for a given magnetization $\vec{\mathcal{M}}$ the field that it produces.

In most materials diamagnetism and paramagnetism are very weak effects and can only be detected by sensitive measurements and strong magnetic fields. In *non-ferromagnetic* materials, the weakness of the magnetization allows us to neglect the magnetic field produced by magnetization. In contrast, in iron, nickel or cobalt the forces are between 10^4 and 10^5 greater.

5.1.4 Magnetostatic field of a magnetized material

We consider a sample of magnetic dipoles. According to the formula (4.42), the vector potential is given by,

$$\mathbf{A}(\mathbf{r}) = \frac{\mu_0}{4\pi}\sum_k \frac{\mathbf{m}\times(\mathbf{r}-\mathbf{r}')}{|\mathbf{r}-\mathbf{r}'|^3} \longrightarrow \frac{\mu_0}{4\pi}\int_{\mathcal{V}} dV' \frac{\vec{\mathcal{M}}\times(\mathbf{r}-\mathbf{r}')}{|\mathbf{r}-\mathbf{r}'|^3} \;, \tag{5.16}$$

where we introduced the dipole moment distribution $\vec{\mathcal{M}}(\mathbf{r}')$ via $\mathbf{m}_k \rightarrow \vec{\mathcal{M}}dV'$. As in the electrostatic case, we can rewrite the integral in the form,

$$\begin{aligned}\mathbf{A}(\mathbf{r}) &= \frac{\mu_0}{4\pi}\int_{\mathcal{V}} \vec{\mathcal{M}}(\mathbf{r}')\times\nabla'\frac{1}{|\mathbf{r}-\mathbf{r}'|}dV' \\ &= \frac{\mu_0}{4\pi}\left[-\int_{\mathcal{V}}\nabla'\times\frac{\vec{\mathcal{M}}(\mathbf{r}')}{|\mathbf{r}-\mathbf{r}'|}dV' + \int_{\mathcal{V}}\frac{1}{|\mathbf{r}-\mathbf{r}'|}\nabla'\times\vec{\mathcal{M}}(\mathbf{r}')dV'\right] \\ &= \frac{\mu_0}{4\pi}\oint_{\partial\mathcal{V}}\frac{\vec{\mathcal{M}}(\mathbf{r}')\times d\mathbf{S}'}{|\mathbf{r}-\mathbf{r}'|} + \frac{\mu_0}{4\pi}\int_{\mathcal{V}}\frac{1}{|\mathbf{r}-\mathbf{r}'|}\nabla'\times\vec{\mathcal{M}}(\mathbf{r}')dV' \;.\end{aligned} \tag{5.17}$$

Comparing these terms with the formula (4.27), we find that the first term looks like the potential of a surface current, while the second term looks like the potential of a volume current. Defining,

$$\boxed{\vec{\kappa}_b \equiv \vec{\mathcal{M}}\times\mathbf{n}_S} \quad \text{and} \quad \boxed{\mathbf{j}_b \equiv \nabla\times\vec{\mathcal{M}}} \;, \tag{5.18}$$

we obtain,

$$\mathbf{A}(\mathbf{r}) = \frac{\mu_0}{4\pi}\oint_{\partial\mathcal{V}}\frac{\vec{\kappa}_b}{|\mathbf{r}-\mathbf{r}'|}dS' + \frac{\mu_0}{4\pi}\int_{\mathcal{V}}\frac{\mathbf{j}_b}{|\mathbf{r}-\mathbf{r}'|}dV' \;. \tag{5.19}$$

The meaning of this result is that the potential (and therefore the field) of a magnetized object is the same as the one produced by a volume current distribution $\mathbf{j}_b$ plus a surface current distribution $\vec{\kappa}_b$. Instead of integrating the contributions of all individual infinitesimal dipoles, as in Eq. (5.17), we can try to find these bound currents, and then calculate the fields they produce, as we did in the previous chapter.

5.1.5 The H-field

In the previous section we found that the phenomenon of magnetization of a body can be understood as being due to *localized currents* inside the material, $\mathbf{j}_b = \nabla \times \vec{\mathcal{M}}$, and on the surface of the body, $\vec{\kappa}_b = \vec{\mathcal{M}} \times \hat{n}_S$. The magnetization field is the magnetic field produced by these currents. In addition, there are obviously *free currents*, such as those generated by the motion of free electrons in a metal.

5.1.5.1 Ampère's law in magnetized materials

Ampère's law can now be generalized for arbitrary media,

$$\frac{1}{\mu_0}\nabla \times \vec{\mathcal{B}} = \mathbf{j} = \mathbf{j}_b + \mathbf{j}_f = \nabla \times \vec{\mathcal{M}} + \mathbf{j}_f \ , \tag{5.20}$$

where $\vec{\mathcal{B}}$ is the total magnetic field. Defining a new field $\vec{\mathcal{H}}$, sometimes called *magnetic excitation*,

$$\boxed{\vec{\mathcal{H}} \equiv \mu_0^{-1}\vec{\mathcal{B}} - \vec{\mathcal{M}}} \ , \tag{5.21}$$

we can now write,

$$\nabla \times \vec{\mathcal{H}} = \mathbf{j}_f \ . \tag{5.22}$$

The field $\vec{\mathcal{H}}$ is that part of the magnetic field, which comes only from free currents. We can also define the *magnetic susceptibility* χ_μ via [5],

$$\vec{\mathcal{M}} = \chi_\mu \vec{\mathcal{H}} \ , \tag{5.23}$$

or the *permeability* μ via,

$$\vec{\mathcal{B}} = \mu\vec{\mathcal{H}} = \mu_0(1 + \chi_\mu)\vec{\mathcal{H}} \ . \tag{5.24}$$

Note, that the divergence of the *magnetization does not necessarily vanish*, since the susceptibility may depend on position, $\chi_\mu = \chi_\mu(\mathbf{r})$,

$$\nabla \cdot \vec{\mathcal{H}} = \mu_0^{-1}\nabla \cdot \vec{\mathcal{B}} - \nabla \cdot \vec{\mathcal{M}} = -\nabla \cdot (\chi_\mu \vec{\mathcal{H}}) \neq 0 \ . \tag{5.25}$$

Hence, $\vec{\mathcal{H}}$ generally can not be derived from a vector potential, and Biot-Savart's law is not valid for $\vec{\mathcal{H}}$. In anisotropic materials the susceptibility and the permeability must be understood as tensors.

5.1.5.2 Boundary conditions involving magnetic materials

The integral version of Eq. (5.25), $\oint \vec{\mathcal{H}} \cdot d\mathbf{S} = -\oint \vec{\mathcal{M}} \cdot d\mathbf{S}$, allows us to determine the behavior of the magnetic excitation near interfaces,

$$H_{top}^{\perp} - H_{bottom}^{\perp} = -M_{top}^{\perp} + M_{bottom}^{\perp} \ . \tag{5.26}$$

On the other hand Ampère's law, $\nabla \times \vec{\mathcal{H}} = \mathbf{j}_f$, yields,

$$\vec{\mathcal{H}}_{top}^{\parallel} - \vec{\mathcal{H}}_{bottom}^{\parallel} = \vec{\kappa}_f \times \hat{\mathbf{n}} \ . \tag{5.27}$$

This is in contrast to the behavior of the magnetic $\vec{\mathcal{B}}$ field at interfaces described by Eqs. (4.30), (4.32), and (4.34). Do the Excs. 5.1.7.7 to 5.1.7.9.

[5] Note, that this definition is not symmetric with that of the electric susceptibility (3.20).

5.1.6 Magnetic susceptibility and permeability

Materials respond to applied magnetic fields $\vec{\mathcal{H}}$ generating a magnetization $\vec{\mathcal{M}}$, such that the total magnetic field is $\vec{\mathcal{B}} = \mu_0\vec{\mathcal{H}} + \mu_0\vec{\mathcal{M}}$. The behavior of a material depends on the value of its susceptibility. In vacuum $\chi_\mu = 0$, for typical diamagnets $\chi_\mu \lesssim 0$, for superconductors $\chi_\mu = -1$, for paramagnets $\chi_\mu \gtrsim 0$, and for ferromagnets $\chi_\mu \gg 1$.

Typical values are listed in the following table:

material	$\chi_\mu[10^{-5}]$	type of magnetism
superconductor	-10^5	dia-
carbon	-2.1	Langevin dia-
copper	-1	Landau dia-
water	-0.9	Langevin dia-
hydrogen	-0.00022	Langevin dia-
oxygen (gas)	0.2	para-
sodium (metal)	0.7	Pauli para-
magnesium	1.2	Pauli para-
lithium	1.4	Pauli para-
cesium	5.1	Pauli para-
platinum	28	
oxygen(liquid)	390	
gadolinium	48000	ferro-
iron		ferro-

5.1.6.1 Linear media

In many materials, as long as the applied magnetic field is not too strong, the magnetization is proportional to the field, $\vec{\mathcal{M}} \propto \vec{\mathcal{B}}$, i.e. the magnetic susceptibility depends on the material's microscopic properties and external factors, such as temperature, but not on the applied field, $\chi_\mu \neq \chi_\mu(\vec{\mathcal{B}})$. Hence, linear media can be characterized by a constant,

$$\mu_r \equiv \frac{\mu}{\mu_0} , \tag{5.28}$$

called *relative permeability*.

5.1.6.2 The role of temperature in paramagnetism

Experiments show, that in inhomogeneous magnetic fields, paramagnetic materials are attracted toward high field regions, but with a force that decreases with temperature. This is understood by the Zeeman effect: The dipole moment can only adopt a few possible (quantized) values corresponding to levels of well-defined positive or negative energy (called Zeeman sub-levels). At high temperature all Zeeman sub-levels are equally populated, such that the total force cancels. At low temperature the populations are distributed according to Boltzmann's law, $n_k/n_l = e^{-(E_k-E_l)/k_BT}$, that is, the lower levels (which are precisely the *high-field seekers*) dominate.

Example 47 (*Paramagnetism of hot samples*): As an example, we consider atoms with two possible orientations for the permanent magnetic moment, $\mathbf{m}\cdot\vec{\mathcal{B}} = \pm m\mathcal{B}$. The magnetization produced by $n = n_+ + n_-$ atoms is then $\vec{\mathcal{M}} = n_+\mathbf{m}_+ + n_-\mathbf{m}_-$. The two orientations are populated according to Boltzmann's law $n_+/n_- = e^{-2m\mathcal{B}/k_BT}$, such that,

$$\frac{\vec{\mathcal{M}}}{n} = \frac{e^{m\mathcal{B}/k_BT} - e^{-m\mathcal{B}/k_BT}}{e^{m\mathcal{B}/k_BT} + e^{-m\mathcal{B}/k_BT}}\mathbf{m} \simeq \frac{m\mathcal{B}}{k_BT}\mathbf{m} \ .$$

For weak fields, we obtain the *Curie law*,

$$\chi_\mu = \frac{M}{H} \simeq \frac{nm^2\mathcal{B}}{k_BTH} \simeq \frac{\mu_0 nm^2}{k_BT} \sim T^{-1} \ .$$

For strong fields, the magnetization saturates. Assuming $m \simeq \mu_B$ (see Exc. 5.1.7.4), we estimate for a metal with $n \approx 10^{22}\,\text{cm}^{-3}$ at room temperature, $\chi_\mu \approx 2.6\times 10^{-4}$ [6].

5.1.6.3 Ferromagnetism

In a linear medium the alignment of the magnetic dipoles is maintained by the application of an external field. There are, however, magnetic materials that do not depend on applied fields. This phenomenon of 'frozen' magnetization is called *ferromagnetism*. As in the case of paramagnetism, ferromagnets develop dipoles associated with the spins of unpaired electrons, but in addition, the dipoles strongly interact with each other and, for reasons that can only be understood within a quantum theory, like to orient themselves in parallel [7].

The correlation is so strong that within regions called *Weiss domains* almost 100% of the dipoles are aligned. On the other hand, a block of ferromagnetic material consists of many spatially separated domains, each domain having a magnetization pointing in a random direction, such that the block as a whole does not exhibit macroscopic magnetization. Inside a Weiss domain the magnetization is so strong that even a strong external magnetic field can not influence the alignment. On the other hand, at the boundaries between Weiss domains the alignment is not well defined, such that the external field can exert a torque $\tau = \mathbf{m}\times\vec{\mathcal{B}}$ shifting the boundaries in a way to favor those domains, which are already aligned. For a sufficiently strong field one domain will prevail and the ferromagnetic material saturate.

Experiments show that the alignment is not fully reversible, that is, not all Weiss domains return to their initial orientation (before the external magnetic field was

[6] In metals free electrons contribute to paramagnetism. In metals the Curie law does not apply, but χ is found to be almost constant. The reason is, that the Boltzmann distribution is inappropriate for electrons, so we need to use the Fermi-Dirac distribution. The energy distribution $\rho(\epsilon)n_{FD}(\epsilon)$ of the electrons depends on the orientation of their spin with respect to the applied magnetic field: electrons with (anti-)parallel spin see their energy increased (reduced). To maintain a uniform E_F, electrons with parallel spin will flip it to antiparallel spin, such that the entire system is slightly *high-field seeking*. This is called *Pauli paramagnetism*. This effect always competes with diamagnetism, which involves all electrons and has opposite sign.

[7] The survival of domains in thermal reservoirs can not be understood by classical interactions between dipoles, but we need to contemplate band structure models. In particular, the $3d$ orbital bands provide electrons to the ferromagnetic elements Fe, Co, Ni. These bands are so close that the exchange interaction influences the orientation of spins in neighboring bands, which induces correlations between the spins of neighboring atoms.

applied). Consequently, the material remains permanently magnetized. This effect is called *remanescence*.

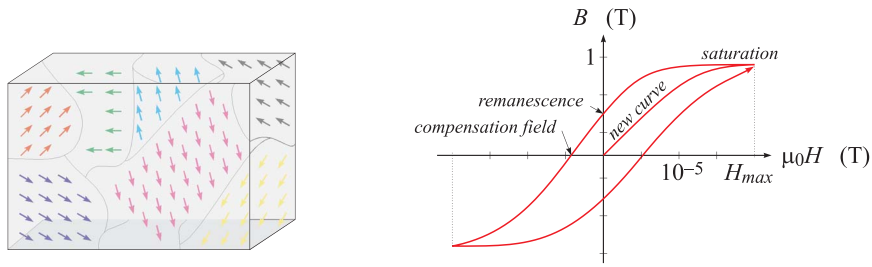

Figure 5.4: Hysteresis curve of magnetization. To allow for a comparison of the scales we plot in real units (Tesla) the applied field ($\vec{\mathcal{H}} \propto I$ in the case of a solenoid) versus the obtained field ($\vec{\mathcal{B}} \simeq \vec{\mathcal{M}}$).

To compensate for remanescence, it is necessary to apply a *compensation field* oriented in the opposite direction (see Fig. 5.4) [8] Beyond the compensation field we observe saturation in the opposite direction. Finally, returning to the initial situation, we draw a curve called *hysteresis curve*, which indicates that magnetization does not only depend on the applied magnetic field, but also on the 'history' of applied fields. Fig. 5.4 shows how an applied field can be dramatically amplified by ferromagnetism.

As already discussed, temperature tends to randomize the alignment of atomic dipoles. At low temperature the heat will not be sufficient to misalign the dipoles within the Weiss domains. But interestingly, beyond a well-defined temperature (the *Curie temperature* of iron is 770 C), the iron undergoes an abrupt phase transition to a paramagnetic state.

Note, that there are also antiferromagnetic materials (MnO_2), where neighboring atoms have antiparallel spins.

Example 48 (*Microscopic theory of induced dipoles*): The permittivity and relative permeability of a dense gas can be connected to the microscopic quantities through the *Clausius-Mossotti formula*,

$$\varepsilon_r = \frac{1+\frac{2}{3}\frac{N}{V}\alpha_{pol,e}}{1-\frac{1}{3}\frac{N}{V}\alpha_{pol,e}} \quad , \quad \mu_r = \frac{1+\frac{2}{3}\frac{N}{V}\alpha_{pol,m}}{1-\frac{1}{3}\frac{N}{V}\alpha_{pol,m}} \quad , \tag{5.29}$$

that is, to the susceptibilities,

$$\chi_\varepsilon = \varepsilon_r - 1 = \frac{\frac{N}{V}\alpha_{pol,e}}{1-\frac{1}{3}\frac{N}{V}\alpha_{pol,e}} \quad , \quad \chi_\mu = \mu_r - 1 = \frac{\frac{N}{V}\alpha_{pol,m}}{1-\frac{1}{3}\frac{N}{V}\alpha_{pol,m}} \quad , \tag{5.30}$$

where the induced electric and magnetic polarizabilities are,

$$\alpha_{pol,e} = \frac{2d_{fi}}{|\vec{\mathcal{E}}_p|}\rho_{if} \quad , \quad \alpha_{pol,m} = \frac{2m_{fi}}{|\vec{\mathcal{B}}_p|}\rho_{if} \ . \tag{5.31}$$

d_{fi} and m_{fi} are the dipole moments for electric and magnetic transitions and ρ_{if} the coherences excited in these transitions, which can be calculated from

[8] In practice, to demagnetize an iron block, we apply an alternating voltage gradually reducing its amplitude.

the Bloch equations. The relative strength between magnetic and electrical transitions is,

$$\frac{2\mu_B}{cea_B} = \alpha \; . \tag{5.32}$$

5.1.7 Exercises

5.1.7.1 Ex: Dipole in an inhomogeneous field

Derive the formula for the force on a dipole in an inhomogeneous field.

5.1.7.2 Ex: Langevin diamagnetism

An electron circulates around its atomic nucleus on an orbit of radius R.
a. Calculate the magnetic dipole moment generated by this movement as a function of velocity.
b. Now a weak magnetic field $\vec{\mathcal{B}}$ is slowly turned on perpendicular to the orbital plane. Calculate the increase of the electron's velocity due to the electric field induced by turning on the magnetic field using Faraday's law.
c. Show that the increase in kinetic energy, ΔE_{kin}, corresponds to the interaction energy between the electronic dipole moment and the magnetic field.
d. Does the turning on of the magnetic field change the radius of the electronic orbit? Justify your answer!

5.1.7.3 Ex: Magnetic susceptibility

By molecular magnetism it is possible to lift any objects in a sufficiently strong magnetic field. Estimate the magnetic field $|\vec{\mathcal{B}}|$ and the field gradient $\nabla|\vec{\mathcal{B}}|^2$ (one may estimate $\nabla|\vec{\mathcal{B}}|^2 = 2|\vec{\mathcal{B}}|\nabla|\vec{\mathcal{B}}| \simeq |\vec{\mathcal{B}}|^2/l$ with $l \simeq 10\,\text{cm}$ as the typical length for such strong magnetic fields), needed to lift a frog. Water is predominantly diamagnetic with $\chi_\mu \simeq -0.9 \cdot 10^{-5}$ is the magnetic susceptibility of water.

Figure 5.5: Magnetic susceptibility.

5.1.7.4 Ex: Larmor precession of a Bohr atom in a magnetic field

As a model of the Larmor precession, consider the Bohr's atom model: An electron flying on circular orbits around a proton. Only certain discrete orbits with the radii $r_n = n^2 a_B$, where $a_B = 4\pi\varepsilon_0 \frac{\hbar^2}{m_e e^2}$, are allowed. The movement of the electron on

these orbits is not accompanied by radiative emission.
a. Calculate the velocity of the electron in its ground state $n = 1$ and compare the result with the speed of light in vacuum c.
b. What is the orbital momentum $\mathbf{L}$ of the electron in a hydrogen atom in this state?
c. Relate the magnetic moment $\mathbf{m}_L$ due to the circular current generated by the electron to the orbital momentum $\mathbf{L}$.
d. Placed in a magnetic field of $\mathcal{B} = 1\,\mathrm{T}$ the atom suffers a torque, which creates a precession of the angular momentum vector $\mathbf{L}$ around the direction of the $\vec{\mathcal{B}}$-field. Determine the frequency of this Larmor precession from $\omega_L = \dot{L}/(L\sin\theta)$, where θ is the angle between $\mathbf{m}_L$ and $\vec{\mathcal{B}}$. ($\hbar = 1.034\cdot10^{-34}\,\mathrm{Js}$, $e = 1.602\cdot10^{-19}\,\mathrm{C}$, $\varepsilon_0 = 8.854\cdot10^{-8}\,\mathrm{As/Vm}$.

5.1.7.5 Ex: H-field of a cylindrical current wire

A cylindrical wire with radius a and permeability μ is traversed by a constant current density $\mathbf{j}$.
a. Calculate the absolute values and the directions of the $\vec{\mathcal{H}}$ and $\vec{\mathcal{B}}$-fields in- and outside the wire using Stokes law.
b. The electric field $\vec{\mathcal{E}}$ within the wire and the current $\mathbf{j}$ are connected by Ohm's law $\mathbf{j} = \sigma\vec{\mathcal{E}}$, where σ is the electrical conductivity. What is the value and direction of the Poynting vector $\mathbf{s}$ on the wire surface?
c. Calculate the total energy flow across the surface of a piece of wire of length L. Show that the energy flow corresponds exactly to the power converted, in this piece of wire, to ohmic heat.
Help: The energy conservation law of electrodynamics is given by: $-\frac{\partial u}{\partial t} = \nabla\cdot\mathbf{s} + \mathbf{j}\cdot\vec{\mathcal{E}}$, where $u = \frac{1}{2}(\vec{\mathcal{E}}\cdot\vec{\mathcal{D}} + \vec{\mathcal{B}}\cdot\vec{\mathcal{H}})$ is the total energy density, $\mathbf{s} = \vec{\mathcal{E}}\times\vec{\mathcal{H}}$ the flow of energy, and $\mathbf{j}\cdot\vec{\mathcal{E}}$ the work done by the field on the electric current density.

5.1.7.6 Ex: Ferromagnetism

a. Make a scheme of the dependence of the magnetization $\mathcal{M}$ of a ferromagnetic material on the magnetic 'excitation' $\mathcal{H}$ with the initial condition $\mathcal{M} = \mathcal{H} = 0$ and letting $\mathcal{H}(t)$ cycle through $0 \to \mathcal{H}_{max} \to -\mathcal{H}_{max} \to \mathcal{H}_{max}$. Indicate the remaining magnetization in the scheme.
b. How does the magnetization of a ferromagnet change when we heat it up above the Curie temperature T_C? How does the magnetic susceptibility behave in this case χ_m?
c. It explains the order of the atomic magnetic moments in ferro-, antiferro- and ferrimagnets and its influence on their magnetization.

5.1.7.7 Ex: Rectangular toroidal coil

A circular coil is made of a core with rectangular cross-sectional area, $A = h(r_2 - r_1)$, on which two coils are densely wound on top of each other, one with the number of turns N_1 and the other with N_2. Establishes a relationship for the mutual inductance L of the two coils.
Help: To calculate the mutual inductance, invoke the flux equation for the case that

the coil N_1 is traversed by the current I_1, that is, $\oint \mathcal{H} \cdot d\mathbf{s} = N_1 I_1$ and calculate the induced flux Φ.

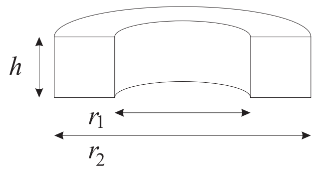

Figure 5.6: Rectangular toroidal coil.

5.1.7.8 Ex: Toroidal coil

Consider a toroidal coil with the average radius R, which consists of N turns carrying the current I. The coil is filled with an iron core of permeability μ.
a. Calculate the amplitude of the fields $\mathcal{H}$ and $\mathcal{B}$ inside the coil.
b. Now consider a core with an air gap d with $d \ll R$ interrupting the torus. Calculate once again the fields $\mathcal{H}$ and $\mathcal{B}$ within the slot.

5.1.7.9 Ex: Toroidal coil

A slotted steel ring has the dimensions: $b = 20\,\text{mm}$, $r = 80\,\text{mm}$, $a = 15\,\text{mm}$, and $d = 1\,\text{mm}$ (see the figure).
a. Calculate, first without air gap, for a magnetic flux density $\mathcal{B}$ the total magnetic flux Ψ_M and the corresponding $\mathcal{H}$ field. What is the amount of current I required generate this flux in a coil of N turns?
b. How must $\mathcal{H}$ and I be modified, if the ring is interrupted by a 1 mm wide air gap, to reach the same flux? Use $\mathcal{B} = 1.2\,\text{T}$, $N = 300$, $\mu_r = 650$.

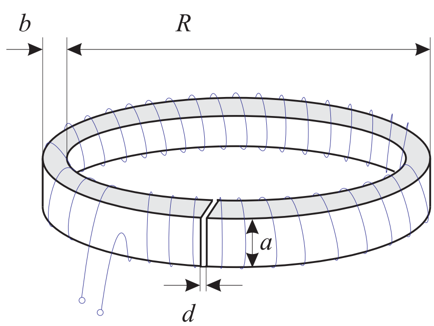

Figure 5.7: Toroidal coil.

5.2 Induction of currents and inductance

We have already seen that the fundamental cause of current $\mathbf{j}$ is a motion of charges Q [see Eq. (3.37)]. To incite charges to move we need a force,

$$\boxed{\mathbf{j} = \varsigma\frac{\mathbf{F}}{Q}} , \tag{5.33}$$

where ς is a proportionality factor called *conductivity* and $\mathbf{F}$ is the Coulomb-Lorentz force, such that,

$$\boxed{\mathbf{j} = \varsigma(\vec{\mathcal{E}} + \mathbf{v} \times \vec{\mathcal{B}})} . \tag{5.34}$$

The first part, $\mathbf{j} = \varsigma\vec{\mathcal{E}}$, is Ohm's law already discussed in Sec. 3.3. Now, in addition to taking into account the Coulomb force acting on electrons traveling in conductors, let us also consider the Lorentz force.

5.2.1 The electromotive force

When we consider a closed electric circuit with a current source and a consumer, knowing the slow average velocity of the electrons carrying the current (see Exc. 3.3.3.3), it is not immediately obvious why the current starts to flow simultaneously in all parts of the circuit. The explanation is that if this were not the case, charges would accumulate in parts of the circuit creating local imbalances. The consequence of this would be the creation of electric fields working to eliminate the imbalances. These fields $\vec{\mathcal{E}}$ are superposed to the electromotive force $\mathbf{f}_0$ exerted by the current source. If the source has an internal resistance, as schematized in Fig. 5.8(a), part of the electromotive force $\mathbf{f}_i$ is spent on it,

$$\mathbf{f}_i = \mathbf{f}_0 + \vec{\mathcal{E}} . \tag{5.35}$$

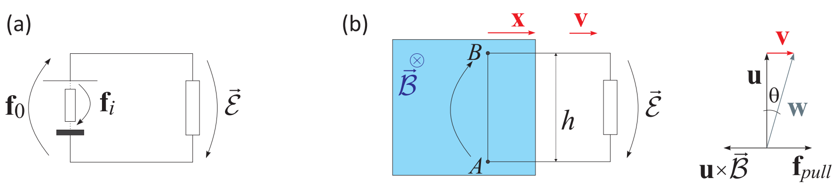

Figure 5.8: (a) Illustration of the electromotive force $\mathbf{f}_0$ exerted by an arbitrary voltage source, the force $\mathbf{f}_i$ spent on the internal resistance of the source, and the electrostatic force $\vec{\mathcal{E}}$ on the circuit. (b) Electromotive force $\mathbf{f}_0$ generated by the motion of a part of the circuit inside a magnetic field.

In the case of an ideal source, $\mathbf{f}_i = 0$, the path integral along the circuit,

$$\mathcal{E} \equiv \int_+^- \mathbf{f}_0 \cdot d\mathbf{l} = -\int_+^- \vec{\mathcal{E}} \cdot d\mathbf{l} = U , \tag{5.36}$$

yields exactly the voltage.

The electromotive force can be caused by batteries, photocells, generators, etc. In the case of a generator, the electromotive force is the Lorentz force acting on the free charges of a conductor moved within an applied magnetic field. Let us consider the setup schematized in Fig. 5.8(b). When the part of the conductor between the points A and B (length h) is moved to the right with velocity $\mathbf{v}$ within the magnetic field $\vec{\mathcal{B}}$, positive charges are accelerated upwards, as in the case of the Hall effect. We obtain an electromotive force,

$$\mathcal{E} \equiv \oint \mathbf{f}_L \cdot d\mathbf{l} = hv\mathcal{B} \;, \tag{5.37}$$

which acts as a source of voltage. Of course, it is not the magnetic field which does the work through the Lorentz force, but the person pushing the conductor: Calling u the velocity along the conductor acquired by the accelerated charges, this velocity creates inside the magnetic field an electromotive force $\mathbf{u} \times \vec{\mathcal{B}}$ against the motion of the conductor exerting per unit of charge the work,

$$\int \mathbf{f}_{pull} \cdot d\mathbf{l}_w = -\int (\mathbf{u} \times \vec{\mathcal{B}}) \cdot d\mathbf{l}_w = \int u\mathcal{B}\hat{\mathbf{e}}_x \cdot d\mathbf{l}_w \tag{5.38}$$
$$= \int_0^h \frac{v}{\tan\theta}\mathcal{B}\cos(90^\circ - \theta)\frac{dh}{\cos\theta} = hv\mathcal{B} = \mathcal{E} \;.$$

We find that the work exerted per unit of charge exactly compensates the electromotive force.

Applying the definition of the magnetic flux (4.12), to the situation illustrated in Fig. 5.8(b),

$$\Psi_M = \int \vec{\mathcal{B}} \cdot d\mathbf{S} = \mathcal{B}hx \;, \tag{5.39}$$

we can reshape the Eq. (5.37),

$$h\mathcal{B}v = -h\mathcal{B}\dot{x} = \boxed{-\frac{d\Psi_M}{dt} = \mathcal{E}} \;. \tag{5.40}$$

Hence, the temporal variation of the magnetic flux induces a *counteracting* electromotive force. This is known as *Lenz's rule*.

5.2.2 The Faraday-Lenz law

In a series of experiments *Michael Faraday* demonstrated that the relationship (5.40) can be generalized to any geometry of the circuit immersed in a magnetic field, to any velocity of the motion, and even to time-varying geometries. The applications of this effect are innumerable, see Exc. 5.2.3.1 to 5.2.3.23. Relating the electromotive force on one side to the generation of a voltage (5.36), $\mathcal{E} = \oint \vec{\mathcal{E}} \cdot d\mathbf{l}$, and on the other side to the variation of the flux (5.40), $\mathcal{E} = -\frac{d\Psi_M}{dt}$, we can write,

$$\boxed{\oint \vec{\mathcal{E}} \cdot d\mathbf{l} = -\frac{\partial}{\partial t}\int \vec{\mathcal{B}} \cdot d\mathbf{S}} \;. \tag{5.41}$$

In the differential version we get,

$$\boxed{\nabla \times \vec{\mathcal{E}} = -\frac{\partial \vec{\mathcal{B}}}{\partial t}} \ . \tag{5.42}$$

Note that, without temporal variations of the magnetic field, we recover electrostatics, $\nabla \times \vec{\mathcal{E}} = 0$.

5.2.2.1 Mutual inductance

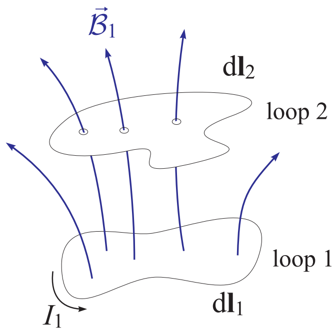

Figure 5.9: Indução.

Here, we consider two loops of arbitrary shapes. The first loop carries the current I_1 and produces a magnetic field, which we can calculate, for example, by Biot-Savart's law,

$$\vec{\mathcal{B}}_1 = \frac{\mu_0 I_1}{4\pi} \oint \frac{d\mathbf{l}_1 \times (\mathbf{r} - \mathbf{r}')}{|\mathbf{r} - \mathbf{r}'|^3} \ . \tag{5.43}$$

The part of the magnetic flux passing through the second loop is,

$$\Psi_{M2} = \int \vec{\mathcal{B}}_1 \cdot d\mathbf{S}_2 \equiv M_{21} I_1 \ , \tag{5.44}$$

where M_{21} is a constant that depends only on the geometry of the two loops. It is called *mutual inductance* and can be expressed as,

$$\begin{aligned} M_{21} &= \frac{1}{I_1} \int \nabla \times \mathbf{A}_1 \cdot d\mathbf{S}_2 = \frac{1}{I_1} \oint \mathbf{A}_1 \cdot d\mathbf{l}_2 \\ &= \frac{1}{I_1} \oint \left(\frac{\mu_0 I_1}{4\pi} \oint \frac{d\mathbf{l}_1}{|\mathbf{r} - \mathbf{r}'|} \right) \cdot d\mathbf{l}_2 = \frac{\mu_0}{4\pi} \oint \oint \frac{d\mathbf{l}_1 \cdot d\mathbf{l}_2}{|\mathbf{r} - \mathbf{r}'|} \ . \end{aligned} \tag{5.45}$$

The symmetry of this formula suggests,

$$M_{21} = M_{12} = M \ . \tag{5.46}$$

We can drop the indices and call both constants M. The conclusion of this is that, regardless of the shapes and positions of the loops, the flux through loop 2 when we throw a current I into the loop 1 is identical to the flux through 1 when we throw the same current I into 2,

$$I_1 = I_2 = I \Longrightarrow \int \vec{\mathcal{B}}_1 \cdot d\mathbf{S}_2 = \int \vec{\mathcal{B}}_2 \cdot d\mathbf{S}_1 \; . \tag{5.47}$$

Example 49 (*Dynamo*): We consider a rotating coil set in motion by a crank inside a magnetic field, as shown in the figure. The voltage wasted by the resistor is,

$$U = \oint \vec{\mathcal{E}} \cdot d\mathbf{l} = -\frac{d}{dt}\Psi_M = -\frac{d}{dt}\int \vec{\mathcal{B}} \cdot d\mathbf{A} = -\frac{d}{dt}\mathcal{B}A\cos\omega t = \omega\mathcal{B}A\sin\omega t \; .$$

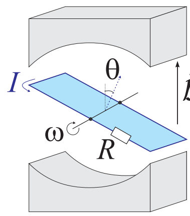

Figure 5.10: Schematic of a generator of alternating voltage (or dynamo).

5.2.2.2 Self-inductance

The magnetic flux produced by the current in loop 1 not only traverses the second loop, but also the first loop itself. Therefore, any variation of the flux will also induce an electromotive force in this loop 1,

$$\Psi_{M1} = M_{11}I_1 \equiv LI_1 \; , \tag{5.48}$$

where the constant L is called *self-inductance*. With the law of Lenz-Faraday,

$$\mathcal{E} = -\frac{d\Psi_M}{dt} = -L\dot{I} \; . \tag{5.49}$$

Example 50 (*Self-inductance of a solenoid*): Consider the solenoid shown in Fig. 5.11. With the formula of the example 43 we calculate the magnetic flux,

$$\Psi_M = \int \vec{\mathcal{B}} \cdot d\mathbf{A} = \mu I\frac{N}{l}\, N\pi R^2 \; .$$

Comparing with the formula (5.48), we find self-inductance,

$$L = \mu\frac{N^2}{l}\,\pi R^2$$

5.2.3 Exercises

5.2.3.1 Ex: Application of the Faraday-Lenz law

The current in a coil characterized by the inductance $L = 1\,\mathrm{mH}$ is linearly reduced in one second from 1 A to 0. Calculate the induced voltage.

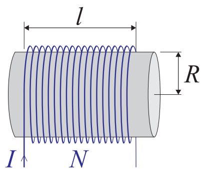

Figure 5.11: Scheme of a solenoid characterized by a self-inductance L.

5.2.3.2 Ex: Breathing charge distribution

A radially symmetric charge distribution varies over time as $\lambda(t)$ in a 'breathing oscillation',

$$\varrho(\mathbf{r},t) = \varrho_0\lambda(t)\frac{1}{r^2}e^{-a\lambda(t)r} \ ,$$

where $\varrho_0 = const.$ and $a = const.$
a. What is the value of the total charge?
b. Calculate the current density $\mathbf{j}(\mathbf{r},t)$, which corresponds to $\varrho(\mathbf{r},t)$ from the continuity equation.
c. Determine $\vec{\mathcal{E}}(\mathbf{r},t)$ from the ansatz $\vec{\mathcal{E}}(\mathbf{r},t) = \mathcal{E}(r,t)\frac{\mathbf{r}}{r}$ (radial symmetry).
d. Calculate the corresponding magnetic field $\vec{\mathcal{B}}$.
e. Show that the solutions for $\vec{\mathcal{E}}$ and $\vec{\mathcal{B}}$ satisfy Maxwell's equations.

5.2.3.3 Ex: Law of induction

a. Explain the concept of magnetic flux across an area F. How does magnetic flux depend on the choice of surface?
b. What is the form of Faraday's induction law? What are the experimental observations underlying this law?
c. What is the physical content of Lenz's law?
d. What is Maxwell's displacement current? Give a physical justification for this current.
e. Write down Maxwell's equations.
f. What is the motivation for introducing the electromagnetic potentials Φ and $\mathbf{A}$?
g. What is the allowed gauge transformation for electromagnetic potentials?
h. What is the meaning of the Lorentz gauge? What advantages does it offer?
i. Formulate the energy conservation law of electrodynamics.
j. What is the physical meaning of the Poynting vector?

5.2.3.4 Ex: Induction and Lorentz force

Two parallel metal rods are tilted by an angle φ with respect to the ground (see diagram). Between the rods a third movable rod of mass m and length L placed at right angles glides without friction. A homogeneous magnetic field $\vec{\mathcal{B}}$ crosses perpendicularly the plane defined by the three rods. The parallel rods are connected at the top end by a capacitor C, such that a closed current circuit is formed together with the transverse rod.
a. Set up the equation of motion for the transverse rod.

b. Determine the solution $x(t)$ of the equation of motion for the initial condition $x(0) = v(0) = 0$.

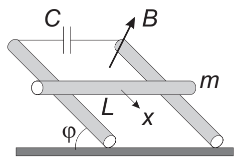

Figure 5.12: Induction.

5.2.3.5 Ex: Magnetic flux and induction

Consider the conductive ring of radius l and negligible electrical resistance shown in the figure. Perpendicular to the plane of the ring there is a homogeneous magnetic field $\vec{\mathcal{B}}$. A rod 2 rotates with angular frequency ω. Calculate the current I across the resistance R of another resting rod 1.

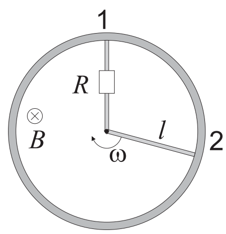

Figure 5.13: Induction.

5.2.3.6 Ex: Induction

Consider the conductive loop at right angle shown in the figure. There is a homogeneous magnetic field given by,

$$\vec{\mathcal{B}}(\mathbf{r}) = \mathcal{B}_0 \hat{e}_y \ .$$

The conductive loop rotates around the bending axis (z-axis) with constant angular frequency.ω.
a. What is the voltage induced in the loop as a function of time?
b. Calculate the time average of the induced voltage.

5.2.3.7 Ex: Induction

A circular ring with radius R rotates with constant angular velocity ω around a diameter. Perpendicular to the rotation axis there is a magnetic field $\vec{\mathcal{B}}$.
a. Calculate the voltage induced in the ring as a function of time.
b. The ring consists of a metallic wire with conductivity σ. What current $I(t)$ flows through the ring, assuming the current is evenly distributed across the cross section of the wire?

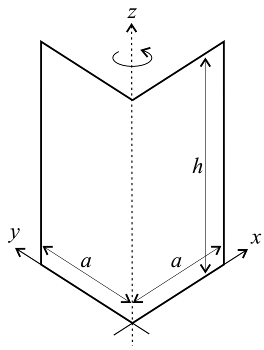

Figure 5.14: Induction.

5.2.3.8 Ex: Induction

An equidistant triangle-shaped conductive loop (edge length S) in the xy-plane is 'immersed' with constant velocity $\mathbf{v} = v\hat{\mathbf{e}}_x$ starting at the tip into a homogeneous magnetic field $\vec{\mathcal{B}} = \mathcal{B}\hat{\mathbf{e}}_z$ ($\mathcal{B}$ is constant) (see diagram) until being completely inside the magnetic field.
a. Calculate the maximum voltage induced in the loop.
b. Make a scheme of the time evolution of the induced voltage.

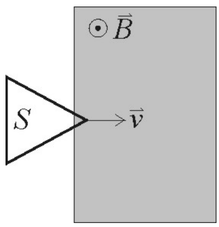

Figure 5.15: Induction.

5.2.3.9 Ex: Induction

A rectangular conducting loop with height $2a$ and width $2b$ rotates with angular velocity ω around the z-axis. At time $t = 0$ the conducting loop is in the xz-plane. In addition, the loop is exposed to the inhomogeneous time-varying magnetic field $\vec{\mathcal{B}}(\mathbf{r}, t) = \mathcal{B}_0 t z^2 \hat{\mathbf{e}}_x$.
a. Show, $\nabla \cdot \vec{\mathcal{B}}(\mathbf{r}, t) = 0$.
b. Calculate the magnetic flux $\Psi(\mathbf{r}, t) = \int \vec{\mathcal{B}} \cdot d\mathbf{F}$ through the rotating loop as a function of time.
c. What is the value of the voltage $U_{ind}(t)$ induced in the loop as a function of time?

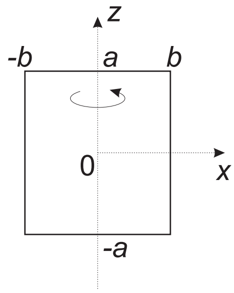

Figure 5.16: Induction.

5.2.3.10 Ex: Induction in a coil

Calculate the magnetic $\mathcal{B}$-field in the middle and at the end of a coil of length $L = 1\,\mathrm{m}$. The number of turns is $N = 2000$, the radius $r = 2\,\mathrm{cm}$, and the current through the coil $I = 5\,\mathrm{A}$. To do this first calculate, using the Biot-Savart law, the magnetic field $\mathcal{B}_1(0, 0, z)$ of a single circular conductor with radius r located at a point z_1 of the coil's symmetry axis. Use the formula obtained for $\mathcal{B}_1$ to describe the magnetic field generated by a coil element dz.

5.2.3.11 Ex: Induction in a rectangular mesh

A rectangular conducting loop has the length a and the width b. In the same plane defined by the loop, parallel to a distance d is a straight conductor traversed by a current I, as shown in the figure.
a. Calculate the magnetic field produced by the current.
b. Calculate the flux through the loop.
c. Calculate the self-inductance imposed on the current circuit by the existence of the loop.
d. Linearize the expression of self-inductance for $b/d \ll 1$.

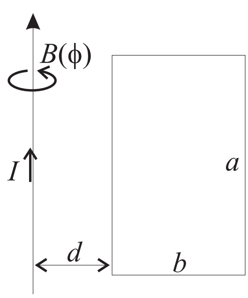

Figure 5.17: Induction.

5.2.3.12 Ex: Falling rod

A metal rod of $L = 1\,\mathrm{m}$ length falls in the gravitational field of the Earth. At time $t = 0$ the initial velocity is 0. The rod is oriented parallel to the ground. Perpendicular to the rod and parallel to the ground there is a magnetic field $\vec{\mathcal{B}}$ with the absolute value $2 \cdot 10^{-5}\,\mathrm{T}$.
a. What voltage is induced between the ends of the rod as a function of the distance traveled h?
b. What value is obtained for the voltage after a fall of $5\,\mathrm{m}$?

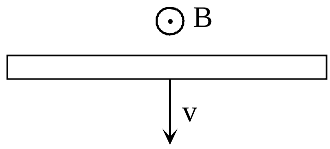

Figure 5.18: Induction.

5.2.3.13 Ex: Sliding rod

We consider two parallel metal rails (distance $d = 10\,\mathrm{cm}$) inclined by an angle ϕ with respect to the ground. Between the rails slides a frictionless rod (mass $M = 100$ g). At a right angle to the plane defined by the rails there is a homogeneous magnetic field $\mathcal{B}$ (amplitude: $0.1\,\mathrm{T}$). We sent a current of $I = 9.8\,\mathrm{A}$ through the rails and through the rod. What is the maximum allowable value of ϕ necessary to let the rod move upward along the rails?

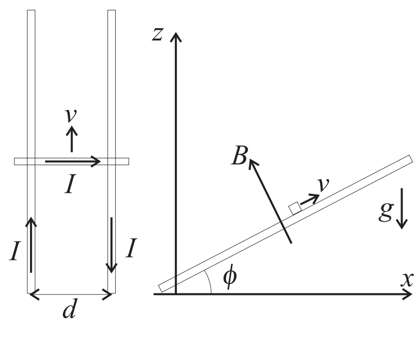

Figure 5.19: Sliding rod.

5.2.3.14 Ex: Conductive ring in oscillating magnetic field

A circular conductive loop (inductance L, resistance R) is traversed by an oscillating magnetic flux, $\Psi = \Psi_0 e^{\imath\omega t}$.
a. Calculate the amplitude of the current in the conductor as well as its phase relative to Ψ.
b. What is the average power dissipated in the conductor? Also discuss the limiting

cases $\omega \to 0$ and $\omega \to \infty$.
Help: Start setting up an equivalent circuit incorporating a voltage source, a resistance, and an inductance.

5.2.3.15 Ex: Self-inductance of a current loop

Calculate the self-inductance of a current loop.

5.2.3.16 Ex: Potentials

Be given are scalar potential and vector potential:

$$\Phi(\mathbf{r},t) = b\frac{\mathbf{r}\hat{\mathbf{e}}_z}{r^3}e^{\imath\omega t} \qquad \text{and} \qquad A(\mathbf{r},t) = \imath kb\frac{e^{\imath kr}}{r^3}e^{\imath\omega t}\hat{\mathbf{e}}_z ,$$

where $\omega = ck$ and $r = |\mathbf{r}|$. Calculate the corresponding electric field $\vec{\mathcal{E}}(\mathbf{r},t)$ and the magnetic field $\vec{\mathcal{B}}(\mathbf{r},t)$.

5.2.3.17 Ex: Motion-induced electromotive force

In the figure a conductive rod of mass m and negligible resistance is free to slide without friction along two parallel rails that have negligible resistances, are separated by a distance ℓ, and connected by a resistance R. The rails are attached to a long plane inclined by an angle θ from the horizontal. There is a magnetic field pointing upwards as shown.
a. Show that there is a retarding force directed upward on the inclined plane given by $F = (\mathcal{B}^2\ell^2 v\cos^2\theta)/R$.
b. Show that the terminal velocity of the stick is $v_t = mgR\sin\theta/(\mathcal{B}^2\ell^2\cos^2\theta)$.

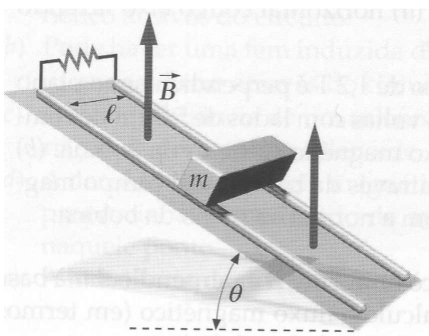

Figure 5.20: Motion-induced electromotive force.

5.2.3.18 Ex: Induction

An insulated wire with resistance of 18.0 Ω/m and length of 9.0 m will be used to build a resistor. First the wire is bent in half and doubled, and then the double wire is wound into a cylindrical shape (see figure) to create a 25 cm long, 2.0 cm diameter helix. Determine the resistance and inductance of this twisted wire resistor.

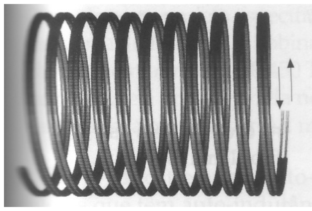

Figure 5.21: Induction.

5.2.3.19 Ex: *R*-*L*-circuit

In the circuit shown in the figure the inductor has negligible internal resistance, and the switch S has been left open for a long time. Now, the switch is closed.
a. Determine the current in the battery, the current in the 100 Ω resistor, and the current in the inductance immediately after the switch has been closed.
b. Determine the current in the battery, the current in the 100 Ω resistor, and the current in the inductance a long time after the switch has been closed.
c. After being closed for a long time, the key is now opened again. Determine the current in the battery, the current in the 100 Ω resistor, and the current in the inductance immediately after the switch has been opened.
d. Determine the current in the battery, the current in the 100 Ω resistor, and the current in the inductance a long time after the key has been reopened.

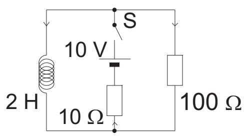

Figure 5.22: Circuit.

5.2.3.20 Ex: Low pass filter

The circuit shown in the figure is an example of a *low-pass filter*. (Consider that the output is connected to a load that conducts negligible current.)
a. If the input voltage is given by $V_{in} = V_{in,pico} \cos \omega t$, shows that the output voltage is $V_{out} = V_L \cos(\omega t - \phi)$, where $V_L = V_{in,pico}/\sqrt{1 + (\omega RC)^{-2}}$.
b. Discuss the trend in the limiting cases $\omega \to 0$ and $\omega \to \infty$.

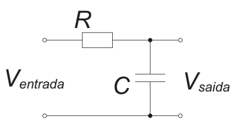

Figure 5.23: Low pass filter.

5.2.3.21 Ex: Notch filter

The circuit shown in the figure is a *cutoff filter*. (Consider that the output is connected to a load carrying a negligible current.)
a. Show that the cutoff filter rejects signals in a frequency band centered in $\omega = 1/\sqrt{LC}$.
How does the width of the rejected frequency band depend on R?

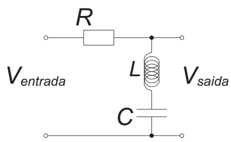

Figure 5.24: Notch filter.

5.2.3.22 Ex: Effective power

Show that the expression $P_{med} = R\mathcal{E}_{rms}^2/Z^2$ provides the correct result for a circuit containing only one ideal *ac*-generator and
a. one resistor R,
b. one capacitor C and
c. one inductance L. In the given expression, P_{med} is the average power supplied by the generator, $\mathcal{E}_{rms}$ is the average quadratic value of the emf-generator.

5.2.3.23 Ex: R-L-C-circuit

In the circuit shown in the figure the ideal generator produces a voltage of 115 V when operated at 60 Hz. What is the *rms*-voltage between the points
a. A and B, b. B and C, c. C and D, d. A and C, and e. B and D?

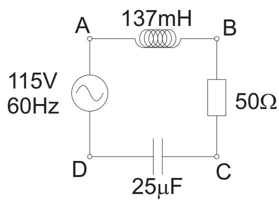

Figure 5.25: Circuit.

5.3 Magnetostatic energy

To calculate the magnetostatic energy stored in a magnetic field we will proceed as follows: We will look for a general expression guessed by analogy with the electrostatic energy, $W = \frac{1}{2}\int \varrho\Phi dV$, and show that, applied to a current-carrying loop, this expression gives the correct result. The analogous formula is,

$$W = \frac{1}{2}\int \mathbf{j}\cdot\mathbf{A}dV \ . \tag{5.50}$$

5.3.1 Energy density of a magnetostatic field

The energy of a current distribution can be rewritten using Ampere's law,

$$W = \frac{1}{2\mu_0}\int (\nabla\times\vec{\mathcal{B}})\cdot\mathbf{A}dV \ . \tag{5.51}$$

Integration by parts allows transferring the derivative from $\vec{\mathcal{B}}$ to $\mathbf{A}$,

$$W = \frac{1}{2\mu_0}\left[-\oint(\mathbf{A}\times\vec{\mathcal{B}})\cdot d\mathbf{S} + \int \vec{\mathcal{B}}\cdot(\nabla\times\mathbf{A})dV\right] \ . \tag{5.52}$$

The surface integral can be neglected because we can choose the integration volume $\mathcal{V}$ to be arbitrarily large. Expressing the rotation by the field,

$$W = \frac{1}{2\mu_0}\int \vec{\mathcal{B}}^2 dV = \frac{1}{2\mu_0}\int u dV \ , \tag{5.53}$$

and introducing the *energy density*,

$$\boxed{u \equiv \frac{1}{2\mu_0}\vec{\mathcal{B}}^2} \ . \tag{5.54}$$

It may seem strange, that we need energy to build up a magnetic field which in turn can not exert work. On the other hand, to create this magnetic field, we have to ramp it up from zero which, according to Faraday's law induces an electric field. This field, in turn, can work. Initially there is no $\vec{\mathcal{E}}$ and at the end of the process there is no $\vec{\mathcal{E}}$ neither; but in between, while $\vec{\mathcal{B}}$ is being constructed, there is. The work has to be exerted against the $\vec{\mathcal{E}}$-field.

5.3.2 Inductors and storage of magnetostatic energy

Using the magnetostatic energy formula,

$$W = \frac{1}{2}\int \mathbf{j}\cdot\mathbf{A}dV = \frac{1}{2}\oint \mathbf{I}\cdot\mathbf{A}dl = \frac{I}{2}\oint \mathbf{A}\cdot d\mathbf{l} = \frac{I}{2}\int(\nabla\times\mathbf{A})\cdot d\mathbf{S} = \frac{I}{2}\int \vec{\mathcal{B}}\cdot d\mathbf{S} = \frac{I}{2}\Psi_M \ . \tag{5.55}$$

Finally, considering a coil and using the formula (5.48),

$$\boxed{W = \frac{1}{2}LI^2} \ , \tag{5.56}$$

which corresponds to the power,

$$\frac{dW}{dt} = -\mathcal{E}I = LI\frac{dI}{dt} \ . \tag{5.57}$$

5.3.3 Exercises

5.3.3.1 Ex: Switching processes

Consider the RL-circuit show in the figure, where the ohmic resistor $R = R(t)$ varies over time. Let τ be the length of the switching-on process starting at time $t = 0$. The resistance be,

$$R(t) = \begin{cases} \infty & \text{for } t < 0 \\ R_0\tau/t & \text{for } 0 \leq t \leq \tau \\ R_0 \text{for } \tau \leq t \end{cases} .$$

a. Set up for the time intervals $t \in [0, \tau]$ and $t \in [\tau, \infty]$ separate differential equations for the current $I(t)$.
b. Solve the differential equations (using a simple ansatz or a method of variable separation) and connect the solutions continuously at $t = \tau$. What is the condition for fast or slow switching?

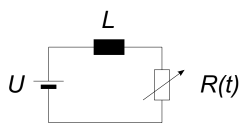

Figure 5.26: Circuit.

5.3.3.2 Ex: Current density of a rotating charge

The surface of a hollow sphere with radius R carries a uniformly distributed charge Q. The sphere rotates with the constant angular velocity ω around one of its diameters.
a. Determine the current density $\mathbf{j}(\mathbf{r})$ generated by this movement.
b. Calculate the magnetic moment produced by $\mathbf{j}$.
c. Derive the components of the potential vector $\mathbf{A}(\mathbf{r})$ and the magnetic field $\vec{\mathcal{B}}(\mathbf{r})$.

5.3.3.3 Ex: Train track

The two iron rails of a toy train have a thickness of $d = 5\,\text{mm}$ and a reciprocal distance of $a = 50\,\text{mm}$ They are connected by a metal rod of mass $m = 0.5\,\text{g}$, which is movable without friction in a direction perpendicular to the rails. A current applied to the rails, which also runs through the metal rod, causes the rod to accelerate along the rails.
a. Calculate the magnetic field between the two rails, if through them runs the same current I but in inverse directions. Neglect inhomogeneities at the ends of the rails and the magnetic field generated by the current passing through the rod.
b. How strong is the force accelerating the rod along the rails?
c. What current would be needed to accelerate the rod over a distance of $l = 5\,\text{m}$, up to a speed of $10\,\text{m/s}$? Ignore all friction effects.

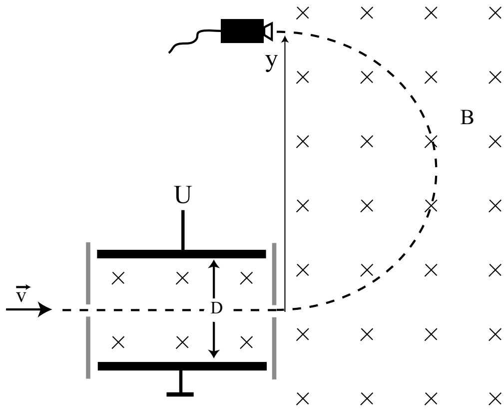

Figure 5.27: Circuit.

5.3.3.4 Ex: Mass spectrometer

A mass spectrometer consists, as shown in the figure, of a plate capacitor with $D =$ 5 mm distance between the electrodes, placed within a magnetic field $\mathcal{B} = 0.4\,\text{T}$ with homogeneous amplitude. A mixture of isotopes of carbon ion $^{12}C^+$ and $^{14}C^+$ penetrates the capacitor through a circular slot. After transit through the capacitor the ions move in the magnetic field on a semicircular path and are counted by a detector, whose distance y from the slot can be varied.
a. What voltage should be applied to the plates of the capacitor to ensure that only ions with the velocity $v = 10^5$ m/s can exit the capacitor through the second slot?
b. At what distances y can the two isotopes be detected respectively?

5.3.3.5 Ex: Transformer

Consider two similar coils with number of turns N_1 and N_2 connected by an iron yoke. In the first coil we apply a time-varying voltage U_1. Therefore, in this coil (called primary) runs a current I_1, producing a magnetic flux Ψ, which is transmitted entirely through the iron yoke to the second (second) coil. Here, a voltage U_2 is induced.
a. Calculate the ratio U_2/U_1 as a function of the number of turns. What is the behavior of the phase between U_1 and U_2.
b. What are the phases of the currents I_1 and I_2 running through the coils with respect to phases of the voltages? What is the consequence for the average power in the coils?

5.3.3.6 Ex: Resonant L-R-C-circuit

Consider an excited LRC serial circuit. The components of the oscillating circuit have the values $R = 5\,\Omega$, $C = 10\,\mu\text{F}$, $L = 1\,\text{H}$, and $U = 30\,\text{V}$.
a. At what excitation frequency ω_a does the amplitude of the current have its maximum value? Give the value of the current?
b. At what angular frequencies ω_{a1} and ω_{a2} does the amplitude of the current have

exactly half the maximum value? What is therefore the FWHM width of the resonance curve for this oscillating circuit? Show that the width of the resonance curve is given by,

$$\frac{\omega_{a1} - \omega_{a2}}{\omega_a} = R\sqrt{\frac{3C}{L}} \ .$$

c. Make a scheme of some resonance curves for various values of R.

5.3.3.7 Ex: Inductive circuit

Consider the circuit shown in the figure, which consists of a coil L, a voltage source U, and an ohmic resistor $R = 100\,\Omega$. The coil is a long solenoid with 50 turns per cm and an inductance of 200 mH. For times $t < 0$ there is no current flow through the solenoid. At time $t = 0$, the voltage is suddenly increased from 0 to 10 V. How long does it take the magnetic field in the solenoid to reach the value $\pi \cdot 10^{-4}$ T?

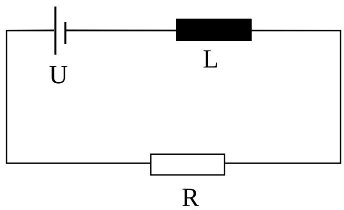

Figure 5.28: Circuit.

5.3.3.8 Ex: Inductive circuit

Consider the circuit shown in the figure, which consists of a coil L, a voltage source $U_0 = 10$ V, and three ohmic resistors $R = 100\,\Omega$. The coil is a long solenoid with 50 turns per cm and an inductance of 200 mH. Initially, the switch is open for a long time. Then at time $t = 0$, it is closed.
a. What is the initial value of the magnetic field in the solenoid while the switch is still open?
b. Using Kirchhoff's laws, derive the formula describing the temporal evolution of the field after the switch has been closed.
c. Determine the field for long times after the switch has been closed.

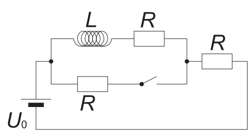

Figure 5.29: Circuit.

5.3.3.9 Ex: Conductive circular rings

Consider two infinitely thin conducting rings. They are concentric with radii a and b ($a < b$) and arranged in the xy-plane with a common center at the coordinate origin. The inner ring carries a homogeneously distributed charge $+q$ (that is, with linear constant charge density), the outer ring carries the homogeneously distributed charge $-q$.
a. First, write the charge density $\rho(\mathbf{r}) = \rho(r, \phi, z)$ in cylindrical coordinates. Now, let the inner ring rotate with the constant angular velocity ω about the symmetry axis (that is, the z-axis). Write the resulting current density also in cylindrical coordinates. **Help:** $\mathbf{j}(\mathbf{r}) = \rho(\mathbf{r}) \cdot \mathbf{v}(\mathbf{r})$ where $\mathbf{v}(\mathbf{r})$ is the velocity at the position $\mathbf{r}$. b. Determine by an explicit calculation the dipolar magnetic moment $\mathbf{m} = \frac{1}{2}\int d^3r\ \mathbf{r} \times \mathbf{j}(\mathbf{r})$ of the rotating ring.

5.4 Alternating current

5.4.1 Electromagnetic oscillations

We have already met the plate capacitor as the most basic device for storing electrostatic energy in an (homogeneous) electric field. Similarly, the solenoid is the most basic device for storing magnetostatic energy in a (homogeneous) magnetic field. Placing a solenoid with inductance L and a capacitor with capacitance C in an electric circuit we find that electric energy can be converted into magnetic energy (and vice versa) in an analogous way as potential energy can be converted into kinetic energy (and vice versa) in a mass-spring system. This can generate (electromagnetic) oscillations.

Example 51 (*Oscillating circuits*): Let us first consider a circuit with a coil and a capacitor connected in series. Kirchhoff's law of meshes requires, $U_{ind} = U_C$, which gives,

$$-L\frac{dI}{dt} = \frac{Q}{C}$$

or

$$L\ddot{I} + C^{-1}I = 0 \ .$$

We now consider a circuit with a battery, a switch, a coil, and a resistor in series. Kirchhoff's law of meshes requires, $U_0 = -U_{ind} + U_R = L\dot{I} + RI$, which gives,

$$\frac{dI}{I - U_0/R} = -\frac{R}{L}dt$$

with the solution

$$I(t) = \frac{U_0}{R} + \left(I_0 - \frac{U_0}{R}\right)e^{-Rt/L} \ ,$$

where we choose the initial current $I_0 = 0$.

5.4.2 Alternating current circuits

To discuss alternating voltages, we consider the circuit shown in Fig. 5.30 fed by a voltage source, $U(t) = U_0 e^{\imath\omega t}$. To simplify the mathematical expressions we adopt a complex notation. The objective is to calculate the current for the various types of consumers Z that we already got to know. In the case of an ohmic resistance we have,

$$I = \frac{U_0}{R} e^{\imath\omega t} = \frac{U}{R} . \tag{5.58}$$

Hence,

$$Z = \frac{U}{I} = R . \tag{5.59}$$

In the case of a capacitance we have,

$$I = \dot{Q} = CU_0 \frac{d}{dt} e^{\imath\omega t} = \imath\omega CU . \tag{5.60}$$

Hence,

$$Z = \frac{U}{I} = \frac{1}{\imath\omega C} . \tag{5.61}$$

In the case of an inductance we have,

$$I = \int_0^t LU_0 e^{\imath\omega t} dt = \frac{U}{\imath\omega L} . \tag{5.62}$$

Hence,

$$Z = \frac{U}{I} = \imath\omega L . \tag{5.63}$$

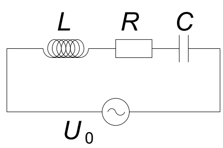

Figure 5.30: *L-R-C* circuit powered by an alternating voltage.

These results can be interpreted graphically (plotting Im U versus Re U) or analytically substituting $\imath = e^{\imath\pi/2}$. For the above three cases we obtain,

$$R = \frac{U_0 e^{\imath\omega t}}{I_0 e^{\imath\omega t + \pi/2}} \quad , \quad L\omega = \frac{U_0 e^{\imath\omega t}}{I_0 e^{\imath\omega t + \imath\pi/2}} \quad , \quad \frac{1}{C\omega} = \frac{U_0 e^{\imath\omega t}}{I_0 e^{\imath\omega t - \imath\pi/2}} . \tag{5.64}$$

This means that in the case of an inductance or capacitance, the voltage is not in phase with the current but has, respectively, an advance or a delay of 90°.

In cases of combinations of resistors and reactants the expression to calculate this phase shift becomes more complicated and may vary with the frequency imposed by the alternating source. Let us see how to calculate it at the example of the *L-R-C* circuit in series, writing in the same way as before,

$$Z = \frac{U}{I} = \imath L\omega + R + \frac{1}{\imath C\omega} = |Z| e^{\imath\phi} . \tag{5.65}$$

Hence,

$$|Z| = ZZ^* = \sqrt{R^2 + \left(L\omega - \frac{1}{\imath C\omega}\right)^2} \qquad \text{and} \qquad \tan\phi = \frac{\sin\phi}{\cos\phi} = \frac{L\omega - \frac{1}{C\omega}}{R} \; . \quad (5.66)$$

A resonance is met when $\omega = 1/\sqrt{LC}$. Other combinations of components are treated in the same way.

5.4.3 Exercises

5.4.3.1 Ex: High-pass filter

The circuits shown in the figure are called (a) first-order and (b) second-order high-pass filter. Calculate for both cases the ratio of output voltage U_a and input voltage U_e. Suppose that $U_e(t) = U_e \cos\omega t$ and $U_a(t) = U_a \cos(\omega t + \phi)$. Plot the result as a function of frequency on a logarithmic graph with the y-axis $\log(U_a/U_e)$ and the x-axis $\log\omega$. (This graph is called 'Bode diagram'.) What is the phase shift ϕ as a function of frequency?

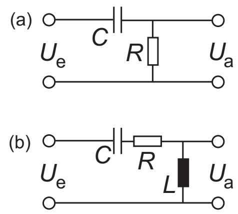

Figure 5.31: High pass.

5.4.3.2 Ex: Band and notch filter

The circuits shown in the figure are called (a) bandpass and (b) notch filter. Calculate

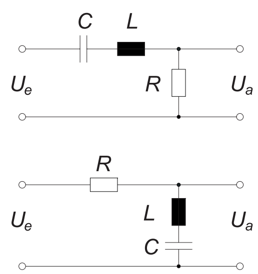

Figure 5.32: Filter.

for both cases the output voltage $U_a(t)$ under the condition that the input voltage is a sinusoidal oscillation, $U_e(t) = U_0 \cos\omega t$. Draw the amplitude of the output voltages as a function of frequency.

a. How do the amplitudes behave in the resonant case?
b. Discuss the limiting cases (i) $L \to 0$ resp., (ii) $C \to \infty$ based on transfer functions.

5.4.3.3 Ex: Coaxial cable

A coaxial cable consists of a cylindrical conductor of radius a and a thin cylindrical waveguide of radius $b > a$. Between the conductors there is a voltage difference of U, and inside them flow currents in opposite directions I. Calculate the Poynting vector in the empty space and the power carried through the cable.
Help: Calculate the electric field between the conductors using Gauß' law and the magnetic field between the conductors using Ampere law.

5.4.3.4 Ex: *ac*-resistance

Calculate the work performed by an alternating current $I = I_0 \sin \omega t$ on a conductor with ohmic resistance R over a time period T. Make a scheme of the evolution in a diagram power versus time.

5.4.3.5 Ex: *ac*-motor

An alternating voltage motor provides with an alternating voltage of $U = 220\,\text{V}$ at $f = 50\,\text{Hz}$ with the power $P = UI \cos \phi = 2.2\,\text{kW}$. The power factor of the engine is $\cos \phi = 0.6$ and the efficiency $\eta = P_{out}/P_{in} = 0.89$.
a. What current does the motor receive?
b. Which capacitor must be connected in parallel to the terminals of the motor in order to increase the power factor to a value of $\cos \phi = 0.9$? Sketch the current pointer in the $U - I$-plane.

5.4.3.6 Ex: Displacement current

a. Explain the significance of the continuity equation,

$$\oint \mathbf{j} \cdot d\mathbf{S} + \frac{d}{dt} \int \rho dV = 0 \ .$$

b. Consider an enclosed area $S_1 + S_2$, because here the continuity equation has the form,

$$\oint \mathbf{j} \cdot d\mathbf{S} - \frac{d}{dt} \int \vec{\mathcal{D}} \cdot d\vec{\mathcal{D}} V = 0 \ .$$

Show that holds,

$$\oint_C \vec{\mathcal{H}} \cdot d\mathbf{l} = \int_{S_2} \frac{d}{dt} \int \vec{\mathcal{D}} \cdot d\mathbf{S} \ .$$

Help: No field lines penetrate through the area S_1, and no current flows through the area S_2.

5.4.3.7 Ex: Resonant LC-circuit

The capacitor of an undamped oscillating electromagnetic circuit has the capacity $C = 22$ nF. The eigenfrequency of the circuit is $f_0 = 5735\,\text{Hz}$. At time $t = 0$ the capacitor has its maximum charge: $Q_0 = 0.33\,\mu\text{C}$.
a. Derive for the undamped oscillating circuit the differential equation for $Q(t)$ from the energy conservation law and determine the solution. Write down the equation for eigenfrequency f.
b. Calculate inductance of the coil.
c. Set up equations for the energy content of the coil and and the capacitor as a function of time t.
d. Calculate the instant of time t_2, at which the energy content of the coil is, for the second time, half the energy content of the capacitor.

5.4.3.8 Ex: Resonant LRC-circuit

The oscillating LRC-circuit shown in 5.30 is excited by the alternating voltage source $U(t) = U_0 \cos \omega t$.
a. Calculate the total impedance Z as a function of ω and prepare graphs of the amplitude response $|Z(\omega)|$ and the phase response $\phi(\omega) = \arctan \frac{\mathfrak{Im}\ Z(\omega)}{\mathfrak{Re}\ Z(\omega)}$.
b. Establish the differential equation for the current. Start by solving the homogeneous differential equation and then the inhomogeneous one.

5.4.3.9 Ex: Resonant LRC-circuit

The components of an RLC-circuit (see 5.30) have the values $R = 5\ \Omega$, $C = 10\,\mu\text{F}$, $L = 1\,\text{H}$, and $U = 30\,\text{V}$.
a. At what angular frequency ω_a does the current amplitude have its maximum value? What is the corresponding current?
b. At what angular frequencies ω_{a1} and ω_{a2} does the amplitude of the current have half the maximum value? What is the relative half-width of the resonance curve for this resonant circuit?
c. Show with the help of the formulas of (b) that the relative half-width of each resonance curve is given by,

$$\frac{\Delta_a}{\omega} = R\sqrt{\frac{3C}{L}}\ ,$$

where Δ_a is the width of the resonance profile at half the maximum amplitude.
d. Prepare schemes of the resonance profile for various values of R. When is the current circuit predominantly capacitive and when inductive?
e. Show that the damping term $e^{-Rt/2L}$ (containing L but not C!) can be written in a more symmetrical form in L and C as follows,

$$e^{-\pi R \frac{t}{T} \sqrt{\frac{C}{L}}}\ .$$

Here, T is the period of oscillation when we neglect resistance. What is the SI-unit of the term $\sqrt{C/L}$?
f. Show, based on the result (e), that the condition for a smaller relative energy loss per oscillation cycle is: $R \ll \sqrt{L/C}$.

5.4.3.10 Ex: Resonant LRC-circuit

Consider a dampened oscillating RLC-circuit. The charge $\bar{q}$ on the capacitor is described by the differential equation,

$$L\frac{d^2\bar{q}}{dt^2} + R\frac{d\bar{q}}{dt} + \frac{1}{C}\bar{q} = 0 \ .$$

a. Use the ansatz $\bar{q} = q_0 e^{\imath\omega t}$ and show that,

$$\omega_{1,2} = \imath\frac{R}{2L} \pm \omega' \qquad \text{where} \qquad \omega' = \omega_0\sqrt{1 - \frac{R^2C}{4L}}$$

with $\omega_0 = 1/\sqrt{LC}$ solves the differential equation.
b. Since this is a second order differential equation, we need two boundary conditions to determine the general solution of the form,

$$\bar{q}(t) = a\bar{q}_1(t) + b\bar{q}(t) \qquad \text{with} \qquad \bar{q}_{1,2} = \bar{q}_0 e^{-\frac{R}{2L}t} e^{\pm\imath\omega' t} \ .$$

Use the conditions $\bar{q}(0) = 0$ and $\dot{\bar{q}}(0) = I_0$ and determine the coefficients a and b. What is the solution for the charge $\bar{q}(t)$ in this case, and for the current $I(t) = \dot{\bar{q}}(t)$?
c. Sketch the evolution of the charge and the current on the capacitor for the following set of parameters and interpret the curves. What is the respective duration T of an oscillation period? Give for each of the following parameter sets the respective general solution before entering the values:
i. $I_0 = 1\,\text{mA}$, $R = 10\,\Omega$, $L = 1\,\text{mH}$, $C = 0.1\,\mu\text{F}$
ii. $I_0 = 1\,\text{mA}$, $R = 200\,\Omega$, $L = 1\,\text{mH}$, $C = 0.1\,\mu\text{F}$
iii. $I_0 = 1\,\text{mA}$, $R = 500\,\Omega$, $L = 1\,\text{mH}$, $C = 0.1\,\mu\text{F}$

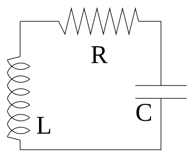

Figure 5.33: Resonant LRC-circuit.

5.4.3.11 Ex: Magnetized sphere

We consider a sphere with radius R magnetized such that, inside the sphere, the magnetic field density is given by $\vec{\mathcal{B}} = \mathcal{B}_0\hat{\mathbf{e}}_z$. The outer space is empty, that is, there are no currents, such that rot $\vec{\mathcal{B}} = 0$ and div $\vec{\mathcal{B}} = 0$. Therefore, we can let for the outer space,

$$\vec{\mathcal{B}} = -\text{grad}\Psi \quad \text{and} \quad \Psi(r,\vartheta,\varphi) = \sum_{l=0}^{\infty}\alpha_l\frac{P_l(\cos\vartheta)}{r^{l+1}} \ ,$$

with P_l the Legendre polynomials and r, ϑ and φ the usual spherical coordinates. Consider the boundary conditions for $\mathcal{B}_r$, $\mathcal{B}_\theta$ as well as for $\mathcal{H}_r$ and $\mathcal{H}_\theta$ at the transition between the inner and outer space of the sphere. Determine from this the expansion coefficients α_l as well as the magnetization $\vec{\mathcal{M}}$ inside the sphere. With this we finally get the magnetic field density $\vec{\mathcal{B}}$ magnetic $\vec{\mathcal{H}}$-field in the inner and outer space.

5.4.3.12 Ex: Magnetic dipole moving through a conductive loop

What is the current signal produced by a ^{87}Rb Bose-Einstein condensate with its spin being polarized in the state $|F, m_F\rangle = |2, 2\rangle$ when it falls through a SQUID? Assume that the SQUID has the diameter $2a = 3\,\text{cm}$, the condensate consists of $N = 100000$ atoms and has a constant velocity of $v_z = 10\,\text{cm/s}$.

5.4.3.13 Ex: Electric current and magnetism

a. How are current and current density defined? What is a 'current line'?
b. What conditions should charge and current densities meet in magnetostatics?
c. How is the magnetic field $\vec{\mathcal{B}}$ defined empirically?
d. Writes the general form of Ampère's law. How is Ampère's law expressed in the case of two parallel conductors carrying currents I_1 and I_2?
e. What does the Ampère's law say?
f. What is the magnetic moment of an arbitrary, flat, closed current circuit?
g. What are the force and thye torque on a magnetic dipole in an external field $\vec{\mathcal{B}}(\mathbf{r})$.
h. Explain the term 'magnetization current density'.
i. What are the macroscopic equations of the magnetostatic field?
j. What is diamagnetism and paramagnetism? What differentiates these two phenomena? What is ferromagnetism?

5.4.3.14 Ex: Electro-motor

Consider the electromotor of the scheme. Two pairs of Helmholtz coils aligned along the x- and y-axes are powered by alternating currents, $I_x(t) = I_0 \cos\omega t$ and $I_y(t) = I_0 \sin\omega t$, respectively. In the field there is a rotating rectangular coil traversed by a constant current I. The inertial moment of the coil is $\mathcal{I}$.
a. Show that the field in the center is given by $\mathcal{B}_x(0) = \frac{-8}{5\sqrt{5}} \frac{\mu_0 I_x \hat{\mathbf{e}}_x}{R}$.
b. Describes the temporal behavior of the magnetic field.
c. Relate the torque with the angular acceleration of the coil.
d. Calculate the instantaneous torque acting on the coil.
e. Suppose that the coil initially rotates with an angular velocity Ω such that, $\theta(t) = \theta_0 + \Omega t$. How you should choose Ω and the initial angle θ_0 to ensure an always positive torque? **Help:** $\sin\alpha\cos\beta + \cos\alpha\sin\beta = \sin(\alpha+\beta)$
f. Calculate the voltage induced in the coil. **Help:** $\sin\alpha\sin\beta + \cos\alpha\cos\beta = \cos(\alpha-\beta)$
g. Suppose the coil has an ohmic resistance ...

5.4.3.15 Ex: Magnetism

A given magnetic material is composed of N non-interacting atoms, whose magnetic moments μ can point in three possible directions, as shown in the figure, μx, μy, and $-\mu x$. The system is in thermal equilibrium at temperature T and subject to a uniform magnetic field oriented along the y-direction, $\vec{\mathcal{H}} = \mathcal{H}\hat{\mathbf{e}}_y$, so the energy levels corresponding to a single atom are $\varepsilon_0 = -\mu\mathcal{H}$, $\varepsilon_1 = 0$, and $\varepsilon_2 = 0$.
a. Get the canonical partition function z for one atom, the canonical partition function Z of the system, and the Helmholtz free energy f per atom.
b. Determine the mean energy $u \equiv \langle\varepsilon_n\rangle$ and the entropy s/k_B per atom.

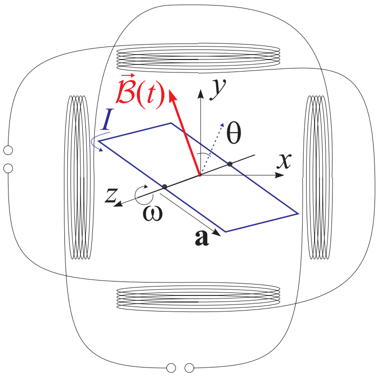

Figure 5.34: Electro-motor.

c. Get magnetization per atom $\mathbf{m} \equiv \langle \vec{\mu}_n \rangle = m_x \hat{x} + m_y \hat{y}$.
d. Verify that the isothermal susceptibility $\chi_T \equiv (\partial m_y / \partial \mathcal{H})_T \propto 1/T$ at zero field obeys Curie's law of paramagnetism, $\chi_T(\mathcal{H} \to 0) \propto 1/T$.

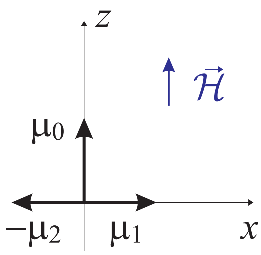

Figure 5.35:

5.5 Further reading

D.J. Griffiths, *Introduction to Electrodynamics* [ISBN]

D. Halliday, R. Resnick, and J. Walker, *Fundamentals of Physics* [ISBN]

H.M. Nussenzveig, *Curso de Física Básica: Eletromagnetismo (Volume 3)* [ISBN]

Chapter 6

Maxwell's equations

In the first part of the course, we derived the laws of electromagnetism from experimental observations related to the Coulomb force on electric charges and the Lorentz force on electric currents. We have found that these forces can be understood by introducing electric fields $\vec{\mathcal{E}}$ and magnetic fields $\vec{\mathcal{B}}$, to which the laws of electromagnetism apply. These laws were all known before Maxwell. These are,

$$\begin{array}{rcll} \nabla\times\vec{\mathcal{B}} & = & \mu_0\mathbf{j} & \textit{Ampère's law} \text{ leading to } \textit{Biot-Savart's law} \\ \nabla\times\vec{\mathcal{E}} & = & -\partial_t\vec{\mathcal{B}} & \textit{Faraday's law} \\ \nabla\cdot\vec{\mathcal{E}} & = & \varepsilon_0^{-1}\varrho & \textit{Gauß' law} \text{ leading to } \textit{Poisson's law} \text{ and } \textit{Coulomb's law} \\ \nabla\cdot\vec{\mathcal{B}} & = & 0 & \text{absence of magnetic monopoles} \end{array} . \tag{6.1}$$

As we will show shortly, well-behaved vector fields are entirely defined by their divergences and rotations, so that we can expect that the set of laws (6.1) be complete, that is, it should be able to describe all electromagnetic phenomena.

However, by comparing the laws of Faraday and Ampère, we perceive an inconsistency: taking the divergences of the rotations, we expect them to zero:

$$0=\nabla\cdot(\nabla\times\vec{\mathcal{E}})=\nabla\cdot\left(-\frac{\partial\vec{\mathcal{B}}}{\partial t}\right)=-\frac{\partial}{\partial t}(\nabla\cdot\vec{\mathcal{B}}) \tag{6.2}$$
$$0=\nabla\cdot(\nabla\times\vec{\mathcal{B}})=\mu_0(\nabla\cdot\mathbf{j})=-\mu_0\frac{\partial\varrho}{\partial t}\neq 0\ ,$$

where the last step makes use of the continuity equation (3.38). For temporal variations of the charge distribution the second equation can not be correct.

Maxwell's idea for solving the problem was to simply subtract from Ampère's law the term that prevents the second equation (6.2) from zeroing. With

$$\boxed{\nabla\times\vec{\mathcal{B}}=\mu_0\mathbf{j}+\varepsilon_0\mu_0\frac{\partial\vec{\mathcal{E}}}{\partial t}}\ , \tag{6.3}$$

we verify,

$$\nabla\cdot(\nabla\times\vec{\mathcal{B}})=\mu_0\nabla\cdot\mathbf{j}+\varepsilon_0\mu_0\frac{\partial\nabla\cdot\vec{\mathcal{E}}}{\partial t}=\mu_0\left(\nabla\cdot\mathbf{j}+\frac{\partial\varrho}{\partial t}\right)=0\ , \tag{6.4}$$

where, once more, we used the continuity equation. The Eq. (6.3) could be called *Maxwell's law* and the surface integral of the additional term,

$$\varepsilon_0 \frac{\partial}{\partial t} \oint_{\mathcal{S}} \vec{\mathcal{E}} \cdot d\mathbf{S} \equiv \oint_{\mathcal{S}} \mathbf{j}_d \cdot d\mathbf{S} = I_d \ . \tag{6.5}$$

is named *displacement current*. We will study consequences of this law in the Excs. 6.1.5.1 and 6.1.5.2.

Example 52 (*Necessity of a displacement current*): We consider the circuit shown in Fig. 6.1. On the one hand, the current passing through the Ampèrian loop must be independent of the shape of the enclosed area,

$$I = \int_{\mathcal{S}} \mathbf{j} \cdot d\mathbf{S} = \tfrac{1}{\mu_0} \oint_{\partial\mathcal{S}} \vec{\mathcal{B}} \cdot d\mathbf{l} \ .$$

On the other hand, we know that the current can not cross the capacitor and must accumulate on one of the electrodes.
The problem is solved by identifying the electric field, which is developing due to the accumulated charge,

$$\frac{\partial Q}{\partial t} = \varepsilon_0 \frac{\partial}{\partial t} \int_{\mathcal{V}} \nabla \cdot \vec{\mathcal{E}} dV = \varepsilon_0 \frac{\partial}{\partial t} \int_{\partial\mathcal{V}} \vec{\mathcal{E}} \cdot d\mathbf{S} \equiv I_d \ ,$$

with a *displacement current* I_d.

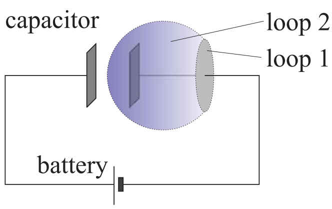

Figure 6.1: Necessity for a displacement current: The magnetic field at the edge of the loops 1 and 2 can not depend on the shape of the chosen surface.

6.1 The fundamental laws of electrodynamics

With these results we can finally summarize the *Maxwell equations* as,

$$\boxed{\begin{array}{lrcl} \text{(i)} & \nabla \times \vec{\mathcal{B}} - \varepsilon_0\mu_0\partial_t\vec{\mathcal{E}} & = & \mu_0\mathbf{j} \\ \text{(ii)} & \nabla \times \vec{\mathcal{E}} + \partial_t\vec{\mathcal{B}} & = & 0 \\ \text{(iii)} & \nabla \cdot \vec{\mathcal{E}} & = & \varepsilon_0^{-1}\varrho \\ \text{(iv)} & \nabla \cdot \vec{\mathcal{B}} & = & 0 \end{array}} \ . \tag{6.6}$$

These equations form the complete basis of the electrodynamical theory initially motivated by the empirical observation of forces acting on features of matter identified as *charges* and *currents*, that is, the electric (Coulomb) force and magnetic (Lorentz) force,

$$\mathbf{F}_{Lor} = Q(\vec{\mathcal{E}} + \mathbf{v} \times \vec{\mathcal{B}}) \ , \tag{6.7}$$

where $\vec{\mathcal{E}}$ is a *polar vector* ($\vec{\mathcal{E}} = -\vec{\mathcal{E}}_{mirrored}$) [1] and $\vec{\mathcal{B}}$ is an *axial vector* ($\vec{\mathcal{B}} = \vec{\mathcal{B}}_{mirrored}$). The electric field $\vec{\mathcal{E}}$ and the magnetic field $\vec{\mathcal{B}}$ and their field equations were 'invented' to explain the Coulomb-Lorentz force. They are only observable through their action on charged particles. According to the *Helmholtz theorem* discussed in the next section, arbitrary (but well-behaved) field vectors are fully defined by their divergence and rotation properties. That is exactly what Maxwell's equations do with the electric and magnetic fields.

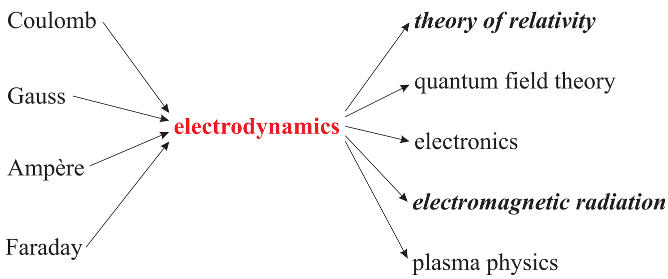

Figure 6.2: Construction and application of the theory of electrodynamics.

Once we know the fundamental laws of electromagnetism [2], we can reverse the reasoning by placing them as postulates and deriving the observable phenomena from them. This will be the procedure of this second part of the course of electromagnetism.

Example 53 (*Derivation of electro- and magnetostatics from Maxwell's equations*): For static systems we can let $\dot{\mathbf{E}} = \dot{\mathbf{B}} = 0$. In particular for the electrostatic case, we ignore currents, $\mathbf{j} = 0$, and for the magnetostatic case we ignore charges, $\varrho = 0$. Maxwell's equations then simplify considerably and can often be replaced by the Poisson equations,

$$-\nabla \cdot \vec{\mathcal{E}} = \nabla \cdot (\nabla \Phi) = \nabla^2 \Phi = -\varepsilon_0^{-1} \varrho$$
$$-\nabla \times \vec{\mathcal{B}} = -\nabla \times (\nabla \times \mathbf{A}) = \nabla^2 \mathbf{A} - \nabla(\cancelto{0}{\nabla \cdot \mathbf{A}}) = -\mathbf{j} \ ,$$

where the divergence of $\mathbf{A}$ is set to zero in the Coulomb gauge.

We will apply Maxwell's equations to solve the Excs. 6.1.5.3 to Excs. 6.1.5.5. In the Excs. 6.1.5.6, 6.1.5.7, and 6.1.5.8 we study implications of a supposed existence of *magnetic charges* or *magnetic monopoles*.

[1]Mirroring means inversion of the dynamic quantities $\mathbf{v} \to -\mathbf{v}$, $\mathbf{F}_{Lor} \to -\mathbf{F}_{Lor}$. Examples for polar vectors are $\mathbf{r}$, $\mathbf{p}$, $\vec{\mathcal{E}}$. Examples for axial vectors are $\mathbf{L}$, ω, $\vec{\mathcal{B}}$. We have for axial vectors $\mathbf{a}_i$ and polar vectors $\mathbf{p}_i$, the following relations,

$$\mathbf{a}_1 \times \mathbf{a}_2 = \mathbf{a}_3 \quad , \quad \mathbf{p}_1 \times \mathbf{p}_2 = \mathbf{a}_3 \quad , \quad \mathbf{p}_1 \times \mathbf{a}_2 = \mathbf{p}_3 \ .$$

[2]We note, that Maxwell's laws can be deduced from more fundamental principles, including the conservation laws for energy, momentum, angular momentum, and charge and the relativistic Lorentz transform.

6.1.1 Helmholtz's theorem

The *Helmholtz theorem* says that, knowing the divergence and the rotation of an unknown vector field $\mathbf{F}$, we can reconstruct this field under the condition that the divergence and the rotation disappear sufficiently fast in the infinity [3] and that $|\mathbf{F}|$ disappears at least as fast as $1/r^2$. That is, knowing the scalar field,

$$D(\mathbf{r}) \equiv \nabla \cdot \mathbf{F}(\mathbf{r}) \tag{6.8}$$

and the vectorial field,

$$\mathbf{C}(\mathbf{r}) \equiv \nabla \times \mathbf{F}(\mathbf{r}) \ , \tag{6.9}$$

the field $\mathbf{F}$ is completely defined. Note that obviously, $\nabla \cdot \mathbf{C} = 0$.

To prove this, we show that,

$$\mathbf{F} = -\nabla\Phi + \nabla \times \mathbf{A} \ , \tag{6.10}$$

where

$$\Phi(\mathbf{r}) \equiv \frac{1}{4\pi}\int_{\mathbb{R}^3} \frac{D(\mathbf{r}')}{|\mathbf{r}-\mathbf{r}'|}dV' \qquad \text{and} \qquad \mathbf{A}(\mathbf{r}) \equiv \frac{1}{4\pi}\int_{\mathbb{R}^3} \frac{\mathbf{C}(\mathbf{r}')}{|\mathbf{r}-\mathbf{r}'|}dV' \ , \tag{6.11}$$

meets the requirements (6.8) and (6.9). The divergence is,

$$\begin{aligned}\nabla_{\mathbf{r}} \cdot \mathbf{F} &= -\nabla^2_{\mathbf{r}}\Phi + \cancelto{0}{\nabla_{\mathbf{r}} \cdot \nabla_{\mathbf{r}} \times \mathbf{A}} \qquad (6.12)\\ &= -\frac{1}{4\pi}\int D(\mathbf{r}')\nabla^2_{\mathbf{r}}\left(\frac{1}{|\mathbf{r}-\mathbf{r}'|}\right)dV' = \int D(\mathbf{r}')\delta^3(\mathbf{r}-\mathbf{r}')dV' = D(\mathbf{r}) \ .\end{aligned}$$

We verify,

$$\begin{aligned}4\pi\nabla_{\mathbf{r}} \cdot \mathbf{A} &= \int \mathbf{C}(\mathbf{r}') \cdot \nabla_{\mathbf{r}}\frac{1}{|\mathbf{r}-\mathbf{r}'|}dV' = -\int \mathbf{C}(\mathbf{r}') \cdot \nabla_{\mathbf{r}'}\frac{1}{|\mathbf{r}-\mathbf{r}'|}dV' \qquad (6.13)\\ &= -\int \frac{1}{|\mathbf{r}-\mathbf{r}'|}\cancelto{\nabla\cdot\nabla\times\mathbf{F}=0}{\nabla_{\mathbf{r}'} \cdot \mathbf{C}(\mathbf{r}')}dV' - \oint \frac{1}{|\mathbf{r}-\mathbf{r}'|}\mathbf{C}(\mathbf{r}') \cdot d\mathbf{S}' \longrightarrow 0 \ ,\end{aligned}$$

because the surface integral can be arbitrarily reduced by choosing very distant surfaces $\mathbf{r}' \to \infty$. Finally, the rotation is,

$$\begin{aligned}\nabla_{\mathbf{r}} \times \mathbf{F} &= \cancelto{0}{-\nabla_{\mathbf{r}} \times \nabla_{\mathbf{r}}\Phi} + \nabla_{\mathbf{r}} \times \nabla_{\mathbf{r}} \times \mathbf{A} = -\nabla^2_{\mathbf{r}}\mathbf{A} + \nabla_{\mathbf{r}}(\cancelto{0}{\nabla_{\mathbf{r}} \cdot \mathbf{A}}) \qquad (6.14)\\ &= -\frac{1}{4\pi}\int \mathbf{C}(\mathbf{r}')\nabla^2_{\mathbf{r}}\left(\frac{1}{|\mathbf{r}-\mathbf{r}'|}\right)dV' = \int \mathbf{C}(\mathbf{r}')\delta^3(\mathbf{r}-\mathbf{r}')dV' = \mathbf{C}(\mathbf{r}) \ ,\end{aligned}$$

using rules of vector analysis summarized in (10.88).

6.1.2 Potentials in electrodynamics

In electrodynamics, two fields are required to describe the Coulomb and Lorentz forces, the electric and the magnetic field. With Helmholtz's theorem we can now

[3] Faster than $1/r$ in order to guarantee that the integrals (6.8) and (6.9) converge.

declare that four equations are necessary and sufficient to completely characterize these fields through the following rotations and divergences,

$$\text{rot } \vec{\mathcal{B}} = ... \quad , \quad \text{rot } \vec{\mathcal{E}} = ... \quad , \quad \text{div } \vec{\mathcal{E}} = ... \quad , \quad \text{div } \vec{\mathcal{B}} = ... \; . \tag{6.15}$$

These equations are precisely those of Maxwell. In addition, the derivation of the preceding section showed that

> *each vector field which disappears fast enough at long distances can be expressed as the sum of the gradient of a scalar function and rotation of a vector function,*

since,

$$\mathbf{F} = -\nabla\Phi + \nabla \times \mathbf{A} = -\nabla \frac{1}{4\pi} \int_{\mathbb{R}^3} \frac{D(\mathbf{r}')}{|\mathbf{r} - \mathbf{r}'|} dV' + \nabla \times \frac{1}{4\pi} \int_{\mathbb{R}^3} \frac{\mathbf{C}(\mathbf{r}')}{|\mathbf{r} - \mathbf{r}'|} dV' \; . \tag{6.16}$$

The functions Φ and $\mathbf{A}$ are called *scalar potential* and *vector potential*, respectively.

Irrotational fields, that is, fields without vortices are conservative and can be expressed by the gradient of a scalar field,

$$\nabla \times \mathbf{F} = 0 \quad \Longleftrightarrow \quad \mathbf{A} = 0 \quad \Longleftrightarrow \quad \mathbf{F} = -\nabla\Phi \quad \Longleftrightarrow \quad \oint \mathbf{F} \cdot d\mathbf{l} = 0 \; . \tag{6.17}$$

Example 54 (*Potentials in electrostatics*): Electrostatics is an example for an irrotational field, since Maxwell's electrostatic equations are precisely, $\nabla \times \vec{\mathcal{E}} = 0$ and $\nabla \cdot \vec{\mathcal{E}} = D = \varrho/\varepsilon_0$. Therefore, there is an electric potential Φ, such that $-\nabla\Phi = \vec{\mathcal{E}}$.

Fields without divergences, that is, without sources or sinks, can be expressed by the rotation of a vector field,

$$\nabla \cdot \mathbf{F} = 0 \quad \Longleftrightarrow \quad \Phi = 0 \quad \Longleftrightarrow \quad \mathbf{F} = \nabla \times \mathbf{A} \quad \Longleftrightarrow \quad \oint \mathbf{F} \cdot d\mathbf{S} = 0 \; . \tag{6.18}$$

Example 55 (*Potentials in magnetostatics*): Magnetostatics is an example for a field without divergences, since Maxwell's magnetostatic equations are precisely, $\nabla \times \vec{\mathcal{B}} = \mathbf{C} = \mu_0 \mathbf{j}$ and $\nabla \cdot \vec{\mathcal{B}} = 0$. Therefore, there is a vector potential $\mathbf{A}$, such that $\nabla \times \mathbf{A} = \vec{\mathcal{B}}$.

We will train the calculation with potentials in Excs. 6.1.5.9 and 6.1.5.10.

6.1.3 The macroscopic Maxwell equations

Electric and magnetic fields and electromagnetic waves survive in vacuum. Maxwell's equations (6.6) are formulated for this environment. On the other hand, we saw in the first part of the course, that charges (3.17) and currents (5.20) that are free or localized in a medium generate a polarization and a magnetization of the medium which can influence the fields.

In this section, we will repeat the derivation of the equations (3.18), respectively, (5.21) in a more stringent way from a microscopic model of matter. We suppose matter to be made of molecules, each one being constructed from atoms composed of positively charged nuclei orbited by negatively charged electrons. On each of these elementary particles considered as point-like, the electromagnetic field diverges. But doing this statement, we are talking about microscopic electromagnetic fields, which can not be measured by macroscopic probes which, are composed of atoms themselves. We can not directly measure microscopic quantities with a macroscopic apparatus.

According to the model of matter already formulated by Democritus 300 years before Christ, we suppose the space between the elementary particles to be empty, such that we can assume the validity of Maxwell's equations for vacuum in a *microscopic environment*, that is, we believe in the equations (6.6) for the fields $\vec{\mathcal{E}}_{mic}$ and $\vec{\mathcal{B}}_{mic}$, where the subscript *mic* indicates the presence of localized or moving point-like charges. A macroscopic measurement apparatus will always deliver an effective mean value, averaged in space and time, of electromagnetic quantities. We will show in the following [47] how, via spatial averaging of Maxwell's microscopic equations, it is possible to deduce Maxwell's macroscopic equations taking account of polarization and magnetization (3.18), respectively, (5.21).

We obtain the spatial average by smearing out the microscopic quantities within a characteristic volume defined by a spherically symmetric function $f(r)$, chosen to cancel out exponentially at sufficiently large distances [4]. The reach of this function must be adapted to the resolution of the macroscopic device. For example, the resolution limit for devices based on optics will limit the reach of the function $f(r)$ to some $100\,\text{nm}$ [5]. The spatial average of the electromagnetic quantities $\vec{\mathcal{E}}_{mic}(\mathbf{r},t)$, $\vec{\mathcal{B}}_{mic}(\mathbf{r},t)$, $\varrho_{mic}(\mathbf{r},t)$, and $\mathbf{j}_{mic}(\mathbf{r},t)$ is then,

$$\langle X_{mic}(\mathbf{r},t)\rangle \equiv \int_{\mathbb{R}^3} d^3\mathbf{r}' f(\mathbf{r}') X_{mic}(\mathbf{r}-\mathbf{r}',t) \ . \tag{6.19}$$

The macroscopic fields are defined as the averages of the respective microscopic fields:

$$\vec{\mathcal{E}}(\mathbf{r},t) \equiv \langle \vec{\mathcal{E}}_{mic}(\mathbf{r},t)\rangle \qquad \text{and} \qquad \vec{\mathcal{B}}(\mathbf{r},t) \equiv \langle \vec{\mathcal{B}}_{mic}(\mathbf{r},t)\rangle \ , \tag{6.20}$$

where macroscopic quantities do not have the subscript *mic*.

Now, taking the averages of the microscopic Maxwell equations, we obtain,

$$\begin{array}{lrcl} \text{(i)} & \langle \nabla \times \vec{\mathcal{B}}_{mic}(\mathbf{r},t)\rangle - \varepsilon_0\mu_0 \left\langle \frac{\partial \vec{\mathcal{E}}_{mic}(\mathbf{r},t)}{\partial t} \right\rangle & = & \mu_0 \langle \mathbf{j}_{mic}(\mathbf{r},t)\rangle \\ \text{(ii)} & \langle \nabla \times \vec{\mathcal{E}}_{mic}(\mathbf{r},t)\rangle + \left\langle \frac{\partial \vec{\mathcal{B}}_{mic}(\mathbf{r},t)}{\partial t} \right\rangle & = & 0 \\ \text{(iii)} & \langle \nabla \cdot \vec{\mathcal{E}}_{mic}(\mathbf{r},t)\rangle & = & \frac{1}{\varepsilon_0}\langle \varrho_{mic}(\mathbf{r},t)\rangle \\ \text{(iv)} & \langle \nabla \cdot \vec{\mathcal{B}}_{mic}(\mathbf{r},t)\rangle & = & 0 \end{array} \ . \tag{6.21}$$

However,

$$\begin{aligned} \langle \nabla \cdot \vec{\mathcal{E}}_{mic}(\mathbf{r},t)\rangle &= \nabla \cdot \langle \vec{\mathcal{E}}_{mic}(\mathbf{r},t)\rangle = \nabla \cdot \vec{\mathcal{E}}(\mathbf{r},t) \\ \langle \nabla \times \vec{\mathcal{E}}_{mic}(\mathbf{r},t)\rangle &= \nabla \times \langle \vec{\mathcal{E}}_{mic}(\mathbf{r},t)\rangle = \nabla \times \vec{\mathcal{E}}(\mathbf{r},t) \ , \end{aligned} \tag{6.22}$$

[4] An example for a normalized smoothing function is $f(\mathbf{r}') \equiv (a/\pi)^{3/2} e^{-ar'^2}$, as it satisfies $\int_{\mathbb{R}^3} f(\mathbf{r}') d^3r' = 1$.

[5] In contrast, X-rays with a resolution of about $10\,\text{nm}$ allow for an analysis of the microscopic structure of matter.

and analogously for $\vec{\mathcal{B}}_{mic}$, since ∇ acts only on $\mathbf{r}$ and not on the integration variable $\mathbf{r}'$. On the other hand, the partial time-derivative also does not act on $\mathbf{r}$ nor on $\mathbf{r}'$,

$$\left\langle \frac{\partial \vec{\mathcal{E}}_{mic}(\mathbf{r},t)}{\partial t} \right\rangle = \frac{\partial}{\partial t}\langle \vec{\mathcal{E}}_{mic}(\mathbf{r},t)\rangle = \frac{\partial \vec{\mathcal{E}}(\mathbf{r},t)}{\partial t} \ , \tag{6.23}$$

and analogously for $\vec{\mathcal{B}}_{mic}$. Thus, we already deduced the two homogeneous macroscopic Maxwell equations (ii) and (iv), and the set of equations (6.21) simplifies to:

$$\begin{array}{llcl} \text{(i)} & \nabla\times\vec{\mathcal{B}}(\mathbf{r},t) - \varepsilon_0\mu_0\partial_t\vec{\mathcal{E}}(\mathbf{r},t) & = & \mu\langle \mathbf{j}_{mic}(\mathbf{r},t)\rangle \\ \text{(ii)} & \nabla\times\vec{\mathcal{E}}(\mathbf{r},t) + \partial_t\vec{\mathcal{B}}(\mathbf{r},t) & = & 0 \\ \text{(iii)} & \nabla\cdot\vec{\mathcal{E}}(\mathbf{r},t) & = & \frac{1}{\varepsilon_0}\langle \varrho_{mic}(\mathbf{r},t)\rangle \\ \text{(iv)} & \nabla\cdot\vec{\mathcal{B}}(\mathbf{r},t) & = & 0 \end{array} \ , \tag{6.24}$$

but we still need to calculate $\langle \varrho_{mic}(\mathbf{r},t)\rangle$ and $\langle \mathbf{j}_{mic}(\mathbf{r},t)\rangle$.

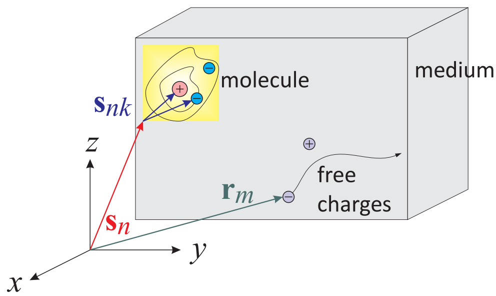

Figure 6.3: Charges localized in molecules and free charges.

To do so we imagine that, as illustrated in Fig. 6.3, there are N charges in each molecule of the material and, for simplicity, we also assume the material to be a pure substance, that is to say, composed of identical molecules. Be $\vec{\mathcal{S}}_n$ the position of the n-th molecule, measured from an arbitrary origin of the coordinate system. Thus, the k-th charge q_{kn} of the n-th molecule is at the point $\vec{\mathcal{S}}_{kn}$, with respect to the position vector of the molecule $\vec{\mathcal{S}}_n$. This means that, with respect to the origin of the coordinate system, the position of the charge q_{kn} is given by $\vec{\mathcal{S}}_{kn} + \vec{\mathcal{S}}_n$. We will also allow for free charges, q_m, at positions $\mathbf{r}_m$. As all the charges can move, all their positions $\mathbf{r}_m(t)$, $\vec{\mathcal{S}}_n(t)$, and $\vec{\mathcal{S}}_{kn}(t)$ must be considered as functions of time.

First, we will calculate the charge density,

$$\varrho_{mic}(\mathbf{r},t) = \sum_m q_m\delta^{(3)}(\mathbf{r}-\mathbf{r}_m) + \sum_{n,k} q_{kn}\delta^{(3)}(\mathbf{r}-\vec{\mathcal{S}}_{kn}-\vec{\mathcal{S}}_n) \ , \tag{6.25}$$

and using the definition of the spatial average (6.19),

$$\langle \varrho_{mic}(\mathbf{r},t)\rangle = \underbrace{\sum_m q_m f(\mathbf{r}-\mathbf{r}_m)}_{\varrho(\mathbf{r},t)} + \sum_{n,k} q_{kn} f(\mathbf{r}-\vec{\mathcal{S}}_{kn}-\vec{\mathcal{S}}_n) \ , \tag{6.26}$$

where we recall, that the first term represents the macroscopic density of free charges $\varrho(\mathbf{r},t)$. Typically, $|\vec{\mathcal{S}}_{kn}|$ is on the order of some Angströms only, and therefore the 'smoothing' function $f(\mathbf{r}-\vec{\mathcal{S}}_{kn}-\vec{\mathcal{S}}_n)$ does not appreciably differ from $f(\mathbf{r}-\vec{\mathcal{S}}_n)$, such that we can approximate:

$$f(\mathbf{r}-\vec{\mathcal{S}}_{kn}-\vec{\mathcal{S}}_n) \simeq f(\mathbf{r}-\vec{\mathcal{S}}_n) - \vec{\mathcal{S}}_{kn}\cdot\nabla f(\mathbf{r}-\vec{\mathcal{S}}_n) + \tfrac{1}{2}(\vec{\mathcal{S}}_{kn}\cdot\nabla)^2 f(\mathbf{r}-\vec{\mathcal{S}}_n) \ , \tag{6.27}$$

and, with this approximation, obtain,

$$\begin{aligned}
\langle\varrho_{mic}(\mathbf{r},t)\rangle &\simeq \varrho(\mathbf{r},t) + \sum_{n,k} q_{kn} f(\mathbf{r}-\vec{\mathcal{S}}_n) - \sum_{n,k} q_{kn}\vec{\mathcal{S}}_{kn}\cdot\nabla f(\mathbf{r}-\vec{\mathcal{S}}_n) \\
&\quad + \sum_{n,k} q_{kn}\tfrac{1}{2}(\vec{\mathcal{S}}_{kn}\cdot\nabla)^2 f(\mathbf{r}-\vec{\mathcal{S}}_n) \\
&= \varrho(\mathbf{r},t) + \cancelto{0}{\sum_{n,k} q_{kn}} f(\mathbf{r}-\vec{\mathcal{S}}_n) - \nabla\cdot\sum_n\left(\sum_k q_{kn}\vec{\mathcal{S}}_{kn}\right) f(\mathbf{r}-\vec{\mathcal{S}}_n) \\
&\quad + \tfrac{1}{6}\sum_n \nabla\cdot\left[\cancelto{0}{\left(3\sum_k q_{kn}\vec{\mathcal{S}}_{kn}\vec{\mathcal{S}}_{kn}\right)}\cdot\nabla f(\mathbf{r}-\vec{\mathcal{S}}_n)\right] \\
&= \varrho(\mathbf{r},t) - \nabla\cdot\sum_n \mathbf{d}_n f(\mathbf{r}-\vec{\mathcal{S}}_n) \ .
\end{aligned} \tag{6.28}$$

In the last line we assumed that each molecule is neutral,

$$\sum_k q_{kn} = 0 \ , \tag{6.29}$$

we use the definition of the electric dipole moment of the n-th molecule,

$$\mathbf{d}_n = \sum_k q_{kn}\vec{\mathcal{S}}_{kn} \ , \tag{6.30}$$

and we suppose, to simplify our calculations below, that the electric quadrupole momentum of the n-th molecule,

$$\overset{\leftrightarrow}{Q}_n \equiv 3\sum_k q_{kn}\vec{\mathcal{S}}_{kn}\vec{\mathcal{S}}_{kn} \overset{!}{=} \overset{\leftrightarrow}{0} \ , \tag{6.31}$$

is zero, that is, that the molecules of the material have zero electric quadrupolar momentum. As shown in the discussion of the relationship (??), the polarization of a medium is the sum of the individual instantaneous dipole moments of each molecule,

$$\vec{\mathcal{P}}_{mic}(\mathbf{r},t) = \sum_n \mathbf{d}_n\delta^{(3)}(\mathbf{r}-\vec{\mathcal{S}}_n) \ , \tag{6.32}$$

With these observations, we conclude that,

$$\langle\vec{\mathcal{P}}_{mic}(\mathbf{r},t)\rangle = \sum_n \mathbf{d}_n f(\mathbf{r}-\vec{\mathcal{S}}_n) \ , \tag{6.33}$$

and, identifying this quantity in the expression (6.28), we get,

$$\langle\varrho_{mic}(\mathbf{r},t)\rangle \simeq \varrho(\mathbf{r},t) - \nabla\cdot\vec{\mathcal{P}}(\mathbf{r},t) \ , \tag{6.34}$$

where we introduced the abbreviation, $\vec{\mathcal{P}}(\mathbf{r},t) \equiv \langle\vec{\mathcal{P}}_{mic}(\mathbf{r},t)\rangle$, analogously to the electrostatic case. The macroscopic Gauß law (6.21)(iii) becomes then,

$$\nabla\cdot\vec{\mathcal{E}}(\mathbf{r},t) = \tfrac{1}{\varepsilon_0}[\varrho(\mathbf{r},t) - \nabla\cdot\vec{\mathcal{P}}(\mathbf{r},t)] \ , \tag{6.35}$$

that is,

$$\nabla\cdot\vec{\mathcal{D}}(\mathbf{r},t) = \varrho(\mathbf{r},t) \ , \tag{6.36}$$

where we defined the field of *electric displacement* as,

$$\boxed{\vec{\mathcal{D}}(\mathbf{r},t) \equiv \varepsilon_0\vec{\mathcal{E}}(\mathbf{r},t) + \vec{\mathcal{P}}(\mathbf{r},t)} \ . \tag{6.37}$$

Let us now calculate, $\langle\mathbf{j}_{mic}(\mathbf{r},t)\rangle$. From the very definition of the microscopic current we have,

$$\mathbf{j}_{mic}(\mathbf{r},t) \equiv \varrho_{mic}(\mathbf{r},t)\mathbf{v}_{mic}(\mathbf{r},t) \ , \tag{6.38}$$

where $\mathbf{v}_{mic}(\mathbf{r},t)$ is the velocity field of the charges of the material medium. By inserting the expression (6.25) for the charge density,

$$\begin{aligned}\mathbf{j}_{mic}(\mathbf{r},t) &= \sum_m q_m\delta^{(3)}(\mathbf{r}-\mathbf{r}_m)\mathbf{v}_{mic}(\mathbf{r},t) + \sum_{n,k} q_{kn}\delta^{(3)}(\mathbf{r}-\vec{\mathcal{S}}_{kn}-\vec{\mathcal{S}}_n)\mathbf{v}_{mic}(\mathbf{r},t) \\ &= \sum_m q_m\dot{\mathbf{r}}_m\delta^{(3)}(\mathbf{r}-\mathbf{r}_m) + \sum_{n,k} q_{kn}(\dot{\mathbf{s}}_{kn}+\dot{\mathbf{s}}_n)\delta^{(3)}(\mathbf{r}-\vec{\mathcal{S}}_{kn}-\vec{\mathcal{S}}_n) \ ,\end{aligned} \tag{6.39}$$

where the field of charge velocities calculated exactly at the location of the m-th charge gives the value of its velocity,

$$\delta^{(3)}(\mathbf{r}-\mathbf{x})\mathbf{v}_{mic}(\mathbf{r},t) = \delta^{(3)}(\mathbf{r}-\mathbf{x})\dot{\mathbf{x}} \ .$$

We can now evaluate the average (6.19),

$$\langle\mathbf{j}_{mic}(\mathbf{r},t)\rangle = \underbrace{\sum_m q_m\dot{\mathbf{r}}_m f(\mathbf{r}-\mathbf{r}_m)}_{\to\,\mathbf{j}(\mathbf{r},t)} + \sum_{n,k} q_{kn}(\dot{\mathbf{s}}_{kn}+\dot{\mathbf{s}}_n)f(\mathbf{r}-\vec{\mathcal{S}}_{kn}-\vec{\mathcal{S}}_n) \ , \tag{6.40}$$

where we recall, that the first term represents the macroscopic density of free current $\mathbf{j}(\mathbf{r},t)$. Approximating again,

$$f(\mathbf{r}-\vec{\mathcal{S}}_{kn}-\vec{\mathcal{S}}_n) \simeq f(\mathbf{r}-\vec{\mathcal{S}}_n) - \vec{\mathcal{S}}_{kn}\cdot\nabla f(\mathbf{r}-\vec{\mathcal{S}}_n) \ , \tag{6.41}$$

and, with this approximation, we obtain,

$$\langle\mathbf{j}_{mic}(\mathbf{r},t)\rangle \simeq \mathbf{j}(\mathbf{r},t) + \sum_{n,k} q_{kn}(\dot{\mathbf{s}}_{kn}+\dot{\mathbf{s}}_n)f(\mathbf{r}-\vec{\mathcal{S}}_n) - \sum_{k,n} q_{kn}(\dot{\mathbf{s}}_{kn}+\dot{\mathbf{s}}_n)\vec{\mathcal{S}}_{kn}\cdot\nabla f(\mathbf{r}-\vec{\mathcal{S}}_n) \ . \tag{6.42}$$

As we are now working to obtain the macroscopic Ampère-Maxwell equation, we need to let appear in the above results the rotation of the magnetization, in addition to the time derivative of the polarization. Recalling that the magnetic dipole moment of the n-th molecule $\vec{\mu}_n$ is defined by equation (4.43) as,

$$\vec{\mu}_n \equiv \tfrac{1}{2}\sum_k q_{kn}\vec{\mathcal{S}}_{kn} \times \dot{\mathbf{s}}_{kn} \ , \tag{6.43}$$

based on the relationship (5.15), we can write magnetization as the sum of the instantaneous magnetic dipole moments of every molecule,

$$\vec{\mathcal{M}}_{mic}(\mathbf{r},t) = \sum_n \vec{\mu}_n \delta^{(3)}(\mathbf{r}-\vec{\mathcal{S}}_n) \ , \tag{6.44}$$

Thus, we want to identify, in the expression for $\langle \mathbf{j}_{mic}(\mathbf{r},t)\rangle$, the rotation of $\langle \vec{\mathcal{M}}_{mic}(\mathbf{r},t)\rangle$:

$$\begin{aligned}\nabla \times \langle \vec{\mathcal{M}}_{mic}(\mathbf{r},t)\rangle &= \nabla \times \sum_n \vec{\mu}_n f(\mathbf{r}-\vec{\mathcal{S}}_n) = -\sum_n \vec{\mu}_n \times \nabla f(\mathbf{r}-\vec{\mathcal{S}}_n) \\ &= -\tfrac{1}{2}\sum_{n,k} q_{kn}(\vec{\mathcal{S}}_{kn} \times \dot{\mathbf{s}}_{kn}) \times \nabla f(\mathbf{r}-\vec{\mathcal{S}}_n) \\ &= -\tfrac{1}{2}\sum_{n,k} q_{kn}\dot{\mathbf{s}}_{kn}[\vec{\mathcal{S}}_{kn}\cdot\nabla f(\mathbf{r}-\vec{\mathcal{S}}_n)] + \tfrac{1}{2}\sum_{n,k} q_{kn}\vec{\mathcal{S}}_{kn}[\dot{\mathbf{s}}_{kn}\cdot\nabla f(\mathbf{r}-\vec{\mathcal{S}}_n)] \ ,\end{aligned} \tag{6.45}$$

using the BAC-CAB rule (10.87)(v), and continuing,

$$\begin{aligned}\nabla \times \langle \vec{\mathcal{M}}_{mic}(\mathbf{r},t)\rangle &= -\sum_{n,k} q_{kn}\dot{\mathbf{s}}_{kn}\vec{\mathcal{S}}_{kn}\cdot\nabla f(\mathbf{r}-\vec{\mathcal{S}}_n) + \tfrac{1}{2}\sum_n\left[\sum_k q_{kn}\frac{d}{dt}(\vec{\mathcal{S}}_{kn}\vec{\mathcal{S}}_{kn})\right]\cdot\nabla f(\mathbf{r}-\vec{\mathcal{S}}_n) \\ &= -\sum_{n,k} q_{kn}\dot{\mathbf{s}}_{kn}\vec{\mathcal{S}}_{kn}\cdot\nabla f(\mathbf{r}-\vec{\mathcal{S}}_n) + \tfrac{1}{6}\sum_n\left[\frac{d}{dt}\left(\cancelto{0}{3\sum_k q_{kn}\vec{\mathcal{S}}_{kn}\vec{\mathcal{S}}_{kn}}\right)\right]\cdot\nabla f(\mathbf{r}-\vec{\mathcal{S}}_n) \ .\end{aligned} \tag{6.46}$$

The second term is zero again because, as in (6.31), we are assuming that $\overset{\leftrightarrow}{Q}_n \overset{!}{=} \overset{\leftrightarrow}{0}$. Continuing the calculation (6.42),

$$\begin{aligned}\langle \mathbf{j}_{mic}(\mathbf{r},t)\rangle = \mathbf{j}(\mathbf{r},t) &+ \sum_{n,k} q_{kn}\dot{\mathbf{s}}_{kn} f(\mathbf{r}-\vec{\mathcal{S}}_n) + \cancelto{0}{\sum_{n,k} q_{kn}}\,\dot{\mathbf{s}}_n f(\mathbf{r}-\vec{\mathcal{S}}_n) \\ &+ \nabla \times \langle \vec{\mathcal{M}}_{mic}(\mathbf{r},t)\rangle - \sum_{n,k} q_{kn}\dot{\mathbf{s}}_n\vec{\mathcal{S}}_{kn}\cdot\nabla f(\mathbf{r}-\vec{\mathcal{S}}_n) \ .\end{aligned} \tag{6.47}$$

The third term disappears, because again we are assuming that the total charge of every molecule is zero, $\sum_k q_{kn} = 0$. The partial temporal derivative of the polarization is given by the expression (6.33),

$$\begin{aligned}\frac{\partial \vec{\mathcal{P}}(\mathbf{r},t)}{\partial t} &= \frac{\partial}{\partial t}\sum_{n,k} q_{kn}\vec{\mathcal{S}}_{kn} f(\mathbf{r}-\vec{\mathcal{S}}_n) = \sum_{n,k} q_{kn}\frac{\partial \vec{\mathcal{S}}_{kn}}{\partial t} f(\mathbf{r}-\vec{\mathcal{S}}_n) + \sum_{n,k} q_{kn}\vec{\mathcal{S}}_{kn}\frac{\partial}{\partial t} f(\mathbf{r}-\vec{\mathcal{S}}_n) \\ &= \sum_{n,k} q_{kn}\dot{\mathbf{s}}_{kn} f(\mathbf{r}-\vec{\mathcal{S}}_n) - \sum_{n,k} q_{kn}\vec{\mathcal{S}}_{kn}\dot{\mathbf{s}}_n\cdot\nabla f(\mathbf{r}-\vec{\mathcal{S}}_n) \ .\end{aligned} \tag{6.48}$$

We can use this result to replace the second term in equation (6.47),

$$\langle \mathbf{j}_{mic}(\mathbf{r},t)\rangle \simeq \mathbf{j}(\mathbf{r},t) + \nabla\times\langle\vec{\mathcal{M}}_{mic}(\mathbf{r},t)\rangle + \frac{\partial\vec{\mathcal{P}}(\mathbf{r},t)}{\partial t} + \sum_{n,k} q_{kn}[\vec{\mathcal{S}}_{kn}\dot{\mathbf{s}}_n\cdot\nabla f(\mathbf{r}-\vec{\mathcal{S}}_n) - \dot{\mathbf{s}}_n\vec{\mathcal{S}}_{kn}\cdot\nabla f(\mathbf{r}-\vec{\mathcal{S}}_n)] \ . \tag{6.49}$$

Note, that the last term of this expression is identical to (6.45) with the difference, that the electronic velocities $\dot{\mathbf{s}}_{kn}$ of that expression or now replaced by the molecular velocities $\dot{\mathbf{s}}_n$.

Now let us suppose that the material itself is not in motion, so that the (averaged absolute) velocities of the molecules, $\dot{\mathbf{s}}_n$, are much smaller than the (averaged absolute) velocities of the charges in every molecule, $\dot{\mathbf{s}}_{kn}$. With this, we can neglect the last term of the above equation in comparison to the first,

$$\mu_0\langle\mathbf{j}_{mic}(\mathbf{r},t)\rangle \simeq \mu_0\mathbf{j}(\mathbf{r},t) + \mu_0\frac{\partial\vec{\mathcal{P}}(\mathbf{r},t)}{\partial t} + \mu_0\nabla\times\langle\vec{\mathcal{M}}_{mic}(\mathbf{r},t)\rangle \ . \tag{6.50}$$

The Ampère-Maxwell equation, then reads in its spatial average (6.21)(i),

$$\begin{aligned}\nabla\times\vec{\mathcal{B}}(\mathbf{r},t) &= \mu_0\langle\mathbf{j}_{mic}(\mathbf{r},t)\rangle + \varepsilon_0\mu_0\left\langle\frac{\partial\vec{\mathcal{E}}_{mic}(\mathbf{r},t)}{\partial t}\right\rangle \\ &= \mu_0\mathbf{j}(\mathbf{r},t) + \mu_0\frac{\partial\vec{\mathcal{P}}(\mathbf{r},t)}{\partial t} + \mu_0\nabla\times\langle\vec{\mathcal{M}}_{mic}(\mathbf{r},t)\rangle + \varepsilon_0\mu_0\frac{\partial\vec{\mathcal{E}}(\mathbf{r},t)}{\partial t} \ ,\end{aligned} \tag{6.51}$$

or,

$$\nabla\times[\vec{\mathcal{B}}(\mathbf{r},t) - \mu_0\nabla\times\langle\vec{\mathcal{M}}_{mic}(\mathbf{r},t)\rangle] = \mu_0\mathbf{j}(\mathbf{r},t) + \mu_0\frac{\partial}{\partial t}[\varepsilon\vec{\mathcal{E}}(\mathbf{r},t) + \vec{\mathcal{P}}(\mathbf{r},t)] \ , \tag{6.52}$$

Introducing the abbreviation,

$$\vec{\mathcal{M}}(\mathbf{r},t) \equiv \langle\vec{\mathcal{M}}_{mic}(\mathbf{r},t)\rangle \ , \tag{6.53}$$

defining *magnetic excitation* field,

$$\boxed{\vec{\mathcal{H}}(\mathbf{r},t) \equiv \tfrac{1}{\mu_0}\vec{\mathcal{B}}(\mathbf{r},t) - \vec{\mathcal{M}}(\mathbf{r},t)} \ , \tag{6.54}$$

and recognizing the electric displacement field, $\vec{\mathcal{D}}(\mathbf{r},t) = \varepsilon_0\vec{\mathcal{E}}(\mathbf{r},t) + \vec{\mathcal{P}}(\mathbf{r},t)$, we obtain,

$$\nabla\times\vec{\mathcal{H}}(\mathbf{r},t) = \frac{\partial\vec{\mathcal{D}}(\mathbf{r},t)}{\partial t} + \mathbf{j}(\mathbf{r},t) \ , \tag{6.55}$$

which is the macroscopic Ampère-Maxwell equation.

The above derivations show that $\vec{\mathcal{P}}$ and $\vec{\mathcal{M}}$ do not exist as exact physical quantities in the microscopic sense. They are artifacts of a process of smearing out the microscopic charges and currents over smooth macroscopic distributions, with the aim of facilitating the calculation with macroscopic quantities.

6.1.4 The fundamental laws in polarizable and magnetizable materials

The derivations made in the previous chapter led to Maxwell's macroscopic equations, which correspond to the Maxwell equations for vacuum complemented by material equations characterizing the medium. In short,

$$\boxed{\begin{array}{lrcl} \text{(i)} & \nabla\times\vec{\mathcal{H}} & = & \partial_t\vec{\mathcal{D}}+\mathbf{j} \\ \text{(ii)} & \nabla\times\vec{\mathcal{E}} & = & -\partial_t\vec{\mathcal{B}} \\ \text{(iii)} & \nabla\cdot\vec{\mathcal{D}} & = & \varrho \\ \text{(iv)} & \nabla\cdot\vec{\mathcal{B}} & = & 0 \end{array}} \quad . \tag{6.56}$$

The fields are related by the macroscopic *polarization* and *magnetization*,

$$\vec{\mathcal{P}}=\vec{\mathcal{D}}-\varepsilon_0\vec{\mathcal{E}} \qquad \text{and} \qquad \vec{\mathcal{M}}=\mu_0^{-1}\vec{\mathcal{B}}-\vec{\mathcal{H}}\ . \tag{6.57}$$

For a given free charge density distribution $\varrho(\mathbf{r},t)$ and a free current density distribution $\mathbf{j}(\mathbf{r},t)$, the above six equations (6.56) and (6.57) define the six components of the fields unambiguously. In vacuum $\varepsilon_0\vec{\mathcal{E}}=\vec{\mathcal{D}}$ and $\mu_0^{-1}\vec{\mathcal{B}}=\vec{\mathcal{H}}$ Maxwell's equations simplify. In material media, however, the secondary quantities $\vec{\mathcal{D}}$ and $\vec{\mathcal{H}}$ are not equal to the fields.

Depending on its structure, a medium may have (or not) bound or free charges and currents, responding in a specific way to applied electric and magnetic fields and giving rise to a wide variety of features. For example, a medium is *non-conductive* when, even in the presence of electric fields applied to the medium, there is no flux of current. A medium is *linear* when the polarization and the magnetization depend linearly on the electric and magnetic fields, respectively. A medium is *homogeneous* when the susceptibilities do not vary across the medium. When the directions of induced polarization and magnetization are parallel, respectively, to the electric and magnetic fields, the medium is said to be *isotropic*, otherwise it is said to be *anisotropic*.

Depending on the type of material and its properties the equations do sometimes simplify. For example, we have for a

medium	condition
dielectric	$\vec{\mathcal{D}}=\varepsilon\vec{\mathcal{E}}$, $\vec{\mathcal{P}}=\chi_\varepsilon\varepsilon_0\vec{\mathcal{E}}$, $\varepsilon=1+\chi_\varepsilon$
non-linear dielectric	$\vec{\mathcal{D}}=\vec{\mathcal{D}}(\vec{\mathcal{E}})\not\propto\vec{\mathcal{E}}$
dia- and paramagnetic	$\vec{\mathcal{B}}=\mu\vec{\mathcal{H}}$, $\vec{\mathcal{M}}=\chi_\mu\vec{\mathcal{H}}$, $\mu=1+\chi_\mu$
non-linear magnetic	$\vec{\mathcal{B}}=\vec{\mathcal{B}}(\vec{\mathcal{H}})\not\propto\vec{\mathcal{B}}$
neutral	$\rho=0$
isolating	$\mathbf{j}=0$
ohmic	$\mathbf{j}=\sigma\vec{\mathcal{E}}$
non ohmic	$\mathbf{j}=\mathbf{j}(\vec{\mathcal{E}})\not\propto\vec{\mathcal{E}}$

The material equations define the material constants, that is, the *permittivity* ε, the *permeability* μ, and the *conductivity* σ. These quantities are scalar for isotropic media and tensors for anisotropic media. Resolve the Exc. 6.1.5.11.

6.1.5 Exercises

6.1.5.1 Ex: Displacement current

Consider a straight big conducting wire of radius a with a small transverse gap of width $w \ll a$ carrying a constant current I. Find the magnetic field in the gap for distances of the symmetry axis $r < a$ as a function of the current.

6.1.5.2 Ex: Plate capacitor

A disk-shaped plate capacitor with radius R, distance d, and $\varepsilon = 1$ is charged by a constant current I.
a. Calculate from the continuity equation, neglecting edge effects, the temporal variation of the charges on the plates $q(t)$, respectively, $-q(t)$.
b. Calculate the temporal variation of the electric field between the plates and Maxwell's displacement current density.
c. Calculate the magnetic field $\vec{\mathcal{B}}$ between the plates along a circular path Γ inside $(\rho < R)$ and outside $(\rho > R)$ the capacitor.
d. Show that the $\vec{\mathcal{B}}$-field between the plates is, for $\rho > R$, equal to the $\vec{\mathcal{B}}$-field produced by the charging current I around the conductors feeding the capacitor.

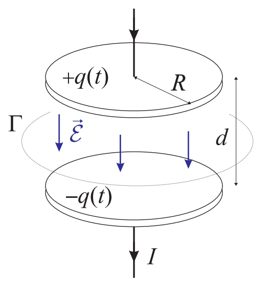

Figure 6.4: Plate capacitor.

6.1.5.3 Ex: Maxwell's equations for a particular charge and current density distribution

Determine the charge and current density distributions producing the fields,

$$\vec{\mathcal{E}}(\mathbf{r},t) = -\frac{1}{4\pi\varepsilon_0}\frac{q}{r^2}\Theta(vt-r)\hat{\mathbf{e}}_r \qquad \text{and} \qquad \vec{\mathcal{B}}(\mathbf{r},t) = 0 \ ,$$

where Θ is the Heavyside function and v is a constant. Show that the fields satisfy all Maxwell equations. Describe the physical situation producing these fields.

6.1.5.4 Ex: Atomic diamagnetism

An electron (charge q) orbits a nucleus (charge Q) at a distance r, the centripetal acceleration being provided by the Coulomb attraction. Now, a small magnetic field $d\mathcal{B}$ is slowly ramped up, perpendicular to the plane of the orbit. Show that the increase of the kinetic energy, dT, transferred to the electron via the induced electric field, is exactly the one necessary to keep the circular motion on the original radius r. (This allows us, in the discussion of *diamagnetism*, to assume a fixed electron radius.)

6.1.5.5 Ex: Variable charge with constant current

Suppose that $\mathbf{j}(\mathbf{r})$ is constant over time, but not $\varrho(\mathbf{r},t)$. Such conditions can prevail, for example, during the charging process of a capacitor.
a. Show that the charge density at any point is a linear function of time: $\varrho(\mathbf{r},t) = \varrho(\mathbf{r},0) + \dot{\varrho}(\mathbf{r},0)t$.
b. Despite the fact that this configuration is not electrostatic or magnetostatic, both the Coulomb law and the Biot-Savart law remain valid, since they satisfy Maxwell's equations. Show in particular that,

$$\vec{\mathcal{B}}(\mathbf{r}) = \frac{\mu_0}{4\pi}\int \frac{\mathbf{j}(\mathbf{r}') \times \hat{\mathbf{e}}_R}{R^2} d^3r'$$

with $R \equiv |\mathbf{r} - \mathbf{r}'|$ obeys Ampère's law including Maxwell's displacement term.

6.1.5.6 Ex: Force on magnetic monopoles

In free space Maxwell's equations are perfectly symmetric under the operation $\vec{\mathcal{E}} \to \vec{\mathcal{B}} \to -\varepsilon_0\mu_0\vec{\mathcal{E}}$. But the existence of charges and electric currents breaks this symmetry. The introduction of 'magnetic charges' and 'magnetic currents' would restore the symmetry, but they were never observed [6]. In this exercise we assume the existence of a 'Coulomb law' for 'magnetic charges' q_m,

$$\mathbf{F} = \frac{\mu_0}{4\pi}\frac{q_{m_1}q_{m_2}}{|\mathbf{r}-\mathbf{r}'|^3}(\mathbf{r}-\mathbf{r}') \ .$$

a. Find the force law for a magnetic charge moving with velocity $\mathbf{v}$ through electric and magnetic fields $\vec{\mathcal{E}}$ and $\vec{\mathcal{B}}$ [79].
b. One of the methods used to search for magnetic monopoles in laboratory [20] consists of passing them through a wire loop with the self-inductance L. What current would be induced in the circuit by the passage of a magnetic monopole?

[6] Dirac showed that the existence of magnetic charges would explain the quantization of charge.

6.1.5.7 Ex: Duality transform

a. In the case of existing magnetic charges and currents, Maxwell's equations would take the form,

$$\begin{aligned}
&\text{(i)} && \nabla \times \vec{\mathcal{B}} - \varepsilon_0\mu_0\partial_t\vec{\mathcal{E}} = \mu_0\mathbf{j}_e \\
&\text{(ii)} && \nabla \times \vec{\mathcal{E}} + \partial_t\vec{\mathcal{B}} = -\mu_0\mathbf{j}_m \\
&\text{(iii)} && \nabla \cdot \vec{\mathcal{E}} = \varepsilon_0^{-1}\varrho_e \\
&\text{(iv)} && \nabla \cdot \vec{\mathcal{B}} = \mu_0\varrho_m \ .
\end{aligned}$$

Show that these equations are invariant under the *duality transform* given by,

$$\begin{pmatrix} \vec{\mathcal{E}}' \\ c\vec{\mathcal{B}}' \end{pmatrix} = \begin{pmatrix} \cos\alpha & \sin\alpha \\ -\sin\alpha & \cos\alpha \end{pmatrix} \begin{pmatrix} \vec{\mathcal{E}} \\ c\vec{\mathcal{B}} \end{pmatrix} \quad , \quad \begin{pmatrix} cq'_e \\ q'_m \end{pmatrix} = \begin{pmatrix} \cos\alpha & \sin\alpha \\ -\sin\alpha & \cos\alpha \end{pmatrix} \begin{pmatrix} cq_e \\ q_m \end{pmatrix} \ ,$$

where α is an arbitrary rotation angle in the $\mathcal{E}$-$\mathcal{B}$ space. Densities of charges and currents transform in the same way as q_e and q_m. This means, in particular, that if you would know the fields produced by an electric charge configuration, you could immediately (using $\alpha = 90^\circ$) deduce the fields produced by a corresponding arrangement of the magnetic charge.
b. Show that the force law derived in Exc. 6.1.5.6,

$$\mathbf{F} = q_e(\vec{\mathcal{E}} + \mathbf{v} \times \vec{\mathcal{B}}) + q_m(\vec{\mathcal{B}} - \tfrac{1}{c^2}\mathbf{v} \times \vec{\mathcal{E}})$$

is also invariant under duality transformation.

6.1.5.8 Ex: Quantization of magnetic monopoles

a. Show that the vector potential,

$$\mathbf{A} = \frac{g(1-\cos\theta)}{r\sin\theta}\hat{\mathbf{e}}_\phi$$

produces a Coulomb-type magnetic field [76].
b. Calculate the magnetic flux across the solid angle delimited by the polar angle θ.
c. Calculate the vector potential $\mathbf{A}'$ obtained by a gauge transformation with the gauge field $\chi = 2g\phi$.
d. Now consider the vector potential defined by $\mathbf{A}'' \equiv \mathbf{A}$ for $\theta \leq \frac{\pi}{2}$ and $\mathbf{A}'' \equiv \mathbf{A}'$ for $\theta \geq \frac{\pi}{2}$. This potential has no more singularity. Derive, from the condition that the transformation $U_{cl} = e^{-\imath e\chi/\hbar}$ be unique, the value of the magnetic charge.

6.1.5.9 Ex: Green's identities

Be ϕ and ψ two continuously differentiable functions and V a volume with the border ∂V. Show with the help of Gauß' theorem,
a.

$$\int_{\mathcal{V}} \left[\phi\nabla^2\psi + (\nabla\phi)\cdot(\nabla\psi)\right]\, dV = \int_{\partial\mathcal{V}} \phi(\nabla\psi)\, d\mathbf{S} \ ,$$

b.

$$\int_{\mathcal{V}} \left[\phi\nabla^2\psi - \psi\nabla^2\phi\right]\, dV = \int_{\partial\mathcal{V}} \left[\phi\nabla\psi - \psi\nabla\phi\right]\, d\mathbf{S} \ .$$

6.1.5.10 Ex: Decomposition of vector fields

Be $\mathbf{F}(\mathbf{r},t)$ an arbitrary vector field defined on $\mathbb{R}$, which tends (along with its derivatives) to zero in sufficiently high order, when $|\mathbf{r}| \to \infty$. This field can be decomposed into a sum of a longitudinal and a transverse component, $\mathbf{F} = \mathbf{F}_l + \mathbf{F}_t$ with $\nabla\times\mathbf{F}_l = 0$ and $\nabla\cdot\mathbf{F}_t = 0$.
a. Prove,

$$\mathbf{F}_l(\mathbf{r},t) = -\frac{1}{4\pi}\nabla\int\frac{\nabla'\cdot\mathbf{F}(\mathbf{r}',t)}{|\mathbf{r}-\mathbf{r}'|}d^3r' \quad \text{and} \quad \mathbf{F}_t(\mathbf{r},t) = +\frac{1}{4\pi}\nabla\times\nabla\times\int\frac{\mathbf{F}(\mathbf{r}',t)}{|\mathbf{r}-\mathbf{r}'|}d^3r' \ .$$

Help: Begin showing that,

$$\mathbf{F}(\mathbf{r},t) = -\frac{1}{4\pi}\triangle\int\frac{\mathbf{F}(\mathbf{r}',t)}{|\mathbf{r}-\mathbf{r}'|}d^3r'$$

and use the vector identity,

$$\nabla\times\nabla\times\mathbf{A} = \nabla(\nabla\cdot\mathbf{A}) - \triangle\mathbf{A} \ .$$

b. Show that the vector field $\mathbf{F}(\mathbf{r})$ is unequivocally given by its sources, $\nabla\cdot\mathbf{F}(\mathbf{r})$, and vertices, $\nabla\times\mathbf{F}(\mathbf{r})$.

6.1.5.11 Ex: Conductivity of seawater

Sea water has at the frequency $v = 4\cdot 10^8\,\text{Hz}$ the permittivity $\varepsilon = 81\varepsilon_0$, the permeability $\mu = \mu_0$, and the resistivity $\rho = 0.23\,\Omega\text{m}$. What is the ratio between the conduction current and the displacement current? **Help:** Consider a parallel-plate capacitor immersed in seawater and driven by a voltage $V_0\cos(2\pi\nu t)$.

6.2 Conservation laws in electromagnetism

The importance of *conservation laws* and *symmetries* lies in their universal validity and their independence of a particular theory (mechanics, electrodynamics, ..). They often allow the derivation of laws, which are specific for a theory and of equations of motion for particular systems. For example, in classical mechanics, we can derive Newtonian axioms from the conservation of linear momentum, and in electrodynamics, as we shall see later, we can derive Maxwell's equations from the principles of Lorentz invariance, gauge invariance, and electric charge conservation, as expressed by the continuity equation. The question which we will elucidate in the following sections will be that of the validity of other mechanical conservation laws in electrodynamics, that is, the laws of energy, linear momentum, and angular momentum conservation.

In the context of preparing the deductions, let us defined some important quantities [7],

$$\begin{array}{lll} \text{(i)} & u = \frac{1}{2}(\vec{\mathcal{E}}\cdot\vec{\mathcal{D}}+\vec{\mathcal{B}}\cdot\vec{\mathcal{H}}) & \textit{energy density} \\ \text{(ii)} & \vec{\mathcal{S}} = \vec{\mathcal{E}}\times\vec{\mathcal{H}} & \textit{energy flux} \text{ or } \textit{Poynting vector} \\ \text{(iii)} & \mathbf{f} = \varrho\vec{\mathcal{E}}+\mathbf{j}\times\vec{\mathcal{B}} & \textit{Lorentz force density} \\ \text{(iv)} & \vec{\wp}^A = \varepsilon_0\mu_0\vec{\mathcal{S}} = \frac{1}{c^2}\vec{\mathcal{E}}\times\vec{\mathcal{H}} & \textit{Abraham momentum density} \\ \text{(iv)} & \vec{\wp}^M = \vec{\mathcal{D}}\times\vec{\mathcal{B}} & \textit{Minkowski momentum density} \\ \text{(v)} & \vec{\ell} = \mathbf{r}\times\vec{\wp} & \textit{angular momentum density} \\ \text{(vi)} & \overleftrightarrow{\mathbf{T}} = \vec{\mathcal{D}}\otimes\vec{\mathcal{E}}+\vec{\mathcal{H}}\otimes\vec{\mathcal{B}}-\frac{1}{2}u\mathbb{I} & \textit{Maxwell stress tensor}\ . \end{array} \tag{6.58}$$

All fields are time-dependent. From Maxwell's equations we derive the *electrodynamical continuity equation*, the *Poynting theorem*, and the conservation of linear and angular momentum. Resolve the Exc. 6.2.5.1.

6.2.1 Charge conservation and continuity equation

Calculating the divergence of Maxwell's first equation and using the third,

$$\nabla\cdot(\nabla\times\vec{\mathcal{H}}) = \partial_t\nabla\cdot\vec{\mathcal{D}}+\nabla\cdot\mathbf{j} = \boxed{\partial_t\varrho+\nabla\cdot\mathbf{j}=0}\ . \tag{6.59}$$

This law describes *charge conservation* in electrodynamics.

6.2.2 Energy conservation and Poynting's theorem

The time derivative of the energy density (6.58)(i) is,

$$\partial_t u = \frac{1}{2}(\vec{\mathcal{E}}\cdot\partial_t\vec{\mathcal{D}}+\vec{\mathcal{D}}\cdot\partial_t\vec{\mathcal{E}}+\vec{\mathcal{B}}\cdot\partial_t\vec{\mathcal{H}}+\vec{\mathcal{H}}\cdot\partial_t\vec{\mathcal{B}}) = \vec{\mathcal{E}}\cdot\partial_t\vec{\mathcal{D}}+\vec{\mathcal{H}}\cdot\partial_t\vec{\mathcal{B}}\ , \tag{6.60}$$

supposing $\vec{\mathcal{D}}=\varepsilon\vec{\mathcal{E}}$ and $\vec{\mathcal{H}}=\vec{\mathcal{B}}/\mu$ with time- and space-independent $\varepsilon,\mu = const$. The divergence of the Poynting vector is,

$$\nabla\cdot\vec{\mathcal{S}} = \nabla\cdot(\vec{\mathcal{E}}\times\vec{\mathcal{H}}) = \vec{\mathcal{H}}\cdot(\nabla\times\vec{\mathcal{E}})-\vec{\mathcal{E}}\cdot(\nabla\times\vec{\mathcal{H}}) = -\vec{\mathcal{H}}\cdot\partial_t\vec{\mathcal{B}}-\vec{\mathcal{E}}\cdot(\partial_t\vec{\mathcal{D}}+\mathbf{j})\ . \tag{6.61}$$

With this we immediately see,

$$\boxed{\partial_t u+\nabla\cdot\vec{\mathcal{S}} = -\mathbf{j}\cdot\vec{\mathcal{E}}}\ . \tag{6.62}$$

To better understand this theorem, we calculate the work exerted by the Coulomb-Lorentz force per unit time on a test charge q,

$$\frac{dW}{dt} = \frac{d}{dt}\int_{\mathcal{C}}\mathbf{F}\cdot d\mathbf{l} = \frac{d}{dt}\int q(\vec{\mathcal{E}}+\cancelto{0}{\mathbf{v}\times\vec{\mathcal{B}}})\cdot\mathbf{v}dt = q\mathbf{v}\cdot\vec{\mathcal{E}}\ . \tag{6.63}$$

[7]The question of the correct expression for the momentum density is difficult and will be dealt with later.

The current generated by the charge can be derived from the parametrization $\mathbf{j}(\mathbf{r}) = q\mathbf{v}\delta^3(\mathbf{r}-\mathbf{r}')$. Thus, we derive the *Poynting theorem*,

$$\frac{dW}{dt} = \int_{\mathcal{V}} \vec{\mathcal{E}} \cdot \mathbf{j} dV = -\frac{d}{dt}\int_{\mathcal{V}} u dV - \int_{\mathcal{V}} \nabla \cdot \vec{\mathcal{S}} dV = -\frac{dU_{erg}}{dt} - \oint_{\partial\mathcal{V}} \vec{\mathcal{S}} \cdot d\mathbf{S} \ . \tag{6.64}$$

This theorem postulates *energy conservation*. That is, the electromagnetic energy U_{erg} within a volume $\mathcal{V}$ can only change 1. by diffusion out of the volume via a flux $\int \vec{\mathcal{S}} \cdot d\mathbf{S}$ of the Poynting vector, or 2. when mechanical work W is done on the volume or when the electromagnetic energy in the volume is dissipated into other forms of energy, for example heat. We apply the Poynting theorem to a current-carrying wire in Exc. 6.2.5.2.

Example 56 (*Derivation of Ohm's law by the Poynting vector*): The current flux through a wire exerts *work*, because the wire heats up. We calculate the energy transferred to the wire per unit time via the Poynting vector. The electric field (assumed to be uniform) along the wire (length L and radius a) is,

$$\mathcal{E} = \frac{U}{L} \ ,$$

where U is the voltage between the ends of the wire. The magnetic field at the surface of the wire is,

$$\mathcal{B} = \frac{\mu_0 I}{2\pi a} \ .$$

Therefore, the absolute value of the Poynting vector is,

$$s = \frac{1}{\mu_0}\mathcal{E}\mathcal{B} = \frac{UI}{2\pi a L} \ .$$

pointing into the wire, $\vec{\mathcal{S}} \propto -\hat{\mathbf{e}}_r$. The energy per unit of time passing through the surface of the wire is therefore,

$$\int \vec{\mathcal{S}} \cdot d\mathbf{S} = s(2\pi a L) = UI \ ,$$

confirming previously obtained results. As the fields are stationary, the electromagnetic energy does not vary with time, neither, $\partial_t U_{erg} = 0$.

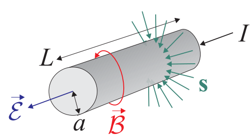

Figure 6.5: Energy flux into the wire causes heating.

6.2.3 Conservation of linear momentum and Maxwell's stress tensor

The interaction between two charges is described by the Coulomb-Lorentz force. However, when these charges accelerate each other mutually, they generate non-stationary fields, so that the force laws of Coulomb and Biot-Savart do not apply. We will see later, how to generalize these laws.

Nevertheless, at first glance, the Coulomb force seems compatible with the third Newton law: *actio* = *reactio*, but not with the Lorentz force.

Example 57 (*Linear momentum of the electromagnetic field*): To see this, we consider two charged particles with trajectories,

$$\mathbf{l}_1(t) = vt\hat{\mathbf{e}}_y \quad , \quad \mathbf{l}_2(t) = vt\hat{\mathbf{e}}_x \ .$$

Charge 1 produces a field $\vec{\mathcal{B}}_1$ at the position of charge 2 and vice versa. At time $t = 0$, when they collide, the forces become orthogonal:

$$\mathbf{F}_{12} = q\mathbf{v}_2 \times \vec{\mathcal{B}}_1 \perp q\mathbf{v}_1 \times \vec{\mathcal{B}}_2 = \mathbf{F}_{21} \ .$$

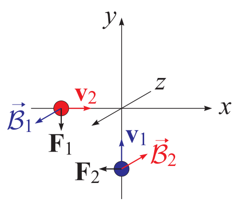

Figure 6.6: The Lorentz forces exerted by approaching charges are mutually orthogonal.

Obviously, in electrodynamics, the Lorentz force flagrantly violates Newton's third law in way to raise questions about the validity of momentum conservation. The solution is that in electrodynamics, *the electromagnetic field itself may lose or gain momentum* and should be included in the formulation of a law of momentum conservation. Moreover, the field does not move instantaneously, but propagates at the speed of light and is subject to retardation effects. The law *actio* = *reactio* postulates the existence of forces acting at a distance that, as we nowadays know, do not exist [8]. We shall return to this problem in the discussion of the relativistic Lorentz transformation.

6.2.3.1 Maxwell's tress tensor

We now consider the Lorentz force density, which we will try to express totally in terms of fields, eliminating the charge and current densities [63],

$$\mathbf{f} = \varrho\vec{\mathcal{E}} + \mathbf{j} \times \vec{\mathcal{B}} = \vec{\mathcal{E}}(\nabla \cdot \vec{\mathcal{D}}) + \left(\nabla \times \vec{\mathcal{H}} - \frac{\partial \vec{\mathcal{D}}}{\partial t}\right) \times \vec{\mathcal{B}} \ . \tag{6.65}$$

We reformulate the last term,

$$-\frac{\partial \vec{\mathcal{D}}}{\partial t} \times \vec{\mathcal{B}} = \vec{\mathcal{D}} \times \frac{\partial \vec{\mathcal{B}}}{\partial t} - \frac{\partial}{\partial t}(\vec{\mathcal{D}} \times \vec{\mathcal{B}}) = -\vec{\mathcal{D}} \times (\nabla \times \vec{\mathcal{E}}) - \frac{\partial}{\partial t}(\vec{\mathcal{D}} \times \vec{\mathcal{B}}) \ . \tag{6.66}$$

[8] One of the important changes of paradigm in the history of physics is from interaction at a distance to local interaction. Newton was a supporter of non-local interaction for gravity. Ironically he argued against waves in favor of particles for light. Today the opinion thinks the other way round: Particles are mediators of local interactions, while only waves can mediate non-local features.

Knowing $\vec{\mathcal{H}}(\nabla\cdot\vec{\mathcal{B}})=0$, we can add this term to the force without cost,

$$\mathbf{f}=\vec{\mathcal{E}}(\nabla\cdot\vec{\mathcal{D}})-\vec{\mathcal{D}}\times(\nabla\times\vec{\mathcal{E}})+\vec{\mathcal{H}}(\nabla\cdot\vec{\mathcal{B}})-\vec{\mathcal{B}}\times(\nabla\times\vec{\mathcal{H}})-\frac{\partial}{\partial t}(\vec{\mathcal{D}}\times\vec{\mathcal{B}})\ . \tag{6.67}$$

We use the rule from vector analysis,

$$\begin{aligned}\nabla(\vec{\mathcal{E}}\cdot\vec{\mathcal{D}})&=\vec{\mathcal{E}}\times(\nabla\times\vec{\mathcal{D}})+\vec{\mathcal{D}}\times(\nabla\times\vec{\mathcal{E}})+(\vec{\mathcal{E}}\cdot\nabla)\vec{\mathcal{D}}+(\vec{\mathcal{D}}\cdot\nabla)\vec{\mathcal{E}}\\&=2\vec{\mathcal{D}}\times(\nabla\times\vec{\mathcal{E}})+2(\vec{\mathcal{E}}\cdot\nabla)\vec{\mathcal{D}}\ ,\end{aligned} \tag{6.68}$$

and analogously for $\vec{\mathcal{B}}\cdot\vec{\mathcal{H}}$. The second equation holds, because for $\vec{\mathcal{D}}=\varepsilon\vec{\mathcal{E}}$ with $\varepsilon=const$, we can arbitrarily exchange the order of products between $\vec{\mathcal{D}}$ and $\vec{\mathcal{E}}$. We also assume $\mu=const$, which allows us to exchange the order of products between $\vec{\mathcal{H}}$ and $\vec{\mathcal{B}}$. We use the rule (6.68) to replace the terms with vector products in equation (6.67),

$$\begin{aligned}\mathbf{f}&=\vec{\mathcal{E}}(\nabla\cdot\vec{\mathcal{D}})-\tfrac{1}{2}\nabla(\vec{\mathcal{E}}\cdot\vec{\mathcal{D}})+(\vec{\mathcal{E}}\cdot\nabla)\vec{\mathcal{D}}\\&\quad+\vec{\mathcal{H}}(\nabla\cdot\vec{\mathcal{B}})-\tfrac{1}{2}\nabla(\vec{\mathcal{H}}\cdot\vec{\mathcal{B}})+(\vec{\mathcal{H}}\cdot\nabla)\vec{\mathcal{B}}-\partial_t\vec{\mathcal{D}}\times\vec{\mathcal{B}}\ .\end{aligned} \tag{6.69}$$

The last term is nothing more than the time derivative of the *Minkowski momentum density* of the electromagnetic field defined in (6.58), $\vec{\wp}^M\equiv\vec{\mathcal{D}}\times\vec{\mathcal{B}}$, which still awaits interpretation.

Now we introduce the *Maxwell stress tensor* (in Minkowski's form) by [9],

$$\boxed{T^M_{ij}\equiv\mathcal{D}_i\mathcal{E}_j+\mathcal{H}_i\mathcal{B}_j-\tfrac{\delta_{ij}}{2}(\vec{\mathcal{E}}\cdot\vec{\mathcal{D}}+\vec{\mathcal{H}}\cdot\vec{\mathcal{B}})}\ . \tag{6.70}$$

Defining the divergent of a matrix, we obtain using Einstein's sum convention,

$$\begin{aligned}(\nabla\cdot\overset{\leftrightarrow}{\mathbf{T}})_j&\equiv(\partial_iT_{ij})_j=\Big(\partial_i(\mathcal{D}_i\mathcal{E}_j)+\partial_i(\mathcal{H}_i\mathcal{B}_j)-\partial_i\tfrac{\delta_{ij}}{2}(\vec{\mathcal{E}}\cdot\vec{\mathcal{D}}+\vec{\mathcal{H}}\cdot\vec{\mathcal{B}})\Big)_j\\&=\Big(\mathcal{E}_j\nabla\cdot\vec{\mathcal{D}}+\vec{\mathcal{D}}\cdot\nabla\mathcal{E}_j+\mathcal{B}_j\nabla\cdot\vec{\mathcal{H}}+\vec{\mathcal{H}}\cdot\nabla\mathcal{B}_j-\tfrac{1}{2}\partial_j(\vec{\mathcal{E}}\cdot\vec{\mathcal{D}}+\vec{\mathcal{H}}\cdot\vec{\mathcal{B}})\Big)_j\ .\end{aligned} \tag{6.71}$$

These terms coincide with those of the equation (6.69) except for the last one. Now, we can reshape the Lorentz force,

$$\boxed{-\partial_t\vec{\wp}^M+\nabla\cdot\overset{\leftrightarrow}{\mathbf{T}}=\mathbf{f}}\ . \tag{6.72}$$

The mechanical force acting on a volume $\mathcal{V}$,

$$\mathbf{F}=\oint_{\partial\mathcal{V}}\overset{\leftrightarrow}{\mathbf{T}}\cdot d\mathbf{S}-\frac{d}{dt}\int_{\mathcal{V}}\vec{\wp}^M dV\ , \tag{6.73}$$

can be expressed by a momentum flux escaping the volume plus a 'stress' acting on its surface in every direction. The diagonal components T_{ii} represent 'pressures' and the non-diagonal 'shear stresses'. In static situations only the stress results in forces.

[9] In matrix notation,

$$\nabla\cdot\overset{\leftrightarrow}{T}=\begin{pmatrix}\frac{d}{dx}&\frac{d}{dy}&\frac{d}{dz}\end{pmatrix}\begin{pmatrix}T_{xx}&T_{xy}&T_{xz}\\T_{yx}&T_{yy}&T_{xz}\\T_{zx}&T_{zy}&T_{zz}\end{pmatrix}\ .$$

Example 58 (*Force on a charged body*): As an example of application of the stress tensor we calculate the force exerted by a solid uniformly charged (charge Q) sphere of radius R on its own upper part. The volume of the upper hemisphere is enclosed by two surfaces: one hemispheric surface and a flat one. In Cartesian coordinates,

$$\hat{\mathbf{e}}_r = \hat{\mathbf{e}}_x \sin\theta\cos\phi + \hat{\mathbf{e}}_y \sin\theta\sin\phi + \hat{\mathbf{e}}_z \cos\theta \ ,$$

for the hemispherical surface, we write the electric field and the surface element as,

$$\vec{\mathcal{E}} = \frac{1}{4\pi\varepsilon_0}\frac{Q}{R^2}\hat{\mathbf{e}}_r \qquad \text{and} \qquad d\mathbf{a} = \hat{\mathbf{e}}_r R^2 \sin\theta d\theta d\phi \ .$$

We calculate the stress tensor,

$$\overleftrightarrow{\mathbf{T}} = \varepsilon_0 \begin{pmatrix} \mathcal{E}_x^2 - \frac{1}{2}\mathcal{E}^2 & \mathcal{E}_x\mathcal{E}_y & \mathcal{E}_x\mathcal{E}_z \\ \mathcal{E}_x\mathcal{E}_y & \mathcal{E}_y^2 - \frac{1}{2}\mathcal{E}^2 & \mathcal{E}_y\mathcal{E}_z \\ \mathcal{E}_x\mathcal{E}_z & \mathcal{E}_y\mathcal{E}_z & \mathcal{E}_z^2 - \frac{1}{2}\mathcal{E}^2 \end{pmatrix}$$

$$= \varepsilon_0 \left(\frac{1}{4\pi\varepsilon_0}\frac{Q}{R^2}\right)^2 \begin{pmatrix} \sin^2\theta\cos^2\phi - \frac{1}{2} & \sin^2\theta\cos\phi\sin\phi & \cos\theta\sin\theta\cos\phi \\ \sin^2\theta\cos\phi\sin\phi & \sin^2\theta\sin^2\phi - \frac{1}{2} & \cos\theta\sin\theta\sin\phi \\ \cos\theta\sin\theta\cos\phi & \cos\theta\sin\theta\sin\phi & \cos^2\theta - \frac{1}{2} \end{pmatrix} \ .$$

The integral of the tensor over the surface can be evaluated by Maple,

$$\int \overleftrightarrow{\mathbf{T}} d\mathbf{a} = \int_0^{2\pi}\int_0^{\pi/2} \overleftrightarrow{\mathbf{T}}\hat{\mathbf{e}}_r R^2 \sin\theta d\theta d\phi = \frac{Q^2}{32\pi\varepsilon_0 R^2}\hat{\mathbf{e}}_z \ .$$

For the flat surface we write,

$$\vec{\mathcal{E}} = \frac{1}{4\pi\varepsilon_0}\frac{Q}{R^3} r\hat{\mathbf{e}}_r \qquad \text{and} \qquad d\mathbf{a} = -\hat{\mathbf{e}}_z r dr d\phi \ .$$

Now we calculate with $\theta = \pi/2$,

$$\overleftrightarrow{\mathbf{T}} = \varepsilon_0 \frac{1}{(4\pi\varepsilon_0)^2}\frac{Q^2}{R^6} \begin{pmatrix} r^2\cos^2\phi - \frac{1}{2} & r^2\cos\phi\sin\phi & 0 \\ r^2\cos\phi\sin\phi & r^2\sin^2\phi - \frac{1}{2} & 0 \\ 0 & 0 & -\frac{1}{2}r^2 \end{pmatrix} \ .$$

The integral over the surface gives,

$$\int \overleftrightarrow{\mathbf{T}} d\mathbf{a} = -\int_0^{2\pi}\int_0^{R} \overleftrightarrow{\mathbf{T}}\hat{\mathbf{e}}_z r dr d\phi = \frac{Q^2}{64\pi\varepsilon_0 R^2}\hat{\mathbf{e}}_z \ .$$

Combining the results we obtain the force by the equation (6.73),

$$\mathbf{F} = \oint_{\text{hemisphere}} \overleftrightarrow{\mathbf{T}} d\mathbf{a} = \frac{3Q^2}{64\pi\varepsilon_0 R^2}\hat{\mathbf{e}}_z \ .$$

The result of this example demonstrates, how we can reduce the calculation of a force acting on a volume to an integral over the surface enclosing the volume. We will calculate other examples in Excs. 6.2.5.3 to 6.2.5.6.

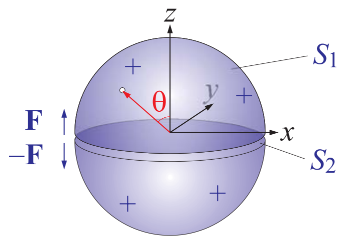

Figure 6.7: Electrostatic forces inside a charged sphere.

6.2.3.2 Conservation of linear momentum

According to Newton's second law, $\mathbf{F} = \partial_t \mathbf{p}_{mec}$ or $\mathbf{f} = \partial_t \vec{\wp}_{mec}$, the Lorentz force produces a variation of the *mechanical momentum*. In addition, there is a momentum $\mathbf{p}^M = \int_\mathcal{V} \vec{\wp}^M dV$, which must be attributed to the *electromagnetic field*, since it only exists in the presence of both electric and magnetic fields. $\mathbf{p}_{mec}$ and $\mathbf{p}^M$ can be interconverted, as in the example of the photonic recoil received by an atom upon an absorption process. But the sum of the mechanical momentum and the momentum of the field can only change through the term $\nabla \cdot \overleftrightarrow{\mathbf{T}}$. This is the law of *linear momentum conservation*. Evidently, $-\overleftrightarrow{\mathbf{T}}$ is the momentum flux density, playing a role similar to the one of the current density $\mathbf{j}$ in the continuity equation or of the energy flux density $\vec{\mathcal{S}}$ in Poynting's theorem. $-T_{ij}$ is the momentum per unit area and time in the direction i passing a surface oriented in j-direction.

We note two very different roles of the Poynting vector: In the energy conservation equation $\vec{\mathcal{S}}$ is the energy per unit area and time carried by electromagnetic fields, while in the momentum conservation equation, $\vec{\wp}^M = \varepsilon_0\mu_0\vec{\mathcal{S}}$ is the momentum per unit volume stored in these fields. Similarly, $\overleftrightarrow{\mathbf{T}}$ plays two roles: $\overleftrightarrow{\mathbf{T}}$ is the electromagnetic stress (i.e. a force per unit area or pressure) acting on a surface, while $-\overleftrightarrow{\mathbf{T}}$ describes the momentum flux (momentum current density) carried by these fields.

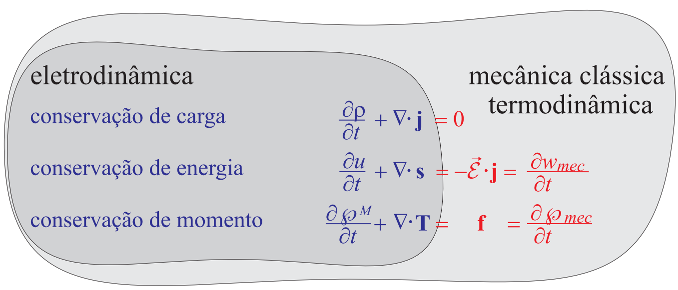

Figure 6.8: The laws of energy and momentum conservation connect the theories of electrodynamics with classical mechanics and thermodynamics.

Forces exerted by (non-radiating) fields on particles can be interpreted as being due to a scattering of 'virtual particles'. For example, the electrostatic force between charged particles and the magnetostatic force between magnetic dipoles are caused by an exchange of virtual photons. These photons carry momentum that is transferred via recoil in a scattering event. Since the photon has no mass, the electric (respectively, magnetic) potential has infinite range.

The photonic concept can be extended to electromagnetic fields, as demonstrated by *Max Planck* in his discussion of the blackbody radiation. The spontaneous emission of a photon during the decay of an excited atom, postulated by *Albert Einstein*, is forbidden in 'classical' quantum mechanics, and requires quantization of the electromagnetic field for its explanation. The quantized energy packets, called (real) photons, also carry momentum, which can be transferred to bodies absorbing the radiation. The fact that light beams can exert forces is nowadays commonly exploited in techniques for cooling atomic gases. This process is called *radiation pressure* and will be discussed in the next chapter.

Example 59 (*The Abraham-Minkowski dilemma*): The expression $\vec{\wp}^A = \frac{1}{c^2}\vec{\mathcal{E}} \times \vec{\mathcal{H}}$ for the momentum flux in dielectric media was proposed by Abraham in 1909, but it is not obvious that this expression is correct. In fact, in the same year 1909 Minkowski proposed the expression $\vec{\wp}^M = \vec{\mathcal{D}} \times \vec{\mathcal{B}}$, and until today this *Abraham-Minkowski dilemma* is not satisfactorily solved [12, 97]. See also (watch talk).

In an (over-)simplified way, we may illustrate the dilemma by the fact that even the correct expression for the photonic momentum within a dielectric is unknown. For, knowing that the phase velocity is reduced in a dielectric medium, $c \to c/n$, we could derive from the kinetic momentum in vacuum, $p = m\frac{c}{n}$, where the mass follows from Einstein's formula, $m = \frac{\hbar\omega}{c^2}$. That is, the photonic momentum within a dielectric medium should be,

$$p = \frac{\hbar\omega}{nc} \;.$$

This is Abraham's conclusion, which emphasizes the corpuscular aspect of the photon. On the other side, starting with de Broglie's expression, $p = \frac{h}{\lambda}$, using the dispersion relation, $\lambda = \frac{c}{n\nu}$, we would conclude that the photonic momentum within a dielectric medium must be,

$$p = \frac{n\hbar\omega}{c} \;,$$

which is Minkowski's result emphasizing the undulating features of the photon. In fact, the dilemma arises because, a priori, it is not clear whether the correct expression for the momentum carried by an electromagnetic wave is,

$$\vec{\wp}^A = \tfrac{1}{c^2}\mathbf{S} = \tfrac{1}{c^2}\vec{\mathcal{E}} \times \vec{\mathcal{H}} \qquad \text{or} \qquad \vec{\wp}^M = \vec{\mathcal{D}} \times \vec{\mathcal{B}} \;.$$

In vacuum there is no difference, but in the case of a plane wave inside a dielectric medium, $\vec{\mathcal{E}}(\mathbf{r},t) = \mathcal{E}_0\hat{\mathbf{e}}_x \cos\omega(t - \frac{n}{c}z)$ and $\vec{\mathcal{B}}(\mathbf{r},t) = \frac{n}{c}\hat{\mathbf{e}}_z \times \vec{\mathcal{E}}(\mathbf{r},t)$, we calculate,

$$\begin{aligned}
\wp^A &\equiv \tfrac{1}{c^2}\overline{\vec{\mathcal{E}} \times \vec{\mathcal{H}}} = \tfrac{1}{\mu_0 c^2}\overline{\vec{\mathcal{E}} \times \vec{\mathcal{B}}} = \tfrac{1}{\mu_0 c^2}\mathcal{E}_0^2\hat{\mathbf{e}}_z\tfrac{n}{c}\overline{\cos^2\omega(t - \tfrac{n}{c}z)} \\
&= \tfrac{1}{\mu_0 c^2}\mathcal{E}_0^2\hat{\mathbf{e}}_z\tfrac{n}{c}\tfrac{1}{2} = \tfrac{1}{\varepsilon_0\mu_0 c^2} - \hat{\mathbf{e}}_z\tfrac{u}{nc} = \hat{\mathbf{e}}_z\tfrac{u}{nc} \\
\wp^M &\equiv \overline{\vec{\mathcal{D}} \times \vec{\mathcal{B}}} = \varepsilon_0\overline{\vec{\mathcal{E}} \times \vec{\mathcal{B}}} = \varepsilon_0\mu_0 c^2\vec{\wp}^A = n^2\vec{\wp}^A \;.
\end{aligned}$$

6.2.4 Conservation of angular momentum of the electromagnetic field

The *angular momentum conservation* (6.58) is also ruled by Maxwell's equations. But its derivation is complicated [42, 47] and will not be reproduced here. In Exc. 6.2.5.7 we calculate the angular momentum stored in a static combination of electric and magnetic fields. In Exc. 6.2.5.8 we calculate the torque acting on charges due to a temporal variation of electromagnetic fields. Finally, in Exc. 6.2.5.9 we try classical discussion of the intrinsic angular momentum (spin) of the electron.

Example 60 (*Angular momentum of electromagnetic fields*): Imagine a very long solenoid with radius R, n windings per unit length, and carrying the current I. Coaxially to the solenoid there are two long cylindrical layers of length d. The first one, of radius a, lies inside the solenoid and carries a charge $+Q$ evenly distributed over the surface; the other one, of radius b, is outside the solenoid and carries the charge $-Q$, as shown in Fig. 6.9. We suppose $d \gg b$. When the current in the solenoid is gradually reduced, the cylinders begin to rotate. The question is, where does the angular momentum come from?

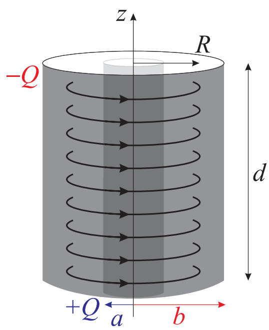

Figure 6.9: Device with a solenoid and charged cylinders illustrating the conservation of angular momentum.

Let us first calculate the angular momentum stored in the electric and magnetic field before we started to reduce the current. In the region between the cylinders, $a < \rho < b$, we had the electric field $\vec{\mathcal{E}} = \frac{Q}{2\pi\varepsilon_0 d}\frac{\hat{\mathbf{e}}_\rho}{\rho}$, and in the inner region of the solenoid, $\rho < R$, the magnetic field, $\vec{\mathcal{B}} = \mu_0 nI\hat{\mathbf{e}}_z$. Therefore, in the region $a < \rho < R$, the momentum density (6.58) was,

$$\vec{\wp} = \varepsilon_0\vec{\mathcal{E}} \times \vec{\mathcal{B}} = -\frac{\mu_0 QnI}{2\pi\rho d}\hat{\mathbf{e}}_\phi$$

The angular momentum density,

$$\vec{\ell} = \mathbf{r} \times \vec{\wp} = -\frac{\mu_0 nIQ}{2\pi d}\hat{\mathbf{e}}_z \ ,$$

was constant, which facilitates the calculation of the total orbital angular momentum,

$$\mathbf{L} = \int \vec{\ell} dV = \vec{\ell}\pi(R^2 - a^2)d = -\tfrac{1}{2}\mu_0 nIQ(R^2 - a^2)\hat{\mathbf{e}}_z \ .$$

Apparently, the existence of an orbital angular momentum is conditioned to the presence of both, a charge and a current.
Now, when the current is turned off, the variation of the magnetic field induces a circumferential electric field, given by Faraday's law:

$$\vec{\mathcal{E}} = -\tfrac{1}{2}\mu_0 n \frac{dI}{dt}\hat{\mathbf{e}}_\phi \begin{cases} \rho & \text{for} \quad \rho < R \\ \frac{R^2}{\rho} & \text{for} \quad \rho > R \end{cases} .$$

The Coulomb force exerted by the electric field on the charged outer cylinder produces a torque on the cylinder,

$$\mathbf{N}_b = \mathbf{r} \times (-Q\vec{\mathcal{E}}) = \tfrac{1}{2}\mu_0 n Q R^2 \frac{dI}{dt}\hat{\mathbf{e}}_z \ ,$$

so that it receives the angular momentum,

$$\mathbf{L}_b = \int_0^\infty \mathbf{N}_b dt = \tfrac{1}{2}\mu_0 n Q R^2 \hat{\mathbf{e}}_z \int_I^0 \frac{dI}{dt} dt = -\tfrac{1}{2}\mu_0 n I Q R^2 \hat{\mathbf{e}}_z \ .$$

In the same way, we obtain for the inner cylinder,

$$\mathbf{N}_a = -\tfrac{1}{2}\mu_0 n Q a^2 \frac{dI}{dt}\hat{\mathbf{e}}_z \quad , \quad \mathbf{L}_a = \tfrac{1}{2}\mu_0 n I Q a^2 \hat{\mathbf{e}}_z \ .$$

Hence, we verify that $\mathbf{L} = \mathbf{L}_a + \mathbf{L}_b$. The angular momentum lost by the fields is precisely equal to the angular momentum acquired by the cylinders, that is, the total angular momentum is conserved.

6.2.5 Exercises

6.2.5.1 Ex: Poynting vector for free charges and currents

Write down the Poynting vector and the momentum density for the case, that there are only free *charges and currents*.

6.2.5.2 Ex: Energy flux in a current-carrying wire

A cylindrical wire with radius a and permeability μ is traversed by a constant current density $\mathbf{j}$. The electric field $\vec{\mathcal{E}}$ inside the wire and the current density $\mathbf{j}$ are connected by Ohm's law $\mathbf{j} = \varsigma\vec{\mathcal{E}}$, where ς is the electrical conductivity.
a. What absolute value and which direction does the Poynting vector $\vec{\mathcal{S}}$ have in the wire and on the wire surface?
b. Calculate the total energy flux running through the surface of a piece of wire of length l. Show that this flux of energy is precisely the power dissipated within this piece for the production of ohmic heat.
Help: The law of energy conservation in electrodynamics is given by $-\frac{du}{dt} = \nabla\vec{\mathcal{S}} + \mathbf{j}\cdot\vec{\mathcal{E}}$, where $u = \frac{1}{2}(\vec{\mathcal{E}}\cdot\vec{\mathcal{D}} + \vec{\mathcal{B}}\cdot\vec{\mathcal{H}})$ is the total energy density, $\vec{\mathcal{S}} = \vec{\mathcal{E}} \times \vec{\mathcal{H}}$ the energy flux and $\mathbf{j}\cdot\vec{\mathcal{E}}$ the work exerted on the electric current density.

6.2.5.3 Ex: Intrinsic force in a rotating charged shell via Maxwell's tensor

Calculate the attractive magnetic force between the north and south hemispheres of a uniformly charged spherical shell (radius R and surface charge density Q) rotating with the angular velocity ω. Use the result of Exc. 4.3.3.1 (clicking on the title).

6.2.5.4 Ex: Coulomb force via Maxwell's tensor

Consider two equal (or opposite) point charges q, separated by distance $2a$. Construct the plane which is equidistant from the two charges. Determine the mutual force between the charges.

6.2.5.5 Ex: Force on a current distribution in a magnetic field

The force felt by a current distribution $\mathbf{j}(\mathbf{r})$ in an external magnetic field is,

$$\mathbf{F} = \int_{\mathcal{V}} d^3r'\mathbf{j}(\mathbf{r}') \times \vec{\mathcal{B}}(\mathbf{r}') \ .$$

Show that this force can also be written as an integral over the surface $\mathcal{S} \equiv \partial\mathcal{V}$ enclosing the volume $\mathcal{V}$:

$$F_j = \oint_{\mathcal{S}} \sum_{i=1}^{3} dS_i \ T_{ij} \qquad \text{with} \qquad T_{ij} = \tfrac{1}{\mu_0}\left(\mathcal{B}_i\mathcal{B}_j - \tfrac{1}{2}\mathcal{B}^2\delta_{ij}\right) \ .$$

6.2.5.6 Ex: Force on the plates of a capacitor

Consider an infinite parallel-plate capacitor, with the lower plate (at $z = -d/2$) carrying the charge density $-\sigma$ and the upper plate (at $z = +d/2$) carrying the charge density σ. Determine the stress tensor in the region between the plates.

6.2.5.7 Ex: Angular momentum of an electromagnetic field

Assuming the existence of an electric charge q_e and a magnetic monopole q_m, calculate the total angular momentum stored in the fields,

$$\vec{\mathcal{E}} = \frac{q_e}{4\pi\varepsilon_0}\frac{\hat{\mathbf{e}}_r}{R^2} \qquad \text{and} \qquad \vec{\mathcal{B}} = \frac{\mu_0 q_m}{4\pi}\frac{\hat{\mathbf{e}}_r}{R^2} \ ,$$

when the two charges are separated by a distance d.

6.2.5.8 Ex: Torque on a demagnetized or discharged iron sphere

We imagine an iron sphere of radius R carrying a charge Q and a uniform magnetization $\vec{\mathcal{M}} = \mathcal{M}\hat{\mathbf{e}}_z$. The sphere is initially at rest.
a. Calculate the angular momentum stored in the electromagnetic fields.
b. Suppose the sphere is gradually (and uniformly) demagnetized (perhaps by heating it beyond the Curie point). Use Faraday's law to determine the induced electric field and find the torque that this field exerts on the sphere. Calculate the total angular momentum transferred to the sphere during demagnetization.
c. Suppose that, instead of demagnetizing the sphere, we discharge it by connecting the north pole of the sphere via a wire to Earth. Suppose that the current flows on the surface in such a way, that the charge density remains uniform. Use the Lorentz force law to determine the torque on the sphere and calculate the total angular momentum given to the sphere during the discharge. (The magnetic field is discontinuous on the surface ... does this matter?)

6.2.5.9 Ex: Magnetic moment of the electron

In relativistic quantum mechanics the magnetic moment of the electron has the value,

$$\mu = g\mu_B \frac{1}{2} = \frac{e\hbar}{2mc} = 9.28 \cdot 10^{-25}\,\mathrm{T\ m}^3 \ .$$

This exercise aims to show that the classical interpretation of this magnetic moment, as being due to a rotating charge distribution, leads to intrinsic contradictions. Let us regard the electron as a sphere of mass m_e with radius r_e carrying the charge e homogeneously distributed over its surface. It rotates around its z-axis with the angular velocity ω. Classically, the movement of the surface charge causes a magnetic moment.
a. Calculate the total energy contained in the electromagnetic fields.
b. Calculate the total angular momentum contained in the fields.
c. According to Einstein's formula, $W_{ED} = m_e c^2$, the energy in the fields must contribute to the mass of the electron. Lorentz and other scientists have speculated that the entire mass of the electron could be understood in this way. Suppose, furthermore, that the rotational angular momentum (spin) of the electron is entirely attributable to the electromagnetic fields: $L_{ED} = \hbar/2$. From these two premisses, determine the radius and the angular velocity of the electron, as well as the product ωr_e. Does this classical model make sense?
d. Determine the magnetic moment of the rotating electron.

6.3 Potential formulation of electrodynamics

6.3.1 The vector and the scalar potential

All quantities involved in Maxwell's equations for vacuum, the fields $\vec{\mathcal{E}}(\mathbf{r},t)$ and $\vec{\mathcal{B}}(\mathbf{r},t)$ as well as charge ($\rho(\mathbf{r},t)$) and current ($\mathbf{j}(\mathbf{r},t)$) distributions they depend on space and time. Knowing that the divergence of a field is zero everywhere, $\nabla\cdot\vec{\mathcal{B}} = 0$, we conclude that this field must be the rotation of another field. That is, there is a vector field $\mathbf{A}(\mathbf{r},t)$, such that,

$$\vec{\mathcal{B}}(\mathbf{r},t) = \nabla \times \mathbf{A}(\mathbf{r},t) \ . \tag{6.74}$$

Substituting the so-called *vector potential* $\mathbf{A}(\mathbf{r},t)$ in Faraday's law, $\nabla\times\vec{\mathcal{E}} = -\frac{\partial\vec{\mathcal{B}}}{\partial t}$, we obtain,

$$\nabla \times \vec{\mathcal{E}} = -\frac{\partial}{\partial t}(\nabla\times\mathbf{A}) = -\nabla\times\frac{\partial\mathbf{A}}{\partial t} \ . \tag{6.75}$$

Hence,

$$\nabla \times \left(\vec{\mathcal{E}} + \frac{\partial\mathbf{A}}{\partial t}\right) = 0 \ . \tag{6.76}$$

Now, since the rotational field within the parentheses is null everywhere, it follows that there exists a scalar field $\Phi(\mathbf{r},t)$, called *scalar potential*, such that,

$$\vec{\mathcal{E}} + \frac{\partial\mathbf{A}}{\partial t} = -\nabla\Phi \ . \tag{6.77}$$

The minus sign in front of the gradient of $\Phi(\mathbf{r},t)$, is introduced to recover the electrostatic case when $\mathbf{A}(\mathbf{r},t)$ does not depend on time. In summary, if we know the vector and scalar potentials, we can calculate the fields $\vec{\mathcal{E}}(\mathbf{r},t)$ and $\vec{\mathcal{B}}(\mathbf{r},t)$ following the prescription expressed by the equations:

$$\boxed{\vec{\mathcal{E}}(\mathbf{r},t) = -\nabla\Phi(\mathbf{r},t) - \frac{\partial\mathbf{A}(\mathbf{r},t)}{\partial t} \qquad \text{and} \qquad \vec{\mathcal{B}}(\mathbf{r},t) = \nabla\times\mathbf{A}(\mathbf{r},t)} \,. \tag{6.78}$$

6.3.2 Gauge transformation

Substituting the expression for the electric field by the vector and scalar potentials in Gauß' law, $\nabla\cdot\vec{\mathcal{E}} = \frac{\varrho}{\varepsilon_0}$,

$$\frac{\varrho}{\varepsilon_0} = \nabla\cdot\left(-\nabla\Phi - \frac{\partial\mathbf{A}}{\partial t}\right) = -\nabla^2\Phi - \frac{\partial\nabla\cdot\mathbf{A}}{\partial t} \,. \tag{6.79}$$

Replacing the fields $\vec{\mathcal{E}}(\mathbf{r},t)$ and $\vec{\mathcal{B}}(\mathbf{r},t)$ by the potentials defined in (6.78), within the law of Ampère-Maxwell, $\nabla\times\vec{\mathcal{B}} = \mu_0\mathbf{j} + \varepsilon_0\mu_0\frac{\partial\vec{\mathcal{E}}}{\partial t}$, we obtain,

$$\nabla\times(\nabla\times\mathbf{A}) = \nabla(\nabla\cdot\mathbf{A}) - \nabla^2\mathbf{A} = \mu_0\mathbf{j} - \frac{1}{c^2}\frac{\partial}{\partial t}\left(-\nabla\Phi - \frac{\partial\mathbf{A}}{\partial t}\right) \,. \tag{6.80}$$

that is,

$$\nabla^2\mathbf{A} - \frac{1}{c^2}\frac{\partial\mathbf{A}^2}{\partial t^2} - \nabla\left(\nabla\cdot\mathbf{A} + \frac{1}{c^2}\frac{\partial\Phi}{\partial t}\right) = -\mu_0\mathbf{j} \,. \tag{6.81}$$

The coupled differential equations (6.79) and (6.81) allow us, in principle, to derive a set of potentials Φ and $\mathbf{A}$, generated by a charge and current distribution ϱ and $\mathbf{j}$, from which the fields $\vec{\mathcal{E}}$ and $\vec{\mathcal{B}}$ can be calculated. However, these *potentials are not unique*. To see this, let us suppose new potentials,

$$\Phi_1 \equiv \Phi - \frac{\partial\chi}{\partial t} \qquad \text{and} \qquad \mathbf{A}_1 \equiv \mathbf{A} + \nabla\chi \,. \tag{6.82}$$

Obviously, these potentials produce the same fields, since,

$$\vec{\mathcal{B}}_1 = \nabla\times(\mathbf{A}+\nabla\chi) = \vec{\mathcal{B}} \,, \tag{6.83}$$

using the expressions (6.78) and,

$$\vec{\mathcal{E}}_1 = -\nabla\left(\Phi - \frac{\partial\chi}{\partial t}\right) - \frac{\partial}{\partial t}(\mathbf{A}+\nabla\chi) = -\nabla\Phi - \frac{\partial}{\partial t}\mathbf{A} = \vec{\mathcal{E}} \,. \tag{6.84}$$

Thus, it is clear that the fields are the same for an infinite number of different potentials, provided they follow from each other by a so-called *gauge transform*,

$$\boxed{\mathbf{A} \longrightarrow \mathbf{A} + \nabla\chi \qquad \text{and} \qquad \Phi \longrightarrow \Phi - \partial_t\chi} \,. \tag{6.85}$$

This *gauge invariance* leaves the observable fields $\vec{\mathcal{E}}$ and $\vec{\mathcal{B}}$ invariant.

The freedom of choosing an appropriate gauge field can be employed to simplify the set of equations (6.79) and (6.81) for particular problems, as we will discuss in the following sections.

6.3.2.1 Lorentz gauge

We note that if the expression within the brackets of Eq. (6.81) were zero,

$$\boxed{\nabla\cdot\mathbf{A}+\frac{1}{c^2}\frac{\partial\Phi}{\partial t}\overset{!}{=}0} \tag{6.86}$$

we would have from the equations (6.79) and (6.81) 'wave' type equations for the potentials,

$$\nabla^2\Phi-\frac{1}{c^2}\frac{\partial^2\Phi}{\partial t^2}=-\frac{\varrho}{\varepsilon_0} \quad\text{and}\quad \nabla^2\mathbf{A}-\frac{1}{c^2}\frac{\partial^2\mathbf{A}}{\partial t^2}=-\mu_0\mathbf{j}\ . \tag{6.87}$$

To analyze the viability of the expression (6.86), we apply a gauge transformation,

$$\nabla\cdot(\mathbf{A}+\nabla\chi)+\frac{1}{c^2}\frac{\partial(\Phi-\partial_t\chi)}{\partial t}=\nabla^2\chi-\frac{1}{c^2}\frac{\partial^2\chi}{\partial t^2}=0\ . \tag{6.88}$$

Hence, imposing the additional condition (6.86) is legal, because it can always be satisfied by a simple gauge transformation with a field χ satisfying the wave equation (6.88).

The equation (6.86) is known as the *Lorentz gauge*. We emphasize that *it is not necessary to postulate the equation*, but it is always possible to find a scalar function χ, which allows the use of new potentials, giving the same $\vec{\mathcal{E}}$ and $\vec{\mathcal{B}}$ fields and satisfying this equation [10].

Introducing the notation of the *d'Alembert operator*,

$$\Box\equiv\nabla^2-\varepsilon_0\mu_0\frac{\partial^2}{\partial t^2}\ , \tag{6.89}$$

the wave equations (6.87) become,

$$\Box\Phi=-\varepsilon_0^{-1}\varrho \quad\text{and}\quad \Box\mathbf{A}=-\mu_0\mathbf{j}\ . \tag{6.90}$$

They generalize the electro- and magnetostatic equations (6.6) to include temporal variations simply by replacing the Laplacian with a d'Alembertian. The democratic treatment of Φ and $\mathbf{A}$ by a Poisson-like equation in four space-time dimensions is particularly interesting in the context of special relativity. We study examples of the Lorentz gauge in Excs. 4.3.3.6 to 4.3.3.8 and 6.3.8.1 to 6.3.8.7.

6.3.2.2 Coulomb gauge, transverse and longitudinal currents

Another condition that can be applied to the potentials in order to simplify the differential equations (6.86) and (6.88) consists in setting,

$$\boxed{\nabla\cdot\mathbf{A}\overset{!}{=}0}\ . \tag{6.91}$$

[10] E.g. choosing χ such that $\nabla\chi=-\mathbf{A}$ and $c^{-1}\partial_t\chi=\phi$.

This is called the *Coulomb gauge*. With this condition we obtain from (6.79) the *Poisson equation* as well as an equation for the vector potential,

$$-\nabla^2\Phi = \frac{\varrho}{\varepsilon_0} \tag{6.92}$$
$$-\nabla^2\mathbf{A} + \frac{1}{c^2}\left(\frac{\partial^2\mathbf{A}}{\partial t^2} + \frac{\partial}{\partial t}\nabla\Phi\right) = \mu_0\mathbf{j} \; .$$

These two equations determine the vector and scalar potentials if the current and charge density distributions are specified [11]. The first Eq. (6.92) is solved by *Coulomb's law*, letting $\Phi(\infty) = 0$,

$$\Phi(\mathbf{r},t) = \frac{1}{4\pi\varepsilon_0}\int\frac{\varrho(\mathbf{r}',t)}{|\mathbf{r}-\mathbf{r}'|}d^3r' \; . \tag{6.93}$$

It is important to be aware that, unlike in electrostatics, we need to know also $\mathbf{A}(\mathbf{r},t)$ to be able to calculate the field $\vec{\mathcal{E}}(\mathbf{r},t)$ through the formula (6.78).

It may seem strange that the scalar potential in Coulomb's gauge is determined by the instantaneous charge distribution: Moving an electron at a point $\mathbf{r}'$, the potential at a distant point, $\Phi(\mathbf{r})$, immediately captures this change, not being limited by the speed limit for the transmission of information postulated by special relativity. The explanation is, that Φ is not an observable physical quantity. To infer a change of ϱ, we must measure $\vec{\mathcal{E}}$, which depends on $\mathbf{A}$ as well. Somehow it is encoded into the Coulomb gauge that, while $\Phi(\mathbf{r})$ instantly reflects all variations of $\varrho(\mathbf{r}')$, the vector potential depends in a much more complicated way on these variations, such that the combination $-\nabla\Phi - \partial\mathbf{A}/\partial t$ only responds to the variations after a long enough time for information to arrive.

The advantage of the Coulomb gauge is that the scalar potential is simple to calculate. The disadvantage is that, in addition to the non-causal appearance of Φ, it is particularly difficult to calculate $\mathbf{A}$: The differential equation for $\mathbf{A}$ in the Coulomb gauge is (6.81).

In order to obtain an equation involving only the vector field and the current density, we use Helmholtz's theorem to write the current density as the sum of *transverse* and *longitudinal* components,

$$\mathbf{j} = \mathbf{j}_T + \mathbf{j}_L \; , \tag{6.94}$$

where the terms 'transverse' and 'longitudinal' are defined by the following two conditions,

$$\boxed{\nabla\cdot\mathbf{j}_T = 0 \qquad \text{and} \qquad \nabla\times\mathbf{j}_L = 0} \; . \tag{6.95}$$

Calculating the rotation of the second equation (6.92) we see that the term containing the gradient of the scalar potential vanishes. Hence,

$$-\nabla^2\mathbf{A} + \frac{1}{c^2}\frac{\partial^2\mathbf{A}}{\partial t^2} = \mu_0\mathbf{j}_T \; , \tag{6.96}$$

which shows that the transverse component of $\mathbf{j}$ is fully associated only with the vector potential. Now, substituting this result into the second equation (6.92) we are left with,

$$\varepsilon_0\frac{\partial}{\partial t}\nabla\Phi = \mathbf{j}_L \; . \tag{6.97}$$

[11] The determination still leaves the freedom to add fields satisfying $\nabla^2\Theta = 0$.

That is, the longitudinal component of $\mathbf{j}$ is fully associated to the scalar potential. The solution of Eq. (6.96) requires some preparation and will be given in the following sections.

6.3.3 Green's function

A useful tool for solving Laplace equations, such as derived in Eq. (6.87) or (6.96), is the *Green's function*. The dynamics of physical systems are often described by differential equations of the type,

$$\mathcal{L}u(\mathbf{r}) = \varrho(\mathbf{r}) \ , \tag{6.98}$$

where $\mathcal{L} = \mathcal{L}(\mathbf{r})$ is a linear *differential operator*. While this operator has a very generic form, the behavior of a particular system depends on the choice of the function ϱ. The Laplace equation, where $\mathcal{L}(\mathbf{r}) \equiv \nabla^2$ and ϱ is a particular charge distribution is an example.

One method of solving this differential equation is to first solve the following equation,

$$\mathcal{L}\mathcal{G}(\mathbf{r}, \mathbf{x}) = \delta^3(\mathbf{r} - \mathbf{x}) \ , \tag{6.99}$$

where $\mathcal{G}(\mathbf{r}, \mathbf{x})$ is called the Green function of the operator. In general, the Green function is not unique. However, in practice, some combination of symmetry, boundary conditions and/or other externally imposed criteria can make the Green function unique.

Green functions are useful tools for solving wave and diffusion equations. In quantum mechanics, the Green function of the Hamiltonian is intrinsically connected to the concept of density of states. If the operator is invariant under translations, that is, if $\mathcal{L}$ has constant coefficients with respect to $\mathbf{r}$, then the Green function can be taken as the convolution [12],

$$\mathcal{G}(\mathbf{r}, \mathbf{x}) = \mathcal{G}(\mathbf{r} - \mathbf{x}) \ . \tag{6.100}$$

If such a function $\mathcal{G}$ can be found for the operator $\mathcal{L}$, then multiplying Eq. (6.99) for the Green function by $\varrho(\mathbf{x})$, and then integrating by the variable $\mathbf{x}$, we obtain:

$$\int \mathcal{L}\mathcal{G}(\mathbf{r}, \mathbf{x})\varrho(\mathbf{x})d^3x = \int \delta^3(\mathbf{r} - \mathbf{x})\varrho(\mathbf{x})d^3x = \varrho(\mathbf{r}) = \mathcal{L}u(\mathbf{r}) \ , \tag{6.101}$$

comparing the result with the Eq. (6.98). As we assume, that the operator $\mathcal{L} = \mathcal{L}(\mathbf{r})$ is linear and acts only on the variable $\mathbf{r}$ (and not on the integration variable $\mathbf{x}$), we can put $\mathcal{L}$ out of the integral on the right side. We conclude,

$$u(\mathbf{r}) = \int \mathcal{G}(\mathbf{r}, \mathbf{x})\varrho(\mathbf{x})d^3x \ . \tag{6.102}$$

Hence, we can obtain the function $u(\mathbf{r})$ from the Green function $\mathcal{G}(\mathbf{r}, \mathbf{x})$, determined by Eq. (6.99), and the source term $\varrho(\mathbf{x})$.

[12] In this case, the Green function is the same as the *pulse response* in the theory of time-independent linear systems.

The Green function, also called the fundamental solution associated with the operator $\mathcal{L}$, can be considered as the inversion of $\mathcal{L} \equiv \mathcal{G}^{-1}$. Not every operator $\mathcal{L}$ admits a Green function. In practice, not only calculating the Green function can be difficult for a particular operator, but also evaluating the integral in Eq. (6.102). In Exc. 6.3.8.8 we will get to know a Green function of the wave equation.

Example 61 (*Solving the Laplace equation by Green's method*): The Laplace equation is,

$$\nabla^2\Phi(\mathbf{r}) = -\varepsilon_0^{-1}\varrho(\mathbf{r}) \ .$$

The Green function,

$$\mathcal{G}(\mathbf{r},\mathbf{r}') = \mathcal{G}(\mathbf{r}-\mathbf{r}') = -\frac{1}{4\pi|\mathbf{r}-\mathbf{r}'|} \ ,$$

resolves the Poisson equation,

$$\nabla^2\mathcal{G}(\mathbf{r}-\mathbf{r}') = \delta^3(\mathbf{r}-\mathbf{r}') \ .$$

Therefore, the solution of the Laplace equation is,

$$\Phi(\mathbf{r}) = \frac{1}{4\pi\varepsilon_0}\int\frac{\varrho(\mathbf{r}')d^3r'}{|\mathbf{r}-\mathbf{r}'|} \ .$$

To solve the wave equations (6.90), we need to find the Green function for a spatio-temporal differential operator $\mathcal{L}(\mathbf{r},t) = \Box$. We will do this in the example 62, but for now, in the following section, we will adopt more empirical arguments.

6.3.4 Retarded potentials of continuous charge distributions

In the Lorentz gauge Φ and $\mathbf{A}$ satisfy the inhomogeneous wave equations (6.90) incorporating a 'source' term. We will use in the following exclusively the Lorentz gauge within which the entire electrodynamics comes down to solving (6.90).

But before that, let us take a look at the static situation, where the equations (6.90) reduce to Poisson equations,

$$\nabla^2\Phi = -\varepsilon_0^{-1}\varrho \qquad \text{and} \qquad \nabla^2\mathbf{A} = -\mu_0\mathbf{j} \ , \tag{6.103}$$

with the known solutions,

$$\Phi(\mathbf{r}) = \frac{1}{4\pi\varepsilon_0}\int\frac{\varrho(\mathbf{r}')}{|\mathbf{r}-\mathbf{r}'|}d^3r' \qquad \text{and} \qquad \mathbf{A}(\mathbf{r}) = \frac{\mu_0}{4\pi}\int\frac{\mathbf{j}(\mathbf{r}')}{|\mathbf{r}-\mathbf{r}'|}d^3r' \ . \tag{6.104}$$

In the dynamic case, the charge confined in the volume dV' (see Fig. 6.10) can move, but for the information on this movement to reach the point of observation $\mathbf{r}$ it takes a time determined by the propagation velocity of the light: $|\mathbf{r}-\mathbf{r}'|/c$. Introducing the distance R between the position of the charge and the observation point and the time retardation t_r by,

$$\mathbf{R} \equiv \mathbf{r}-\mathbf{r}' \qquad \text{and} \qquad t_r \equiv t - \tfrac{R}{c} \ , \tag{6.105}$$

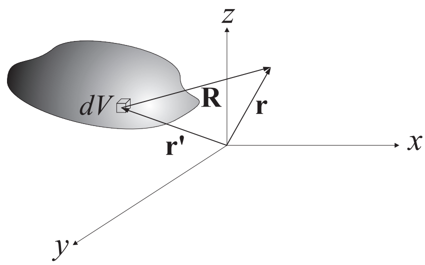

Figure 6.10: Geometry of source and the observation point.

we expect the following generalization of the equation (6.104),

$$\boxed{\Phi(\mathbf{r},t) = \frac{1}{4\pi\varepsilon_0}\int\frac{\varrho(\mathbf{r}',t_r)}{R}d^3r' \quad\text{and}\quad \mathbf{A}(\mathbf{r}) = \frac{\mu_0}{4\pi}\int\frac{\mathbf{j}(\mathbf{r}',t_r)}{R}d^3r'} \;, \tag{6.106}$$

called *retarded potential*.

The argument given above seems reasonable, but does not represent a stringent derivation, which will be given in the following. In fact, the same argument applied to the fields $\vec{\mathcal{E}}$ and $\vec{\mathcal{B}}$ would give false results, as we shall see later.

To verify the correctness of the assertion (6.106) we can simply show that it satisfies the wave equation (6.90) and the Lorentz gauge (6.89). However, this is not trivial, since the integral expressions depend on $\mathbf{r}$ explicitly (via the distance R in the denominator) and implicitly (via the retarded time t_d). Here, we present the calculation for the scalar potential,

$$\nabla_r\Phi(\mathbf{r}) = \frac{1}{4\pi\varepsilon_0}\int\nabla_r\frac{\varrho(\mathbf{r}',t-\frac{|\mathbf{r}-\mathbf{r}'|}{c})}{|\mathbf{r}-\mathbf{r}'|}d^3r' \tag{6.107}$$
$$= \frac{1}{4\pi\varepsilon_0}\int\left[\frac{1}{R}\nabla_r\varrho+\varrho\nabla_r\frac{1}{R}\right]d^3r' = \frac{1}{4\pi\varepsilon_0}\int\left[\frac{1}{R}\frac{-\dot\varrho}{c}\frac{\mathbf{R}}{R}+\varrho\frac{-\mathbf{R}}{R^3}\right]d^3r' \;.$$

The divergence of the gradient,

$$\nabla_r^2\Phi(\mathbf{r}) = \frac{1}{4\pi\varepsilon_0}\int\left[\frac{-\dot\varrho}{c}\left(\nabla_r\cdot\frac{\mathbf{R}}{R^2}\right)-\frac{\mathbf{R}}{R^2}\cdot\left(\frac{\nabla_r\dot\varrho}{c}\right)-(\nabla_r\varrho)\cdot\frac{\mathbf{R}}{R^3}-\varrho\left(\nabla_r\cdot\frac{\mathbf{R}}{R^3}\right)\right]d^3r'$$
$$= \frac{1}{4\pi\varepsilon_0}\int\left[\cancel{\frac{-\dot\varrho}{c}\frac{1}{R^2}}-\frac{\mathbf{R}}{R^2}\cdot\left(\frac{-\ddot\varrho\mathbf{R}}{c^2R}\right)-\cancel{\left(-\frac{\dot\varrho\mathbf{R}}{cR}\right)\cdot\frac{\mathbf{R}}{R^3}}-\varrho4\pi\delta^3(\mathbf{R})\right]d^3r'$$
$$= \frac{1}{4\pi\varepsilon_0}\int\left[\frac{\ddot\varrho}{c^2R}-4\pi\varrho\delta^3(\mathbf{R})\right]d^3r' = \frac{1}{c^2}\frac{\partial^2\Phi}{\partial t^2}-\frac{\varrho(\mathbf{r},t)}{\varepsilon_0} \;, \tag{6.108}$$

where we replaced in the last line the integral of $\ddot\varrho/c^2R$ by the expression (6.106), reproduces the wave equation. In Exc. 6.3.8.9 we verify that the retarded potentials (6.106) satisfy the Lorentz gauge.

It is interesting to note that the same calculation can be made for advanced times, where the potential would be affected by a *future* movement of the charge, $t_a = t + \frac{R}{c}$. But this would violate causality.

Example 62 (*Resolution of the wave equation by the Greens function*): We showed in the previous section that in the Lorentz gauge, given the sources ϱ and $\mathbf{j}$, all we have to do to find the scalar and vector potentials is to solve wave type differential equations (6.87),

$$\nabla^2\psi(\mathbf{r},t) - \frac{1}{c^2}\frac{\partial^2\psi(\mathbf{r},t)}{\partial t^2} = f(\mathbf{r},t) \ ,$$

where ψ is a variable to denote the fields Φ or $\mathbf{A}$ and f to denote the sources ϱ or $\mathbf{j}$. First, we want to find a particular solution of this equation. To this end, we use the Green function $\mathcal{G}(\mathbf{r},t,\mathbf{r}',t')$, which by definition satisfies,

$$\boxed{\nabla^2\mathcal{G}(\mathbf{r},t,\mathbf{r}',t') - \frac{1}{c^2}\frac{\partial^2}{\partial t^2}\mathcal{G}(\mathbf{r},t,\mathbf{r}',t') = \delta^{(3)}(\mathbf{r}-\mathbf{r}')\delta(t-t')} \ .$$

We can perform the Fourier transform with respect to the variable t and obtain,

$$\nabla^2 g(\mathbf{r},\omega,\mathbf{r}',t') + \frac{\omega^2}{c^2}g(\mathbf{r},\omega,\mathbf{r}',t') = \delta^{(3)}(\mathbf{r}-\mathbf{r}')\frac{e^{\imath\omega t'}}{2\pi} \ ,$$

where we used the integral representation of the Dirac delta function, i.e.,

$$\delta(t-t') = \frac{1}{2\pi}\int_{-\infty}^{\infty} e^{-\imath\omega(t-t')}d\omega$$

and we defined,

$$\mathcal{G}(\mathbf{r},t,\mathbf{r}',t') \equiv \int_{-\infty}^{\infty} e^{-\imath\omega t}g(\mathbf{r},\omega,\mathbf{r}',t')d\omega \ .$$

As we will explain later, instead of solving the above differential equation, we will modify it:

$$\nabla^2 g_\eta(\mathbf{r},\omega,\mathbf{r}',t') + (k_0+\imath\eta)^2 g_\eta(\mathbf{r},\omega,\mathbf{r}',t') = \delta^{(3)}(\mathbf{r}-\mathbf{r}')\frac{e^{\imath\omega t'}}{2\pi} \ ,$$

with $k_0 \equiv \omega/c$ assuming positive and negative values for ω: We can now take the Fourier transform with respect to the variable $\mathbf{r}$ and obtain,

$$-k^2\bar{g}_\eta(\mathbf{k},\omega,\mathbf{r}',t') + (k_0+\imath\eta)^2\bar{g}_\eta(\mathbf{k},\omega,\mathbf{r}',t') = \frac{e^{-\imath\mathbf{k}\cdot\mathbf{r}'+\imath\omega t'}}{(2\pi)^4} \ ,$$

where we used,

$$\delta^{(3)}(\mathbf{r}-\mathbf{r}') = \frac{1}{(2\pi)^3}\int_{\mathbb{R}^3} e^{\imath\mathbf{k}\cdot(\mathbf{r}-\mathbf{r}')}d^3k \ ,$$

and defined,

$$g_\eta(\mathbf{r},\omega,\mathbf{r}',t') \equiv \int e^{\imath\mathbf{k}\cdot\mathbf{r}}\bar{g}_\eta(\mathbf{k},\omega,\mathbf{r}',t')d^3k \ .$$

Hence,

$$\bar{g}_\eta(\mathbf{k},\omega,\mathbf{r}',t') = \frac{e^{-\imath\mathbf{k}\cdot\mathbf{r}'+\imath\omega t'}}{(2\pi)^4[-k^2+(k_0+\imath\eta)^2]} \ ,$$

and therefore,

$$g_\eta(\mathbf{r},\omega,\mathbf{r}',t') = \int \frac{e^{-\imath\mathbf{k}\cdot(\mathbf{r}-\mathbf{r}')+\imath\omega t'}}{(2\pi)^4[-k^2+(k_0+\imath\eta)^2]}d^3k \ .$$

Note that, if we had not modified the original equation (i.e. set $\eta = 0$), the integral above would not converge, and we could not find a Green function by the present method. Now, however, the Green function is,

$$\mathcal{G}_\eta(\mathbf{r}-\mathbf{r}', t-t') = \int_{-\infty}^{\infty} e^{-\imath\omega t} g_\eta(\mathbf{r},\omega,\mathbf{r}',t')d\omega = \int d^3k \int_{-\infty}^{\infty} d\omega \frac{e^{\imath\mathbf{k}\cdot(\mathbf{r}-\mathbf{r}')-\imath\omega(t-t')}}{(2\pi)^4[-k^2+(k_0+\imath\eta)^2]} \ ,$$

or yet,

$$\mathcal{G}_\eta(\mathbf{r},t) = \int d^3k \int_{-\infty}^{\infty} \frac{d\omega\ e^{\imath\mathbf{k}\cdot\mathbf{r}-\imath\omega t}}{(2\pi)^4[-k^2+(k_0+\imath\eta)^2]} = \frac{1}{(2\pi)^4}\int_{-\infty}^{\infty} d\omega e^{-\imath\omega t}\int \frac{d^3k\ e^{\imath\mathbf{k}\cdot\mathbf{r}}}{[k^2-(k_0+\imath\eta)^2]} \ .$$

In polar coordinates, choosing the orientation of the **k**-vector space such that k_z is parallel to the vector **r**,

$$\begin{aligned}\int d^3k \frac{e^{\imath\mathbf{k}\cdot\mathbf{r}}}{[k^2-(k_0+\imath\eta)^2]} &= \int_0^\infty k^2 dk \frac{1}{[k^2-(k_0+\imath\eta)^2]}\int_0^{2\pi} d\phi_k \int_0^\pi d\theta_k \sin\theta_k e^{\imath\mathbf{k}\cdot\mathbf{r}} \\ &= \int_0^\infty dk \frac{k^2}{[k^2-(k_0+\imath\eta)^2]}\int_0^{2\pi} d\phi_k \int_0^\pi d\theta_k \sin\theta_k e^{\imath kr\cos\theta_k} \\ &= \int_0^\infty dk \frac{2\pi k^2}{[k^2-(k_0+\imath\eta)^2]}\int_{-1}^{1} du e^{\imath kru} \\ &= \frac{2\pi}{\imath r}\int_0^\infty dk \frac{k}{[k^2-(k_0+\imath\eta)^2]}(e^{\imath kr}-e^{-\imath kr}) \ ,\end{aligned}$$

where we used the substitution $u \equiv \cos\theta_k$. Since,

$$\int_0^\infty dk \frac{ke^{-\imath kr}}{[k^2-(k_0+\imath\eta)^2]} = -\int_{-\infty}^0 dk \frac{ke^{\imath kr}}{[k^2-(k_0+\imath\eta)^2]} \ ,$$

we can write,

$$\int d^3k \frac{e^{\imath\mathbf{k}\cdot\mathbf{r}}}{[k^2-(k_0+\imath\eta)^2]} = \frac{2\pi}{\imath r}\int_{-\infty}^\infty dk \frac{ke^{\imath kr}}{[k^2-(k_0+\imath\eta)^2]} \ .$$

The poles of this integral are given by,

$$Z_\pm = \pm(k_0+\imath\eta) \ .$$

We consider the integral in the complex plane:

$$\oint_\mathcal{C} \frac{Ze^{\imath rZ}}{(Z-Z_+)(Z-Z_-)}dZ \ ,$$

where the contour is closed over the upper complex half-plane. When $\eta \to 0^+$ [see Fig. 6.11(a)], we get,

$$\oint_\mathcal{C} \frac{Ze^{\imath rZ}}{(Z-Z_+)(Z-Z_-)}dZ = 2\pi\imath\frac{Z_+e^{\imath rZ_+}}{Z-Z_+} = \imath\pi e^{\imath k_0 r} \ .$$

When $\eta \to 0^-$ [see Fig. 6.11(b)], we get,

$$\oint_\mathcal{C} \frac{Ze^{\imath rZ}}{(Z-Z_+)(Z-Z_-)}dZ = \imath\pi e^{-\imath k_0 r} \ .$$

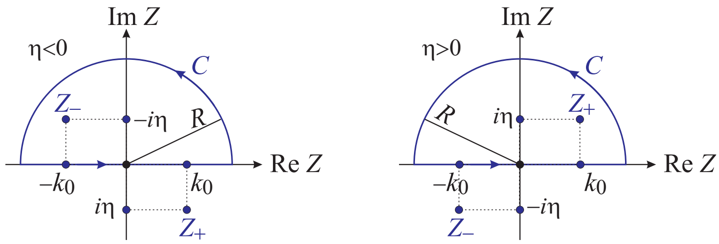

Figure 6.11: Illustration of the integration path.

But, with the closed contour over the upper complex half-plane,

$$\int_{-\infty}^{\infty} dk \frac{ke^{\imath kr}}{[k^2-(k_0+\imath\eta)^2]} = \oint_C \frac{Ze^{\imath rZ}}{(Z-Z_+)(Z-Z_-)} dZ = \imath\pi e^{\pm\imath k_0 r} \ .$$

With these results, we can conclude that,

$$\int d^3k \frac{e^{\imath \mathbf{k}\cdot\mathbf{r}}}{[k^2-(k_0+\imath\eta)^2]} = \frac{2\pi^2}{r} e^{\pm\imath k_0 r} \ ,$$

and hence,

$$\mathcal{G}_\pm(\mathbf{r},t) = -\frac{1}{(2\pi)^4}\int_{-\infty}^{\infty} d\omega e^{-\imath\omega t}\frac{2\pi^2}{r}e^{\pm\imath k_0 r} = -\frac{1}{8\pi^2 r}\int_{-\infty}^{\infty} d\omega e^{-\imath\omega(t\mp\frac{r}{c})} = -\frac{1}{4\pi r}\delta(t\mp\tfrac{r}{c}) \ .$$

Thus, we also have,

$$\mathcal{G}_\pm(\mathbf{r}-\mathbf{r}',t-t') = -\frac{1}{4\pi}\frac{1}{|\mathbf{r}-\mathbf{r}'|}\delta(t-t'\mp\tfrac{|\mathbf{r}-\mathbf{r}'|}{c}) \ .$$

There are, therefore, two possible solutions to the problem:

$$\psi(\mathbf{r},t) = \int d^3r' \int_{-\infty}^{\infty} dt' \mathcal{G}_\pm(\mathbf{r}-\mathbf{r}',t-t') f(\mathbf{r}',t')$$
$$= -\frac{1}{4\pi}\int \frac{d^3r'}{|\mathbf{r}-\mathbf{r}'|}\int_{-\infty}^{\infty} dt'\delta(t'-t\pm\tfrac{|\mathbf{r}-\mathbf{r}'|}{c}) f(\mathbf{r}',t') = -\frac{1}{4\pi}\int d^3r' \frac{f(\mathbf{r}',t\mp\frac{|\mathbf{r}-\mathbf{r}'|}{c})}{|\mathbf{r}-\mathbf{r}'|} \ .$$

In this case, we will use retarded rather than advanced solutions, i.e.,

$$\Phi(\mathbf{r},t) = \frac{1}{4\pi\varepsilon_0}\int \frac{\varrho(\mathbf{r}',t-\frac{|\mathbf{r}-\mathbf{r}'|}{c})}{|\mathbf{r}-\mathbf{r}'|} d^3\mathbf{r}' \quad \text{and} \quad \mathbf{A}(\mathbf{r},t) = \frac{\mu_0}{4\pi}\int \frac{\mathbf{j}(\mathbf{r}',t-\frac{|\mathbf{r}-\mathbf{r}'|}{c})}{|\mathbf{r}-\mathbf{r}'|} d^3\mathbf{r}' \ .$$

6.3.5 Retarded fields in electrodynamics and Jefimenko's equations

From the retarded potentials (6.106) we can determine the fields through equations (6.78),

$$\vec{\mathcal{E}}(\mathbf{r},t) = -\nabla_r\Phi - \frac{\partial \mathbf{A}}{\partial t} = -\frac{1}{4\pi\varepsilon_0}\int\left[\frac{1}{R}\frac{-\dot\varrho}{c}\frac{\mathbf{R}}{R} + \varrho\frac{-\mathbf{R}}{R^3}\right] d^3r' - \frac{\mu_0}{4\pi}\int\frac{\dot{\mathbf{j}}(\mathbf{r}',t_r)}{R} d^3r' \ ,$$

using the result (6.107). With $c^2 = 1/\varepsilon_0\mu_0$ we obtain the time-dependent generalization of Coulomb's law,

$$\boxed{\vec{\mathcal{E}}(\mathbf{r},t) = \frac{1}{4\pi\varepsilon_0}\int\left[\frac{\varrho(\mathbf{r}',t_r)}{R^2}\hat{\mathbf{e}}_R + \frac{\dot{\varrho}(\mathbf{r}',t_r)}{cR}\hat{\mathbf{e}}_R - \frac{\dot{\mathbf{j}}(\mathbf{r}',t_r)}{c^2R}\right]d^3r'} \ . \tag{6.109}$$

In static situations the second and third term cancel, $\varrho(\mathbf{r}',t') = \varrho(\mathbf{r}')$ becomes independent of time, and we recover the electrostatic Coulomb law.

We now calculate the magnetic field via the rotation,

$$\vec{\mathcal{B}}(\mathbf{r},t) = \nabla_r\times\mathbf{A} = \frac{\mu_0}{4\pi}\int\left[\frac{1}{R}(\nabla_r\times\mathbf{j}) - \mathbf{j}\times\nabla_r\left(\frac{1}{R}\right)\right]d^3r' \ . \tag{6.110}$$

With,

$$\begin{aligned}[\nabla_r\times\mathbf{j}(\mathbf{r}',t-\tfrac{R}{c})]_x &= \frac{\partial j_z}{\partial y} - \frac{\partial j_y}{\partial z} = \dot{j}_z\frac{\partial t_r}{\partial y} - \dot{j}_y\frac{\partial t_r}{\partial z} \\ &= -\frac{1}{c}\left(\dot{j}_z\frac{\partial R}{\partial y} - \dot{j}_y\frac{\partial R}{\partial z}\right) = \left[\frac{1}{c}\dot{\mathbf{j}}\times\nabla_r R\right]_x = \left[\frac{1}{c}\dot{\mathbf{j}}\times\frac{\mathbf{R}}{R}\right]_x \ .\end{aligned} \tag{6.111}$$

Thus, the time-dependent generalization of the Biot-Savart law is,

$$\boxed{\vec{\mathcal{B}}(\mathbf{r},t) = \frac{\mu_0}{4\pi}\int\left[\frac{\mathbf{j}(\mathbf{r}',t_r)}{R^2} + \frac{\dot{\mathbf{j}}(\mathbf{r}',t_r)}{cR}\right]\times\frac{\mathbf{R}}{R}d^3r'} \ . \tag{6.112}$$

The equations (6.109) and (6.112) are the (causal) solutions of Maxwell's equations published by *Jefimenko* in 1966. In practice, these equations are of limited utility, since it is usually easier to calculate the retarded potentials, instead of going directly to the fields. However, they provide the satisfying sensation of a closed theory. We note that the simple replacement of the times t by t_r made for the potentials in (6.106) does not apply to the fields, as it would only produce the first terms of Jefimenko's expressions.

In the Excs. 6.3.8.10 and 6.3.8.11 we evaluate the fields for slow current variations.

6.3.6 The Liénard-Wiechert potentials

The goal now is to calculate the retarded electromagnetic potentials produced by a moving point charge q along a predefined path $\mathbf{w}(t)$. The presence of the charge at a time t_r at a point $\mathbf{w}(t_r)$, called the *retarded position* of this trajectory, has an impact on an arbitrary point of space $\mathbf{r}$ at a time t given by,

$$t = t_r + \tfrac{|\mathbf{r}-\mathbf{w}(t_r)|}{c} \ . \tag{6.113}$$

At a given instant of time t, the potentials $\Phi(\mathbf{r},t)$ and $\mathbf{A}(\mathbf{r},t)$ evaluated at the point $\mathbf{r}$ *depend only on a single point* of the trajectory $\mathbf{w}(t_r)$ occupied by the charge in the past. The equation (6.106) now allows you to calculate the potentials. For a given trajectory $\mathbf{w}(t')$ the charge and current densities are parametrized by,

$$\boxed{\varrho(\mathbf{r}',t') = q\delta^3(\mathbf{r}'-\mathbf{w}(t')) \qquad \text{and} \qquad \mathbf{j}(\mathbf{r}',t') = \mathbf{v}\varrho(\mathbf{r}',t')} \ . \tag{6.114}$$

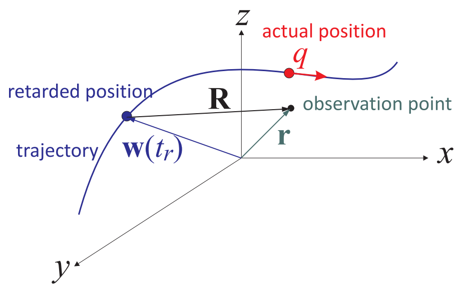

Figure 6.12: Retardation of potentials.

However, we need the density at the retarded time t_r [13],

$$\varrho(\mathbf{r}',t_r)=q\int\delta^3(\mathbf{r}'-\mathbf{w}(t'))\delta(t'-t_r)dt' \ . \tag{6.115}$$

We obtain,

$$\begin{aligned}\Phi(\mathbf{r},t)&=\frac{q}{4\pi\varepsilon_0}\int\frac{\varrho(\mathbf{r}',t_r)}{|\mathbf{r}-\mathbf{r}'|}d^3r'=\frac{q}{4\pi\varepsilon_0}\int\int\frac{\delta^3(\mathbf{r}'-\mathbf{w}(t'))}{|\mathbf{r}-\mathbf{r}'|}\delta(t'-t_r)d^3r'dt' \\ &=\frac{q}{4\pi\varepsilon_0}\int\frac{1}{|\mathbf{r}-\mathbf{w}(t')|}\delta(t'-(t-\tfrac{|\mathbf{r}-\mathbf{w}(t')|}{c}))dt' \ ,\end{aligned} \tag{6.116}$$

where spatial integration replaced $\mathbf{r}'=\mathbf{w}(t')$.

To evaluate a function $\delta(g(x))$ which depends on another function $g(x)$, we make the substitution,

$$u\equiv g(x) \qquad \text{with} \qquad du=\tfrac{dg}{dx}dx \ , \tag{6.117}$$

such that,

$$\int\delta(g(x))dx=\int\frac{\delta(u)}{|dg/dx|}du=\frac{1}{\left|\frac{dg(x_0)}{dx}\right|} \ , \tag{6.118}$$

where x_0 is defined by $u=g(x_0)=0$. Applied to our problem, we identify,

$$u=g(t')=t'-\left(t-\tfrac{|\mathbf{r}-\mathbf{w}(t')|}{c}\right)=t'-t_r \ . \tag{6.119}$$

That is, the time when $u=g(t')=0$ is simply $t'=t_r$. Now, the time derivative is,

$$\frac{dg}{dt'}=1+\frac{1}{c}\frac{d}{dt'}|\mathbf{r}-\mathbf{w}(t')|=1-\frac{\mathbf{v}(t')}{c}\cdot\frac{\mathbf{r}-\mathbf{w}(t')}{|\mathbf{r}-\mathbf{w}(t')|} \ , \tag{6.120}$$

with $\mathbf{v}\equiv\dot{\mathbf{w}}$. With this, the expression (6.116) becomes,

$$\Phi=\frac{q}{4\pi\varepsilon_0}\int\frac{1}{|\mathbf{r}-\mathbf{w}(t')|}\frac{\delta(u)}{\left|\frac{dg}{dt'}\right|}du=\frac{q}{4\pi\varepsilon_0}\frac{1}{|\mathbf{r}-\mathbf{w}(t_r)|}\frac{1}{|1-\frac{\mathbf{v}(t_r)}{c}\cdot\frac{\mathbf{r}-\mathbf{w}(t_r)}{|\mathbf{r}-\mathbf{w}(t_r)|}|} \ , \tag{6.121}$$

[13] Can not simply replace $t'\to t_r$ in the argument of $\mathbf{w}(t')$, because t_r implicitly depends on $\mathbf{w}(t')$ via the expression (6.113).

where the application of the $\delta(u)$ function comes down to replacing t' by t_r. Finally, recalling the abbreviation $\mathbf{R} \equiv \mathbf{r} - \mathbf{w}(t_r)$,

$$\boxed{\Phi(\mathbf{r},t) = \frac{1}{4\pi\varepsilon_0}\frac{qc}{Rc - \mathbf{R}\cdot\mathbf{v}}} \quad \text{and} \quad \boxed{\mathbf{A}(\mathbf{r},t) = \frac{\mu_0}{4\pi}\frac{qc\mathbf{v}}{Rc - \mathbf{R}\cdot\mathbf{v}} = \frac{\mathbf{v}}{c^2}\Phi(\mathbf{r},t)} , \tag{6.122}$$

where the vector potential is obtained in an analogous way. These are the so-called *Liénard-Wiechert potentials* [14]. In Exc. 6.3.8.12 we calculate the potentials of a point charge in uniform motion.

6.3.7 The fields of a moving point charge

Fields produced by a moving point charge are calculated from the potentials (6.122) using (6.78). The calculation is complicated, because we must evaluate both, distance and speed,

$$\mathbf{R} = \mathbf{r} - \mathbf{w}(t_r) \quad \text{and} \quad \mathbf{v} = \dot{\mathbf{w}}(t_r) \tag{6.123}$$

at the retarded time, which is implicitly defined by the equation,

$$R = |\mathbf{r} - \mathbf{w}(t_r)| = c(t - t_r) \; . \tag{6.124}$$

We start with the gradient of the scalar potential (6.122),

$$\nabla\Phi = \frac{qc}{4\pi\varepsilon_0}\frac{-1}{(Rc - \mathbf{R}\cdot\mathbf{v})^2}\nabla(Rc - \mathbf{R}\cdot\mathbf{v}) \; , \tag{6.125}$$

and evaluate both terms separately. Using (6.124) we find,

$$\nabla(Rc) = -c^2\nabla t_r \; , \tag{6.126}$$

where we leave the calculation of the gradient of retarded time for later. Also, using the rule (10.88)(ix), we find,

$$\nabla(\mathbf{R}\cdot\mathbf{v}) = (\mathbf{R}\cdot\nabla)\mathbf{v} + (\mathbf{v}\cdot\nabla)\mathbf{R} + \mathbf{R}\times(\nabla\times\mathbf{v}) + \mathbf{v}\times(\nabla\times\mathbf{R}) \; . \tag{6.127}$$

The first term of this expression gives,

$$(\mathbf{R}\cdot\nabla)\mathbf{v}(t_r) = R_x\frac{\partial t_r}{\partial x}\frac{d\mathbf{v}}{dt_r} + R_y\frac{\partial t_r}{\partial y}\frac{d\mathbf{v}}{dt_r} + R_z\frac{\partial t_r}{\partial z}\frac{d\mathbf{v}}{dt_r} = \mathbf{a}(\mathbf{R}\cdot\nabla t_r) \; , \tag{6.128}$$

where $\mathbf{a} \equiv \dot{\mathbf{v}}$ is the acceleration at the retarded time. The second term is,

$$(\mathbf{v}\cdot\nabla)\mathbf{R} = (\mathbf{v}\cdot\nabla)\mathbf{r} - (\mathbf{v}\cdot\nabla)\mathbf{w} = \mathbf{v} - \mathbf{v}(\mathbf{v}\cdot\nabla t_r) \; . \tag{6.129}$$

Now, using,

$$\nabla\times\mathbf{v} = \left(\frac{\partial t_r}{\partial y}\frac{dv_z}{dt_r} - \frac{\partial t_r}{\partial z}\frac{dv_y}{dt_r}\right)\hat{\mathbf{e}}_x + ... = -\mathbf{a}\times\nabla t_r \; , \tag{6.130}$$

[14] We get the same result from the argument, that light needs a finite time to cross the volume of the charge distribution $d^3r' = dV'$, such that the volume appears stretched at the time instant t_r, $dV' \longrightarrow \frac{dV'}{1-\hat{\mathbf{e}}_r\cdot\mathbf{v}/c}$.

the third term becomes,

$$\mathbf{R} \times (\nabla \times \mathbf{v}) = -\mathbf{R} \times (\mathbf{a} \times \nabla t_r) \ . \tag{6.131}$$

Finally, using,

$$\nabla \times \mathbf{R} = \cancelto{0}{\nabla \times \mathbf{r}} - \nabla \times \mathbf{w} = \mathbf{v} \times \nabla t_r \ , \tag{6.132}$$

the fourth term is,

$$\mathbf{v} \times (\nabla \times \mathbf{R}) = \mathbf{v} \times (\mathbf{v} \times \nabla t_r) \ . \tag{6.133}$$

With these results the expression (6.127) becomes,

$$\begin{aligned}\nabla(\mathbf{R} \cdot \mathbf{v}) &= \mathbf{a}(\mathbf{R} \cdot \nabla t_r) + \mathbf{v} - \mathbf{v}(\mathbf{v} \cdot \nabla t_r) - \mathbf{R} \times (\mathbf{a} \times \nabla t_r) + \mathbf{v} \times (\mathbf{v} \times \nabla t_r) \\ &= \mathbf{v} + (\mathbf{R} \cdot \mathbf{a} - v^2)\nabla t_r \ ,\end{aligned} \tag{6.134}$$

using in the last step the rule $\mathbf{A} \times (\mathbf{B} \times \mathbf{C}) = \mathbf{B}(\mathbf{A} \cdot \mathbf{C}) - \mathbf{C}(\mathbf{A} \cdot \mathbf{B})$. Now, we calculate ∇t_r,

$$\begin{aligned}\nabla t_r &= -\tfrac{1}{c}\nabla R = -\tfrac{1}{c}\nabla\sqrt{\mathbf{R} \cdot \mathbf{R}} = -\frac{1}{2c\sqrt{\mathbf{R} \cdot \mathbf{R}}}\nabla(\mathbf{R} \cdot \mathbf{R}) \\ &= -\frac{1}{cR}[(\mathbf{R} \cdot \nabla)\mathbf{R} \ + \ \mathbf{R} \times (\nabla \times \mathbf{R})] \\ &= -\frac{1}{cR}[(\mathbf{R} \cdot \nabla)\mathbf{r} - (\mathbf{R} \cdot \nabla)\mathbf{w} \ + \ \mathbf{R} \times (\nabla \times \mathbf{R})] \\ &= -\frac{1}{cR}[\mathbf{R} - \mathbf{v}(\mathbf{R} \cdot \nabla t_r) \ + \ \mathbf{R} \times (\mathbf{v} \times \nabla t_r)] = -\frac{1}{cR}[\mathbf{R} - (\mathbf{R} \cdot \mathbf{v})\nabla t_r)] \ .\end{aligned} \tag{6.135}$$

To get $(\mathbf{R} \cdot \nabla)\mathbf{w}$ we did a calculation similar to (6.128) and $\nabla \times \mathbf{R}$ was already calculated in (6.132). Solving the result (6.135) by ∇t_r,

$$\nabla t_r = -\frac{\mathbf{R}}{cR - \mathbf{R} \cdot \mathbf{v}} \ . \tag{6.136}$$

Finally, the gradient of the scalar potential (6.125) is,

$$\nabla\Phi = \frac{1}{4\pi\varepsilon_0}\frac{qc}{(cR - \mathbf{R} \cdot \mathbf{v})^3}\left[(cR - \mathbf{R} \cdot \mathbf{v})\mathbf{v} - (c^2 - v^2 + \mathbf{R} \cdot \mathbf{a})\mathbf{R}\right] \ . \tag{6.137}$$

A similar calculation for the temporal derivative of the vector potential gives the result,

$$\frac{\partial \mathbf{A}}{\partial t} = \frac{1}{4\pi\varepsilon_0}\frac{qc}{(cR - \mathbf{R} \cdot \mathbf{v})^3}\left[(cR - \mathbf{R} \cdot \mathbf{v})(-\mathbf{v} + \frac{R}{c}\mathbf{a}) + \frac{R}{c}(c^2 - v^2 + \mathbf{R} \cdot \mathbf{a})\mathbf{v}\right] \ . \tag{6.138}$$

The rotation of the vector potential yields,

$$\begin{aligned}\nabla \times \mathbf{A} &= \frac{1}{c^2}\nabla \times (\Phi\mathbf{v}) = \frac{1}{c^2}[\Phi(\nabla \times \mathbf{v}) - \mathbf{v}(\nabla\Phi)] \\ &= -\frac{1}{c}\frac{q}{4\pi\varepsilon_0}\frac{1}{(\mathbf{R} \cdot \mathbf{u})^3}\mathbf{R} \times [(c^2 - v^2)\mathbf{v} + (\mathbf{R} \cdot \mathbf{a})\mathbf{v} + (\mathbf{R} \cdot \mathbf{u})\mathbf{a}] \ ,\end{aligned} \tag{6.139}$$

using the expressions (6.130) and (6.137) and introducing the abbreviation $\mathbf{u} \equiv c\hat{\mathbf{e}}_R - \mathbf{v}$.

Combining these results with equations (6.78), we find the fields,

$$\boxed{\vec{\mathcal{E}}(\mathbf{r},t) = \frac{q}{4\pi\varepsilon_0}\frac{R}{(\mathbf{R}\cdot\mathbf{u})^3}[(c^2-v^2)\mathbf{u} + \mathbf{R}\times(\mathbf{u}\times\mathbf{a})]}\ , \tag{6.140}$$

and,

$$\boxed{\vec{\mathcal{B}}(\mathbf{r},t) = \tfrac{1}{c}\hat{\mathbf{e}}_R \times \vec{\mathcal{E}}(\mathbf{r},t)}\ . \tag{6.141}$$

Obviously, the magnetic field of a point charge is always perpendicular to the electric field and to the vector of the retarded point. The first term in $\vec{\mathcal{E}}$ (involving $(c^2-v^2)\cdot\mathbf{u}$) falls off like $1/R^2$. If the velocity $\mathbf{v}$ and the acceleration $\mathbf{a}$ were zero, this term survives and reduces to the old electrostatic result (2.3). For this reason, this term is called the generalized Coulomb field. The second term (involving $\mathbf{R}\times(\mathbf{u}\times\mathbf{a})$) falls off like $1/R$ and thus becomes dominant at large distances. As we will see in Sec. 8.4, this is the term responsible for electromagnetic radiation.

Knowing the fields generated by the moving charge q we can, by the laws of the *Coulomb force* and the *Lorentz force*, determine the force acting on a test particle Q located at $\mathbf{r}$ and moving with velocity $\mathbf{V}$,

$$\begin{aligned}\mathbf{F}(\mathbf{r},t) = \frac{qQ}{4\pi\varepsilon_0}\frac{R}{(\mathbf{R}\cdot\mathbf{u})^3}\Big\{&[(c^2-v^2)\mathbf{u} + \mathbf{R}\times(\mathbf{u}\times\mathbf{a})] \\ &+ \frac{\mathbf{V}}{c}\times\left[\hat{\mathbf{e}}_R\times[(c^2-v^2)\mathbf{u}+\mathbf{R}\times(\mathbf{u}\times\mathbf{a})]\right]\Big\}\ ,\end{aligned} \tag{6.142}$$

where $\mathbf{r}$, $\mathbf{u}$, $\mathbf{v}$, and $\mathbf{a}$ are all evaluated at the retarded time. The entire classical electrodynamics is contained in this equation because, since the charge is quantized, we can apply the superposition principle and calculate the impact of any charge distribution on a test particle Q. However, in view of the complexity of (6.142), the necessary effort seems huge. The scheme 6.13 summarizes the fundamental laws of electrodynamics.

Resolve the Excs. 6.3.8.13 to 6.3.8.16.

Example 63 (*Electric and magnetic fields generated by a uniformly moving charge*): Letting $\mathbf{a} = 0$ in (6.140),

$$\vec{\mathcal{E}}(\mathbf{r},t) = \frac{q}{4\pi\varepsilon_0}\frac{R}{(\mathbf{R}\cdot\mathbf{u})^3}(c^2-v^2)\mathbf{u}\ ,$$

we can express the position of the charge at the retarded time by its constant velocity, $\dot{\mathbf{w}} = \mathbf{v}$. We calculate using the definition of $\mathbf{u}$,

$$R\mathbf{u} = c\mathbf{R} - R\mathbf{v} = c\mathbf{R} - R\dot{\mathbf{w}} = c(\mathbf{r} - \mathbf{v}t_r) - c(t-t_r)\mathbf{v} = c(\mathbf{r}-\mathbf{v}t)\ .$$

The square of the relationship $|\mathbf{r} - \mathbf{v}t_r| = c(t-t_r)$ resolved by t_r gives,

$$t_r = \frac{(c^2t - \mathbf{r}\cdot\mathbf{v}) \pm \sqrt{(c^2t-\mathbf{r}\cdot\mathbf{v})^2 + (c^2-v^2)(r^2-c^2t^2)}}{c^2-v^2}\ ,$$

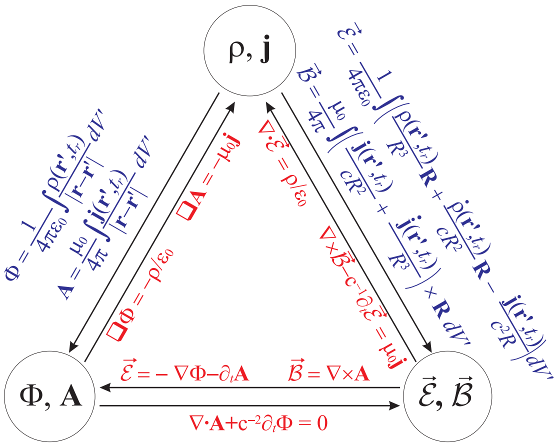

Figure 6.13: Organization chart of the fundamental laws of electrodynamics. Compare with the corresponding charts in electrostatics Fig. 2.9 and magnetostatics Fig. 4.13.

where we only consider the sign $-$. With this we calculate,

$$\begin{aligned}\mathbf{R}\cdot\mathbf{u} &= Rc - \mathbf{R}\cdot\mathbf{v} = c^2(t-t_r) - (\mathbf{r}-\mathbf{v}t_r)\cdot\mathbf{v} = c^2t - \mathbf{r}\cdot\mathbf{v} - (c^2-v^2)t_r \\ &= \sqrt{(c^2t-\mathbf{r}\cdot\mathbf{v})^2 + (c^2-v^2)(r^2-c^2t^2)} \\ &= \sqrt{(c^2-v^2)(\mathbf{r}-\mathbf{v}t)^2 + [(\mathbf{r}-\mathbf{v}t)\cdot\mathbf{v}]^2} \\ &= \sqrt{(c^2-v^2)d^2 + (\mathbf{d}\cdot\mathbf{v})^2} = d\sqrt{c^2-v^2+v^2\cos^2\theta} = dc\sqrt{1-\tfrac{v^2}{c^2}\sin^2\theta}\ ,\end{aligned}$$

where the abbreviation $\mathbf{d}\equiv\mathbf{r}-\mathbf{v}t$ is the vector between $\mathbf{r}$ and the *actual position* of the particle and θ is the angle between $\mathbf{d}$ and $\mathbf{v}$. Then,

$$\vec{\mathcal{E}}(\mathbf{r},t) = \frac{q}{4\pi\varepsilon_0}\frac{1-v^2/c^2}{(1-\frac{v^2}{c^2}\sin^2\theta)^{3/2}}\frac{\hat{\mathbf{e}}_d}{d^2}\ .$$

Note that $\vec{\mathcal{E}}$ points along the distance $\mathbf{d}$. This is an extraordinary coincidence; after all, the 'message' came from the retarded position. Because of the $\sin^2\theta$ in the denominator, the field of a charge moving fast is flattened like a pancake in the direction perpendicular to the motion (see Fig. 6.14). In the forward and backward directions $\vec{\mathcal{E}}$ is reduced by a factor $(1-v^2/c^2)$ with respect to the field of a charge at rest; in the perpendicular direction is amplified by a factor $1/\sqrt{1-v^2/c^2}$.
To get $\vec{\mathcal{B}}$ we calculate,

$$\hat{\mathbf{e}}_R = \frac{\mathbf{r}-\mathbf{v}t_r}{R} = \frac{(\mathbf{r}-\mathbf{v}t)+(t-t_r)\mathbf{v}}{R} = \frac{\mathbf{d}}{R}+\frac{\mathbf{v}}{c}\ ,$$

and hence,

$$\vec{\mathcal{B}} = \tfrac{1}{c}(\hat{\mathbf{e}}_R\times\vec{\mathcal{E}}) = \tfrac{1}{c^2}(\mathbf{v}\times\vec{\mathcal{E}})\ .$$

The $\vec{\mathcal{B}}$-field lines form circles around the charge, as shown in Fig. 6.14. At low velocities, $v\ll c$,

$$\vec{\mathcal{E}}(\mathbf{r},t) = \frac{q}{4\pi\varepsilon_0}\frac{\mathbf{d}}{d^2} \quad , \quad \vec{\mathcal{B}} = \frac{\mu_0 q}{4\pi}\frac{\mathbf{v}\times\hat{\mathbf{e}}_d}{d^2}\ .$$

we recover the laws of Coulomb and Biot-Savart for point charges.

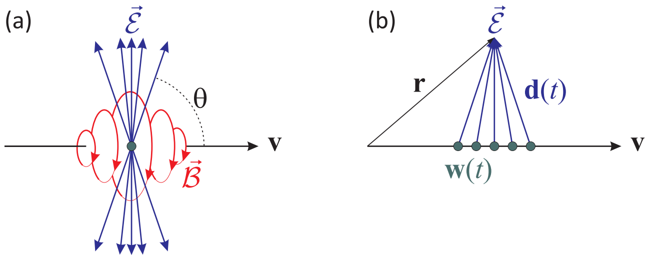

Figure 6.14: (a) Electric and magnetic field generated by of a point charge in uniform motion. (b) Electric field seen from an observation point **r** fixed in space.

6.3.8 Exercises

6.3.8.1 Ex: Potentials, fields and the Lorentz gauge

Consider a scalar field and a vector field of the form,

$$\Phi(\mathbf{r},t) = cd\frac{\mathbf{r}\cdot\hat{\mathbf{e}}_z}{r^3}e^{\imath\omega t} \qquad \text{and} \qquad \mathbf{A}(\mathbf{r},t) = \imath kd\frac{e^{\imath kr}}{r}e^{\imath\omega t}\ \hat{\mathbf{e}}_z \ .$$

where $k = \omega/c$.
a. Calculate the corresponding fields $\vec{\mathcal{B}}$ and $\vec{\mathcal{E}}$.
b. Show that for small r the given potentials satisfy the Lorentz gauge.

6.3.8.2 Ex: Fields, potentials, and the gauge transformation

Find the charge and current distributions producing the following potential,

$$\Phi(\mathbf{r},t) = 0 \qquad \text{and} \qquad \mathbf{A}(\mathbf{r},t) = \frac{\mu_0 k}{4c}(ct-|x|)^2\hat{\mathbf{e}}_z\ \Theta(|x|-ct) \ ,$$

where $k = const$.

6.3.8.3 Ex: Fields derived from potentials

Show that the differential equations for Φ and $\mathbf{A}$ can be written in a more symmetric form as,

$$\Box\Phi + \frac{\partial L}{\partial t} = -\frac{\varrho}{\varepsilon_0} \qquad \text{and} \qquad \Box\mathbf{A} - \nabla L = -\mu_0\mathbf{j} \ ,$$

where $L \equiv \nabla\cdot\mathbf{A} + \varepsilon_0\mu_0\frac{\partial\Phi}{\partial t}$.

6.3.8.4 Ex: Fields derived from potentials

a. Find the fields and the charge and current distributions corresponding to,

$$\Phi(\mathbf{r},t) = 0 \qquad \text{and} \qquad \mathbf{A}(\mathbf{r},t) = -\frac{1}{4\pi\varepsilon_0}\frac{qt}{r^2}\hat{\mathbf{e}}_r \ .$$

b. Use the gauge function $\chi = -\frac{1}{4\pi\varepsilon_0}\frac{qt}{r}$ to transform the potentials in (a), and comment the result.
c. Check whether the potentials are in the Lorentz or in the Coulomb gauge.

6.3.8.5 Ex: Fields derived from potentials

a. Suppose $\Phi = 0$ and $\mathbf{A} = A_0 \sin(kx - \omega t)\hat{\mathbf{e}}_y$, where A_0, ω, and k are constants. Find $\vec{\mathcal{E}}$ and $\vec{\mathcal{B}}$, and verify, that they satisfy Maxwell's equations in vacuum. What conditions should be imposed to ω and k?
b. Check whether the potentials are in the Lorentz or in the Coulomb gauge.

6.3.8.6 Ex: Other gauges

Check the viability of a gauge defined by $\Phi \equiv 0$ and a gauge defined by $\mathbf{A} \equiv 0$.

6.3.8.7 Ex: Coulomb gauge

a. Show that the vector potential can be expressed by the magnetic field as,

$$\mathbf{A}(\mathbf{r}, t) = \nabla \times \int \frac{\vec{\mathcal{B}}(\mathbf{r}', t)}{4\pi|\mathbf{r} - \mathbf{r}'|} d^3r' \ .$$

Show that, given by this expression, the potential vector satisfies the Coulomb gauge.
b. Show that for uniform and constant magnetic fields,

$$\mathbf{A}(\mathbf{r}, t) = -\tfrac{1}{2}\mathbf{r} \times \vec{\mathcal{B}} \ .$$

Why can't you use the formula in (a) to solve the problem?

6.3.8.8 Ex: Green function

Show that $G(\mathbf{r}, \mathbf{r}') = \frac{e^{\imath k|\mathbf{r}-\mathbf{r}'|}}{4\pi|\mathbf{r}-\mathbf{r}'|}$ is the Green function of the operator $\mathcal{L} = \nabla^2 + k^2$.

6.3.8.9 Ex: Gauge of retarded potentials

Confirm, that retarded potentials (6.106) are in the Lorentz gauge.

6.3.8.10 Ex: Jefimenko with constant current

Suppose that $\mathbf{j}(\mathbf{r})$ is constant in time, such that $\varrho(\mathbf{r}, t) = \varrho(\mathbf{r}, 0) + \dot{\varrho}(\mathbf{r}, 0)t$. Demonstrate the validity of Coulomb's law with the charge density evaluated at the *non-retarded* time.

6.3.8.11 Ex: Jefimenko with slowly varying current

Suppose a current density varying sufficiently slowly so that we can ignore all higher derivatives of the Taylor expansion $\mathbf{j}(\mathbf{r}, t_r) = \mathbf{j}(\mathbf{r}, t) + (t_r - t)\dot{\mathbf{j}}(\mathbf{r}, t_r) + \ldots$. Demonstrate the validity of the Biot-Savart law with the charge density evaluated at the *non-retarded* time. This means that the quasi-static approximation is much better than could have expected.

6.3.8.12 Ex: Potentials of a point charge in uniform motion

a. Calculate the potentials (6.122) produced by the uniform motion, $w(t) = \mathbf{v}t$, of a charge q.
b. Verify that these potentials satisfy the Lorentz gauge.

6.3.8.13 Ex: Liénard-Wiechert potentials for a rotating charge

A particle of charge q moves circularly with constant angular velocity ω in the center of the x-y-plane. At time $t = 0$ the charge is at the position $(a, 0)$. Find the Liénard-Wiechert potentials for the points of the z-axis.

6.3.8.14 Ex: Point charge moving on a straight line

Assume that a point charge q is constrained to move along the x-axis. Calculate the fields at points on the axis in front of and behind the charge.

6.3.8.15 Ex: Charge on a hyperbolic motion

Determine the Liénard-Wiechert potentials for a charge on a hyperbolic motion, i.e. $\mathbf{w}(t) = \hat{\mathbf{e}}_x\sqrt{b^2 + c^2t^2}$.

6.3.8.16 Ex: Actio=reactio with the Lorentz force

Suppose that two charges in uniform motion, the first one along the x-axis and the second along the y-axis, are at the origin at time $t = 0$. Calculate the reciprocal Coulomb-Lorentz forces.

6.4 Further reading

J.D. Jackson, *Classical Electrodynamics* [ISBN]

D.J. Griffiths, *Introduction to Electrodynamics* [ISBN]

Chapter 7

Electromagnetic waves

The phenomenon of waves is usually introduced in undergraduate Physics courses. We already discussed that, unlike classical longitudinal or transverse waves, *electromagnetic waves* do not require a propagation medium, but move through the vacuum with the speed of light. And we showed that the wave equation is form-invariant to the Lorentz, but not to the Galilei transform [1].

The electromagnetic waves are generated when charges change their positions. Therefore, the theory of electromagnetic waves is also a consequence of electrodynamic theory, which is summarized in the *Maxwell equations*. In this chapter we will consider these equations as given and deduce from them the properties of electromagnetic waves.

7.1 Wave propagation

By *wave* we mean the propagation of a perturbation $f(\mathbf{r},t)$, which can be a scalar or vector quantity. When it propagates in one dimension, the wave is described by the *wave equation*,

$$\frac{\partial^2 f}{\partial z^2} = \frac{1}{v^2}\frac{\partial^2 f}{\partial t^2} \;, \tag{7.1}$$

where v is the propagation velocity of the wave. The most common waveform is the sine wave,

$$f(z,t) = A\cos(kz-\omega t+\delta) = \mathfrak{Re}\;[\tilde{A}e^{\imath(kz-\omega t)}] = \mathfrak{Re}\;\tilde{f}(z,t) \;, \tag{7.2}$$

in complex notation (often ornamented by a tilde) introducing the complex amplitude $\tilde{A} \equiv Ae^{\imath\delta}$. The wave equation satisfies the superposition principle allowing for the expansion of any wave type according to,

$$\tilde{f}(z,t) = \int_{-\infty}^{\infty} \tilde{A}(k)e^{\imath(kz-\omega t)}dk \;. \tag{7.3}$$

We will show in Exc. 7.1.8.1, that all functions satisfying $f(z,t) = g(z \pm vt)$ automatically obey the wave equation. The most general solution of the wave equation is given by,

$$f(z,t) = g_1(z-vt) + g_2(z+vt) \;. \tag{7.4}$$

We show this in the following example directly generalizing to three dimensions.

[1] See script on *Vibrations and waves* (2020), Sec. 2.2.3.

Example 64 (*General solution of the wave equation*): The three-dimensional wave equation is,

$$\frac{1}{c^2}\frac{\partial^2 f}{\partial t^2} - \nabla^2 f = 0 \ .$$

Using for the Dirac function the representation, $\delta^{(3)}(\mathbf{r}-\mathbf{r}') = \frac{1}{(2\pi)^3}\int d^3k e^{\imath\mathbf{k}\cdot(\mathbf{r}-\mathbf{r}')}$, we can write,

$$f(\mathbf{r},t) = \int_{V_\infty} d^3r'\delta^{(3)}(\mathbf{r}-\mathbf{r}')f(\mathbf{r}',t)$$
$$= \int d^3k e^{\imath\mathbf{k}\cdot\mathbf{r}} \int_{V_\infty} d^3r' \tfrac{e^{-\imath\mathbf{k}\cdot\mathbf{r}'}}{(2\pi)^3} f(\mathbf{r}',t) = \int d^3k e^{\imath\mathbf{k}\cdot\mathbf{r}} A(\mathbf{k},t) \ ,$$

where $A(\mathbf{k},t) \equiv \int_{V_\infty} d^3r' \frac{1}{(2\pi)^3} e^{-\imath\mathbf{k}\cdot\mathbf{r}'} f(\mathbf{r}',t)$ is the Fourier transform of f. Applying the operator $\nabla^2 - \frac{1}{c^2}\frac{\partial^2}{\partial t^2}$ to the expression for f gives,

$$0 = \frac{1}{c^2}\frac{\partial^2 f}{\partial t^2} - \nabla^2 f = \frac{1}{c^2}\int d^3k e^{\imath\mathbf{k}\cdot\mathbf{r}} \frac{\partial^2 A(\mathbf{k},t)}{\partial t^2} - \int d^3k A(\mathbf{k},t)\nabla^2 e^{\imath\mathbf{k}\cdot\mathbf{r}}$$
$$= \int d^3k e^{\imath\mathbf{k}\cdot\mathbf{r}} \left[\frac{1}{c^2}\frac{\partial^2 A(\mathbf{k},t)}{\partial t^2} + k^2 A(\mathbf{k},t)\right] \ .$$

Hence,

$$\frac{1}{c^2}\frac{\partial^2 A(\mathbf{k},t)}{\partial t^2} + k^2 A(\mathbf{k},t) = 0 \ .$$

The general solution of this equation can be written as,

$$A(\mathbf{k},t) = a(\mathbf{k})e^{\imath kct} + b(\mathbf{k})e^{-\imath kct} \ ,$$

where $a(\mathbf{k})$ and $b(\mathbf{k})$ are arbitrary functions of $\mathbf{k}$. Thus, the general solution for f is given by,

$$f(\mathbf{r},t) = \int a(\mathbf{k})e^{\imath\mathbf{k}\cdot\mathbf{r}+\imath kct}d^3k + \int b(\mathbf{k})e^{\imath\mathbf{k}\cdot\mathbf{r}-\imath kct}d^3k \ .$$

Since f is a real quantity, $f(\mathbf{r},t)^* = f(\mathbf{r},t)$, we must have,

$$a(-\mathbf{k})^* = b(\mathbf{k}) \ ,$$

and,

$$f(\mathbf{r},t) = \mathfrak{Re}\left[\int 2b(\mathbf{k})e^{\imath\mathbf{k}\cdot\mathbf{r}-\imath kct}d^3k\right] \ .$$

The scalar functions $e^{\imath\mathbf{k}\cdot\mathbf{r}-\imath kct}$ satisfy the wave equation for all $\mathbf{k}$.

Waves of vector quantities must be characterized by a *polarization vector* $\hat{\epsilon} \equiv \mathbf{b}/b$. Therefore, we define,

$$\vec{\mathcal{E}} = \mathfrak{Re}\ \vec{\tilde{\mathcal{E}}} \qquad \text{with} \qquad \vec{\tilde{\mathcal{E}}}(\mathbf{r},t) = \hat{\epsilon}\mathcal{E}_0 e^{\imath\mathbf{k}\cdot\mathbf{r}-\imath kct} \ , \tag{7.5}$$

where $\mathcal{E}_0$ is real and $\omega \equiv kc$, as the vector functions forming the functional basis for the fields. These functions represent plane waves, because on a wavefront, the value of $\vec{\tilde{\mathcal{E}}}(\mathbf{r},t)$ is fixed, and this occurs only when $e^{\imath\mathbf{k}\cdot\mathbf{r}-\imath kct}$ is constant [2].

[2]We shall see later that, when a wave passes through zones with different propagation velocities v, the amplitude $\mathbf{A}$ and the polarization $\hat{\epsilon}$ may change. However, any change must be such that $\tilde{\mathbf{F}}(z_0,t)$ and the derivative $\tilde{\mathbf{F}}'(z_0,t)$ are continuous at the transition point z_0.

To calculate the magnetic field from the complex representation of the electric field, we write first,

$$\vec{\mathcal{B}} = \mathfrak{Re}\,\vec{\tilde{\mathcal{B}}} \qquad \text{with} \qquad \vec{\tilde{\mathcal{B}}}(\mathbf{r},t) = \hat{\epsilon}'\mathcal{B}_0 e^{\imath\mathbf{k}'\cdot\mathbf{r}-\imath k'ct} \;, \tag{7.6}$$

where $\vec{\tilde{\mathcal{B}}}$ is the magnetic plane wave, since both $\vec{\tilde{\mathcal{E}}}$ as well as $\vec{\tilde{\mathcal{B}}}$ satisfy the same wave equation. With Maxwell's equations in the absence of sources, it is obvious that,

$$\mathbf{k} = \mathbf{k}' \;, \tag{7.7}$$

because the equations that couple $\vec{\tilde{\mathcal{E}}}$ and $\vec{\tilde{\mathcal{B}}}$ must be satisfied at every point of space and at every instant of time.

7.1.1 Helmholtz's equation

Electromagnetic waves differ from classical longitudinal or transverse waves in several aspects. For example, they do not require a propagation medium, but move through the vacuum at extremely high speed. Being exactly $c = 299792458$ m/s the speed of light is so high, that the laws of classical mechanics are no longer valid. And because there is no propagation medium, in vacuum all inertial systems are equivalent, and this will have important consequences for the Doppler effect. We will show that the electromagnetic wave equation almost comes out as a corollary of the theory of special relativity.

We have shown earlier how the periodic conversion between kinetic and potential energy in a pendulum can propagate in space, when the pendulum is coupled to other pendulums hung in an array, and that this model explains the propagation of a pulse along a string. We also discussed, how electric and magnetic energy can be interconverted in an electronic L-C circuit constiting of a capacitor (storing electrical energy) and an inductance (a coil storing magnetic energy). The law of electrodynamics describing the transformation of electric field variations into magnetic energy is *Ampère's law*, and the law describing the transformation of magnetic field variations into electric energy is *Faraday's law*,

$$\frac{\partial\vec{\mathcal{E}}}{\partial t} \curvearrowright \vec{\mathcal{B}}(t) \qquad , \qquad \frac{\partial\vec{\mathcal{B}}}{\partial t} \curvearrowright -\vec{\mathcal{E}}(t) \;. \tag{7.8}$$

Extending the L-C circuit to an array, it is possible to show that the electromagnetic oscillation propagates along the array. This model describes well the propagation of electromagnetic energy along a coaxial cable or the propagation of light in free space.

The *electrical energy* stored in the capacitor and the *magnetic energy* stored in the coil are given by,

$$E_{ele} = \tfrac{\varepsilon_0}{2}|\vec{\mathcal{E}}|^2 \qquad , \qquad E_{mag} = \tfrac{1}{2\mu_0}|\vec{\mathcal{B}}|^2 \;, \tag{7.9}$$

where the constants $\varepsilon_0 = 8.854\cdot 10^{-12}$ As/Vm and $\mu_0 = 4\pi\cdot 10^{-7}$ Vs/Am are called *vacuum permittivity* and *vacuum permeability*. The constant $Z_0 \equiv \sqrt{\mu_0/\varepsilon_0}$ is called *vacuum impedance*.

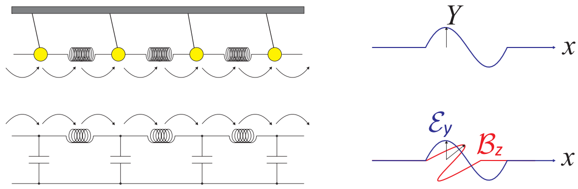

Figure 7.1: Analogy between propagation of mechanical waves (above) and electromagnetic waves (below).

From Maxwell's equations in free space,

$$\nabla\times\vec{\mathcal{B}}-\varepsilon_0\mu_0\partial_t\vec{\mathcal{E}}=0 \qquad \text{and} \qquad \nabla\times\vec{\mathcal{E}}+\partial_t\vec{\mathcal{B}}=0\ , \tag{7.10}$$

deriving the first and inserting this into the second, and using the fact that the divergences vanish,

$$\frac{1}{c^2}\frac{\partial^2\vec{\mathcal{E}}}{\partial t^2}=\frac{1}{\varepsilon_0\mu_0c^2}\frac{\partial}{\partial t}\nabla\times\vec{\mathcal{B}}=-\nabla\times(\nabla\times\vec{\mathcal{E}})=-\nabla(\nabla\cdot\vec{\mathcal{E}})+\nabla^2\vec{\mathcal{E}}=\nabla^2\vec{\mathcal{E}} \tag{7.11}$$
$$\frac{1}{c^2}\frac{\partial^2\vec{\mathcal{B}}}{\partial t^2}=-\frac{1}{c^2}\frac{\partial}{\partial t}\nabla\times\vec{\mathcal{E}}=-\frac{1}{\varepsilon_0\mu_0c^2}\nabla\times(\nabla\times\vec{\mathcal{B}})=-\nabla(\nabla\cdot\vec{\mathcal{B}})+\nabla^2\vec{\mathcal{B}}=\nabla^2\vec{\mathcal{B}}\ .$$

These are the homogeneous *Helmholtz equations*. We will check in Exc. 7.1.8.2, that

- electromagnetic waves (in free space) are transverse;
- the amplitude of the electric field, the magnetic field, and the direction of propagation are orthogonal;
- the propagation velocity is the speed of light, because $c^2=1/\varepsilon_0\mu_0$.

7.1.2 The polarization of light

A consequence of the requirement, $\nabla\cdot\vec{\mathcal{E}}=0=\nabla\cdot\vec{\mathcal{B}}$, following from Maxwell's equations in vacuum is, that the electromagnetic waves are transverse with orthogonal electric and magnetic fields. This is easy to see in the case of plane wave:

$$0=\nabla\cdot\vec{\mathcal{E}}=\vec{\mathcal{E}}_0\cdot\nabla e^{\imath(\mathbf{k}\cdot\mathbf{r}-\omega t)}=\imath\vec{\mathcal{E}}_0\cdot\mathbf{k}e^{\imath(\mathbf{k}\cdot\mathbf{r}-\omega t)}\ , \tag{7.12}$$

and analogously for $\vec{\mathcal{B}}$. We conclude,

$$\boxed{\mathbf{k}\cdot\vec{\mathcal{E}}=0=\mathbf{k}\cdot\vec{\mathcal{B}}}\ . \tag{7.13}$$

In addition, from Faraday's law,

$$\vec{\mathcal{B}}_0\ \imath\omega e^{\imath(\mathbf{k}\cdot\mathbf{r}-\omega t)}=-\frac{\partial\vec{\mathcal{B}}}{\partial t}=\nabla\times\vec{\mathcal{E}}=-\vec{\mathcal{E}}_0\times\nabla e^{\imath(\mathbf{k}\cdot\mathbf{r}-\omega t)}=-\vec{\mathcal{E}}_0\times\imath\mathbf{k}e^{\imath(\mathbf{k}\cdot\mathbf{r}-\omega t)}\ . \tag{7.14}$$

together with an analogous result obtained from Ampère-Maxwell's law, we can summarize,

$$\boxed{\vec{\mathcal{B}}=\tfrac{\mathbf{k}}{\omega}\times\vec{\mathcal{E}} \qquad \text{and} \qquad \vec{\mathcal{E}}=-\tfrac{c^2\mathbf{k}}{\omega}\times\vec{\mathcal{B}}}\ . \tag{7.15}$$

We conclude that the fields $\vec{\mathcal{E}}$ and $\vec{\mathcal{B}}$ and the propagation wavevector are all mutually orthogonal for waves in free space. In the Excs. 7.1.8.3 and 7.1.8.4 we study the polarization of light.

Example 65 (*Circular polarization*): Let us study the example of polarized light,

$$\vec{\tilde{\mathcal{E}}} = (\mathcal{E}_x \hat{\mathbf{e}}_x + \imath\mathcal{E}_y \hat{\mathbf{e}}_y) e^{\imath k_z z - \imath\omega t} \ .$$

If $\mathcal{E}_x = \mathcal{E}_y$, we have circular polarization. If $\mathcal{E}_x \neq \mathcal{E}_y$, the polarization is said to be elliptical. The reason is easily seen by taking the real part of the plane wave:

$$\vec{\mathcal{E}} = \mathfrak{Re}\ \vec{\tilde{\mathcal{E}}} = \mathcal{E}_x \hat{\mathbf{e}}_x \cos(k_z z - \omega t) - \mathcal{E}_y \hat{\mathbf{e}}_y \sin(k_z z - \omega t) \ .$$

In the plane defined by $z = z_0$, with z_0 constant, the electric field vector describes an ellipse as time passes; the ellipse is a circle if $\mathcal{E}_x = \mathcal{E}_y$.
Other polarizations are possible in free space although sometimes a bit more difficult to realize in practice, for example, radial polarization,

$$\vec{\tilde{\mathcal{E}}} = \mathcal{E}_0 \hat{\mathbf{e}}_r e^{\imath k_z z - \imath\omega t} \qquad \text{and} \qquad \vec{\tilde{\mathcal{B}}} = \mathcal{B}_0 \hat{\mathbf{e}}_\theta e^{\imath k_z z - \imath\omega t} \ .$$

7.1.2.1 Polarization optics

A laser generally has a well-defined polarization, for example, linear or circular. The polarizations can be transformed into each other through *birefringent optical elements*, such as birefringent waveplates, Fresnel rhombs, or electro-optical modulators. Superpositions of different polarizations can be separated with polarizing *beam splitters*.

It is important to distinguish between the *polarization*, which is always specified in relation to a fixed coordinate system, and *helicity*, i.e. the rotation direction of the polarization vector with respect to the propagation direction of the light beam. The polarization of a beam propagating in z-direction can easily be expressed by a vector of complex amplitude,

$$\vec{\mathcal{E}}(\mathbf{r}, t) = \begin{pmatrix} a \\ b \\ 0 \end{pmatrix} e^{\imath\mathbf{k}\cdot\mathbf{r} - \imath\omega t} = \begin{pmatrix} 1 \\ e^{-\imath\phi}|b|/|a| \\ 0 \end{pmatrix} |a| e^{\imath\mathbf{k}\cdot\mathbf{r} - \imath\omega t} \ . \tag{7.16}$$

The angle $\phi = \arctan \frac{\mathfrak{Im}\ ab^*}{\mathfrak{Re}\ ab^*}$ determines the polarization of the light beam. The polarization is linear for $\phi = 0$ and circular for $\phi = \pi/2$. $|b|/|a|$ then gives the degree of ellipticity. A device rotating the (linear) polarization of a light beam (e.g. a sugar solution) is described by the so-called *Jones matrix* (we restrict ourselves to the xy-plane orthogonal to the propagation direction),

$$M_{rotator}(\phi) = \begin{pmatrix} \cos\phi & \sin\phi \\ -\sin\phi & \cos\phi \end{pmatrix} \ , \tag{7.17}$$

where ϕ is the angle of rotation. For birefringent half-waveplates the rotation angle is independent on the propagation direction. In devices called *Faraday rotators*, in contrast, the sign of the rotation angle depends on the propagation direction of the laser beam,

$$M_{Faraday}(\phi) = \begin{pmatrix} \cos\phi & \mathbf{k}\cdot\hat{\mathbf{e}}_z\sin\phi \\ -\mathbf{k}\cdot\hat{\mathbf{e}}_z\sin\phi & \cos\phi \end{pmatrix} , \tag{7.18}$$

A *polarizer* projects the polarization to a specific axis. In case of a polarizer aligned to the x-axis the Jones matrix is,

$$M_{polarizer} = \begin{pmatrix} 1 & 0 \\ 0 & 0 \end{pmatrix} , \tag{7.19}$$

while for an arbitrary axis given by the angle ϕ, it is,

$$M_{polarizer}(\phi) = \begin{pmatrix} \cos\phi & \sin\phi \\ -\sin\phi & \cos\phi \end{pmatrix} \begin{pmatrix} 1 & 0 \\ 0 & 0 \end{pmatrix} \begin{pmatrix} \cos\phi & \sin\phi \\ -\sin\phi & \cos\phi \end{pmatrix}^{-1} . \tag{7.20}$$

A birefringent crystal acts only on one of the two optical axes. Assuming that only the y-axis is optically active, its Jones's matrix is,

$$M_{\theta\text{-waveplate}} = \begin{pmatrix} 1 & 0 \\ 0 & e^{\imath\theta} \end{pmatrix} . \tag{7.21}$$

For $\theta = 2\pi/n$ we obtain a so-called λ/n-*waveplate*. When we rotate the waveplate (and therefore the optically active about the inactive axis) by an angle ϕ, the Jones matrix becomes [3],

$$\begin{aligned} M_{\theta\text{-waveplate}}(\phi) &= \begin{pmatrix} \cos\phi & \sin\phi \\ -\sin\phi & \cos\phi \end{pmatrix} \begin{pmatrix} 1 & 0 \\ 0 & e^{\imath\theta} \end{pmatrix} \begin{pmatrix} \cos\phi & \sin\phi \\ -\sin\phi & \cos\phi \end{pmatrix}^{-1} \\ &= \begin{pmatrix} \cos^2\phi + e^{\imath\theta}\sin^2\phi & -\sin\phi\cos\phi + e^{\imath\theta}\sin\phi\cos\phi \\ -\sin\phi\cos\phi + e^{\imath\theta}\sin\phi\cos\phi & \sin^2\phi + e^{\imath\theta}\cos^2\phi \end{pmatrix} . \end{aligned} \tag{7.22}$$

We use in most cases $\lambda/4$-waveplates,

$$M_{\lambda/4}(\phi) = \begin{pmatrix} \cos^2\phi + \imath\sin^2\phi & (-1+\imath)\sin\phi\cos\phi \\ (-1+\imath)\sin\phi\cos\phi & \sin^2\phi + \imath\cos^2\phi \end{pmatrix} \tag{7.23}$$

or $\lambda/2$-waveplates,

$$M_{\lambda/2}(\phi) = \begin{pmatrix} \cos 2\phi & -\sin 2\phi \\ -\sin 2\phi & -\cos 2\phi \end{pmatrix} . \tag{7.24}$$

Note that interestingly $M_{\lambda/2}(\phi)^2 = \mathbb{I}$.

Example 66 (*Generating circular polarization*): We can use $\lambda/4$-waveplates to create, from linearly polarized light, circularly polarized light. Choosing an angle $\theta = 45^\circ$ we get from (7.23),

$$M_{\lambda/4}(\pm\pi/4)\begin{pmatrix} 1 \\ 0 \end{pmatrix} = \begin{pmatrix} \frac{1}{2}+\frac{1}{2}\imath & \mp\frac{1}{2}\pm\frac{1}{2}\imath \\ \mp\frac{1}{2}\pm\frac{1}{2}\imath & \frac{1}{2}+\frac{1}{2}\imath \end{pmatrix}\begin{pmatrix} 1 \\ 0 \end{pmatrix} = \frac{e^{\imath\pi/4}}{\sqrt{2}}\begin{pmatrix} 1 \\ \pm\imath \end{pmatrix} .$$

[3] See script on *Optical spectroscopy* (2020), Sec. 2.3.1.

Example 67 (*Polarization behavior of upon reflection from a mirror*): A light beam reflected from a mirror under normal incidence does not changes its polarization vector, but only its wavevector. This can be interpreted as conservation of the angular momentum of light upon reflection. One consequence of this is, that $\sigma^\pm$ light turns into $\sigma^\pm$ light upon reflection.

Example 68 (*Action of birefringent waveplates as a function of propagation direction*): The Jones matrices for λ/n-waveplates *do not depend* on the propagation direction, simply because the wavevector does not appear in the expressions. That is, the polarization $\hat{\epsilon} = \hat{\mathbf{e}}_x$ of a beam propagating towards $\pm k\hat{\mathbf{e}}_z$ is transformed by a $M_{\lambda/4}(\pi/4)$ waveplate into σ^+-polarized light regardless of the propagation direction. A consequence of this is that a beam traversing the waveplate $M_{\lambda/4}(\pi/4)$ twice in the round-trip (e.g. being reflected by a mirror) will undergo a rotation of amplitude by 90°,

$$M_{\lambda/4}(\tfrac{\pi}{2})\begin{pmatrix}1\\0\end{pmatrix} = \begin{pmatrix}\imath\\0\end{pmatrix}$$

$$M_{\lambda/4}(\tfrac{\pi}{4})M_{\lambda/4}(\tfrac{\pi}{4}) = \begin{pmatrix}0 & -1\\-1 & 0\end{pmatrix} .$$

This feature is often used to separate counterpropagating light fields via a polarizing beamsplitter.
On the other hand, for $\lambda/2$-waveplates, it is easy to check the following results,

$$M_{\lambda/2}(\tfrac{\pi}{4})\begin{pmatrix}1\\0\end{pmatrix} = \begin{pmatrix}0\\-1\end{pmatrix}$$

$$M_{\lambda/2}(\tfrac{\pi}{8})\begin{pmatrix}1\\0\end{pmatrix} = \tfrac{1}{\sqrt{2}}\begin{pmatrix}1\\-1\end{pmatrix} .$$

In addition, for any ϕ,

$$M_{\lambda/2}(\phi)M_{\lambda/2}(\phi) = \begin{pmatrix}1 & 0\\0 & 1\end{pmatrix} .$$

Thus, the double passage through a $\lambda/2$-waveplate cancels its effect.

7.1.3 The energy density and flow in plane waves

The energy densities stored in the electric field and the magnetic field are given by,

$$u_{ele} = \tfrac{\varepsilon_0}{2}|\vec{\mathcal{E}}|^2 \quad , \quad u_{mag} = \tfrac{1}{2\mu_0}|\vec{\mathcal{B}}|^2 . \tag{7.25}$$

In the case of a monochromatic wave parametrized by $\vec{\mathcal{E}}(\mathbf{r},t) = \vec{\mathcal{E}}_0\cos(\mathbf{k}\cdot\mathbf{r}-\omega t)$ the calculus (7.15) shows that $|\vec{\mathcal{B}}| = \frac{k}{\omega}|\vec{\mathcal{E}}| = \frac{1}{c}|\vec{\mathcal{E}}|$, such that the average energy density is,

$$\langle u(\mathbf{r})\rangle = \left\langle|\varepsilon_0\vec{\mathcal{E}}_0\cos(\mathbf{k}\cdot\mathbf{r}-\omega t)|^2\right\rangle = \tfrac{1}{2}\varepsilon_0|\vec{\mathcal{E}}_0|^2 = \tfrac{1}{2\mu_0}|\vec{\mathcal{B}}_0|^2 , \tag{7.26}$$

consistent with the expressions (6.58). When the wave propagates, it carries with it this amount of energy. The energy flux density is calculated by the *Poynting vector*,

$$\langle\vec{\mathcal{S}}(\mathbf{r})\rangle = \tfrac{1}{\mu_0}\left\langle\vec{\mathcal{E}}(\mathbf{r},t)\times\vec{\mathcal{B}}(\mathbf{r},t)\right\rangle = \tfrac{1}{2}c\varepsilon_0|\vec{\mathcal{E}}_0|^2\hat{\mathbf{e}}_k . \tag{7.27}$$

The absolute value is the *intensity* of the light field,

$$\langle I(\mathbf{r},t)\rangle = \langle|\vec{\mathcal{S}}(\mathbf{r},t)|\rangle \ . \tag{7.28}$$

In addition, a radiation field can have linear momentum. In vacuum, the momentum is connected to the Poynting vector,

$$\langle\wp\rangle = \left\langle c\varepsilon_0|\vec{\mathcal{E}}(\mathbf{r},t)|^2\hat{\mathbf{e}}_k\right\rangle = c\varepsilon_0|\vec{\mathcal{E}}_0|^2\hat{\mathbf{e}}_k \ . \tag{7.29}$$

but in dielectric media things are different, as we will see later. The *momentum density* is responsible for the *radiation pressure*. When light hits the surface A of a perfect absorber, it transfers, during the time interval Δt, the momentum $\Delta\mathbf{p} = \langle\wp\rangle Ac\Delta t$ to the body. Thus, the pressure is,

$$P = \frac{1}{A}\frac{\Delta p}{\Delta t} = \frac{\varepsilon_0\mathcal{E}_0^2}{2} = \frac{I}{c} \ . \tag{7.30}$$

Note that for a perfect reflector the pressure is doubled.

In Exc. 7.1.8.5 we show a trick how to quickly calculate the temporal average of expressions containing products of oscillating field. We solve problems about the radiative pressure in Excs. 7.1.8.6 to 7.1.8.8. In the Excs. 7.1.8.10 to 7.1.8.12 we calculate u and $\vec{\mathcal{S}}$ for various types of waves.

7.1.3.1 Spherical waves

Other wave geometries are possible (see Exc. 7.1.8.13). For example, it is easy to show that spherical scalar fields of the type $\Phi(\mathbf{r},t) = \Phi_0\frac{e^{\imath(kr-\omega t)}}{r}$ and spherical vector fields of the type $\mathbf{A}(\mathbf{r},t) = \mathbf{A}_0\frac{e^{\imath(kr-\omega t)}}{r}$ satisfy the wave equation,

$$\begin{aligned} 0 &= \nabla^2\Phi - \frac{1}{c^2}\frac{\partial^2\Phi}{\partial t^2} \\ &= \frac{1}{r^2}\frac{\partial}{\partial r}\left(r^2\frac{\partial\Phi}{\partial r}\right) + \cancelto{0}{\frac{1}{r^2\sin\theta}\frac{\partial}{\partial\theta}\left(\sin\theta\frac{\partial\Phi}{\partial\theta}\right)} + \cancelto{0}{\frac{1}{r^2\sin^2\theta}\frac{\partial^2\Phi}{\partial\phi^2}} - \frac{1}{c^2}\frac{\partial^2\Phi}{\partial t^2} \\ &= -k^2\Phi + \frac{\omega^2}{c^2}\Phi \ . \end{aligned} \tag{7.31}$$

This also applies to electric and magnetic fields,

$$\vec{\mathcal{E}}(\mathbf{r},t) \stackrel{?}{=} \vec{\mathcal{E}}_0\frac{e^{\imath(kr-\omega t)}}{r} \quad \text{and} \quad \vec{\mathcal{B}}(\mathbf{r},t) \stackrel{?}{=} \vec{\mathcal{B}}_0\frac{e^{\imath(kr-\omega t)}}{r} \ . \tag{7.32}$$

But it does not mean that these fields obey Maxwell's equations. In fact, the simplest possible spherical wave corresponds a the dipole radiation, which will be discussed in the next chapter. We will find in Exc. 8.1.6.3 that the expressions for electric dipole radiation satisfy Maxwell's equations and in Exc. 7.1.8.14, that the expressions (7.32) do not satisfy them. In Excs. 7.1.8.15 and 7.1.8.16 we will deepen this discussion.

7.1.4 Slowly varying envelope approximation

The slowly varying envelope approximation [6] (SVEA) is the assumption that the envelope of a forward-traveling wave pulse varies slowly in time and space compared to a period or wavelength. This requires the spectrum of the signal to be narrow-banded. The SVEA is often used because the resulting equations are in many cases easier to solve than the original equations, reducing the order of all (or some) of the highest-order partial derivatives. But the validity of the assumptions which are made need to be justified.

For example, consider the electromagnetic wave equation:

$$\nabla^2 \mathcal{E} - \mu_0 \varepsilon_0 \frac{\partial^2 \mathcal{E}}{\partial t^2} = 0 \ . \tag{7.33}$$

If k_0 and ω_0 are the wave number and angular frequency of the (characteristic) carrier wave for the signal $\mathcal{E}(\mathbf{r}, t)$, the following representation is useful:

$$\mathcal{E}(\mathbf{r}, t) = \mathfrak{Re}\left[\mathcal{E}_0(\mathbf{r}, t) e^{\imath(\mathbf{k}_0 \cdot \mathbf{r} - \omega_0 t)}\right] \ . \tag{7.34}$$

In the SVEA it is assumed that the complex amplitude $\mathcal{E}_0(\mathbf{r}, t)$ only varies slowly with $\mathbf{r}$ and t. This inherently implies that $\mathcal{E}_0(\mathbf{r}, t)$ represents waves propagating forward, predominantly in the $\mathbf{k}_0$ direction. As a result of the slow variation of $\mathcal{E}_0(\mathbf{r}, t)$, when taking derivatives, the highest-order derivatives may be neglected [19]:

$$|\nabla^2 \mathcal{E}_0| \ll |\mathbf{k}_0 \cdot \nabla \mathcal{E}_0| \quad \text{and} \quad \left|\frac{\partial^2 \mathcal{E}_0}{\partial t^2}\right| \ll \left|\omega_0 \frac{\partial \mathcal{E}_0}{\partial t}\right| \ . \tag{7.35}$$

Consequently, the wave equation is approximated in the SVEA as,

$$2\imath \mathbf{k}_0 \cdot \nabla \mathcal{E}_0 + 2\imath \omega_0 \mu_0 \varepsilon_0 \frac{\partial \mathcal{E}_0}{\partial t} - (k_0^2 - \omega_0^2 \mu_0 \varepsilon_0) \mathcal{E}_0 = 0 \ . \tag{7.36}$$

It is convenient to choose k_0 and ω_0 such that they satisfy the dispersion relation, $k_0^2 - \omega_0^2 \mu_0 \varepsilon_0 = 0$. This gives the following approximation to the wave equation,

$$\mathbf{k}_0 \cdot \nabla \mathcal{E}_0 + \omega_0 \mu_0 \varepsilon_0 \frac{\partial \mathcal{E}_0}{\partial t} = 0 \ . \tag{7.37}$$

This is a hyperbolic partial differential equation, like the original wave equation, but now of first-order instead of second-order. It is valid for coherent forward-propagating waves in directions near the k_0-direction. The space and time scales over which $\mathcal{E}_0$ varies are generally much longer than the spatial wavelength and temporal period of the carrier wave. A numerical solution of the envelope equation thus can use much larger space and time steps, resulting in significantly less computational effort.

Example 69 (*Parabolic SVEA approximation*): Assuming that the wave propagation is dominantly in z-direction, and k_0 is taken in this direction. The SVEA is only applied to the second-order spatial derivatives in the z-direction and time. If $\nabla_\perp = \hat{\mathbf{e}}_x \partial/\partial x + \hat{\mathbf{e}}_y \partial/\partial y$ is the gradient in the x-y plane, the result is [91],

$$k_0 \frac{\partial \mathcal{E}_0}{\partial z} + \omega_0 \mu_0 \varepsilon_0 \frac{\partial \mathcal{E}_0}{\partial t} - \tfrac{1}{2} \imath \nabla_\perp^2 \mathcal{E}_0 = 0 \ .$$

This is a parabolic partial differential equation. This equation has enhanced validity as compared to the full SVEA: it represents waves propagating in directions significantly different from the z-direction. It is the starting point of the theory of Gaussian beams, which will be studied in Sec. 7.4.1.

7.1.5 Plane waves in linear dielectrics and the refractive index

In dielectric (non-conducting) media we have $\varrho = 0$ and $\mathbf{j} = 0$ but $\dot{\vec{\mathcal{E}}}, \dot{\vec{\mathcal{B}}} \neq 0$. If the medium is linear and homogeneous, the permittivity ε and the permeability μ are constant, and we can substitute $\vec{\mathcal{D}} = \varepsilon\vec{\mathcal{E}}$ and $\vec{\mathcal{H}} = \mu^{-1}\vec{\mathcal{B}}$. Thus, Maxwell's equations (6.56) become equal to those holding for vacuum (6.6) but with the generalizations $\varepsilon_0 \to \varepsilon$ and $\mu_0 \to \mu$. Therefore, the wave equations remain valid,

$$\left(\frac{1}{c_n^2}\frac{\partial^2}{\partial t^2} - \nabla^2\right)\vec{\mathcal{E}} = 0 = \left(\frac{1}{c_n^2}\frac{\partial^2}{\partial t^2} - \nabla^2\right)\vec{\mathcal{B}} , \tag{7.38}$$

with the propagation velocity now reading,

$$c_n = \frac{1}{\sqrt{\varepsilon\mu}} = \frac{c}{n} , \tag{7.39}$$

where we defined the index of refraction,

$$n \equiv \sqrt{\frac{\varepsilon\mu}{\varepsilon_0\mu_0}} . \tag{7.40}$$

In dielectric media, we must use the original definitions for the energy and momentum densities and flows (6.58). The polarization and magnetization of the medium may cause new phenomena. For example, in anisotropic optical media the Poynting vector is not necessarily parallel to the wave vector. Resolve the Excs. 7.1.8.17 to 7.1.8.22.

7.1.6 Reflection and transmission by interfaces and Fresnel's formulas

So far we have considered homogenous media. An interesting question is, what happens when a field traverses regions characterized by different ε and μ. The boundary conditions can be discussed from the integral form of the Maxwell equations, which follow immediately from the differential form via the theorems of Gauss and Stokes:

$$\begin{array}{lrcl} \text{(i)} & \oint_{\partial\mathcal{S}} \vec{\mathcal{H}}\cdot d\mathbf{l} &=& \frac{d}{dt}\int_{\mathcal{S}} \vec{\mathcal{D}}\cdot d\mathbf{S} + I_{enc} \\ \text{(ii)} & \oint_{\partial\mathcal{S}} \vec{\mathcal{E}}\cdot d\mathbf{l} &=& -\frac{d}{dt}\int_{\mathcal{S}} \vec{\mathcal{B}}\cdot d\mathbf{S} \\ \text{(iii)} & \oint_{\partial\mathcal{V}} \vec{\mathcal{D}}\cdot d\mathbf{S} &=& Q_{enc} \\ \text{(iv)} & \oint_{\partial\mathcal{V}} \vec{\mathcal{B}}\cdot d\mathbf{S} &=& 0 \end{array} . \tag{7.41}$$

Let us consider two media with different permittivities $\varepsilon_{1,2}$ and permeabilities $\mu_{1,2}$ joined together at an interface. The closed path $\partial\mathcal{S}$ around a surface $\mathcal{S}$ and the closed surface $\partial\mathcal{V}$ around a volume $\mathcal{V}$ are chosen such as to cross the interface, as illustrated in Figs. 2.10 and 4.14. The surface integrals in equations (i) and (ii) vanish in the limit, where we choose the path $\partial\mathcal{S}$ very close to the interface.

From these equations, and as already shown in the derivations of the static equations (2.37), (2.39), (4.30), and (4.32), we have for linear media and in the absence of free surface charges σ_f and free surface currents $\mathbf{k}_f$,

$$\begin{array}{llcl} \text{(i)} & \frac{1}{\mu_1}\vec{\mathcal{B}}_1^{\parallel} - \frac{1}{\mu_2}\vec{\mathcal{B}}_2^{\parallel} & = & |\mathbf{k}_f \times \hat{\mathbf{e}}_n| \longrightarrow 0 \\ \text{(ii)} & \vec{\mathcal{E}}_1^{\parallel} - \vec{\mathcal{E}}_2^{\parallel} & = & 0 \\ \text{(iii)} & \varepsilon_1\vec{\mathcal{E}}_1^{\perp} - \varepsilon_2\vec{\mathcal{E}}_2^{\perp} & = & \sigma_f \longrightarrow 0 \\ \text{(iv)} & \vec{\mathcal{B}}_1^{\perp} - \vec{\mathcal{B}}_2^{\perp} & = & 0 \end{array} \quad . \tag{7.42}$$

We will use these equations to establish the theory of reflection and refraction.

7.1.6.1 Normal incidence

Electromagnetic waves can be guided by interfaces (waveguides). From Maxwell's equations we can deduce useful rules for the behavior of waves near interfaces. First, we consider a plane wave propagating in the direction z within a dielectric medium characterized by the refraction index n_1,

$$\vec{\mathcal{E}}_i(z,t) = \hat{\mathbf{e}}_x \mathcal{E}_i e^{\imath(k_{z1}z-\omega t)} \quad , \quad \vec{\mathcal{B}}_i(z,t) = \hat{\mathbf{e}}_y \frac{n_1\mathcal{E}_i}{c} e^{\imath(k_{z1}z-\omega t)} \ . \tag{7.43}$$

At position $z = 0$ there be a partially reflecting interface, as shown in Fig. 7.2(a). The reflected part is,

$$\vec{\mathcal{E}}_r(z,t) = \hat{\mathbf{e}}_x \mathcal{E}_r e^{\imath(-k_{z1}z-\omega t)} \quad , \quad \vec{\mathcal{B}}_r(z,t) = -\hat{\mathbf{e}}_y \frac{n_1\mathcal{E}_r}{c} e^{\imath(-k_{z1}z-\omega t)} \ . \tag{7.44}$$

The negative sign comes from the relation $\vec{\mathcal{B}}(\mathbf{r},t) = \frac{1}{c}\mathbf{k} \times \vec{\mathcal{E}}(\mathbf{r},t)$. The transmitted part is,

$$\vec{\mathcal{E}}_t(z,t) = \hat{\mathbf{e}}_x \mathcal{E}_t e^{\imath(k_{z2}z-\omega t)} \quad , \quad \vec{\mathcal{B}}_r(z,t) = \hat{\mathbf{e}}_y \frac{n_2\mathcal{E}_t}{c} e^{\imath(k_{z2}z-\omega t)} \ . \tag{7.45}$$

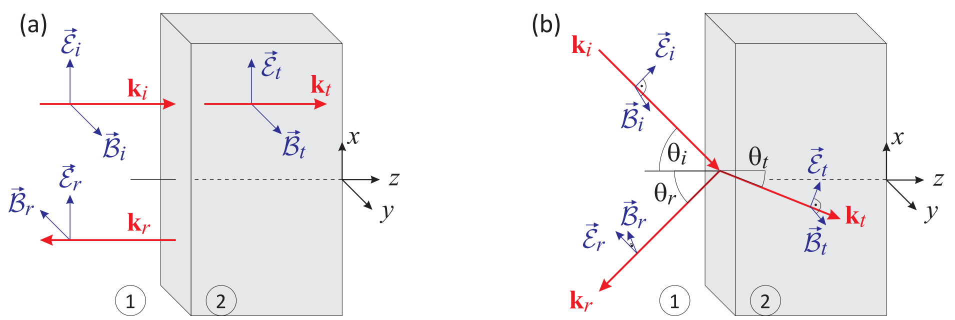

Figure 7.2: Electric and magnetic fields reflected and transmitted at an interface under (a) normal and (b) inclined incidence.

At the position $z = 0$ the total radiation must satisfy the boundary conditions. Since under normal incidence, there are only parallel components,

$$\vec{\mathcal{E}}_i(0,t) + \vec{\mathcal{E}}_r(0,t) = \vec{\mathcal{E}}_t(0,t) \quad , \quad \tfrac{1}{\mu_1}[\vec{\mathcal{B}}_i(0,t) + \vec{\mathcal{B}}_r(0,t)] = \tfrac{1}{\mu_2}\vec{\mathcal{B}}_t(0,t) \ . \tag{7.46}$$

Dividing all terms by $e^{-\imath\omega t}$,

$$\mathcal{E}_i + \mathcal{E}_r = \mathcal{E}_t \quad , \quad \tfrac{n_1}{\mu_1 c}[\mathcal{E}_i - \mathcal{E}_r] = \tfrac{n_2}{\mu_2 c}\mathcal{E}_t \ . \tag{7.47}$$

Solving the system of equations,

$$\boxed{\frac{\mathcal{E}_r}{\mathcal{E}_i} = \frac{1-\beta}{1+\beta} \quad , \quad \frac{\mathcal{E}_t}{\mathcal{E}_i} = \frac{2}{1+\beta}} \ , \tag{7.48}$$

defining

$$\beta \equiv \frac{\mu_1 n_2}{\mu_2 n_1} \ . \tag{7.49}$$

Example 70 (*Reflection on an air-glass interface*): We consider an air-glass interface, $n_1 = 1$ and $n_2 = 1.5$. Taking $\mu_1 = \mu_2 = \mu_0$ we have $\beta = 1.5$, and we calculate that the interface reflects the energy,

$$R \equiv \frac{I_r}{I_i} = \frac{\varepsilon_1 c_1 |\vec{\mathcal{E}}_r|^2}{\varepsilon_1 c_1 |\vec{\mathcal{E}}_i|^2} = \left(\frac{1-\beta}{1+\beta}\right)^2 = 0.04 \ ,$$

and transmits the energy,

$$T \equiv \frac{I_t}{I_i} = \frac{\varepsilon_2 c_2 |\vec{\mathcal{E}}_t|^2}{\varepsilon_1 c_1 |\vec{\mathcal{E}}_i|^2} = \frac{\varepsilon_2 c_2}{\varepsilon_1 c_1}\left(\frac{2}{1+\beta}\right)^2 = 0.96 \ .$$

We check $R + T = 1$.

7.1.6.2 Inclined incidence and geometric optics

When the wave strikes perpendicular to the interface, the polarization of the light is irrelevant. This is no longer true for inclined incidence, as shown in Fig. 7.2(b). In this case the Eqs. (7.43)-(7.45) must be generalized,

$$\vec{\mathcal{E}}_m(\mathbf{r},t) = \vec{\mathcal{E}}_{0m} e^{\imath(\mathbf{k}_m\cdot\mathbf{r}-\omega t)} \quad , \quad \vec{\mathcal{B}}_m(\mathbf{r},t) = \frac{n_m}{c}\hat{\mathbf{k}}_m \times \vec{\mathcal{E}}_m(\mathbf{r},t) \ , \tag{7.50}$$

for $m = i, r, t$. Obviously the frequency is the same for all waves, such that by inserting each wave into the wave equation we find,

$$k_i c_i = k_r c_r = k_t c_t = \omega \ , \tag{7.51}$$

with $c_m \equiv c/n_m$ and $c_i = c_r \equiv c_1$ and $c_t \equiv c_2$. We now need to join the fields $\vec{\mathcal{E}}_i + \vec{\mathcal{E}}_r$ and $\vec{\mathcal{B}}_i + \vec{\mathcal{B}}_r$ of one side of the interface with the fields $\vec{\mathcal{E}}_t$ and $\vec{\mathcal{B}}_t$ of the other side at the plane $z = 0$, respecting the boundary conditions (7.42). We get generic expressions,

$$(\cdot)e^{\imath(\mathbf{k}_i\cdot\mathbf{r}-\omega t)} + (\cdot)e^{\imath(\mathbf{k}_r\cdot\mathbf{r}-\omega t)} = (\cdot)e^{\imath(\mathbf{k}_t\cdot\mathbf{r}-\omega t)} \quad \text{at} \quad z = 0 \tag{7.52}$$

at all times t, where $(\cdot) \equiv \varepsilon_m \vec{\mathcal{E}}_m^{\perp}, \vec{\mathcal{E}}_m^{\parallel}, \vec{\mathcal{B}}_m^{\perp}, \frac{1}{\mu_m}\vec{\mathcal{B}}_m^{\parallel}$. Since the equation (7.52) must be valid at any point (x,y) of the plane $z = 0$, the exponential factors must be equal,

$$e^{\imath\mathbf{k}_i\cdot\mathbf{r}} = e^{\imath\mathbf{k}_r\cdot\mathbf{r}} = e^{\imath\mathbf{k}_t\cdot\mathbf{r}} \ , \tag{7.53}$$

that is,

$$\boxed{\mathbf{k}_i \cdot \hat{\mathbf{e}}_x = \mathbf{k}_r \cdot \hat{\mathbf{e}}_x = \mathbf{k}_t \cdot \hat{\mathbf{e}}_x \qquad \text{and} \qquad \mathbf{k}_i \cdot \hat{\mathbf{e}}_y = \mathbf{k}_r \cdot \hat{\mathbf{e}}_y = \mathbf{k}_t \cdot \hat{\mathbf{e}}_y} \ , \tag{7.54}$$

that is, the wavevectors $\mathbf{k}_i$, $\mathbf{k}_r$, $\mathbf{k}_t$ and the normal vector $\hat{\mathbf{e}}_z$ of the interface are in the same plane. We can orient the coordinate system such that $\mathbf{k}_i \cdot \hat{\mathbf{e}}_y \equiv 0$ (see Fig. 7.2). Defining the angles of incidence, reflection and refraction, we find,

$$\mathbf{k}_m \cdot \hat{\mathbf{e}}_x = k_i \sin\theta_i = k_r \sin\theta_r = k_t \sin\theta_t \ . \tag{7.55}$$

With (7.51) we deduce the *law of reflection*:

$$\boxed{\theta_i = \theta_r} \ , \tag{7.56}$$

and the *law of refraction* or *Snell's law*:

$$\boxed{\frac{\sin\theta_t}{\sin\theta_i} = \frac{n_1}{n_2}} \ . \tag{7.57}$$

The equations (7.54), (7.56), and (7.57) form the basis of geometric optics.

7.1.6.3 Polarization behavior and Fresnel's formulas

Going back to the condition (7.52) and eliminating the exponentials, we get,

$$\begin{aligned}
\text{for } \vec{\mathcal{B}}_m^{\parallel} &: & \tfrac{1}{\mu_1}\vec{\mathcal{B}}_i \cdot \hat{\mathbf{e}}_{x,y} + \tfrac{1}{\mu_1}\vec{\mathcal{B}}_r \cdot \hat{\mathbf{e}}_{x,y} &= \tfrac{1}{\mu_2}\vec{\mathcal{B}}_t \cdot \hat{\mathbf{e}}_{x,y} \\
\text{for } \vec{\mathcal{E}}_m^{\parallel} &: & \vec{\mathcal{E}}_i \cdot \hat{\mathbf{e}}_{x,y} + \vec{\mathcal{E}}_r \cdot \hat{\mathbf{e}}_{x,y} &= \vec{\mathcal{E}}_t \cdot \hat{\mathbf{e}}_{x,y} \\
\text{for } \vec{\mathcal{E}}_m^{\perp} &: & \varepsilon_1\vec{\mathcal{E}}_i \cdot \hat{\mathbf{e}}_z + \varepsilon_1\vec{\mathcal{E}}_r \cdot \hat{\mathbf{e}}_z &= \varepsilon_2\vec{\mathcal{E}}_t \cdot \hat{\mathbf{e}}_z \\
\text{for } \vec{\mathcal{B}}_m^{\perp} &: & \vec{\mathcal{B}}_i \cdot \hat{\mathbf{e}}_z + \vec{\mathcal{B}}_r \cdot \hat{\mathbf{e}}_z &= \vec{\mathcal{B}}_t \cdot \hat{\mathbf{e}}_z \ .
\end{aligned} \tag{7.58}$$

We again orient the coordinate system such that $\mathbf{k}_i \cdot \hat{\mathbf{e}}_y \equiv 0$. We first assume, that the polarization of the incident field is within the plane of incidence (that is, the plane spanned by the vectors $\mathbf{k}_i$ and $\mathbf{k}_r$), that is, $\vec{\mathcal{E}}_i \cdot \hat{\mathbf{e}}_y = 0 = \vec{\mathcal{B}}_i \cdot \hat{\mathbf{e}}_x$. This is called *p-polarization*. In this case, the conditions (7.58) become,

$$\begin{aligned}
\tfrac{1}{\mu_1}\vec{\mathcal{B}}_i \cdot \hat{\mathbf{e}}_y + \tfrac{1}{\mu_1}\vec{\mathcal{B}}_r \cdot \hat{\mathbf{e}}_y = \tfrac{1}{\mu_1}\mathcal{B}_i + \tfrac{1}{\mu_1}\mathcal{B}_r = \tfrac{1}{\mu_1 c_1}(\mathcal{E}_i - \mathcal{E}_r) &\overset{!}{=} \tfrac{1}{\mu_2 c_2}\mathcal{E}_t = \tfrac{1}{\mu_2}\mathcal{B}_t = \tfrac{1}{\mu_2}\vec{\mathcal{B}}_t \cdot \hat{\mathbf{e}}_y \\
\vec{\mathcal{E}}_i \cdot \hat{\mathbf{e}}_x + \vec{\mathcal{E}}_r \cdot \hat{\mathbf{e}}_x = \mathcal{E}_i \cos\theta_i + \mathcal{E}_r \cos\theta_r = (\mathcal{E}_i + \mathcal{E}_r)\cos\theta_r &\overset{!}{=} \mathcal{E}_t \cos\theta_t = \vec{\mathcal{E}}_t \cdot \hat{\mathbf{e}}_x \\
\varepsilon_1\mathcal{E}_i \sin\theta_i + \varepsilon_1\mathcal{E}_r \sin\theta_r = \varepsilon_1(\mathcal{E}_i - \mathcal{E}_r)\sin\theta_i &\overset{!}{=} \varepsilon_2\mathcal{E}_t \sin\theta_t \\
0 &\overset{!}{=} 0 \ .
\end{aligned} \tag{7.59}$$

Using the abbreviation (7.49) and introducing another abbreviation,

$$\alpha \equiv \frac{\cos\theta_t}{\cos\theta_i} = \frac{\sqrt{1 - (n_1/n_2)^2 \sin^2\theta_i}}{\cos\theta_i} \ , \tag{7.60}$$

and solving the system of equations (7.59), we find *Fresnel's formula* for p-polarization [4],

$$r_p \equiv \left.\frac{\mathcal{E}_r}{\mathcal{E}_i}\right|_p = \frac{\alpha-\beta}{\alpha+\beta} = \frac{n_1\cos\theta_t - n_2\cos\theta_i}{n_1\cos\theta_t + n_2\cos\theta_i} \quad \text{and} \quad t_p \equiv \left.\frac{\mathcal{E}_t}{\mathcal{E}_i}\right|_p = \frac{2}{\alpha+\beta} \ . \tag{7.61}$$

We now assume that the polarization of the incident field is perpendicular to the plane of incidence, $\vec{\mathcal{E}}_i \cdot \hat{\mathbf{e}}_x = 0 = \vec{\mathcal{B}}_i \cdot \hat{\mathbf{e}}_y$. This is called *s-polarization*. In this case the equations (7.58) yield,

$$\begin{aligned}
\tfrac{1}{\mu_1}\vec{\mathcal{B}}_i\cdot\hat{\mathbf{e}}_x + \tfrac{1}{\mu_1}\vec{\mathcal{B}}_r\cdot\hat{\mathbf{e}}_x = \tfrac{1}{\mu_1 c_1}(\mathcal{E}_i\cos\theta_i - \mathcal{E}_r\cos\theta_r) &\overset{!}{=} \tfrac{1}{\mu_2 c_2}\mathcal{E}_t\cos\theta_t = \tfrac{1}{\mu_2}\vec{\mathcal{B}}_t\cdot\hat{\mathbf{e}}_x \\
\vec{\mathcal{E}}_i\cdot\hat{\mathbf{e}}_y + \vec{\mathcal{E}}_r\cdot\hat{\mathbf{e}}_y = \mathcal{E}_i + \mathcal{E}_r &\overset{!}{=} \mathcal{E}_t = \vec{\mathcal{E}}_t\cdot\hat{\mathbf{e}}_y \\
0 &\overset{!}{=} 0 \\
\mathcal{B}_i\sin\theta_i + \mathcal{B}_r\sin\theta_r = \tfrac{1}{c_1}(\mathcal{E}_i - \mathcal{E}_r)\sin\theta_i &\overset{!}{=} \tfrac{1}{c_2}\mathcal{E}_t\sin\theta_t = \mathcal{B}_t\sin\theta_t \ .
\end{aligned} \tag{7.62}$$

Similar to the case of p-polarization we obtain the Fresnel formulas for s-polarization,

$$r_s \equiv \left.\frac{\mathcal{E}_r}{\mathcal{E}_i}\right|_s = -\frac{1-\alpha\beta}{1+\alpha\beta} = -\frac{n_1\cos\theta_i - n_2\cos\theta_t}{n_1\cos\theta_i + n_2\cos\theta_t} \quad \text{and} \quad t_s \equiv \left.\frac{\mathcal{E}_t}{\mathcal{E}_i}\right|_s = \frac{\sqrt{\alpha\beta}}{1+\alpha\beta} \ . \tag{7.63}$$

See also Exc. 7.1.8.23.

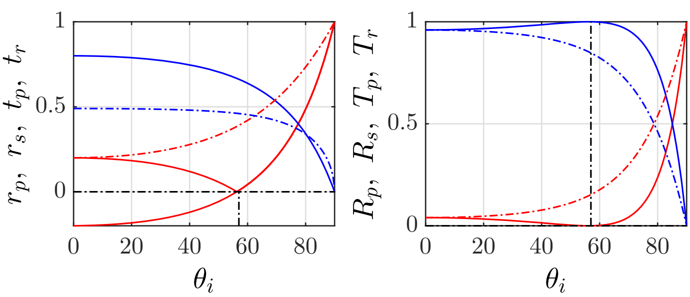

Figure 7.3: (code) Fresnel formulas for the transmitted (blue) and reflected (red) amplitude (left) and intensity (right). The dotted curve holds for s-polarization and the solid curve for p-polarization.

The power flux density incident on the interface is the projection of the intensity, $\vec{\mathcal{S}} \cdot \hat{\mathbf{e}}_z$. Therefore the intensities are,

$$I_m = \tfrac{1}{2}\varepsilon_1 c_m \mathcal{E}_m^2 \cos\theta_m \ , \tag{7.64}$$

[4] Using Snell's law (7.57) the Fresnel formulas can also be written as,

$$r_p^2 = \frac{\tan^2(\theta_i-\theta_t)}{\tan^2(\theta_i\theta_t)} \quad \text{and} \quad r_s^2 = \frac{\sin^2(\theta_i-\theta_t)}{\sin^2(\theta_i+\theta_t)}$$

$$t_p^2 = \frac{\sin 2\theta_i \sin 2\theta_t}{\sin^2(\theta_i+\theta_t)\cos^2(\theta_i-\theta_t)} \quad \text{and} \quad t_s^2 = \frac{\sin 2\theta_i \sin 2\theta_t}{\sin^2(\theta_i+\theta_t)} \ .$$

with $m = i, r, t$. Thus the reflection and the transmission are for p-polarization,

$$R_p = \left(\frac{\mathcal{E}_r}{\mathcal{E}_i}\right)_p^2 = \left(\frac{\alpha-\beta}{\alpha+\beta}\right)^2 \quad \text{and} \quad T_p = \frac{\varepsilon_2 c_2}{\varepsilon_1 c_1}\frac{\cos\theta_t}{\cos\theta_i}\left(\frac{\mathcal{E}_t}{\mathcal{E}_i}\right)_p^2 = \alpha\beta\left(\frac{2}{\alpha+\beta}\right)^2 = 1 - R_p \ . \tag{7.65}$$

For s-polarization we have,

$$R_s = \left(\frac{\mathcal{E}_r}{\mathcal{E}_i}\right)_s^2 = \left(\frac{1-\alpha\beta}{1+\alpha\beta}\right)^2 \quad \text{and} \quad T_s = \frac{\varepsilon_2 c_2}{\varepsilon_1 c_1}\frac{\cos\theta_t}{\cos\theta_i}\left(\frac{\mathcal{E}_t}{\mathcal{E}_i}\right)_s^2 = \alpha\beta\left(\frac{2}{1+\alpha\beta}\right)^2 = 1 - R_s \ . \tag{7.66}$$

7.1.6.4 The Brewster angle

For an angle of incidence of $\theta_i = 0°$ ($\alpha = 1$) we recover the expressions (7.48). For $\theta_i = 90°$ ($\alpha \to \infty$), all light is reflected. Looking at the formula (7.61) it is interesting to note the existence of an angle, where the reflection vanishes for the case of the s-polarization. It is given by $\alpha = \beta$, that is,

$$\sin^2\theta_{i,B} \equiv \sin^2\theta_i = \frac{1-\beta^2}{(n_1/n_2)^2 - \beta^2} \ . \tag{7.67}$$

θ_B is the *Brewster angle*. When $\mu_1 \simeq \mu_2$ we can simplify to,

$$\boxed{\theta_{i,B} = \arcsin\frac{1-\beta^2}{(n_1/n_2)^2 - \beta^2} \simeq \arctan\frac{n_2}{n_1}} \ . \tag{7.68}$$

That is, a p-polarized beam of light traveling in a vacuum and encountering a dielectric with refractive index $n_2 = 1.5$ under the angle of $\theta_{i,B} \approx 56.3°$ is fully transmitted. This is seen in Fig. 7.3(right), where the reflected intensity I_r/I_0 of p-polarized light vanishes at a specific angle, and illustrated in Fig. 7.4(a).

7.1.6.5 Internal total reflection and the Goos-Hänchen shift

We now consider a light beam traveling in a dielectric with refractive index n_1 and encountering an interface to an optically less dense medium, $n_2 < n_1$, as illustrated in Fig. 7.4(b). Increasing the angle of incidence θ_i, according to Snell's law (7.57) we will come to a point, where the outgoing angle reaches $\theta_t = 90°$. Snell's law gives the critical angle for this to happen,

$$\boxed{\theta_{i,tot} = \arcsin\frac{n_2}{n_1}} \ . \tag{7.69}$$

For an index of refraction $n_1 = 1.5$ this angle is $\theta_{i,tot} \approx 41.8°$. Above this angle, $\theta_i > \theta_{i,tot}$, all energy is reflected by the optically denser medium. This phenomenon of *total internal reflection* is used e.g. to guide light in optical fibers. Nevertheless, the fields do not completely disappear in the medium 2 but form, a so-called *evanescent wave*, which is exponentially attenuated and does not carry energy into the medium 2. A quick way to construct the evanescent wave consists in simply extending to the complex domain the formulas obtained for inclined incidence of light on interfaces. For $\theta_i > \theta_{i,tot}$,

$$\sin\theta_t = \frac{n_1}{n_2}\sin\theta_i > \frac{n_1}{n_2}\sin\theta_{i,tot} = \sin\theta_{t,tot} = 1 \ , \tag{7.70}$$

Obviously θ_t can no longer be interpreted as an angle! We will show in Exc. 7.1.8.24 that, for the geometry illustrated in Fig. 7.4(b), the electric field generated in region 2 is given by,

$$\vec{\tilde{\mathcal{E}}}_t(\mathbf{r},t) = \vec{\tilde{\mathcal{E}}}_0 e^{-\kappa z} e^{\imath(kx-\omega t)} \ , \tag{7.71}$$

where

$$\kappa \equiv \tfrac{\omega}{c}\sqrt{(n_1\sin\theta_i)^2 - n_2^2} \qquad \text{and} \qquad k \equiv \tfrac{\omega n_1}{c}\sin\theta_i \ . \tag{7.72}$$

(7.71) is a wave propagating in x-direction, parallel to the interface, and being atten-

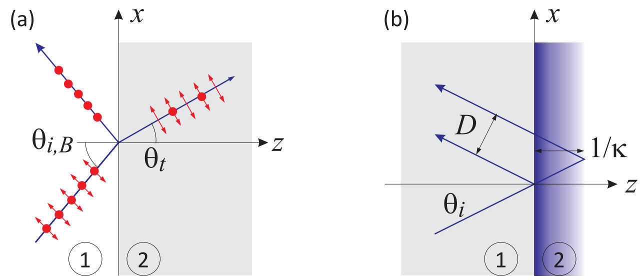

Figure 7.4: (a) Illustration of the effect of the Brewster angle on the polarization of light. (b) Illustration of the Goos-Hänchen shift.

uated in z-direction. The penetration depth of is κ^{-1}. Also in Exc. 7.1.8.24 we will show that for both polarizations p and s the reflection coefficient is 1, which confirms that there is no energy transported into the medium 2.

Example 71 (*The Goos-Hänchen shift*): The fact that the light wave penetrates region 2 up to a depth of κ^{-1} causes a transverse displacement of the wave known as *Goos-Hänchen shift* named after *Gustav Goos* and *Hilda Hänchen*. From Fig. 7.4 it is easy to verify that this displacement is of the order of magnitude $D \simeq \frac{2}{\kappa}\sin\theta_i$. It can be measured taking a beam of light with finite radial extent.

7.1.7 Transfer matrix formalism

For a propagating wave the amplitude of the field at a point $z = 0$ can be related to another point z via $\vec{\mathcal{E}}_z = M\vec{\mathcal{E}}_0$, where M is a phase factor of the type $e^{\imath kz}$. A counter-propagating wave (e.g. generated by partial reflection at an interface) suffers, over the same distance, a phase shift of $e^{-\imath kz}$. Since both waves interfere, it is useful to set up a model describing in a compact manner the amplitude and phase variations of the two counterpropagating waves along the optical axis. The *transfer matrix formalism* represents such a model.

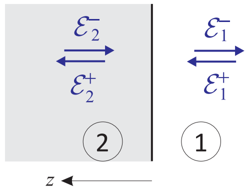

Figure 7.5: Illustration of the transfer matrix formalism.

7.1.7.1 The $\mathcal{T}$-matrix

Let us consider a beam of light propagating along the z-axis toward $+\infty$ through an inhomogeneous dielectric medium described by the refractive index $n(z)$. Each interface where the refractive index varies causes a partial reflection of the beam into the opposite direction. The fields reflected at different positions z interfere constructively or destructively depending on the accumulated phase. To address the problem mathematically, we divide the medium into layers treated as homogeneous and delimited by interfaces located at positions z, as shown in Fig. 7.5. We define the complex transfer matrix $\mathcal{T}_{12}$ describing the transition between from medium 1 to medium 2 by,

$$\boxed{\begin{pmatrix}\mathcal{E}_2^+\\ \mathcal{E}_2^-\end{pmatrix}=\mathcal{T}_{12}\begin{pmatrix}\mathcal{E}_1^+\\ \mathcal{E}_1^-\end{pmatrix}}\ . \tag{7.73}$$

Here, the fields $\mathcal{E}^\pm$ propagate toward $\pm\infty$. That is, the fields $\mathcal{E}_1^+$ and $\mathcal{E}_2^-$ move toward the interface and the fields $\mathcal{E}_1^-$ and $\mathcal{E}_2^+$ move away from the interface. In (7.48) we showed that the reflectivity and the transmissivity of the interface for a transition from region 1 to region 2 are given by,

$$r_{12}=\frac{n_1-n_2}{n_1+n_2}\qquad\text{and}\qquad t_{12}=\frac{2n_1}{n_1+n_2}\ . \tag{7.74}$$

Obviously, we have $r_{21}=-r_{12}$ and $t_{21}=\frac{n_2}{n_1}t_{12}$. Therefore,

$$\mathcal{E}_2^+=t_{12}\mathcal{E}_1^++r_{21}\mathcal{E}_2^-\qquad\text{and}\qquad\mathcal{E}_1^-=t_{21}\mathcal{E}_2^-+r_{12}\mathcal{E}_1^+\ , \tag{7.75}$$

that is,

$$\mathcal{E}_2^+=\left(t_{12}-\tfrac{r_{12}r_{21}}{t_{21}}\right)\mathcal{E}_1^++\tfrac{r_{21}}{t_{21}}\mathcal{E}_1^-\qquad\text{and}\qquad\mathcal{E}_2^-=-\tfrac{r_{12}}{t_{21}}\mathcal{E}_1^++\tfrac{1}{t_{21}}\mathcal{E}_1^-\ . \tag{7.76}$$

The matrix, therefore, is,

$$\boxed{\mathcal{T}_{12}=\begin{pmatrix}t_{12}-\frac{r_{12}r_{21}}{t_{21}} & \frac{r_{21}}{t_{21}}\\ -\frac{r_{12}}{t_{21}} & \frac{1}{t_{21}}\end{pmatrix}=\frac{1}{2n_2}\begin{pmatrix}n_2+n_1 & n_2-n_1\\ n_2-n_1 & n_2+n_1\end{pmatrix}}\ . \tag{7.77}$$

The determinant is $\det\mathcal{T}=\frac{t_{12}}{t_{21}}=\frac{n_1}{n_2}$.

The simple propagation over a distance Δz through a homogeneous medium simply causes a phase shift, since $\mathcal{E}_z^+=e^{\imath kz}\mathcal{E}_0^+$ and $\mathcal{E}_0^-=e^{\imath kz}\mathcal{E}_z^-$. The corresponding transfer matrix is,

$$\boxed{\mathcal{T}_{\Delta z} = \begin{pmatrix} e^{\imath k\Delta z} & 0 \\ 0 & e^{-\imath k\Delta z} \end{pmatrix}} . \tag{7.78}$$

Absorption losses can attenuate the beam. This can be taken into account via an absorption coefficient α in the matrix,

$$\boxed{\mathcal{T}_{abs} = \begin{pmatrix} e^{-\alpha} & 0 \\ 0 & e^{\alpha} \end{pmatrix}} . \tag{7.79}$$

satisfying $\det \mathcal{T} = 1$.

7.1.7.2 AR and HR coating

Concatenating the matrices (7.77) and (7.78), $\mathcal{M} = \mathcal{T}_{\Delta z}\mathcal{T}_{12}\mathcal{T}_{abs}$, we can now describe the transmission of a light beam through a dielectric layer with refractive index n_2 and thickness Δz.

Example 72 (*Anti-reflection coating*): Here we consider the transition between a medium n_0 through a thin layer n_1 of thickness $\lambda/4$ to a medium n_2. The transition is described by the concatenation of three matrices,

$$\begin{pmatrix} \mathcal{E}_2^+ \\ 0 \end{pmatrix} = \mathcal{T}_{12}\mathcal{T}_{\lambda/4}\mathcal{T}_{01} \begin{pmatrix} \mathcal{E}_0^+ \\ \mathcal{E}_0^- \end{pmatrix} = \begin{pmatrix} M_{11} & M_{12} \\ M_{21} & M_{22} \end{pmatrix} \begin{pmatrix} \mathcal{E}_0^+ \\ \mathcal{E}_0^- \end{pmatrix} = \begin{pmatrix} M_{11} - \frac{M_{12}M_{21}}{M_{22}} \\ 0 \end{pmatrix} \mathcal{E}_0^+ .$$

The total matrix is,

$$\begin{aligned} \mathcal{M} &= \frac{1}{2n_2} \begin{pmatrix} n_2 + n_1 & n_2 - n_1 \\ n_2 - n_1 & n_2 + n_1 \end{pmatrix} \begin{pmatrix} e^{\imath\pi/2} & 0 \\ 0 & e^{-\imath\pi/2} \end{pmatrix} \frac{1}{2n_1} \begin{pmatrix} n_1 + n_0 & n_1 - n_0 \\ n_1 - n_0 & n_1 + n_0 \end{pmatrix} \\ &= \frac{\imath}{2n_1 n_2} \begin{pmatrix} n_1^2 + n_0 n_2 & n_1^2 - n_0 n_2 \\ -n_1^2 + n_0 n_2 & -n_1^2 - n_0 n_2 \end{pmatrix} . \end{aligned}$$

Finally, we obtain the fields,

$$\begin{aligned} \mathcal{E}_2^+ &= M_{11} - \frac{M_{12}M_{21}}{M_{22}} \mathcal{E}_0^+ = \frac{2\imath n_0 n_1}{n_1^2 + n_0 n_2} \mathcal{E}_0^+ \overset{n_1^2 \equiv n_0 n_2}{\longrightarrow} \frac{\imath n_0}{n_1} \mathcal{E}_0^+ \\ \mathcal{E}_0^- &= -\frac{M_{21}}{M_{22}} \mathcal{E}_0^+ = \frac{n_1^2 - n_0 n_2}{n_1^2 + n_0 n_2} \mathcal{E}_0^+ \overset{n_1^2 \equiv n_0 n_2}{\longrightarrow} 0 . \end{aligned}$$

Choosing $n_1^2 \equiv n_0 n_2$ we can cancel out the reflection and maximize the transmission. We check,

$$\begin{aligned} T &= \frac{I_t}{I_i} = \frac{\varepsilon_2 c_2 |\mathcal{E}_2^+|^2}{\varepsilon_0 c_0 |\mathcal{E}_0^+|^2} = \frac{\frac{n_2^2}{c^2} \frac{c}{n_2} \left| \frac{2\imath n_0 n_1}{n_1^2 + n_0 n_2} \right|^2}{\frac{n_0^2}{c^2} \frac{c}{n_0}} = \frac{4 n_0 n_1^2 n_2}{(n_1^2 + n_0 n_2)^2} \\ R &= \frac{I_r}{I_i} = \frac{\varepsilon_0 c_0 |\mathcal{E}_0^-|^2}{\varepsilon_0 c_0 |\mathcal{E}_0^+|^2} = \left| \frac{n_1^2 - n_0 n_2}{n_1^2 + n_0 n_2} \right|^2 = 1 - T . \end{aligned}$$

Fig. 7.6 shows the transmission through a stack of dielectric layers. The transfer matrix is,

$$\mathcal{M} = (\mathcal{T}_{21}\mathcal{T}_{\Delta z_2}\mathcal{T}_{abs}\mathcal{T}_{12}\mathcal{T}_{\Delta z_1}\mathcal{T}_{abs})^N\mathcal{T}_{01} \ . \tag{7.80}$$

We observe a large reflection band (600..660 nm) called one-dimensional *photonic band gap*. Dielectric mirrors can, nowadays, achieve reflections up to $R = 99.9995\%$, while the reflectivity of metal mirrors is always limited by losses.

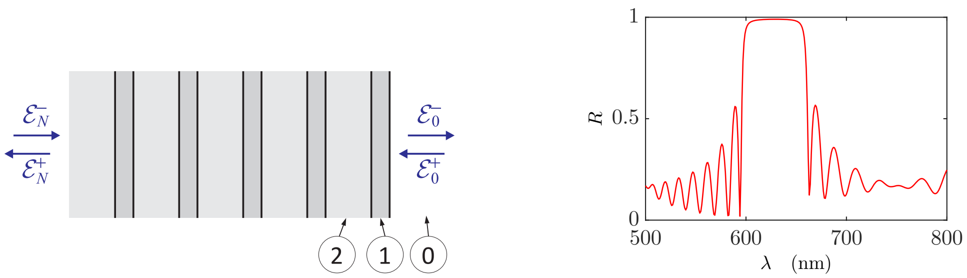

Figure 7.6: (code) Reflection by a high reflecting mirror made of 10 layers with $n_1 = 2.4$ and $\Delta z_1 = 80$ nm alternating with 10 layers with $n_2 = 1.5$ and $\Delta z_2 = 500$ nm. The absorption coefficient for each layer is supposed to be $\alpha = 0.2\%$. The beam impinges from vacuum, $n_0 = 1$.

Example 73 (*Use of transfer matrices in cavities*): The transfer matrix formalism can be used for *impedance matching* the reflection of optical cavities [5]. In order to deserve the label *mode*, a geometric configuration of a cavity must be self-consistent, that is, any field $\mathcal{E}^{\pm}(z)$ wanting to fill the mode must be the same after a round-trip around the cavity.

We proceed to calculating the real and imaginary parts of the transfer matrices,

$$\begin{pmatrix} \mathcal{E}_z^+ + \mathcal{E}_z^- \\ \mathcal{E}_z^+ - \mathcal{E}_z^- \end{pmatrix} = \mathcal{M} \begin{pmatrix} \mathcal{E}_0^+ + \mathcal{E}_0^- \\ \mathcal{E}_0^+ - \mathcal{E}_0^- \end{pmatrix} \ .$$

For example, the phase shift due to free space propagation is described by the matrix,

$$\mathcal{M}_{phase} = \begin{pmatrix} \cos kz & \imath \sin kz \\ \imath \sin kz & \cos kz \end{pmatrix} \ .$$

Reflection and transmission from a classical object with can be written as, $\vec{\mathcal{E}}_z^+ = t_a\mathcal{E}_0^+ + r_a\vec{\mathcal{E}}_z^-$ and $\mathcal{E}_0^- = t_a\vec{\mathcal{E}}_z^- - r_a\mathcal{E}_0^+$, where $r_a^2 + t_a^2 = 1$. Transforming to the basis $\mathcal{E}_j^+ \pm \mathcal{E}_j^-$, we obtain,

$$\mathcal{M}_{pump} = \begin{pmatrix} \frac{1+r_a}{t_a} & 0 \\ 0 & \frac{1-r_a}{t_a} \end{pmatrix} \ .$$

Let us assume that the cavity is pumped from one side by the field $\mathcal{E}_{in}$. We get after a round-trip,

$$\begin{pmatrix} \mathcal{E}^+ + \mathcal{E}^- \\ \mathcal{E}^+ - \mathcal{E}^- \end{pmatrix} = \mathcal{M} \begin{pmatrix} \mathcal{E}^+ + \mathcal{E}^- \\ \mathcal{E}^+ - \mathcal{E}^- \end{pmatrix} + t_{in} \begin{pmatrix} \mathcal{E}_{in}^+ + \mathcal{E}_{in}^- \\ \mathcal{E}_{in}^+ - \mathcal{E}_{in}^- \end{pmatrix} = t_{in}(1-\mathcal{M})^{-1} \begin{pmatrix} \mathcal{E}_{in}^+ + \mathcal{E}_{in}^- \\ \mathcal{E}_{in}^+ - \mathcal{E}_{in}^- \end{pmatrix} \ .$$

[5] Not to be confused with *phase matching* of optical cavities, which is an important requirement for coupling light efficiently into a cavity, but must be treated within the theory of Gaussian optics.

The phase minimum of the determinant $\det(1-\mathcal{M})$ determines the eigenvalues of the cavity. For a round-trip with losses in the mirrors the determinant is $\det(1-\mathcal{M}_{phase}\mathcal{M}_{loss}) = 2-(t_c+t_c^{-1})\cos\phi$, where t_c is the total transmission coefficient of the cavity. Phase minima always occur when $\phi = 2\pi n$. The amplification of the intensity at theses phases is given by,

$$\frac{I_{cav}}{I_{in}} = \frac{|\mathcal{E}^+ + \mathcal{E}^-|^2}{|\mathcal{E}_{in}^+ + \mathcal{E}_{in}^-|^2} = \frac{t_{in}^2}{(1-t_c)^2} \ .$$

Exc. 7.1.8.25 can be solved using transfer matrices.

The transfer matrix formalism can also be applied to modeling the passage of a laser beam through a gas of two levels atoms periodically organized in one dimension like a stack of pancakes [89, 81]. One only has to consider that the variation of the density of the gas along the optical axis generates a spatial modulation of the refractive index [6].

7.1.8 Exercises

7.1.8.1 Ex: Wave equation and Galilei transform

Show that any function of the form $y(x,t) = f(x-vt)$ or $y(x,t) = g(x+vt)$ satisfies the wave equation.

7.1.8.2 Ex: Plane waves

Consider a set of solutions for plane electromagnetic waves in vacuum, whose fields (electric or magnetic) are described by the real part of the functions $\mathbf{u}(\mathbf{r},t) = \mathbf{A}e^{\imath(\mathbf{k}\cdot\mathbf{r}-\omega t)}$, with constant phase $(\mathbf{k}\cdot\mathbf{r}-\omega t)$. In these expressions, $\mathbf{k}$ is the wavevector (determining the propagation direction of the wave) and $\omega = vk$ is the angular frequency, where $v = 1/\sqrt{\varepsilon\mu}$ is the propagation velocity of the waves.
a. Show that the divergent $\mathbf{u}(x,t)$ satisfies: $\nabla\cdot\mathbf{u} = \imath\mathbf{k}\cdot\mathbf{u}$;
b. Show that the rotation $\mathbf{u}(x,t)$ satisfies: $\nabla\times\mathbf{u} = \imath\mathbf{k}\times\mathbf{u}$;
c. Show that the waves are transverse and that the vectors $\vec{\mathcal{E}}$, $\vec{\mathcal{B}}$, and $\mathbf{k}$ are mutually perpendicular.

7.1.8.3 Ex: Polarization of a wave in vacuum

A transverse electromagnetic wave propagates through an isotropic, non-conducting medium without charges (vacuum) in positive z-direction. The projection of the vector of the electric field on the plane x-y has the form,

$$\vec{\mathcal{E}} = \vec{\mathcal{E}}_0\sin(kz-\omega t) = (\mathcal{E}_{0x}, \mathcal{E}_{0y}, 0)\sin(kz-\omega t) \ .$$

a. Illustrate the motion of the electric field vector by a scheme. How is the wave polarized?
b. Show from Maxwell's equations, that the magnetic field vector can be written as,

$$\vec{\mathcal{B}}(\mathbf{r},t) = \frac{1}{\omega}(\mathbf{k}\times\vec{\mathcal{E}})$$

[6] We will discuss this system in [7] .

with the wavevector $\mathbf{k} = k\hat{\mathbf{e}}_z$.
c. Calculate the energy flux of the wave (Poynting vector) $\vec{\mathcal{S}}(\mathbf{r}, t)$ as a function of the (phase) velocity of the wave c_0. How does the phase change in other media ($\mu \neq \mu_0$ and $\varepsilon \neq \varepsilon_0$)? What does this mean for $\vec{\mathcal{S}}(\mathbf{r}, t)$.

7.1.8.4 Ex: Jones matrices for a three-beam MOT

A three-beam magneto-optical trap (MOT) is characterized by the fact that each of three linearly polarized laser beams passes through a $\lambda/4$-waveplate rotated in a way to leave them circularly polarized. Then the beam traverses the MOT a first time, behind the MOT it passes through a second waveplate, and being finally reflected by a mirror, it makes all the way back, as shown in the figure. Show that the polarization of the laser beam at the position of the mirror is always *linear* independently of the rotation angle of the second waveplate.

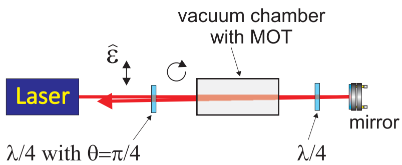

Figure 7.7: One of three retroreflected beams of a MOT.

7.1.8.5 Ex: Temporal average of waves in complex notation

In complex notation there is a practical recipe for finding the temporal average of a product of waves. Consider $f(\mathbf{r}, t) = \cos(\mathbf{k}\cdot\mathbf{r} - \omega t + \delta_a)$ and $g(\mathbf{r}, t) = \cos(\mathbf{k}\cdot\mathbf{r} - \omega t + \delta_b)$. Show $\overline{fg} = \frac{1}{2}\mathfrak{Re}\,(\tilde{f}\tilde{g}^*)$. Note, that this only works, when the two waves have the same wavevector $\mathbf{k}$ and the same frequency ω, but they may have arbitrary amplitudes and phases. For example,

$$\langle u \rangle = \frac{1}{4}\mathfrak{Re}\,(\varepsilon_0 \vec{\tilde{\mathcal{E}}} \cdot \vec{\tilde{\mathcal{E}}}^* + \frac{1}{\mu_0}\vec{\tilde{\mathcal{B}}} \cdot \vec{\tilde{\mathcal{B}}}^*) \qquad \text{and} \qquad \langle \vec{\mathcal{S}} \rangle = \frac{1}{2\mu_0}\mathfrak{Re}\,(\vec{\tilde{\mathcal{E}}} \times \vec{\tilde{\mathcal{B}}}^*) \ .$$

7.1.8.6 Ex: Radiation pressure of a plane wave

A plane electromagnetic wave impinges vertically on a plane.
a. Show that the radiation pressure exerted on a surface is equal to the energy density in the incident beam. Does this ratio depend on the reflected part of the radiation?
b. Now consider a beam of small massive balls of mass m incident on a plane. What is the relationship between the mean pressure on the surface and the kinetic energy in this case?

7.1.8.7 Ex: Radiation pressure of solar light

Estimate the radiation pressure force exerted by the Sun on the Earth, and compare this force to the gravitational force on Earth and at the atmospheric pressure. (The

intensity of sunlight at the Earth's orbit is $I = 1.37\,\mathrm{kW/m^2}$).
b. Repeat part (a) for Mars, which has an average distance of $2.28 \cdot 10^8$ km from the Sun and has a radius of 3400 km.
c. What is the exerted radiation pressure when light strikes a perfect absorber (reflector)?

7.1.8.8 Ex: Radiation pressure of a point-like emitter onto a plane

A punctual and intense source of light isotropically radiates 1.0 MW. The source is located 1.0 m above an infinite and perfectly reflecting plane. Determine the force that the radiation pressure exerts on the plane.

7.1.8.9 Ex: Maxwell's tensor for a plane wave

Find all the elements of Maxwell's stress tensor for a monochromatic plane wave traveling in z-direction and being linearly polarized in y-direction. Interpret the result remembering that $\overleftrightarrow{T}$ represents a momentum flux density. How is $\overleftrightarrow{T}$ related to the energy density in this case?

7.1.8.10 Ex: Superposition of waves

Suppose $Ae^{\imath ax} + Be^{\imath bx} = Ce^{\imath cx}\ \forall x$. Prove that $a = b = c$ and $A + B = C$.

7.1.8.11 Ex: Poynting vector of a superposition of two waves

The electric fields of two harmonic electromagnetic waves of angular frequencies ω_1 and ω_2 are given by $\vec{\mathcal{E}}_1 = \mathcal{E}_{10}\cos(k_1x - \omega_1 t)\hat{\mathbf{e}}_y$ and by $\vec{\mathcal{E}}_2 = \mathcal{E}_{20}\cos(k_2x - \omega_2 t + \delta)\hat{\mathbf{e}}_y$. For the superposition of these two waves, determine
a. the instantaneous Poynting vector and
b. the temporal average of the Poynting vector.
c. Repeat parts (a) and (b) for an inverted propagation direction of the second wave, i.e. $\vec{\mathcal{E}}_2 = \mathcal{E}_{20}\cos(k_2x + \omega_2 t + \delta)\hat{\mathbf{e}}_y$.

7.1.8.12 Ex: Poynting vector of a standing wave

The electric field $\vec{\mathcal{E}}(\mathbf{r}, t)$ of a standing electromagnetic wave in vacuum be given by,

$$\vec{\mathcal{E}}(\mathbf{r}, t) = \mathfrak{Re}\ \left(\mathcal{E}_0\hat{\mathbf{e}}_x e^{\imath(kz-\omega t)} - \mathcal{E}_0\hat{\mathbf{e}}_x e^{\imath(-kz-\omega t)}\right) = 2\mathcal{E}_0 \sin kz \sin \omega t \hat{\mathbf{e}}_x$$

with $\mathcal{E}_0 \in \mathbb{R}$.
a. Determine the corresponding magnetic field $\vec{\mathcal{B}}(\mathbf{r}, t)$.
b. Calculate the Poynting vector $\vec{\mathcal{S}}(\mathbf{r}, t)$. What follows for the energy flow $\bar{s}$ of the standing electromagnetic wave in the temporal average, that is, calculate

$$\bar{s} = \frac{\int dt\ s}{\int dt}\ ,$$

where both integrals should be evaluated between $t = 0$ and $t = 2\pi/\omega$.

7.1.8.13 Ex: Phase fronts of planar and spherical waves

Describes the phase front for (a) a plane wave and (b) a spherical wave.

7.1.8.14 Ex: Fake spherical wave

We verified in class, that spherical waves of the form

$$\vec{\mathcal{E}}_\pm(\mathbf{r},t) = \vec{\mathcal{E}}_0 \frac{1}{r} e^{\imath(kr\pm\omega t)} \qquad \text{and} \qquad \vec{\mathcal{B}}_\pm(\mathbf{r},t) = \vec{\mathcal{B}}_0 \frac{1}{r} e^{\imath(kr\pm\omega t)}$$

with $\omega = ck$, $c^2 = 1/(\varepsilon_0\mu_0)$ satisfy the Helmholtz equation. Argue, why nevertheless, they can not be electromagnetic waves. Check whether such waves satisfy the homogeneous Maxwell equations.

7.1.8.15 Ex: Spherical wave

Consider a spherical electromagnetic wave,

$$\vec{\mathcal{E}}(\mathbf{r},t) = \vec{\mathcal{E}}_0(r,\theta) e^{\imath(kr-\omega t)} \qquad \text{and} \qquad \vec{\mathcal{B}}(\mathbf{r},t) = \vec{\mathcal{B}}_0(r,\theta) e^{\imath(kr-\omega t)} \ .$$

Show that the validity of Maxwell's equations for $\nabla \cdot \vec{\mathcal{E}} = 0 = \nabla \cdot \vec{\mathcal{B}}$ for the case of vanishing charge and current densities implies that $\vec{\mathcal{E}}$, $\vec{\mathcal{B}}$, and $\hat{\mathbf{e}}_r$ are mutually orthogonal (transversality).

7.1.8.16 Ex: Spherical wave in a neutral dielectric medium

a. Show that spherical waves $\vec{\mathcal{E}}(\mathbf{r},t) = \frac{\vec{\mathcal{E}}_0}{r} e^{\imath(kr-\omega t)}$ solve the wave equation in a vacuum, when $\omega = ck$. The Laplace operator in spherical coordinates is,

$$\nabla^2 = \frac{1}{r^2}\frac{\partial}{\partial r}\left(r^2 \frac{\partial}{\partial r}\right) + \frac{1}{r^2}\Delta_{\theta,\phi} \ .$$

The second term only acts on the parts that depend on the angles. Verify that $\Delta_{\theta,\phi}\vec{\mathcal{E}} \equiv 0$.

b. Show that the wave equations have the form,

$$\nabla^2 \vec{\mathcal{E}} - \frac{1}{c^2}\frac{\partial^2 \vec{\mathcal{E}}}{\partial t^2} = \frac{1}{\varepsilon_0 c^2}\frac{\partial^2 \vec{\mathcal{P}}}{\partial t^2} \ ,$$

when the wave does not propagate in a vacuum, but in a neutral dielectric medium (i.e. without free charges). Assume the simple case that the dielectric displacement $\vec{\mathcal{D}} = \varepsilon_0\vec{\mathcal{E}} + \vec{\mathcal{P}}$ has the form,

$$\vec{\mathcal{P}} = \varepsilon_0 \chi \vec{\mathcal{E}} \ .$$

What is the form of the wave equations in this case? How do you change the phase velocity c of the wave? You can identify the meaning of the quantity $n \equiv \sqrt{1+\chi}$?

7.1.8.17 Ex: Refraction in a bath of water

An observer stands at the edge of a basin filled with water down to a depth of $h = 2.81$ m. He looks at an object lying on the bottom. At what depth h' appears the image of the object, if the direction of observation in which the observer perceives the image forms with the normal direction to the water surface an angle of $\alpha = 60°$? Prepare a scheme.

7.1.8.18 Ex: Poynting vector of a partially reflected wave

A plane wave $\vec{\mathcal{E}}_{in}(z,t)$ which is linearly polarized in x-direction runs along the z-axis from $-\infty$ towards an interface ($z = 0$-plane). At the interface, a part r of the wave is reflected without phase shift.
a. Give the amplitudes of the electric and the magnetic field in the half-space $z < 0$ in real numbers.
b. Give the Poynting vector $\vec{\mathcal{S}}(z,t)$ and its time average.

7.1.8.19 Ex: Energy flow upon refraction

Two infinitely extended media with relative dielectric constants ϵ_1 and ϵ_2 and permeabilities $\mu_1 = \mu_2 = \mu_0$, that is, with refraction indices $n_1 = \sqrt{\epsilon_1}$ and $n_2 = \sqrt{\epsilon_2}$, be separated by the $z = 0$-plane. Coming from the medium n_1 traveling in x-direction a linearly polarized plane wave with frequency ω and wavenumber k_1 hits the interface perpendicularly. The amplitude is $\mathcal{E}_0$.
a. Use the continuity of the normal components of $\vec{\mathcal{D}}$ and $\vec{\mathcal{B}}$, as well as of the tangential components of $\vec{\mathcal{E}}$ and $\vec{\mathcal{H}}$, at the interface to calculate the amplitudes of refracted part and the reflected part of the incident wave.
b. The energy flux is defined by the temporal average of the real part of the Poynting vector $\vec{\mathcal{S}}$: $\vec{\varphi} \equiv \mathfrak{Re}\,[\vec{\mathcal{E}} \times \vec{\mathcal{H}}^*]$. Calculate the incident, reflected, and refracted energy fluxes. What is the total flux in front and behind of the interface?
c. Determine the reflection coefficient r (the ratio between the absolute values of the reflected and incident fluxes) and the transmission coefficient t (the ratio between the absolute values of the transmitted and incident fluxes).

7.1.8.20 Ex: Birefringent crystal

An optically anisotropic crystal has in the x-direction the dielectric constant ε_1 (that is, the refractive index $n_1 = c\sqrt{\varepsilon_1\mu_1}$) and in the y-direction ε_2, respectively, n_2. A linearly polarized plane wave with frequency ω propagating in z-direction impinges, coming from the vacuum, at normal incidence on a disc of thickness d of this material in such a way, that the plane of the polarization forms with the x and y-axes an angle of $45°$. What is the polarization of the plane wave after the transition through the disk? How should we choose d, so that the wave is circularly polarized? Express this thickness in terms of the vacuum wavelength.

7.1.8.21 Ex: Glass cube

At the center of a glass cube of length $d = 10\,\text{mm}$ with the refractive index $n = 1.5$ there is a small spot. Which parts should the surfaces be covered so that the spot is invisible from outside the cube regardless of the direction of vision? Neglect the light refracted out of the cube after a first reflection inside the cube.

7.1.8.22 Ex: Total internal reflection

a. We consider the transition of a beam of light from an optically dense medium (1) to a more dilute medium (2). Extending the theory of light refraction at interfaces

beyond the angle of total internal reflection (7.70), derive the expression for the electric field in the medium (2).
b. Noting that α [from Eq. (7.60)] is now imaginary, use the equation (7.61) to calculate the reflection coefficient for the polarization parallel to the plane of incidence [8].
c. Do the same for polarization that is perpendicular to the plane of incidence.
d. In case of perpendicular polarization, show that the (real) evanescent fields are,

$$\vec{\mathcal{E}}(\mathbf{r},t) = \mathcal{E}_0 e^{-\kappa z}\cos(kx-\omega t)\hat{\mathbf{e}}_y \quad , \quad \vec{\mathcal{B}}(\mathbf{r},t) = \mathcal{E}_0 e^{-\kappa z}[\kappa\sin(kx-\omega t)\hat{\mathbf{e}}_x + k\cos(kx-\omega t)\hat{\mathbf{e}}_z] \; .$$

e. Verify that the fields in (d) satisfy all Maxwell equations without sources.
f. For the fields in (d), construct the Poynting vector and show that, on average, no energy is transmitted in z-direction.

7.1.8.23 Ex: Fresnel formulae

Rewrite the Fresnel formulae (7.61) and (7.63) in terms of the wavevectors of the incident, reflected and transmitted waves.

7.1.8.24 Ex: The Goos-Hänchen effect

The Goos-Hänchen shift is an optical phenomenon in which a linearly polarized light beam with finite transverse extension suffers, under total internal reflection from a plane interface, a small lateral displacement within the plane of incidence. The effect is due to an interference of the partial waves composing the finite-sized beam, hitting the interface under different angles and thus undergoing different phase shifts upon reflection. The sum of the reflected waves with different phase shifts form an interference pattern transverse to the mean propagation direction leading to a lateral displacement of the beam. Thus, the Goos-Hänchen effect is a coherence phenomenon [40, 41, 47].
To describe this phenomenon quantitatively, we consider a linearly polarized light beam of wavelength λ, with finite transverse size. This beam is fully internally reflected at the interface between two non-permeable media with refractive indices n_1 and $n_2 < n_1$. The relationship between the reflected and incident amplitudes is a complex number, which can be expressed by $\mathcal{E}_0''/\mathcal{E}_0 = e^{\imath\phi(\theta_i,\theta_{i,total})}$ for the angle of incidence $\theta_i > \theta_{i,total}$, where $\sin\theta_{i,total} = \frac{n_2}{n_1}$.
a. Show that for a beam of 'monochromatic' radiation in z-direction with an electric field amplitude of $\mathcal{E}(x)e^{\imath kz-\imath\omega t}$, where $\mathcal{E}(x)$ is smooth and finite in transverse direction (albeit extending over many wavelengths), the first approximation in terms of plane waves is,

$$\vec{\mathcal{E}}(x,z,t) = \hat{\epsilon}\int A(\kappa)e^{\imath\kappa x+\imath kz-\imath\omega t}d\kappa \; ,$$

where $\hat{\epsilon}$ is a polarization vector and $A(\kappa)$ is the Fourier transform of $\mathcal{E}(x)$ with respect to κ around $\kappa = 0$ small compared to k. The finite-sized beam consists of plane waves with a small range of angles of incidence centered around the valor predicted by geometric optics.

[8] We observe 100% reflection, which is better than on a conductive surface.

b. Consider the reflected beam and show that for $\theta_i > \theta_{i,total}$ the electric field can be expressed approximately as,

$$\vec{\mathcal{E}}_r(x,z,t) = \hat{\epsilon}_r \mathcal{E}(\xi - \delta\xi) e^{\imath \mathbf{k}_r \cdot \mathbf{r} - \imath\omega t + \imath\phi(\theta_i)} \ ,$$

where $\hat{\epsilon}_r$ is a polarization vector, ξ is the coordinate perpendicular to $\mathbf{k}_r$, which is the reflected wavevector and $\delta\xi = -\frac{1}{k}\frac{d\phi(\theta_i)}{d\theta_i}$.
c. With the Fresnel expressions for the phases $\phi(\theta_i)$ and for the two polarization states of the plane, show that the lateral displacements of the beams with respect to the position predicted by geometric optics are,

$$\mathcal{D}_s = \frac{\lambda}{\pi}\frac{\sin\theta_i}{\sqrt{\sin^2\theta_i - \sin^2\theta_{i,total}}} \qquad \text{and} \qquad \mathcal{D}_p = \mathcal{D}_s \frac{\sin^2\theta_{i,total}}{\sin^2\theta_i - \cos^2\theta_i \sin^2\theta_{i,total}} \ .$$

7.1.8.25 Ex: Interfaces

A light field of angular frequency ω passes from a medium (1), through a slab of thickness d representing a medium (2), to a medium (3). All three media are linear and homogeneous. Calculate the transmission coefficient between the media 1 and 3 for normal incidence.

7.2 Optical dispersion in material media

7.2.1 Plane waves in conductive media

When there are free charges in the propagation medium, we can not neglect neither ϱ_f nor $\mathbf{j}_f$ in the Maxwell equations used to describe the wave propagation, because the electric field of the wave will itself generate a current $\mathbf{j}_f = \varsigma\vec{\mathcal{E}}$, where ς is the conductivity introduced in Eq. (3.41). Thus, for linear media we must use the complete equations (6.6).

For a homogeneous and linear medium, the continuity equation gives,

$$\frac{\partial\varrho_f}{\partial t} = -\nabla\cdot\mathbf{j}_f = -\varsigma\nabla\cdot\vec{\mathcal{E}} = -\frac{\varsigma}{\varepsilon}\varrho_f \ , \tag{7.81}$$

with the solution

$$\varrho_f(t) = e^{-(\varsigma/\varepsilon)t}\varrho_f(0) \ . \tag{7.82}$$

Therefore, every initial free charge density $\varrho_f(0)$ diffuses within a characteristic time $\tau = \varepsilon/\varsigma$. This reflects the familiar fact that free charges in a conductor migrate to its edges with a speed that depends on the conductivity ς. For a good conductor, the relaxation time is much shorter than other characteristic times of the system, e.g. for oscillatory systems $\tau \ll \omega^{-1}$. In stationary situations we can assume, $\varrho = 0$, such that the relevant Maxwell equations,

$$\begin{array}{lrcl}
\text{(i)} & \nabla\times\vec{\mathcal{B}} - \varepsilon\mu\partial_t\vec{\mathcal{E}} & = & \mu\varsigma\vec{\mathcal{E}} \\
\text{(ii)} & \nabla\times\vec{\mathcal{E}} + \partial_t\vec{\mathcal{B}} & = & 0 \\
\text{(iii)} & \nabla\cdot\vec{\mathcal{E}} & = & 0 \\
\text{(iv)} & \nabla\cdot\vec{\mathcal{B}} & = & 0
\end{array} \ , \tag{7.83}$$

only differ from the Maxwell equations for dielectric media by the existence of the term $\mu\varsigma\vec{\mathcal{E}}$.

Letting the rotation operator act on equations (i) and (ii) and exploiting the disappearance of the field divergences we obtain generalized wave equations,

$$\nabla^2\vec{\mathcal{E}} = \varepsilon\mu\frac{\partial^2\vec{\mathcal{E}}}{\partial t^2} + \varsigma\mu\frac{\partial\vec{\mathcal{E}}}{\partial t} \quad \text{and} \quad \nabla^2\vec{\mathcal{B}} = \varepsilon\mu\frac{\partial^2\vec{\mathcal{B}}}{\partial t^2} + \varsigma\mu\frac{\partial\vec{\mathcal{B}}}{\partial t} . \tag{7.84}$$

These equations still accept plane wave solutions,

$$\vec{\mathcal{E}}(z,t) = \vec{\mathcal{E}}_0 e^{\imath(\tilde{k}z-\omega t)} \quad \text{and} \quad \vec{\mathcal{B}}(z,t) = \vec{\mathcal{B}}_0 e^{\imath(\tilde{k}z-\omega t)} , \tag{7.85}$$

but this time the wavevector is complex,

$$\tilde{k}^2 = \varepsilon\mu\omega^2 + \imath\varsigma\mu\omega , \tag{7.86}$$

which can easily be verified by inserting a plane wave into the wave equations (7.84). The root of this expression gives,

$$\boxed{\begin{aligned} \tilde{k} = k + \imath\kappa \qquad \text{with} \qquad & k \equiv \omega\sqrt{\frac{\varepsilon\mu}{2}}\left(\sqrt{1+\left(\frac{\varsigma}{\varepsilon\omega}\right)^2}+1\right)^{1/2} \\ \text{and} \qquad & \kappa \equiv \omega\sqrt{\frac{\varepsilon\mu}{2}}\left(\sqrt{1+\left(\frac{\varsigma}{\varepsilon\omega}\right)^2}-1\right)^{1/2} \end{aligned}} . \tag{7.87}$$

The imaginary part results in an attenuation of the wave in z-direction:

$$\vec{\tilde{\mathcal{E}}}(z,t) = \vec{\tilde{\mathcal{E}}}_0 e^{-\kappa z} e^{\imath(kz-\omega t)} \quad \text{and} \quad \vec{\tilde{\mathcal{B}}}(z,t) = \vec{\tilde{\mathcal{B}}}_0 e^{-\kappa z} e^{\imath(kz-\omega t)} . \tag{7.88}$$

The typical attenuation distance, κ^{-1}, called *skin depth*, measures the penetration depth of the wave in a conductor, while the real part k determines the propagation of the wave. As before, the equations (7.83)(iii) and (iv) exclude components perpendicular to the interface. The wave only has transverse components, that is, parallel to the interface, so that we can let the electric field be along $\hat{\mathbf{e}}_x$,

$$\vec{\tilde{\mathcal{E}}}(z,t) = \tilde{\mathcal{E}}_0 \hat{\mathbf{e}}_x e^{-\kappa z} e^{\imath(kz-\omega t)} \quad \text{and} \quad \vec{\tilde{\mathcal{B}}}(z,t) = \tilde{\mathcal{B}}_0 \hat{\mathbf{e}}_y e^{-\kappa z} e^{\imath(kz-\omega t)} . \tag{7.89}$$

By the equation (7.83)(ii) we verify,

$$\tilde{\mathcal{B}}_0 = \frac{\tilde{k}}{\omega}\tilde{\mathcal{E}}_0 . \tag{7.90}$$

Expressing the wavevector and the complex amplitudes by phase factors,

$$\tilde{k} = Ke^{\imath\phi} \quad , \quad \tilde{\mathcal{E}}_0 = \mathcal{E}_0 e^{\imath\delta_E} \quad , \quad \tilde{\mathcal{B}}_0 = \mathcal{B}_0 e^{\imath\delta_B} , \tag{7.91}$$

with $K, \mathcal{E}_0, \mathcal{B}_0 \in \mathbb{R}$, we finally find,

$$\mathcal{B}_0 e^{\imath\delta_B} = \frac{Ke^{\imath\phi}}{\omega}\mathcal{E}_0 e^{\imath\delta_E} , \tag{7.92}$$

that is,

$$\frac{\mathcal{B}_0}{\mathcal{E}_0} = \frac{K}{\omega} = \frac{\sqrt{k^2+\kappa^2}}{\omega} = \sqrt{\varepsilon\mu\sqrt{1+\left(\frac{\varsigma}{\varepsilon\omega}\right)^2}} \tag{7.93}$$

and

$$\vec{\mathcal{E}}(z,t) = \mathcal{E}_0\hat{\mathbf{e}}_x e^{-\kappa z}\cos(kz-\omega t+\delta_E) \tag{7.94}$$
$$\vec{\mathcal{B}}(z,t) = \mathcal{B}_0\hat{\mathbf{e}}_y e^{-\kappa z}\cos(kz-\omega t+\delta_E+\phi)\ ,$$

as illustrated in Fig. 7.8. Such a wave is called *evanescent wave*. From Eqs. (7.93) and (7.87) we immediately deduce,

$$K \overset{\varsigma\to 0}{\longrightarrow} \frac{\omega}{c_n} \quad \text{and} \quad \phi = \arctan\frac{\kappa}{k} \overset{\varsigma\to 0}{\longrightarrow} 0 \tag{7.95}$$
$$K \overset{\varsigma\to\infty}{\longrightarrow} \infty \quad \text{and} \quad \phi \overset{\varsigma\to\infty}{\longrightarrow} \tfrac{\pi}{4}\ .$$

Do the Exc. 7.2.7.1 and 7.2.7.2.

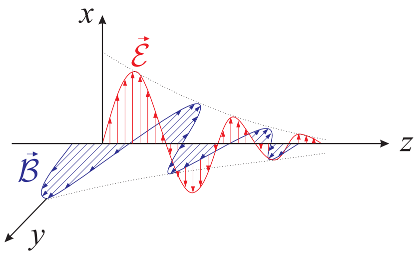

Figure 7.8: Attenuation of a wave by a conducting medium.

7.2.1.1 Reflection by a conductive surface

In the presence of free charges and currents the boundary conditions derived in (7.42) must be generalized,

$$\begin{array}{llcl} \text{(i)} & \frac{1}{\mu_1}\vec{\mathcal{B}}_1^{\parallel} - \frac{1}{\mu_2}\vec{\mathcal{B}}_2^{\parallel} & = & \mathbf{k}_f\times\hat{\mathbf{e}}_n \\ \text{(ii)} & \vec{\mathcal{E}}_1^{\parallel} - \vec{\mathcal{E}}_2^{\parallel} & = & 0 \\ \text{(iii)} & \varepsilon_1\vec{\mathcal{E}}_1^{\perp} - \varepsilon_2\vec{\mathcal{E}}_2^{\perp} & = & \sigma_f \\ \text{(iv)} & \vec{\mathcal{B}}_1^{\perp} - \vec{\mathcal{B}}_1^{\perp} & = & 0 \end{array}\ , \tag{7.96}$$

where σ_f is the density of free surface charges, $\mathbf{k}_f$ is the density of free surface currents, and $\hat{\mathbf{e}}_n$ the normal vector of the surface pointing into the direction of medium 1 (compare with Fig. 4.14).

We now assume that the interface at $z=0$ separates the dielectric medium 1 from the conductive medium 2. A monochromatic plane wave is partially reflected and transmitted, as discussed above,

$$\begin{aligned}
\vec{\tilde{\mathcal{E}}}_i(z,t) &= \tilde{\mathcal{E}}_{0i}\hat{\mathbf{e}}_x e^{\imath(k_1z-\omega t)} \quad , \quad & \vec{\tilde{\mathcal{B}}}_i(z,t) &= -\tfrac{1}{c_1}\tilde{\mathcal{E}}_{0i}\hat{\mathbf{e}}_y e^{\imath(k_1z-\omega t)} \\
\vec{\tilde{\mathcal{E}}}_r(z,t) &= \tilde{\mathcal{E}}_{0r}\hat{\mathbf{e}}_x e^{\imath(-k_1z-\omega t)} \quad , \quad & \vec{\tilde{\mathcal{B}}}_r(z,t) &= \tfrac{1}{c_1}\tilde{\mathcal{E}}_{0r}\hat{\mathbf{e}}_y e^{\imath(k_1z-\omega t)} \quad , \\
\vec{\tilde{\mathcal{E}}}_t(z,t) &= \tilde{\mathcal{E}}_{0t}\hat{\mathbf{e}}_x e^{\imath(\tilde{k}_2z-\omega t)} \quad , \quad & \vec{\tilde{\mathcal{B}}}_t(z,t) &= \tfrac{\tilde{k}_2}{\omega}\tilde{\mathcal{E}}_{0t}\hat{\mathbf{e}}_y e^{\imath(\tilde{k}_2z-\omega t)}
\end{aligned} \tag{7.97}$$

Obviously, the transmitted wave penetrating the conductive medium is attenuated.

The boundary conditions at $z=0$ become, for the considered case ($\vec{\mathcal{E}}^\perp = 0 = \vec{\mathcal{B}}^\perp$) and with $\mathbf{k}_f = 0$,

$$\begin{aligned}
&\text{(i)} & \tfrac{1}{\mu_1 c_1}(\mathcal{E}_{0i} - \mathcal{E}_{0r}) &= \tfrac{\tilde{k}_2}{\mu_2\omega}\mathcal{E}_{0t} \\
&\text{(ii)} & \tilde{\mathcal{E}}_{0i} + \tilde{\mathcal{E}}_{0r} &= \tilde{\mathcal{E}}_{0t} \\
&\text{(iii)} & 0 &= \sigma_f \\
&\text{(iv)} & 0 &= 0 \,.
\end{aligned} \quad , \tag{7.98}$$

Defining,

$$\tilde{\beta} \equiv \frac{\mu_1\tilde{k}_2}{\mu_2 k_1} \ , \tag{7.99}$$

we derive,

$$\frac{\tilde{\mathcal{E}}_{0r}}{\tilde{\mathcal{E}}_{0i}} = \frac{1-\tilde{\beta}}{1+\tilde{\beta}} \quad \text{and} \quad \frac{\tilde{\mathcal{E}}_{0t}}{\tilde{\mathcal{E}}_{0i}} = \frac{2}{1+\tilde{\beta}} \ . \tag{7.100}$$

The formulas are formally similar to (7.48), but they are complex. For a bad conductor ($\varsigma = 0 \ \rightarrow \ \kappa = 0$) we recover the equation (7.48). For a perfect conductor ($\varsigma = \infty \ \rightarrow \ \kappa = \infty \ \rightarrow \ \tilde{\beta} = \imath\infty$) we find $\tilde{\mathcal{E}}_{0r} = -\tilde{\mathcal{E}}_{0i}$ and $\tilde{\mathcal{E}}_{0t} = 0$. That is, the wave is fully reflected with a phase change of 180° [9].

7.2.2 Linear and quadratic dispersion

The refractive index may depend on the wavelength. Even the *refractive index of air* exhibits dispersion, as shown in Fig. 7.9 [10].

We consider a superposition of two waves,

$$\begin{aligned}
Y_1(x,t) + Y_2(x,t) &= a\cos(k_1x - \omega_1 t) + a\cos(k_2x - \omega_2 t) \\
&= 2a\cos\left[\tfrac{(k_1-k_2)x}{2} - \tfrac{(\omega_1-\omega_2)t}{2}\right]\cos\left[\tfrac{(k_1+k_2)x}{2} - \tfrac{(\omega_1+\omega_2)t}{2}\right] \ .
\end{aligned} \tag{7.101}$$

The resulting wave can be seen as a wave of frequency $\frac{1}{2}(\omega_1+\omega_2)t$ and wavelength $\frac{1}{2}(k_1+k_2)$ whose amplitude is modulated by an envelope of frequency $\frac{1}{2}(\omega_1-\omega_2)t$ and wavelength $\frac{1}{2}(k_1-k_2)x$.

---

[9] The 'skin depth' in silver (for optical frequencies) is in the order of 10 nm. For this reason, thin layers of good conductors already represent good mirrors.

[10] The refractive index of air can be calculated by the formula $n = 1 + (n_s - 1)\frac{0.00185097}{1+0.003661}\frac{P}{T}$ with $n_s = \sqrt{1 + \frac{4.334446\cdot10^{-4}\lambda^2}{\lambda^2-3.470339\cdot10^{-3}} + \frac{1.118728\cdot10^{-4}\lambda^2}{\lambda^2-1.394001\cdot10^{-2}}}$, where T is the temperature in Celsius and P the atmospheric pressure in mbar.

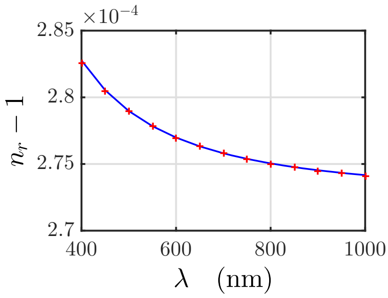

Figure 7.9: (code) Refractive index of air. The crosses were calculated by the Cauchy formula (7.146), with $A = 0.0002725$ and $B = 0.0059$.

In the absence of dispersion the *phase velocities* of the two waves and the propagation velocity of the envelope, called *group velocity*, are equal,

$$c = \frac{\omega_1}{k_1} = \frac{\omega_2}{k_2} = \frac{\omega_1 - \omega_2}{k_1 - k_2} = \frac{\Delta\omega}{\Delta k} = v_g \ . \tag{7.102}$$

But the phase velocities of the two harmonic waves may be different, $c = c(k)$, such that the frequency depends on the wavelength, $\omega = \omega(k)$. In this case, the group velocity also varies with the wavelength,

$$v_g = \frac{d\omega}{dk} = \frac{d}{dk}(kc) = c + k\frac{dc}{dk} \ . \tag{7.103}$$

Often, this variation is not very strong, such that it is possible to expand around an average value ω_0 of the spectral region of interest,

$$\boxed{\begin{aligned} \omega(k) &= \omega_0 + \left.\frac{d\omega}{dk}\right|_{k_0} \cdot (k - k_0) + \frac{1}{2}\left.\frac{d^2\omega}{dk^2}\right|_{k_0} \cdot (k - k_0)^2 \\ &\equiv \omega_0 + v_g(k - k_0) + \beta(k - k_0)^2 \end{aligned}} \ . \tag{7.104}$$

Generally, $v_g < c$, in which situation we speak of *normal dispersion*. But there are situations of *anomalous dispersion*, where $v_g > c$, e.g. close to resonances or when the wave under study is a *matter wave* characterized by quadratic dispersion [11], $\hbar\omega = (\hbar k)^2/2m$.

Example 74 (*Rectangular wave packet with linear dispersion*): As an example we determine the shape of the wavepacket for a rectangular amplitude distribution, $A(k) = A_0\chi_{[k_0-\Delta k/2, k_0+\Delta k/2]}$, subject to linear dispersion (expan-

[11] Since $c = \frac{\omega}{c} = \frac{\hbar k}{2m} < \frac{\hbar k}{m} = v_g$.

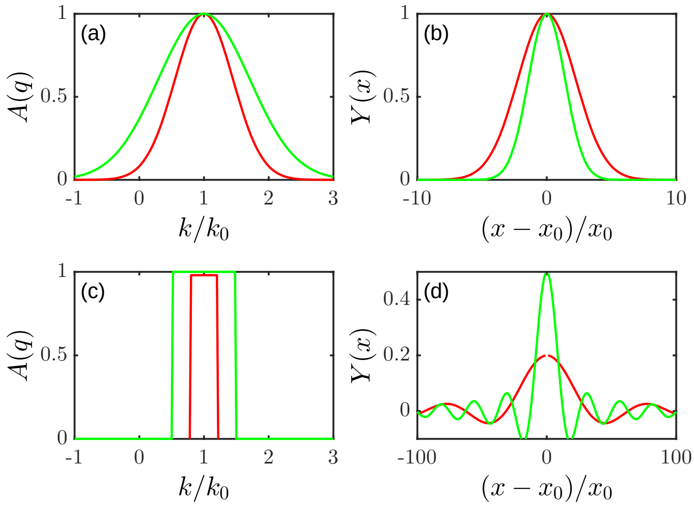

Figure 7.10: (code) Gaussian amplitude distribution (a,b) and rectangular distribution (c,d) in momentum space (a,c) and in position space (b,d).

sion up to the linear term in Eq. (7.104)). Via the Fourier theorem,

$$\begin{aligned}
Y(x,t) &= \int_{-\infty}^{\infty} A(k)e^{\imath(kx-\omega t)}dk = A_0\int_{k_0-\Delta k/2}^{k_0+\Delta k/2} e^{\imath(kx-\omega_0 t+v_g(k-k_0)t)}dk \\
&= A_0 e^{\imath(k_0x-\omega_0 t)}\int_{k_0-\Delta k/2}^{k_0+\Delta k/2} e^{\imath(k-k_0)(x-v_g t)}dk \\
&= A_0 e^{\imath(k_0x-\omega_0 t)}\int_{-\Delta k/2}^{\Delta k/2} e^{\imath k(\overbrace{x-v_g t}^{u})}dk \\
&= A_0\frac{e^{\imath u\Delta k/2}-e^{-\imath u\Delta k/2}}{\imath u}e^{\imath(k_0x-\omega_0 t)} = 2A_0\frac{\sin\frac{u\Delta k}{2}}{u}e^{\imath(k_0x-\omega_0 t)} \equiv A(x,t)e^{\imath(k_0x-\omega_0 t)} \ .
\end{aligned}$$

The envelope $A(x,t)$ has the shape of a 'sinc' function, such that the wave intensity is,

$$|Y(x,t)|^2 = A_0^2\Delta k^2\ \text{sinc}^2\left[\tfrac{\Delta k}{2}(x-v_g t)\right] \ .$$

Obviously, the *wave packet* is at any time t localized in space, as illustrated by the lower graphs of Figs. 7.10. It *moves with group velocity*, v_g, but it does not spread.

The last example showed, that linear dispersion does not lead to spreading (or diffusion) of a wavepacket, as opposed to quadratic dispersion, which we will show in the following example.

Example 75 (*Dispersion of a Gaussian wavepacket subject to quadratic dispersion*): Quadratic dispersion causes spreading of wavepackets. We show this at the example of the Gaussian wavepacket, $A(k) = A_0e^{-\alpha(k-k_0)^2}$, expanding the dispersion relation (7.104) up to the quadratic term. Via the Fourier theorem,

$$\begin{aligned}
Y(x,t) &= \int_{-\infty}^{\infty} A(k)e^{\imath(kx-\omega t)}dk = A_0 e^{\imath(k_0x-\omega_0 t)} \int_{-\infty}^{\infty} e^{\imath(k-k_0)(x-v_gt)-(\alpha+\imath\beta t)(k-k_0)^2}dk \\
&= A_0 e^{\imath(k_0x-\omega_0 t)} \int_{-\infty}^{\infty} e^{\imath k(\overbrace{x-v_gt}^{u})-(\overbrace{\alpha+\imath\beta t}^{v})k^2}dk \\
&\equiv A_0 e^{\imath(k_0x-\omega_0 t)} \int_{-\infty}^{\infty} e^{\imath ku-vk^2}dk = A_0\sqrt{\tfrac{\pi}{v}}e^{\imath(k_0x-\omega_0 t)}e^{-u^2/4v} \ .
\end{aligned}$$

The absolute square of the solution describes the spatial energy distribution of the packet,

$$|Y(x,t)|^2 = A_0^2\frac{\pi}{\sqrt{vv^*}}e^{-u^2/4v-u^2/4v^*} = A_0^2\frac{\pi}{x_0\sqrt{\alpha/2}}e^{-(x-v_gt)^2/x_0^2} \ ,$$

with $x_0 \equiv \sqrt{2\alpha}\sqrt{1+\frac{\beta^2}{\alpha^2}t^2}$. Obviously, for long times the pulse spreads with constant velocity. Since the constant α gives the initial width of the pulse, we realize that an initially compressed pulse spreads faster. Therefore, the angular coefficient of the dispersion relation determines the group velocity, while the curvature determines the spreading velocity. See upper graphs of Figs. 7.10.

Resolve the Excs. 7.2.7.3 to 7.2.7.5.

7.2.3 Microscopic dispersion and the Lorentz model

Obviously, the structure that we assume for the matter also influences its reaction to electromagnetic waves, which interact differently with the charged components of the matter. The planetary model proposed by *E. Rutherford* considers matter to be made of atoms, which in turn are composed of *bound electrons* orbiting small positively charged nuclei. On the other side, metals have free electrons. The inertia of the charged particles (free or bound electrons, ions) being accelerated by incident electromagnetic waves is the reason for the dispersion phenomena that we will treat in the following sections.

Thomson scattering is the elastic scattering of light (photons) by free or quasi-free electrically charged particles (that is, weakly bound as compared to photon energies). A charged particle is prompted by the field of an electromagnetic wave to perform harmonic oscillations within the plane spanned by the electric and the magnetic field vectors. As the oscillation is an accelerated motion, the particle simultaneously re-emits energy in the form of an electromagnetic wave with the same frequency (dipole radiation). Thomson scattering does not consider photonic recoil, that is, there is no transfer of momentum from the photon to the electron, which is only a good assumption when the energy of the incident photons is small enough, that is, $\hbar\omega \ll m_ec^2$, so that the wavelength of the electromagnetic radiation is much longer than the Compton wavelength $\lambda \gg \lambda_C = h/mc \simeq 2.4\,\text{pm}$ of the electron (which is the case for optical wavelengths). For higher energies, it is necessary to take the recoil of the electron into consideration (as done in the case of Compton scattering) [12].

[12] Thomson scattering can be considered the limiting case of *Compton scattering* for small photon energies. The Thomson model holds for free electrons in a metal, whose resonant frequency tends, due to the absence of restoring forces, to zero. Scattering by bound electrons is called *Rayleigh*

7.2.3.1 Lorentz model

In classical physics the scattering of light by charges is described by the *Lorentz model* [43]. Assuming a harmonic electric field, $\vec{\mathcal{E}}(t) = \vec{\mathcal{E}}_0 e^{-\imath\omega t}$, we derive a force acting on an electron harmonically bound to a potential [13],

$$\mathbf{F} = -e\vec{\mathcal{E}}(t) \tag{7.105}$$

with e the elementary charge. The equation of motion is that of a damped harmonic oscillator:

$$m_e\ddot{\mathbf{r}} + m_e\gamma_\omega\dot{\mathbf{r}} + m_e\omega_0^2\mathbf{r} = -e\vec{\mathcal{E}}(t) \tag{7.106}$$

with the mass m_e of the electron, the damping γ_ω (by collisions, radiative losses, etc.), and a resonance frequency ω_0. We note, that the damping may depend on the excitation frequency.

After some time, when the transient processes are damped out, the electrons oscillate with the angular frequency ω of the external field. For this inhomogeneous solution we make the ansatz:

$$\mathbf{r}(t) = \mathbf{r}_e e^{-\imath\omega t} \tag{7.107}$$

with the constant complex amplitude $\mathbf{r}_e$. Inserting this into the equation of motion, we obtain for the atomic dipole moment induced by the electromagnetic field [14]:

$$\boxed{\mathbf{d}(t) \equiv -e\mathbf{r}(t) = \frac{e^2/m_e}{\omega_0^2 - \omega^2 - \imath\gamma_\omega\omega}\vec{\mathcal{E}}(t) \equiv \alpha_{pol}(\omega)\vec{\mathcal{E}}(t)}\ , \tag{7.108}$$

where we used the *electric polarizability* α_{pol} introduced in (3.6) and relating the amplitudes of the field and the dipole moment. The imaginary term in the denominator means that the oscillation of $\mathbf{d}$ is out of phase with $\vec{\mathcal{E}}$ being delayed by an angle

$$\varphi = \arctan\frac{\gamma_\omega\omega}{\omega_0^2 - \omega^2}\ , \tag{7.109}$$

which is very small when $\omega \ll \omega_0$ and approaches π when $\omega \gg \omega_0$ [88]. This is illustrated in Fig. 7.13(left).

The temporal average of the dipole moment is,

$$\sqrt{\overline{d^2}} = \alpha_{pol}\mathcal{E}_0\sqrt{\tfrac{1}{T}\int_0^T \cos^2\omega t dt} = \alpha_{pol}\mathcal{E}_0\sqrt{\tfrac{1}{2}} \equiv d_0\sqrt{\tfrac{1}{2}}\ . \tag{7.110}$$

To calculate the emitted radiation we must borrow a result from future lessons: From the electromagnetic fields (8.40) of an oscillating dipole we will derive the expression for the Poynting vector (8.44),

$$\langle\vec{\mathcal{S}}\rangle = \tfrac{1}{\mu_0}\langle\vec{\mathcal{E}}\times\vec{\mathcal{B}}\rangle = \frac{\mu_0 d_0^2\omega^4}{16\pi^2 c}\frac{\sin^2\theta}{r^2}\hat{\mathbf{e}}_r = \frac{d_0^2\omega^4}{32\pi^2\varepsilon_0 c^3}\frac{\sin^2\theta}{r^2}\hat{\mathbf{e}}_r\ . \tag{7.111}$$

---

scattering.
In practice, Thomson scattering is used to determine the electron density through the intensity and temperature of the spectral distribution of scattered radiation assuming a Maxwell distribution for the electron velocities.

[13] Let us imagine for the sake of illustration that the displacement of the electron from its equilibrium position generates (to first order) an elastic restoring force with resonances at certain frequencies.

[14] See script on *Vibrations and waves* (2020), Sec. 1.3.

Obviously, the radiation is not isotropic, but concentrated in directions perpendicular to the dipole moment. In fact, the spherical harmonic function ($\sin\theta$), responsible for this toroidal angular distribution, is precisely the p-wave [15]. The total power radiated by the dipole can be derived from the Poynting vector,

$$\boxed{P = \int_0^{2\pi}\int_0^{\pi} \langle\vec{S}\rangle \cdot \hat{\mathbf{e}}_r r^2 \sin\theta d\theta d\phi = \frac{\mu_0 d_0^2\omega^4}{32\pi^2 c}\, 2\pi \int_0^{\pi} \sin^3\theta d\theta = \frac{\mu_0\omega^4 d_0^2}{12\pi c}} \quad , \tag{7.112}$$

knowing $\int_0^\pi \sin^3 x dx = \frac{4}{3}$. This result is known as the *Larmor formula*.

7.2.3.2 Thompson and Rayleigh scattering

We now imagine that the dipole is excited by an incident wave of intensity,

$$I = \tfrac{1}{2}\varepsilon_0 c\vec{\mathcal{E}}_0^2 \ , \tag{7.113}$$

and scatters the radiation to a solid angle $d\Omega$, such that the angular distribution of scattered power is,

$$\frac{dP}{d\Omega} = |\langle\vec{S}\rangle| r^2 \ . \tag{7.114}$$

We can now calculate the differential *scattering cross section* inserting the polarizability (7.108),

$$\begin{aligned} \frac{d\sigma}{d\Omega} &= \frac{dP/d\Omega}{I} = \frac{d_0^2\omega^4\sin^2\theta}{32\pi^2\varepsilon_0 c^3 r^2} r^2 \frac{1}{\frac{1}{2}\varepsilon_0 c\mathcal{E}_0^2} = \frac{|\alpha_{pol}|^2\mathcal{E}_0^2\omega^4\sin^2\theta}{16\pi^2\varepsilon_0^2 c^4\mathcal{E}_0^2} \\ &= \left|\frac{e^2/m_e}{\omega_0^2-\omega^2-\imath\gamma_\omega\omega}\right|^2 \frac{\omega^4\sin^2\theta}{16\pi^2\varepsilon_0^2 c^4} = \frac{r_e^2\omega^4\sin^2\theta}{(\omega_0^2-\omega^2)^2+\gamma_\omega^2\omega^2} \ , \end{aligned} \tag{7.115}$$

where we defined the abbreviation,

$$r_e \equiv \frac{1}{4\pi\varepsilon_0}\frac{e^2}{m_e c^2} \approx 2.8\cdot 10^{-15}\,\text{m} \tag{7.116}$$

being the *classical electron radius*. The total cross section,

$$\boxed{\sigma(\omega) = \int_{\mathbb{R}^2} \frac{d\sigma}{d\Omega} d\Omega = \frac{8\pi}{3} r_e^2 \frac{\omega^4}{(\omega_0^2-\omega^2)^2+\gamma_\omega^2\omega^2}} \ , \tag{7.117}$$

describes a resonance of Lorentzian profile.

We have the following limiting cases:

- $\omega \gg \omega_0$ Thomson scattering ,
- $\omega = \omega_0$ resonance fluorescence ,
- $\omega \ll \omega_0$ Rayleigh scattering .

[15] $Y_1^{\pm 1}(\theta,\phi) = \mp\frac{1}{2}\sqrt{\frac{3}{2\pi}} e^{\pm\imath\phi}\sin\theta$.

A *Thomson cross section* follows in the limit of high energies in comparison with the eigenfrequency, $\omega \gg \omega_0 \gg \gamma_\omega$ from the Lorentz model [16],

$$\sigma_{Thom} = \frac{8\pi}{3} r_e^2 \approx 6.65 \cdot 10^{-29}\,\mathrm{m}^2 \quad . \tag{7.118}$$

Example 76 (*Rayleigh scattering and the blue sky*): We consider the scattering cross section (7.117). For $\omega \to \omega_0$ we obtain a resonant amplification of the cross session of ω^2/γ_ω^2. The resonances of the particles in the atmosphere are in the blue region of the electromagnetic spectrum. Therefore, the visible frequencies are $\omega \ll \omega_0$, and the cross session is $\propto \omega^4$. For this reason, the blue region dominates. The sky just does not look violet, because the eyes are not sensitive for these colors.
The dependence on the observation angle $\propto \sin^2\theta$, where $\theta = \angle(\hat{\epsilon}, \mathbf{k}_s)$ is only valid for polarized light. For non-polarized light, which can be understood as a superposition of two waves with orthogonal polarization, the dependence is $\propto 1 + \cos^2\vartheta$, where $\vartheta = \angle(\mathbf{k}, \mathbf{k}_s)$.

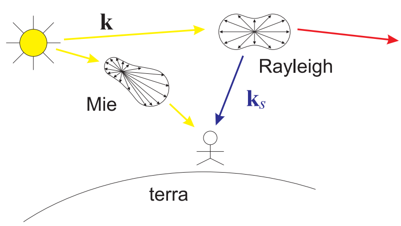

Figure 7.11: Dependence of the Rayleigh and Mie scattering on the observation angle.

Rayleigh scattering dominates for molecules and small scattering objects, $< \lambda/10$. *Mie scattering* is more important for $> \lambda/10$, e.g. water drops. This type of scattering is governed by boundary conditions defined by the surfaces of objects. The angular distributions are strongly oriented in forward direction, particularly when the objects are large. Therefore, this type of scattering only dominates at small angles with respect to the sun, where we observe a bleaching of the blue color of the sky).

7.2.3.3 Atomic polarizability

In atoms, the damping rate γ_ω is due to the radiative energy loss (given by Larmor's formula). It is calculated as the ratio between the classically radiated power and the kinetic energy of the electron orbiting the nucleus,

$$\gamma_\omega = \frac{P}{E_{kin}} = \frac{\mu_0 e^2 a^2/12\pi c}{m_e \omega^2 r^2/2} \ , \tag{7.119}$$

[16] A better approximation for small energies is obtained by expansion of the Klein-Nishina formula,

$$\sigma(\nu) = \sigma_{Thom}\left(1 - 2\alpha + \tfrac{56}{5}\alpha^2 + \dots\right)$$

with the factor $\alpha = \frac{h\nu}{m_e c^2}$.

where $a = \omega^2 r$ is the acceleration of the electron. We get [43] [17],

$$\boxed{\gamma_\omega = \frac{e^2\omega^2}{6\pi\varepsilon_0 m_e c^3}} \ . \tag{7.120}$$

Defining $\Gamma \equiv \gamma_{\omega_0}$ and inserting into equation (7.108), we can calculate the polarizability within the Lorentz model,

$$\alpha_{pol} = 6\pi\varepsilon_0 c^3 \frac{\Gamma/\omega_0^2}{\omega_0^2 - \omega^2 - \imath(\omega^3/\omega_0^2)\Gamma} \ . \tag{7.121}$$

Close to narrow resonances we can approximate $(\omega_0+\omega) \rightarrow 2\omega_0$ and $(\omega^3/\omega_0^2)\Gamma \rightarrow \omega_0\Gamma$ in the denominator of the formula (7.121). Hence, the *polarizability* simplifies to,

$$\boxed{\frac{\alpha_{pol}}{\varepsilon_0} \simeq \frac{6\pi}{k_0^3}\frac{-1}{\imath + 2\Delta/\Gamma}} \ , \tag{7.122}$$

defining the detuning $\Delta \equiv \omega - \omega_0$. Resolve the Excs. 7.2.7.6 to 7.2.7.9.

7.2.4 Classical theory of radiative forces

The Lorentz model permits a classical calculation of the forces exerted by a radiation wave on an electric dipole moment oscillating with the excitation frequency ω [47, 43] [18]. With the dipole moment given by equation (7.108) and the polarizability given by equation (7.121) we can write the dipolar interaction potential as the time-average,

$$\boxed{U_{dip}(\mathbf{r}) = -\frac{1}{2}\overline{\mathbf{d}\cdot\vec{\mathcal{E}}} = -\frac{1}{2\varepsilon_0 c}I(\mathbf{r})\mathfrak{Re}\ \alpha_{pol}} \ , \tag{7.123}$$

with the field intensity $I = 2\varepsilon_0 c|\vec{\mathcal{E}}|^2$. The factor $\frac{1}{2}$ takes into account the fact, that the dipole moment is induced rather than permanent, as shown in equation (3.10).

Therefore, the potential energy of the atom in the field is proportional to the intensity $I(\mathbf{r})$ and the real part of the polarizability, which describes the *in-phase* component of the dipolar oscillation, being responsible for the dispersive properties of the interaction. The dipole force comes from the gradient of the interaction potential,

$$\mathbf{F}_{dip}(\mathbf{r}) = -\nabla U_{dip}(\mathbf{r}) = \frac{1}{\varepsilon_0 c}\nabla I(\mathbf{r})\mathfrak{Re}\ \alpha_{pol} \ . \tag{7.124}$$

It is a conservative force proportional to the intensity gradient of the light field. As illustrated in Fig. 7.12, below resonance ($\omega < \omega_0$) the induced electric dipole will be

[17] In quantum mechanics we learn, that the rate for spontaneous emission is, $\Gamma = d^2k^3/3\pi\varepsilon_0\hbar$. This rate coincides with Eq. (7.120) when we assume an amplitude for the electron's oscillation equal to the size of the ground state of a harmonic oscillator,

$$d_0 = er = e\sqrt{\frac{\hbar}{m_e\omega}} = \overline{d^2}\sqrt{2} \ .$$

[18] In principle, we could also use Maxwell's stress tensor.

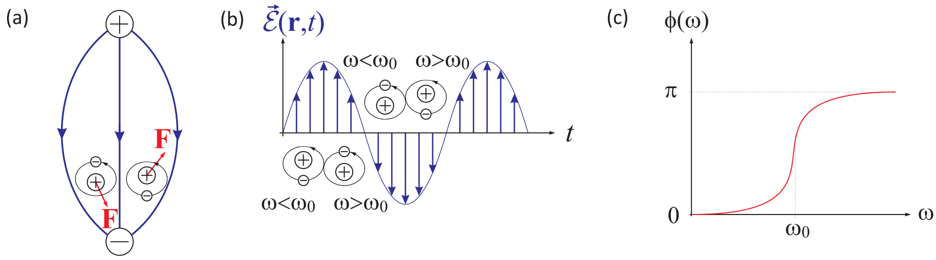

Figure 7.12: (a) Lorentz force on electric dipoles in an electrostatic field gradient. (b) Orientation of induced dipoles in an electromagnetic field. (c) Phase-shift of a harmonic oscillator with a resonance frequency at ω_0 driven at frequency ω.

oriented parallel to the electric field such as to minimize its energy by seeking strong field regions. Above resonance ($\omega > \omega_0$) the orientation is reversed so that the dipole can minimize its energy by seeking low field regions.

The power of the field absorbed by the dipolar oscillator (and reemitted as dipolar radiation) is given by,

$$P_{abs} = \overline{\dot{\mathbf{d}} \cdot \vec{\mathcal{E}}} = 2\omega \mathfrak{Im}\ \tilde{\mathbf{d}} \cdot \tilde{\vec{\mathcal{E}}} = -\frac{\omega}{\varepsilon_0 c} I(\mathbf{r}) \mathfrak{Im}\ \alpha_{pol} \ . \tag{7.125}$$

The absorption results from the imaginary part of the polarizability, which describes the *out of phase* component of the dipolar oscillation. Considering the light as a stream of photons with energy $\hbar\omega$, the absorptive part can be interpreted in terms of photon absorption processes followed by spontaneous reemission. The corresponding scattering rate is,

$$\boxed{\Gamma_{sct}(\mathbf{r}) = \frac{P_{abs}}{\hbar\omega} = \frac{1}{\hbar\varepsilon_0 c} I(\mathbf{r}) \mathfrak{Im}\ \alpha_{pol}} \ . \tag{7.126}$$

We emphasize that these expressions are valid for any polarizable neutral particle exposed to an oscillating electric field, provided that saturation effects can be neglected. That it, the expressions hold for atoms and molecules excited near or far from resonances, as well as for a classical antenna [19].

Inserting the polarizability (7.121) in the expressions (7.123) for the dipolar potential and (7.126) for the (Rayleigh) scattering rate we obtain, for the case of large detunings in comparison to the transition linewidth, $\Delta \gg \Gamma$, and negligible saturation,

$$\begin{aligned} U_{dip}(\mathbf{r}) &= -\frac{1}{2\varepsilon_0 c} I(r) \mathfrak{Re}\ \frac{6\pi\varepsilon_0 c^3 \Gamma/\omega_0^2}{\omega_0^2 - \omega^2 - \imath(\omega^3/\omega_0^2)\Gamma} \\ &\simeq -\frac{3\pi c^2}{\omega_0^2} I(\mathbf{r}) \frac{\Gamma}{\omega_0^2 - \omega^2} = -\frac{3\pi c^2}{2\omega_0^3} I(\mathbf{r}) \left(\frac{\Gamma}{\omega_0 - \omega} + \frac{\Gamma}{\omega_0 + \omega} \right) \ , \end{aligned} \tag{7.127}$$

[19] An important difference between quantum and classical oscillators is the possible occurrence of saturation. When the intensity of the driving field is too high, the excited state becomes strongly populated and the derived results are no longer valid. However, for large detunings we are far below the saturation, such that the expressions can be used even for quantum oscillators.

and

$$\hbar\Gamma_{sct}(\mathbf{r}) = \frac{1}{\varepsilon_0 c} I(\mathbf{r}) \mathfrak{Im}\, \frac{6\pi\varepsilon_0 c^3 \Gamma/\omega_0^2}{\omega_0^2 - \omega^2 - \imath(\omega^3/\omega_0^2)\Gamma} \tag{7.128}$$
$$\simeq \frac{-6\pi c^2 \Gamma^2 \omega^3}{\omega_0^4} I(\mathbf{r}) \frac{1}{(\omega_0^2-\omega^2)^2} = \frac{-3\pi c^2}{2\omega_0^3}\left(\frac{\omega}{\omega_0}\right)^3 I(\mathbf{r}) \left(\frac{\Gamma}{\omega_0-\omega} + \frac{\Gamma}{\omega_0+\omega}\right)^2 .$$

These expressions exhibit two resonant contributions: In addition to the usual resonance at $\omega = \omega_0$, there is a so-called *counter-rotating* term resonant at $\omega = -\omega_0$. In most applications the radiation source is tuned relatively close to the resonance at ω_0, such that the counter-rotating term can be neglected, which simplifies the expressions to,

$$\boxed{U_{dip}(\mathbf{r}) = \frac{3\pi c^2}{2\omega_0^3}\frac{\Gamma}{\Delta} I(\mathbf{r}) \qquad \text{and} \qquad \hbar\Gamma_{sct}(\mathbf{r}) = \frac{3\pi c^2}{2\omega_0^3}\frac{\Gamma^2}{\Delta^2} I(\mathbf{r})} . \tag{7.129}$$

The obvious relationship between the scattering rate and the dipolar potential,

$$\hbar\Gamma_{sct} = \frac{\Gamma}{\Delta} U_{dip} , \tag{7.130}$$

is a direct consequence of the profound relationship between the absorptive and dispersive responses of the oscillator. We furthermore emphasize the following relevant points:

- The sign of the detuning: Below an atomic resonance ('red detuning', $\Delta < 0$) the dipolar potential is negative and the interaction attracts the atom to regions of high intensity, e.g. toward the optical axis of a Gaussian light beam or towards the anti-nodes of a standing light wave. Above the atomic resonance ('blue detuning', $\Delta > 0$) is the opposite; the atom is repelled out of high-intensity regions.

- Intensity and detuning-dependence: The dipolar potential is $\propto I/\Delta$, while the scattering rate is $\propto I/\Delta^2$. Therefore, dipolar optical traps are generally realized at large detunings and high intensities in order to reduce the scattering rate while maintaining the potential depth.

7.2.4.1 Microscopic model of the susceptibility, anomalous dispersion

Until now we considered a single valence electron bound to a nucleus. If there are several electrons, the relationship (7.108) must be generalized. Electrons located at different orbitals of a molecule feel different spring constants f_j, natural frequencies ω_j, and damping coefficients γ_j. In the presence of several electrons per molecule and N molecules per volume unit, the polarization $\vec{\mathcal{P}}$ is given by the real part of (3.12),

$$\vec{\tilde{\mathcal{P}}} = \frac{Nq^2}{m}\left(\sum_j \frac{f_j}{\omega_j^2 - \omega^2 - \imath\gamma_j\omega}\right)\vec{\tilde{\mathcal{E}}} . \tag{7.131}$$

In equation (3.20) we defined the electric susceptibility χ_ε as proportionality constant between the electric field and the polarization. In the case considered here, $\vec{\mathcal{P}}$ *is not* *proportional* to $\vec{\mathcal{E}}$ (strictly speaking, it is not a linear medium), because there is a phase shift between $\vec{\mathcal{P}}$ and $\vec{\mathcal{E}}$. But at least the *complex* polarization $\tilde{\vec{\mathcal{P}}}$ *is proportional to the complex field* $\tilde{\vec{\mathcal{E}}}$, which suggests the introduction of a *complex susceptibility* $\tilde{\chi}_\varepsilon$,

$$\tilde{\vec{\mathcal{P}}} = \varepsilon_0 \tilde{\chi}_\varepsilon \tilde{\vec{\mathcal{E}}} \ . \tag{7.132}$$

All manipulations made so far remain valid, if we assume that the physical polarization is the real part of $\tilde{\vec{\mathcal{P}}}$, in the same way as the physical field is the real part of $\tilde{\vec{\mathcal{E}}}$. In particular, the proportionality between $\tilde{\vec{\mathcal{D}}}$ and $\tilde{\vec{\mathcal{E}}}$ is the complex permittivity $\tilde{\varepsilon} = \varepsilon_0(1+\tilde{\chi}_\varepsilon)$, and the complex dielectric constant (in this model) is,

$$\tilde{\epsilon} \equiv \frac{\tilde{\varepsilon}}{\varepsilon_0} = 1 + \frac{Nq^2}{m\varepsilon_0} \sum_j \frac{f_j}{\omega_j^2 - \omega^2 - \imath\gamma_j\omega} \ . \tag{7.133}$$

Generally, the imaginary part is despicable; however, when ω is very close to one of the resonant frequencies ω_j, it will play a crucial role, as we shall see later.

In a dispersive medium the wave equation for a given frequency is,

$$\nabla^2 \tilde{\vec{\mathcal{E}}} = \tilde{\varepsilon}\mu_0 \frac{\partial^2 \tilde{\vec{\mathcal{E}}}}{\partial t^2} \ . \tag{7.134}$$

It admits plane wave solutions as before,

$$\tilde{\vec{\mathcal{E}}}(z,t) = \tilde{\vec{\mathcal{E}}}_0 e^{\imath(\tilde{k}z - \omega t)} \ , \tag{7.135}$$

with the complex wavenumber,

$$\tilde{k} = \omega\sqrt{\tilde{\varepsilon}\mu_0} = \tfrac{\omega}{c}\sqrt{\tilde{\epsilon}} \ . \tag{7.136}$$

Writing $\tilde{k}$ in terms of its real and imaginary parts, $\tilde{k} = k + \imath\kappa$, the plane wave becomes,

$$\tilde{\vec{\mathcal{E}}}(z,t) = \tilde{\vec{\mathcal{E}}}_0 e^{-\kappa z} e^{\imath(kz-\omega t)} \ . \tag{7.137}$$

Obviously, the wave is attenuated (this is not surprising, since the damping absorbs energy). Since the intensity is proportional to $\vec{\mathcal{E}}^2$ (and consequently to $e^{-2\kappa z}$), the quantity,

$$\alpha \equiv 2\kappa \tag{7.138}$$

is called *absorption coefficient*. The relationship,

$$I \propto e^{-\alpha z} \tag{7.139}$$

is called the *Lambert-Beer law*. However, the velocity of the wave is ω/k, and the *refraction index* is,

$$n = \frac{ck}{\omega} \ . \tag{7.140}$$

In the present case k and κ have nothing to do with conductivity, as in the case of Eq. (7.87); but they are determined by the parameters of our damped harmonic oscillator. For gases, the second term in (7.133) is small, and we can approximate the square root (7.136) by the first term of the binomial expansion $\sqrt{1+\tilde{\chi}_\varepsilon} \simeq 1 + \frac{1}{2}\tilde{\chi}_\varepsilon$. Hence,

$$\tilde{k} = \frac{\omega}{c}\sqrt{\tilde{\epsilon}} \simeq \frac{\omega}{c}\left(1+\frac{\tilde{\chi}_\varepsilon}{2}\right) = \frac{\omega}{c}\left(1+\frac{Nq^2}{2m\varepsilon_0}\sum_j \frac{f_j}{\omega_j^2-\omega^2-\imath\gamma_j\omega}\right) . \tag{7.141}$$

therefore,

$$\boxed{\begin{array}{lllll} n & = & \mathfrak{Re}\,\sqrt{\epsilon} & \simeq & 1+\dfrac{Nq^2}{2m\varepsilon_0}\displaystyle\sum_j \frac{f_j(\omega_j^2-\omega^2)}{(\omega_j^2-\omega^2)^2+\gamma_j^2\omega^2} \\ \alpha & = & \dfrac{2\omega}{c}\mathfrak{Im}\,\sqrt{\epsilon} & \simeq & \dfrac{Nq^2\omega^2}{m\varepsilon_0 c}\displaystyle\sum_j \frac{f_j\gamma_j}{(\omega_j^2-\omega^2)^2+\gamma_j^2\omega^2} \end{array}} . \tag{7.142}$$

In Fig. 7.13 we plot the refractive index and the absorption coefficient in the neighborhood of one of the resonances $\omega_0 = \omega_j$. In most cases the refractive index gradually increases with frequency, which is consistent with our experience in optics (Fig. 7.9). However, near a resonance the refraction index drops abruptly. Being atypical, this behavior is called *anomalous dispersion*. We observe that the region of anomalous dispersion ($\omega_1 < \omega < \omega_2$ in the figure) coincides with the region of maximum absorption. In fact, the material can be almost opaque in this spectral region. The reason is, we now excite the electrons on their 'preferred' frequency; the amplitude of their oscillation is relatively large, and therefore much energy is dissipated by the damping mechanism.

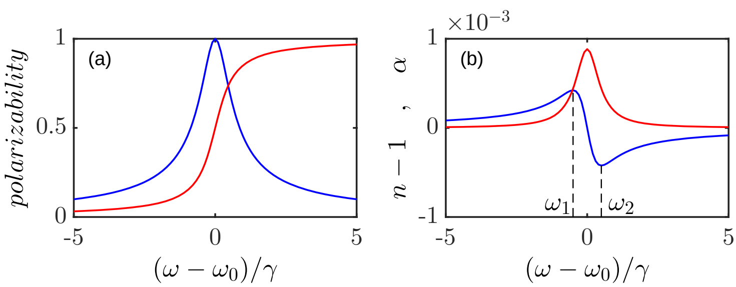

Figure 7.13: (code) (a) Profile of the polarizability $|\alpha_{pol}|$ (blue curve) and of the phase shift $\arctan \frac{\mathfrak{Im}\ \alpha_{pol}}{\pi\mathfrak{Re}\ \alpha_{pol}}$ (red curve). (b) Refractive index (blue curve) and the absorption (red curve). In the spectral region between ω_1 and ω_2 we have anomalous dispersion.

The refractive index n plotted in Fig. 7.13 may be below 1 above the resonance, suggesting that the *velocity of the wave exceeds* c. But we must remember that energy propagates at the group velocity, which is always below c. The graph does not include the contributions of other terms in the sum, because they are negligible when the resonances are narrow or distant from each other. Out of the resonances, the damping can be ignored, and the formula for the refractive index simplifies:

$$n = 1 + \frac{Nq^2}{2m\varepsilon_0}\sum_j \frac{f_j}{\omega_j^2-\omega^2} . \tag{7.143}$$

For most substances the natural frequencies ω_j are distributed across the spectrum in a chaotic way. In transparent materials, the resonances are in the ultraviolet regime, such that the visible frequencies ω are far below the resonances, $\omega \ll \omega_j$. In this case,

$$\frac{1}{\omega_j^2 - \omega^2} \simeq \frac{1}{\omega_j^2}\left(1 + \frac{\omega^2}{\omega_j^2}\right) . \tag{7.144}$$

and (7.143) adopts the form,

$$n = 1 + \frac{Nq^2}{2m\varepsilon_0}\sum_j \frac{f_j}{\omega_j^2} + \omega^2 \frac{Nq^2}{2m\varepsilon_0}\sum_j \frac{f_j}{\omega_j^4} . \tag{7.145}$$

Or, in terms of vacuum wavelengths ($\lambda = 2\pi c/\omega$):

$$\boxed{n = 1 + A\left(1 + \frac{B}{\lambda^2}\right)} . \tag{7.146}$$

This is the *Cauchy formula*; the constant A is called the *refraction coefficient* and B is called *dispersion coefficient*. The Cauchy equation applies reasonably well to most gases in the optical regime. Fig. 7.9 shows the example of the refractive index of air.

The Lorentz model certainly does not account for all dispersion phenomena in non-conductive media. But at least, it indicates how the damped harmonic motion of electrons can generate a dispersive refractive index, and it also explains why n is usually a slowly increasing function of ω with occasional 'anomalous' regions.

Example 77 (*Energy density and Poynting vector in a dielectric medium*): The energy density in vacuum, $\bar{u} = \frac{\varepsilon_0}{4}|\vec{\mathcal{E}}|^2 + \frac{1}{4\mu_0}|\vec{\mathcal{B}}|^2$, becomes in a dielectric medium,

$$\bar{u}^{(\chi)} = \frac{1}{4}\mathfrak{Re}\left(\varepsilon\vec{\mathcal{E}}\cdot\vec{\mathcal{E}}^* + \frac{1}{\mu_0}\vec{\mathcal{B}}\cdot\vec{\mathcal{B}}^*\right) = \frac{\mathfrak{Re}\ \varepsilon}{4}|\vec{\mathcal{E}}|^2 + \frac{1}{4\mu_0}\left|\frac{k+\imath\kappa}{\omega}\vec{\mathcal{E}}\right|^2$$
$$= \frac{\varepsilon_0}{4}(1+\chi_e')\mathcal{E}_0^2 + \frac{\varepsilon_0}{4\omega^2}|k+\imath\kappa|^2\mathcal{E}_0^2 = (k^2-\kappa^2+k^2+\kappa^2)\frac{\varepsilon_0}{4}\mathcal{E}_0^2 = \frac{\varepsilon_0}{2}\frac{k^2}{\omega^2}\mathcal{E}_0^2 ,$$

where we only consider the real part of the susceptibility χ_ε. On the other hand, the Poynting vector is,

$$\bar{I} = \frac{1}{2\mu_0}\mathfrak{Re}\ [\vec{\mathcal{E}}\times\vec{\mathcal{B}}^*] = \frac{\varepsilon_0 c^2}{2}\mathcal{E}_0^2\left[e^{-2\omega\kappa z/c}\mathfrak{Re}\ \frac{k+\imath\kappa}{\omega}\right] = \frac{\varepsilon_0 c^2}{2}\frac{k}{\omega}\mathcal{E}_0^2 e^{-2\omega\kappa z/c} .$$

7.2.4.2 The Fresnel-Fizeau effect

Naively, the index of refraction is due to a finite time lag between photon absorption and emission. The time spend in an excited state slows down the light propagation velocity. If during this time the atom travels, the atomic velocity adds to (or reduces) the light propagation velocity. This effect which is known as *Fresnel-Fizeau effect* is an internal degrees of freedom effect. Consider a medium with the index of refraction n

(measured in the moving frame) which is moving with velocity v. The copropagation velocity of light is for $v \ll c$,

$$c_v = \frac{c}{n_{rf}} \frac{c + n_{rf}v}{c + v/n_{rf}} \approx \frac{c}{n_{rf}} + v\left(1 - \frac{1}{n_{rf}^2}\right) . \tag{7.147}$$

This is the Fresnel 'drag' coefficient. In particular, it is easy to show that,

$$c_{-v} < c/n_{rf} < c_v < c . \tag{7.148}$$

Expressing the refraction index by the susceptibility, $n_{rf} = \sqrt{1+\chi_\varepsilon} \approx 1 + \frac{1}{2}\chi_\varepsilon$, we get,

$$\frac{c_v - c_{-v}}{2v} = 1 - \frac{1}{n_{rf}^2} = \frac{\chi_\varepsilon}{1+\chi_\varepsilon} . \tag{7.149}$$

Knowing that,

$$\chi_\varepsilon = \frac{2nd^2}{3\varepsilon_0\hbar} \frac{\Delta + \imath\Gamma}{4\Delta^2 + 2\Omega^2 + \Gamma^2} \quad \text{and} \quad d = \sqrt{\frac{3\pi\varepsilon_0\hbar\Gamma}{k^3}} \tag{7.150}$$

$$\mathfrak{Re}\ \chi_\varepsilon = \frac{2\pi\Gamma n}{k^3} \frac{\Delta}{4\Delta^2 + 2\Omega^2 + \Gamma^2}$$

it follows,

$$\frac{c_v - c_{-v}}{2v} = \frac{1}{1 + \left(\frac{2\pi\Gamma n}{k^3} \frac{\Delta}{4\Delta^2 + 2\Omega^2 + \Gamma^2}\right)^{-1}} . \tag{7.151}$$

For small detunings within the natural linewidth,

$$\frac{c_v - c_{-v}}{2v} \approx \frac{1}{1 + \frac{k^3}{2\pi n} \frac{\Gamma}{\Delta}} , \tag{7.152}$$

a long excited state lifetime is advantageous. For very large detunings and $\Omega \to 0$,

$$\frac{c_v - c_{-v}}{2v} \approx \frac{1}{1 + \frac{2k^3}{\pi n} \frac{\Delta}{\Gamma}} . \tag{7.153}$$

This shows that (far from resonance) the effect increases for large densities, broad linewidths and smaller detunings. For example, the *Rb* D_1 line for typical conditions the coefficient is $\frac{2k^3}{\pi n} \approx 1000$ [20].

7.2.5 Light interaction with metals and the Drude model

The *Drude model* is based on a classical kinetic theory of non-interacting electrons in a metal. Since the conduction electrons are considered to be free, the Drude oscillator is

[20] For the high-finesse ring-cavity CARL experiment this means that the Fresnel-Fizeau effect is negligible. Far from resonance the atoms do not spend time in the excited state. The adiabatic elimination of the internal degrees of freedom removes the effect from the theoretical model. It also means that the counter-propagating modes of the ring-cavity do not split because of the atomic velocity, $n_{rf+} = n_{rf-}$. The calculation shows that the back-scattered light is not perfectly resonant, but that this shift is negligibly small.

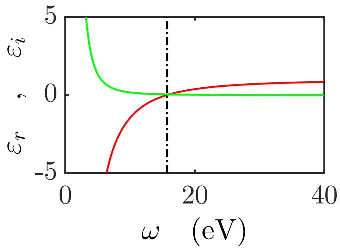

Figure 7.14: (code) Real (red) and imaginary (green) parts of the dielectric function as a function of the excitation frequency.

an extension of the Lorentz model of a single oscillator to the case, when the restoring force and the atomic resonance frequency are zero, $\Gamma_0 = \omega_0 = 0$. The equation of motion is,

$$m\frac{d\mathbf{v}}{dt} + m\Gamma_d\mathbf{v} = -e\vec{\mathcal{E}} \ , \tag{7.154}$$

where $m\frac{d\mathbf{v}}{dt}$ is the force accelerating the electron, $m\Gamma_d\mathbf{v}$ is the friction due to collisions with ions of the crystalline lattice and $-e\vec{\mathcal{E}} = -e\vec{\mathcal{E}}_0 e^{\imath\omega t}$ is the Coulomb force exerted by the oscillating field. We find,

$$\mathbf{v} = \mathbf{v}_0 e^{\imath\omega t} = -\frac{e}{m}\frac{\vec{\mathcal{E}}_0}{\imath\omega + \Gamma_d}e^{\imath\omega t} \ . \tag{7.155}$$

The current density corresponding to the motion of n electrons per unit volume is,

$$\mathbf{j}_c(\omega) = -ne\mathbf{v} = \frac{ne^2}{m(\Gamma_d + \imath\omega)}\vec{\mathcal{E}} \ . \tag{7.156}$$

In addition we have the current that corresponds to the electric displacement in vacuum,

$$\mathbf{j}_d(\omega) = \frac{\partial\vec{\mathcal{D}}}{\partial t} = \imath\omega\varepsilon_0\vec{\mathcal{E}} \ , \tag{7.157}$$

where $\vec{\mathcal{D}} = \varepsilon_0\vec{\mathcal{E}}$. The total current density is given by,

$$\mathbf{j}(\omega) = \mathbf{j}_c(\omega) + \mathbf{j}_d(\omega) = \left[\frac{ne^2}{m(\Gamma_d + \imath\omega)} + \imath\omega\varepsilon_0\right]\vec{\mathcal{E}} \ . \tag{7.158}$$

Assuming the total current as being created by a total electric displacement, $\vec{\mathcal{D}}_{tot} = \tilde{\varepsilon}\vec{\mathcal{E}}$, where again the electric field and the displacement are related by a complex permittivity, we find,

$$\mathbf{j}(\omega) = \frac{\partial\vec{\mathcal{D}}_{tot}}{\partial t} = \imath\omega\tilde{\varepsilon}\vec{\mathcal{E}} \ , \tag{7.159}$$

and comparing the last two expressions,

$$\left[\frac{ne^2}{m(\Gamma_d + \imath\omega)} + \imath\omega\varepsilon_0\right]\vec{\mathcal{E}} = \imath\omega\tilde{\varepsilon}(\omega)\vec{\mathcal{E}} \ . \tag{7.160}$$

Resolving by $\tilde{\varepsilon}$,

$$\boxed{\tilde{\epsilon}(\omega) = 1 - \frac{\omega_p^2}{\imath\omega\Gamma_d - \omega^2}} \; , \tag{7.161}$$

where

$$\omega_p \equiv \sqrt{\frac{ne^2}{m\varepsilon_0}} \tag{7.162}$$

is called the *plasma frequency*, which corresponds to the energy, where $\epsilon(\omega_p) \simeq 0$. Separated into real and imaginary parts,

$$\epsilon'(\omega) = 1 - \frac{\omega_p^2}{\Gamma_d^2 + \omega^2} \quad , \quad \epsilon''(\omega) = \frac{\omega_p^2 \Gamma_d}{\omega(\Gamma_d^2 + \omega^2)} \tag{7.163}$$

For $\omega < \omega_p$ and small Γ_d, the real part ϵ' is negative. No electric field can penetrate the metal, which therefore becomes fully reflecting.
For $\omega = \omega_p$, the real part ϵ' is zero. That is, the electrons oscillate in phase with the field along the propagation distance in the metal.
For $\omega \gg \omega_p$, the imaginary (absorptive) part ε'' disappears at high frequencies.

For metals, usually we have $\omega_p = (2\pi)$ 1000...4000 THz and $\Gamma_d \approx 100\,\text{s}^{-1}$. Note that the model can not describe semiconductors.

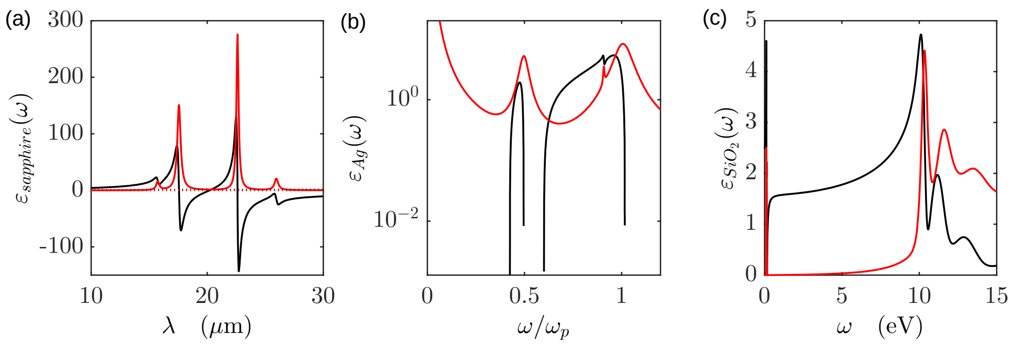

Figure 7.15: (code) Examples of frequency-dependent permittivities for (a) sapphire [33, **?**], (b) silver [77], and (c) amorphous glas [30].

7.2.6 Causality connecting $\vec{\mathcal{D}}$ with $\vec{\mathcal{E}}$ and the Kramers-Kronig relations

A consequence of the dispersion of $\varepsilon(\omega)$ is the temporarily nonlocal connection between the displacement $\vec{\mathcal{D}}$ and the electric field $\vec{\mathcal{E}}$. Calculating the Fourier transform of,

$$\vec{\mathcal{D}}(\mathbf{r},\omega) = \varepsilon(\omega)\vec{\mathcal{E}}(\mathbf{r},\omega) = \varepsilon_0[1 + \chi_\varepsilon(\omega)]\vec{\mathcal{E}}(\mathbf{r},\omega) \; , \tag{7.164}$$

we obtain, using the convolution theorem,

$$\vec{\mathcal{D}}(\mathbf{r},t) = \frac{1}{\sqrt{2\pi}}\int_{-\infty}^{\infty}\varepsilon(\omega)\vec{\mathcal{E}}(\mathbf{r},\omega)e^{-\imath\omega t}d\omega \tag{7.165}$$
$$= \varepsilon_0\vec{\mathcal{E}}(\mathbf{r},t) + \frac{\varepsilon_0}{\sqrt{2\pi}}\int_{-\infty}^{\infty}\chi_\varepsilon(\omega)\vec{\mathcal{E}}(\mathbf{r},\omega)e^{-\imath\omega t}d\omega$$
$$= \varepsilon_0\vec{\mathcal{E}}(\mathbf{r},t) + \frac{\varepsilon_0}{\sqrt{2\pi}}\int_{-\infty}^{\infty}\chi_\varepsilon(\tau)\vec{\mathcal{E}}(\mathbf{r},t-\tau)d\tau \ ,$$

where $\chi_\varepsilon(\tau)$ is the Fourier transform of the electric susceptibility. This results shows that the displacement field $\vec{\mathcal{D}}$ depends on all values the incident electric field $\vec{\mathcal{E}}$ had at all times. Only if $\chi_\varepsilon(\omega)$ were independent of ω would we have $\chi_\varepsilon(\tau) \propto \delta(\tau)$.

Example 78 (*Simple model of the susceptibility*): To illustrate the implications of equation (7.165) we consider a permittivity of the following form,

$$\frac{\varepsilon(\omega)}{\varepsilon_0} = \frac{\omega_p}{\omega_0^2 - \omega^2 - \imath\gamma\omega} \ . \tag{7.166}$$

The kernel related to the susceptibility,

$$\chi_\varepsilon(\tau) = \frac{\omega_p^2}{2\pi}\int_{-\infty}^{\infty}\frac{e^{-\imath\omega\tau}d\tau}{\omega_0^2 - \omega^2 - \imath\gamma\omega} \ , \tag{7.167}$$

can be evaluated by contour integration, the result being,

$$\chi_\varepsilon(\tau) = \omega_p^2 e^{-\gamma\tau/2}\frac{\sin\tau\sqrt{\omega_0^2 - (\gamma/2)^2}}{\sqrt{\omega_0^2 - (\gamma/2)^2}}\Theta(\tau) \ , \tag{7.168}$$

where $\Theta(\tau)$ is the Heaviside function.

This example shows that the displacement field $\vec{\mathcal{D}}$ only depends on the electric field at *past times*, which is fortunate as it allows causality to be respected.

7.2.6.1 The Kramers-Kronig relations

The *Kramers-Kronig relations* are bidirectional mathematical relations, connecting the real and imaginary parts of any complex function that is an *analytic function* on the upper half-plane [21]. These relationships are often used to calculate the real part of response functions in physical systems from the imaginary part (or vice versa). This works because, in stable physical systems, *causality and analyticity* are equivalent conditions. Be $\chi(\omega)$ a complex function of the complex variable ω. We assume this function to be analytic in the upper closed half-plane of ω and to disappear as $1/|\omega|$ or faster for $|\omega| \to \infty$. The Kramers-Kronig relations are given by,

$$\boxed{\mathfrak{Re}\ \chi(\omega) = \frac{1}{\pi}\mathcal{P}\int_{-\infty}^{\infty}\frac{\mathfrak{Im}\ \chi(\omega')}{\omega'-\omega}d\omega' \quad \text{and} \quad \mathfrak{Im}\ \chi(\omega) = -\frac{1}{\pi}\mathcal{P}\int_{-\infty}^{\infty}\frac{\mathfrak{Re}\ \chi(\omega')}{\omega'-\omega}d\omega'} \ , \tag{7.169}$$

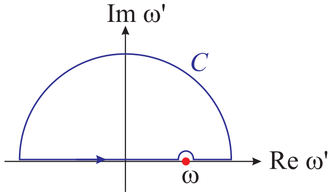

Figure 7.16: Path of the contour integral illustrating Cauchy's theorem.

where $\mathcal{P}$ denotes the *Cauchy principal value*. Thus, the real and imaginary parts of such a function are not independent, and the complete function can be reconstructed from only one of its parts.

For any analytic function χ defined on the upper closed half-plane, the function $\omega' \to \chi(\omega')/(\omega' - \omega)$ where $\omega \in \mathbb{R}$, will also be analytic in the upper half-plane. The *Cauchy's residue theorem* for integration consequently says, that

$$\oint \frac{\chi(\omega')}{\omega' - \omega} d\omega' = 0 \ . \tag{7.170}$$

We chose the contour to follow the real axis, making a loop around the pole at $\omega' = \omega$, and a large semicircle in the upper half-plane, as shown in Fig. 7.16. We now decompose the integral into its contributions along each one of these three paths and then evaluate the limits. The length of the semicircular path increases proportionally to $|\omega'|$, but the integral along it disappears in this limit, since $\chi(\omega')$ disappears at least as fast as $1/|\omega'|$. Letting the size of the semicircle go to zero we get,

$$0 = \oint \frac{\chi(\omega')}{\omega' - \omega} d\omega' = \mathcal{P} \int_{-\infty}^{\infty} \frac{\chi(\omega')}{\omega' - \omega} d\omega' - \imath\pi\chi(\omega) \ . \tag{7.171}$$

The second term in the last expression is obtained using the Sokhotski-Plemelj theorem of residues. After rearrangement we arrive at the compact form of the Kramers-Kronig relations,

$$\chi(\omega) = \frac{1}{\imath\pi} \mathcal{P} \int_{-\infty}^{\infty} \frac{\chi(\omega')}{\omega' - \omega} d\omega' \ . \tag{7.172}$$

The imaginary unit in the denominator makes the connection between the real and the imaginary components. Finally, we separate $\chi(\omega)$ and the equation (7.172) into their real and imaginary parts, and we get the expressions from above (7.169).

7.2.6.2 Physical interpretation in terms of causality

We can apply the Kramers-Kronig formalism to response functions. In certain linear and time-invariant physical systems or signal processing applications, the response function $h(t)$ describes, how some time-dependent property of the system, responds to a force $F(t')$ pulsed during a time t'. For example, the property of the system can be the angle of a pendulum and the force applied by a motor kicking the pendulum.

[21] A function is analytic if and only if its Taylor series about a point $\mathbf{r}_0$ converges to the function in some neighborhood for every $\mathbf{r}_0$ in its domain. Hence, analytic functions must be infinitely differentiable.

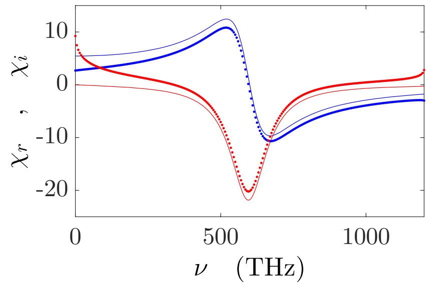

Figure 7.17: (code) Real (blue) and imaginary (red) parts of the susceptibility. The dashed curves are calculated by the Kramers-Kronig formulas.

The response function must be zero for $t < 0$, since the system can not respond to the force before it has been applied. It can be shown that this request for causality *in time domain* implies *in frequency domain*, that the Fourier transform $\chi(\omega)$ of $h(t)$ is analytical inside the upper half-plane. Furthermore, if we subject the system to an oscillating force with a frequency much higher than its highest resonance frequency, there will be almost no time for the system to respond before the forcing has alternated the direction, and hence the frequency response $\chi(\omega)$ converges to zero, when ω becomes very large. From these physical considerations, we see that $\chi(\omega)$ will normally satisfy the conditions necessary for the Kramers-Kronig relations to apply.

The frequency response of a system forced to generate an impulse response $h(t)$ is given by the Fourier-transform,

$$\chi(\omega) = \frac{1}{\sqrt{2\pi}} \int_{-\infty}^{\infty} h(t)e^{-\imath\omega t}dt = \mathcal{F}[h(t)] \ , \tag{7.173}$$

which for an electrical system corresponds to its impedance. Now, the boundary condition of causality can be implemented with the use of the Heaviside step function $\Theta(t)$,

$$\chi(\omega) = \frac{1}{\sqrt{2\pi}} \int_{-\infty}^{\infty} h(t)\Theta(t)e^{-\imath\omega t}dt = \mathcal{F}[h(t)\Theta(t)] = \mathcal{F}[h(t)\Theta(t)\Theta(t)] \ . \tag{7.174}$$

Note that the implementation of causality via the Heaviside step function is directly implemented when replacing the Fourier transform by the Laplace transform. Applying the convolution theorem to the Fourier transform and using the Fourier transform of the Heaviside function we get [22],

$$\boxed{\chi(\omega) = \mathcal{F}[h(t)\Theta(t)] \star \mathcal{F}[\Theta(t)] = \chi(\omega) \star (\mathcal{F}\Theta)(\omega) = \chi(\omega) \star \left(\frac{1}{2\pi\imath\omega} + \frac{1}{2}\delta(\omega)\right)} \ . \tag{7.175}$$

This equality can be considered an early or raw form of the Kramers-Kronig relations and will turn out to be equivalent to them. To see this, we carry out the convolution explicitly,

$$\chi(\omega) = \frac{1}{2\pi} \int_{-\infty}^{\infty} \frac{\chi(\omega')d\omega'}{\imath(\omega-\omega')} + \frac{1}{2}\chi(\omega) \ , \tag{7.176}$$

[22] $\mathcal{F}[\Theta(t)] = \frac{1}{\imath\sqrt{2\pi}\omega} + \sqrt{\frac{\pi}{2}}\delta(\omega)$

or isolating $\chi(\omega)$,

$$\chi(\omega) = \frac{1}{\pi}\int_{-\infty}^{\infty}\frac{\chi(\omega')d\omega'}{\imath(\omega-\omega')} . \tag{7.177}$$

This is the frequency response of causal systems being invariant under a Hilbert-transform. It is equivalent to the Kramers-Kronig relations (7.169). Rewriting it for only positive integration limits, the integral splits up like,

$$\chi(\omega) = \frac{1}{\pi}\int_{0}^{\infty}\frac{\chi(\omega')d\omega'}{\imath(\omega-\omega')} + \frac{1}{\pi}\int_{0}^{\infty}\frac{\chi(-\omega')d\omega'}{\imath(\omega+\omega')} . \tag{7.178}$$

From the definition of the Fourier integral of the real quantity $h(t)$ follows directly $\chi(-\omega) = \chi^*(\omega)$, that is, the positive frequency response determines the negative frequency response. Therefore,

$$\begin{aligned}\chi(\omega) &= \frac{1}{\pi}\int_{0}^{\infty}\frac{\chi(\omega')(\omega+\omega')+\chi^*(\omega')(\omega-\omega')}{\imath(\omega^2-\omega'^2)}d\omega' \\ &= \frac{1}{\pi}\int_{0}^{\infty}\frac{\omega'\mathfrak{Im}\ \chi(\omega') - \imath\omega\mathfrak{Re}\ \chi^*(\omega')}{\omega^2-\omega'^2}d\omega' .\end{aligned} \tag{7.179}$$

from which we obtain the Kramers-Kronig relations for the real and imaginary parts in a format, where they are useful for physically realistic response functions,

$$\boxed{\mathfrak{Re}\ \chi(\omega) = \frac{2}{\pi}\int_{0}^{\infty}\frac{\omega'\mathfrak{Im}\ \chi(\omega')}{\omega^2-\omega'^2}d\omega' \quad \text{and} \quad \mathfrak{Im}\ \chi(\omega) = \frac{-2}{\pi}\int_{0}^{\infty}\frac{\omega\mathfrak{Re}\ \chi(\omega')}{\omega^2-\omega'^2}d\omega'} . \tag{7.180}$$

The imaginary part of a response function describes, being *out of phase* with the driving force, how a system dissipates energy. The Kramers-Kronig relations imply that observing the *dissipative* response of a system is sufficient to determine its (reactive) *in-phase* response, and vice versa.

7.2.7 Exercises

7.2.7.1 Ex: Skin depth

a. Consider a piece of glass containing some free charges. How long does it take for the charges to migrate to the surface?
b. Suppose you were designing a microwave experiment at a frequency of 10^{10} Hz. How thick would you make a silver coating?
c. Find the wavelength and propagation velocity in copper for radio waves at 1 MHz. Compare with the corresponding values in air (or vacuum).

7.2.7.2 Ex: Complex refractive index

A light wave described by the electric field $\mathcal{E}_i = \mathcal{E}_0 e^{\imath k_0 z}$ comes from the vacuum and impinges on a metal surface characterized by the complex refractive index $n = n' + \imath n''$. Determine from the relation $n = \sqrt{\epsilon}$ the relative dielectric constant ϵ.
a. At what depth the field falls to e^{-1}, if $\mathcal{E}_{met} \simeq 0.05\mathcal{E}_0$ and $k_{met} = nk_0$.
b. Now despise the penetrating field, $|\mathcal{E}_{met}| \simeq 0$, and consider the reflected field $\mathcal{E}_r = \mathcal{E}_0 e^{-\imath kx + \imath\Delta\phi}$. Calculate the intensity resulting from the superposition of $\mathcal{E}_i$ and $\mathcal{E}_r$.

7.2.7.3 Ex: Fourier expansion

The Fourier inversion theorem says that,

$$f(z) = \int_{-\infty}^{\infty} A(k)e^{\imath kz}dk \qquad \Longleftrightarrow \qquad A(k) = \tfrac{1}{2\pi}\int_{-\infty}^{\infty} f(z)e^{-\imath kz}dz \ .$$

Use the theorem to determine $A(k)$ for the wavepacket given by $f(z,t) = \int_{-\infty}^{\infty} A(k)e^{\imath[kz-\omega(k)t]}dk$ as a function of the real parts $\mathfrak{Re}\ f(z,0)$ and $\mathfrak{Re}\ \dot{f}(z,0)$.

7.2.7.4 Ex: Electromagnetic wave

In a dispersionless medium ($\varepsilon = \varepsilon_0$ and $\mu = \mu_0$) we have for a component $u(x,t)$ of an electromagnetic wave (here without dimension),

$$u(x,t) = \frac{1}{\sqrt{2\pi}}\int_{-\infty}^{\infty} dk A(k)e^{\imath kx - \imath\omega(k)t} \quad \text{with} \quad \omega(k) = ck \ ,$$

and

$$A(k) = \frac{1}{\sqrt{2\pi}}\int_{-\infty}^{\infty} dx u(x,0)e^{-\imath kx} \ .$$

a. Show that $u(x,t)$ satisfies the one-dimensional wave equation for vacuum.
b. Calculate the spectral distribution $A(k)$ for $u(x,t) = e^{\imath k_0 x - \imath\omega_0 t}$.
c. Calculate the spectral distribution $A(k)$ for $\{u(x,t) = e^{\imath k_0 x - \imath\omega_0 t}$ for $-L < x - (\omega_0/k_0)t < L$ and 0 else$\}$.
d. Calculate $u(x,t)$, when $u(x,0) = \int_{-a}^{+a}\delta(x-a)da$.
e. Try to understand in an elementary way the relation of part (c) between the bandwidth and the length of the wavepacket. Perform the transition to the limit $L \to \infty$ explicitly. For the case (d) discuss the propagation of the wavepacket in space.
Formulas:

$$\delta(k_0 - k) = \frac{1}{2\pi}\int_{-\infty}^{\infty} dx e^{\imath(k_0-k)x} = \frac{1}{\pi}\lim_{L\to\infty}\frac{\sin(k_0-k)}{k_0-k}$$

$$\Theta(a) = \frac{1}{2\pi\imath}\int_{-\infty}^{\infty} dk\frac{e^{\imath ka}}{k} = \begin{cases} 1 & \text{for } a > 0 \\ 0 & \text{else} \end{cases} \ .$$

7.2.7.5 Ex: Phase and group velocity

Let us study the one-dimensional motion of a wavepacket in x-direction, which spreads in infinite space. The law of dispersion is given by $\omega = \omega(k)$. The motion of a wavepacket is then described by,

$$u(x,t) = \frac{1}{\sqrt{2\pi}}\int_{-\infty}^{\infty} dk A(k)e^{\imath kx - \imath\omega(k)t} \ ,$$

where the spectral distribution $A(k)$ is given by shape of the wavepacket at time $t = 0$:

$$A(k) = \frac{1}{\sqrt{2\pi}} \int_{-\infty}^{\infty} dx u(x,0) e^{-\imath kx} \ .$$

The maximum of $A(k)$ be at $k = k_0$. We call $v_{ph} = \omega(k)/k$ the *phase velocity* and $v_{gr} = [d\omega(k)/dk]_{k_0}$ the *group velocity*, because in specific idealized situations a wavepacket propagates precisely at this speed. In the following we consider a propagation of the wavepacket given by,

$$u(x,0) = c \exp\left\{-\frac{x^2}{2a^2} + \imath k_0 x\right\}$$

for a medium characterized by the dispersion relation $\omega(k) = b^2k^2$ (for a de Broglie matter wave).

a. Plot the shape of the wavepacket at time $t = 0$ via the intensity distribution $|u(x,0)|^2$. The 'width' of a Gaussian profile is given by the points, where the profile fell to $(1/e)$ of the maximum value. Calculate the width $\triangle x(t = 0)$ of the intensity distribution.

b. Calculate the spectral distribution $A(k)$ and the width $\triangle k$ of the corresponding intensity distribution $|A(k)|^2$.

c. Now calculate $u(x,t)$ at a later time t. Express $u(x,t)$ in the form $u(x,t) = \alpha e^{-(x-\beta t)^2/\gamma} e^{\imath(k_0 x - \omega(k_0)t)} e^{\imath\phi}$, where α, β, γ, and ϕ are real quantities which, nevertheless, may depend on t and x.

d. Calculate the intensity distribution $|u(x,t)|^2$ at time t. At what speed does the maximum move? Calculate the width $\triangle x(t)$ of the intensity distribution. What is the temporal evolution of $\triangle x(t)\triangle k$?

e. Compare $|u(x,t)|^2$ width $|u(x,0)|^2$.

Help:

$$\int_{-\infty}^{+\infty} dx \ e^{-ax^2+bx+c} = \sqrt{\tfrac{\pi}{a}} \exp\left[\tfrac{b^2+4ac}{4a}\right] \ .$$

7.2.7.6 Ex: Radiation force acting on a small dielectric particle

The polarizability of a small ($a \ll \lambda$) dielectric particle with complex refraction index $n_p = \mathfrak{Re}\ n_p - \imath\frac{\alpha\lambda}{4\pi}$ immersed in a medium of refraction index n_m is given by,

$$\alpha_{rad} = \frac{4\pi a^3 \frac{n_p^2 - n_m^2}{n_p^2 + 2n_m^2} n_m^2 \varepsilon_0}{1 - \frac{n_p^2 - n_m^2}{n_p^2 + 2n_m^2}\left[\left(\frac{n_m\omega_0}{c}a\right)^2 - \frac{2}{3}\imath\left(\frac{n_m\omega_0}{c}a\right)^3\right]} \ .$$

Calculate the total force acting on it when subject to an electromagnetic field.

7.2.7.7 Ex: Lorentz model

Based on the Lorentz model, derive the differential equation for the oscillation amplitude of the electrons and calculate the response of the matter reacting via a polarization $P = Nex$, where N is the number of electrons and x their oscillation amplitude.

Calculate the absorptive part $\mathfrak{Im}\ \chi$ and the dispersive part $\mathfrak{Re}\ \chi$ of the susceptibility $\chi \equiv P/\varepsilon_0\mathcal{E}$.
With this calculate the index of refraction n and the coefficient of absorption α in the Lorentz model.

7.2.7.8 Ex: Lorentz force on a single atomic dipole

Calculate the Lorentz force on a single atom within the dipole approximation from the expression [46],

$$\mathbf{F} = \int d^3r[\varrho(\mathbf{r})\vec{\mathcal{E}}(\mathbf{r}) + \mathbf{j}(\mathbf{r}) \times \vec{\mathcal{B}}(\mathbf{r})] \ .$$

7.2.7.9 Ex: The Faraday effect

Derive the *Faraday effect* from the Lorentz model using the following procedure:
a. Formulate the equation of motion for the position $\mathbf{s}$ of a bound electron according to (7.106) in the presence of a homogeneous magnetic field $\vec{\mathcal{B}} = \mathcal{B}\hat{\mathbf{e}}_z$ and an electromagnetic wave characterized by $\vec{\mathcal{E}}(z,t) = \mathcal{E}(z)\hat{\epsilon}e^{-\imath\omega t}$ and assumed to be initially linearly polarized in x-direction.
b. Express the motion of the electron in the xy-plane in a new basis given by $\hat{\mathbf{e}}_\pm = \frac{1}{\sqrt{2}}(\hat{\mathbf{e}}_x \pm \imath\hat{\mathbf{e}}_y)$.
c. Solve the equations of motion for the decoupled components $s_\pm(z,t) \equiv s_x \mp \imath s_y$ and determine the susceptibility.
d. Calculate the electric field and the angle by which the linear polarization vector is rotated as a function of z.

7.2.7.10 Ex: Complex refraction index and extinction coefficient

a. Derive the relations $n'^2 - n''^2 = 1 + \chi'_\varepsilon$ and $2n'n'' = \chi_\varepsilon$. **Note:** In a transparent dielectric medium there is no absorption, such that, $n'^2 = 1 + \chi'_\varepsilon = \frac{\varepsilon}{\varepsilon_0}$.
b. Calculate the *absorption coefficient* for a light field traversing a dielectric medium.

7.3 Plasmons, waveguides and resonant cavities

7.3.1 Green's tensor for wave propagation in dielectric media

The electromagnetic field in the presence of macroscopic dielectrics is governed by an inhomogeneous vector Helmholtz equation. Defining the permittivity and the permeability as tensor fields $\vec{\mathcal{D}}(\mathbf{r},\omega) = \epsilon(\mathbf{r},\omega)\varepsilon_0\vec{\mathcal{E}}(\mathbf{r},\omega)$ and $\vec{\mathcal{B}}(\mathbf{r},\omega) = \mu(\mathbf{r},\omega)\mu_0\vec{\mathcal{H}}(\mathbf{r},\omega)$ the Maxwell equations (6.6), become after a temporal Fourier transform,

$$\begin{aligned} \nabla \times \vec{\mathcal{H}} &= -\imath\omega\epsilon\varepsilon_0\vec{\mathcal{E}} + \mathbf{j} \\ \nabla \times \vec{\mathcal{E}} &= \imath\omega\mu\mu_0\vec{\mathcal{H}} \\ \nabla \cdot \epsilon\varepsilon_0\vec{\mathcal{E}} &= \varrho \\ \nabla \cdot \mu\mu_0\vec{\mathcal{H}} &= 0 \ . \end{aligned} \quad (7.181)$$

It is easy to see, that the *inhomogeneous Helmholtz equation* [52, 64, 17],

$$\boxed{\left[\nabla\times\frac{1}{\mu(\mathbf{r},\omega)}\nabla\times-\frac{\omega^2}{c^2}\epsilon(\mathbf{r},\omega)\right]\vec{\mathcal{E}}(\mathbf{r},\omega)=\imath\omega\mu_0\mathbf{j}(\mathbf{r},\omega)} \tag{7.182}$$

satisfies the above Maxwell equations with $\vec{\mathcal{E}}(\mathbf{r},\omega)\to 0$ for $r\to\infty$. Using the Green's function formalism, the solution to the Helmholtz equation can be given by,

$$\vec{\mathcal{E}}(\mathbf{r},\omega)=\imath\omega\mu_0\int_V d^3r'\mathcal{G}(\mathbf{r},\mathbf{r}',\omega)\cdot\mathbf{j}(\mathbf{r}',\omega)\ , \tag{7.183}$$

where the *Green's tensor* is the solution to

$$\boxed{\left[\nabla_\mathbf{r}\times\frac{1}{\mu(\mathbf{r},\omega)}\nabla_\mathbf{r}\times-\frac{\omega^2}{c^2}\epsilon(\mathbf{r},\omega)\right]\mathcal{G}(\mathbf{r},\mathbf{r}',\omega)=\delta^{(3)}(\mathbf{r}-\mathbf{r}')\mathbb{I}} \tag{7.184}$$

together with the boundary condition $\mathcal{G}(\mathbf{r},\mathbf{r}',\omega)\to 0$ for $|\mathbf{r}-\mathbf{r}'|\to\infty$. The volume of integration V is a small volume surrounding the point $\mathbf{r}=\mathbf{r}'$ in order to avoid the singularity.

The Green's tensor represents the electric field radiated at position $\mathbf{r}$ by three orthogonal dipoles located at $\mathbf{r}'$.

7.3.1.1 Bulk medium

Let us now consider the simplest case of a bulk medium, i.e. an infinitely extended, homogeneous dielectric independent of $\mathbf{r}$, that is, $\epsilon(\mathbf{r},\omega)=\epsilon(\omega)$ and $\mu(\mathbf{r},\omega)=\mu(\omega)$. In this case, the Helmholtz equation further simplifies to,

$$[\nabla_\mathbf{r}\times\nabla_\mathbf{r}\times-k(\omega)^2]\vec{\mathcal{E}}_b(\mathbf{r},\omega)=\imath\omega\mu_0\mathbf{j}(\mathbf{r},\omega) \tag{7.185}$$

with $k(\omega)^2=\frac{\omega^2}{c^2}\mu(\omega)\epsilon(\omega)$ defined at $\mathbf{r}$. The Green tensor is then the solution to,

$$\nabla_\mathbf{r}\times\nabla_\mathbf{r}\times\mathcal{G}_b(\mathbf{r},\mathbf{r}',\omega)-k^2\mathcal{G}_b(\mathbf{r},\mathbf{r}',\omega)=\delta^{(3)}(\mathbf{r}-\mathbf{r}')\mathbb{I}\ . \tag{7.186}$$

7.3.1.2 The scalar Helmholtz equation

The bulk medium vector Helmholtz equation (7.186) can be reduced to a scalar Helmholtz equation. To that end, we take its divergence and find,

$$\nabla\cdot\mathcal{G}_b(\mathbf{r},\mathbf{r}',\omega)=-\tfrac{1}{k^2}\nabla\delta^{(3)}(\mathbf{r}-\mathbf{r}')\ . \tag{7.187}$$

Using this identity and expanding,

$$\nabla_\mathbf{r}\times\nabla_\mathbf{r}\times\mathcal{G}_b=\begin{pmatrix}\partial_x^2-\triangle & \partial_x\partial_y & \partial_x\partial_z\\ \partial_x\partial_y & \partial_y^2-\triangle & \partial_y\partial_z\\ \partial_x\partial_z & \partial_y\partial_z & \partial_z^2-\triangle\end{pmatrix}\begin{pmatrix}G_{xx} & G_{xy} & G_{xz}\\ G_{yx} & G_{yy} & G_{yz}\\ G_{zx} & G_{zy} & G_{zz}\end{pmatrix}=(\nabla\otimes\nabla-\mathbb{I}\triangle)\,\mathcal{G}_b\ , \tag{7.188}$$

we may write,

$$[\Delta + k^2]\mathcal{G}_b(\mathbf{r},\mathbf{r}',\omega) = \nabla\nabla\cdot\mathcal{G}_b(\mathbf{r},\mathbf{r}',\omega) - \nabla\times\nabla\times\mathcal{G}_b(\mathbf{r},\mathbf{r}',\omega) + k^2\mathcal{G}_b(\mathbf{r},\mathbf{r}',\omega)$$
$$= \nabla\nabla\cdot\mathcal{G}_b(\mathbf{r},\mathbf{r}',\omega) - \delta^{(3)}(\mathbf{r}-\mathbf{r}')\mathbb{I}$$
$$= -\tfrac{1}{k^2}\nabla\nabla\delta^{(3)}(\mathbf{r}-\mathbf{r}') - \delta^{(3)}(\mathbf{r}-\mathbf{r}')\mathbb{I} = -\left[\mathbb{I} + \tfrac{1}{k^2}\nabla\nabla\right]\delta^{(3)}(\mathbf{r}-\mathbf{r}') \ . \tag{7.189}$$

The vector Helmholtz equation can hence be solved by writing,

$$\mathcal{G}_b(\mathbf{r},\mathbf{r}',\omega) = \left[\mathbb{I} + \tfrac{1}{k^2}\nabla\nabla\right]g(\mathbf{r},\mathbf{r}',\omega) \ , \tag{7.190}$$

where the scalar Green function g obeys the scalar Helmholtz equation,

$$\boxed{[\triangle + k^2]g(\mathbf{r},\mathbf{r}',\omega) = -\delta^{(3)}(\mathbf{r}-\mathbf{r}')} \ , \tag{7.191}$$

the solution of which is simply,

$$g(\mathbf{r},\mathbf{r}',\omega) = \frac{e^{\imath k|\mathbf{r}-\mathbf{r}'|}}{4\pi|\mathbf{r}-\mathbf{r}'|} \ , \tag{7.192}$$

where the boundary condition at infinity implies that k must have a positive imaginary part, $k = \sqrt{\varepsilon(\omega)}\frac{\omega}{c}$ with $\mathfrak{Im}\ k > 0$. Combining these results, we obtain the Green tensor of a bulk medium [69, 17],

$$\mathcal{G}_b(\mathbf{r},\mathbf{r}',\omega) = \left[\mathbb{I} + \tfrac{1}{k^2}\nabla\nabla\right]\frac{e^{\imath k|\mathbf{r}-\mathbf{r}'|}}{4\pi|\mathbf{r}-\mathbf{r}'|} \tag{7.193}$$
$$= \frac{\delta^{(3)}(\mathbf{R})\mathbb{I}}{3k^2} - \frac{e^{\imath kR}}{4\pi k^2R^3}\left\{[1-\imath kR-(kR)^2]\mathbb{I} - [3-3\imath kR-(kR)^2]\hat{\mathbf{e}}_R\otimes\hat{\mathbf{e}}_R\right\} \ ,$$

with $\mathbf{R} \equiv \mathbf{r}-\mathbf{r}'$, as will be shown in Exc. 7.3.7.1. The real and imaginary part are (for $\mathbf{R} \neq 0$),

$$\tfrac{4\pi}{k}\mathfrak{Re}\ \mathcal{G}_b(\mathbf{r},\mathbf{r}',\omega_0) = (\mathbb{I}-\hat{\mathbf{e}}_R\otimes\hat{\mathbf{e}}_R)\frac{\cos kR}{kR} - (\mathbb{I}-3\hat{\mathbf{e}}_R\otimes\hat{\mathbf{e}}_R)\left(\frac{\sin kR}{k^2R^2} - \frac{\cos kR}{k^3R^3}\right)$$
$$\tfrac{4\pi}{k}\mathfrak{Im}\ \mathcal{G}_b(\mathbf{r},\mathbf{r}',\omega_0) = (\mathbb{I}-\hat{\mathbf{e}}_R\otimes\hat{\mathbf{e}}_R)\frac{\sin kR}{kR} + (\mathbb{I}-3\hat{\mathbf{e}}_R\otimes\hat{\mathbf{e}}_R)\left(\frac{\cos kR}{k^2R^2} - \frac{\sin kR}{k^3R^3}\right) \ . \tag{7.194}$$

Furthermore is is possible to show [17],

$$\mathfrak{Re}\ \mathcal{G}_b(\mathbf{r},\mathbf{r},\omega) = 0 \qquad \text{and} \qquad \mathfrak{Im}\ \mathcal{G}_b(\mathbf{r},\mathbf{r},\omega) = \frac{k}{6\pi}\mathbb{I} \ . \tag{7.195}$$

Example 79 (*Electric field of a point dipole in an inhomogeneous dielectric*): Parametrizing the current generated by a point dipole located at $\mathbf{r} = \mathbf{r}_s$ by

$$\mathbf{j}(\mathbf{r},\omega) = -\imath\omega\mathbf{d}_s\delta^{(3)}(\mathbf{r}-\mathbf{r}_s) \ , \tag{7.196}$$

the generated electric field in an environment characterized by the Green function $\mathcal{G}(\mathbf{r},\mathbf{r}_s,\omega)$ can be evaluated from Eq. (7.183),

$$\vec{\mathcal{E}}(\mathbf{r},\mathbf{r}_s,\omega) = \omega^2\mu_0\mathcal{G}(\mathbf{r},\mathbf{r}_s)\cdot\mathbf{d}_s \ . \tag{7.197}$$

Using the solution (7.193) for bulk media we find,

$$\vec{\mathcal{E}}_b(\mathbf{r},\mathbf{r}_s,\omega) = \omega^2\mu_0\left[-\frac{e^{\imath kR}}{4\pi k^2R^3}\left\{[1-\imath kR-(kR)^2]\mathbb{I}-[3-3\imath kR-(kR)^2]\hat{\mathbf{e}}_R\otimes\hat{\mathbf{e}}_R\right\}\right]\cdot\mathbf{d}_s \; . \tag{7.198}$$

with $k = k(\omega)$.

7.3.1.3 Bulk medium Green tensor projected on particular orientations

The Green tensor can be used to relate two dipoles $\hat{\mathbf{e}}_d$ and $\hat{\mathbf{e}}'_d$ respectively located at $\mathbf{r}$ and $\mathbf{r}'$. Using the identity,

$$R^2\hat{\mathbf{e}}'^*_d(\hat{\mathbf{e}}_R\otimes\hat{\mathbf{e}}_R)\hat{\mathbf{e}}_d = \begin{pmatrix}d'_x & d'_y & d'_z\end{pmatrix}\begin{pmatrix}x^2 & xy & xz\\ xy & y^2 & yz\\ xz & yz & z^2\end{pmatrix}\begin{pmatrix}d_x\\ d_y\\ d_z\end{pmatrix} = (\hat{\mathbf{e}}'_d\cdot\hat{\mathbf{e}}_R)(\hat{\mathbf{e}}_d\cdot\hat{\mathbf{e}}_R)\;, \tag{7.199}$$

we calculate from (7.194),

$$\begin{aligned}
&\tfrac{4\pi}{k}\hat{\mathbf{e}}'^*_d\;\mathfrak{Re}\;\mathcal{G}_b(\mathbf{r},\mathbf{r}',\omega)\;\hat{\mathbf{e}}_d \\
&= [\hat{\mathbf{e}}'_d\cdot\hat{\mathbf{e}}_d-(\hat{\mathbf{e}}'_d\cdot\hat{\mathbf{e}}_R)(\hat{\mathbf{e}}_R\cdot\hat{\mathbf{e}}_d)]\frac{\cos kR}{kR}-[\hat{\mathbf{e}}'_d\cdot\hat{\mathbf{e}}_d-3(\hat{\mathbf{e}}'_d\cdot\hat{\mathbf{e}}_R)(\hat{\mathbf{e}}_R\cdot\hat{\mathbf{e}}_d)]\left(\frac{\sin kR}{k^2R^2}-\frac{\cos kR}{k^3R^3}\right) \\
&\tfrac{4\pi}{k}\hat{\mathbf{e}}'^*_d\;\mathfrak{Im}\;\mathcal{G}_b(\mathbf{r},\mathbf{r}',\omega)\;\hat{\mathbf{e}}_d \\
&= [\hat{\mathbf{e}}'_d\cdot\hat{\mathbf{e}}_d-(\hat{\mathbf{e}}'_d\cdot\hat{\mathbf{e}}_R)(\hat{\mathbf{e}}_R\cdot\hat{\mathbf{e}}_d)]\frac{\sin kR}{kR}+[\hat{\mathbf{e}}'_d\cdot\hat{\mathbf{e}}_d-3(\hat{\mathbf{e}}'_d\cdot\hat{\mathbf{e}}_R)(\hat{\mathbf{e}}_R\cdot\hat{\mathbf{e}}_d)]\left(\frac{\cos kR}{k^2R^2}-\frac{\sin kR}{k^3R^3}\right)\;.
\end{aligned} \tag{7.200}$$

Note that dipole moment is complex in the case of circular polarization. The formula (7.200) simplifies when the dipoles are parallel,

$$\begin{aligned}
\tfrac{4\pi}{k}\hat{\mathbf{e}}^*_d\;\mathfrak{Re}\;\mathcal{G}_b(\mathbf{r},\mathbf{r}',\omega)\;\hat{\mathbf{e}}_d &= [1-(\hat{\mathbf{e}}_d\cdot\hat{\mathbf{e}}_R)^2]\frac{\cos kR}{kR}-[1-3(\hat{\mathbf{e}}_d\cdot\hat{\mathbf{e}}_R)^2]\left(\frac{\sin kR}{k^2R^2}+\frac{\cos kR}{k^3R^3}\right) \\
\tfrac{4\pi}{k}\hat{\mathbf{e}}^*_d\;\mathfrak{Im}\;\mathcal{G}_b(\mathbf{r},\mathbf{r}',\omega)\;\hat{\mathbf{e}}_d &= [1-(\hat{\mathbf{e}}_d\cdot\hat{\mathbf{e}}_R)^2]\frac{\sin kR}{kR}+[1-3(\hat{\mathbf{e}}_d\cdot\hat{\mathbf{e}}_R)^2]\left(\frac{\cos kR}{k^2R^2}-\frac{\sin kR}{k^3R^3}\right)\;.
\end{aligned} \tag{7.201}$$

7.3.1.4 Dispersion relation in anisotropic media

A homogeneous medium can still be anisotropic if,

$$\epsilon(\mathbf{r},\omega)=\epsilon(\omega) \qquad \text{although} \qquad \epsilon(\omega)\cdot\hat{\mathbf{e}}_r\neq const\;. \tag{7.202}$$

Then, $\epsilon(\omega)$ and $\mu(\omega)$ still need to be represented by tensors, which however do not depend on coordinates. The Helmholtz equation then simplifies to,

$$\left[\nabla_{\mathbf{r}}\times\nabla_{\mathbf{r}}\times-\frac{\omega^2}{c^2}\mu(\omega)\epsilon(\omega)\right]\vec{\mathcal{E}}_b(\mathbf{r},\omega)=\imath\omega\mu_0\mathbf{j}(\mathbf{r},\omega)\;, \tag{7.203}$$

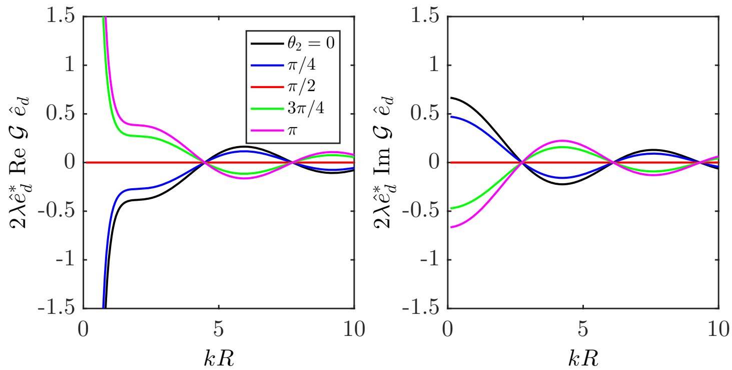

Figure 7.18: (code) Real and imaginary part of the bulk Green tensor for various orientations of the dipoles: $\hat{\mathbf{e}}_d'^* = \hat{\mathbf{e}}_x$ and $\hat{\mathbf{e}}_d$ as indicated in the legend.

in analogy to (7.185). Assuming no currents, $\mathbf{j}(\mathbf{r},\omega) = 0$, and plane electromagnetic waves, $\vec{\mathcal{E}}_b(\mathbf{r},\omega) = \vec{\mathcal{E}}_0(\omega)e^{\imath\mathbf{k}\cdot(\mathbf{r}-\mathbf{r}')}$, we obtain with the identity (7.188),

$$0 = \left[\nabla_{\mathbf{r}} \otimes \nabla_{\mathbf{r}} - \mathbb{I}\triangle - \frac{\omega^2}{c^2}\mu\epsilon\right] \vec{\mathcal{E}}_0 e^{\imath\mathbf{k}\cdot(\mathbf{r}-\mathbf{r}')} \tag{7.204}$$

$$= \left[-\mathbf{k} \otimes \mathbf{k} + k^2 - \frac{\omega^2}{c^2}\mu\epsilon\right] \vec{\mathcal{E}}_0 e^{\imath\mathbf{k}\cdot(\mathbf{r}-\mathbf{r}')} \ ,$$

where $\mu\epsilon$ is to be understood as a product between two matrices. From this we derive the dispersion relation,

$$0 = \left| -k_i k_j + k^2 \delta_{ij} - \frac{\omega^2}{c^2}(\mu)_{il}(\epsilon)_{lj} \right| \ , \tag{7.205}$$

for $i, j = x, y, z$.

We will discuss anisotropic homogeneous media in the context of hyperbolic metamaterials in Sec. 7.3.3.

7.3.1.5 Interaction between dipoles near dielectric media

The vector Green tensor describes the interaction between two points in space via an electromagnetic field. It can be used to solve a variety of problems, for example,

- the interaction between dipoles in free space;
- the modification of a dipole due to the presence of a dielectric boundary (Purcell effect);
- the modification of the interaction between dipoles due to the presence of a dielectric boundary.

The linearity of Maxwell's equations allows us to exploit the superposition principle applying it to the Green tensor. For example, we can express the interaction between two point dipoles $\mathbf{r}_1$ and $\mathbf{r}_2$ near a dielectric boundary by simply adding to the bulk tensor for their interaction in free space $\mathcal{G}_b(\mathbf{r}_1, \mathbf{r}_2, \omega)$ a tensor $\mathcal{G}_d(\mathbf{r}_1, \mathbf{r}_2, \omega)$ accounting for the presence of the dielectric,

$$\boxed{\mathcal{G} = \mathcal{G}_b + \mathcal{G}_d} . \tag{7.206}$$

7.3.2 Plasmons at metal-dielectric interfaces

A *surface plasmon polariton* (SPP) or simply *plasmon* is an electromagnetic wave in the infrared or visible spectral regime, which propagates along a metal-dielectric or metal-air interface. The term SPP explains that the wave involves both, the motion of charges in the metal and electromagnetic waves in the air or the dielectric.

SPPs are a type surface waves, guided along the interface in a similar way as light can be guided by an optical fiber. The wavelengths of SPPs are shorter than that of the incident light, which created them. Thus, they can be more localized and more intense. Perpendicularly to the interface, they are confined to the scale of a wavelength. The propagation of SPPs along the interface is limited by absorption losses in the metal or by photon scattering into other directions, e.g. into free space.

SPPs can be excited by electronic or photonic bombardment. For a photon to excite an SPP, both must have the same frequency and the same momentum. However, at a given frequency, a free space photon has less momentum than an SPP because the two have different dispersion relations (see below). Therefore, a photon coming from free space can not directly couple to an SPP. For the same reason, an SPP (on a perfectly smooth metal surface) can not emit photons into free space (assumed uniform). This incompatibility is analogous to the absence of transmission at total internal reflection.

However, the coupling of photons to SPPs can be achieved using a coupling medium, such as a dielectric or a grating, designed to match the wavevectors of photons and SPPs, until their momenta coincide. For example, a glass prism may be positioned against a thin metal film in Kretschmann configuration, as shown in Fig. 7.19(a). Single insulated surface defects, such as isolated or periodic grooves, slits or elevations, provide a mechanism coupling free space radiation and SPPs, which then can exchange energy.

7.3.2.1 Fields and plasmonic dispersion relation

The properties of a SPP can be derived from Maxwell's equations. Let $z > 0$ be the space occupied by the dielectric and $z < 0$ the space occupied by the metal. The electric and magnetic fields must obey Maxwell's equations and, in particular, the boundary conditions (7.42)(i-iv) at the interface. We will show in Exc. 7.3.7.2, that the fields must have the following form:

$$\boxed{\vec{\mathcal{H}}_n(\mathbf{r}, t) = \begin{pmatrix} 0 \\ 1 \\ 0 \end{pmatrix} \mathcal{H}_0 e^{\imath k_x x + \imath k_{z,n}|z| - \imath\omega t} \quad , \quad \vec{\mathcal{E}}_n(\mathbf{r}, t) = \begin{pmatrix} \pm k_{z,n} \\ 0 \\ -k_x \end{pmatrix} \frac{\mathcal{H}_0}{\omega\varepsilon_n} e^{\imath k_x x + \imath k_{z,n}|z| - \imath\omega t}} , \tag{7.207}$$

under the condition that,

$$\frac{k_{z,\mathrm{m}}}{\varepsilon_\mathrm{m}} = -\frac{k_{z,\mathrm{d}}}{\varepsilon_\mathrm{d}} , \tag{7.208}$$

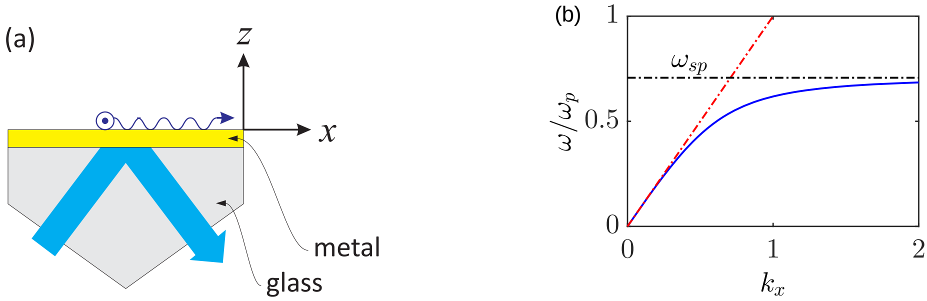

Figure 7.19: (code) (a) Kretschmann configuration of attenuated total reflection for the coupling of surface plasmons. The component of the scattered wavevector parallel to the surface forms SPPs, which then propagate along the metal-dielectric interface. (b) Dispersion curve for a SPP (blue). At low k_x it approaches the photonic dispersion curve (red).

where n indicates the material ($n = \mathrm{m}$ for the metal and $n = \mathrm{d}$ for the dielectric). This condition guarantees the continuity of the electric field parallel to the boundary. Upper signs apply to the dielectric region ($z > 0$) and lower signs to the metallic region ($z < 0$). That is, SPPs are always transverse magnetic waves (TM). The wavevector $\mathbf{k}$ is complex. In case of a lossless SPP, the k_x component is real and the k_z component imaginary,

$$k_{z,m} = \imath\kappa_{z,\mathrm{m}} \ , \tag{7.209}$$

such that the wave propagates along the x-direction and decays exponentially toward $\pm z$. While k_x is always the same in both materials, $k_{z,\mathrm{m}}$ is generally different from $k_{z,\mathrm{d}}$. Entering the fields (7.207) in the wave equation,

$$\nabla^2\vec{\mathcal{H}}_n = \varepsilon_n\mu_n\frac{\partial^2\vec{\mathcal{H}}_n}{\partial t^2} \ , \tag{7.210}$$

we easily verify that,

$$k_x^2 + k_{z,n}^2 = \omega^2\varepsilon_n\mu_n = \epsilon_n\left(\frac{\omega}{c}\right)^2 \ , \tag{7.211}$$

where we assume $\mu_n = \mu_0$ and $\varepsilon_n = \varepsilon_0\epsilon_n$, where the 'breve' denotes relative permittivities. Solving the two equations (7.211) for $n = \mathrm{m}, \mathrm{d}$ together with the relationship (7.208), we obtain the dispersion relation for a plasmon wave propagating on the surface,

$$\boxed{k_x = \frac{\omega}{c}\sqrt{\frac{\epsilon_\mathrm{d}\epsilon_\mathrm{m}}{\epsilon_\mathrm{d}+\epsilon_\mathrm{m}}}} \ . \tag{7.212}$$

To apply this relation in practice, we must specify the two permittivities ϵ_n. For simplicity, we assume $\epsilon_\mathrm{d} = 1$, and for ϵ_m we resort to the *Drude model* using (7.161), where for now we despise the attenuation $\Gamma_d = 0$,

$$\epsilon_m(\omega) = 1 - \frac{\omega_p^2}{\omega^2} \ , \tag{7.213}$$

where ω_p is the plasma frequency (7.162). Joining the expressions (7.212) and (7.213) we obtain,

$$ck_x = \sqrt{\frac{\omega^2 - \omega_p^2}{2\omega^2 - \omega_p^2}} \ . \tag{7.214}$$

This relationship is plotted in Fig. 7.19(b).

At low k_x, the SPP behaves like a photon, but as k_x increases, the dispersion relation becomes flatter and reaches an asymptotic limit ω_{sp} called 'surface plasma frequency'. If $\omega < \omega_{sp}$, the SPP has a shorter wavelength than the radiation in the free space, such that the components $k_{z,\mathrm{m}}$ are purely imaginary and exhibit evanescent decay. The plasma frequency at the surface ($\epsilon_\mathrm{d} = 1$) is,

$$\omega_{sp} = \lim_{k_x \to \infty} \omega = \frac{\omega_p}{\sqrt{2}} \ . \tag{7.215}$$

7.3.2.2 Absorption of plasmons

The formula (7.213) predicts $\varepsilon_\mathrm{m} < 0$ below the plasmon frequency. Electromagnetic waves propagating in metals suffer damping due to ohmic losses and interactions between the electrons and the atoms of the metallic lattice. These effects appear as an imaginary component of the dielectric function. To take this into account, we express the dielectric function of a metal in the complex plane,

$$\epsilon_\mathrm{m} = \epsilon'_\mathrm{m} + \imath\epsilon''_\mathrm{m} \ . \tag{7.216}$$

Generally, we have, $|\epsilon'_\mathrm{m}| \gg \epsilon''_\mathrm{m}$, such that the wavevector can be expressed in terms of its real and imaginary components as (see Exc. 7.3.7.3),

$$k_x = k'_x + \imath k''_x = \frac{\omega}{c}\sqrt{\frac{\epsilon_d\epsilon'_\mathrm{m}}{\epsilon_\mathrm{d} + \epsilon'_\mathrm{m}}} + \imath\frac{\omega}{c}\sqrt{\frac{\epsilon_d\epsilon'_\mathrm{m}}{\epsilon_\mathrm{d} + \epsilon'_\mathrm{m}}}^3 \frac{\epsilon''_\mathrm{m}}{2(\epsilon'_\mathrm{m})^2} \ . \tag{7.217}$$

The wavevector gives us insight into the physically significant properties of the electromagnetic wave, such as its spatial extent and mode matching conditions.

7.3.2.3 Distance of propagation and depth of penetration

As an SPP propagates along the surface, it loses energy to the metal due to absorption. The intensity of the surface plasmon decays with the square of the electric field, therefore, over a distance x, the intensity decreases by a factor of $e^{-2k_x x}$. The propagation length is defined as the distance, where the SPP intensity has decreased by a factor of $1/e$. This condition is satisfied at a length $L = \frac{1}{2k''_x}$.

Likewise, the electric field decays perpendicular to the surface of the metal. At low frequencies, the penetration depth of the SPP into the metal is commonly approximated using the skin depth formula. In a dielectric, the field will decay much more slowly. The decay depth in the metal and the dielectric medium can be expressed as

$$z_n = \frac{\lambda}{2\pi}\left(\frac{|\epsilon'_\mathrm{m}| + \epsilon_\mathrm{d}}{\epsilon_n^2}\right)^{1/2} \ , \tag{7.218}$$

where n indicates the propagation medium. SPPs are very sensitive to small perturbations within the skin depth and, therefore, are often used to probe surface inhomogeneities. Resolve the Exc. 7.3.7.4.

7.3.3 Negative refraction and metamaterials

The general dispersion relation for anisotropic media has been derived in (7.205),

$$\boxed{\left|\tfrac{\omega^2}{c^2}\epsilon_{il}\mu_{lj} - k^2\delta_{ij} + k_ik_j\right| = 0} , \tag{7.219}$$

which, for isotropic media simplifies to $\frac{\omega^2}{c^2}n^2 = k^2$, where $n^2 = \epsilon\mu$. Apparently, inverting the signs of both, the permittivity and the permeability, $\varepsilon, \mu < 0$ has no effect on the equations. However, one can show [94], that inserting into the first and second Maxwell equations,

$$\begin{aligned} \nabla \times \vec{\mathcal{H}} &= \partial_t \vec{\mathcal{D}} \quad , \quad \nabla \times \vec{\mathcal{E}} = -\partial_t \vec{\mathcal{B}} \\ \text{with} \quad \vec{\mathcal{D}} &= \varepsilon \vec{\mathcal{E}} \quad , \quad \vec{\mathcal{B}} = \mu \vec{\mathcal{H}} \end{aligned} \tag{7.220}$$

a plane wave, $\vec{\mathcal{E}}, \vec{\mathcal{D}}, \vec{\mathcal{B}}, \vec{\mathcal{H}} \propto e^{\imath(\mathbf{k}\cdot\mathbf{r}-\omega t)}$,

$$\mathbf{k} \times \vec{\mathcal{H}}_0 = -\omega\varepsilon\vec{\mathcal{E}}_0 \quad , \quad \mathbf{k} \times \vec{\mathcal{E}}_0 = \omega\mu\vec{\mathcal{H}}_0 , \tag{7.221}$$

one obtains for $\varepsilon, \mu > 0$, a right-handed triplet of vectors $\mathbf{k}$, $\vec{\mathcal{E}}$, $\vec{\mathcal{H}}$, whereas for $\varepsilon, \mu < 0$ one obtains a left-handed triplet. Defining the handedness via,

$$p \equiv \frac{(\mathbf{k} \times \vec{\mathcal{E}}) \cdot \vec{\mathcal{H}}}{|(\mathbf{k} \times \vec{\mathcal{E}}) \cdot \vec{\mathcal{H}}|} , \tag{7.222}$$

if $p = \pm 1$, we call the material is right(left)-handed. The energy flux,

$$\vec{\mathcal{S}} = \vec{\mathcal{E}} \times \vec{\mathcal{H}} \tag{7.223}$$

is parallel to $\mathbf{k}$ for right-handed materials and anti-parallel for left-handed, which means that phase and group velocities are reversed. Also, in left-handed materials we expect a reversed Doppler effect.

At the interface between two materials with different handednesses, $\varepsilon_1, \mu_1 > 0$ and $\varepsilon_2, \mu_2 < 0$, the equations (7.42) must still hold,

$$\begin{array}{ll} \text{(i)} & \vec{\mathcal{H}}_1^{\|} = \vec{\mathcal{H}}_2^{\|} \\ \text{(ii)} & \vec{\mathcal{E}}_1^{\|} = \vec{\mathcal{E}}_2^{\|} \\ \text{(iii)} & \varepsilon_1\vec{\mathcal{E}}_1^{\perp} = \varepsilon_2\vec{\mathcal{E}}_2^{\perp} \\ \text{(iv)} & \mu_1\vec{\mathcal{H}}_1^{\perp} = \mu_2\vec{\mathcal{H}}_2^{\perp} \end{array} . \tag{7.224}$$

but now, the signs of $\mathcal{E}_2^{\perp}$ and $\mathcal{H}_2^{\perp}$ are inverted. We calculate,

$$\vec{\mathcal{E}}_0 \times \vec{\mathcal{H}}_0 = \frac{1}{\omega\mu}\vec{\mathcal{E}}_0 \times (\mathbf{k} \times \vec{\mathcal{E}}_0) = \frac{1}{\omega\mu}[\mathbf{k}(\vec{\mathcal{E}}_0 \cdot \vec{\mathcal{E}}_0) - \vec{\mathcal{E}}_0(\mathbf{k} \cdot \vec{\mathcal{E}}_0)] = \frac{\mathcal{E}_0^2}{\omega\mu}\mathbf{k} \upuparrows -\vec{\mathcal{S}} . \tag{7.225}$$

As a consequence Snell's law (7.57) must be corrected,

$$\frac{\sin\theta_t}{\sin\theta_i} = \frac{n_1}{n_2} = \frac{p_2}{p_1}\left|\sqrt{\frac{\varepsilon_2\mu_2}{\varepsilon_1\mu_1}}\right| . \tag{7.226}$$

The *complex refractive index*,

$$n = n' + \imath n'' = c\sqrt{\varepsilon\mu} = c\sqrt{(\varepsilon' + \imath\varepsilon'')(\mu' + \imath\mu'')} = c\sqrt{|\varepsilon\mu|}e^{\imath\phi/2} \tag{7.227}$$

can have negative real part, $\mathfrak{Re}\ n < 0$, if the angle is $\phi > \pi$, that is, if,

$$\sin\phi = \frac{\mathfrak{Im}\ \varepsilon\mu}{|\varepsilon\mu|} = \frac{\varepsilon''\mu' + \varepsilon'\mu''}{|\varepsilon\mu|} < 0 \ . \tag{7.228}$$

Since the absorption is necessarily $\varepsilon'', \mu'' > 0$, the condition (7.228) is satisfied if $\varepsilon', \mu' < 0$. More generally, a sufficient but not necessary condition for *negative refraction* is,

$$\varepsilon'|\mu' + \imath\mu''| + \mu'|\varepsilon' + \imath\varepsilon''| < 0 \ . \tag{7.229}$$

The direction of the phase velocity is $\mathbf{k}$, while the energy flows along $\vec{\mathcal{S}} = \vec{\mathcal{E}} \times \vec{\mathcal{H}}$. For $n' > 0$ the dispersive medium is called *right-handed*, because $\mathbf{k}$, $\vec{\mathcal{E}}$ and $\vec{\mathcal{H}}$ form a tripod. For $n' < 0$ the medium is called *left-handed*, because $-\mathbf{k}$, $\vec{\mathcal{E}}$ and $\vec{\mathcal{H}}$ form a tripod, that is, $\mathbf{k}$ and $\vec{\mathcal{S}}$ are contrary. We will check this in Exc. 7.3.7.5. Such media are always very dispersive.

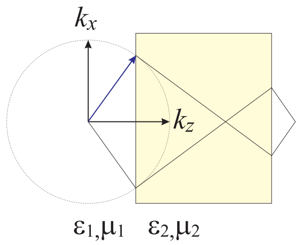

Figure 7.20: Refraction at the interface between 'right-handed' and 'left-handed' media.

Left-handed media have attracted much attention, because of the theoretical possibility of performing *perfect lenses* with a focusing power not being limited by diffraction. Left-handed media are studied in non-homogeneous and non-isotropic *metamaterials* [23], but there are also ideas on how to design them in homogeneous and isotropic atomic gases [24]

7.3.3.1 Hyperbolic metamaterials

Hyperbolic metamaterials (HMM) are artificial media with sub-optical-wavelength nano-structuring, which exhibit unusual optical properties. In particular, they are characterized by extreme anisotropy, behaving like dielectrics when illuminated from one side and like metals when illuminated from another. As already mentioned in Sec. 7.3.1, in a hyperbolic metamaterial the dispersion relation is anisotropic, corresponding to permittivity and permeability tensors of the form,

$$\varepsilon = \begin{pmatrix} \varepsilon_\perp & & \\ & \varepsilon_\perp & \\ & & \varepsilon_{\shortparallel} \end{pmatrix} \qquad \text{and} \qquad \mu = \begin{pmatrix} \mu_\perp & & \\ & \mu_\perp & \\ & & \mu_{\shortparallel} \end{pmatrix} \ . \tag{7.230}$$

[23] See [70, 71, 85, 58, 59, 61, 60, 72, 7, 93, 24, 18, 57, 84, 53].
[24] See the script *Quantum Mechanics* of the same author .

In the case $\varepsilon_\perp\varepsilon_\shortparallel < 0$ or $\mu_\perp\mu_\shortparallel < 0$ the dispersion relation,

$$\frac{k_x^2+k_y^2}{\varepsilon_\shortparallel}+\frac{k_z^2}{\varepsilon_\perp}=\frac{(\omega/c)^2}{\varepsilon_0}\ , \tag{7.231}$$

becomes hyperbolic [25]. In Exc. 7.3.7.7 we derive from the Maxwell equations, allowing for an anisotropic (but homogeneous) permittivity tensor, the hyperbolic dispersion relation.

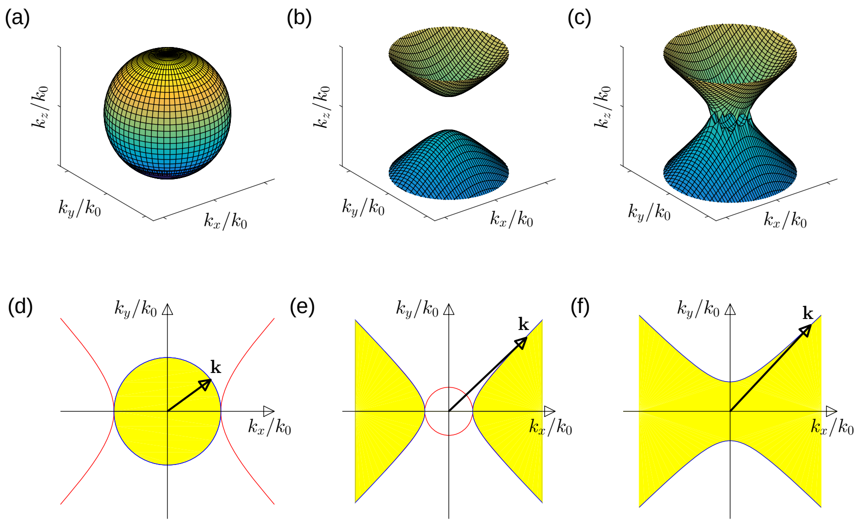

Figure 7.21: Isofrequency surfaces of hyperbolic dispersion relations. (a) Isotropic dielectric ($\varepsilon_\perp = \varepsilon_\shortparallel$); (b) two-sheeted hyperboloid ($\varepsilon_\perp < 0$ and $\varepsilon_\shortparallel > 0$); (c) one-sheeted hyperboloid ($\varepsilon_\perp > 0$ and $\varepsilon_\shortparallel < 0$). (d-f) Projection of the two-dimensional isofrequency surfaces shown in (a-c) on the $k_y = 0$ plane. The yellow-shaded areas correspond to lossy regions (real parts).

Example 80 (*Interest of hyperbolic metamaterials*): Hyperbolic metamaterials are investigated for their potential interest in engineering the decay routes of quantum emitters by manipulating the local density-of-states. The reason is, that HMMs allow for the propagation of modes with wavevectors (known as high-k modes) much higher than the free-space wavevector. Thus, the evanescent waves (also with high-k) of an emitter couple more easily to a sufficiently close HMM, and thus emitting their photons faster.
The elementary cells of a metamaterial are often complicated, and a stratification is helpful to describe its response to incident light. For example, many features of an HMM can be grasped by frequency-dependent effective permittivity and permeability tensors.

In Exc. 7.3.7.8 we show, that the effective permittivity of a nanostructure having the shape of a stack of alternating intrinsically homogeneous layers with permittivities

[25] Note that a more correct treatment would need to account for the polarizations of the electric and magnetic fields. We leave this to an upcoming version of the script.

ε_d and ε_m and thicknesses $d_d, d_m \ll \lambda$ [see Fig. 7.22(b)] is given by [80],

$$\varepsilon_{\shortparallel} = \frac{\varepsilon_d d_d + \varepsilon_m d_m}{d_d + d_m} \qquad \text{and} \qquad \frac{1}{\varepsilon_\perp} = \frac{d_d/\varepsilon_d + d_m/\varepsilon_m}{d_d + d_m} \ . \tag{7.232}$$

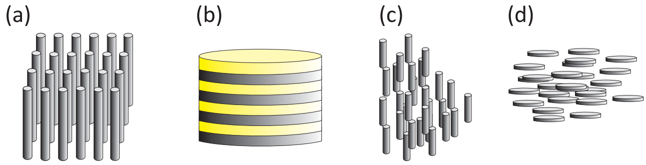

Figure 7.22: Hyperbolic dispersion materials. In order to achieve a negative permittivity in a given direction, the electrons must move freely along it, like in a metal.

Example 81 (*Anisotropy of a metamaterial*): For example, choosing $d_m = d_d$, $\varepsilon_d = 1$ and $\varepsilon_m = -2$, we obtain $\varepsilon_{\shortparallel} = \frac{1}{4}$ and $\varepsilon_\perp = -\frac{1}{2}$.

In Exc. 7.3.7.9 we discuss, whether it is possible to realize a hyperbolic dispersion relation in an atomic gas.

7.3.4 Wave guides

The presence of conductive interfaces influences the propagation of electromagnetic waves. Interfaces, which influence the propagation direction of electromagnetic waves are called *waveguides*. Let us consider a waveguide such as the one illustrated in Figs. 7.23. In the volume enclosed by the waveguide, supposedly perfectly conductive ($\vec{\mathcal{E}} = 0 = \vec{\mathcal{B}}$ inside the wave guide material), every electromagnetic field must satisfy the boundary conditions (7.42), that is, we have,

$$\boxed{\vec{\mathcal{E}}^{\parallel} = 0 \qquad \text{and} \qquad \vec{\mathcal{B}}^{\perp} = 0} \tag{7.233}$$

on all interior surfaces of the waveguide. Free surface charges and currents will automatically be generated in such a way as to endorse these conditions, and all conclusions derived in the following sections are basically corollaries of these boundary conditions.

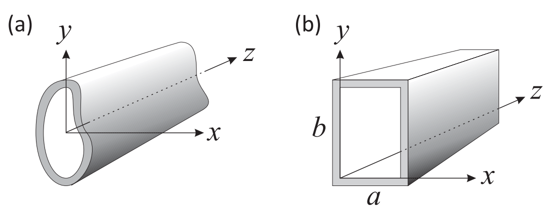

Figure 7.23: Waveguides of arbitrarily (i) and rectangular (ii) shape.

Let us now consider monochromatic waves propagating along a tube oriented in z-direction,

$$\vec{\mathcal{E}}(x,y,z,t) = \vec{\mathcal{E}}(x,y)e^{\imath(k_z z - \omega t)} \qquad \text{and} \qquad \vec{\mathcal{B}}(x,y,z,t) = \vec{\mathcal{B}}(x,y)e^{\imath(k_z z - \omega t)} \ . \tag{7.234}$$

Obviously, the $\vec{\mathcal{E}}$ and $\vec{\mathcal{B}}$ fields must simultaneously satisfy the vacuum Maxwell equations (6.6) inside the guide and the boundary conditions (7.233). To implement these conditions, we reformulate Maxwell's equations. We insert (7.234) and the expansions $\vec{\mathcal{E}}(x,y) = \sum_{k=x,y,z} \mathcal{E}_k(x,y)\hat{\mathbf{e}}_k$ and $\vec{\mathcal{B}}(x,y) = \sum_{k=x,y,z} \mathcal{B}_k(x,y)\hat{\mathbf{e}}_k$ in the Maxwell equations (6.6)(i) and (ii) and obtain,

$$\begin{array}{llcl llcl} \text{(i)} & \partial_y\mathcal{E}_z - \imath k_z\mathcal{E}_y & = & \imath\omega\mathcal{B}_x & \text{(ii)} & \partial_y\mathcal{B}_z - \imath k_z\mathcal{B}_y & = & -\imath\frac{\omega}{c^2}\mathcal{E}_x \\ \text{(iii)} & \imath k_z\mathcal{E}_x - \partial_x\mathcal{E}_z & = & \imath\omega\mathcal{B}_y & \text{(iv)} & \imath k_z\mathcal{B}_x - \partial_x\mathcal{B}_z & = & -\imath\frac{\omega}{c^2}\mathcal{E}_y \\ \text{(v)} & \partial_x\mathcal{E}_y - \partial_y\mathcal{E}_x & = & \imath\omega\mathcal{B}_z & \text{(vi)} & \partial_x\mathcal{B}_y - \partial_y\mathcal{B}_x & = & -\imath\frac{\omega}{c^2}\mathcal{E}_z\ . \end{array} \tag{7.235}$$

Inserting the component $\mathcal{B}_y$ of the third into the second equation, the $\mathcal{B}_x$ of the first into the fourth equation, the $\mathcal{E}_y$ of the fourth into the first equation, and the $\mathcal{E}_x$ of the second in the third equation, we arrive at,

$$\begin{array}{lrcl} \text{(i)} & \mathcal{E}_x & = & \frac{\imath}{(\omega/c)^2-k_z^2}(k_z\partial_x\mathcal{E}_z + \omega\partial_y\mathcal{B}_z) \\ \text{(ii)} & \mathcal{E}_y & = & \frac{\imath}{(\omega/c)^2-k_z^2}(k_z\partial_y\mathcal{E}_z - \omega\partial_x\mathcal{B}_z) \\ \text{(iii)} & \mathcal{B}_x & = & \frac{\imath}{(\omega/c)^2-k_z^2}(k_z\partial_x\mathcal{B}_z - \frac{\omega}{c^2}\partial_y\mathcal{E}_z) \\ \text{(iv)} & \mathcal{B}_y & = & \frac{\imath}{(\omega/c)^2-k_z^2}(k_z\partial_y\mathcal{B}_z + \frac{\omega}{c^2}\partial_x\mathcal{E}_z)\ . \end{array} \tag{7.236}$$

And inserting these equations into Maxwell's equations (iii) and (iv), we arrive at,

$$\left[\frac{\partial^2}{\partial x^2} + \frac{\partial^2}{\partial y^2} + (\omega/c)^2 - k_z^2\right]\mathcal{E}_z = 0 = \left[\frac{\partial^2}{\partial x^2} + \frac{\partial^2}{\partial y^2} + (\omega/c)^2 - k_z^2\right]\mathcal{B}_z\ . \tag{7.237}$$

Hence, we can solve the waveguide problem by first solving the wave equations for the components $\mathcal{E}_z$ and $\mathcal{B}_z$ and then inserting the solutions into Eqs. (7.236) in order to obtain the other field components.

When $\mathcal{E}_z = 0$ we call these waves *transverse electric waves* (TE), when $\mathcal{B}_z = 0$ we call them *transverse magnetic waves* (TM), and when $\mathcal{E}_z = 0 = \mathcal{B}_z$ we call them *transverse electro-magnetic waves* (TEM). TEM waves can not exist in a hollow waveguide, as we will show in Exc. 7.3.7.10.

7.3.4.1 Waveguide with constant rectangular cross section

Here, we consider the transmission of TE waves through a waveguide of constant rectangular cross-section, as shown in Fig. 7.23(ii). Similarly to the procedure for solving the Laplace equation in electrostatics, we make a separation ansatz for the variables in a way suggested by the symmetry of the problem, that is, we assume the existence of two functions X and Y, such that inserting the ansatz

$$\mathcal{E}_z = 0 \quad \text{and} \quad \mathcal{B}_z = X(x)Y(y)\ , \tag{7.238}$$

in the wave equation,

$$Y\frac{d^2X}{dx^2} + X\frac{d^2Y}{dy^2} + [(\omega/c)^2 - k_z^2] = 0\ , \tag{7.239}$$

leaves us with,

$$\frac{1}{X}\frac{d^2X}{dx^2} = -k_x^2 \quad \text{and} \quad \frac{1}{Y}\frac{d^2Y}{dy^2} = -k_y^2 \quad \text{with} \quad -k_x^2-k_y^2+(\omega/c)^2-k_z^2 = 0\ . \tag{7.240}$$

$\mathcal{B}_x$ must vanish on the surfaces at $x = 0, a$ and, because of (7.236)(iii) $\partial_x \mathcal{B}_z$ as well, such that $dX/dx = 0$, that is, X is a cosine. In the same way, $\mathcal{B}_y$ must vanish on the surfaces at $y = 0, b$, such that Y is a cosine. Therefore, the solution is,

$$\mathcal{B}_z = \mathcal{B}_0 \cos k_x x \cos k_y y \qquad \text{with} \qquad k_x = \tfrac{m\pi}{a} \qquad \text{and} \qquad k_y = \tfrac{n\pi}{b} \ . \tag{7.241}$$

With this, the wavevector becomes,

$$k_z = \sqrt{(\omega/c)^2 - \pi^2[(m/a)^2 + (n/b)^2]} \ . \tag{7.242}$$

Consequently, the frequency must be higher than,

$$\omega > c\pi\sqrt{(m/a)^2 + (n/b)^2} \equiv \omega_{mn} \ , \tag{7.243}$$

to avoid exponentially attenuated fields. The frequency ω_{mn} is called *cut-off frequency*. The components $\mathcal{B}_x$ and $\mathcal{B}_y$ can be determined from (7.236)(iii) and (iv),

$$\boxed{\begin{aligned} \vec{\mathcal{E}} &= \mathcal{E}_0 \begin{pmatrix} \frac{\imath\omega k_y}{k_x^2+k_y^2} \cos k_x x \sin k_y y \\ \frac{-\imath\omega k_x}{k_x^2+k_y^2} \sin k_x x \cos k_y y \\ 0 \end{pmatrix} e^{\imath(k_z z - \omega t)} \\ \vec{\mathcal{B}} &= \mathcal{B}_0 \begin{pmatrix} \frac{\imath k_z k_x}{k_x^2+k_y^2} \sin k_x x \cos k_y y \\ \frac{\imath k_z k_y}{k_x^2+k_y^2} \cos k_x x \sin k_y y \\ \cos k_x x \cos k_y y \end{pmatrix} e^{\imath(k_z z - \omega t)} \end{aligned}} \ . \tag{7.244}$$

Inserting ω_{mn} in the dispersion relation (7.242), we notice that the formula for the phase propagation velocity,

$$c = \frac{\omega}{k_z} = \frac{c}{\sqrt{1 - (\omega_{mn}/\omega)^2}} > c \ , \tag{7.245}$$

predicts a velocity above the speed of light. However, the group velocity,

$$v_g = \frac{1}{dk_z/d\omega} = c\sqrt{1 - (\omega_{mn}/\omega)^2} < c \ , \tag{7.246}$$

is slower. Resolve Exc. 7.3.7.11 and 7.3.7.12 [26].

7.3.5 The coaxial line

We have already mentioned the possibility of TEM waves in a *coaxial waveguide*, as shown in Fig. 7.24. Inserting $\mathcal{E}_z = 0 = \mathcal{B}_z$ in the equations (7.235) we obtain,

$$\begin{array}{rcl} c\mathcal{B}_y = \mathcal{E}_x & \text{and} & c\mathcal{B}_x = -\mathcal{E}_y \\ \partial_x\mathcal{E}_y - \partial_y\mathcal{E}_x = & 0 & = \partial_x\mathcal{B}_y - \partial_y\mathcal{B}_x \\ \partial_x\mathcal{E}_x + \partial_y\mathcal{E}_y = & 0 & = \partial_x\mathcal{B}_x + \partial_y\mathcal{B}_y \end{array} \ , \tag{7.247}$$

where we join the Maxwell equations (iii) and (iv) in the last line. In Exc. 7.3.7.13

[26] Rectangular waveguides are used, for example, in radio detection and ranging (RADAR) systems to guide microwave signals from a synthesizer to an antenna.

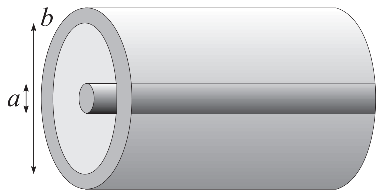

Figure 7.24: Guia de onda coaxial.

we will show that,

$$\vec{\mathcal{E}}(\rho,\phi,z,t) = \frac{A\cos(k_z z - \omega t)}{\rho}\hat{\mathbf{e}}_\rho \quad \text{and} \quad \vec{\mathcal{B}}(\rho,\phi,z,t) = \frac{A\cos(k_z z - \omega t)}{c\rho}\hat{\mathbf{e}}_\phi \ , \tag{7.248}$$

satisfies Maxwell's equations. Solve Exc. 7.3.7.14.

7.3.6 Cavities

An *optical resonator* consists of an arrangement of mirrors reflecting light beams in such a way as to form a closed path. Light which entered the cavity carries out many round-trips before it is transmitted again through a (partially reflecting) mirror, scattered out of the cavity mode or absorbed by impurities in the mirrors. Thus, the light power is considerably increased. That is, cavities can store light. Do Exc. 7.3.7.15 to 7.3.7.17.

In order to resonate in a cavity, a light beam must satisfy the boundary condition, that the mirror surfaces coincide with nodes of the standing light wave formed by the beam and its reflections at the mirrors. Therefore, in a cavity of length L, only a discrete spectrum of wavelengths $N\lambda/2 = L$ can be resonantly amplified, where N is a natural number. Because of this property, cavities are often used as frequency filters or optical spectrum analyzers: Only frequencies close to $\nu = N\delta_{fsr}$ are transmitted, where $\delta_{fsr} = c/2L$ is the called the *free spectral range* of the cavity.

A cavity is characterized on one hand by its geometry, that is, the curvature and the distance of its mirrors, and on the other hand by its finesse, which is given by the reflectivity of its mirrors. Let us first study the finesse and postpone the discussion of its geometry to Sec. 7.4.1. Treating the cavity as a multiple path interferometer (or *Fabry-Perot cavity*), we can derive an expression for the reflected and transmitted intensity as a function of frequency,

$$(k+\Delta k)L = \frac{(\omega_c+\Delta)L}{c} = \frac{\omega_c+\Delta}{2\delta_{fsr}} = \pi N + \frac{\Delta}{2\delta_{fsr}} \ . \tag{7.249}$$

The so-called *Airy formulas* for reflection and transmission are,

$$\boxed{\begin{aligned} I_{refl} &= I_{in}\frac{(2F/\pi)^2\sin^2(\Delta/2\delta_{fsr})}{1+(2F/\pi)^2\sin^2(\Delta/2\delta_{fsr})} \\ I_{trns} &= I_{in}\frac{1}{1+(2F/\pi)^2\sin^2(\Delta/2\delta_{fsr})} \end{aligned}} \ , \tag{7.250}$$

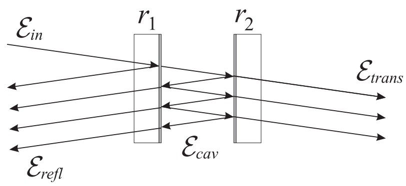

Figure 7.25: Multiple interference in an optical cavity of two mirrors characterized by reflectivities $r_{1,2}$.

where $R = |r|^2$ is the reflectivity of a mirror and Δ the detuning between the laser and the cavity (in radians/s). We will derive the formulas in Exc. 7.3.7.18. The transmission curve of the cavity has a finite bandwidth κ_{int}, which depends on the reflectivity of the mirrors. The *finesse* of the cavity is defined by,

$$F \equiv \frac{2\pi\delta_{fsr}}{\kappa_{int}} = \frac{\pi\sqrt{R}}{1-R} \ . \tag{7.251}$$

Note that δ_{fsr} is given in terms of a real frequency, while κ_{int} is a radiant [27].

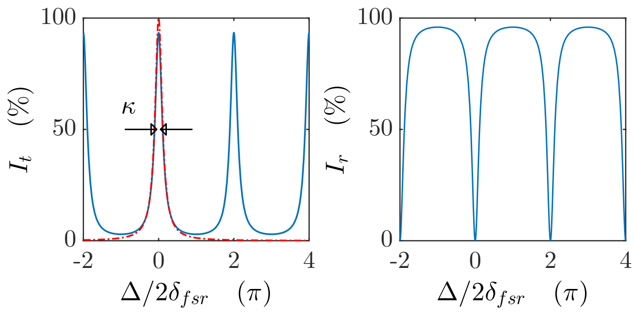

Figure 7.26: (code) Transmission and reflection of a resonator. The chosen mirror reflectivities are $R = 70\%$, the absorption losses $S = 1\%$. The red dash-dotted line is the Lorentzian approximation. Apparently, it fails off resonance.

The Airy formula was derived under the assumption of plane waves, but this assumption is not always realistic. Indeed, as we will show in Sec. 7.4.1, light propagates in transversely delimited modes and is subject to diffraction. We will see, that the resonance of a cavity not only depends on the order number N of the *longitudinal mode*, but also on the order of the *transverse mode*. The free space modes are TEM-modes.

7.3.6.1 Damping of the cavity

The decay time τ of the cavity is defined by the number of 'round-trips' with reflections at both mirrors R_1 and R_2, that a light beam can do before its intensity falls to e^{-1} of its original value [99](p.148):

$$I(\tau) = I_0\sqrt{R_1R_2}^{c\tau/2L} \stackrel{!}{=} e^{-1}I_0 \ . \tag{7.252}$$

[27] Note, that κ_{int} is defined as the FWHM of the intensity transmission curve.

Letting $R_1 = R_2 = 1 - T$, this yields,

$$\tau = \frac{2L}{c} \frac{\ln e^{-1}}{\ln R_1 R_2} = \frac{1}{\delta_{fsr}} \frac{-1}{\ln(1-T)^2} \simeq \frac{1}{\delta_{fsr}} \frac{1}{2T} \tag{7.253}$$
$$= \frac{1}{2\delta_{fsr}} \frac{1}{1-\sqrt{R_1 R_2}} \simeq \frac{F}{2\pi\delta_{fsr}} = \frac{1}{\kappa_{int}} \; ,$$

approximating $\sqrt{R} \simeq 1$. Hence, κ_{int} has also the meaning of a intensity decay constant [28].

7.3.7 Exercises

7.3.7.1 Ex: Green function for vector Helmholtz equation

Derive the expression (7.193) in Cartesian coordinates.

7.3.7.2 Ex: The fields of a plasmon

From the ansatz,

$$\vec{\mathcal{H}}_n(\mathbf{r}, t) = \begin{pmatrix} 0 \\ \mathcal{H}_{y,n} \\ 0 \end{pmatrix} e^{\imath k_x x + \imath k_{z,n}|z| - \imath\omega t}$$

for a plasmonic wave, with $n = \text{m}$ in the metallic region ($z < 0$) and $n = \text{d}$ in the dielectric region ($z > 0$), construct the electric and magnetic fields on both sides of a metal-dielectric interface.

7.3.7.3 Ex: Absorption of plasmons

Derive the expression (7.217).

7.3.7.4 Ex: Poynting vector of plasmons

At the interface between the vacuum and a metal surface there live solutions of the Maxwell equations, which decay exponentially in z-direction. We consider in this exercise only those parts of the waves, which live on the vacuum side $z > 0$, as illustrated in Fig. 7.19(a). The magnetic field, in this scheme, takes the following form:

$$\vec{\mathcal{H}}(\mathbf{r}, t) = \begin{pmatrix} 0 \\ \mathcal{H}_0 \\ 0 \end{pmatrix} \cos(kx - \omega t) e^{-\kappa z} \;\; (z > 0) \; .$$

a. Derive with the help of Maxwell's equation $\nabla \times \vec{\mathcal{H}} - \frac{\partial \vec{\mathcal{D}}}{\partial t} = \mathbf{j}$ the corresponding electric field $\vec{\mathcal{E}}(\mathbf{r}, t)$ in the half-space $z > 0$.
b. Calculate the Poynting vector $\vec{\mathcal{S}}(\mathbf{r}, t)$ in the half-space $z > 0$.
c. Calculate the total energy flow in x-direction. To do this, calculate the average over an oscillation period and integrate over the half-space $z > 0$.

[28] It should not be confused with the electric field *amplitude* decay rate defined as $\kappa = \kappa_{int}/2$.

7.3.7.5 Ex: Negative refraction

Show that a medium with negative refractive index is left-handed and allows for perfect focusing.

7.3.7.6 Ex: Negative refraction in chiral media

In a *chiral medium* the electric polarization $\vec{\mathcal{P}}$ couples to the magnetic field $\vec{\mathcal{H}}$ of an electromagnetic wave and the magnetization $\vec{\mathcal{M}}$ couples to the electric field $\vec{\mathcal{E}}$ like,

$$\vec{\mathcal{P}} = \varepsilon_0\chi_\varepsilon\vec{\mathcal{E}} + \tfrac{1}{c}\xi_{EH}\vec{\mathcal{H}} \qquad \text{and} \qquad \vec{\mathcal{M}} = \tfrac{1}{c}\xi_{HE}\vec{\mathcal{E}} + \chi_m\vec{\mathcal{H}} \ ,$$

where ξ_{EH} and ξ_{HE} are the complex chirality coefficients. Show that a chiral medium allows for a negative refraction coefficient.

7.3.7.7 Ex: Hyperbolic metamaterials

Hyperbolic metamaterials are artificial media with sub-wavelength nanostructuring below exhibiting uncommon optical properties, such as an extreme anisotropy giving rise to permittivity and permeability tensors of the form,

$$\epsilon = \begin{pmatrix} \varepsilon_\perp & & \\ & \varepsilon_\perp & \\ & & \varepsilon_\shortparallel \end{pmatrix} \qquad \text{and} \qquad \mu = \begin{pmatrix} \mu_\perp & & \\ & \mu_\perp & \\ & & \mu_\shortparallel \end{pmatrix} \ .$$

In the case $\varepsilon_\perp\varepsilon_\shortparallel < 0$ or $\mu_\perp\mu_\shortparallel < 0$ the dispersion relation,

$$\frac{k_x^2 + k_y^2}{\varepsilon_\shortparallel} + \frac{k_z^2}{\varepsilon_\perp} = \frac{(\omega/c)^2}{\varepsilon_0} \ ,$$

becomes hyperbolic.
Derive from the Maxwell equations, allowing for an anisotropic (but homogeneous) permittivity tensor, the hyperbolic dispersion relation.

7.3.7.8 Ex: Stacked layer metamaterial

Show that the effective permittivity of a nanostructure having the shape of an alternating stack of two different but intrinsically homogenous layers with the permittivity ε_d and ε_m and thicknesses $d_d, d_m \ll \lambda$ is given by,

$$\varepsilon_\perp = \frac{\varepsilon_d d_d + \varepsilon_m d_m}{d_d + d_m} \qquad \text{and} \qquad \varepsilon_\shortparallel = \frac{d_d/\varepsilon_d + d_m/\varepsilon_m}{d_d + d_m} \ .$$

7.3.7.9 Ex: Hyperbolic dispersion relation in gases

Discuss, whether it is possible to realize a hyperbolic dispersion relation in an atomic gas.

7.3.7.10 Ex: TEM waves in a hollow wave guide

Verify that TEM waves can not occur in hollow waveguides. Do not use the already derived results (7.236).

7.3.7.11 Ex: The TE_{00} mode in the rectangular waveguide

Show that the TE_{00} mode can not occur in a rectangular waveguide.

7.3.7.12 Ex: Cut-off frequency

Calculate the radial size of a hollow rectangular wave guide capable of guiding a (i) 60 Hz signal, (ii) a 10 MHz signal, and (iii) a 9.1 GHz signal.

7.3.7.13 Ex: Cylindrical waveguide

Show that the fields (7.248) satisfy the Maxwell equations with the boundary conditions (7.233) [42](p.411).

7.3.7.14 Ex: Propagation of a TEM mode along a coaxial cable

A transmission line made of two concentric circular metallic cylinders with conductivity ρ and skin depth δ is filled with a lossless uniform dielectric (ε, μ). A TEM mode propagates along this line.
a. Show that the time averaged energy flux along the line is,

$$P = \sqrt{\frac{\mu}{\varepsilon}} \pi a^2 |\mathcal{H}_0|^2 \ln \frac{b}{a} \ ,$$

where H_0 is the maximum value of the azimuthal magnetic field on the surface of the inner conductor.
b. Show that the transmitted power is attenuated along the line like,

$$P(z) = P_0 e^{-2\gamma z} \ ,$$

where,

$$\gamma = \frac{1}{2\sigma\delta} \sqrt{\frac{\varepsilon}{\mu}} \frac{a^{-1} + b^{-1}}{ln(b/a)} \ .$$

c. The characteristic impedance Z_0 of the line is defined as the ratio between the voltage between the cylinders and the current flowing in axial direction inside one of the cylinders at any position z. Show that for this line,

$$Z_0 = \frac{1}{2\pi} \sqrt{\frac{\mu}{\varepsilon}} \ln \frac{b}{a} \ .$$

d. Show that the resistance and the serial inductance per unit length of the line are,

$$R = \frac{1}{2\pi\sigma\delta} \left(\frac{1}{a} + \frac{1}{b} \right) \quad , \quad L = \frac{\mu}{2\pi} \ln \frac{b}{a} + \frac{\mu_c \delta}{4\pi} \left(\frac{1}{a} + \frac{1}{b} \right) \ ,$$

where μ_c is the permeability of the conductor. The correction for the inductance comes from the penetration of the flux into the conductors by the distance of the order δ.

7.3.7.15 Ex: Resonant cavity

Consider a perfectly conducting resonant cavity having the shape of a 3D rectangular box with the volume defined by $x \in [0, L_x]$, $y \in [0, L_y]$, and $z \in [0, L_z]$. Show that the resonant frequencies for both the TE and TM modes are given by $\omega_{n_x,n_y,n_z} = c\pi\sqrt{(n_x/L_x)^2 + (n_y/L_y)^2 + (n_z/L_z)^2}$ for integers n_i. Find the associated electric and magnetic fields.

7.3.7.16 Ex: Spherical holes in conductors such as cavities

A spherical hole of radius a in a conductive medium may serve as an electromagnetic resonant cavity.
a. Assuming infinite conductivity, determine the transcendental equations for the characteristic frequencies $\omega_{\ell m}$ of the cavity for TE and TM modes.
b. Calculate numerical values for the wavelength $\lambda_{\ell m}$ in units of the radius a for the four lowest modes for TE and TM waves.
c. Explicitly calculate the electric and magnetic fields inside the cavity for the lowest TE mode and the lowest TM mode.

7.3.7.17 Ex: Schumann resonances

A resonant cavity consists of the void space between two perfectly conducting and concentric spherical layers. The smaller one has the external radius a, the larger one the internal radius b. The azimuthal magnetic field has a radial dependence given by spherical Bessel functions, $j_\ell(kr)$ and $n_\ell(kr)$, where $k = \omega/c$.
a. Write the transcendental equation for the characteristic frequencies of the cavity for arbitrary ℓ.
b. For $\ell = 1$ use the explicit forms of the spherical Bessel functions to show that the characteristic frequencies are given by,

$$\frac{\tan kh}{kh} = \frac{k^2 + (ab)^{-1}}{k^2 + ab(k^2 - a^{-2})(k^2 - b^{-2})} ,$$

where $h = b - a$.
c. For $h/a \ll 1$, verify that the result of part (b) reproduces the frequency found in [47], Sec. 8.9, and determine the first-order corrections in h/a.
Now, we apply this cavity as a model for the atmosphere enclosed by the Earth's surface and its ionosphere.
d. For the Schumann resonances of Sec. 8.9 calculate the values Q under the assumption that the Earth has the conductivity σ_e and the ionosphere the conductivity σ_i with corresponding skin depths δ_e and δ_i. Show that in the lowest order in h/a the value Q is given by $Q = Nh/(\delta_e + \delta_i)$ and determine the numerical factor N for all ℓ.
e. For the lowest Schumann resonance evaluate the value Q assuming $\sigma_e = 0.1\ (\Omega m)^{-1}$, $\sigma_e = 10^{-5}\ (\Omega m)^{-1}$, $h = 100$ km.
f. Discuss the validity of the approximations used in part (a) for the parameter regime used in part (b).

7.3.7.18 Ex: Airy formula

To derive the *Airy formulas*, consider a light field described by $\mathcal{E}_{in}$ incident on a Fabry-Pérot cavity of length L. The cavity mirrors are glass substrates having a surface with dielectric coating. The surfaces of the two mirrors are characterized by the transmission rates t_1, t_2 and reflection rates r_1, r_2. Note, that the reflected wave suffers a phase shift of π, when the reflection occurs at a denser medium $n > 1$. Disregard energy losses by absorption.

7.4 Beam and wave optics

While the propagation of high wavelength radiation is dominated by diffraction effects, we observe that visible light tends to form bundles that apparently propagate (in homogeneous media) in a straight line. With the invention of the laser, the optical regime has become the preferred spectral regime for many spectroscopic applications. Therefore, we will dedicate the following section to the propagation of laser beams, which is understood within the theory of Gaussian optics.

7.4.1 Gaussian optics

At first glance, one might think that the propagation of laser light is well described by the laws of geometrical optics. Closer inspection, however, shows that a laser beam in many ways behaves more like a wave, although its energy is concentrated near an optical axis. The fields satisfy the wave equation. By inserting the propagating wave $u = \psi_z(x,y)e^{\imath(kz-\omega t)}$, we obtain an equation similar to the Schrödinger equation [49],

$$0 = \left[\frac{1}{c^2}\frac{\partial^2}{\partial t^2} - \nabla^2\right]\psi e^{\imath(kz-\omega t)} = e^{\imath(kz-\omega t)}\left(2\imath k\frac{\partial\psi}{\partial z} - \nabla^2\psi\right) . \tag{7.254}$$

Neglecting the second derivative for z, we obtain,

$$\left[2\imath k\frac{\partial}{\partial z} - \left(\frac{\partial^2}{\partial x^2} + \frac{\partial^2}{\partial y^2}\right)\right]\psi = 0 . \tag{7.255}$$

To describe a Gaussian beam, we choose an exponential ansatz and introduce two parameters that may vary along the propagation axis z: $\varphi(z)$ is a complex phase shift and $q(z)$ a complex parameter, whose imaginary part describes the diameter of the beam. Inserting the ansatz

$$\psi = e^{-\imath\left[\varphi(z)+k(x^2+y^2)/2q(z)\right]} \tag{7.256}$$

into the Schrödinger equation, we obtain,

$$\begin{aligned}0 &= 2\imath k e^{-\imath[\varphi+k(x^2+y^2)/2q]}\left(-\imath\frac{\partial\varphi}{\partial z} + \frac{\imath k(x^2+y^2)}{2q^2}\frac{\partial q}{\partial z}\right) - 2e^{-\imath[\varphi+k(x^2+y^2)/2q]}\frac{-\imath k}{q} \\ &\quad - e^{-\imath[\varphi+k(x^2+y^2)/2q]}\left(\frac{-\imath kx}{q}\right)^2 - e^{-\imath[\varphi+k(x^2+y^2)/2q]}\left(\frac{-\imath ky}{q}\right)^2 .\end{aligned} \tag{7.257}$$

This leads directly to the equation,

$$0 = (q' - 1)\frac{\imath k(x^2 + y^2)}{q^2} - 2\imath\varphi' + \frac{2}{q} \ . \tag{7.258}$$

For Eq. (7.258) to be valid at all x and y, we need $q' = 1$ and $\varphi' = \frac{-\imath}{q}$. Integrating q', we find,

$$q(z) = q_0 + z \ . \tag{7.259}$$

It is practical to introduce real beam parameters

$$\boxed{\frac{1}{q} \equiv \frac{1}{R} - \imath\frac{\lambda}{\pi w^2}} \ . \tag{7.260}$$

Inserting this into the ansatz (7.256),

$$\psi = e^{-\imath\varphi - \imath\frac{k(x^2+y^2)}{2R^2} - \frac{(x^2+y^2)}{w^2}} \ , \tag{7.261}$$

it becomes clear that $R(z)$ is the radius of curvature and $w(z)$ is the diameter of the beam. Evaluating q_0 at the position of the focus (beam waist), where $R = \infty$, we get from (7.259) along with the definition (7.260),

$$\frac{1}{\frac{1}{R_z} - \imath\frac{\lambda}{\pi w_z^2}} = q(z) = q_0 + z = \frac{1}{\frac{1}{\infty} - \imath\frac{\lambda}{\pi w_0^2}} + z = \imath\frac{\pi w_0^2}{\lambda} + z \ , \tag{7.262}$$

The separation of this result into a real part and an imaginary part gives,

$$\frac{z}{R} + \frac{w_0^2}{w^2} = 1 \qquad \text{and} \qquad \frac{\pi w^2}{\lambda R} = \frac{\lambda z}{\pi w_0^2} \ . \tag{7.263}$$

Solving the second equation for $1/R$ and replacing this in the first equation gives an equation for w,

$$\boxed{w^2 = w_0^2\left[1 + \left(\frac{\lambda z}{\pi w_0^2}\right)^2\right]} \ . \tag{7.264}$$

This expression can now be replaced in the second equation,

$$\boxed{R = z\left[1 + \left(\frac{\pi w_0^2}{\lambda z}\right)^2\right]} \ . \tag{7.265}$$

We call $z_R \equiv q_0$ the *Rayleigh length*. Now we integrate φ',

$$\begin{aligned}\varphi = \int_0^z \frac{-\imath}{q}dz = \int_0^z \frac{-\imath dz}{\imath z_R + z} &= -\imath\int_0^z \frac{z dz}{z_R^2 + z^2} - \int_0^z \frac{z_R dz}{z_R^2 + z^2} \\ &= -\frac{\imath}{2}\ln\frac{z_R^2 + z^2}{z_R^2} - \arctan\frac{z}{z_R} = -\imath\ln\frac{w}{w_0} - \arctan\frac{\lambda z}{\pi w_0^2} \ .\end{aligned} \tag{7.266}$$

Hence,

$$\boxed{\psi(\mathbf{r}) = \frac{w_0}{w} e^{\imath \arctan(-z/q_0) - \imath k(x^2+y^2)/2q}} \ . \tag{7.267}$$

We note that the function $|\psi|^2$ is normalized by the radial integral,

$$\begin{aligned} \int |\psi|^2 dxdy &= \frac{w_0^2}{w^2} \int |e^{-k(x^2+y^2)/2q(z)}|^2 dxdy \\ &= \frac{w^2}{w_0^2} \left(\int_{-\infty}^{\infty} e^{-2x^2/w^2} dx \right)^2 = \frac{\pi w_0^2}{2} \ , \end{aligned} \tag{7.268}$$

which is independent of z and thus ensures conservation of energy along the beam. The intensity profile of a Gaussian beam is proportional to $|\psi|^2$ and normalized to the total power P, that is,

$$\boxed{I(\mathbf{r}) = \frac{2P}{\pi w_0^2} |\psi(\mathbf{r})|^2 = \frac{2P}{\pi w(z)^2} e^{-2(x^2+y^2)/w(z)^2}} \ . \tag{7.269}$$

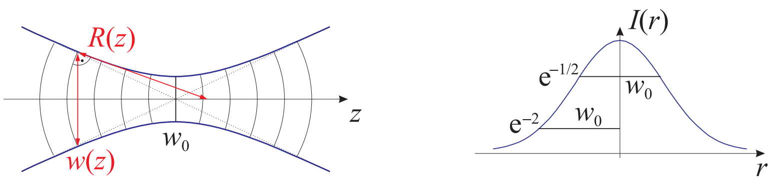

Figure 7.27: (Left) Propagation of the beam along the optical axis. (Right) Cross section of the Gaussian beam.

The above treatment shows that modes do not only exist in cavities but also in free space. In Excs. 7.4.4.1 and 7.4.4.2 we are dealing with modes of Gaussian light beams that are often used in laser beam optics.

Example 82 (*Gaussian optics*): The expansion of the Gaussian beam $\mathcal{E}(\mathbf{r}) = \mathcal{E}_0 e^{-(x^2+y^2)/w(z)^2 - z^2/z_R^2}$ into plane waves simply is,

$$\mathcal{E}(\mathbf{k}) = \int \mathcal{E}(\mathbf{r}) e^{\imath \mathbf{k}\cdot\mathbf{r}} d^3r = \mathcal{E}_0 e^{-(k_x^2+k_y^2)w(z)^2 - k_z^2 z_R^2} \ .$$

7.4.1.1 Optical components

In *geometrical optics* (or ray optics) we work a lot with *transfer matrices* $\mathcal{M}$ defined by their feature of transforming the two-component vector, which consists of the distance of a ray from the optical axis $y(z)$ and its divergence $y'(z)$ [29]:

$$\begin{pmatrix} y(z) \\ y'(z) \end{pmatrix} = \mathcal{M} \begin{pmatrix} y(0) \\ y'(0) \end{pmatrix} \ . \tag{7.270}$$

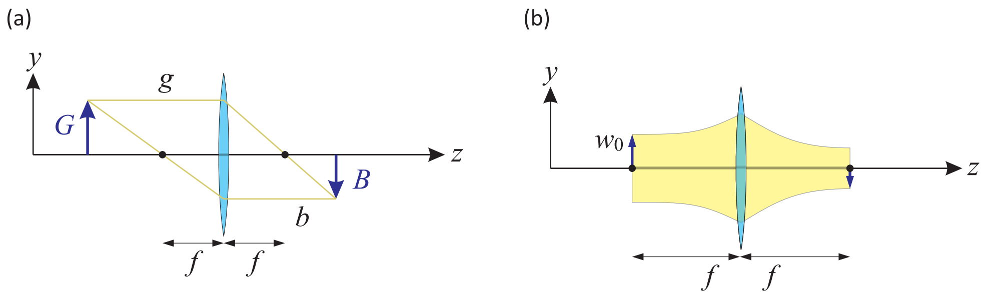

Figure 7.28: (a) Image formation through a lens with ray optics. (b) Focusing a laser beam with Gaussian optics.

Now, it is possible to show that the same matrix $\mathcal{M}$ can describe the transformation of a Gaussian beam through optical components along the optical axis, provided that we apply the transformation to the beam parameter q in the following way:

$$\boxed{q(z) = \frac{M_{11}q(0) + M_{12}}{M_{21}q(0) + M_{22}}} . \tag{7.271}$$

Hence, the transfer matrices allow us to calculate, how the parameters R and w transform along the optical axis through optical elements or in free propagation. The most common optical elements are lenses, crystals, prisms, mirrors, and cavities. For example, the matrix for free propagation of a beam over a distance d is,

$$\mathcal{M}_{dist} = \begin{pmatrix} 1 & d \\ 0 & 1 \end{pmatrix} , \tag{7.272}$$

and the matrix describing the passage through a thin lens with focal length f,

$$\mathcal{M}_{lens} = \begin{pmatrix} 1 & 0 \\ -1/f & 1 \end{pmatrix} . \tag{7.273}$$

In Exc. 7.4.4.3 we use these matrices to derive the lens equations in ray optics and Gaussian optics.

7.4.1.2 Modes of a linear cavity

We will now apply the formalism of the transfer matrices to calculate the modal structure of a linear cavity. Let $\mathcal{M}$ be the matrix describing the round-trip of a beam of light in the cavity. For the cavity to be stable, the fields must be stationary. This is only possible if the mode geometry is self-consistent. That is, at any position z, the beam parameter $q(z) = q_z$ must satisfy [49],

$$q_z = \frac{M_{11}q_z + M_{12}}{M_{21}q_z + M_{22}} . \tag{7.274}$$

[29]Note that these matrices have nothing to do with the matrices describing the transmission and reflection of electric and magnetic fields by interfaces.

Using, $M_{11}M_{22} - M_{12}M_{21} = 1$, the condition (7.274) can be solved by,

$$\frac{1}{q_z} = \frac{M_{22} - M_{11}}{2M_{12}} \pm \frac{\imath}{2M_{12}}\sqrt{4 - (M_{11} + M_{22})^2} \ , \tag{7.275}$$

or separating the real part from the imaginary part according to the definition (7.260) of the beam parameter,

$$w_z^2 = \frac{2\lambda M_{12}}{\pi\sqrt{4 - (M_{11} + M_{22})^2}} \quad \text{and} \quad R_z = \frac{2M_{12}}{M_{22} - M_{11}} \ . \tag{7.276}$$

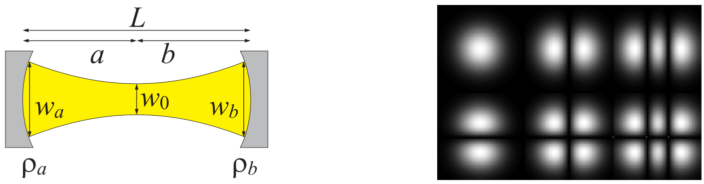

Figure 7.29: (code) (Left) Scheme of a linear cavity. (Right) Radial profiles of the lowest order transverse Hermite-Gaussian modes TEM_{mn} of a linear cavity.

We now consider the cavity of length L schematized in Fig. 7.29. It consists of two mirrors with radii of curvature ρ_a and ρ_b. The transfer matrix for a round-trip beginning and ending at the position of mirror 'a' is,

$$\mathcal{M} = \begin{pmatrix} 1 & 0 \\ -1/f_a & 1 \end{pmatrix}\begin{pmatrix} 1 & L \\ 0 & 1 \end{pmatrix}\begin{pmatrix} 1 & 0 \\ -1/f_b & 1 \end{pmatrix}\begin{pmatrix} 1 & L \\ 0 & 1 \end{pmatrix} \tag{7.277}$$
$$= \frac{1}{f_a f_b}\begin{pmatrix} f_a(f_b - L) & f_a L(2f_b - L) \\ L - f_b - f_a & L(L - 2f_b) + f_a(f_b - L) \end{pmatrix} ,$$

where $f_k = -\rho_k/2$ are the focal lengths of the mirrors. With (7.276) we obtain the diameter w_a and the radius of curvature R_a of the beam at the position of the mirror 'a',

$$w_a^2 = \frac{2\lambda f_a L(2f_b - L)}{\pi\sqrt{4f_a^2 f_b^2 - (L^2 - 2f_a L - 2f_b L + 2f_a f_b)^2}} \quad \text{and} \quad R_a = -2f_a \ . \tag{7.278}$$

Applying the second equation (7.263), we find,

$$\frac{\lambda a}{\pi w_0^2} = \frac{\pi w_a^2}{\lambda R_a} = \frac{L(2f_b - L)}{\sqrt{4f_a^2 f_b^2 - (L^2 - 2f_a L - 2f_b L + 2f_a f_b)^2}} \ , \tag{7.279}$$

and analogously for $\lambda b/\pi w_0^2$. We replace $f_k = \rho_k/2$ and introduce the abbreviation,

$$x_a \equiv \frac{\pi w_a^2}{\lambda R_a} = \frac{\frac{2L}{\rho_a}\left(1 - \frac{L}{\rho_b}\right)}{\sqrt{1 - \left(1 - \frac{2L}{\rho_a} - \frac{2L}{\rho_b} + \frac{2L^2}{\rho_a\rho_b}\right)^2}} \ , \tag{7.280}$$

and analogously for x_b. With the help of MAPLE we calculate,

$$\frac{x_a x_b - 1}{\sqrt{(1+x_a^2)(1+x_b^2)}} = \sqrt{1-\frac{L}{\rho_a}}\sqrt{1-\frac{L}{\rho_b}} \ . \tag{7.281}$$

The phase shift between the waist of the beam and mirror 'a' is given by the real part of the formula (7.266). The phase shift accumulated between the mirrors 'a' and 'b' is,

$$\begin{aligned} \varphi &= \varphi_a + \varphi_b = \arctan x_a + \arctan x_b \\ &= \pi - \arccos\frac{x_a x_b - 1}{\sqrt{1+x_a^2}\sqrt{1+x_b^2}} = \pi - \arccos\sqrt{1-\frac{L}{\rho_a}}\sqrt{1-\frac{L}{\rho_b}} \ , \end{aligned} \tag{7.282}$$

where we used tabulated trigonometric relationships to convert the arctan into a arccos.

The spectrum of transverse modes follows from the condition, that the total phase is a multiple of π, i.e.,

$$N = \frac{kL+\varphi}{\pi} = \frac{2L\nu}{c} + \frac{\varphi}{\pi} \ , \tag{7.283}$$

that is,

$$\boxed{\frac{\nu}{\delta_{fsr}} = N - 1 + \frac{1}{\pi}\arccos\sqrt{\left(1-\frac{L}{\rho_a}\right)\left(1-\frac{L}{\rho_b}\right)}} \ , \tag{7.284}$$

where we used the *free spectral range* $\delta_{fsr} \equiv c/2L$. This formula represents a generalization of the previously derived formula (7.249), which only holds in the limit of plane waves, $\rho_k \rightarrow \infty$.

The diameter of the beam waist in the cavity is,

$$w_0 = \sqrt[4]{\left(\frac{\lambda}{\pi}\right)^2 \frac{L(\rho_a-L)(\rho_b-L)(\rho_a+\rho_b-L)}{(\rho_a+\rho_b-2L)^2}} \ . \tag{7.285}$$

For optimum coupling, the geometries of the Gaussian light beam and of the cavity must be matched, i.e. the diameter and divergence of the laser beam must be adjusted to the cavity mode, e.g. using a suitable arrangement of lenses. In Exc. 7.4.4.4, we will extend the calculation to ring cavities.

7.4.1.3 Hermite-Gaussian transverse modes

We can generalize the ansatz (7.256) to allow for more complicated radial intensity distributions described by the functions g and h,

$$\psi = g\left(\frac{x}{w}\right) h\left(\frac{y}{w}\right) e^{-\imath\left[\varphi(z)+k(x^2+y^2)/2q(z)\right]} \ . \tag{7.286}$$

Inserting the ansatz into the equation (7.255), we will show in Exc. 7.4.4.5, that the solution is given by,

$$\psi(x,y,z) = \frac{w_0}{w} H_m\left(\frac{\sqrt{2}x}{w}\right) H_n\left(\frac{\sqrt{2}y}{w}\right) e^{\imath(m+n+1)\arctan\frac{2z}{kw_0^2} - r^2\left(\frac{1}{w^2}+\frac{\imath k}{2R}\right)} \ . \tag{7.287}$$

Fig. 7.29(right) shows radial profiles of the lowest order transverse Hermite-Gaussian modes TEM_{mn} of a linear cavity.

In the presence of higher-order transverse modes TEM_{mn} the cavity spectrum becomes,

$$\boxed{\frac{\nu}{\delta_{fsr}} = N - 1 + \frac{m+n+1}{\pi}\arccos\sqrt{\left(1-\frac{L}{\rho_a}\right)\left(1-\frac{L}{\rho_b}\right)}} \ . \tag{7.288}$$

This formula can be derived using the self-consistency requirement for the light beam circulating inside the cavity. It represents yet another generalization of the formula (7.249) and lifts the degeneracy of the longitudinal modes described by the Airy formula and exhibited in Fig. 7.26. On the other hand, a *confocal cavity* with degenerate transverse modes, $\rho_a = \rho_b = L$, is particularly suited to work as a spectrum analyzer.

7.4.1.4 Splitting of TEM_{mn} modes having the same $m + n$

In a cylindrically symmetric mode, all modes TEM_{mn} with the same $m+n$ are degenerate. If however cylindrical symmetry is broken, e.g. due to alignment imperfection or in the case of a ring cavity, the degeneracy is lifted [86]. If the problem of tilted incidence of the beams onto a mirror surface can be boiled down to assuming elliptically shaped mirrors, i.e. mirrors having different radii of curvatures in two orthogonal axis, the different phase shifts for the two axis can be calculated, as discussed in Exc. 7.4.4.4 and in Ref. [32]:

$$\nu/\delta_{fsr} = (q+1) + 2\frac{2m+1}{2\pi}\phi_h + 2\frac{2n+1}{2\pi}\phi_v \ . \tag{7.289}$$

where $\phi_k = \arccos\sqrt{\left(1-\frac{2a}{\rho_k}\right)\left(1-\frac{b}{\rho_k}\right)}$ for $k = h, v$. The splitting between the TEM_{01} and TEM_{10} modes is,

$$\tfrac{2}{\pi}\arccos\sqrt{\left(1-\tfrac{2a}{\rho_h}\right)\left(1-\tfrac{b}{\rho_h}\right)} - \tfrac{2}{\pi}\arccos\sqrt{\left(1-\tfrac{2a}{\rho_v}\right)\left(1-\tfrac{b}{\rho_v}\right)} \ . \tag{7.290}$$

The splitting observed for ring cavities is on the same order as the free spectra range.

Furthermore, different phase shifts in the dielectric surfaces lead to different resonance conditions [54]. Since, according to Fresnel's formulas, s and p-polarized light fields have different reflectivities under inclined incidence on mirrors, they also suffer different phase shifts and, hence, exhibit different eigenfrequencies of the cavity. In high-finesse ring cavities this leads to a dramatic splitting of s and p-polarized modes, which can be on the order of the free spectral range itself.

7.4.2 Non-Gaussian beams

The Hermite-Gaussian ansatz (7.286) to solve the wave equation represents only one possibility. But we nowadays know a large variety of beams with different transverse distributions of intensity, polarization and angular momentum. Examples are transverse Gaussian modes with Cartesian or circular symmetry, Bessel modes, Laguerre-Gaussian modes with angular momentum, and modes with radial or azimuthal polarization.

7.4.2.1 Bessel beams

Ideally, a *Bessel beam* (BB) is a non-diffracting monochromatic solution to the scalar wave equation in cylindrical coordinates carrying an infinite amount of energy [31, 62]. Inserting into the wave equation,

$$\left(\frac{1}{c^2}\frac{\partial^2}{\partial t^2} - \nabla^2\right)\psi(\mathbf{r},t) = 0 \tag{7.291}$$

the ansatz,

$$\psi(\mathbf{r},t) = e^{\imath(\beta z-\omega t)}\int_0^{2\pi} A(\phi)e^{\imath\alpha(x\cos\phi+y\sin\phi)}d\phi \ , \tag{7.292}$$

we get the dispersion relation,

$$\alpha^2+\beta^2 = \frac{\omega^2}{c^2} \ . \tag{7.293}$$

For β real the intensity profile does not vary along the z-axis,

$$|\psi(\mathbf{r},t)|^2 = \left|\int_0^{2\pi} A(\phi)e^{\imath\alpha(x\cos\phi+y\sin\phi)}d\phi\right|^2 = |\psi(x,y,z=0,t)|^2 \ . \tag{7.294}$$

For axial symmetry $A(\phi) = A$, we get what is called the 2^{st} type 0-order Bessel beam,

$$\psi(\mathbf{r},t) = Ae^{\imath(\beta z-\omega t)}\int_0^{2\pi} e^{\imath\alpha(x\cos\phi+y\sin\phi)}d\phi = Ae^{\imath(\beta z-\omega t)}J_0(\alpha\rho) \ . \tag{7.295}$$

For $0 < \alpha \leq \omega/c$ we get a non-trivial solution decaying like $(\alpha\rho)^{-1}$.

In its simplest form, the electric field of an arbitrary ν-th order BB with wavelength λ can be written as,

$$\mathcal{E}(\rho,\phi,z) = A_0\exp(\imath k_z z)J_\nu(k_\rho\rho)\exp(\imath\nu\phi) \ , \tag{7.296}$$

where A_0 is the electric field strength and J_ν is the ν-th order Bessel function of the first kind. In Eq. (7.296), k_z and k_ρ are the longitudinal and transverse wave numbers satisfying the dispersion relation $k^2 = k_z^2 + k_\rho^2 = (2\pi/\lambda)^2$, such that $k_z = k\cos\theta$ and $k_\rho = k\sin\theta$, being θ the axicon angle associated to the tilted plane of waves propagating along the surface of a cone of half-angle θ in the angular spectrum decomposition. Cylindrical coordinates (ρ,ϕ,z) have been adopted, and a time harmonic factor $e^{\imath\omega t}$ has been omitted for brevity. For our purposes, the Rayleigh range is an essential parameter to be considered since the non-diffracting beam must propagate through a 20 cm long differential vacuum tube to minimize losses of atoms during their guidance to the science chamber. The maximum propagation distance up to which a BB can overcome diffraction is given by $Z_{max} = 2\pi R\bar{r}/\lambda$, where R is the aperture radius and $\bar{r}$ is the beam radius [31]. It should be noticed that, in general, Z_{max} is much greater than the Rayleigh range of a Gaussian beam with an equivalent beam waist radius $w_g = \bar{r}$.

Example 83 (*Frozen Bessel beams*): Certain superposition of these non-diffracting Bessel beams have interesting properties,

$$\psi(\mathbf{r},t) = e^{-\imath\omega t}\sum_{n=-N}^{N} A_n J_0(k_{\rho n}\rho)e^{\imath\beta_n z} \ . \tag{7.297}$$

A *frozen Bessel beam* can be constructed by a continuous superposition of 0^{th}-order scalar BBs over the longitudinal wavenumber k_z, as given by the following integral solution of the scalar Helmholtz equation with azimuthal symmetry,

$$\Psi_0(\rho,z,t) = e^{-\imath\omega t}\int_{-k}^{k} S(k_z)J_0(\rho\sqrt{k^2-k_z^2})e^{-\imath k_z z}dk_z \ , \tag{7.298}$$

where $k\equiv\omega/c$ and $k_\rho^2\equiv\omega^2/c^2-k_z$ is the transverse wave number. The quantity k_ρ^2 must be positive since evanescent waves do come into play.
Higher-order Bessel beams can be constructed via [101, 100],

$$\Psi_1(\rho,\phi,z) = \mathcal{U}\Psi_0(\rho,z) \qquad \text{with} \qquad \mathcal{U}\equiv e^{\imath\phi}\left(\frac{\partial}{\partial\rho}+\frac{\imath}{\rho}\frac{\partial}{\partial\phi}\right) \ , \tag{7.299}$$

Apparently, they can carry angular orbital momentum.

7.4.3 Fourier optics

In the following sections we will derive from the general Huygens principle an expression describing the propagation of phase fronts. We will also show how it can be used for numerical calculations of phase front propagation.

7.4.3.1 Rayleigh-Sommerfeld solution

We consider the propagation of monochromatic light from a 2D planar source of area Σ indicated by the coordinates ξ and η, as illustrated in Fig. 7.30. The field distribution in the source plane is given by $\psi_0(\xi,\eta)$, and the field $\psi_z(x,y)$ in a distant observation plane can be predicted using the first Rayleigh-Sommerfeld diffraction solution [39, 95],

$$\boxed{\psi_z(x,y) = \frac{1}{\imath\lambda}\iint_\Sigma \frac{z}{r_{12}}\frac{e^{\imath kr_{12}}}{r_{12}}\psi_0(\xi,\eta)d\xi d\eta} \ . \tag{7.300}$$

The formula will be derived from the wave equation in Exc. 7.4.4.6. Here, z is the distance between the centers of the source and observation coordinate systems and

$$r_{12} = \sqrt{z^2+(x-\xi)^2+(y-\eta)^2} \tag{7.301}$$

is the distance between a position on the source plane and a position in the observation plane, with the planes assumed to be parallel.

Expression (7.300) is a statement of the *Huygens-Fresnel principle*, which supposes that the source acts as an infinite collection of fictitious point sources located at (ξ,η), each one producing a spherical wave. The interference of the spherical waves at any observation position (x,y), expressed by the projection onto the propagation axis z in (7.300), can be written as a two-dimensional convolution integral,

$$\psi_z(x,y) = \iint_\Sigma h_z(x-\xi,y-\eta)\psi_0(\xi,\eta)d\xi d\eta = (h_z*\psi_0)(x,y) \ , \tag{7.302}$$

where the general form of the *Rayleigh-Sommerfeld impulse response*,

$$h_z(x,y) = \frac{z}{\imath\lambda}\frac{e^{\imath kr}}{r^2} \ , \tag{7.303}$$

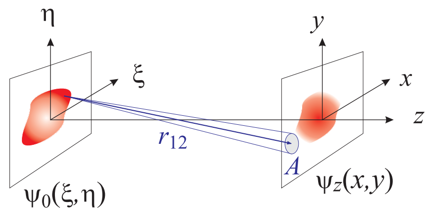

Figure 7.30: Propagation geometry for parallel source and observation planes. Every point of the source plane generates a spherical wave $\propto e^{\imath k r_{12}}/r_{12}$. The projection of the field within a solid angle element onto the xy-plane, which is proportional to z/r_{12} generates a new spherical wave propagating further along the z optical axis.

where $r = \sqrt{z^2 + x^2 + y^2}$ is simply the field distribution $\psi_z(x, y)$ observed in case of a point-like source $\psi_0(\xi, \eta) = \delta(\xi)\delta(\eta)$.

The Fourier convolution theorem allows to write Eq. (7.302) as,

$$\psi_z(x, y) = \mathcal{F}^{-1}\{\mathcal{F}[h_z * \psi_0](x, y)\} = \mathcal{F}^{-1}\{\mathcal{F}[h_z(x, y)]\mathcal{F}[\psi_0(x, y)]\} \; , \tag{7.304}$$

where $\mathcal{F}$ denotes the two-dimensional Fourier transform. Introducing the *Rayleigh-Sommerfeld transfer function* H_z, we may also write,

$$\boxed{\begin{aligned} \psi_z(x, y) &= \mathcal{F}^{-1}\{H_z(f_x, f_y) \cdot \mathcal{F}[\psi_0(x, y)]\} \\ \text{where} \quad H_z(f_x, f_y) &= e^{\imath k z \sqrt{1-(\lambda f_x)^2-(\lambda f_y)^2}} \end{aligned}} \; . \tag{7.305}$$

Strictly speaking, $\sqrt{f_x^2 + f_y^2} < \lambda^{-1}$ must be satisfied for propagating field components. The Rayleigh-Sommerfeld expression is the most accurate diffraction solution as, other than the assumption of scalar diffraction, this solution only requires that $r \gg \lambda$, the distance between the source and the observation position, be much greater than a wavelength.

7.4.3.2 Fresnel approximation

Let us simplify the transfer function by expanding the distance (7.301),

$$r_{12} \simeq z + \tfrac{1}{2}\tfrac{(x-\xi)^2}{z} + \tfrac{1}{2}\tfrac{(y-\eta)^2}{z} \; , \tag{7.306}$$

which amounts to assuming a parabolic radiation wave rather than a spherical wave for the fictitious point sources. Furthermore, we use the approximation $r_{12} \simeq z$ in the denominator of Eq. (7.300) to arrive at the Fresnel diffraction expression:

$$\boxed{\psi_z(x, y) = \frac{e^{\imath k z}}{\imath \lambda z} \iint_\Sigma e^{\imath k[(x-\xi)^2+(y-\eta)^2]/2z} \psi_0(\xi, \eta) d\xi d\eta} \; . \tag{7.307}$$

This expression is also a convolution of the form in Eq. (7.302), where the impulse response is,

$$h_z(x, y) = \frac{e^{\imath k z}}{\imath \lambda z} e^{\imath k \rho^2/2z} \; , \tag{7.308}$$

and the transfer function is,

$$H_z(f_x, f_y) = e^{\imath kz} e^{-\imath \pi z \lambda (f_x^2 + f_y^2)} \ . \tag{7.309}$$

The expressions in Eqs. (7.305) are again applicable in this case for computing diffraction results.

Another useful form of the Fresnel diffraction expression is obtained by moving the quadratic phase term in x and y outside the integrals:

$$\psi_z(x, y) = \frac{e^{\imath kz}}{\imath \lambda z} e^{\imath k(x^2+y^2)/2z} \iint_{\Sigma} e^{\imath k(\xi^2+\eta^2)/2z} e^{-\imath k(x\xi + y\eta)/z} \psi_0(\xi, \eta) d\xi d\eta \ . \tag{7.310}$$

7.4.3.3 Fraunhofer approximation

Fraunhofer diffraction, which refers to diffraction patterns in a regime that is commonly known as the 'far field', is arrived at by approximating the chirp term multiplying the initial field within the integrals of Eq. (7.310) as unity. The assumption involved is,

$$z \gg \max[\tfrac{k}{2}(\xi^2 + \eta^2)] \tag{7.311}$$

and results in the Fraunhofer diffraction expression:

$$\boxed{\begin{aligned} \psi_z(x, y) &= \frac{e^{\imath kz}}{\imath \lambda z} e^{\imath k\rho^2/2z} \iint_{\Sigma} e^{-\imath k(x\xi + y\eta)/z} \psi_0(\xi, \eta) d\xi d\eta \\ &= \frac{e^{\imath kz}}{\imath \lambda z} e^{\imath \frac{k}{2z}\rho^2} (\mathcal{F}\psi_0)(\tfrac{kx}{z}, \tfrac{ky}{z}) \end{aligned}} \ . \tag{7.312}$$

Along with multiplicative factors out front, the Fraunhofer expression can be recognized simply as a Fourier transform of the source field. The condition of Eq. (7.311), typically, requires very long propagation distances relative to the source support size. However, a form of the Fraunhofer pattern also appears in the propagation analysis involving lenses. The Fraunhofer diffraction expression is a powerful tool and finds use in many applications such as laser beam propagation, image analysis, and spectroscopy.

The Fraunhofer expression cannot be written as a convolution integral, so there is no impulse response or transfer function. But, since it is a scaled version of the Fourier transform of the initial field, it can be relatively easy to calculate, and as with the Fresnel expression, the Fraunhofer approximation is often used with success in situations where Eq. (7.311) is not satisfied. For simple source structures such as a plane-wave illuminated aperture, the Fraunhofer result can be useful even when Eq. (7.311) is violated by more than a factor of 10, particularly if the main quantity of interest is the irradiance pattern at the receiving plane. Using the *Fresnel number* defined as,

$$N_F = \frac{\max(\xi^2 + \eta^2)}{z\lambda} \ , \tag{7.313}$$

the commonly accepted requirement for the Fraunhofer region is $N_F \ll 1$.

7.4.3.4 Propagation of phase fronts across optical elements

To propagate an optical phase front located at z_0, we conveniently start from a Gaussian laser beam,

$$\psi_{Gauss}(\rho) = e^{-\rho^2/w_0^2} \; . \tag{7.314}$$

with $\rho = \sqrt{x^2+y^2}$ the distance from the optical axis. For a given total power the electric field is obtained via normalization,

$$\mathcal{E}_0 = \sqrt{\frac{P}{\frac{1}{2}\varepsilon_0 c \int |u|^2 d^2\rho}} \; , \tag{7.315}$$

where $\eta \equiv \sqrt{\mu_0/\varepsilon_0} = 1/(\varepsilon_0 c)$ is the vacuum impedance.

Optical elements can shape the phase front of a light beam by phase shift or absorption. If the element can be assumed to be thin we may neglect the axial displacement, $\Delta z \simeq 0$, and simply multiply the phase front with an xy-matrix,

$$\boxed{\psi'_z(x,y) = e^{-\alpha_{component}(x,y)}\psi_z(x,y)} \; , \tag{7.316}$$

where $\alpha(x,y) = \sigma(x,y) + \imath\delta(x,y)$. For instance, a *pinhole* with radius R will transform a phase front like,

$$\alpha_{pinhole}(\rho) = \infty\Theta(\rho - R) \; , \tag{7.317}$$

where Θ is the Heavyside function. A *thin lens* with focal distance f will transform a phase front like,

$$\alpha_{lens}(\rho) = \imath\tfrac{k}{R}\rho^2 = \imath\tfrac{k}{2f}\rho^2 \; , \tag{7.318}$$

where R is the radius of the spherical lens. For an *axicon* of base angle α made of material with refractive index n_{refr},

$$\alpha_{axicon}(\rho) = \imath k(n_{refr} - 1)\rho\tan\alpha \; . \tag{7.319}$$

In Exc. 7.4.4.9 we will derive the phase front transformation matrices for other interesting optical components. We will do a numerical simulation in 7.4.4.10.

7.4.4 Exercises

7.4.4.1 Ex: Gaussian light mode

The light of a laser propagates in light modes called Gaussian. A beam propagating along $\hat{\mathbf{e}}_z$ and linearly polarized along $\hat{\mathbf{e}}_x$ is described by the potential vector, $\mathbf{A}(\mathbf{r},t) = \hat{\mathbf{e}}_x u(\mathbf{r}) e^{\imath(\omega t - kz)}$, where $u(\mathbf{r}) = \frac{u_0}{w(z)} e^{-(x^2+y^2)/w(z)^2}$ is the energy density and $w(z) = w_0\sqrt{1 + (\lambda z/\pi w_0^2)^2}$ the diameter of the beam at the position z. Calculate the Poynting vector in the Lorentz gauge, $\Phi = -\frac{c^2}{\imath\omega}\nabla\cdot\mathbf{A}$.

7.4.4.2 Ex: Volume and power of a Gaussian beam mode

a. Derive the expression for the mode volume V_m of a Gaussian beam of length L from the definition $I(0)V_m = \int I(\mathbf{r})dV$.

b. In quantum mechanics we learn, that the zero point energy of the harmonic oscillator is $\hbar\omega/2$. Use this notion to calculate the maximum electric field amplitude $\mathcal{E}_1(0)$ created by a single photon in terms of the mode volume.
c. A linear cavity of length L has the free spectral range $\delta_{fsr} = c/2L$. Express the power of the beam in terms of the number of photons contained in the cavity.

7.4.4.3 Ex: The lens in ray and wave optics

a. Use the transfer matrices (7.272) and (7.273) to derive the lens equations of geometric optics from the relation (7.270).
b. Now, use the transfer matrices (7.272) and (7.273) to derive, from the relation (7.270), the transformation of a Gaussian beam. How do the waists behave upon transformation?
c. You have a laser of $\lambda = 632\,\text{nm}$ wavelength producing a Gaussian beam of diameter $w_1 = 1\,\text{mm}$ in its waist. Now, you want to match the beam into a cavity, whose mode (defined by the radii of curvature of the mirrors) has a waist of diameter $w_2 = 100\,\mu\text{m}$. To do this, you have at your disposal a lens of $f = 500\,\text{mm}$ focal distance. Using the formulas derived in (b), determine, how the distances d_1 (between the location of the waist of the laser beam and the lens) and d_2 (between the lens and the location of the waist of the cavity) must be chosen.

7.4.4.4 Ex: Transverse modes of a ring cavity

In this exercise we consider a ring cavity made of a plane input coupler and two identical curved high-reflectors (radius of curvature $\rho = 2f$) forming an isosceles triangle. Let $a = L/(2+\sqrt{2})$ be the two short distances and $b = L/(1+\sqrt{2})$ the long one, so that $L = 2a + b$.
a. How many waists does the cavity modes have, and where are they located?
b. Derive the round-trip matrix starting from the location of any one of the waists.
c. Calculate the waists.
d. Calculate the transverse mode spectrum, and prepare a plot for $\rho = 30\,\text{cm}$ and $L = 8.7\,\text{cm}$.
e. The above results presume cylindrical symmetry. However, incidence on curved mirrors under a tilted angle θ produces astigmatism. This can be accounted for by assuming different radii of curvature for the horizontal and vertical axis:

$$R_h = R\cos\theta \qquad \text{and} \qquad R_v = R/\cos\theta \;. \tag{7.320}$$

Calculate the impact waist sizes in the horizontal and vertical axis.

7.4.4.5 Ex: Transverse Hermite-Gauss modes

Derive the spectrum of Hermite-Gauss transverse modes.

7.4.4.6 Ex: Derivation of the Rayleigh-Sommerfeld formula

Derive the Rayleigh-Sommerfeld formula (7.300).

7.4.4.7 Ex: Phasefront distorsion by an axicon and a thin lens

Calculate the phasefront distortion suffered by a plane wave upon traversing (a) an axicon with base angle α and (b) a thin lens with focal length f.

7.4.4.8 Ex: Transmission through a pinhole

Calculate the light field distribution after a circular pinhole of radius a.

7.4.4.9 Ex: Transmission through a various optical components

Calculate the phase front transformation matrix
a. for a Fresnel zone plate
b. for a Laguerre-Gauss zone plate.

7.4.4.10 Ex: Numerical phasefront propagation

Numerical phasefront propagation through a thin lens.

7.5 Further reading

7.5.1 on optics

H. Kogelnik et al., *Laser Beams and Resonators* [DOI]

D.G. Voelz, *Computational Fourier Optics: a MATLAB tutorial* [ISBN]

P.R. Berman, *Optical Faraday rotation* [DOI]

G. Labeyrie et al., *Large Faraday rotation of resonant light in a cold atomic cloud* [DOI]

W.J. Wild et al., *Goos-Haenchen shifts from absorbing media* [DOI]

7.5.2 on metamaterials

J. Sinova et al., *Spin Hall effects* [DOI]

J.B. Pendry, *Negative refraction makes a perfect lens* [DOI]

J.B. Pendry, *A chiral route to negative refraction* [DOI]

S.M. Rytov, *Electromagnetic properties of a finely stratified medium* [DOI]

P. Szarek, *Electric permittivity in individual atomic and molecular systems through direct associations with electric dipole polarizability and chemical hardness* [DOI]

V.G. Veselago, *The electrodynamics of substances with simultaneously negative values of E and M* [DOI]

A. Poddubny et al., *Hyperbolic metamaterials* [DOI]

P. Shekhar et al., *Strong Coupling in Hyperbolic Metamaterials* [DOI]

H.N.S. Krishnamoorthy et al., *Topological transitions in metamaterials* [DOI]

Chapter 8

Radiation

In the previous sections we discussed the propagation of electromagnetic waves, but we do not say how these waves were produced in the first place. For now, we only know, that it need's accelerated charges or varying currents. Now, we will show how such 'sources' can emit energy by 'radiating' electromagnetic waves.

To begin with, let us consider sources located near the origin and confined within a sphere of radius r. The total power crossing the sphere's surface is the integral of the Poynting vector,

$$P(r) = \oint \vec{\mathcal{S}} \cdot d\mathbf{a} = \tfrac{1}{\mu_0} \oint (\vec{\mathcal{E}} \times \vec{\mathcal{B}}) \cdot d\mathbf{a} \ . \tag{8.1}$$

The radiated power is then the energy per unit area transported to infinity without ever returning,

$$P_{rad} = \lim_{r\to\infty} P(r) \ . \tag{8.2}$$

Now, the area of the sphere's surface is $4\pi r^2$ such that, in order to have non-vanishing radiation, the Poynting vector must decrease (for large r) no faster than as $1/r^2$. Following the Coulomb law, electrostatic fields decrease like $1/r^2$ or faster, when the total enclosed charge is zero. And Biot-Savart's law states that magnetostatic fields decrease at least as fast as $1/r^2$, such that $|\vec{\mathcal{S}}| \propto 1/r^4$, for static configurations. Hence, static sources do not radiate. On the other hand, Jefimenko's equations (6.109) and (6.112) indicate the existence of time-dependent terms (involving $\dot{\varrho}$ and $\dot{\mathbf{j}}$), which are proportional to $1/r$. These are the terms responsible for electromagnetic radiation. To study the radiation we choose the parts of $\vec{\mathcal{E}}$ and $\vec{\mathcal{B}}$ going as $1/r$ at large distances from the source, combine them to terms going as $1/r^2$ in the Poynting vector $\vec{\mathcal{S}}$, and integrate $\vec{\mathcal{S}}$ on a large spherical surface taking the limit $r \to \infty$.

8.1 Multipolar expansion of the radiation

8.1.1 The radiation of an arbitrary charge distribution

In this section we will calculate the radiation emitted by arbitrary time-dependent variations of charge and current distributions, but which are confined within a small volume near the origin. The retarded scalar potential is according to (6.106),

$$\Phi(\mathbf{r}, t) = \frac{1}{4\pi\varepsilon_0} \int \frac{\varrho(\mathbf{r}', t - R/c)}{R} d^3r' \ , \tag{8.3}$$

where $R = \sqrt{r^2 + r'^2 - 2\mathbf{r}\cdot\mathbf{r}'}$, as illustrated in Fig. 6.10. Within the small source approximation, $r' \ll r$, we have,

$$R \simeq r\left(1 - \frac{\mathbf{r}\cdot\mathbf{r}'}{r^2}\right) \qquad \text{and} \qquad \frac{1}{R} \simeq \frac{1}{r}\left(1 + \frac{\mathbf{r}\cdot\mathbf{r}'}{r^2}\right) \;, \tag{8.4}$$

such that, defining,

$$t_0 \equiv t - \tfrac{r}{c} \;, \tag{8.5}$$

we obtain,

$$\varrho(\mathbf{r}', t - R/c) \simeq \varrho(\mathbf{r}', t - \tfrac{r}{c} + \tfrac{\hat{\mathbf{e}}_r\cdot\mathbf{r}'}{c}) \equiv \varrho(\mathbf{r}', t_0 + \tfrac{\hat{\mathbf{e}}_r\cdot\mathbf{r}'}{c}) \;. \tag{8.6}$$

Expanding ϱ in a Taylor series around the retarded time at the origin t_0, we get,

$$\varrho(\mathbf{r}', t - R/c) \simeq \varrho(\mathbf{r}', t_0) + \dot{\varrho}(\mathbf{r}', t_0)\tfrac{\hat{\mathbf{e}}_r\cdot\mathbf{r}'}{c} + \ldots \;. \tag{8.7}$$

Substituting the numerator and denominator in the formula (8.3) by the expansions (8.4) and (8.7) we get up to the first order,

$$\Phi(\mathbf{r}, t) = \frac{1}{4\pi\varepsilon_0 r}\left[\int \varrho(\mathbf{r}', t_0)d^3r' + \frac{\hat{\mathbf{e}}_r}{r}\cdot\int \mathbf{r}'\varrho(\mathbf{r}', t_0)d^3r' + \frac{\hat{\mathbf{e}}_r}{c}\cdot\frac{d}{dt}\int \mathbf{r}'\varrho(\mathbf{r}', t_0)d^3r'\right] \;. \tag{8.8}$$

The first integral is simply the charge [1], the other two represent the electric dipole at time t_0,

$$\Phi(\mathbf{r}, t) = \frac{1}{4\pi\varepsilon_0}\left[\frac{Q}{r} + \frac{\hat{\mathbf{e}}_r\cdot\mathbf{d}(t_0)}{r^2} + \frac{\hat{\mathbf{e}}_r\cdot\dot{\mathbf{d}}(t_0)}{cr}\right] \;. \tag{8.9}$$

In the static case, the first two terms are the contributions of the monopole and dipole to the multipolar expansion of Φ, the third term would not be present.

The vector potential,

$$\mathbf{A}(\mathbf{r}, t) = \frac{\mu_0}{4\pi}\int \frac{\mathbf{j}(\mathbf{r}', t - R/c)}{R}d^3r' \;, \tag{8.10}$$

is easily expanded up to first order by,

$$\mathbf{A}(\mathbf{r}, t) \simeq \frac{\mu_0}{4\pi r}\int \mathbf{j}(\mathbf{r}', t_0)d^3r' \;, \tag{8.11}$$

since, as we will show in Exc. 8.1.6.1,

$$\boxed{\mathbf{A}(\mathbf{r}, t) \simeq \frac{\mu_0}{4\pi}\frac{\dot{\mathbf{d}}(t_0)}{r}} \;, \tag{8.12}$$

that is, $\mathbf{d} \sim \mathbf{r}'$ is already of first order in $\mathbf{r}'$.

Now we must calculate the fields. Again, we are interested in the radiation zone (that is, in fields surviving great distances from the source), discarding all terms in $\vec{\mathcal{E}}$ and $\vec{\mathcal{B}}$ which decrease like $1/r^2$ or faster, which will not be the case for the first term

[1] The charge is evaluated at time t_0, but since it is conserved, it stays the same at all times.

(Coulomb) and the second term in (8.9). Therefore, considering the abbreviation (8.5), we obtain,

$$\nabla\Phi \simeq \frac{1}{4\pi\varepsilon_0}\nabla\frac{\hat{\mathbf{e}}_r\cdot\dot{\mathbf{d}}(t_0)}{rc} = \frac{1}{4\pi\varepsilon_0}\left[\cancelto{0}{\frac{\dot{\mathbf{d}}(t_0)}{cr^2}} + \frac{\hat{\mathbf{e}}_r\cdot\ddot{\mathbf{d}}(t_0)}{cr}\nabla t_0 - \cancelto{0}{\frac{2\hat{\mathbf{e}}_r\cdot\dot{\mathbf{d}}(t_0)}{cr^2}\hat{\mathbf{e}}_r}\right]$$
$$\simeq \frac{1}{4\pi\varepsilon_0}\frac{\hat{\mathbf{e}}_r\cdot\ddot{\mathbf{d}}(t_0)}{cr}\left(-\frac{\hat{\mathbf{e}}_r}{c}\right) . \tag{8.13}$$

Similarly,

$$\nabla\times\mathbf{A} = \nabla\times\frac{\mu_0}{4\pi}\frac{\dot{\mathbf{d}}(t_0)}{r} = \frac{\mu_0}{4\pi}\left[\frac{1}{r}\nabla\times\dot{\mathbf{d}}(t_0) + \left(\nabla\frac{1}{r}\right)\times\dot{\mathbf{d}}(t_0)\right] \tag{8.14}$$
$$= \frac{\mu_0}{4\pi}\left[-\frac{\ddot{\mathbf{d}}(t_0)}{r}\times\nabla t_0 - \cancelto{0}{\frac{\hat{\mathbf{e}}_r\times\dot{\mathbf{d}}(t_0)}{r^2}}\right] = -\frac{\mu_0}{4\pi}\frac{\ddot{\mathbf{d}}(t_0)}{r}\times\left(\frac{-\hat{\mathbf{e}}_r}{c}\right) = -\frac{\mu_0}{4\pi}\frac{\hat{\mathbf{e}}_r\times\ddot{\mathbf{d}}(t_0)}{cr} .$$

and,

$$\frac{\partial\mathbf{A}}{\partial t} \simeq \frac{\mu_0}{4\pi}\frac{\ddot{\mathbf{d}}(t_0)}{r} . \tag{8.15}$$

Hence, the Eqs. (6.78) tell us,

$$\vec{\mathcal{E}}(\mathbf{r},t) \simeq \frac{\mu_0}{4\pi r}[(\hat{\mathbf{e}}_r\cdot\ddot{\mathbf{d}}(t_0))\hat{\mathbf{e}}_r - \ddot{\mathbf{d}}(t_0)] = \frac{\mu_0}{4\pi r}[\hat{\mathbf{e}}_r\times(\hat{\mathbf{e}}_r\times\ddot{\mathbf{d}}(t_0)] \tag{8.16}$$
$$\vec{\mathcal{B}}(\mathbf{r},t) \simeq -\frac{\mu_0}{4\pi cr}[\hat{\mathbf{e}}_r\times\ddot{\mathbf{d}}(t_0)] .$$

In spherical coordinates,

$$\vec{\mathcal{E}}(r,\theta,\phi,t) \simeq \frac{\mu_0\ddot{d}(t_0)}{4\pi}\frac{\sin\theta}{r}\hat{\mathbf{e}}_\theta \quad\text{and}\quad \vec{\mathcal{B}}(r,\theta,\phi,t) \simeq \frac{\mu_0\ddot{d}(t_0)}{4\pi c}\frac{\sin\theta}{r}\hat{\mathbf{e}}_\phi . \tag{8.17}$$

The Poynting vector is,

$$\boxed{\vec{\mathcal{S}} \simeq \tfrac{1}{\mu_0}\vec{\mathcal{E}}\times\vec{\mathcal{B}} = \frac{\mu_0\ddot{d}(t_0)^2}{16\pi^2 c}\frac{\sin^2\theta}{r^2}\hat{\mathbf{e}}_r} , \tag{8.18}$$

which is a result that we already used in (7.111). And for total radiated power we get the *Larmor formula*,

$$P \simeq \oint\vec{\mathcal{S}}\cdot d\mathbf{a} = \frac{\mu_0\ddot{d}(t_0)}{6\pi c} . \tag{8.19}$$

The calculation is equivalent to a multipolar expansion of the retarded potentials up to the lowest order in r' which can still radiate, and which turns out to be an electric dipole radiation. Multipolar orders of radiation usually only come into play, when for some reason (e.g. a selection rule) the electric dipole radiation cancels. The next multipolar order will be, as we will soon see, a combination of magnetic dipole and quadrupolar electric radiation.

8.1.2 Multipolar expansion of retarded potentials

In order to simplify the multipolar treatment, we use the superposition principle, allowing us to decompose any temporal oscillation of a charge distribution into harmonic oscillations,

$$\varrho(\mathbf{r},t_r) = \varrho(\mathbf{r})e^{-\imath\omega t_r} \quad \text{and} \quad \mathbf{j}(\mathbf{r},t_r) = \mathbf{j}(\mathbf{r})e^{-\imath\omega t_r} \ . \tag{8.20}$$

By inserting these dependencies into the *retarded potentials* (6.106), we obtain with $t_r = t - |\mathbf{r}-\mathbf{r}'|/c$,

$$\Phi(\mathbf{r}) = \frac{1}{4\pi\varepsilon_0}\int \varrho(\mathbf{r}_r)\frac{e^{\imath k|\mathbf{r}-\mathbf{r}'|}}{|\mathbf{r}-\mathbf{r}'|}d^3r' \quad \text{and} \quad \mathbf{A}(\mathbf{r}) = \frac{\mu_0}{4\pi}\int \mathbf{j}(\mathbf{r}')\frac{e^{\imath k|\mathbf{r}-\mathbf{r}'|}}{|\mathbf{r}-\mathbf{r}'|}d^3r' \ , \tag{8.21}$$

with $k = \omega/c$ and implying $\Phi(\mathbf{r},t) = \Phi(\mathbf{r})e^{-\imath\omega t}$ and $\mathbf{A}(\mathbf{r},t) = \mathbf{A}(\mathbf{r})e^{-\imath\omega t}$.

From these expressions we can, knowing the sources (8.20), calculate the fields via the expressions (6.78) or alternatively (based only on the vector potential) via,

$$\vec{\mathcal{B}} = \nabla\times\mathbf{A} \quad \text{and} \quad \vec{\mathcal{E}} = \tfrac{\imath c^2}{\omega}\nabla\times\vec{\mathcal{B}} \quad \text{and} \quad \vec{\mathcal{B}} = \tfrac{-\imath}{\omega}\nabla\times\vec{\mathcal{E}} \ , \tag{8.22}$$

where $\vec{\mathcal{E}}$ is evaluated outside the source. We will consider sources which are small (size d) compared to the wavelength λ and distinguish three regions characterized by fields with very different properties:

• near-field (or static) zone	$r' < d \ll r \ll \lambda$
• intermediate (or inductive) zone	$r' < d \ll r \sim \lambda$
• far-field (or radiative) zone	$r' < d \ll \lambda \ll r$

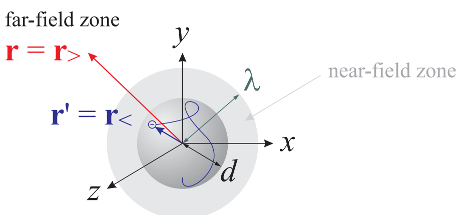

Figure 8.1: Geometry of source ($r' < d$) and observer ($r > d$) coordinates.

To handle the expression (8.21) we expand the Green function into spherical harmonics,

$$\frac{e^{\imath k|\mathbf{r}-\mathbf{r}'|}}{4\pi|\mathbf{r}-\mathbf{r}'|} = \imath k\sum_{\ell=0}^{\infty} h_\ell^{(1)}(kr_>)j_\ell(kr_<)\sum_{m=-\ell}^{\ell} Y_{\ell m}^*(\theta',\phi')Y_{\ell m}(\theta,\phi) \ , \tag{8.23}$$

where (placing the observer out of the source region) $r_< \equiv \min(r,r') = r'$ and $r_> \equiv \max(r,r') = r$. j_ℓ and $h_\ell^{(1)}$ are the *Bessel functions* and *Hankel functions* of the first type. This formula can be simplified by the sum rule,

$$\sum_{m=-\ell}^{\ell} Y_{\ell m}^*(\hat{\mathbf{e}}_{r'})Y_{\ell m}(\hat{\mathbf{e}}_r) = \frac{2\ell+1}{4\pi}P_\ell(\hat{\mathbf{e}}_{r'}\cdot\hat{\mathbf{e}}_r) \ , \tag{8.24}$$

where P_ℓ are *Legendre polynomials*. We write,

$$\frac{e^{\imath k|\mathbf{r}-\mathbf{r}'|}}{|\mathbf{r}-\mathbf{r}'|} = \imath k \sum_{\ell=0}^{\infty}(2\ell+1)h_\ell^{(1)}(kr)j_\ell(kr')P_\ell(\hat{\mathbf{e}}_{r'}\cdot\hat{\mathbf{e}}_r) \ . \tag{8.25}$$

For observation points $\mathbf{r}$ out of the source (which is certainly satisfied in the limit $r' \ll r$) the Eq. (8.21) becomes,

$$\mathbf{A}(\mathbf{r}) = \frac{\mu_0}{4\pi}(2\ell+1)\imath k \sum_{\ell=0}^{\infty} h_\ell^{(1)}(kr)\int \mathbf{j}(\mathbf{r}')j_\ell(kr')P_\ell(\hat{\mathbf{e}}_{r'}\cdot\hat{\mathbf{e}}_r)d^3r' \ . \tag{8.26}$$

Since we will always be considering the limit $kr' \ll 1$, we can expand the Bessel function for small arguments,

$$j_\ell(x) \overset{x\rightarrow 0}{\longrightarrow} \frac{x^\ell}{(2\ell+1)!!}\left(1-\frac{x^2}{2(2\ell+3)}+...\right) \ . \tag{8.27}$$

We obtain for the vector potential,

$$\boxed{\mathbf{A}(\mathbf{r}) \simeq \frac{\mu_0}{4\pi}\imath k \sum_{\ell=0}^{\infty}\frac{1}{(2\ell-1)!!}h_\ell^{(1)}(kr)\int \mathbf{j}(\mathbf{r}')(kr')^\ell P_\ell(\hat{\mathbf{e}}_{r'}\cdot\hat{\mathbf{e}}_r)d^3r'} \ . \tag{8.28}$$

Now, let us discuss the limiting cases by comparing the observation distance r with the wavelength. In the *near-field zone*, where $kr \ll 1$, we can also expand the Bessel function for small arguments,

$$n_\ell(x) \overset{x\rightarrow 0}{\longrightarrow} -\frac{(2\ell-1)!!}{x^{\ell+1}}\left(1-\frac{x^2}{2(1-2\ell)}+...\right) \tag{8.29}$$
$$\text{and} \qquad h_\ell^{(1)}(x) = j_\ell(x)+\imath n_\ell(x) \overset{x\rightarrow 0}{\longrightarrow} \imath n_\ell(x) \ ,$$

resulting in the vector potential,

$$\boxed{\mathbf{A}(\mathbf{r}) \overset{kr\rightarrow 0}{\longrightarrow} \frac{\mu_0}{4\pi}k\sum_{\ell=0}^{\infty}\frac{1}{(kr)^{\ell+1}}\int \mathbf{j}(\mathbf{r}')(kr')^\ell P_\ell(\hat{\mathbf{e}}_{r'}\cdot\hat{\mathbf{e}}_r)d^3r'} \ . \tag{8.30}$$

This formula could already have been derived by approximating the exponential of the formula (8.21) by $e^{\imath k|\mathbf{r}-\mathbf{r}'|} \simeq 1$ and expanding the following Green function into spherical harmonics [2],

$$\frac{1}{4\pi|\mathbf{r}-\mathbf{r}'|} = \sum_{\ell=0}^{\infty}\sum_{m=-\ell}^{\ell}\frac{1}{2\ell+1}\frac{r_<^\ell}{r_>^{\ell+1}}Y_{\ell m}^*(\theta',\phi')Y_{\ell m}(\theta,\phi) \ . \tag{8.31}$$

[2]This expansion is obtained by expanding the Legendre polynomials in the expansion (2.91),

$$\frac{1}{|\mathbf{r}-\mathbf{r}'|} = \frac{1}{r}\sum_{\ell=0}^{\infty}\frac{r_<^\ell}{r_>^{\ell+1}}P_\ell(\cos\theta') \qquad \text{with} \qquad P_\ell(\cos\theta') = \frac{4\pi}{2\ell+1}\sum_{m=\ell}^{\ell}Y_{\ell m}^*(\theta',\phi')Y_{\ell m}(\theta,\phi) \ ,$$

.

The absence of propagating terms in the expression (8.30) (the wave vector k can be eliminated from the expression (8.30)) demonstrates the *quasi-static* character of the fields within the near zone, that is, apart from a uniform and harmonic oscillation described by $e^{-\imath\omega t}$. The radial components depend on the details of the source's geometry. The scalar and vector potentials are of the form already derived in electrostatics (2.92) and magnetostatics (4.39).

On the other hand, in *far-field zone*, where $kr \gg 1$, the exponential in (8.21) oscillates rapidly and determines the behavior of vector potential. Here, we must resort to the complete expression (8.28), but we can expand the Hankel functions like,

$$h_\ell^{(1)}(x) = (-\imath)^{\ell+1}\frac{e^{\imath x}}{x}\sum_{m=0}^{\ell}\frac{\imath^m}{m!(2x)^m}\frac{(\ell+m)!}{(\ell-m)!}~. \tag{8.32}$$

Knowing,

$$\begin{aligned} h_0^{(1)}(x) &= -\imath\frac{e^{\imath x}}{x} \quad , \quad P_0(x) = 1 \\ h_1^{(1)}(x) &= -\frac{e^{\imath x}}{x}\left(1-\frac{1}{\imath x}\right) \quad , \quad P_1(x) = x~. \end{aligned} \tag{8.33}$$

we calculate the potentials,

$$\begin{aligned} \mathbf{A}_{\ell=0}(\mathbf{r}) &\simeq \frac{\mu_0}{4\pi}\frac{e^{\imath kr}}{r}\int\mathbf{j}(\mathbf{r}')d^3r' \\ \mathbf{A}_{\ell=1}(\mathbf{r}) &\simeq -\frac{\mu_0}{4\pi}\imath k\frac{e^{\imath kr}}{r}\left(1-\frac{1}{\imath kr}\right)\int\mathbf{j}(\mathbf{r}')\mathbf{r}'\cdot\hat{\mathbf{e}}_r d^3r'~, \end{aligned} \tag{8.34}$$

We will see in the following sections that $\mathbf{A}_{\ell=0}$ is the potential for electric dipole radiation and $\mathbf{A}_{\ell=1}$ the potential for magnetic dipole radiation and electric quadrupolar radiation.

Example 84 (*The far-field limit*): Assuming that the spatial extent of the radiation source is small, $r' \lesssim d \ll r$, it is sufficient to approximate directly in the expression (8.21),

$$|\mathbf{r}-\mathbf{r}'| \simeq r - \hat{\mathbf{e}}_r\cdot\mathbf{r}'~.$$

Moreover, if only the principal term in kr is desired [3], the inverse distance in (8.21) can be replaced by r. Then, the vector potential is,

$$\lim_{kr\to\infty}\mathbf{A}(\mathbf{r}) = \frac{\mu_0}{4\pi}\frac{e^{\imath kr}}{r}\int\mathbf{j}(\mathbf{r}')e^{-\imath k\hat{\mathbf{e}}_r\cdot\mathbf{r}'}d^3r'~.$$

This shows that, in the far-field zone, the vector potential behaves like a spherically expanding wave modulated by an angular coefficient. It is easy to show, that the fields calculated from (8.22) are transverse to the radius vector and fall off as $1/r$. They correspond thus to the radiation fields. If the size of the source is small compared to a wavelength, it is appropriate to expand the exponential in the integral in (8.25) in powers of k,

$$\lim_{kr\to\infty}\mathbf{A}(\mathbf{r}) = \frac{\mu_0 k}{4\pi}\sum_n\frac{(-\imath)^n}{n!}\frac{e^{\imath kr}}{kr}\int\mathbf{j}(\mathbf{r}')(\hat{\mathbf{e}}_r\cdot k\mathbf{r}')^n d^3r'~.$$

[3] The expansion by $\frac{1}{kr}$ gives,

$$\frac{e^{-\imath k\hat{\mathbf{e}}_r\cdot r'}}{kr-k\hat{\mathbf{e}}_r\cdot r'} = \frac{e^{-\imath k\hat{\mathbf{e}}_r\cdot r'}}{kr}\left[\frac{\hat{\mathbf{e}}_r\cdot r'}{r}+\left(\frac{\hat{\mathbf{e}}_r\cdot r'}{r}\right)^2+...\right] \simeq \frac{e^{-\imath k\hat{\mathbf{e}}_r\cdot r'}}{kr}~.$$

The magnitude of the n-th term is given by $\frac{1}{n!}\int \mathbf{j}(\mathbf{r}')(\hat{\mathbf{e}}_r \cdot k\mathbf{r}')^n d^3r'$. Since the order of magnitude of $\mathbf{r}'$ is d, and since we assumed $kr' \ll 1$, consecutive terms decrease rapidly with n. Consequently, the radiation emitted from the source comes mainly from the first terms of the expansion (8.26).

8.1.2.1 The electric monopole

We notice that the lowest order radiation found in the expansion of $\mathbf{A}$ is dipolar. How about monopolar fields? Let us examine the issue of electric monopole fields, when the sources vary in time. The contribution of the electric monopole is obtained by substituting $|\mathbf{r}-\mathbf{r}'| \to |\mathbf{r}| = r$ in the integral (8.21) for the potential Φ. The result is,

$$\Phi_{monopole}(\mathbf{r},t) = \frac{1}{4\pi\varepsilon_0}\frac{e^{\imath kr}}{r}\int \rho(\mathbf{r}')d^3r' = \frac{Q}{4\pi\varepsilon_0}\frac{e^{\imath kr}}{r} \ . \tag{8.35}$$

where $q(t)$ is the total charge of the source. Since the charge is localized in the source (and therefore conserved), the total charge q is independent of time. Thus, the electrical monopole part of the potential of a localized source is necessarily static. Radiation with harmonic temporal dependence, $e^{-\imath\omega t}$, does not have monopolar terms in the fields.

Now let us go back to multipolar fields. Since these fields can be calculated from the vector potential via (8.23), we omit explicit references to the scalar potential in the following.

8.1.3 Radiation of an oscillating electric dipole

Keeping only the first term in (8.30) we get the potential vector (8.33),

$$\mathbf{A}(\mathbf{r}) = \frac{\mu_0}{4\pi}\frac{e^{\imath kr}}{r}\int \mathbf{j}(\mathbf{r}')d^3r' \ . \tag{8.36}$$

which is valid everywhere outside the source. Using the continuity equation we can rewrite it, using a result from Exc. 8.1.6.1,

$$\mathbf{A}(\mathbf{r}) = -\frac{\mu_0}{4\pi}\frac{e^{\imath kr}}{r}\int \mathbf{r}'(\nabla'\cdot\mathbf{j})d^3r' = -\frac{\mu_0}{4\pi}\frac{e^{\imath kr}}{r}\imath\omega\int \mathbf{r}'\varrho(\mathbf{r}')d^3r' \ . \tag{8.37}$$

With the *electric dipole moment*,

$$\mathbf{d} \equiv \int \mathbf{r}'\varrho(\mathbf{r}')d^3r' \ , \tag{8.38}$$

defined in electrostatics we write,

$$\boxed{\mathbf{A}(\mathbf{r}) = -\frac{\mu_0}{4\pi}\frac{e^{\imath kr}}{r}\imath\omega\mathbf{d}} \ . \tag{8.39}$$

We obtain the fields via the equations (8.22),

$$\boxed{\begin{aligned}\vec{\mathcal{B}} &= -\frac{ck^3\mu_0}{4\pi}(\hat{\mathbf{e}}_r \times \mathbf{d})\frac{e^{\imath kr}}{kr}\left(1 - \frac{1}{\imath kr}\right) \\ \vec{\mathcal{E}} &= \frac{k^3}{4\pi\varepsilon_0}\left\{(\hat{\mathbf{e}}_r \times \mathbf{d}) \times \hat{\mathbf{e}}_r\frac{e^{\imath kr}}{kr} + [3\hat{\mathbf{e}}_r(\hat{\mathbf{e}}_r \cdot \mathbf{d}) - \mathbf{d}]\left(\frac{1}{(kr)^3} - \frac{\imath}{(kr)^2}\right)e^{\imath kr}\right\}\end{aligned}} . \tag{8.40}$$

We observe that the magnetic field is transverse to the radius vector $\hat{\mathbf{e}}_r$ at all distances, but that the electric field has components parallel and perpendicular to $\hat{\mathbf{e}}_r$. In Exc. 8.1.6.2 we will derive the fields (8.40) directly from the potentials.

In the radiation zone $kr \gg 1$ the fields adopt the typical behavior,

$$\vec{\mathcal{B}} = -\frac{ck^3\mu_0}{4\pi}(\hat{\mathbf{e}}_r \times \mathbf{d})\frac{e^{\imath kr}}{kr} \quad \text{and} \quad \vec{\mathcal{E}} = \frac{k^3}{4\pi\varepsilon_0}(\hat{\mathbf{e}}_r \times \mathbf{d}) \times \hat{\mathbf{e}}_r\frac{e^{\imath kr}}{kr} . \tag{8.41}$$

In the near-field zone $kr \ll 1$,

$$\vec{\mathcal{B}} = \frac{\imath\omega\mu_0}{4\pi}(\hat{\mathbf{e}}_r \times \mathbf{d})\frac{1}{r^2} \quad \text{and} \quad \vec{\mathcal{E}} = \frac{1}{4\pi\varepsilon_0}[3\hat{\mathbf{e}}_r(\hat{\mathbf{e}}_r \cdot \mathbf{d}) - \mathbf{d}]\frac{1}{r^3} , \tag{8.42}$$

does not have the propagation term $e^{\imath kr}$. The electric field, apart from its temporal oscillations, is just a static electric dipole. The magnetic field is, apart from a constant $Z_0 \equiv \sqrt{\mu_0/\varepsilon_0}$ called *vacuum impedance*, smaller by a factor kr than the electric field in the region where $kr \ll 1$. Thus, the fields in the near-field zone are of predominantly electrical nature. The magnetic field disappears, obviously, in the static limit $k \to 0$. In this case, the near-field zone extends to infinity.

The Poynting vector in the far-field due to the oscillation of the dipole moment $\mathbf{d}$ is, inserting (8.41),

$$\begin{aligned}\vec{\mathcal{S}} &= \frac{1}{2\mu_0}\vec{\mathcal{E}} \times \vec{\mathcal{B}}^* = -\frac{ck^4}{32\pi^2\varepsilon_0 r^2}\{[\hat{\mathbf{e}}_r \times \mathbf{d}) \times \hat{\mathbf{e}}_r] \times (\hat{\mathbf{e}}_r \times \mathbf{d})\} \\ &= -\frac{ck^4}{32\pi^2\varepsilon_0 r^2}(d^2 - d_r^2)\hat{\mathbf{e}}_r = -\frac{ck^4}{32\pi^2\varepsilon_0 r^2}\hat{\mathbf{e}}_r d^2 \sin^2\theta .\end{aligned} \tag{8.43}$$

The radiated power is given by the absolute value of (8.43) per solid angle element [4]. If the components of $\mathbf{d}$ all have the same phase, the angular distribution is a typical dipole pattern,

$$\frac{dP}{d\Omega} = \frac{c}{32\pi^2\varepsilon_0}k^4|\mathbf{d}|^2\sin^2\theta . \tag{8.44}$$

where the angle θ is measured from the direction of $\mathbf{d}$. The total radiated power, regardless of the relative phases of the components of $\mathbf{d}$, is,

$$P = \frac{cZ_0}{12\pi\varepsilon_0}|\mathbf{d}|^2 = \frac{\mu_0}{12\pi c}|\mathbf{d}|^2 , \tag{8.45}$$

[4]When writing angular distributions of radiation, we will always exhibit the polarization explicitly by writing the absolute square of a vector that is proportional to the electric field. If the angular distribution of a particular polarization is desired, it can then be obtained by taking the scalar product of the vector with the appropriate polarization vector before the square.

which is half of the value calculated in the derivation of the Larmor formula (8.19), because in (8.43) we choose to calculate directly the temporal average of the Poynting vector.

Resolve the 8.1.6.3. In Exc. 8.1.6.4 we will verify the gauge of the dipolar potential and in Exc. 8.1.6.5 we calculate the fields of a linear antenna.

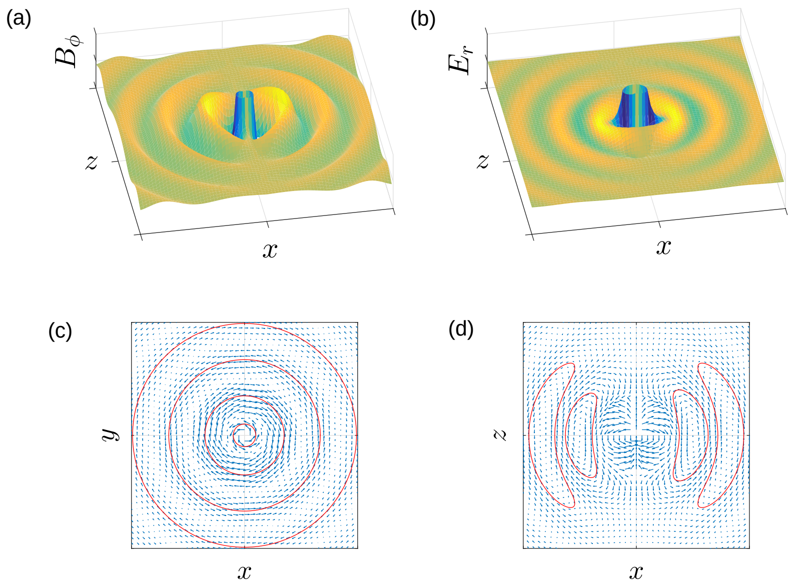

Figure 8.2: (code) Electric dipole radiation patterns. (a) Cut through $\vec{\mathcal{B}}_\phi$, (b) cut through $\vec{\mathcal{E}}_r$, (c) field lines of $\vec{\mathcal{B}}$ in the xy-plane, and (d) field lines of $\vec{\mathcal{E}}$ in the xz-plane. A movie can be seen at (watch movie).

Example 85 (*Linear antenna*): As an example, we calculate the power radiated by an oscillating charge $\varrho(\mathbf{r},t) = Q\delta(x)\delta(y)\delta(z - z_0 e^{-\imath\omega t})$. The dipole moment is,

$$\mathbf{d} = \int \mathbf{r}'\varrho(\mathbf{r}',t)dV' = Q\hat{\mathbf{e}}_z z_0 e^{-\imath\omega t} .$$

Inserted into the formula (8.45),

$$P = \frac{cZ_0 Q^2 z_0^2}{12\pi\varepsilon_0} .$$

Example 86 (*Linear antenna*): As another example we calculate the power radiated by a simple linear antenna, characterized by a current distribution $\mathbf{j}(\mathbf{r},t) = I_0\hat{\mathbf{e}}_z\delta(x)\delta(y)(1 - 2|z|/a)e^{-\imath\omega t}$. The dipole moment is,

$$\mathbf{d} = \frac{\imath}{\omega}\int \mathbf{j}dV' = \frac{\imath}{\omega}I_0\hat{\mathbf{e}}_z e^{-\imath\omega t}\int_{-a/2}^{a/2}\mathbf{j}dV'\left(1 - \frac{2|z'|}{a}\right)dz' = \frac{\imath I_0 a}{2\omega}\hat{\mathbf{e}}_z e^{-\imath\omega t} .$$

Inserted into the formula (8.45),

$$P = \frac{Z_0 I_0^2(ka)^2}{48\pi} .$$

8.1.4 Magnetic dipole and electric quadrupole radiation

The term $\ell = 1$ in the expansion (8.28) leads to the second vector potential (8.34),

$$\mathbf{A}(\mathbf{r}) = -\imath\frac{\mu_0}{4\pi}\imath k h_1^{(1)}\int \mathbf{j}(\mathbf{r}')(\hat{\mathbf{e}}_r\cdot\mathbf{r}')d^3r' = \frac{\mu_0}{4\pi}\frac{e^{\imath kr}}{r}\left(\frac{1}{r}-\imath k\right)\int \mathbf{j}(\mathbf{r}')(\hat{\mathbf{e}}_r\cdot\mathbf{r}')d^3r' \ . \tag{8.46}$$

This vector potential can be written as the sum of two terms: one gives a transverse magnetic field and the other gives a transverse electric field. These physically distinct contributions can be separated by rewriting the integrand in (8.46) as the sum of a part, which is symmetric about an exchange of $\mathbf{j}$ and $\mathbf{r}'$, and an antisymmetric part. Therefore,

$$(\hat{\mathbf{e}}_r\cdot\mathbf{r}')\mathbf{j} = \tfrac{1}{2}[(\hat{\mathbf{e}}_r\cdot\mathbf{r}')\mathbf{j} + (\hat{\mathbf{e}}_r\cdot\mathbf{j})\mathbf{r}'] - \hat{\mathbf{e}}_r\times\tfrac{1}{2}(\mathbf{r}'\times\mathbf{j}) \ , \tag{8.47}$$

using the rule $B(AC) - C(AB)$. The second (antisymmetric) part is recognizable as the magnetization due to the current $\mathbf{j}$:

$$\vec{\mathcal{M}} = \tfrac{1}{2}(\mathbf{r}'\times\mathbf{j}) \ . \tag{8.48}$$

We will see, that the first (symmetric) term is related to the electric quadrupole moment density.

8.1.4.1 Magnetic dipole radiation

Considering, for the moment, only the magnetization term, we get the vector potential,

$$\boxed{\mathbf{A}(\mathbf{r}) = \frac{\imath k\mu_0}{4\pi}(\hat{\mathbf{e}}_r\times\mathbf{m})\frac{e^{\imath kr}}{r}\left(1-\frac{1}{\imath kr}\right)} \ , \tag{8.49}$$

where $\mathbf{m}$ is the *magnetic dipole moment*,

$$\mathbf{m} = \int \vec{\mathcal{M}}d^3r = \tfrac{1}{2}\int(\mathbf{r}\times\mathbf{j})d^3r \ . \tag{8.50}$$

The fields can be determined by observing that the vector potential (8.49) is proportional to the magnetic field (8.40) of an electric dipole (except that we have to exchange the electric by the magnetic dipole moment). Thus, we can use the calculations we already made and transfer the results to the fields of a magnetic dipole via Eqs. (8.22):

$$\boxed{\begin{aligned}\vec{\mathcal{B}} &= \frac{k^3\mu_0}{4\pi}\left\{(\hat{\mathbf{e}}_r\times\mathbf{m})\times\hat{\mathbf{e}}_r\frac{e^{\imath kr}}{kr} + [3\hat{\mathbf{e}}_r(\hat{\mathbf{e}}_r\cdot\mathbf{m})-\mathbf{m}]\left(\frac{1}{(kr)^3}-\frac{\imath}{(kr)^2}\right)e^{\imath kr}\right\}\\ \vec{\mathcal{E}} &= -\frac{ck^3\mu_0}{4\pi}(\hat{\mathbf{e}}_r\times\mathbf{m})\frac{e^{\imath kr}}{kr}\left(1-\frac{1}{\imath kr}\right)\end{aligned}} \ . \tag{8.51}$$

In Exc. 8.1.6.6 we will derive the fields (8.51) directly from the potentials.

All arguments concerning the behavior of the fields in the near-field and far-field regions are the same as those proposed for the electric dipole radiation with the modifications,

$$\vec{\mathcal{E}}^{(M1)} \overset{\mathbf{m}\leftrightarrow c\mathbf{d}}{\longleftrightarrow} c\vec{\mathcal{B}}^{(E1)} \\ c\vec{\mathcal{B}}^{(M1)} \overset{\mathbf{m}\leftrightarrow c\mathbf{d}}{\longleftrightarrow} \vec{\mathcal{E}}^{(E1)} \ . \tag{8.52}$$

Likewise, the radiation pattern and the total radiated power are the same for the two types of dipole. The only difference in the radiation fields are their polarizations. For an electric dipole, the electric field vector lies in the plane defined by $\hat{\mathbf{e}}_r$ and $\mathbf{d}$, whereas for a magnetic dipole, it is perpendicular to the plane defined by $\hat{\mathbf{e}}_r$ and $\mathbf{m}$.

8.1.4.2 Electric quadrupole radiation

The integral of the symmetric term in (8.47) can be transformed using the continuity equation and integrating by parts:

$$\tfrac{1}{2}\int[(\hat{\mathbf{e}}_r\cdot\mathbf{r}')\mathbf{j}+(\hat{\mathbf{e}}_r\cdot\mathbf{j})\mathbf{r}']d^3r' = -\tfrac{\imath\omega}{2}\int\mathbf{r}'(\hat{\mathbf{e}}_r\cdot\mathbf{r}')\varrho(\mathbf{r}')d^3r' \ . \tag{8.53}$$

This will be demonstrated in Exc. 8.1.6.1. Since this integral involves the second moments of charge density, it corresponds to a quadrupolar electric radiation source. The potential vector is,

$$\boxed{\mathbf{A}(\mathbf{r}) = -\frac{\mu_0 ck^2}{8\pi}\frac{e^{\imath kr}}{r}\left(1-\frac{1}{\imath kr}\right)\int\mathbf{r}'(\hat{\mathbf{e}}_r\cdot\mathbf{r}')\varrho(\mathbf{r}')d^3r'} \ . \tag{8.54}$$

The expressions for the fields are a bit complicated, such that we focus on the radiation zone, where it is easy to verify that,

$$\vec{\mathcal{B}} = \nabla\times\mathbf{A} = \imath k\hat{\mathbf{e}}_r\times\mathbf{A} \quad , \quad \vec{\mathcal{E}} = \imath ck(\hat{\mathbf{e}}_r\times\mathbf{A})\times\hat{\mathbf{e}}_r \ . \tag{8.55}$$

Consequently, the magnetic field is,

$$\vec{\mathcal{B}} = -\frac{\imath ck^3\mu_0}{8\pi}\frac{e^{\imath kr}}{r}\int(\hat{\mathbf{e}}_r\times\mathbf{r}')(\hat{\mathbf{e}}_r\cdot\mathbf{r}')\varrho(\mathbf{r}')d^3re' \ . \tag{8.56}$$

With the definition of the tensor of the quadrupolar moment,

$$Q_{\alpha\beta} \equiv \int(3x_\alpha x_\beta - r^2\delta_{\alpha\beta})\varrho(\mathbf{r}')d^3r' \ , \tag{8.57}$$

the integral (8.56) can be written as,

$$\hat{\mathbf{e}}_r\times\int\mathbf{r}'(\hat{\mathbf{e}}_r\cdot\mathbf{r}')\varrho(\mathbf{r}')d^3\mathbf{r}' = \tfrac{1}{3}\hat{\mathbf{e}}_r\times\mathbf{Q}(\hat{\mathbf{e}}_r) \ , \tag{8.58}$$

where the vector $\mathbf{Q}(\hat{\mathbf{e}}_r)$ is defined via its components,

$$Q_\alpha = \sum_{\alpha\beta} Q_{\alpha\beta}\hat{\mathbf{e}}_\beta \ . \tag{8.59}$$

We note that its magnitude and direction depend on the direction of observation as well as on the properties of the source. With these definitions, we get the magnetic field,

$$\vec{\mathcal{B}} = -\frac{\imath ck^3\mu_0}{24\pi}\frac{e^{\imath kr}}{r}\hat{\mathbf{e}}_r \times \mathbf{Q}(\hat{\mathbf{e}}_r) \ , \tag{8.60}$$

and the time-averaged power radiated into a solid angle,

$$\frac{dP}{d\Omega} = \frac{c^2 Z_0}{1152\pi^2}k^6|[\hat{\mathbf{e}}_r \times \mathbf{Q}(\hat{\mathbf{e}}_r)] \times \hat{\mathbf{e}}_r|^2 \ . \tag{8.61}$$

The final expressions are complicated [47], but for the example of a ellipsoidal charge distribution periodically changing its 'aspect ratio', it is possible to show that the angular distribution of the radiation pattern exhibits four lobes,

$$\frac{dP}{d\Omega} = \frac{c^2 Z_0 k^6}{512\pi^2}Q_0^2 \sin^2\theta\cos^2\theta \ , \tag{8.62}$$

and the total radiated power is,

$$P = \frac{c^2 Z_0 k^6}{960\pi}Q_0^2 \ . \tag{8.63}$$

For multipoles of higher order the formulas become more and more complicated. Other techniques based on the multipolar expansion of the wave equation, rather than deriving the radiation patterns directly from the retarded potentials, are more suitable. Resolve the Exc. 8.1.6.7.

8.1.5 Multipolar expansion of the wave equation

The radiation from sources which are small in comparison with the observation distance exhibits a symmetry suggesting a reformulation of the wave equation in spherical coordinates, as we have already done in Sec. 2.6.3. In short, we consider a scalar field $\psi(\mathbf{r},t)$ satisfying the wave equation,

$$\nabla^2\psi - \frac{1}{c^2}\frac{\partial^2\psi}{\partial t^2} = 0 \ . \tag{8.64}$$

The temporal dependency is separated by a Fourier transform,

$$\psi(\mathbf{r},t) = \int_{-\infty}^{\infty}\phi(\mathbf{r},\omega)e^{-\imath\omega t}d\omega \ , \tag{8.65}$$

yielding a distribution of the amplitudes which satisfying the Poisson equation,

$$(\nabla^2 + k^2)\phi(\mathbf{r},\omega) = 0 \ , \tag{8.66}$$

with $\omega^2 = c^2k^2$. Expanding into spherical harmonics by the ansatz,

$$\phi(\mathbf{r},\omega) = \sum_{\ell,m} f_\ell(r)Y_{\ell,m}(\theta,\phi) \ , \tag{8.67}$$

we transform (8.66), where the Laplacian is expressed in spherical coordinates, into a differential equation which is independent of m,

$$\left[\frac{d^2}{dr^2}+\frac{2}{r}\frac{d}{dr}+k^2-\frac{\ell(\ell+1)}{r^2}\right]f_\ell(r)=0\ . \tag{8.68}$$

This equation is precisely the spherical Bessel equation, whose solutions are linear combinations of spherical Bessel and von Neumann functions,

$$A_\ell j_\ell(kr)+B_\ell n_\ell(kr)\ . \tag{8.69}$$

With respect to the spherical part, we note that the spherical harmonics are the eigenfunctions of the square of an angular momentum operator $\hat{\mathbf{L}}$, which can be identified with the angular part of the Laplacian in spherical coordinates,

$$\hat{\mathbf{L}}^2=-\left[\frac{1}{\sin\theta}\frac{\partial}{\partial\sin\theta}\left(\sin\theta\frac{\partial}{\partial\sin\theta}\right)+\frac{1}{\sin^2\theta}\frac{\partial}{\partial\phi}\right]\ , \tag{8.70}$$

and has as eigenvalues the integer numbers $\ell(\ell+1)$,

$$\hat{\mathbf{L}}^2Y_{\ell m}=\ell(\ell+1)Y_{\ell m}\ . \tag{8.71}$$

The Lie algebra ruling the calculation with angular momentum operators will not be reproduced here [5].

Clearly, the simplicity of the multipolar expansion of the wave equation (8.64) into spherical coordinates is due to its scalar nature, and a similar procedure is used to solve the scalar Schrödinger equation for the hydrogen atom. Electromagnetic fields, however, are vectorial which complicates the calculus, as we will see in the following.

8.1.5.1 Multipolar expansion of the fields

Assuming a time dependence as $e^{-\imath\omega t}$ and combining the Maxwell equations for the field rotations to derive the Helmholtz equation, we obtain a set of equations, which is equivalent to the Maxwell equations,

$$(\nabla^2+k^2)\vec{\mathcal{B}}=0 \quad \text{and} \quad \nabla\cdot\vec{\mathcal{B}}=0 \quad \text{with} \quad \vec{\mathcal{E}}=\imath\frac{c}{k}\nabla\times\vec{\mathcal{B}}\ , \tag{8.72}$$

or alternatively,

$$(\nabla^2+k^2)\vec{\mathcal{E}}=0 \quad \text{and} \quad \nabla\cdot\vec{\mathcal{E}}=0 \quad \text{with} \quad \vec{\mathcal{B}}=\imath\frac{1}{ck}\nabla\times\vec{\mathcal{E}}\ . \tag{8.73}$$

Now, we have for any well-behaved vector field $\mathbf{X}$,

$$\nabla^2(\mathbf{r}\cdot\mathbf{X})=\mathbf{r}\cdot(\nabla^2\mathbf{X})+2\nabla\cdot\mathbf{X}\ . \tag{8.74}$$

Applying this relation to the electromagnetic fields, we find,

$$\boxed{(\nabla^2+k^2)(\mathbf{r}\cdot\vec{\mathcal{B}})=0 \quad \text{and} \quad (\nabla^2+k^2)(\mathbf{r}\cdot\vec{\mathcal{E}})=0}\ . \tag{8.75}$$

[5] See the treatment of spherical potentials in the script *Quantum Mechanics* by the same author Scripts/QuantumMechanicsScript .

The *transverse magnetic field* and the *transverse electric field* can be rewritten by the rotation of the equations (8.72) respectively (8.73),

$$\begin{array}{ll} \mathbf{r}\cdot\vec{\mathcal{B}} & = \frac{\imath}{ck}\mathbf{r}\cdot(\nabla\times\vec{\mathcal{E}}) = \frac{\imath}{ck}(\mathbf{r}\times\nabla)\cdot\vec{\mathcal{E}} \equiv \frac{1}{ck}\mathbf{L}\cdot\vec{\mathcal{E}} \\ \mathbf{r}\cdot\vec{\mathcal{E}} & = \frac{\imath c}{k}\mathbf{r}\cdot(\nabla\times\vec{\mathcal{B}}) = \frac{\imath c}{k}(\mathbf{r}\times\nabla)\cdot\vec{\mathcal{B}} \equiv \frac{c}{k}\mathbf{L}\cdot\vec{\mathcal{B}} \end{array} , \tag{8.76}$$

defining in this way the operator for the orbital angular momentum $\mathbf{L}$.

These scalar fields can now be expanded as demonstrated in (8.67) and (8.69). That is, we can expand the transverse parts of electric and magnetic fields into magnetic (electric) multipoles as,

$$\begin{array}{lllll} \mathbf{r}\cdot\vec{\mathcal{B}}^{(M)}_{\ell m} & = \frac{\ell(\ell+1)}{k}g_\ell(kr)Y_{\ell m}(\theta,\phi) = \frac{1}{ck}\mathbf{L}\cdot\vec{\mathcal{E}}^{(M)}_{\ell m} & \text{and} & \mathbf{r}\cdot\vec{\mathcal{E}}^{(M)}_{\ell m} & = 0 \\ \mathbf{r}\cdot\vec{\mathcal{E}}^{(E)}_{\ell m} & = -Z_0\frac{\ell(\ell+1)}{k}f_\ell(kr)Y_{\ell m}(\theta,\phi) = \frac{c}{k}\mathbf{L}\cdot\vec{\mathcal{B}}^{(E)}_{\ell m} & \text{and} & \mathbf{r}\cdot\vec{\mathcal{B}}^{(E)}_{\ell m} & = 0 \end{array} . \tag{8.77}$$

where g_ℓ is a linear combination of Bessel and Hankel functions and $\ell(\ell+1)/k$ a convenient normalization factor.

We can see (by simplifying the argument a bit) that, by comparing (8.77) with the equation (8.71) the field $\vec{\mathcal{E}}^{(M)}$ must contain the operator $\mathbf{L}$,

$$\boxed{\begin{array}{llllll} \vec{\mathcal{E}}^{(M)} & = & cg_\ell(kr)\mathbf{L}Y_{\ell m}(\theta,\phi) & \text{with} & \vec{\mathcal{B}}^{(M)} & = -\frac{\imath}{ck}\nabla\times\vec{\mathcal{E}}^{(M)}_{\ell m} \\ \vec{\mathcal{B}}^{(E)} & = & \mu_0 g_\ell(kr)\mathbf{L}Y_{\ell m}(\theta,\phi) & \text{with} & \vec{\mathcal{E}}^{(E)} & = -\frac{\imath c}{k}\nabla\times\vec{\mathcal{B}}^{(E)}_{\ell m} \end{array}} . \tag{8.78}$$

The functions,

$$\mathbf{X}_{\ell m}(\theta,\phi) = \frac{1}{\sqrt{\ell(\ell+1)}}\mathbf{L}Y_{\ell m}(\theta,\phi) , \tag{8.79}$$

are known as *vector spherical harmonics*. Combining the expansions into electric and magnetic multipoles we obtain,

$$\begin{aligned} \vec{\mathcal{B}} &= \sum_{\ell m}\left[a^{(E)}_{\ell,m}f_\ell(kr)\mathbf{X}_{\ell,m} - \tfrac{\imath}{k}a^{(M)}_{\ell,m}\nabla\times g_\ell(kr)\mathbf{X}_{\ell m}\right] \\ \vec{\mathcal{E}} &= \sum_{\ell m}\left[\tfrac{\imath}{k}a^{(E)}_{\ell,m}\nabla\times f_\ell(kr)\mathbf{X}_{\ell,m} - a^{(M)}_{\ell,m}g_\ell(kr)\mathbf{X}_{\ell m}\right] . \end{aligned} \tag{8.80}$$

The coefficients can be determined from the radial projections of the fields.

8.1.5.2 Vector spherical harmonics

The *vector spherical harmonics* defined above are a particular case of those defined for the coupling of two spins $\mathbf{L}$ and $\mathbf{S}$ with $S=1$ in the following sense,

$$\boxed{\mathbf{Y}_{j\ell m} = \sum_q \begin{pmatrix} J & 1 & L \\ -m & q & m-q \end{pmatrix} Y^{(\ell)}_{m-q}\hat{\mathbf{e}}_q} , \tag{8.81}$$

where the basis is in Cartesian coordinates,

$$\hat{\mathbf{e}}_0 = \hat{\mathbf{e}}_z \quad \text{and} \quad \hat{\mathbf{e}}_\pm = -\tfrac{1}{\sqrt{2}}(\hat{\mathbf{e}}_x \pm \imath\hat{\mathbf{e}}_y) . \tag{8.82}$$

These functions are tensor operators of rank $(1,\ell)$, since $\mathbf{Y}_{j\ell m} = (Y^{(\ell)} \otimes \hat{\mathbf{e}}^{(1)})^{(j)}_m$. This means they have vectorial properties via $\hat{\mathbf{e}}^{(1)}_q$ and, at the same time, are tensor operators just like the spherical harmonics $Y^{(\ell)}_m$. It is possible to check the following expressions,

$$\begin{aligned}\mathbf{J}^2\mathbf{Y}_{j\ell m} &= j(j+1)\mathbf{Y}_{j\ell m} \\ \mathbf{L}^2\mathbf{Y}_{j\ell m} &= \ell(\ell+1)\mathbf{Y}_{j\ell m} \\ \mathbf{S}^2\mathbf{Y}_{j\ell m} &= 2\mathbf{Y}_{j\ell m} \\ \mathbf{J}_z\mathbf{Y}_{j\ell m} &= m\mathbf{Y}_{j\ell m} \ .\end{aligned} \tag{8.83}$$

Furthermore, comparing (8.83) and (8.79),

$$\begin{aligned}\frac{\mathbf{L}}{\sqrt{\ell(\ell+1)}}Y^{(\ell)}_m &= -\imath\mathbf{Y}_{\ell\ell m} = \mathbf{X}_{\ell m} \\ \frac{\mathbf{r}}{r}Y^{(\ell)}_m &= \imath\sqrt{\frac{\ell+1}{2\ell+1}}\mathbf{Y}_{\ell\ \ell+1\ m} - \imath\sqrt{\frac{l}{2\ell+1}}\mathbf{Y}_{\ell\ \ell-1\ m} \\ 0 &= \mathbf{r}\cdot\mathbf{Y}_{\ell\ell m} = \mathbf{p}\cdot\mathbf{Y}_{\ell\ell m} \ .\end{aligned} \tag{8.84}$$

In 8.1.6.8 we calculate the following examples, $\mathbf{Y}_{000} = 0$ and,

$$r\mathbf{Y}_{110} = \sqrt{\tfrac{3}{16\pi}}\begin{pmatrix}-\imath y\\ \imath x\\ 0\end{pmatrix} \quad , \quad r\mathbf{Y}_{11\pm1} = \sqrt{\tfrac{3}{16\pi}}\begin{pmatrix}z\\ \pm\imath\\ -(x\pm\imath y)\end{pmatrix} \quad , \quad r\mathbf{Y}_{10\pm1} = -\sqrt{\tfrac{1}{24\pi}}\begin{pmatrix}x\\ \pm\imath y\\ 0\end{pmatrix} \ . \tag{8.85}$$

Also,

$$\mathbf{Y}^2_{\kappa\kappa m} = [\kappa(\kappa+1)-m(m+1)]|Y_{\kappa\ m+1}|^2 + 2m^2|Y_{\kappa\ m}|^2 + [\kappa(\kappa+1)-m(m-1)]|Y_{\kappa\ m-1}|^2 \ . \tag{8.86}$$

Applying the formulas [98](Chp. 10.1) to scalar and vector products of vector spherical harmonics, it is possible to derive the energy density $\frac{\varepsilon_0}{2}\vec{\mathcal{E}}^2_{jm\tau} + \frac{1}{2\mu_0}\vec{\mathcal{B}}^2_{jm\tau}$ and the Poynting vector $\varepsilon_0|\vec{\mathcal{E}}_{jm\tau}\times\vec{\mathcal{B}}_{jm\tau}|$. The calculation is complicated, because we must calculate $(3j)$, $\{6j\}$, and $\{9j\}$ coefficients. Considering that the angular distribution is the same for electric and magnetic multipolar radiation, we obtain,

$$u_{jm\tau}(\mathbf{r}) = \frac{1}{2\mu_0}\vec{\mathcal{B}}^2_{jm\tau}(\mathbf{r}) = -\frac{\hbar\omega}{4V}\left(\frac{j+1}{2j+1}\right)^2\frac{(kr)^{2j}}{(2j+1)!!^2}\mathbf{Y}^2_{jjm} \ , \tag{8.87}$$

The question now is, with what polarization ε and under what angle of incidence $\mathbf{k}$ can we excite a particular multipolar transition. The transition can only be excited by a mode, to which it couples and, therefore, into which it can radiate light. Therefore, it is sufficient to analyze the angular distribution and the polarization of spontaneously emitted radiation. In the far-field of a point source the electric and magnetic fields satisfy the Helmholtz equation [98],

$$(\triangle + \mathbf{k}^2)\vec{\mathcal{E}}(\mathbf{r},t) = 0 \ , \tag{8.88}$$

and similarly for the magnetic field $\vec{\mathcal{B}}(\mathbf{r},t)$. An atomic transition $|J,m_J\rangle \leftrightarrow |J+\kappa, m_J+m\rangle$ interacts with the electric or magnetic multipolar part κ of the radiation field. The general solution of the Helmholtz equation, therefore, is expanded into spherical harmonics $Y_{\kappa m}(\theta,\phi)$:

$$\vec{\mathcal{E}} = \sum_{\kappa=0}^{\infty}\sum_{m=-\kappa}^{\kappa}\left(\vec{\mathcal{E}}_m^{(E\kappa)} + \vec{\mathcal{E}}_m^{(M\kappa)}\right) \tag{8.89}$$

and similarly for the magnetic field. The angular distributions of the multipolar electric field components are calculated by,

$$\vec{\mathcal{E}}_m^{(E\kappa)} = -\imath k^{-1}\nabla\times\vec{\mathcal{B}}_m^{(E\kappa)} \tag{8.90}$$

$$\vec{\mathcal{B}}_m^{(E\kappa)} = -\imath\left(\mathbf{k}\times\nabla\right)Y_{\kappa m}(\theta,\phi) \equiv \sqrt{\kappa(\kappa+1)}\mathbf{Y}_{\kappa\kappa m}(\theta,\phi)\ , \tag{8.91}$$

and similarly for the magnetic field. The field components can be expressed by the vector spherical harmonics $\mathbf{Y}_{\kappa\kappa m}$. The angular distribution of the radiated intensity follows from the absolute value of the Poynting vector,

$$I_m^{(E\kappa)}(\mathbf{r}) = \mu_0^{-1}\left|\vec{\mathcal{E}}_m^{(E\kappa)}(\mathbf{r})\times\vec{\mathcal{B}}_m^{(E\kappa)}(\mathbf{r})\right| = \mu_0^{-1}\left|\vec{\mathcal{B}}_m^{(E\kappa)}(\mathbf{r})\right|^2 \propto \mathbf{Y}_{\kappa\kappa m}(\theta,\phi)^2\ . \tag{8.92}$$

The multipolar order of a radiation can, in principle, be determined by measuring its angular distribution. The above distribution integrate over all possible polarizations. If polarized light is used, in order to excite transitions between selected Zeeman levels, the angular intensity distribution of *polarized radiation* must be calculated. The transition rate between two levels $|a\rangle$ and $|b\rangle$ for light incident from a given direction $\mathbf{r}$ with a given polarization $\hat{\varepsilon}$ is, $|\langle b|\hat{\varepsilon}\vec{\mathcal{E}}_m^{(E\kappa)}(\mathbf{r})|a\rangle|^2$, where $\vec{\mathcal{E}}_m^{(E\kappa)}(\mathbf{r}) = -\imath k^{-1}\nabla\times\vec{\mathcal{B}}_m^{(E\kappa)}(\mathbf{r})$. The cases of linear polar polarization (respectively axial) of the light field in relation to the quantization axis are expressed by the fractions $\hat{\varepsilon}_{polar}\cdot\mathbf{Y}_{\kappa\kappa m}$, respectively, $\hat{\varepsilon}_{axial}\cdot\mathbf{Y}_{\kappa\kappa m}$, the absolute square values of which add up to the angular intensity distribution,

$$\begin{aligned}
u_{10} &\sim 4|Y_1^{(1)}|^2 &&= \tfrac{3}{4\pi}2\sin^2\theta\\
u_{1\pm1} &\sim 2|Y_1^{(1)}|^2 + 2|Y_0^{(1)}|^2 &&= \tfrac{3}{4\pi}(1+\cos^2)\\
u_{20} &\sim 12|Y_1^{(2)}|^2 &&= \tfrac{5}{4\pi}18\sin^2\cos^2\\
u_{2\pm1} &\sim 4|Y_2^{(2)}|^2 + 2|Y_1^{(2)}|^2 + 6|Y_0^{(2)}|^2 &&= \tfrac{5}{4\pi}3(4\cos^2 - 3\cos^2 + 1)\\
u_{2\pm2} &\sim 8|Y_2^{(2)}|^2 + 4|Y_1^{(2)}|^2 &&= \tfrac{5}{4\pi}3\sin^2(1+\cos^2)\\
u_{30} &\sim 24|Y_1^{(3)}|^2 &&= \tfrac{7}{4\pi}\tfrac{9}{2}\sin^2(5\cos^2-1)^2\\
u_{3\pm1} &\sim 10|Y_2^{(3)}|^2 + 2|Y_1^{(3)}|^2 + 12|Y_0^{(3)}|^2 &&= \tfrac{7}{4\pi}\tfrac{3}{8}(225\cos^6 - 305\cos^4 + 111\cos^2 + 1)\\
u_{3\pm2} &\sim 6|Y_3^{(3)}|^2 + 8|Y_2^{(3)}|^2 + 10|Y_1^{(3)}|^2 &&= \tfrac{7}{4\pi}\tfrac{15}{4}\sin^2(9\cos^4 - 2\cos^2 + 1)\\
u_{3\pm3} &\sim 18|Y_3^{(3)}|^2 + 6|Y_2^{(3)}|^2 &&= \tfrac{7}{4\pi}\tfrac{45}{8}\sin^4(1+\cos^2)\ .
\end{aligned} \tag{8.93}$$

In the equatorial plane, only the parts $u_{j\pm1}$ contribute; but these disappear in polar direction. All other components lie in the equatorial plane. For non-polarized radiation the angular distribution is uniform,

$$\sum_{m=-j}^{j} u_{jm} \sim \tfrac{2j+1}{4\pi}2(j+1)!\ . \tag{8.94}$$

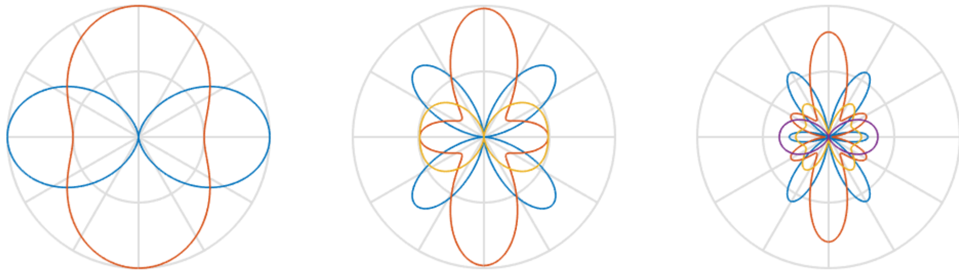

Figure 8.3: (code) Angular dependence of dipolar radiation u_{1m} (left), quadrupolar u_{2m} (center) and u_{3m} octupolar (right) with their respective contributions $m = 0$ (blue), $m = \pm 1$ (red), $m = \pm 2$ (yellow) and $m = \pm 3$ (magenta).

8.1.6 Exercises

8.1.6.1 Ex: Relationship between current density and electric dipole moment

a. For a charge and current configuration contained in a volume $\mathcal{V}$ show that, $\int_{\mathcal{V}} \mathbf{j}dV = \frac{d\mathbf{d}}{dt}$, where $\mathbf{d}$ is the total dipolar moment.
b. Demonstrate the relationship, $\int \mathbf{r}'(\hat{\mathbf{e}}_r \cdot \mathbf{r}')\dot{\varrho}(\mathbf{r}')d^3r' = \int \{\mathbf{j}(\mathbf{r}')(\hat{\mathbf{e}}_r \cdot \mathbf{r}') + \mathbf{r}'[\hat{\mathbf{e}}_r \cdot \mathbf{j}(\mathbf{r}')]\} d^3r'$.

8.1.6.2 Ex: Hertz dipole

A Hertz dipole with vertical orientation is in the focus of a parabolic antenna PA1 and emits electromagnetic radiation with a frequency of 3 GHz. The shape of the antenna is such that the electromagnetic radiation is reflected forming a 'parallel' beam with diameter $d = 3\,\text{m}$. The electric field within the beam can be roughly described by the following formula:

$$\vec{\mathcal{E}}_1(\mathbf{r}, t) = \vec{\mathcal{E}}_0 \cos(\mathbf{k}_1 \cdot \mathbf{r} - \omega t)\ \hat{\mathbf{e}}_z \qquad \text{where} \qquad \mathbf{k}_1 = -k\hat{\mathbf{e}}_x \sin\alpha + k\hat{\mathbf{e}}_y \cos\alpha\ .$$

a. Determine the parameter k using the wave equation.
b. What is the amplitude $\vec{\mathcal{E}}_0$ of the electric field assuming that the parabolic antenna emits a power of 5 W?
c. There is a second Hertz dipole, acting as a detector, oriented orthogonal to $\mathbf{k}_1$. The maximum amplitude of the electric field detected by D2 is around 0.1 V/m. Estimate the angle of the orientation of the dipole with respect to the vertical axis (without calculation, but with a short justification).
d. Now, the emitter dipole D1 is also rotated in such a way that, regardless of the orientation of the dipole D2, it does not receive signals. What is the orientation of the dipole emitter? Give a short justification.
e. The dipole emitter is again oriented vertically. Another parabolic antenna PA2, identical to PA1, is now integrated into the experiment, as shown in the figure. Calculate the power density S on the axis x in the time average. ($\alpha = 5°$)
Help: Addition theorems:

$$\cos(\alpha \pm \beta) = \cos\alpha\cos\beta \mp \sin\alpha\sin\beta \qquad \text{and} \qquad \cos 2\alpha = \cos^2\alpha - \sin^2\alpha$$

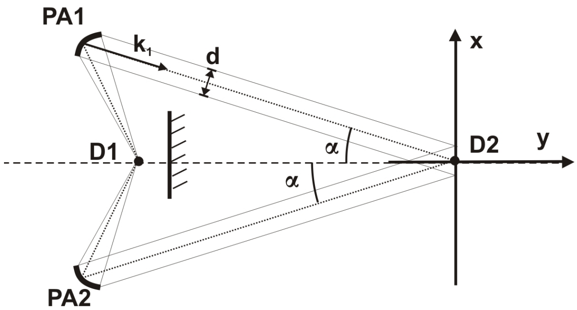

Figure 8.4: Hertz dipole.

8.1.6.3 Ex: Dipolar spherical waves

We derived in class, starting from the relations $\vec{\mathcal{B}} = \nabla \times \mathbf{A}$ and $\vec{\mathcal{E}} = \frac{\imath c}{k}\nabla \times \vec{\mathcal{B}}$, the expressions (8.40) for the magnetic and electric fields of a electric dipole radiation produced by the dipole moment $\mathbf{d} = d\hat{\mathbf{e}}_z$.
a. Show that the magnetic field can be expressed in the form $\vec{\mathcal{B}} = \vec{\mathcal{B}}_\phi(r,\theta)\hat{\mathbf{e}}_\phi$.
b. Show that the electric field can be expressed in the form $\vec{\mathcal{E}} = \vec{\mathcal{E}}_r(r,\theta)\hat{\mathbf{e}}_r + \vec{\mathcal{E}}_\theta(r,\theta)\hat{\mathbf{e}}_\theta$.
c. The purpose of this exercise is to check in spherical coordinates, where the divergence and rotation are given by (1.79) and (1.80), that these fields satisfy Maxwell's equations.

8.1.6.4 Ex: Gauges of dipolar potentials

Verify that the retarded potentials of an oscillating dipole,

$$\Phi(r,\theta,t) = \frac{p_0\cos\theta}{4\pi\varepsilon_0 r}\left\{-\frac{\omega}{c}\sin[\omega(t-r/c)] + \frac{1}{r}\cos[\omega(t-r/c)]\right\}$$
$$\mathbf{A}(r,\theta,t) = -\frac{\mu_0 p_0\omega}{4\pi r}\sin[\omega(t-r/c)]\hat{\mathbf{e}}_z \ ,$$

satisfy the Lorentz gauge.

8.1.6.5 Ex: Electric and magnetic fields of an oscillating electric dipole

Calculate the electric and magnetic fields of an oscillating electric dipole in the dipolar approximation ($kr' \ll 1$) but for arbitrary distances ($kr \lesseqgtr 1$) directly from the retarded potentials in spherical coordinates. Find the Poynting vector and show that the radiation intensity is exactly the same, as the one derived within the far-field approximation ($kr \gg 1$).

8.1.6.6 Ex: Electric and magnetic fields of an oscillating magnetic dipole

Calculate the electric and magnetic fields of an oscillating magnetic dipole in the dipolar approximation ($kr' \ll 1$), but for arbitrary distances ($kr \lesseqgtr 1$) directly from the retarded potentials in spherical coordinates. Compare with the fields of an oscillating electric dipole. Find the Poynting vector and show that the intensity of the radiation is exactly the same, as the one derived within the far-field approximation ($kr \gg 1$).

8.1.6.7 Ex: Spherical harmonics

The spherical harmonic function for $\ell = 2$ and $m = 1$ has the form,

$$Y_{21}(\vartheta,\varphi) = \sqrt{\tfrac{15}{8\pi}} \sin\vartheta\cos\vartheta(\cos\varphi + \imath\sin\varphi) \ .$$

Express the quadrupolar momentum q_{21} as a linear combination in Cartesian coordinates,

$$Q_{ij} = \int \rho(\mathbf{r})(3x_ix_j - \delta_{ij}r^2)\ dr^3 \ .$$

8.1.6.8 Ex: Vector spherical harmonics

Calculate the angular distribution of $E1$ and $M1$ radiation.

8.2 Radiation of point charges

The fundamental structure of matter is based on electromagnetic forces: Electrons are bound to nuclei by the Coulomb-Lorentz force, the orbital motion of the electrons produces magnetic fields, which can interact with the intrinsic spins of electrons and nuclei, external electromagnetic fields can influence the motion of electrons. Therefore, it is of primary interest to understand the radiation emitted by accelerated point-like electric charges.

8.2.1 Power radiated by an accelerated point charge

We derived in an earlier chapter the fields (6.140) and (6.141) produced by an arbitrary moving charge,

$$\vec{\mathcal{E}}(\mathbf{r},t) = \frac{q}{4\pi\varepsilon_0}\frac{R}{(\mathbf{R}\cdot\mathbf{u})^3}[(c^2-v^2)\mathbf{u} + \mathbf{R}\times(\mathbf{u}\times\mathbf{a})] \tag{8.95}$$
$$\vec{\mathcal{B}}(\mathbf{r},t) = \tfrac{1}{c}\mathbf{R}\times\vec{\mathcal{E}}(\mathbf{r},t) \ ,$$

with $\mathbf{u} = c\hat{\mathbf{e}}_r - \mathbf{v}$. We call the first term in (8.95) *velocity field* and the second *acceleration field*. The Poynting vector is,

$$\vec{\mathcal{S}} = \tfrac{1}{\mu_0}(\vec{\mathcal{E}}\times\vec{\mathcal{B}}) = \tfrac{1}{\mu_0 c}[\vec{\mathcal{E}}\times(\mathbf{R}\times\vec{\mathcal{E}})] = \tfrac{1}{\mu_0 c}[\mathcal{E}^2\hat{\mathbf{e}}_r - (\hat{\mathbf{e}}_r\cdot\vec{\mathcal{E}})\vec{\mathcal{E}}] \ . \tag{8.96}$$

However, not all of this energy flow constitutes radiation; part of it is field energy *transported* by the particle as it moves. The *radiated* energy is the part that separates from the charge and propagates to infinity. To calculate the total power radiated by the particle at time t_r we draw a large sphere of radius R, centered on the position of the particle at time t_r, we wait for the appropriate interval,

$$t - t_r \equiv \frac{R}{c} \, , \tag{8.97}$$

for the radiation to reach the sphere and, at that moment, we integrate the Poynting vector on the surface. The notation t_r points to the fact, that this is the retarded time for all points on the sphere at time t. Now, the area of the sphere is proportional to R^2, hence any term in $\vec{\mathcal{S}}$ that goes like $1/R^2$ will produce a finite response, but terms like $1/R^3$ or $1/R^4$ will not contribute in the limit $R \to \infty$. For this reason, only the acceleration field truly radiates:

$$\vec{\mathcal{E}}_{rad} = \frac{q}{4\pi\varepsilon_0} \frac{R}{(\mathbf{R}\cdot\mathbf{u})^3} [\mathbf{R} \times (\mathbf{u} \times \mathbf{a})] \, . \tag{8.98}$$

Since $\vec{\mathcal{E}}_{rad} \perp \mathbf{R}$, the second term in Eq. (8.96) disappears:

$$\vec{\mathcal{S}}_{rad} = \frac{1}{\mu_0 c} \vec{\mathcal{E}}^2_{rad} \hat{\mathbf{e}}_r \, . \tag{8.99}$$

Example 87 (*Radiation at the turning point*): If at time t_r the charge is instantaneously at rest, $\mathbf{v}(t_r) = 0$, for example at the turning points of a harmonic oscillation, then $\mathbf{u} = c\hat{\mathbf{e}}_r$, and,

$$\vec{\mathcal{E}}_{rad} = \frac{q}{4\pi\varepsilon_0 c^2 R} [\hat{\mathbf{e}}_r \times (\hat{\mathbf{e}}_r \times \mathbf{a})] = \frac{\mu_0 q}{4\pi R} [(\hat{\mathbf{e}}_r \cdot \mathbf{a})\hat{\mathbf{e}}_r - \mathbf{a}] \, . \tag{8.100}$$

In this case,

$$\vec{\mathcal{S}}_{rad} = \frac{1}{\mu_0 c} \left(\frac{\mu_0 q}{4\pi R}\right)^2 [a^2 - (\hat{\mathbf{e}}_r \cdot \mathbf{a})^2] \hat{\mathbf{e}}_r = \frac{\mu_0 q^2 a^2}{16\pi^2 c} \frac{\sin^2\theta}{R^2} \, , \tag{8.101}$$

where θ is the angle between $\hat{\mathbf{e}}_r$ and $\mathbf{a}$. No power is radiated in forward or backward directions. Instead, it is emitted in a torus around the instantaneous acceleration, as shown in Fig. 8.5(a).
The total radiated power is evidently,

$$P = \oint \vec{\mathcal{S}}_{rad} \cdot d\mathbf{S} = \frac{\mu_0 q^2 a^2}{16\pi^2 c} \int \frac{\sin^2\theta}{R^2} R^2 \sin\theta d\theta d\phi = \frac{\mu_0 q^2 a^2}{6\pi c} \, . \tag{8.102}$$

This, again, is the *Larmor formula*, which we previously obtained via another route (8.19). Although derived under the assumption that $v = 0$, the equations (8.101) and (8.102) represent a good approximation, since $v \ll c$.

An exact treatment of the case $v \neq 0$ is more difficult for two reasons. The first obvious reason is, that $\vec{\mathcal{E}}_{rad}$ is more complicated, and the second more subtle reason is that $\vec{\mathcal{S}}_{rad}$, which is the rate at which energy passes through the sphere, is not equal to the rate at which the energy separated from the particle. Suppose someone is throwing a stream of bullets through the window of a moving car. The rate N_t at which the bullets hit a stationary target is not the same as the rate N_g at which they left the weapon, because of the movement of the car. In fact, we can easily verify that $N_g = (1 - v/c)N_t$, if the car is moving toward the target, and,

$$N_g = \left(1 - \tfrac{\hat{\mathbf{e}}_r \cdot \mathbf{v}}{c}\right) N_t \tag{8.103}$$

for arbitrary directions (here v is the speed of the car, c is the velocity of the bullets, and $\mathbf{R}$ is a unit vector pointing from the car towards the target). In our case, if dW/dt is the rate at which energy passes through the sphere of radius R, then the rate at which the energy separated from the charge was,

$$\frac{dW}{dt_r} = \frac{dW/dt}{\partial t_r/\partial t} \,. \tag{8.104}$$

We calculate the denominator from the relation (8.97),

$$\begin{aligned}\frac{\partial t_r}{\partial t} &= 1 - \frac{\partial\sqrt{[\mathbf{r}-\mathbf{w}(t_r)]^2}}{c\partial t} = 1 - \frac{-2[\mathbf{r}-\mathbf{w}(t_r)]}{2c\sqrt{[\mathbf{r}-\mathbf{w}(t_r)]^2}} \cdot \frac{\partial \mathbf{w}(t_r)}{\partial t_r}\frac{\partial t_r}{\partial t} \\ &= 1 + \frac{\mathbf{R}}{cR}\cdot\mathbf{v}\frac{\partial t_r}{\partial t} = \frac{1}{1-\hat{\mathbf{e}}_R\cdot\mathbf{v}/c} = \frac{cR}{\mathbf{R}\cdot\mathbf{u}} \,.\end{aligned} \tag{8.105}$$

This factor is precisely that of the relation (8.103) between N_g and N_t; is a purely geometric factor (the same as in the Doppler effect).

Therefore, the power radiated by the particle into an area element, $R^2\sin\theta d\theta d\phi = R^2 d\Omega$ of the sphere is, using the Poynting vector (8.99) and the radiated field (8.98), given by,

$$\frac{dP}{d\Omega} = \frac{\vec{\mathcal{S}}_{rad}}{\partial t_r/\partial t} = \frac{\mathbf{R}\cdot\mathbf{u}}{Rc}\frac{1}{\mu_0 c}\vec{\mathcal{E}}^2_{rad}R^2 = \frac{q^2}{16\pi^2\varepsilon_0}\frac{|\hat{\mathbf{e}}_r\times(\mathbf{u}\times\mathbf{a})|^2}{(\hat{\mathbf{e}}_r\cdot\mathbf{u})^5} \,, \tag{8.106}$$

where $d\Omega = \sin\theta d\theta d\phi$ is the solid angle at which this energy is radiated. Integrating over θ and ϕ to obtain the total radiated power is not easy, such that we simply quote the answer:

$$\boxed{P = \frac{\mu_0 q^2\gamma^6}{6\pi c}\left(a^2 - \left|\frac{\mathbf{v}\times\mathbf{a}}{c}\right|^2\right)} \,, \tag{8.107}$$

where $\gamma \equiv 1/\sqrt{1-v^2/c^2}$. This is *Liénard's generalization* of Larmor's formula, to which it reduces when $v \ll c$. The factor γ^6 means that the radiated power increases enormously as the velocity of the particle approaches the speed of light.

Resolve the Excs. 8.2.3.1 to 8.2.3.5.

8.2.1.1 Bremstrahlung

Suppose that $\mathbf{v}$ and $\mathbf{a}$ be instantaneously collinear (at time t_r), such as for a motion on a straight line. In this case $\mathbf{u}\times\mathbf{a} = (c\hat{\mathbf{e}}_r - \cancel{\mathbf{v}}^{0})\times\mathbf{a}$, then the angular distribution of radiation (8.106) gives,

$$\frac{dP}{d\Omega} = \frac{q^2c^2}{16\pi^2\varepsilon_0}\frac{|\hat{\mathbf{e}}_r\times(\hat{\mathbf{e}}_r\times\mathbf{a})|^2}{(c-\hat{\mathbf{e}}_r\cdot\mathbf{v})^5} \,. \tag{8.108}$$

Now with $|\hat{\mathbf{e}}_r\times(\hat{\mathbf{e}}_r\times\mathbf{a})| = a\sin\theta$ and letting $\mathbf{v}\equiv v\hat{\mathbf{e}}_z$,

$$\frac{dP}{d\Omega} = \frac{\mu_0 q^2 a^2}{16\pi^2 c}\frac{\sin^2\theta}{(1-\beta\cos\theta)^5} \,, \tag{8.109}$$

where $\beta \equiv v/c$. This is consistent with the result (8.101), in the case $v = 0$. However, for very large v ($\beta \approx 1$), the torus of the radiation illustrated in Fig. 8.5(a) is stretched and pushed forward by a factor $(1-\beta\cos\theta)^{-5}$, as indicated in Fig. 8.5(b). Although there is still no radiation in the exact forward direction, most of the radiation is concentrated in an increasingly narrow cone around the forward direction.

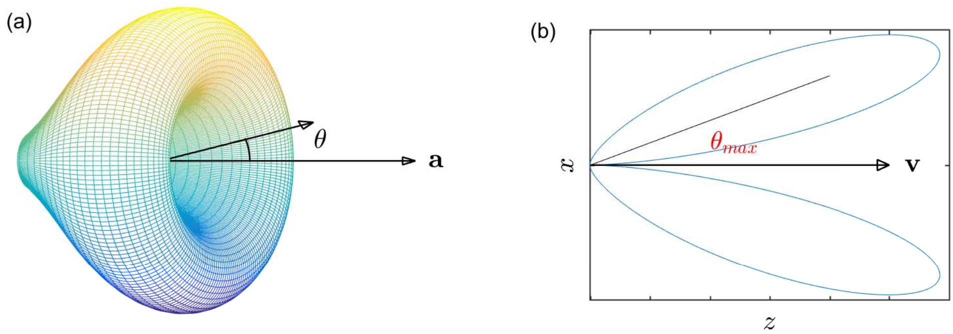

Figure 8.5: (code) (a) Radiation pattern of an accelerated charge. (b) Angular distribution of the bremsstrahlung.

The total emitted power is found by integrating equation (8.110) over all angles:

$$P = \int \frac{dP}{d\Omega}d\Omega = \frac{\mu_0 q^2 a^2}{16\pi^2 c}\int \frac{\sin^2\theta}{(1-\beta\cos\theta)^5}\sin\theta d\theta d\phi \tag{8.110}$$
$$= \frac{\mu_0 q^2 a^2}{8\pi c}\int_{-1}^{+1}\frac{1-x^2}{(1-\beta x)^5}dx = \frac{\mu_0 q^2 a^2}{8\pi c}\tfrac{4}{3}(1-\beta^2)^{-3} = \frac{\mu_0 q^2 a^2 \gamma^6}{6\pi c} \ .$$

This result is consistent with the Liénard's formula (8.107), for the case when **v** and **a** are collinear. Note that the angular distribution of radiation is the same, whether the particle is accelerating or decelerating; it does not depend on **a**, but only on velocity being concentrated in forward direction (with respect to the velocity) in both cases. When a high-speed electron hits a metal target, it decelerates rapidly, releasing what is called bremsstrahlung. This example is essentially the classical theory of *bremsstrahlung*.

We will calculate the *synchrotron radiation* in Exc. 8.2.3.6 and the *Cherenkov radiation* in Exc. 8.2.3.7. A movie illustrating the Cherenkov radiation emission can be viewed at (watch movie).

Example 88 (*Bremsstrahlung of thermal electrons*): The power lost by bremsstrahlung for not extremely relativistic velocities is,

$$P = \frac{\mu_0 q^2 a^2 \gamma^2}{6\pi c} \simeq \frac{\mu_0 q^2 a^2}{6\pi c} \ ,$$

such that,

$$\vec{\mathcal{E}}_{rad} = \int_0^t P dt = \frac{\mu_0 q^2 a^2}{6\pi c}\int_{v_0}^0 \frac{dv}{\dot{v}} = \frac{\mu_0 q^2 a}{6\pi c}\int_{v_0}^0 dv = \frac{\mu_0 q^2 a}{6\pi c}v_0 \ .$$

For an electron in a metal with a free path of $d \approx 3$ nm and a thermal velocity $v_0 = 100000$ m/s the deceleration $a = \frac{v_0^2}{2d}$ leads to a negligible radiated fraction,

$$\frac{\vec{\mathcal{E}}_{rad}}{E_{kin}} = \frac{\frac{\mu_0 q^2 a}{6\pi c} v_0}{\frac{m}{2} v_0^2} = \frac{\mu_0 q^2 a}{3\pi c m v_0} = \frac{\mu_0 q^2}{3\pi c m} \frac{v_0}{2d} \approx 2 \cdot 10^{-10} .$$

8.2.2 Radiation reaction

According to the laws of classical electrodynamics, an accelerated charge radiates. This radiation takes energy, which must come at the expense of the particle's kinetic energy. Under the influence of a given force, therefore, a charged particle accelerates less than a neutral particle of the same mass. The radiation evidently exerts a reactive force $\mathbf{F}_{rad}$ corresponding to a recoil. We will now derive the *radiation reaction* force from energy conservation.

For a non-relativistic particle ($v \ll c$), the total radiated power P is given by the *Larmor formula* (8.102). The conservation of energy suggests that this is also the rate at which the particle loses energy, under the influence of the radiative reaction force $\mathbf{F}_{rad}$:

$$\mathbf{F}_{rad} \cdot \mathbf{v} \overset{?}{=} -\frac{\mu_0 q^2 a^2}{6\pi c} = -P . \tag{8.111}$$

However, this equation is really wrong. For, to derive Larmor's formula, we calculated the radiated power by integrating the Poynting vector on a sphere of 'infinite' radius; in this calculation the velocity fields *did not contribute*, since they fall off very rapidly as a function of R. However, the velocity fields *carry* energy; they simply do not carry it to infinity. As the particle accelerates and decelerates, it exchanges energy with the velocity fields, while another part of the energy is irremediably radiated away by the acceleration fields. The equation (8.111) only takes into account this lost energy, but if we want to know the recoil force exerted by the fields on the charge, we must consider the power lost at each instant of time, not only the radiatively escaping power. (In this sense the term 'radiation reaction' is misleading and should be replaced by 'field reaction'.) In fact, we shall see shortly that F_{rad} is determined by the time derivative of the acceleration and can be nonzero, even if the acceleration is instantaneously zero, such that the particle does not radiate.

The energy lost by the particle during a given time interval, therefore, must equal the energy carried away by radiation plus the extra energy that has been pumped into the velocity fields. However, if we agree to consider only time intervals $[t_1, t_2]$ over which the *system returns to its initial state*, then the energy in the velocity fields is the same at both times, and the only loss is through radiation. Thus, equation (8.111), while instantly incorrect, is valid on average:

$$\int_{t_1}^{t_2} \mathbf{F}_{rad} \cdot \mathbf{v} dt = -\frac{\mu_0 q^2}{6\pi c} \int_{t_1}^{t_2} a^2 dt , \tag{8.112}$$

with the stipulation that the state of the system is identical at times t_1 and t_2. In the case of periodic movements, for example, we must integrate over a total number of complete cycles. Now, the right-hand side of the equation (8.112) can be integrated by parts:

$$\int_{t_1}^{t_2} \mathbf{a}^2 dt = \mathbf{v} \cdot \frac{d\mathbf{v}}{dt}\Big|_{t_1}^{t_2} - \int_{t_1}^{t_2} \frac{d^2\mathbf{v}}{dt^2} \cdot \mathbf{v} dt \ . \tag{8.113}$$

The boundary term cancels, since the velocities and accelerations are identical at t_1 and t_2, then the equation (8.112) can be written in an equivalent way as,

$$\int_{t_1}^{t_2} \left(\mathbf{F}_{rad} - \frac{\mu_0 q^2}{6\pi c} \dot{\mathbf{a}} \right) \cdot \mathbf{v} dt = 0 \ . \tag{8.114}$$

This equation will certainly be satisfied if,

$$\boxed{\mathbf{F}_{rad} = \frac{\mu_0 q^2}{6\pi c} \dot{\mathbf{a}}} \ . \tag{8.115}$$

This is the *Abraham-Lorentz formula* for the radiation reaction force. Obviously, the equation (8.114) does not prove (8.115), because it does not say anything about the component of $\mathbf{F}_{rad}$ perpendicular to $\mathbf{v}$; and only informs us on the time-average of the parallel component for, moreover, very special time intervals.

The Abraham-Lorentz formula has disturbing implications, which are not fully understood nearly a century after the law was first proposed. Let us assume that a particle is not subject to external forces; then Newton's second law tells us,

$$F_{rad} = \frac{\mu_0 q^2}{6\pi c} \dot{a} = ma \ , \tag{8.116}$$

yielding,

$$a(t) = a_0 e^{t/\tau} \qquad \text{with} \qquad \tau = \frac{\mu_0 q^2}{6\pi mc} \ . \tag{8.117}$$

In the case of an electron, $\tau = 6 \cdot 10^{-24}$ s. The acceleration increases spontaneously exponentially with time! This absurd conclusion can be avoided, if we insist that $a_0 = 0$. But it turns out, that the systematic exclusion of such catastrophic solutions has an even more unpleasant consequence: if we now *switch on* an external force, the particle begins to respond to it *before it actually has been switch on* (see Exc. 8.2.3.8 and 8.2.3.9).

Example 89 (*Radiative damping*): Here, we calculate the radiative damping rate τ of a charged particle fixed to a spring by solving the equation of motion,

$$m\ddot{x} = F_{sprng} + F_{rad} + F_{excit} = -m\omega_0^2 x + m\tau \dddot{x} + F_{excit} \ .$$

With the oscillating system, $x(t) = x_0 \cos(\omega t + \delta)$, we have,

$$\dddot{x} = -\omega^2 \dot{x} \ .$$

Therefore,

$$m\ddot{x} + m\omega^2 \tau \dot{x} + m\omega_0^2 x = F_{excit} \ ,$$

and the damping factor is given by $\omega^2 \tau$.

Example 90 (*Radiation reaction*): In previous chapters, the problems of electrodynamics were divided into two classes: one class in which the charge and current sources are specified and the resulting electromagnetic fields are calculated, and the other class in which external electromagnetic fields are specified and the motion of charged particles of currents are calculated. Occasionally, as in the discussion of the bremsstrahlung, the two problems are combined. But the treatment is recursive: first, the motion of a charged particle in an external field is determined neglecting the radiation it emits; then the radiation of the particle is calculated from its (accelerated) trajectory treating the particle as a source of charge and current.

Obviously, this way of dealing with electrodynamical problems can only be approximate. The (accelerated) motion of charged particles within force fields necessarily involves the emission of radiation, removing energy, angular momentum, and momentum from the particles and thus influencing their subsequent motion. Consequently, the motion of radiation sources is (partially) determined by the emission of radiation, and a correct treatment must take account of the reaction of the radiation onto the motion of the sources. Fortunately, for many problems of electrodynamics the radiative reaction is negligibly small. On the other hand, there exists no completely satisfactory classical treatment. The difficulties presented by this problem touch upon fundamental aspects of physics, such as the nature of elementary particles. Nevertheless, there are viable partial solutions with limited regimes of validity. In quantum mechanics, the introduction of renormalization techniques was able to solve the divergences within the theory of *quantum electrodynamics* (QED).

In order to give a gross idea of 'radiative reaction', let us consider a charge q of a point particle distributed in space. For simplicity we choose 'sub-charges' $\frac{q}{2}$ located at two positions $\mathbf{d}_{1,2} = \pm\frac{d}{2}\hat{\mathbf{e}}_y$ and moving in an accelerated way in x-direction, that is, $\mathbf{a} = a\hat{\mathbf{e}}_x$. Only after the calculations will we go to the limit $d \to 0$. So with (6.140) we obtain for the electric field generated by the charge 2 at the place of the charge 1,

$$\begin{aligned}\vec{\mathcal{E}}_1(\mathbf{r},t) &= \frac{q/2}{4\pi\varepsilon_0}\frac{R}{(\mathbf{R}\cdot\mathbf{u})^3}[(c^2-v^2)\mathbf{u}+\mathbf{R}\times(\mathbf{u}\times\mathbf{a})] \\ &= \frac{q/2}{4\pi\varepsilon_0}\frac{R}{(\mathbf{R}\cdot\mathbf{u})^3}[(c^2-v^2+\mathbf{R}\cdot\mathbf{a})\mathbf{u}-\mathbf{a}(\mathbf{R}\cdot\mathbf{u})]\ .\end{aligned}$$

Now, we assume that the charge be instantly at rest, $\mathbf{v} = 0$, that is, $\mathbf{u} \equiv c\hat{\mathbf{e}}_r - \mathbf{v} = c\hat{\mathbf{e}}_r$. In Cartesian coordinates, $\mathbf{R} \equiv l\hat{\mathbf{e}}_x + d\hat{\mathbf{e}}_y$, where $l \equiv x(t) - x(t_r)$ is the distance between the actual position and the retarded position, we can write the x-component of the electric field as,

$$\vec{\mathcal{E}}_{x,1} = \frac{q/2}{4\pi\varepsilon_0}\frac{R}{c^3R^3}[(c^2+\mathbf{R}\cdot\mathbf{a})u_x-(\mathbf{R}\cdot\mathbf{u})a_x] = \frac{q}{8\pi\varepsilon_0c^2}\frac{c^2l-d^2a}{\sqrt{l^2+d^2}^3}\ .$$

By symmetry, $\vec{\mathcal{E}}_{x,1} = \vec{\mathcal{E}}_{x,2}$, such that the force on the dumbbell is,

$$\mathbf{F}_{self} = \frac{q}{2}(\vec{\mathcal{E}}_1+\vec{\mathcal{E}}_2) = \frac{q}{8\pi\varepsilon_0c^2}\frac{c^2l-d^2a}{\sqrt{l^2+d^2}^3}\hat{\mathbf{e}}_x\ .$$

Now, we expand l in terms of the retarded time,

$$l = x(t_r+T) - x(t_r) = \cancelto{0}{vT} + \tfrac{1}{2}aT^2 + \tfrac{1}{6}\dot{a}T^3 + \dots\ ,$$

such that,

$$d = \sqrt{(cT)^2 - l^2} = cT\sqrt{1 - \left(\tfrac{aT}{2c} + \tfrac{\dot{a}T^2}{6c} + ...\right)^2} = cT - \frac{a^2}{8c}T^3 + ... \simeq cT - \frac{a^2}{8c}\left(\frac{d}{c}\right)^3 + ... ,$$

where we replaced, in the last step, the first order solution in the expansion, $T \simeq d/c$, for the third order. Resolving by T,

$$T \simeq \frac{d}{c} + \frac{a^2 d^3}{8c^5} .$$

and inserting into the expansion of l,

$$l \simeq \frac{1}{2}a\left(\frac{d}{c} + \frac{a^2 d^3}{8c^5}\right)^2 + \frac{1}{6}\dot{a}\left(\frac{d}{c} + \frac{a^2 d^3}{8c^5}\right)^3 + ... \simeq \frac{1}{2}a\left(\frac{d}{c}\right)^2 + \frac{1}{6}\dot{a}\left(\frac{d}{c}\right)^3 .$$

With this we obtain for reaction force,

$$\mathbf{F}_{self} \simeq \frac{q}{8\pi\varepsilon_0 c^2}\frac{c^2 l - d^2 a}{\sqrt{l^2 + d^2}^3}\hat{\mathbf{e}}_x \simeq \frac{q}{8\pi\varepsilon_0 c^2}\frac{c^2\left(\frac{1}{2}a\left(\frac{d}{c}\right)^2 + \frac{1}{6}\dot{a}\left(\frac{d}{c}\right)^3\right) - d^2 a}{\sqrt{(..)d^4 + d^2}^3}\hat{\mathbf{e}}_x$$
$$\simeq \frac{q}{4\pi\varepsilon_0 c^2}\left(-\frac{a}{4d} + \frac{\dot{a}}{12c}\right)\hat{\mathbf{e}}_x ,$$

considering that d is small. The acceleration is still expressed in terms of the retarded time, but this is easily remedied by,

$$a(t_r) = a(t) + \dot{a}(t)(t - t_r) = a(t) - \dot{a}(t)\frac{d}{c} .$$

Inserting into the force,

$$\mathbf{F}_{self} \simeq \frac{q}{4\pi\varepsilon_0 c^2}\left(-\frac{a}{4d} + \frac{\dot{a}}{12c}\right)\hat{\mathbf{e}}_x = \frac{q}{4\pi\varepsilon_0}\left(-\frac{a(t)}{4c^2 d} - \frac{-\dot{a}(t)}{4c^3} + \frac{\dot{a}(t)}{12c^3}\right)\hat{\mathbf{e}}_x$$
$$= \frac{q}{4\pi\varepsilon_0}\left(\frac{a(t)}{4c^2 d} + \frac{\dot{a}(t)}{3c^3}\right)\hat{\mathbf{e}}_x .$$

Finally,

$$\mathbf{F} = m_{tot}a + \mathbf{F}_{rad} = \left(m_0 + \frac{1}{4\pi\varepsilon_0}\frac{q^2}{4dc^2}\right)\mathbf{a} + \frac{\mu_0 q^2 \dot{\mathbf{a}}}{12\pi c} ,$$

where m_0 is the sum of the two partial masses. We retrieve the Abraham-Lorentz formula by the second term. The missing factor of 2, when compared to (8.116), comes from the fact that we only consider the mutual reactions of partial charges. The expression in the parentheses corresponds to a correction of the inertial mass of the particle due to the Coulombian repulsion between the charges.

8.2.3 Exercises

8.2.3.1 Ex: Radiation emitted by a rotating electron

A particle with charge q moves with constant angular velocity ω in a circular orbit with radius R around the origin in the plane x-y. Its trajectory therefore is,

$$\mathbf{R}'(t) = R(\hat{\mathbf{e}}'_x \cos\omega t + \hat{\mathbf{e}}'_y \sin\omega t) .$$

a. Calculate the associated (temporary) charge density $\varrho(\mathbf{r}', t)$ and the dipole moment using the general rule,

$$\mathbf{d}(t) = \int \mathbf{r}' \varrho(\mathbf{r}', t) d^3\mathbf{r}' \ .$$

b. The rotating particle can be seen as a source of radiation. At a point $\mathbf{r}$ far from this source, in the dipole approximation, the associated electromagnetic fields are given by,

$$\vec{\mathcal{B}} = \tfrac{\mu_0}{4\pi cr} \hat{\mathbf{e}}_r \times \ddot{\mathbf{d}} \qquad \text{respectively} \qquad \vec{\mathcal{E}} = c\vec{\mathcal{B}} \times \hat{\mathbf{e}}_r \ .$$

Calculate the Poynting vector,

$$\vec{\mathcal{S}} = \tfrac{1}{\mu_0} \vec{\mathcal{E}} \times \vec{\mathcal{B}}$$

as well as its component $\mathcal{S}_n \equiv \hat{\mathbf{e}}_r \cdot \vec{\mathcal{S}}$ in the direction of the point $\mathbf{r}$. **Help:** Use the formula $\mathbf{a} \times \mathbf{b} \times \mathbf{c} = \mathbf{b}(\mathbf{a} \cdot \mathbf{c}) - \mathbf{c}(\mathbf{a} \cdot \mathbf{b})$.
c. Now calculate the time average of $\mathcal{S}_n$ over an orbit of the particle, that is, calculate $\bar{\mathcal{S}}_n = \int dt \mathcal{S}_n \ / \ \int dt$ with the two integrals taken between $t = 0$ and $t = 2\pi/\omega$. Express the result in spherical coordinates, so that $r^2 \bar{\mathcal{S}}_n$ is precisely the average power radiated to the solid angle element $d\Omega$ in the direction $\mathbf{r}$. Now integrate over the entire solid angle and evaluate the total emitted power P.

8.2.3.2 Ex: Rutherford's atom model

In Rutherford's 'classical' atom model a hydrogen atom is described by an electron (charge $-e$) orbiting a nucleus (charge $+e$) in a circular trajectory with constant angular velocity ω. The equilibrium condition is chosen so that the Coulomb force and the centrifugal force compensate each other. However, according to the Exc. 8.2.3.1, such an electron represents a source of radiation. The radiated power decreased the energy of the electron [$dE/dt = -P$ with P taken from Exc. 8.2.3.1(c)]. Derive a differential equation for the temporal variation of the radius $R(t)$ of the electronic orbit, and integrate it with the boundary conditions $t_0 = 0$ and $R(t_0) = a_B$, where $a_B = 0.53 \times 10^{-8}$ cm is the Bohr radius. After what time T do we get $R(T) = 0$?

8.2.3.3 Ex: Dynamics of charged point particles

Consider a point particle with charge q and mass m and general electromagnetic fields in vacuum, $\vec{\mathcal{E}}(\mathbf{r}, t)$ and $\vec{\mathcal{B}}(\mathbf{r}, t)$, which are not perturbed neither by the charge nor the current resulting from the particle's motion. On the particle acts the Coulomb-Lorentz force.
a. What are the equations of motion for the particle? What is the temporal variation of its total kinetic energy? What condition must be satisfied to ensure that the kinetic energy of the particle is temporally constant?
b. We now consider homogeneous fields $\vec{\mathcal{E}}(\mathbf{r}, t) = \mathcal{E}_0 \hat{\mathbf{e}}_z$ and $\vec{\mathcal{B}}(\mathbf{r}, t) = \mathcal{B}_0 \hat{\mathbf{e}}_z$. What are the equations of motion now?
c. The particle is at time $t = 0$ at the origin of the coordinate system and has the velocity $\mathbf{v}_0$. Solve the equations of motion. **Help:** Use the complex variable $\eta = x + \imath y$ and add the equations of motion to obtain a complex equation motion for η of the type $\ddot{\eta} = -\imath\omega\dot{\eta}$ with $\omega = q\vec{\mathcal{B}}_0/(mc)$.
d. How does the kinetic energy of the particle vary over time?

8.2.3.4 Ex: Excitation of an electron by circularly polarized light

Derive the expression for the dipole radiation from the Maxwell equations proceeding in the following way:
a. Derive the equation of motion of a point particle of charge q and mass m in an electromagnetic field ($\vec{\mathcal{E}}$, $\vec{\mathcal{B}}$) neglecting the emission of radiation by the moving charge. Determine the temporal variation of the particle's energy W inside the external field.
b. A circularly polarized monochromatic wave in vacuum is described by the electric field, $\vec{\mathcal{E}}(\mathbf{r},t) = \mathcal{E}[\cos(kz-\omega t)\hat{\mathbf{e}}_x + \sin(kz-\omega t)\hat{\mathbf{e}}_y]$. Calculate the corresponding magnetic field $\vec{\mathcal{B}}(\mathbf{r},t)$.
c. Calculate the Poynting vector $\vec{\mathcal{S}}(\mathbf{r},t)$.
d. For an energy flux of the electromagnetic wave of $10\,\mathrm{W/m^2}$ calculate the amplitudes of the electric and the magnetic field.
e. For the particle of part (a) moving in the fields of part (b) establish the equation of motion.
f. Initially ($t=0$) the particle is at the origin of the coordinate system. How should the initial condition for the velocity be chosen in order to obtain a constant energy for the particle?
g. Determine the momentum $\mathbf{p}$ of the particle and verify that $\mathbf{p}_\perp = p_x\hat{\mathbf{e}}_x + p_y\hat{\mathbf{e}}_y$ coincides at every instant of time with the direction of $\vec{\mathcal{B}}$.
h. Solve the equation of motion with the initial conditions of part (d).
i. What is the form of the particle's trajectory in the x-y plane?

8.2.3.5 Ex: Charge and current densities for radiative atomic transitions

The charge and current densities for radiative atomic transitions from the state $m=0$, $2p$ of hydrogen to the ground state $1s$, are (neglecting the spin),

$$\varrho(r,\theta,\phi,t) = \frac{2e}{\sqrt{6}a_B^4} r e^{-3r/2a_B} Y_{00}Y_{10}e^{-\imath\omega_0 t} \quad , \quad \mathbf{j}(r,\theta,\phi,t) = -\imath v_0\left(\frac{\hat{\mathbf{e}}_r}{2} + \frac{a_B}{z}\hat{\mathbf{e}}_z\right)\varrho(r,\theta,\phi,t) \ ,$$

where $v_0 = \alpha c$ is the orbital velocity of the electron, a_B the Bohr radius, and α the Sommerfeld constant.
a. Show that the effective transitional orbital 'magnetization' is,

$$\vec{\mathcal{M}}_{ef}(r,\theta,\phi,t) = -\imath\frac{\alpha c a_B}{2}\tan\theta(\hat{\mathbf{e}}_x\sin\phi - \hat{\mathbf{e}}_y\cos\phi)\varrho(r,\theta,\phi,t) \ .$$

Calculate $\nabla\cdot\vec{\mathcal{M}}_{ef}$ and evaluate the electric and magnetic dipole moments.
b. In the electric dipole approximation, calculate the temporal average of the total radiated power. Express your response in units of $(\hbar\omega_0)(\alpha^4 c/a_B)$.
c. Interpreting the classically calculated power as the energy of a photon ($\hbar\omega_0$) times the transition probability, numerically evaluate the transition probability in units of reciprocal seconds.
d. If, instead of the semiclassic charge density used above, the electron in the $2p$ state is described by a circular Bohr orbit of radius $2a_B$, rotating with the transition frequency ω_0, what would be the radiated power? Express your answer in the same units as in part (b), and evaluate the ratio of the two powers numerically.

8.2.3.6 Ex: Synchrotron radiation

In the discussion of the Bremsstrahlung in class we assumed that the velocity and the acceleration were (at least instantaneously) *collinear*. Do the same analysis for the case, that they are *perpendicular*. Choose your axes so that v is along the z-axis and a along the x-axis (see Fig. 8.5), such that $\mathbf{v} = v\hat{\mathbf{e}}_z$, $\mathbf{a} = \hat{\mathbf{e}}_x$ and $\mathbf{R} = \sin\theta\cos\phi\hat{\mathbf{e}}_x + \sin\theta\sin\phi\hat{\mathbf{e}}_y + \cos\theta\hat{\mathbf{e}}_z$. Verify whether P is consistent with the Liénard formula.

8.2.3.7 Ex: Cherenkov radiation

Cherenkov radiation is observed, when a charge moves with relativistic velocity within a dielectric medium, which reduces the speed of light below the velocity of the particle. A blue superluminal shock wave is then formed.
a. Calculate the angle θ_c between the propagation direction of the charge and the propagation direction of the shock wavefront.
b. We now imagine the deceleration process of the charge inside the dielectric as being due to a collision with a heavy molecule of the dielectric material. The collision creates a photon emitted under the angle θ_c and the momentum of charge is deflected. We despise the recoil of the molecule. Based on relativistic energy and momentum conservation, calculate the angle θ_c in terms of the momenta of charge before and after the collision and of the radiated frequency.
c. Comparing the results obtained in (a) and (b), calculate the rest mass of the charge.
d. Calculate the retarded Liénard-Wiechert potentials inside and outside of the cone.

8.2.3.8 Ex: Electron subject to gravity

An electron is released from rest and falls under the influence of gravity. Within the first centimeter, what fraction of the lost potential energy is radiated?

8.2.3.9 Ex: Radiation reaction

Including the radiative reaction force (8.115), Newton's second law for a charged particle becomes,

$$a = \tau\dot{a} + \frac{F}{m} \ ,$$

where F is an external force acting on the particle.
a. In contrast to the case of an uncharged particle ($a = F/m$), the acceleration (in the same way as position and velocity) must be a continuous function of time, even when the force changes abruptly. (Physically, the radiative reaction dampens out any rapid variation in a.) Show that a is continuous at any time t by integrating the given equation of motion between $(t-\epsilon)$ and $(t+\epsilon)$ and evaluating the limit $\epsilon \to 0$.
b. A particle be subjected to a constant force F, beginning at time $t = 0$ and remaining until the time T. Find the most general solution $a(t)$ of the equation of motion in each of the three stages: (i) $t < 0$; (ii) $0 < t < T$; and (iii) $t > T$.
c. Impose the continuity condition (a) at times $t = 0$ and $t = T$. Show, that it is possible to *either* eliminate 'runaway-acceleration' in region (iii) *or* avoid 'pre-acceleration' in region (i), but not both.

d. Choosing to eliminate the runaway-acceleration, what will be the acceleration, as a function of time, in each stage (i-iii)? How will the velocity behave, which obviously must be continuous at $t = 0$ and $t = T$. Assume, that the particle was initially at rest: $v(-\infty) = 0$. Prepare schemes of $a(t)$ and $v(t)$ and compare with the behavior of a neutral particle.
e. Repeat (d) choosing the option to eliminate pre-acceleration.

8.3 Diffraction and scattering

Radiation (let us call it 'light' for simplicity) incident on a target (e.g. a charge and current distribution, a dielectric body, an atomic cloud, or anything else) will be absorbed, diffracted or scattered. In the absence of absorption, the entire incident energy must be re-emitted. Whether the re-emission process is best described by *diffraction* or *scattering* models depends on the wavelength λ of light in relation to the size of the target and its structure. When the target is small, we can treat the problem in the lowest (usually dipolar) multipolar order; for a target of comparable size with λ, a complete multipolar treatment is required, and in the limit of a large target, we can resort to semi-geometrical methods to explain deviations from geometric optics caused by diffraction.

The topic of diffraction and scattering is well covered in the literature [47]. Rather than reproducing these theories here, we will give in this course a brief introduction to the *coupled-dipoles model*. This model, which has received much attention in recent years, has proven capable, albeit renouncing of notions such as the refraction index, to give a microscopic view of many macroscopic scattering and diffraction phenomena.

8.3.1 Coupled dipoles model

The electrodynamics contained in Maxwell's macroscopic equations describes the interaction of light with matter characterized by a refractive index $n(\mathbf{r})$. The refractive index is understood as a continuous field, which fully describes the reaction of the target to incident light. On the other hand, we know how the microscopic constituents, that is, the atoms and molecules of the target material, react individually to incident light. In the simplest case, a two-level atom will absorb a photon carrying an electron to a higher orbit, and when the electron returns to the original state, it will emit a photon into an arbitrary direction, that is, isotropically in the time average.

The difficulty now resides in the linking of the macro- and microscopic images, illustrated in Fig. 8.6, to a complete theory. Indeed, all atoms or molecules in the crystal must *cooperate* in some way to generate a refractive index and macroscopic scattering phenomena described by the laws of Snellius, Lambert-Beer, or Ewald-Oseen [14]. The details of how this cooperation works are being studied in several laboratories around the world [82, 83, 26].

From a microscopic point of view, the refractive index is an artifact; it does not exist like an atom exists! Since Democritus' reflections on the nature of matter 350 years before Christ, we know that what does exist are 'atoms and empty space, the remainder is mere opinion'. The index of refraction can help us to simplify the description of how light interacts with macroscopic objects. But this does not always work, and in some circumstances even leads to paradoxical results, that are difficult

Figure 8.6: (Left) Macroscopic refraction and (right) microscopic scattering. See also (watch talk).

to resolve within Maxwell's theory of electromagnetism. This is, for example, the case of the famous Abraham and Minkowski dilemma, which since 1909, when these two physicists proposed different calculations for the photonic momentum inside a dielectric medium leading to different results, still gives rise to debates. But there are also other situations, where microscopic theory is able to describe phenomena beyond the macroscopic approximation of continuous media. These are phenomena due to disorder, such as Anderson's localization of light or the spontaneous synchronization of atomic dipoles in superradiance.

In the simplest version of the coupled-dipoles model we imagine the target as a (more or less dense) sample of point-like two-level atoms, so that the radiation of the atoms can be described in the dipolar limit, $a_B \ll \lambda$, where the Bohr radius gives a typical scale for the extension of the radiation source. We will not reproduce integrally the derivation of the coupled-dipoles model here, which borrows from the theory of quantum mechanics. Instead, we will superficially trace the line of argumentation and justify the results by showing that, in the limit of a smooth distribution of the atomic scatterers, we recover the classical laws of Maxwell's theory.

8.3.1.1 Rayleigh scattering

To describe the Rayleigh scattering from an atom, we need to understand the phenomenon of spontaneous emission. This is usually achieved by the *Weisskopf-Wigner theory* starting from the Hamiltonian describing the interaction of a single two-level atom of the sample (labeled j) interacting with an incident laser,

$$\begin{aligned}\hat{H}_j &= \hbar g_{\mathbf{k}_0}\left(\hat{\sigma}_j e^{-\imath\omega_a t}+\hat{\sigma}_j^\dagger e^{\imath\omega_a t}\right)\left(\hat{a}_{\mathbf{k}_0}^\dagger e^{\imath\omega_0 t-\imath\mathbf{k}_0\cdot\mathbf{r}_j}+\hat{a}_{\mathbf{k}_0}e^{-\imath\omega_0 t+\imath\mathbf{k}_0\cdot\mathbf{r}_j}\right)\\ &\quad+\sum_{\mathbf{k}}\hbar g_{\mathbf{k}}\left(\hat{\sigma}_j e^{-\imath\omega_a t}+\hat{\sigma}_j^\dagger e^{\imath\omega_a t}\right)\left(\hat{a}_{\mathbf{k}}^\dagger e^{\imath\omega_k t-\imath\mathbf{k}\cdot\mathbf{r}_j}+\hat{a}_{\mathbf{k}}e^{-\imath\omega_k t+\imath\mathbf{k}\cdot\mathbf{r}_j}\right)\ .\end{aligned}\tag{8.118}$$

Here, ω_0, ω_a, and ω_k are, respectively, the frequencies of the incident laser, the atomic resonance and the scattered light [6]. $g_{\mathbf{k}_0}$ is the coupling strength between the atom and the incident light mode and $g_k = d\sqrt{\omega/(\hbar\varepsilon_0 V)}$ describes the coupling between the atom and a vacuum mode with the volume V. $\hat{\sigma}_j = |g\rangle\langle e|$ is the lowering operator of the atomic excitation, that is, it describes the transition of the j^{th} atom from the excited state $|e\rangle$ to the ground state $|g\rangle$. $\hat{a}_{\mathbf{k}}$ is the annihilation operator of a photon in the mode $\mathbf{k}$.

[6] We are only considering fixed atoms in space, that is, we do not allow acceleration by photonic recoil.

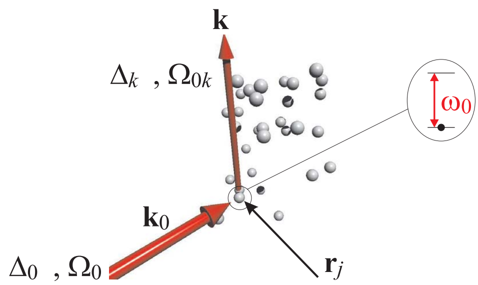

Figure 8.7: Scheme of the interaction of a light beam with a sample of atoms.

Now, considering an incident light mode (e.g. a laser beam) with high power,

$$\hat{a}_{\mathbf{k}_0}|n_0\rangle_{\mathbf{k}_0} = \sqrt{n_0}|n_0-1\rangle_{\mathbf{k}_0} \simeq \alpha_0|n_0\rangle_{\mathbf{k}_0} \ , \tag{8.119}$$

$\hat{a}_{\mathbf{k}_0}$ is approximately an observable, whose amplitude is proportional to the root of the intensity. As $[\hat{a}_{\mathbf{k}_0}, \hat{a}^\dagger_{\mathbf{k}_0}] \simeq 0$, we can disregard the quantum nature and treat the incident light as a classical field by replacing $\Omega_0 \equiv 2\alpha_0 g_{k_0}$, where Ω_0 is the Rabi frequency. The *rotating wave approximation* (RWA) allows us to neglect those terms of the Hamiltonian, which (in the first perturbative order) do not conserve energy, that is, terms proportional to $\hat{\sigma}^-_j\hat{a}$ and $\hat{\sigma}^+_j\hat{a}^\dagger$. Introducing the abbreviations,

$$\Delta_0 \equiv \omega_0 - \omega_a \qquad \text{and} \qquad \Delta_k \equiv \omega_k - \omega_a \ . \tag{8.120}$$

the Hamiltonian becomes,

$$\hat{H} = \tfrac{\hbar}{2}\Omega_0\left(\hat{\sigma}\hat{a}^\dagger_{\mathbf{k}_0}e^{\imath\Delta_0 t} + h.c.\right) + \hbar\sum_{\mathbf{k}}\left(g_k\hat{\sigma}\hat{a}^\dagger_{\mathbf{k}}e^{\imath\Delta_k t} + h.c.\right) \ . \tag{8.121}$$

The system can be found in three states,

$$|\Psi(t)\rangle = \alpha(t)|0\rangle_a|0\rangle_{\mathbf{k}} + \beta(t)|1\rangle_a|0\rangle_{\mathbf{k}} + \sum_{\mathbf{k}}\gamma_{\mathbf{k}}(t)|0\rangle_a|1\rangle_{\mathbf{k}} \ . \tag{8.122}$$

Before the scattering the system is, with the probability amplitude α, in the state $|0\rangle_a|0\rangle_{\mathbf{k}}$. After the absorption of a photon, with the probability amplitude β, the atom is excited $|1\rangle_a|0\rangle_{\mathbf{k}}$. Finally, after the reemission of the photon to a mode $\mathbf{k}$, with the probability amplitude $\gamma_{\mathbf{k}}$, the state of the system is $|0\rangle_a|1\rangle_{\mathbf{k}}$. The temporal evolution of the probability amplitudes is obtained by inserting the Hamiltonian (8.121) and the ansatz (8.122) into the Schrödinger equation,

$$\frac{d}{dt}|\Psi(t)\rangle = -\frac{\imath}{\hbar}\hat{H}|\Psi(t)\rangle \ . \tag{8.123}$$

We get, after a calculation which is not reproduced here [7] and which makes use of the so-called *Markov approximation* postulating that the variation of the amplitudes $\beta_j(t)$

[7] See the script *Quantum Mechanics* by the same author Scripts/QuantumMechanicsScript .

is slower than the evolution of the system given by $e^{\imath(\omega_k-\omega_0)t}$, the following equation of motion for the amplitudes β_j,

$$\boxed{\dot{\beta}_j = \left(\imath\Delta_0 - \frac{\Gamma}{2}\right)\beta_j - \frac{\imath\Omega_0}{2}e^{\imath\mathbf{k}_0\cdot\mathbf{r}_j}} \ . \tag{8.124}$$

This equation correctly describes the dynamics of the probability amplitude of finding an atom exposed to a laser beam and subject to spontaneous emission of its excited state.

8.3.1.2 Collective scattering

In the presence of several atoms, the full Hamiltonian for the atomic cloud is simply obtained by summing over the N atoms [8],

$$\hat{H} = \sum_{j=1}^{N} \hat{H}_j \ . \tag{8.125}$$

Following the same scheme as in the last section, the Schrödinger equation with the Hamiltonian (8.125) where (8.118) can be resolved to the limit of weak excitation: Let us restrict to the situation in which at most a single photon or a single atomic excitation can be in the system. This assumption is realistic, when the time for reemitting a photon is short. The state created by the passage of a single photon is a collective state, because the atomic sample can either be entirely in the ground state before a scattering event, $|g_1,..,g_N\rangle|0\rangle_\mathbf{k}$, or after a scattering event, $|g_1,..,g_N\rangle|1\rangle_\mathbf{k}$, or else any one of the atoms j can be excited, $|g_1,..,e_j,..,g_N\rangle|0\rangle_\mathbf{k}$, during the scattering event. All information on the system is coded in the temporal dependencies of the probability amplitudes for these states, which we obtain through the insertion of the wavefunction [9],

$$\begin{aligned}|\Psi\rangle &= \alpha(t)|g_1\dots g_N\rangle|0\rangle_\mathbf{k} + e^{-\imath\Delta_0 t}\sum_{j=1}^{N}\beta_j(t)|g_1\dots e_j\dots g_N\rangle|0\rangle_\mathbf{k} \\ &+ \sum_\mathbf{k}\gamma_\mathbf{k}(t)|g_1\dots g_N\rangle|1\rangle_\mathbf{k} + \sum_{m,n=1}^{N}\epsilon_{m<n,\mathbf{k}}(t)|g_1\dots e_m\dots e_n\dots g_N\rangle|1\rangle_\mathbf{k} \ .\end{aligned} \tag{8.126}$$

within the Schrödinger equation. What we get is a set of integro-differential equations for the amplitudes α, β, and $\gamma_\mathbf{k}$, which can be solved within the Markov approximation,

$$\boxed{\dot{\beta}_j = \left(\imath\Delta_0 - \frac{\Gamma}{2}\right)\beta_j - \frac{\imath\Omega_0}{2}e^{\imath\mathbf{k}_0\cdot\mathbf{r}_j} - \frac{\Gamma}{2}\sum_{m\neq j}\frac{e^{\imath k_0|\mathbf{r}_j-\mathbf{r}_m|}}{\imath k_0|\mathbf{r}_j-\mathbf{r}_m|}\beta_m} \ . \tag{8.127}$$

[8]We do not consider in this Hamiltonian collisional interactions between the atoms, for example, of the van der Waals type, which can have a great impact at high densities $n \gg \lambda^{-3}$.

[9]The fourth term corresponds to the presence of two simultaneously excited atoms plus a (virtual) photon with 'negative' energy. These states need to be taken into account, if we do not want to make use ofthe RWA approximation.

We note, that the first two terms of this equation correspond to the equation describing the dynamics of a single atom (8.124). The third term corresponds to processes, where photons scattered at an atom are reabsorbed by another atom.

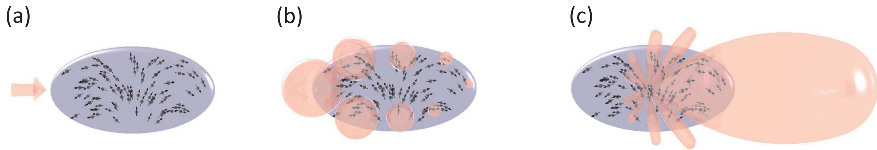

Figure 8.8: Illustration of cooperative scattering: From (a) to (c) a photon traversing an atomic cloud first excites the upstream dipoles, which immediately begin to radiate. The downstream dipoles are excited later on. The phase lag of the reemission processes leads to a radiative emission pattern being strongly peaked into forward direction.

The claim is now that equation (8.127) (or at least its generalization to level systems allowing to take account of the vectorial nature of light) is capable of reproducing all phenomena of macroscopic scattering, usually described by Maxwell's theory, for example, refraction, diffraction, Mie and Bragg scattering, etc. In addition, it correctly describes microscopic scattering phenomena, such as cooperative Rayleigh scattering, Anderson location, photonic band gaps, etc.

8.3.2 The limit of the Mie scattering and the role of the refractive index

In practice, the exploitation of the N coupled equations (8.127) (one for each atom), which needs to be done numerically, is limited by computer capacity to some 100 000 atoms. On the other hand, at least, in the limit of high densities, we may hope, that the atomic cloud be well described by a continuous density distribution,

$$\sum_j \beta_j \to \int \beta(\mathbf{r}')\rho(\mathbf{r}')dV' \ . \tag{8.128}$$

Considering the stationary case, $\dot{\beta}_j = 0$, we arrive at,

$$\frac{\Omega_0}{2}e^{\imath\mathbf{k}_0\cdot\mathbf{r}} = (\Delta_0 + \imath\Gamma)\beta(\mathbf{r}) + \frac{\Gamma}{2}\int \frac{e^{\imath k_0|\mathbf{r}-\mathbf{r}'|}}{k_0|\mathbf{r}-\mathbf{r}'|}\beta(\mathbf{r}')\rho(\mathbf{r}')dV' \ . \tag{8.129}$$

We note that the kernel of the above equation is the Green function of the Helmholtz equation, since,

$$[\nabla^2 + k_0^2]\frac{e^{\imath k_0|\mathbf{r}-\mathbf{r}'|}}{4\pi|\mathbf{r}-\mathbf{r}'|} = -\delta^{(3)}(\mathbf{r}-\mathbf{r}') \ . \tag{8.130}$$

Now, by applying the operator $[\nabla^2 + k_0^2]$ to both sides of equation (8.129), we arrive at,

$$0 = (\Delta_0 + \imath\Gamma)[\nabla^2 + k_0^2]\beta(\mathbf{r}) - 2\pi\Gamma\frac{\beta(\mathbf{r})\rho(\mathbf{r})}{k_0} \ , \tag{8.131}$$

that is [34, 9, 10],

$$\boxed{[\nabla^2 + k_0^2 n(\mathbf{r})^2]\beta(\mathbf{r}) = 0 \qquad \text{defining} \qquad n^2(\mathbf{r}) \equiv 1 - \frac{4\pi\rho(\mathbf{r})}{k_0^3(2\Delta_0/\Gamma + \imath)}} . \qquad (8.132)$$

This is the *Helmholtz equation* of Maxwell's theory. The reappearance of the refractive index $n(\mathbf{r})$ is the price to pay for smoothing the density distribution, and with it we lose all effects related to discretization and cloud disorder. In Exc. 8.3.3.1 we compare the result of the smoothed coupled-dipole model (8.132) to the macroscopic susceptibility derived from the Lorentz model (7.142), and to the Clausius-Mossotti formula (3.28).

Example 91 (*Bragg scattering by partially disordered clouds*): Fig. 8.9 shows the example of Bragg scattering by an atomic cloud. Without disorder we would expect an incident laser beam to be partially reflected and partially transmitted. The simulation of the stationary version of equation (8.127) for the scattering of the cloud illustrated in (a) shows, in addition to transmission and reflection, a random pattern of specular scattering in all directions, which can be attributed to disorder.

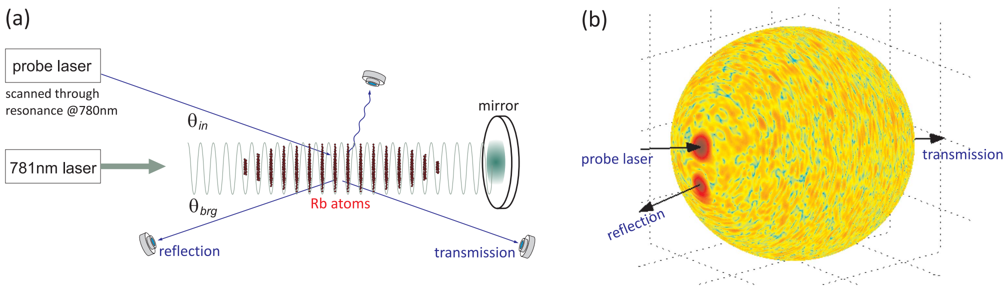

Figure 8.9: (a) Experimental scheme for Bragg reflection by an ordered atomic cloud in a periodic pile of pancakes. (b) Simulation of the stationary cloud scattering equation schematized in (a).

Example 92 (*Collective radiative pressure*): The internal and the global structure of an atomic cloud both dramatically influence the radiative pressure force exerted on its center of mass. We compare two limiting cases [26]: (a) For large dilute clouds, scattering by intrinsic disorder prevails. The more atoms are in the cloud, the more pronounced is the forward scattering of the light. Therefore, the radiative pressure force *per atom* exerted by the incident light decreases with N. (b) For small dense clouds, the scattering is rather governed by the global inhomogeneous shape of the cloud. The more atoms are in the cloud, the greater the variation of the refractive index and the greater the refractive deflection of photons off the optical axis [13]. Therefore, the radiation pressure force per atom exerted by the incident light increases with N, as shown in Fig. 8.10(c).

Microscopic collective scattering depends on one hand on the internal spatial distribution of the scatterers, that is, the intrinsic disorder, and on the other hand on the

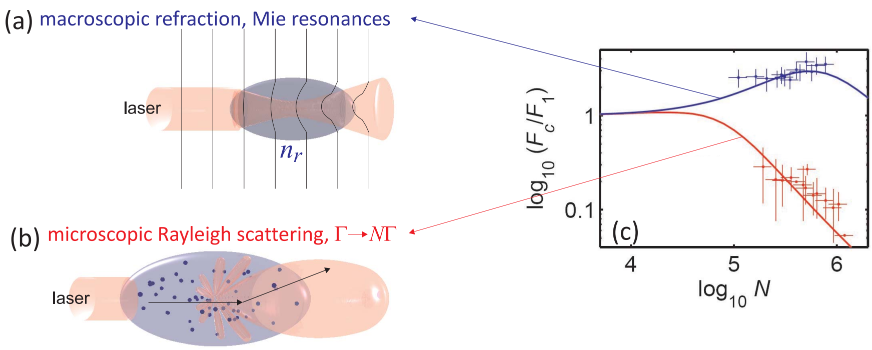

Figure 8.10: (a) Rayleigh scattering by a disordered cloud. (b) Mie scattering via wavefront deformation by the refractive index of an optically dense cloud. (c) Dependence of the radiation pressure force on the number of atoms for the two cases (a) and (b).

global distribution, i.e. the shape and the size of the cloud and its density distribution near the edges, which may be smooth or abrupt. In the limit of despicable disorder, we have seen that the theory of collective scattering is equivalent to Maxwell's macroscopic theory. In this limit, we can describe the cloud of scatterers as a (locally) homogeneous sphere characterized by a refractive index $n(\mathbf{r})$, which varies spatially with the density of the scatterers. Let us assume, for simplicity, a spherical cloud with a homogeneous refraction index $n(\mathbf{r}) = n_0$ inside the cloud and $n(\mathbf{r}) = 1$ outside. The scattering of a plane wave of radiation by a dielectric sphere is known as *Mie scattering* . In Mie's theory we expand the incident plane wave into partial spherical waves,

$$e^{\imath\mathbf{k}\cdot\mathbf{r}} = \sqrt{4\pi}\sum_{\ell=0}^{\infty}\sqrt{2\ell+1}\imath^{\ell}j_{\ell}(kr)Y_{\ell 0}(\hat{\mathbf{e}}_r) \ , \tag{8.133}$$

which must satisfy the boundary condition for electromagnetic waves at the outer edge of the sphere. This is illustrated in Fig. 8.11. Theoretically it should be possible to observe Mie resonances with atomic clouds, albeit strictly speaking, they do not have a surface which could act like an abrupt boundary condition.

8.3.3 Exercises

8.3.3.1 Ex: Coupled dipoles versus Clausius-Mossotti

Compare the result of the smoothed coupled-dipole model (8.132) to the macroscopic susceptibility derived from the Lorentz model (7.142), and to the Clausius-Mossotti formula (3.28).

8.4 Further reading

M.J. Berg et al., *A new explanation of the extinction paradox* [DOI]

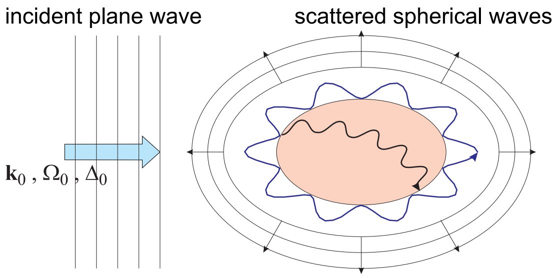

Figure 8.11: Two types of Mie resonances are possible: (i) Waves propagating in the interior of the body and form a stationary wave bounded by the surface and (ii) evanescent waves that propagate on the surface of the body (whispering gallery modes). The resonances of type (ii) require abrupt boundary conditions.

V.C. Ballenegger, *The Ewald-Oseen extinction theorem and extinction lengths* [DOI]

Chapter 9

Theory of special relativity

Until the end of the nineteenth century people believed in the existence of an 'ether', that is, a medium capable of carrying oscillations of the electromagnetic field in a similar way as water transports surface waves or the air propagates the sound. The propagation velocity of the light must then have a certain value c in this ether. But when measured in another inertial system, according to the Galilei transformation, propagation velocity should be the sum of c and the velocity v of the inertial system through the ether. This ether would be fixed to the universe, and the earth would have a velocity v with respect to this ether.

With the objective of measuring the relative velocity between a fixed laboratory and the ether, *Michelson* and *Morley* did an experiment known as *Michelson-Morley experiment*, and which now represents one of the foundations of the theory of special relativity. It consists of a *Michelson interferometer*, which can be rotated in space. If an 'ether' existed, which is not fixed to the Earth, the speed of light must be anisotropic and the interference fringes observed in the interferometer must move when the interferometer is rotated. This was not observed.

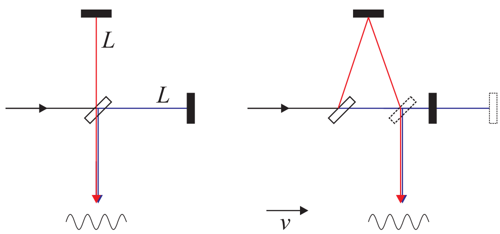

Figure 9.1: Scheme of the Michelson-Morley experiment.

Within the resting system (the ether) the times required for light to travel through each of the interferometer arms are,

$$t_{1,2} = \frac{2L}{c} \ . \tag{9.1}$$

In a frame moving in the direction of one of the arms these times would be,

$$t_1 = \frac{2L}{c}\frac{1}{\sqrt{1-\beta^2}} \qquad \text{and} \qquad t_2 = \frac{L}{c+v} + \frac{L}{c-v} = \frac{2L}{c}\frac{1}{1-\beta^2} \ . \tag{9.2}$$

The experiment confirms the result (9.1) *regardless of the rotation of the interferometer.*

Guided by Michelson's observation it was *Poincaré*, who first proposed the absence of an ether, which motivated *Einstein* to formulate the following postulates:

Law A: *The laws of physics do not depend on a translatory motion of the system as a whole. There is no particular system, in which the 'ether' would be at rest.*

Law B: *The speed of light is constant in all inertial systems and regardless of the speed of the emitting source.*

These postulates revolutionized classical mechanics. The new theory, called the theory of *special relativity*, still contains classical mechanics in the limit of slow velocities, but extends its validity to the limit of velocities approaching the speed of light. Moreover, special relativity reconciles mechanics with electrodynamics in a natural way, as we will show in the following sections.

9.1 Relativistic metric and Lorentz transform

In the theory of relativity, the space represented by the vector $\mathbf{r}$ and the time represented by the scalar ct (where we multiply the universal speed of light for dimensionality reasons) are treated on equal footing. There are other combinations of scalar and vectorial physical quantities such as energy E/c and linear momentum $\mathbf{p}$ which, when combined to a four-dimensional entity, allow for a more symmetrical representation of the fundamental laws of physics. Let us, in the following, set the foundations of this new formalism developed by Poincaré, Lorentz, Einstein, and Minkowski.

9.1.1 Ricci's calculus, Minkowski's metric, and space-time tensors

In the notation of 4-dimensional space-time vectors the physical quantities are described (or combined) by tensors of rank k, e.g. scalars A, vectors A^μ, matrices $A^{\mu\nu}$, and tensors of higher ranks $A^{\mu\nu\lambda\cdots}$. Tensors can be *contravariant*, A^μ, or *covariant*, A_μ, with respect to an index, depending on their behavior regarding the Lorentz transform (as we shall see shortly). Co- (or contra-) variant scalars are independent of the inertial system and, therefore, called *Lorentz invariants*. The contra- and covariant tensors are related by the *Minkowski metric* defined by (see also Sec. 1.4),

$$\boxed{(g^{\mu\nu}) \equiv \begin{pmatrix} 1 & 0 & 0 & 0 \\ 0 & -1 & 0 & 0 \\ 0 & 0 & -1 & 0 \\ 0 & 0 & 0 & -1 \end{pmatrix}} , \tag{9.3}$$

using the *sum rule of Einstein*, which consists in summing over all pairs of co- and contravariant indices,

$$a^\mu a_\mu \equiv \sum\nolimits_\mu a^\mu a_\mu , \tag{9.4}$$

via

$$a^\mu = g^{\mu\nu} a_\nu . \tag{9.5}$$

We note that the first index in a matrix counts the columns and the second index the rows. For flat space-time (that is, without curvature),

$$g_\mu{}^\nu = g_{\mu\alpha}g^{\alpha\nu} = \delta_\mu^\nu \quad , \quad g_{\mu\nu} = g^{\mu\nu} \quad \text{that is} \quad \check{g}^{-1} = \check{g} = \check{g}^\intercal \; , \tag{9.6}$$

where δ_μ^ν is the *Kronecker symbol* and the decoration '∨' denotes a matrix, $\check{a} \equiv (a_{\mu\nu})$. Thus, the identity and the metric are the two faces of the same tensor, $\check{\delta} = \check{g}$. The norm is defined by,

$$\|(a^\mu)\| \equiv \sqrt{a_\mu a^\mu} = \sqrt{a^\mu g_{\mu\nu} a^\nu} \; . \tag{9.7}$$

The product between two contravariant vectors is given by,

$$a^\mu b^\mu \equiv a^\mu g_{\mu\nu} b^\nu \; . \tag{9.8}$$

The tensors are represented by scalars, vectors and matrices. The vector symbol is used for the contravariant column vector,

$$\vec{a} \equiv (a^\mu) = \begin{pmatrix} a^0 \\ \mathbf{a} \end{pmatrix} \quad , \quad \check{a} \equiv (a^{\mu\nu}) = \begin{pmatrix} a^0 & (a^{m0}) \\ (a^{0n}) & (a^{mn}) \end{pmatrix} \; . \tag{9.9}$$

The covariant vector is also represented by a column,

$$\check{g}\vec{a} = (a_\mu) = (g_{\mu\nu}a^\nu) = \begin{pmatrix} a^0 \\ -\mathbf{a} \end{pmatrix} \; . \tag{9.10}$$

Often, Greek letters are used as indices for space-time tensors, while Roman letters are used as indices for spatial components. In order to work with vectors within Minkowski's formalism, we must interpret them as two-dimensional 1×4 matrices,

$$\vec{a} \equiv (a^{\mu 1}) \; , \tag{9.11}$$

where the '1' indicates the number of columns of the matrix. Introducing the *transposition*, denoted by the symbol '$\intercal$', as an exchange of the indices labeling rows and columns,

$$F_{\mu\nu} = (F^\intercal)_{\nu\mu} \; , \tag{9.12}$$

we can represent the transposition of a vector by a 4×1 matrix,

$$\vec{a}^\intercal = (a^{\mu 1})^\intercal = (a^{1\mu}) = \begin{pmatrix} a^0 & \mathbf{a} \end{pmatrix} \; , \tag{9.13}$$

and define the scalar product between vectors in terms of the product between matrices as,

$$\begin{aligned} \vec{a} \cdot \vec{b} \equiv (a^{\mu 1}b_{\mu 1}) &= (a^\intercal)^{1\mu}(b_{\mu 1}) = (a^\intercal)^{1\mu} g_{\mu\nu}(b^{\nu 1}) = \check{a}^\intercal \check{g} \check{b} \\ &= \begin{pmatrix} a^0 & (a^m) \end{pmatrix} \begin{pmatrix} 1 & 0 \\ 0 & (-\delta^{mn}) \end{pmatrix} \begin{pmatrix} a^0 \\ (a^n) \end{pmatrix} \; . \end{aligned} \tag{9.14}$$

We conclude emphasizing that, to be able to multiply tensores as matrices, the indices to be contracted must be adjacent. If necessary, the tensors must be transposed,

$$A^{\mu\alpha} B^\nu{}_\alpha = A^{\mu\alpha} (B^\intercal)_\alpha{}^\nu \; . \tag{9.15}$$

One has to be very careful, because in general $A^{\mu\alpha} \neq A^{\alpha\mu} \neq A_{\alpha\mu} \neq A_{\mu\alpha} \neq A_\alpha^\mu \neq A_\mu{}^\alpha \neq A^\mu{}_\alpha \neq A^\alpha{}_\mu$.

9.1.2 Lorentz transform

We are now in the shape to officially introduce our first explicit space-time vector by combining the physical quantities time and position,

$$\boxed{(r^\mu) \equiv \begin{pmatrix} ct \\ \mathbf{r} \end{pmatrix}} . \tag{9.16}$$

In classical mechanics the transformation to a system moving at velocity $\beta = v/c$ is described by the *Galilei transform* given by,

$$(G^\mu{}_\nu) \equiv \begin{pmatrix} 1 & 0 & 0 & 0 \\ 0 & 1 & 0 & 0 \\ 0 & 0 & 1 & 0 \\ -\beta & 0 & 0 & 1 \end{pmatrix} \quad , \quad (G^\mu{}_\nu)^{-1} = \begin{pmatrix} 1 & 0 & 0 & 0 \\ 0 & 1 & 0 & 0 \\ 0 & 0 & 1 & 0 \\ \beta & 0 & 0 & 1 \end{pmatrix} . \tag{9.17}$$

Example 93 (*Galilei transform*): Let us try out the Galilei transform on the space-time vector (9.16):

$$\begin{pmatrix} ct' \\ x' \\ y' \\ z' \end{pmatrix} = (r'^\mu) = (G^\mu{}_\nu)(r_\nu) = \begin{pmatrix} 1 & 0 & 0 & 0 \\ 0 & 1 & 0 & 0 \\ 0 & 0 & 1 & 0 \\ -\beta & 0 & 0 & 1 \end{pmatrix} \begin{pmatrix} ct \\ x \\ y \\ z \end{pmatrix} = \begin{pmatrix} ct \\ x \\ y \\ z - vt \end{pmatrix} .$$

In classical mechanics wave propagation is conditioned to the existence of a medium. Consequently, different inertial systems are not equivalent and, as will be shown in a later section, the wave equation *is not invariant* to the Galilei transform. Let us therefore look for another transformation, which preserves the shape of the wave equation. We may, for example, request the transformation to ensure that the propagation of the phase fronts of a spherical wave is independent of the inertial system: $c^2t'^2 - \mathbf{r}'^2 = c^2t^2 - \mathbf{r}^2$.

The story of the *Lorentz transform* begins with Poincaré, who introduced the idea of local time: According to him, simultaneity depends on the reference system. Voigt attempted in 1897 for the first time to find a transformation that would conserve the value of c, but it was Lorentz who found a transformation leaving Maxwell's equations invariant and, consequently, Helmholtz's wave equation as well. The Lorentz transform is linear with respect to the preservation of space-time intervals in Minkowski space and, as we will see shortly, it removes the contradictions between classical mechanics and electrodynamics.

Consider a system S' moving through our lab S at a velocity $\mathbf{v} = v\hat{\mathbf{e}}_z$. We define,

$$\beta = \frac{v}{c} \qquad \text{and} \qquad \gamma = \frac{1}{\sqrt{1-\beta^2}} . \tag{9.18}$$

The matrix describing the Lorentz transform from system S to system S' is,

$$\boxed{\check{\Lambda} = (\Lambda^\mu{}_\nu) \equiv \begin{pmatrix} \gamma & 0 & 0 & -\gamma\beta \\ 0 & 1 & 0 & 0 \\ 0 & 0 & 1 & 0 \\ -\gamma\beta & 0 & 0 & \gamma \end{pmatrix}} \quad , \quad \check{\Lambda}^{-1} = (\Lambda^\mu{}_\nu)^{-1} = \begin{pmatrix} \gamma & 0 & 0 & \gamma\beta \\ 0 & 1 & 0 & 0 \\ 0 & 0 & 1 & 0 \\ \gamma\beta & 0 & 0 & \gamma \end{pmatrix} \tag{9.19}$$

that is, the inverse of the transformation matrix is obtained by changing the sign of the velocity, $v \to -v$. For the Lorentz transform tensor we can show,

$$(\Lambda^\mu{}_\nu)^{-1} = g_{\mu\omega}\Lambda^\omega{}_\kappa g^{\kappa\nu} = \Lambda_\mu{}^\nu \qquad \text{that is} \qquad \check{\Lambda}^{-1} = \check{g}\check{\Lambda}\check{g} \tag{9.20}$$
$$\text{and} \qquad \Lambda^\omega{}_\mu g_{\omega\kappa}\Lambda^\kappa{}_\nu = g_{\mu\nu} \qquad \text{that is} \qquad \check{\Lambda}^\intercal\check{g}\check{\Lambda} = \check{g} \ .$$

The transformation from a laboratory reference frame S into a rest frame S' is done by,

$$A'^\mu = \Lambda^\mu{}_\nu A^\nu \ . \tag{9.21}$$

Time-space scalars are always Lorentz invariant. We consider, for example,

$$x'_\mu x'^\mu = \Lambda_\mu{}^\nu x_\nu \Lambda^\mu{}_\omega x^\omega = (\check{\Lambda}^{-1}\check{\Lambda})^\nu{}_\omega x_\nu x^\omega = \mathbb{I}\ x^\omega x_\omega \ . \tag{9.22}$$

For space-time differentials, since,

$$dx'^\mu = \frac{\partial x'^\mu}{\partial x^\nu}dx^\nu \ , \tag{9.23}$$

comparing with the relationship (9.21), we can identify,

$$\Lambda^\mu{}_\nu = \frac{\partial x'^\mu}{\partial x^\nu} \ . \tag{9.24}$$

Contra- and covariant tensors are defined by their different behavior under arbitrary coordinate transformation. For example, in the case of Lorentz transforms,

$$A'_\mu = \frac{\partial x^\nu}{\partial x'^\mu}A_\nu \quad , \quad A'^\mu = \frac{\partial x'^\mu}{\partial x^\nu}A^\nu \ . \tag{9.25}$$

Similarly, tensors or higher rank satisfy,

$$A'_{\mu\nu} = \frac{\partial x^\mu}{\partial x'^\nu}\frac{\partial x^\nu}{\partial x'^\beta}A_{\nu\beta} \quad , \quad A'^{\mu\nu} = \frac{\partial x'^\mu}{\partial x^\nu}\frac{\partial x'^\nu}{\partial x^\beta}A^{\nu\beta} \ , \tag{9.26}$$

and also,

$$A'^{\mu_1..\mu_n}{}_{\nu_1..\nu_m} = \Lambda^{\mu_1}{}_{\omega_1}..\Lambda^{\mu_n}{}_{\omega_n}\Lambda_{\nu_1}{}^{\kappa_1}..\Lambda_{\nu_n}{}^{\kappa_n}A^{\omega_1..\omega_n}{}_{\kappa_1..\kappa_m} \ . \tag{9.27}$$

In Exc. 9.1.7.1 we show that the derivative by a covariant coordinate is contravariant.

Example 94 (*Lorentz transform*): In the limit of slow velocities, $v \ll c$, the Lorentz transform converges to the Galilei transform. This can be seen rewriting the Lorentz transform as,

$$\begin{pmatrix} t' \\ z' \end{pmatrix} = \begin{pmatrix} \gamma & -\frac{\gamma\beta}{c} \\ -\gamma\beta & \gamma \end{pmatrix}\begin{pmatrix} t \\ z \end{pmatrix} \simeq \begin{pmatrix} 1 & 0 \\ -\beta & 1 \end{pmatrix}\begin{pmatrix} t \\ z \end{pmatrix} \ .$$

Example 95 (*Lorentz transform*): We have,

$$\Lambda^\mu{}_\nu = \frac{\partial x'^\mu}{\partial x^\nu} = \left(\frac{\partial x'_\mu}{\partial x_\nu}\right)^{-1} = \left(\frac{\partial x^\nu}{\partial x'^\mu}\right)^{-1} = (\Lambda_\mu{}^\nu)^{-1} \ .$$

9.1.3 Contraction of space

Einstein's theory has important consequences, such as the *contraction of space* and the *dilatation of time*. Let us consider a rod moving through the lab S with velocity v. The rod delimits two points $j = 1, 2$ in space-time for which we measure in the lab (at time $t = t_1 = t_2$) the distance $z_2 - z_1$. The spatio-temporal points are Lorentz-transformed to the system S', in which the rod is at rest (neglecting transverse spatial dimensions), by,

$$\begin{pmatrix} ct'_j \\ z'_j \end{pmatrix} = (\Lambda^\mu{}_\nu) \begin{pmatrix} ct \\ z_j \end{pmatrix} = \begin{pmatrix} \gamma ct - \gamma\beta z_j \\ -\gamma\beta ct + \gamma z_j \end{pmatrix} \ . \tag{9.28}$$

Hence,

$$z'_2 - z'_1 = -\gamma\beta ct + \gamma z_2 + \gamma\beta ct - \gamma z_1 = \gamma(z_2 - z_1) \ . \tag{9.29}$$

Consequently, in the lab the distance seems smaller than in the rest frame [1].

9.1.4 Dilatation of time

We consider a clock flying through the lab S at a velocity v. The clock produces regular time intervals, for which we measure in the lab the duration $t_2 - t_1$. The spatio-temporal points are Lorentz-transformed to the system S' in which the clock is at rest ($z' = z'_1 = z'_2$) via,

$$\begin{pmatrix} ct'_j \\ z' \end{pmatrix} = (\Lambda^\mu{}_\nu) \begin{pmatrix} ct_j \\ z_j \end{pmatrix} = \begin{pmatrix} \gamma ct_j - \gamma\beta z_j \\ -\gamma\beta ct_j + \gamma z_j \end{pmatrix} \ . \tag{9.30}$$

Hence,

$$\begin{aligned} t'_2 - t'_1 &= \gamma t_2 - \gamma\beta\frac{z_2}{c} - \gamma t_1 + \gamma\beta\frac{z_1}{c} \\ &= \gamma t_2 - \beta\left(\frac{z'}{c} + \gamma\beta t_2\right) - \gamma t_1 + \beta\left(\frac{z'}{c} + \gamma\beta t_1\right) = \gamma^{-1}(t_2 - t_1) \ . \end{aligned} \tag{9.31}$$

Consequently, in the lab the time interval seems longer than in the rest frame.

A good illustration of the effect of time dilatation is the *twin paradox*. A twin begins an interstellar voyage aboard a space ship traveling at a constant velocity. Twin B, who remained on Earth calculates, that the time elapsed for his twin A is smaller than his own time. Twin B calculates that the elapsed time for his twin A is shorter. Who's right? Twin A is wrong, because his system must be accelerated when taking off from Earth. Note that only special relativity is required to understand the effect [2]: Take for example, a third person traveling back to Earth after having synchronized its clock with twin A. We calculate in Excs. 9.1.7.2 to 9.1.7.5 examples of temporal dilatation.

---

[1] Alternatively, we can measure the instants of time t_j when the ends of the rod pass by a certain point z of the lab, such that $l = v(t_2 - t_1)$.

[2] [http://de.wikipedia.org/wiki/Zwillingsparadox]

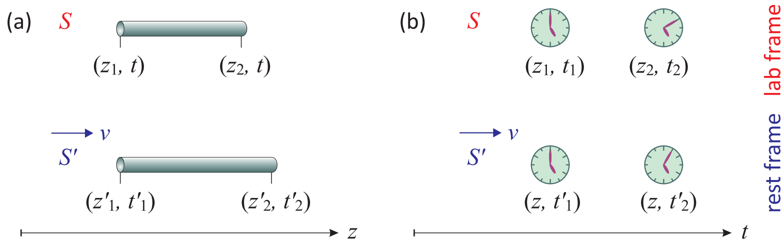

Figure 9.2: Illustration of (a) contraction of space and (b) dilatation of time.

9.1.5 Transformational behavior of the wave equation

In the previous section we have seen that the relativistic metric is based on the co-variant formulation of mechanics with the definition of relativistic space-time vectors. We introduced the *quadri-vectors* of the displacement Δr^μ, of the position (r^μ), and of the gradient (∂^μ),

$$\boxed{(\Delta r^\mu) \equiv \begin{pmatrix} c\Delta t \\ \Delta\mathbf{r} \end{pmatrix} \quad , \quad (r^\mu) \equiv \begin{pmatrix} ct \\ \mathbf{r} \end{pmatrix} \quad , \quad (\partial^\mu) \equiv \begin{pmatrix} \frac{1}{c}\frac{\partial}{\partial t} \\ -\nabla \end{pmatrix}} \ . \tag{9.32}$$

The contraction of quadri-vectors produces Lorentz invariants, such as the *quadri-scalars* of space-time intervals Δs^2, of proper time $\Delta\tau$, of proper distance $|\Delta\vec{S}|$, or of the d'Alembertian $\Box$, given by,

$$\begin{aligned} \Delta s^2 &\equiv \Delta r_\mu \Delta r^\mu = c^2\Delta t^2 - \Delta\mathbf{r}^2 \ , \\ \Delta\tau &\equiv \sqrt{\tfrac{\Delta s^2}{c^2}} \qquad \text{for 'time'-like intervals} \qquad \Delta s^2 > 0 \ , \\ |\Delta\mathbf{s}| &\equiv \sqrt{-\Delta s^2} \qquad \text{for 'space'-like intervals} \qquad \Delta s^2 < 0 \ , \\ \Box &\equiv \partial_\mu \partial^\mu = \tfrac{1}{c^2}\tfrac{\partial^2}{\partial t^2} - \nabla^2 \ . \end{aligned} \tag{9.33}$$

With these definitions we can write the wave equation in the absence of sources,

$$\boxed{\Box\psi = \partial^\mu \partial_\mu \psi = 0} \ . \tag{9.34}$$

The covariant form of the wave equation already shows its compatibility with the Lorentz transform. Nevertheless, we will discuss the transformation properties in the following. These are fundamental, since the propagation of light, whose invariant velocity triggered the theory of relativity, is an undulatory phenomenon.

9.1.5.1 Wave equation under Galilei transformation

The Galilei transformation claims that we obtain the coordinates of an object in a system S' simply by substituting $z \to z'$ and $t \to t'$ with [3],

$$\begin{aligned} t' \equiv t \qquad &\text{and} \qquad z' \equiv z - v_0 t \qquad \text{or} \\ t \equiv t' \qquad &\text{and} \qquad z \equiv z' + v_0 t \ , \end{aligned} \tag{9.35}$$

[3]Note that the Galilei transform (9.17) is unitary because $\det G = 1$.

which implies

$$v' = \frac{\partial z'}{\partial t'} = \frac{\partial z}{\partial t} - v_0 = v - v_0 \; . \tag{9.36}$$

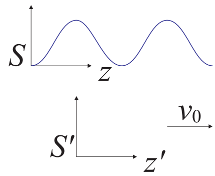

Figure 9.3: Wave in the inertial system S as seen by an observer in the system S' moving at a velocity u.

Newton's classical mechanics is *Galilei invariant*, which means that the fundamental equations of the type,

$$m\dot{v}_i = -\nabla_{x_i} \sum_j V_{ij}(|x_i - x_j|) \; , \tag{9.37}$$

do not change their shape under the *Galilei transform*. In contrast, the wave equation is *not* Galilei invariant. To see this, we consider a wave in the inertial system S, which is resting with respect to the propagation medium, being described by $Y(z,t)$ and satisfying the wave equation,

$$\frac{\partial^2 Y(z,t)}{\partial t^2} = c^2 \frac{\partial^2 Y(z,t)}{\partial z^2} \; . \tag{9.38}$$

An observer sits in the inertial system S' moving with respect to S with the speed v_0, such that $z' = z - v_0 t$. The question now is, what is the equation of motion for this wave described by $Y'(z',t')$, that is, we want to check the validity of

$$\frac{\partial^2 Y'(z',t')}{\partial t'^2} \stackrel{?}{=} c^2 \frac{\partial^2 Y'(z',t')}{\partial z'^2} \; . \tag{9.39}$$

For example, the wave $Y(z,t) = \sin k(z - ct)$ traveling to the right is perceived in the system S', which is also traveling to the right, as $Y'(z',t') = \sin k[z' - (c - v_0)t'] = Y(z,t)$ applying the Galilei transform. Therefore,

$$Y'(z',t') = Y(z,t) \; , \tag{9.40}$$

that is, we expect that the laws valid in S are also valid in S'. We calculate the partial derivatives,

$$\begin{aligned} \frac{\partial Y'(z',t')}{\partial t'} &= \frac{\partial Y(z,t)}{\partial t'} = \frac{\partial t}{\partial t'} \frac{\partial Y(z,t)}{\partial t}\bigg|_{z=const} + \frac{\partial z}{\partial t'} \frac{\partial Y(z,t)}{\partial z}\bigg|_{t=const} = \frac{\partial Y(z,t)}{\partial t} + v_0 \frac{\partial Y(z,t)}{\partial z} \\ \frac{\partial Y'(z',t')}{\partial z'} &= \frac{\partial Y(z,t)}{\partial z'} = \frac{\partial t}{\partial z'} \frac{\partial Y(z,t)}{\partial t}\bigg|_{z=const} + \frac{\partial z}{\partial z'} \frac{\partial Y(z,t)}{\partial z}\bigg|_{t=const} = \frac{\partial Y(z,t)}{\partial z} \; . \end{aligned} \tag{9.41}$$

Therefore, we conclude that the wave equation in the propagating system is modified:

$$\begin{aligned}\frac{\partial^2 Y'(z',t')}{\partial t'^2} &\overset{\rightrightarrows}{=} \frac{\partial^2 Y(z,t)}{\partial t^2} + v_0^2\frac{\partial^2 Y(z,t)}{\partial z^2} + 2v_0\frac{\partial^2 Y(z,t)}{\partial t\partial z} \\ &\overset{\text{eq.onda}}{=} c^2\frac{\partial^2 Y(z,t)}{\partial z^2} + v_0^2\frac{\partial^2 Y(z,t)}{\partial z^2} + 2v_0\frac{\partial^2 Y(z,t)}{\partial t\partial z} \\ &\overset{\leftleftarrows}{=} (c^2 - v_0^2)\frac{\partial^2 Y'(z',t')}{\partial z'^2} + 2v_0\frac{\partial^2 Y'(z',t')}{\partial t'\partial z'} \ .\end{aligned} \tag{9.42}$$

Only in cases where the wave function can be written as $Y(z,t) = f(z-ct) = f(z'-(c-v_0)t') = f'(z'-ct') = Y'(z',t')$, will we obtain a similar wave equation to that of the system S, but with a modified propagation velocity. We calculate,

$$\frac{\partial f'(z'-ct')}{\partial t'} = \frac{\partial f(z'-(c-v_0)t')}{\partial t'} = (v_0-c)\frac{\partial f(z'-(c-v_0)t')}{\partial z'} = (v_0-c)\frac{\partial f'(z'-ct')}{\partial z'} \ , \tag{9.43}$$

and the second derivative,

$$\frac{\partial^2 f'(z'-ct')}{\partial t'^2} = (c-v_0)^2\frac{\partial^2 f'(z'-ct')}{\partial z'^2} \ . \tag{9.44}$$

The observation that the wave equation is not Galilei invariant expresses the fact, that there is a preferential system for the wave to propagate, which is simply the system in which the propagation medium is at rest. Only in this inertial system will a spherical wave propagate isotropically.

Example 96 (*Wave equation under Galilei transformation*): Let us now verify the correctness of the wave equation in the propagating system S' using the example of a sine wave,

$$\begin{aligned}&(c^2-v_0^2)\frac{\partial^2 \sin k[z'-(c-v_0)t']}{\partial z'^2} + 2v_0\frac{\partial^2 \sin k[z'-(c-v_0)t']}{\partial z'\partial t'} \\ &= -k^2(c^2-v_0^2)\sin k[z'-(c-v_0)t'] + 2uk^2(c-v_0)\sin k[z'-(c-v_0)t'] \\ &= -k^2(c-v_0)^2\sin k[z'-(c-v_0)t'] = \frac{\partial^2 \sin k[z'-(c-v_0)t']}{\partial t'^2} \ .\end{aligned}$$

9.1.5.2 Wave equation under Lorentz transformation

The question now is, how to deal with electromagnetic waves which are lacking a propagation medium, as we have already noted and as has been verified by Michelson's famous experiment. If there is no propagation medium, all inertial systems should be equivalent, and the wave equation should be the same in all systems, and so should be the propagation velocity, i.e. the speed of light. These were the consideration of *Henry Poincaré*. To solve the problem we need another transformation than that of *Galileo Galilei*. It was *Hendrik Antoon Lorentz* who found the solution, but the biggest intellectual challenge was to accept all consequences of this new transformation. *Albert Einstein* accepted the challenge and created a new mechanics, which he called *relativistic mechanics*. The wave equation for electromagnetic waves, called the *Helmholtz equation*, being a direct consequence of Maxwell's theory, it is not surprising that the relativistic theory proved not only compatible with electrodynamic theory, but provides a much deeper understanding of the latter.

We begin with the ansatz of a general transformation connecting temporal and spatial coordinates via four unknown parameters, γ, $\tilde{\gamma}$, β, and $\tilde{\beta}$,

$$ct = \gamma(ct' + \beta z') \qquad \text{and} \qquad z = \tilde{\gamma}(z' + \tilde{\beta}ct') \ . \tag{9.45}$$

A similar calculation as the one made for the Galilei transformation now gives the first derivatives,

$$\frac{\partial Y'(z',t')}{c\partial t'} = \frac{\partial Y(z,t)}{c\partial t'} = \frac{\partial t}{\partial t'}\frac{\partial Y(z,t)}{c\partial t}\bigg|_{z=const} + \frac{\partial z}{c\partial t'}\frac{\partial Y(z,t)}{\partial z}\bigg|_{t=const} = \gamma\frac{\partial Y(z,t)}{c\partial t} + \tilde{\gamma}\tilde{\beta}\frac{\partial Y(z,t)}{\partial z} \tag{9.46}$$

$$\frac{\partial Y'(z',t')}{\partial z'} = \frac{\partial Y(z,t)}{\partial z'} = \frac{c\partial t}{\partial z'}\frac{\partial Y(z,t)}{c\partial t}\bigg|_{z=const} + \frac{\partial z}{\partial z'}\frac{\partial Y(z,t)}{\partial z}\bigg|_{t=const} = \gamma\beta\frac{\partial Y(z,t)}{c\partial t} + \tilde{\gamma}\frac{\partial Y(z,t)}{\partial z} \ .$$

The second derivatives and the application of the wave equation in the system S give,

$$\begin{aligned}\frac{\partial^2 Y'(z',t')}{c^2\partial t'^2} &\overset{\Rightarrow}{=} \gamma^2\frac{\partial^2 Y(z,t)}{c^2\partial t^2} + 2\gamma\tilde{\gamma}\tilde{\beta}\frac{\partial^2 Y(z,t)}{c\partial t\partial z} + (\tilde{\gamma}\tilde{\beta})^2\frac{\partial^2 Y(z,t)}{\partial z^2} \\ &\overset{\text{wave eq.}}{=} \gamma^2\frac{\partial^2 Y(z,t)}{\partial z^2} + 2\gamma\tilde{\gamma}\tilde{\beta}\frac{\partial^2 Y(z,t)}{c\partial t\partial z} + (\tilde{\gamma}\tilde{\beta})^2\frac{\partial^2 Y(z,t)}{c^2\partial t^2} \\ &\overset{!}{=} (\gamma\beta)^2\frac{\partial^2 Y(z,t)}{c^2\partial t^2} + 2\gamma\tilde{\gamma}\beta\frac{\partial^2 Y(z,t)}{c\partial t\partial z} + \tilde{\gamma}^2\frac{\partial^2 Y(z,t)}{\partial z^2} \overset{\Leftarrow}{=} \frac{\partial^2 Y'(z',t')}{\partial z'^2} \ .\end{aligned} \tag{9.47}$$

That is, the wave equation in the system S' has the same form [4], under the condition that,

$$\gamma = \tilde{\gamma} \qquad \text{and} \qquad (\gamma\beta)^2 = (\tilde{\gamma}\tilde{\beta})^2 \qquad \text{and} \qquad \beta = \tilde{\beta} \ . \tag{9.48}$$

In addition, the transformation

$$\begin{pmatrix} ct' \\ z' \end{pmatrix} = \Lambda \begin{pmatrix} ct \\ z \end{pmatrix} \qquad \text{with} \qquad \Lambda \equiv \begin{pmatrix} \gamma & \gamma\beta \\ \gamma\beta & \gamma \end{pmatrix} \tag{9.49}$$

has to be unitary, that is,

$$1 = \det\Lambda = \gamma\tilde{\gamma} - \gamma\tilde{\gamma}\beta\tilde{\beta} = \gamma^2(1-\beta^2) \ , \tag{9.50}$$

which allows to relate the parameters γ and β by,

$$\gamma = \frac{1}{\sqrt{1-\beta^2}} \ . \tag{9.51}$$

Finally and obviously, we expect to recover the Galilei transformation at low velocities,

$$ct = \gamma(ct' + \beta z') \to ct' \qquad \text{and} \qquad z = \gamma(z' + \beta ct') \to z' + v_0 t' \ . \tag{9.52}$$

That is, the limit is obtained by $\gamma \to 1$ and $\gamma\beta c \to v_0$, such that,

$$\beta = \frac{v_0}{c} \ . \tag{9.53}$$

[4] Note that the computation is dramatically simplified in the covariant formalism of 4-dimensional *space-time vectors* introduced by *Hermann Minkowski* and *Gregory Ricci-Curbastro*.

The *Lorentz transform* from an inertial system S to another S' is,

$$\begin{aligned} t' &= \gamma\left(t - \tfrac{v_0}{c^2}z\right) \quad \text{and} \quad z' = \gamma(z - v_0 t) \quad \text{or} \\ t &= \gamma\left(t' + \tfrac{v_0}{c^2}z'\right) \quad \text{and} \quad z = \gamma(z' + v_0 t') \ . \end{aligned} \tag{9.54}$$

9.1.6 The Lorentz boost

In this section we will construct the Lorentz transform from *infinitesimal generators* [47]. To begin with we introduce 6 fundamental matrices. The matrices,

$$K_k \equiv \begin{pmatrix} 0 & \hat{\mathbf{e}}_k \\ \hat{\mathbf{e}}_k & \mathbf{0}_3 \end{pmatrix} \ , \tag{9.55}$$

with the unit vectors $\hat{\mathbf{e}}_k = \hat{\mathbf{e}}_x, \hat{\mathbf{e}}_y, \hat{\mathbf{e}}_z$ generate linear boosts and the matrices,

$$S_k \equiv \begin{pmatrix} 0 & \mathbf{0} \\ \mathbf{0} & \mathbf{S}_k \end{pmatrix} \quad \text{with} \quad \mathbf{S}_x \equiv \hat{\mathbf{e}}_z\hat{\mathbf{e}}_y^\dagger - \hat{\mathbf{e}}_y\hat{\mathbf{e}}_z^\dagger \ , \quad \mathbf{S}_y \equiv \hat{\mathbf{e}}_x\hat{\mathbf{e}}_z^\dagger - \hat{\mathbf{e}}_z\hat{\mathbf{e}}_x^\dagger \ , \quad \mathbf{S}_z \equiv \hat{\mathbf{e}}_y\hat{\mathbf{e}}_x^\dagger - \hat{\mathbf{e}}_x\hat{\mathbf{e}}_y^\dagger \ , \tag{9.56}$$

generate spatial rotations around the 3 Cartesian axes. We note that the squares of all matrices S_k and K_k are diagonal and that,

$$[S_i, S_j] = \epsilon_{ijk}S_k \quad , \quad [S_i, K_j] = \epsilon_{ijk}K_k \quad , \quad [K_i, K_j] = -\epsilon_{ijk}S_k \ . \tag{9.57}$$

Example 97 (*Actions of the matrices* K_k *and* S_k): For example, the operation

$$(x'^\mu) = (\mathbb{I}_4 + K_z)^\mu{}_\nu (x^\nu) = \begin{pmatrix} 1 & \hat{\mathbf{e}}_z \\ \hat{\mathbf{e}}_z & \mathbb{I}_3 \end{pmatrix} \begin{pmatrix} ct \\ \mathbf{r} \end{pmatrix}$$

transports a space-time point $(ct, \mathbf{r})$ with light velocity along the z-axis to another point, $(ct', \mathbf{r}') = (ct + z, \mathbf{r} + ct\hat{\mathbf{e}}_z)$. And the operation

$$(x'^\mu) = (\mathbb{I}_4 + S_z)^\mu{}_\nu (x^\nu) = \begin{pmatrix} 1 & \mathbf{0} \\ \mathbf{0} & \mathbb{I}_3 + S_z \end{pmatrix} \begin{pmatrix} ct \\ \mathbf{r} \end{pmatrix} = \begin{pmatrix} ct \\ \begin{pmatrix} 1 & -1 & 0 \\ 1 & 1 & 0 \\ 0 & 0 & 1 \end{pmatrix} \mathbf{r} \end{pmatrix} = \begin{pmatrix} ct \\ x - y \\ y + x \\ z \end{pmatrix}$$

transports a space-time point $(ct, \mathbf{r})$ around the z-axis to another point, $(ct', \mathbf{r}') = (ct, x - y, y + x, z)$.

The *Lorentz boost* can now be written as,

$$\boxed{\begin{aligned} \Lambda = e^L \quad &\text{with} \quad L = -\vec{\omega}\cdot\mathbf{S} - \vec{\zeta}\cdot\mathbf{K} \\ &\text{where} \quad \mathbf{S} \equiv \begin{pmatrix} S_x & S_y & S_z \end{pmatrix} \\ &\text{and} \quad \mathbf{K} \equiv \begin{pmatrix} K_x & K_y & K_z \end{pmatrix} \end{aligned}} \ . \tag{9.58}$$

We verify that,

$$\det \Lambda = \det e^L = e^{\text{Tr } L} = \pm 1 \ . \tag{9.59}$$

Example 98 (*Lorentz-boost without rotation*): For a Lorentz-boost without rotation,

$$\Lambda = e^{-\vec{\zeta}\cdot\mathbf{K}} \qquad \text{with} \qquad \vec{\zeta} = \hat{\mathbf{e}}_\beta \tanh^{-1}\beta \ ,$$

we get,

$$\Lambda = \begin{pmatrix} \gamma & -\gamma\beta_x & -\gamma\beta_y & -\gamma\beta_z \\ -\gamma\beta_x & 1+\frac{(\gamma-1)\beta_x^2}{\beta^2} & \frac{(\gamma-1)\beta_x\beta_y}{\beta^2} & \frac{(\gamma-1)\beta_x\beta_z}{\beta^2} \\ -\gamma\beta_y & \frac{(\gamma-1)\beta_x\beta_y}{\beta^2} & 1+\frac{(\gamma-1)\beta_y^2}{\beta^2} & \frac{(\gamma-1)\beta_y\beta_z}{\beta^2} \\ -\gamma\beta_z & \frac{(\gamma-1)\beta_x\beta_z}{\beta^2} & \frac{(\gamma-1)\beta_y\beta_z}{\beta^2} & 1+\frac{(\gamma-1)\beta_z^2}{\beta^2} \end{pmatrix} = \begin{pmatrix} \gamma & -\gamma\vec{\beta} \\ -\gamma\vec{\beta} & \mathbb{I}_3 + (\gamma-1)\hat{\beta}_i\hat{\beta}_j \end{pmatrix} \ , \tag{9.60}$$

as will be shown in Exc. 9.1.7.6. The Lorentz transform (9.19) into a system moving along the z-axis follows immediately with $\beta_x = \beta_y = 0$.

9.1.6.1 The Thomas precession

We consider the circular motion of an electron around a nucleus about the z-axis subject to a centripetal (Coulombian) force. The nucleus is fixed in the lab frame S, the electron's rest frame S' moves with respect to the lab frame at the instantaneous velocity $\mathbf{v}(t) = c\vec{\beta}(t)$, as illustrated in Fig. 9.4.

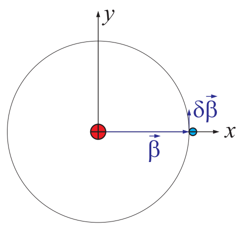

Figure 9.4: Circular motion of an electron around a nucleus.

At time t, when the electron's velocity is $\vec{\beta}(t)$, the Lorentz transform from S to S' is described by [47],

$$x'(t) = \Lambda_{boost}(\vec{\beta})x \ , \tag{9.61}$$

Note, that the nucleus' position does not change in the frame S, $x(t+\delta t) = x(t) = x$. At a later time $t+\delta t$, when the electron's velocity is $\vec{\beta}(t+\delta t) = \vec{\beta}(t) + \delta\vec{\beta}(t)$, the Lorentz transform,

$$x'(t+\delta t) = \Lambda_{boost}(\vec{\beta}+\delta\vec{\beta})x = \Lambda_{boost}(\vec{\beta}+\delta\vec{\beta})\Lambda^{-1}_{boost}(\vec{\beta})x'(t) \tag{9.62}$$

can be expressed as a Lorentz transform from the electron's system S' at time t to the same S' at time $t+\delta t$. From the expression (9.60) for a Lorentz-boost without rotation, setting $\beta_z = 0$, we get for Lorentz-boost in the xy-plane,

$$\Lambda^{\pm 1}_{boost}(\beta_x\hat{\mathbf{e}}_x + \beta_y\hat{\mathbf{e}}_y) = \begin{pmatrix} \gamma & \mp\gamma\beta_x & \mp\gamma\beta_y & 0 \\ \mp\gamma\beta_x & 1+\frac{(\gamma-1)\beta_x^2}{\beta^2} & \frac{(\gamma-1)\beta_x\beta_y}{\beta^2} & 0 \\ \mp\gamma\beta_y & \frac{(\gamma-1)\beta_x\beta_y}{\beta^2} & 1+\frac{(\gamma-1)\beta_y^2}{\beta^2} & 0 \\ 0 & 0 & 0 & 1 \end{pmatrix} \ . \tag{9.63}$$

Now, setting the initial position of the electron along the direction $\vec{\beta}(t) = \beta\hat{\mathbf{e}}_x$, as shown in Fig. 9.4, we get,

$$\Lambda^{-1}_{boost}(\vec{\beta}) = \begin{pmatrix} \gamma & \gamma\beta & 0 & 0 \\ \gamma\beta & \gamma & 0 & 0 \\ 0 & 0 & 1 & 0 \\ 0 & 0 & 0 & 1 \end{pmatrix} , \tag{9.64}$$

and, expanding γ for small velocity changes like,

$$\gamma + \delta\gamma = \frac{1}{\sqrt{1-(\beta+\delta\beta)^2}} \simeq \gamma + \gamma^3\beta\delta\beta , \tag{9.65}$$

we find,

$$\begin{aligned} \Lambda_{boost}(\vec{\beta}+\delta\vec{\beta}) &= \begin{pmatrix} \gamma+\delta\gamma & -(\gamma+\delta\gamma)(\beta+\delta\beta_x) & -(\gamma+\delta\gamma)\delta\beta_y & 0 \\ -(\gamma+\delta\gamma)(\beta+\delta\beta_x) & 1+\frac{(\gamma+\delta\gamma-1)(\beta+\delta\beta_x)^2}{(\beta+\delta\beta_x)^2} & \frac{(\gamma+\delta\gamma-1)(\beta+\delta\beta_x)\delta\beta_y}{(\beta+\delta\beta_x)^2} & 0 \\ -(\gamma+\delta\gamma)\delta\beta_y & \frac{(\gamma+\delta\gamma-1)(\beta+\delta\beta_x)\delta\beta_y}{(\beta+\delta\beta_x)^2} & 1+\frac{(\gamma+\delta\gamma-1)(\delta\beta_y)^2}{(\beta+\delta\beta_x)^2} & 0 \\ 0 & 0 & 0 & 1 \end{pmatrix} \\ &\simeq \begin{pmatrix} \gamma+\gamma^3\beta\delta\beta_x & -\gamma\beta-\gamma^3\delta\beta_x & -\gamma\delta\beta_y & 0 \\ -\gamma\beta-\gamma^3\delta\beta_x & \gamma+\gamma^3\beta\delta\beta_x & \frac{\gamma-1}{\beta}\delta\beta_y & 0 \\ -\gamma\delta\beta_y & \frac{\gamma-1}{\beta}\delta\beta_y & 1 & 0 \\ 0 & 0 & 0 & 1 \end{pmatrix} . \end{aligned} \tag{9.66}$$

Multiplying the matrices (9.65) and (9.66) we get,

$$\Lambda_{Th}(\vec{\beta}+\delta\vec{\beta}) = \Lambda_{boost}(\vec{\beta}+\delta\vec{\beta})\Lambda^{-1}_{boost}(\vec{\beta}) \simeq \begin{pmatrix} 1 & -\gamma^2\delta\beta_x & -\gamma\delta\beta_y & 0 \\ -\gamma^2\delta\beta_x & 1 & \frac{\gamma-1}{\beta}\delta\beta_y & 0 \\ -\gamma\delta\beta_y & -\frac{\gamma-1}{\beta}\delta\beta_y & 1 & 0 \\ 0 & 0 & 0 & 1 \end{pmatrix} . \tag{9.67}$$

This represents an infinitesimal Lorentz transformation that, expressing the components of $\delta\vec{\beta}$ parallel and perpendicular to β by,

$$\delta\vec{\beta}_{\|} = \tfrac{\delta\vec{\beta}\cdot\vec{\beta}}{\beta^2}\vec{\beta} \qquad \text{and} \qquad \delta\vec{\beta}_{\perp} = \delta\vec{\beta} - \tfrac{\delta\vec{\beta}\cdot\vec{\beta}}{\beta^2}\vec{\beta} \tag{9.68}$$

can be written in terms of the matrices **S** and **K** as [5],

$$\boxed{\begin{aligned} \Lambda_{Th}(\vec{\beta}+\delta\vec{\beta}) &= \mathbb{I} - \tfrac{\gamma-1}{\beta^2}(\vec{\beta}\times\delta\vec{\beta})\cdot\mathbf{S} - (\gamma^2\delta\vec{\beta}_{\|} + \gamma\delta\vec{\beta}_{\perp})\cdot\mathbf{K} \\ &\simeq R(\Delta\vec{\Omega})\ \Lambda_{boost}(\Delta\vec{\beta}) \end{aligned}} . \tag{9.69}$$

[5] We note that, for the case $\vec{\beta}(t) = \beta\hat{\mathbf{e}}_x$ Eq. (9.69) can be written as,

$$\Lambda_{Th} = \mathbb{I} - \frac{\gamma-1}{\beta}S_z\delta\beta_y - \gamma^2K_x\delta\beta_x - \gamma K_y\delta\beta_y ,$$

which reproduces exactly Eq. (9.67).

Here, we defined the *commuting* infinitesimal boosts and rotations called *Wigner rotations*,

$$\Lambda_{boost}(\Delta\vec{\beta}) \equiv \mathbb{I} - \Delta\vec{\beta}\cdot\mathbf{K} \qquad \text{and} \qquad R(\Delta\vec{\Omega}) \equiv \mathbb{I} - \Delta\vec{\Omega}\cdot\mathbf{S} \tag{9.70}$$

in terms of velocity and rotation angle,

$$\Delta\vec{\beta} \equiv \gamma^2\delta\vec{\beta}_{\parallel} + \gamma\delta\vec{\beta}_{\perp} \qquad \text{and} \qquad \Delta\vec{\Omega} \equiv \frac{\gamma-1}{\beta^2}\vec{\beta}\times\delta\vec{\beta} \ . \tag{9.71}$$

Clearly, the second line of (9.69) holds to first order in $\delta\vec{\beta}$. Thus, the pure Lorentz boost (9.62) to the frame with velocity $c(\vec{\beta}+\delta\vec{\beta})$ is equivalent to a boost (9.61) to a frame moving with velocity $c\vec{\beta}$, followed by an infinitesimal Lorentz transformation consisting of a boost with velocity $c\vec{\Delta}\beta$ and a rotation $\Delta\vec{\Omega}$.

In summary, we got,

$$\begin{aligned} x'(t+\delta t) &= \Lambda_{boost}(\vec{\beta}+\delta\vec{\beta})x = \Lambda_{boost}(\vec{\beta}+\delta\vec{\beta})\Lambda^{-1}_{boost}(\vec{\beta})x'(t) \\ &= \Lambda_{Th}(\vec{\beta}+\delta\vec{\beta})x'(t) = R(\Delta\Omega)\Lambda_{boost}(\Delta\vec{\beta})x'(t) \ . \end{aligned} \tag{9.72}$$

In terms of the interpretation of the moving frames as successive rest frames of the electron we do not want rotations as well as boosts. Non-relativistic equations of motion can be expected to hold provided the evolution of the rest frame is described by infinitesimal boosts without rotations. We are thus led to consider the rest-frame coordinates at time $t+\delta t$ that are given from those at time t by the boost $\Lambda_{boost}(\Delta\vec{\beta})$ instead of Λ_{Th}. Denoting these coordinates by $\tilde{x}'$ we have,

$$\begin{aligned} \tilde{x}'(t+\delta t) &= \Lambda_{boost}(\Delta\vec{\beta})x'(t) \\ &= R(-\Delta\vec{\Omega})x'(t+\delta t) = R(-\Delta\vec{\Omega})\Lambda_{boost}(\vec{\beta}+\delta\vec{\beta})x \ . \end{aligned} \tag{9.73}$$

The rest system of coordinates defined by $\tilde{x}'$ is rotated by $R(-\Delta\vec{\Omega})$ relative to the boosted laboratory axes x'. If a physical vector $\mathbf{G}$ has a (proper) time rate of change $(d\mathbf{G}/d\tau)$ in the rest frame, the precession of the rest-frame axes with respect to the laboratory makes the vector have a total time rate of change with respect to the laboratory axes of,

$$\left(\frac{d\mathbf{G}}{dt}\right)_{non-rot} = \left(\frac{d\mathbf{G}}{dt}\right)_{rest} + \vec{\omega}_{Th}\times\mathbf{G} \ . \tag{9.74}$$

with

$$\vec{\omega}_{Th} = -\lim_{\delta t\to 0}\frac{\Delta\Omega}{\delta t} = \frac{\gamma^2}{\gamma+1}\frac{\mathbf{a}\times\mathbf{v}}{c^2} \ , \tag{9.75}$$

where $\mathbf{a}$ is the acceleration in the laboratory frame and, to be precise,

$$\left(\frac{d\mathbf{G}}{dt}\right)_{rest} = \gamma^{-1}\left(\frac{d\mathbf{G}}{d\tau}\right)_{rest} \ . \tag{9.76}$$

The *Thomas precession* is purely kinematical in origin. If a component of acceleration exists perpendicular to $\mathbf{v}$, for whatever reason, then there is a Thomas precession, independent of other effects such as precession of the magnetic moment in a magnetic field.

Example 99 (*Circular motion*): Assuming a constant circular motion about the z-axis, as parametrized by $\mathbf{v} = r\dot{\theta}\hat{\mathbf{e}}_\theta$ and $\mathbf{a} = -r\dot{\theta}^2\hat{\mathbf{e}}_r = -\dot{\theta}v\hat{\mathbf{e}}_r$ with $\dot{\theta} = const$, we find,

$$\vec{\omega}_{Th} = \frac{\gamma^2}{\gamma+1}\frac{\mathbf{a}\times\mathbf{v}}{c^2} = \frac{\gamma^2}{\gamma+1}\frac{-\dot{\theta}v^2}{c^2}\hat{\mathbf{e}}_z = -\frac{\gamma^2\beta^2}{\gamma+1}\dot{\theta}\hat{\mathbf{e}}_z = -(\gamma-1)\dot{\theta}\hat{\mathbf{e}}_z \ .$$

9.1.6.2 Spin-Orbit coupling

For electrons in atoms the acceleration is caused by the screened Coulomb field. Thus the Thomas angular velocity is,

$$\vec{\omega}_{Th} \simeq -\frac{1}{2c^2}\frac{\mathbf{r}\times\mathbf{v}}{m}\frac{1}{r}\frac{dV}{dr} = -\frac{1}{2m^2c^2}\mathbf{L}\frac{1}{r}\frac{dV}{dr} \ . \tag{9.77}$$

It is evident that the extra contribution to the energy from the Thomas precession reduces the spin-orbit coupling, yielding,

$$U = \frac{-ge}{2mc}\vec{\mathcal{S}}\cdot\vec{\mathcal{B}} + \frac{(g-1)}{2m^2c^2}\vec{\mathcal{S}}\cdot\mathbf{L}\frac{1}{r}\frac{dV}{dr} \ . \tag{9.78}$$

9.1.7 Exercises

9.1.7.1 Ex: Contravariant partial derivation

Show that the partial derivative by the contravariant coordinate x^μ is covariant.

9.1.7.2 Ex: Time dilatation

Proxima Centauri, which is the closest star to our solar system with a distance of 4.22 light-years from Earth, is a so-called Red Dwarf of class M. At its 34th anniversary, Peter embarks on a journey from Earth to this star. His spaceship flies with a speed of 250000 km/s. How old is Peter when he arrives? What is the age of Peter's twin brother, who remained on Earth at this time?

9.1.7.3 Ex: The twin paradox

Explain the twin paradox by applying the Lorentz transform to the twin traveling on a round-trip to α-Centauri assuming a fixed distance between Earth and α-Centauri.

9.1.7.4 Ex: Muons

In the upper layers of the atmosphere (at 20 km altitude) about 250 muons are generated per square meter and second. After that they move with 99.98% of the speed of light towards the surface of the Earth. Muons at rest have a lifetime of 1.52 µs.
a. Assuming that there were no time dilatation, how many muons would arrive per square meter and second at the surface of the Earth?
b. How many muons actually reach the surface of the Earth?

9.1.7.5 Ex: Atomic clocks

In 1971 atomic clocks were taken by a high-speed aircraft to measure time dilatation directly. How long must an aircraft fly at a speed of 3000 km/h, so that the airplane's clock and a clock fixed on Earth show, due to time dilatation, a difference of one second?

9.1.7.6 Ex: Lorentz-boost without rotation

Derive the matrix (9.60) for the Lorentz-boost without rotation to a system moving in arbitrary direction.

9.2 Relativistic mechanics

9.2.1 The inherent time of an inertial system

The key to constructing relativistic theories is to find the quantities behaving well under Lorentz transformations. We have already defined some quantities in (9.32) and (9.33). But we need more to establish a *relativistic mechanics*. In the following sections we will analyze how other kinematic variables (velocity, momentum, and acceleration) fit into four-vectors. Since these variables are defined through time derivatives, an accurate characterization of the notion of *time intervals* is necessary.

We consider an object following a space-time trajectory. As the evaluation of traveled distances and elapsed time intervals depends on the observer's inertial system, there is no universal parametrization. But there is at least one 'natural' parametrization that all observers can agree on, which is the proper time τ, which is the duration of time felt by the object itself. Due to time dilatation, an observer sitting in some inertial system and measuring the motion of the object with the old-fashioned Newtonian tri-velocity $\mathbf{v}(t)$ infers, that the relation between his own time t and the proper time τ of the particle is given by,

$$\boxed{\frac{dt}{d\tau} = \gamma_v \equiv \frac{1}{\sqrt{1 - v^2/c^2}} > 1} \ . \tag{9.79}$$

Example 100 (*Common velocity under Lorentz transformation*): We could define the *common velocity* of a body via the distance $\mathbf{r}$ covered in a time interval t measured in the laboratory system (in relation to which the body travels with this velocity),

$$(v^\mu) \equiv \frac{d(r^\mu)}{dt} = \begin{pmatrix} c \\ \mathbf{v} \end{pmatrix}$$

However, the contraction of this 4-vector is not a Lorentz invariant because,

$$v_\mu v^\mu = c^2 - v^2 \neq c^2 - v'^2 = v'_\mu v'^\mu \ .$$

On the other hand, the notion of *proper time* allows us to define a true quadri-velocity. We assume that in some inertial system, the body follows the trajectory $r^\mu(\tau)$. Then the quantity,

$$u^\mu \equiv \gamma_v v^\mu = \gamma_v \frac{dr^\mu}{dt} = \gamma_v \frac{d\tau}{dt}\frac{dr^\mu}{d\tau} = \frac{dr^\mu}{d\tau} \quad \text{that is} \quad (u^\mu) = \begin{pmatrix} \gamma_v c \\ \gamma_v \mathbf{v} \end{pmatrix} , \tag{9.80}$$

called *proper velocity* is a Lorentz invariant, since,

$$u_\mu u^\mu = c^2 . \tag{9.81}$$

A useful illustration of the relation between space and time, as proposed by Minkowski, is exhibited in Fig. 9.5. The inner region of the cone represents the space-time points in a lab frame that a moving body can reach within a given time interval. The cone's surface are the points that can be reaches traveling at light speed, and the outer region remains inaccessible.

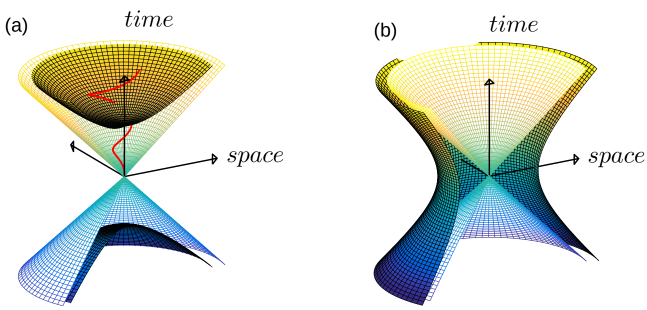

Figure 9.5: Two-dimensional illustration of Minkowski space-time. The cones delimits accessible (inside) from inaccessible (outside) regions. The red curve in (a) represents a possible trajectory for a moving body. The hyperboloid in (a) represents the hyperspace where a system S' with its *proper velocity* v is found after a time τ elapsed in the system S'. The hyperboloid in (b) represents the hyperspace of 'space'-like intervals according to (9.33).

9.2.2 Adding velocities

The Lorentz transformation from system S' moving with respect to another system S with the relative velocity v_0 must be applied to the proper velocity,

$$\begin{pmatrix} \gamma_{v'} c \\ \gamma_{v'} v' \end{pmatrix} = (\Lambda^\mu{}_\nu) \begin{pmatrix} \gamma_v c \\ \gamma_v v \end{pmatrix} = \begin{pmatrix} \gamma & -\gamma\beta \\ -\gamma\beta & \gamma \end{pmatrix} \begin{pmatrix} \gamma_v c \\ \gamma_v v \end{pmatrix} = \gamma_v \gamma \begin{pmatrix} c - \beta v \\ -\beta c + v \end{pmatrix} , \tag{9.82}$$

where we denote $\gamma \equiv \gamma_{v_0}$. Eliminating $\gamma_{v'}$ and resolving by v' we get,

$$v' = \frac{v - v_0}{1 - v_0 v / c^2} . \tag{9.83}$$

Obviously, the speed of light can not be exceeded. The velocity in the system S' is limited to $-c \le v' \le c$, even if $v = c$. Similar calculations can be made for the two transverse directions, and we obtain the general formula reproduced here without proof,

$$\mathbf{v} = \frac{\mathbf{v}' + \mathbf{v}_0\left[\gamma(1+\mathbf{v_0}\cdot\mathbf{v}'/v_0^2) - \mathbf{v}_0\cdot\mathbf{v}'/v_0^2\right]}{\gamma(1+\mathbf{v}_0\cdot\mathbf{v}'/c^2)} . \tag{9.84}$$

We calculate in Exc. 9.2.6.1 an example of relativistic addition of velocities.

9.2.3 Relativistic momentum and rest energy

The *relativistic linear momentum* is given by,

$$\boxed{p^\mu \equiv mu^\mu = m\gamma_v v^\mu \qquad \text{or} \qquad (p^\mu) = \begin{pmatrix} E/c \\ \mathbf{p} \end{pmatrix}} . \tag{9.85}$$

We will show in Exc. 9.2.6.2 that an identification of the momentum p^μ with mv^μ would be inconsistent with the principle of momentum conservation and the principle of relativity. For zero velocity of the particle, $\mathbf{v} = 0$, the first line of the expression (9.85) is the famous Einstein equation on the equivalence of mass and energy,

$$E = mc^2 . \tag{9.86}$$

Thus, the mass is nothing more than the energy of the particle in its rest frame.

Transforming into the rest frame, we have:

$$p'_\mu p'^\mu = \left\|\begin{pmatrix} E/c \\ \mathbf{p} \end{pmatrix}\right\|^2 = \left\|\begin{pmatrix} mc \\ \mathbf{0} \end{pmatrix}\right\|^2 = p_\mu p^\mu , \tag{9.87}$$

yielding,

$$E = \sqrt{m^2c^4 + c^2\mathbf{p}^2} = mc^2\sqrt{1+\gamma_v^2\frac{\mathbf{v}^2}{c^2}} = \gamma_v mc^2 . \tag{9.88}$$

The kinetic energy in the non-relativistic limit follows from a Taylor expansion of the expression (9.88) for low velocities,

$$E_{kin} \equiv E - mc^2 = mc^2(\gamma_v - 1) \simeq \frac{p^2}{2m} - \frac{p^4}{8m^3c^2} . \tag{9.89}$$

Example 101 (*Compton scattering*): Here we consider the interaction of a photon with an electron. The electron has the rest mass m_e. Thus, transforming to the rest frame, we find its energy via, $(p_e)_\mu(p_e)^\mu = E_e^2/c^2 - \mathbf{p}^2 = m_e^2c^4$. The photon has no rest mass. Thus, transforming to the rest frame, we find its energy via, $(p_\gamma)_\mu(p_\gamma)^\mu = (\hbar k)^2 = (\hbar\omega)^2/c^2$.

Now we let the photon with energy $\hbar\omega_i$ bounce off an electron initially at rest. After the collision the photon and the electron move away under angles of $\sin\theta_\gamma$, respectively, $\sin\theta_e$, with respect to the collision axis. As shown in Fig. 9.6, we can choose the collision axis along the z-axis and within the xy-plane. The photon has changed its energy to $\hbar\omega_f$ and its momentum to $\hbar k_f$, the electron now has the momentum $\mathbf{p}_f$. For an elastic collision, energy and linear momentum conservation request,

$$p_i^\mu \equiv \begin{pmatrix} E_i/c \\ p_i^x \\ p_i^y \\ p_i^z \end{pmatrix} = \begin{pmatrix} \hbar\omega_i/c + m_ec \\ 0 \\ 0 \\ \hbar k_i \end{pmatrix} \overset{!}{=} \begin{pmatrix} \hbar\omega_f/c + \sqrt{m_e^2c^2 + p_f^2} \\ -\hbar k_f\sin\theta_\gamma + p_f\sin\theta_e \\ 0 \\ \hbar k_f\cos\theta_\gamma + p_f\cos\theta_e \end{pmatrix} = \begin{pmatrix} E_f/c \\ p_f^x \\ p_f^y \\ p_f^z \end{pmatrix} \equiv p_f^\mu .$$

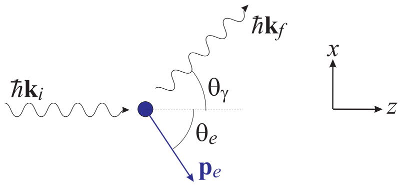

Figure 9.6: Scattering of a photon from an electron.

Solving the second line by θ_e and substituting into the fourth,

$$\frac{\hbar\omega_i}{c} = \hbar k_i = p_f\cos\theta_e + \hbar k_f\cos\theta_\gamma = p_f\sqrt{1-\sin^2\theta_e} + \hbar k_f\cos\theta_\gamma$$
$$= p_f\sqrt{1-\left(\frac{\hbar k_f}{p_f}\right)^2\sin^2\theta_\gamma} + \hbar k_f\cos\theta_\gamma\ .$$

Solving this by p_f,

$$c^2p_f^2 = (\hbar\omega_i - c\hbar k_f\cos\theta_\gamma)^2 - (c\hbar k_f)^2\sin^2\theta_\gamma = (\hbar\omega_i)^2 - 2\hbar\omega_i c\hbar k_f\cos\theta_\gamma + (c\hbar k_f)^2$$
$$= (\hbar\omega_i)^2 - 2\hbar\omega_i\hbar\omega_f\cos\theta_\gamma + (\hbar\omega_f)^2\ .$$

Inserting this result into energy conservation,

$$\hbar\omega_i + m_ec^2 = \hbar\omega_f + \sqrt{m_e^2c^4 + c^2p_f^2} = \hbar\omega_f + \sqrt{m_e^2c^4 + (\hbar\omega_i)^2 - 2\hbar\omega_i\hbar\omega_f\cos\theta_\gamma + (\hbar\omega_f)^2}\ .$$

Solving this by ω_f,

$$\frac{hc}{\lambda_f} = \hbar\omega_f = \frac{1}{(1-\cos\theta_\gamma)/m_ec^2 + 1/\hbar\omega_i}\ ,$$

or defining the *Compton wavelength* of the electron,

$$\lambda_C \equiv \frac{h}{m_ec}$$

we find for the wavelength of the scattered photon,

$$\lambda_f = \lambda_i + \lambda_C(1-\cos\theta_\gamma)\ .$$

Other examples of relativistic collisions will be studied in Excs. 9.2.6.3 to 9.2.6.5.

9.2.4 Relativistic Doppler effect

We have seen at the example of sonic waves, that the magnitude of the Doppler effect depends on who moves with respect to the *medium*: the source or the receiver. Electromagnetic waves, however, propagate in empty space, that is, there is no material medium, ether, or wind. According to Einstein's theory of relativity, there is no absolute motion and the propagation velocity of light is the same for all inertial systems. Therefore, the classical theory of the Doppler effect can not apply to electromagnetic waves.

By the fact that the vector k_μ given by,

$$\boxed{k^\mu \equiv \frac{p^\mu}{\hbar} \qquad \text{that is} \qquad (k^\mu) = \begin{pmatrix} \omega/c \\ \mathbf{k} \end{pmatrix}} \tag{9.90}$$

is a space-time vector,

$$k_\mu k^\mu = \omega^2/c^2 - k^2 = 0 \;, \tag{9.91}$$

we know that this vector transforms like,

$$\begin{pmatrix} \omega/c \\ k \end{pmatrix} = (\Lambda_{\mu\nu})^{-1} \begin{pmatrix} \omega'/c \\ k' \end{pmatrix} = \begin{pmatrix} \gamma & \gamma\beta \\ \gamma\beta & \gamma \end{pmatrix} \begin{pmatrix} \omega'/c \\ k' \end{pmatrix} \tag{9.92}$$

$$= \begin{pmatrix} \gamma\frac{\omega'}{c} + \gamma\beta k' \\ \gamma\beta\frac{\omega'}{c} + \gamma k' \end{pmatrix} = \frac{\omega'}{c}\gamma(1+\beta) \begin{pmatrix} 1 \\ 1 \end{pmatrix} \;,$$

such that,

$$\boxed{\omega = ck = \omega'\sqrt{\frac{1+\beta}{1-\beta}} = \gamma\omega'(1+\beta)} \;. \tag{9.93}$$

Including the transverse motion, we obtain

$$\omega = \gamma\omega'\left(1 + \frac{\mathbf{v}_0 \cdot \mathbf{v}}{vc}\right) \;, \tag{9.94}$$

where $\mathbf{v}_0$ is the speed of the source. It is interesting to note that, even in case of a purely transverse motion $\mathbf{v}_0 \cdot \mathbf{v} = 0$, we observe a Doppler shift.

Example 102 (*Doppler effect on a moving laser*): We now consider a light source flying through the lab S, for example, a laser operating at a frequency ω', which is well-defined by an atomic transition of the active medium. A spectrometer installed in the same rest frame S' as the laser will measure just this frequency. We now ask, what frequency would be measured by a spectrometer installed in the lab frame. The classical response has already been derived for a moving sound source,

$$\omega' = \omega - kv = \omega - \frac{\omega}{c}v = \frac{\omega}{1+\frac{v}{c}} \;,$$

with $k = \omega/c$. Because of time dilatation, we need to multiply by γ,

$$\omega' = \frac{\gamma^{-1}\omega}{1+\frac{v}{c}} = \omega\sqrt{\frac{1-\beta}{1+\beta}} \simeq \omega\left(1 \pm \frac{v}{c} + \frac{v^2}{2c^2}\right) \;.$$

The above example shows that, for non-relativistic velocities, one can distinguish the *first-order Doppler effect* from the *relativistic Doppler effect* due to time dilatation,

$$\boxed{\omega' \simeq \omega \pm kv + \tfrac{1}{2}\omega\beta^2} \;. \tag{9.95}$$

We will study the Doppler effect for the case of ultracold atoms in Excs. 9.2.6.6 to 9.2.6.8.

9.2.5 Relativistic Newton's law

The relativistic form of *Newton's law*,

$$\mathbf{F} = \frac{d\mathbf{p}}{dt} \,, \tag{9.96}$$

with the momentum given by (9.85) defines the *common* relativistic force. However, because it is derived from the momentum with respect to common time, the common force $\mathbf{F}$ *can not* be extended to a Lorentz invariant of the type F^μ. In contrast, *Minkowski force* defined as,

$$\boxed{K_\mu = \frac{dp_\mu}{d\tau} = \frac{\gamma_v dp_\mu}{dt} \qquad \text{that is} \qquad (K^\mu) = \begin{pmatrix} \gamma_v P/c \\ \gamma_v \mathbf{F} \end{pmatrix}} \,, \tag{9.97}$$

is covariant. Nevertheless, we will often be interested in the common force $\mathbf{F}$ acting on moving bodies as measured in a laboratory frame.

The work exerted on a particle increases its kinetic energy, such that,

$$\begin{aligned} W \equiv \int \mathbf{F} \cdot d\mathbf{l} &= \int \frac{d\mathbf{p}}{dt} \cdot d\mathbf{l} = \int \frac{d\mathbf{p}}{dt} \cdot \mathbf{v} \; dt = \int \frac{d}{dt}(\gamma_v m \mathbf{v}) \cdot \mathbf{v} \; dt \\ &= \int (\gamma_v^3 m \dot{\mathbf{v}}) \cdot \mathbf{v} \; dt = \int mc^2 \frac{d\gamma_v}{dt} dt = \int \frac{dE}{dt} dt = E_{final} - E_{initial} \,. \end{aligned} \tag{9.98}$$

Unlike the first two Newton laws, the third one (actio = reactio) does *not* apply in the relativistic regime. Indeed, the simultaneity of 'actions' and reactions' in the forces that two distant bodies A and B exert on each other depends on the velocity of the observer.

9.2.6 Exercises

9.2.6.1 Ex: Adding velocities

Imagine an array of flash lamps at rest in the system S. The lamps are aligned at distances of $\Delta s = 10\,\text{m}$ from each other. The array extends over a distance of many light-years. Now, the lamps are flashed successively (from left to right), so that the light seems to move to the right.
a. At what time interval Δt two adjacent lamps need to flash in order to generate an apparent velocity of $v_1 = 1.2c$?
b. An inertial system S' moves relative to S with velocity $v_2 = -0.56c$ in opposite direction to that of the motion of the flashes. At what velocity the flashes seem to be moving in the system S'?

9.2.6.2 Ex: Covariant momentum

Show that an identification of the momentum p^μ with mv^μ would be inconsistent with the principle of momentum conservation and the principle of relativity.

9.2.6.3 Ex: Inelastic collision

A particle of mass m whose total energy is twice its rest energy collides with an identical particle at rest. If they stick together, what is the mass of the resulting particle compound? What is its velocity?

9.2.6.4 Ex: Relativistic collision

Consider a relativistic completely inelastic frontal collision of two particles moving along the x-axis. Both particles have mass m. Before the collision, an observer A sitting in an inertial frame, notices that the masses move with the same constant velocities but in the opposite direction, that is, the particle 1 moves with velocity v and the particle 2 moves with velocity $-v$. According to another observer B, however, particle 1 is initially at rest.
a. Determine the velocity v'_x of particle 2 measured by observer B before collision.
b. Find the velocities v_A and v'_B of the particle resulting from the collision, measured, respectively, by the observers A and B.
c. Use the relativistic mass-energy conservation and calculate the mass M of the particle resulting from the collision.

9.2.6.5 Ex: γ-rays

γ-rays produced by paired annihilation exhibit considerable Compton scattering. Consider a photon produced with the energy m_0c^2 by the annihilation of an electron and a positron, where m_0 is the rest mass of the electron. Suppose that this photon be scattered by a free electron and that the scattering angle is θ_γ, as shown in Fig. 9.6.
a. Find the maximum possible kinetic energy for the recoiling electron.
b. If the scattering angle were $\theta_\gamma = 120°$, determine the photon energy and the kinetic energy of the electron after the scattering.
c. If $\theta_\gamma = 120°$, what is the direction of motion of the electron after the scattering with respect to the direction of the incident photon?

9.2.6.6 Ex: Second order Doppler shift

The *second order Doppler shift* comes from the relativistic dilation of time. Periodic events occurring in a moving inertial system appear dilated to an observer in another system. Consider a strontium atom, which has a resonance at the wavelength $\lambda = 461\,\text{nm}$, located inside a resonant laser beam from which it absorbs and reemits photons.
a. Assume the atom initially at rest. What will be it's velocity after having absorbed a single photon?
b. Calculate the first and second order Doppler shift for the remitted photon as a function of the emission direction.

9.2.6.7 Ex: Recoil- and Doppler-shift upon photon absorption

Derive the expressions for the recoil- and Doppler-shift upon the absorption of a photon of frequency ω_i by an atom with the initial velocity $\mathbf{v}_i$ using relativistic mechanics.

9.2.6.8 Ex: Recoil- and Doppler-shift upon photon scattering in relativistic mechanics

Derive the expression for the recoil- and Doppler-shift upon the absorption and reemission of a photon of frequency ω_i by an atom with the initial velocity $\mathbf{v}_i$ using relativistic mechanics. Discuss the particular case, $\mathbf{v}_i = 0$.

9.3 Relativistic electrodynamics

9.3.1 Relativistic current and magnetism

To begin with, we introduce the space-time current density by,

$$\boxed{(j^\mu) \equiv \begin{pmatrix} c\varrho \\ \mathbf{j} \end{pmatrix}} \ . \tag{9.99}$$

This notation allows us to formulate the continuity equation as,

$$\boxed{\partial_\mu j^\mu = 0} \ . \tag{9.100}$$

Example 103 (*Electric charge under Lorentz transformation*): In order to convince ourselves that it makes sense to combine charge density and current as quadri-vectors, we consider a situation in which there are only static charges with density ϱ_0 and has no current: $j_\mu = (c\varrho_0 \ \mathbf{0})$. Now, in an inertial system moving at velocity $\mathbf{v}$, the charge density will appear as a current,

$$(j'^\mu) = (\Lambda^\mu{}_\nu j^\nu) = \begin{pmatrix} \gamma c\varrho_0 \\ -c\gamma\beta\varrho_0\hat{\mathbf{e}}_z \end{pmatrix} = \begin{pmatrix} \gamma\varrho \\ -\gamma\varrho\mathbf{v} \end{pmatrix} \ .$$

That is, different observers observe different charge densities. The current $-\gamma\varrho\mathbf{v}$ appears due to the motion of the charge being contrary to the motion of the observer. Moreover, as the charge density is defined per unit volume and the volume is compressed due to Lorentz contraction, the observed charge density $\gamma\varrho_0$ appears to be increased.

The observation that a moving charge gives rise to a current is not new. But the fact that we can transform charge into current through a Lorentz transform already points to the close connection between the phenomena of electricity and magnetism in the theory of relativity: moving electric fields must generate magnetic fields. We will study the details of how this happens shortly. But first, let us have a look at a simple example, where we re-derive the magnetic force purely from the Coulomb force and a Lorentz contraction.

Example 104 (*Electric current under Lorentz transform*): We consider a sample of positive charges $+q$ moving along a conducting wire with velocity $+v$ and a sample of negative charges $-q$ moving in opposite direction with velocity $-v$, as shown Fig. 9.7. If the densities n of positive and negative charges is equal, the total charge density vanishes, while the currents add up to $I = 2nAqv$, where A is the cross section of the wire. We now consider a test particle, also carrying a charge q, which moves parallel to the wire at some velocity v_0. This charge does not feel any electrical force, because the wire is neutral, but we know that it experiences a magnetic force. We will now show, how to find an expression for this force without ever invoking the phenomenon of magnetism. The trick is

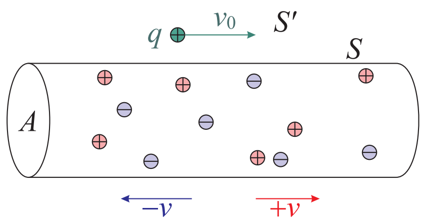

Figure 9.7: Illustration of the relativistic origin of the Lorentz force.

to go to the inertial system S' of the test particle, which means that we have to transform to a velocity v_0. The formula for summing relativistic velocities tells us, that the velocities of the positive and negative charges are now different,

$$v_\pm = \frac{v \mp v_0}{1 \mp v_0 v/c^2} \ .$$

But with this transformation comes a Lorentz contraction modifying the density of the charges. In addition, the different velocities of the positive and negative charges cause that, seen from the system S' (rest frame of the test particle), the wire is no longer neutral. Let us see how this works: First, we introduce the density of positively (negatively) charged particles n_0 in the system S_+ (S_-) in which they are at rest. With this, the charge densities in the lab system S (rest frame of the wire) are,

$$\varrho_\pm = qn_\pm = \gamma_v q n_0 \ .$$

In the system S, the wire is neutral because the positive and negative charges travel at the same velocity, albeit in opposite directions, $\varrho_+ + \varrho_- = 0$. Now, in the system S', the charge densities are,

$$\varrho'_\pm = q\gamma_{v_\pm} n_0 = \frac{1}{\sqrt{1 - \left(\frac{v \mp v_0}{c \mp v v_0/c}\right)^2}} q n_0$$
$$= \frac{-c^2 \pm v v_0}{\sqrt{(c^2 - v^2)(c^2 - v_0^2)}} q n_0 = \left(1 \mp \frac{v_0 v}{c^2}\right) \gamma_{v_0} \gamma_v q n_0 \ ,$$

Since $v_- > v_+$, we have $n'_- > n'_+$, and the wire carries negative charge. That is, the total charge density in the new system is,

$$\varrho' = q(n'_+ - n'_-) = -\frac{2v_0 v}{c^2} \gamma_{v_0} q n_\pm \ .$$

But we know that a line of electric charges creates an electric field (using Gauß' law) of,

$$\vec{\mathcal{E}}'(r) = \frac{\varrho' A}{2\pi\varepsilon_0 r} \hat{\mathbf{e}}_r = -\frac{2v_0 v}{c^2} \gamma_{v_0} q n_\pm \frac{A}{2\pi\varepsilon_0 r} \hat{\mathbf{e}}_r \ ,$$

where r is the radial direction perpendicular to the wire. This means that in its rest frame, the particle experiences a force,

$$F' = q\mathcal{E}'(r) = -v_0\gamma_{v_0}\frac{n_\pm Aq^2 v}{\pi\varepsilon_0 c^2 r} ,$$

where the negative sign tells us, that the force is in radial direction toward the center of the wire for $v_0 > 0$. But if there is a force in one system, there must also be a force in the other one. Transforming back to the lab system S, we conclude that even when the wire is neutral, there will be a force,

$$F = \frac{F'}{\gamma_{v_0}} = -v_0\frac{n_\pm Aq^2 v}{\pi\varepsilon_0 c^2 r} = -v_0 q\frac{\mu_0 I}{2\pi r} .$$

But this agrees precisely with the Lorentz force attracting or repelling two neutral current-carrying wires.

This analysis provides an explicit demonstration of how an electric force in one reference system is interpreted as a magnetic force in another. Another surprising observation is the following. We are accustomed to think of Lorentz contraction as an exotic result, which is only important, when we approach the speed of light. However, the electrons traveling on a wire are very slow, taking about an hour to travel a meter! Nevertheless, we can easily detect the magnetic force between two wires which, as we have seen above, can be directly attributed to the length contraction of the electronic density [6].

9.3.2 Electromagnetic potential and tensor

The shape of the *scalar and vector relativistic potentials* (6.104), as expressed by the laws of Coulomb and Biot-Savart, suggests their combination to a quadri-vector,

$$\boxed{(A^\mu) \equiv \begin{pmatrix} \frac{1}{c}\Phi \\ \mathbf{A} \end{pmatrix}} . \tag{9.101}$$

with this the *gauge transform* defined in (6.85) adopts the form,

$$\boxed{A^\mu \to A^\mu - \partial^\mu\chi} . \tag{9.102}$$

In particular, the *Lorentz gauge* (6.86) becomes,

$$\boxed{\partial_\mu A^\mu = 0} . \tag{9.103}$$

Now, let us have a look at the following antisymmetric construction,

$$\boxed{F^{\mu\nu} \equiv \partial^\mu A^\nu - \partial^\nu A^\mu} . \tag{9.104}$$

[6] The above discussion needs a small adjustment for real wires. In the rest frame of the wire the positive charges, which are ions, are fixed while the electrons move. According to the above explanation, we might think that this will lead to an imbalance of the charge densities. But this is not correct. The current is due to electrons injected by the battery into one end of the battery and drained at the other end in such a way, that the wire remains neutral in the rest frame, with the electron density accurately compensating the ionic density. In contrast, if we moved to a system in which ions and electrons had equal and opposite speeds, the wire would appear charged.

Obviously, this tensor is invariant under gauge transformation, since,

$$F^{\mu\nu} \to \partial^\mu(A^\nu - \partial^\nu\chi) - \partial^\nu(A^\mu - \partial^\mu\chi) = F^{\mu\nu} - \partial^\mu\partial^\nu\chi + \partial^\nu\partial^\mu\chi \ . \tag{9.105}$$

which already suggests, that the components of $F^{\mu\nu}$ have something to do with electromagnetic fields.

In fact, analyzing each component of (9.104) in the light of the equations (6.78), we find the so-called *electromagnetic field tensor*,

$$\check{F} = (F^{\mu\nu}) = \begin{pmatrix} 0 & -\frac{1}{c}\mathcal{E}_x & -\frac{1}{c}\mathcal{E}_y & -\frac{1}{c}\mathcal{E}_z \\ \frac{1}{c}\mathcal{E}_x & 0 & -\mathcal{B}_z & \mathcal{B}_y \\ \frac{1}{c}\mathcal{E}_y & \mathcal{B}_z & 0 & -\mathcal{B}_x \\ \frac{1}{c}\mathcal{E}_z & -\mathcal{B}_y & \mathcal{B}_x & 0 \end{pmatrix} = \begin{pmatrix} 0 & -\frac{1}{c}\vec{\mathcal{E}} \\ \frac{1}{c}\vec{\mathcal{E}} & (-\epsilon_{mnk}\mathcal{B}_k) \end{pmatrix} \ . \tag{9.106}$$

where ϵ_{mnk} it is the Levi-Civita tensor.

9.3.2.1 Maxwell's equations

The dual tensor is,

$$\check{\mathcal{F}} = (\mathcal{F}^{\mu\nu}) = (\tfrac{1}{2}\epsilon^{\mu\nu\alpha\beta}F_{\alpha\beta}) = \begin{pmatrix} 0 & -\mathcal{B}_x & -\mathcal{B}_y & -\mathcal{B}_z \\ \mathcal{B}_x & 0 & \frac{1}{c}\mathcal{E}_z & -\frac{1}{c}\mathcal{E}_y \\ \mathcal{B}_y & -\frac{1}{c}\mathcal{E}_z & 0 & \frac{1}{c}\mathcal{E}_x \\ \mathcal{B}_z & \frac{1}{c}\mathcal{E}_y & -\frac{1}{c}\mathcal{E}_x & 0 \end{pmatrix} = \begin{pmatrix} 0 & -\vec{\mathcal{B}} \\ \vec{\mathcal{B}} & (\frac{1}{c}\epsilon_{mnk}\mathcal{E}_k) \end{pmatrix} \ . \tag{9.107}$$

The spatio-temporal *Maxwell equations* are written,

$$\boxed{\partial_\mu F^{\mu\nu} = \mu_0 j^\nu \quad , \quad \partial_\mu \mathcal{F}^{\mu\nu} = 0} \ . \tag{9.108}$$

The first space-time Maxwell equation incorporates the familiar form of Maxwell's first and third equations,

$$\begin{aligned}(\partial_\mu F^{\mu\nu}) &= \begin{pmatrix} \frac{\partial}{c\partial t} & \nabla \end{pmatrix} \begin{pmatrix} 0 & -\frac{1}{c}\vec{\mathcal{E}} \\ \frac{1}{c}\vec{\mathcal{E}} & (-\epsilon_{mnk}\mathcal{B}_k) \end{pmatrix} = \begin{pmatrix} \frac{1}{c}\nabla\cdot\vec{\mathcal{E}} \\ -\frac{1}{c^2}\frac{\partial}{\partial t}\vec{\mathcal{E}} - \nabla\cdot(\epsilon_{mnk}B_k) \end{pmatrix}^\intercal \qquad (9.109)\\ &= \begin{pmatrix} \frac{1}{c}\nabla\cdot\vec{\mathcal{E}} \\ -\frac{1}{c^2}\frac{\partial}{\partial t}\vec{\mathcal{E}} + (\epsilon_{mkn}\frac{\partial}{\partial x^m}\mathcal{B}_k) \end{pmatrix}^\intercal = \begin{pmatrix} \frac{1}{c}\nabla\cdot\vec{\mathcal{E}} \\ -\frac{1}{c^2}\frac{\partial}{\partial t}\vec{\mathcal{E}} + \nabla\times\vec{\mathcal{B}} \end{pmatrix}^\intercal = \mu_0\begin{pmatrix} c\rho \\ \mathbf{j} \end{pmatrix}^\intercal = (\mu_0 j^\nu) \ ,\end{aligned}$$

using the definition of the vector product,

$$(\mathbf{a}\times\mathbf{b})_k = \epsilon_{mnk}a_m b_n \ . \tag{9.110}$$

The second space-time Maxwell equation incorporates Maxwell's second and fourth equations. With the definition of the Levi-Civita tensor, we can rewrite the equation as,

$$\epsilon^{\mu\nu\kappa\lambda}\partial_\kappa F_{\mu\nu} = \partial_\kappa F_{\mu\nu} + \partial_\mu F_{\nu\kappa} + \partial_\nu F_{\kappa\mu} = 0 \ . \tag{9.111}$$

This form satisfies the requirement of cyclical permutability and also takes into account the fact, that all indexes must be different. If two indexes are equal, for example, $\mu = \kappa$, we would have $\partial_\kappa F_{\mu\mu} + \partial_\mu F_{\mu\kappa} + \partial_\mu F_{\kappa\mu}$. This expression is certainly zero because the field tensor is antisymmetric, $F^{\mu\nu} = -F^{\nu\mu}$.

9.3.3 Lorentz transformation of electromagnetic fields

The rapid motion of the electron within the electrostatic field $\vec{\mathcal{E}}$ of the nucleus produces, according to the theory of relativity, a magnetic field $\vec{\mathcal{B}}'$ in the reference frame of the electron. In atomic physics [7] we learn that this field can interact with the spin of the electron, thus giving rise to a considerable energy shift called the fine structure of the atomic spectrum. We calculate the interaction energy in the following.

In relativistic mechanics defined by the metric (9.3) and the Lorentz transform (9.19) the Maxwell field tensor is given by (9.106). With this we can calculate the field transformed into an inertial system propagating along the z-axis,

$$F'^{\mu\nu} = \Lambda^\mu{}_\alpha F^{\alpha\beta}\Lambda_\beta{}^\nu = \begin{pmatrix} 0 & -\frac{\gamma}{c}\mathcal{E}_x + \gamma\beta\mathcal{B}_y & -\frac{\gamma}{c}\mathcal{E}_y - \gamma\beta\mathcal{B}_x & -\frac{1}{c}\mathcal{E}_z \\ \frac{\gamma}{c}\mathcal{E}_x - \gamma\beta\mathcal{B}_y & 0 & -\mathcal{B}_z & -\gamma\frac{\beta}{c}\mathcal{E}_x + \gamma\mathcal{B}_y \\ \frac{\gamma}{c}\mathcal{E}_y + \gamma\beta\mathcal{B}_x & \mathcal{B}_z & 0 & -\gamma\frac{\beta}{c}\mathcal{E}_y - \gamma\mathcal{B}_x \\ \frac{1}{c}\mathcal{E}_z & \gamma\frac{\beta}{c}\mathcal{E}_x - \gamma B_y & \gamma\frac{\beta}{c}\mathcal{E}_y + \gamma B_x & 0 \end{pmatrix} . \tag{9.112}$$

Using $\mathbf{v} = v_z\hat{\mathbf{e}}_z$, that is $\beta_x = 0 = \beta_y$ and $\beta_z = \beta$, we find,

$$\vec{\mathcal{E}}' = \begin{pmatrix} \mathcal{E}'_x \\ \mathcal{E}'_y \\ \mathcal{E}'_z \end{pmatrix} = \begin{pmatrix} \gamma\mathcal{E}_x - \beta_z c\gamma\mathcal{B}_y \\ \gamma\mathcal{E}_y + \beta_z c\gamma\mathcal{B}_x \\ \mathcal{E}_z \end{pmatrix} = \begin{pmatrix} \gamma\mathcal{E}_x + \gamma c\beta_y\mathcal{B}_z - \gamma c\beta_z\mathcal{B}_y - \frac{\gamma^2}{\gamma+1}\beta_x\vec{\beta}\cdot\mathcal{E} \\ \gamma\mathcal{E}_y + \gamma c\beta_z\mathcal{B}_x - \gamma c\beta_x\mathcal{B}_z - \frac{\gamma^2}{\gamma+1}\beta_y\vec{\beta}\cdot\mathcal{E} \\ \gamma\mathcal{E}_z + \gamma c\beta_x\mathcal{B}_y - \gamma c\beta_y\mathcal{B}_x - \frac{\gamma^2}{\gamma+1}\beta_z\vec{\beta}\cdot\mathcal{E} \end{pmatrix} \tag{9.113}$$

$$\vec{\mathcal{B}}' = \begin{pmatrix} \mathcal{B}'_x \\ \mathcal{B}'_y \\ \mathcal{B}'_z \end{pmatrix} = \begin{pmatrix} \gamma\mathcal{B}_x + \frac{\beta_z}{c}\gamma\mathcal{E}_y \\ \gamma\mathcal{B}_y - \frac{\beta_z}{c}\gamma\mathcal{E}_x \\ \mathcal{B}_z \end{pmatrix} = \begin{pmatrix} \gamma\mathcal{B}_x - \gamma\frac{\beta_y}{c}\mathcal{E}_z + \gamma\frac{\beta_z}{c}\mathcal{E}_y - \frac{\gamma^2}{\gamma+1}\beta_x\vec{\beta}\cdot\mathcal{B} \\ \gamma\mathcal{B}_y - \gamma\frac{\beta_z}{c}\mathcal{E}_x + \gamma\frac{\beta_x}{c}\mathcal{E}_z - \frac{\gamma^2}{\gamma+1}\beta_y\vec{\beta}\cdot\mathcal{B} \\ \gamma\mathcal{B}_z - \gamma\frac{\beta_x}{c}\mathcal{E}_y + \gamma\frac{\beta_y}{c}\mathcal{E}_x - \frac{\gamma^2}{\gamma+1}\beta_z\vec{\beta}\cdot\mathcal{B} \end{pmatrix} .$$

yielding,

$$\boxed{\begin{aligned} \vec{\mathcal{E}}' &= \gamma(\vec{\mathcal{E}} + c\vec{\beta}\times\vec{\mathcal{B}}) - \frac{\gamma^2}{\gamma+1}\vec{\beta}(\vec{\beta}\cdot\vec{\mathcal{E}}) \\ \vec{\mathcal{B}}' &= \gamma(\vec{\mathcal{B}} - \tfrac{1}{c}\vec{\beta}\times\vec{\mathcal{E}}) - \frac{\gamma^2}{\gamma+1}\vec{\beta}(\vec{\beta}\cdot\vec{\mathcal{B}}) \end{aligned}} . \tag{9.114}$$

Although having been derived for the special case $\vec{\beta} = \beta\hat{\mathbf{e}}_z$, this result holds for arbitrary velocities, $\gamma \to 1$, in any direction $\vec{\beta}$. At lower velocities the result simplifies to,

$$\vec{\mathcal{E}}' \simeq \vec{\mathcal{E}} + c\vec{\beta}\times\vec{\mathcal{B}} \qquad \text{and} \qquad \vec{\mathcal{B}}' = \vec{\mathcal{B}} - \tfrac{1}{c}\vec{\beta}\times\vec{\mathcal{E}} . \tag{9.115}$$

The first of these equations is the Coulomb-Lorentz force: In the charge's rest frame the Lorentz part of the force has to disappear. The second equation becomes important only for relativistic velocities. Let us consider, for example, the orbital motion of an electron within the Colombian field generated by a proton. From the point of view of the proton, the motion of the electron corresponds to a circular current producing a magnetic field in the place of the proton, which can be approximated to

[7] See script on *Quantum mechanics* (2023).

first order in v/c by [8],

$$\vec{\mathcal{B}}' \simeq -\frac{\mathbf{v}}{c^2} \times \vec{\mathcal{E}} \,. \tag{9.116}$$

We conclude that magnetism can be seen as a relativistic electrical phenomenon. Do the Exc. 9.3.6.2.

9.3.3.1 Lorentz force

The spatio-temporal *Lorentz force* is,

$$\boxed{K^\mu = \frac{dp^\mu}{d\tau} = qF^{\mu\nu}u_\nu} \,, \tag{9.117}$$

using the definition of the proper velocity (9.80) and of the proper momentum (9.85). Being covariant it is a Minkowski force of the type (9.97). Extracting the spatial components,

$$\mathbf{F} = \frac{d\mathbf{p}}{dt} = \frac{d\mathbf{p}}{\gamma d\tau} = q(\vec{\mathcal{E}} + \mathbf{v} \times \vec{\mathcal{B}}) \,, \tag{9.118}$$

Remembering that $\mathbf{p} = m\gamma\mathbf{v}$ is the relativistic momentum.

The temporal component of the Lorentz force,

$$\frac{dE/c}{dt} = \frac{dE/c}{\gamma d\tau} = \frac{q}{c}\vec{\mathcal{E}} \cdot \mathbf{v} \,, \tag{9.119}$$

simply informs us, that the kinetic energy $m\gamma c^2 - mc^2$ increases under the action of work, and the only the electric field works.

The spatio-temporal *Lorentz force density* is,

$$\boxed{f^u = F^{\mu\nu}j_\nu} \,. \tag{9.120}$$

From this we obtain the equations,

$$\begin{aligned} f^u = F^{\mu\nu}j_\nu &= \begin{pmatrix} 0 & -\frac{1}{c}\vec{\mathcal{E}} \\ \frac{1}{c}\vec{\mathcal{E}} & (-\epsilon_{mnk}\mathcal{B}_k) \end{pmatrix} \begin{pmatrix} c\varrho \\ \mathbf{j} \end{pmatrix} = \begin{pmatrix} -\frac{1}{c}\vec{\mathcal{E}} \cdot \mathbf{j} \\ \varrho\vec{\mathcal{E}} - (\epsilon_{mnk}j_m\mathcal{B}_k) \end{pmatrix} \\ &= \begin{pmatrix} -\frac{1}{c}\vec{\mathcal{E}} \cdot \mathbf{j} \\ \varrho\vec{\mathcal{E}} + \mathbf{j} \times \vec{\mathcal{B}} \end{pmatrix} = \begin{pmatrix} \frac{1}{c}P \\ \mathbf{f} \end{pmatrix} \,. \end{aligned} \tag{9.121}$$

9.3.4 Energy and momentum tensor

The meaning of the 4-dimensional energy-momentum tensor is illustrated with the following matrix,

$$T^{\alpha\beta} = \begin{pmatrix} density & flux & flux & flux \\ flux & pressure & shear & shear \\ fluxo & shear & pressure & shear \\ flux & shear & shear & pressure \end{pmatrix} \,. \tag{9.122}$$

[8] Note, however, that this derivation does not account for the rotation of electrons reference system giving rise to the so-called Thomas precession.

The *Maxwell stress tensor* for an electromagnetic field in the absence of sources is defined by,

$$T^{\mu\nu} = \tfrac{1}{\mu_0}\left(F^{\mu}_{\ \alpha}F^{\alpha\nu} + \tfrac{1}{4}F_{\alpha\beta}F^{\alpha\beta}g^{\mu\nu}\right) \ . \tag{9.123}$$

In matrix notation this gives,

$$(T^{\mu\nu}) = \tfrac{1}{\mu_0}\left(F^{\mu\gamma}g_{\gamma\alpha}F^{\alpha\nu} + \tfrac{1}{4}g_{\alpha\gamma}F^{\gamma\delta}g_{\delta\beta}F^{\alpha\beta}g^{\mu\nu}\right) = \tfrac{1}{\mu_0}\check{F}\check{g}\check{F} + \tfrac{1}{4\mu_0}\left\|\check{F}(\check{g}\check{F}\check{g})\right\|\check{g} \tag{9.124}$$

$$= \begin{pmatrix} u & \frac{1}{c}\vec{\mathcal{S}} \\ \frac{1}{c}\vec{\mathcal{S}} & -(T_{mn}) \end{pmatrix}$$

$$= \begin{pmatrix} u & \frac{1}{c}\mathcal{S}_x & \frac{1}{c}\mathcal{S}_y & \frac{1}{c}\mathcal{S}_z \\ \frac{1}{c}\mathcal{S}_x & -\varepsilon_0\mathcal{E}_x^2 - \frac{1}{\mu_0}\mathcal{B}_x^2 + \frac{1}{\mu_0}\mathcal{B}^2 & -\varepsilon_0\mathcal{E}_x\mathcal{E}_y - \frac{1}{\mu_0}\mathcal{B}_y\mathcal{B}_x & -\varepsilon_0\mathcal{E}_x\mathcal{E}_z - \frac{1}{\mu_0}\mathcal{B}_z\mathcal{B}_x \\ \frac{1}{c}\mathcal{S}_y & -\varepsilon_0\mathcal{E}_x\mathcal{E}_y - \frac{1}{\mu_0}\mathcal{B}_y\mathcal{B}_x & -\varepsilon_0\mathcal{E}_y^2 - \frac{1}{\mu_0}\mathcal{B}_y^2 + \frac{1}{\mu_0}\mathcal{B}^2 & -\varepsilon_0\mathcal{E}_y\mathcal{E}_z - \frac{1}{\mu_0}\mathcal{B}_z\mathcal{B}_y \\ \frac{1}{c}\mathcal{S}_z & -\varepsilon_0\mathcal{E}_x\mathcal{E}_z - \frac{1}{\mu_0}\mathcal{B}_z\mathcal{B}_x & -\varepsilon_0\mathcal{E}_y\mathcal{E}_z - \frac{1}{\mu_0}\mathcal{B}_z\mathcal{B}_y & -\varepsilon_0\mathcal{E}_z^2 - \frac{1}{\mu_0}\mathcal{B}_z^2 + \frac{1}{\mu_0}\mathcal{B}^2 \end{pmatrix}$$

$$+ \left(\tfrac{\varepsilon_0}{2}\mathcal{E}^2 - \tfrac{1}{2\mu_0}\mathcal{B}^2\right)(g^{\mu\nu}) \ ,$$

with the energy density $u = \frac{\varepsilon_0}{2}\mathcal{E}^2 + \frac{1}{2\mu_0}\mathcal{B}^2$, the Poynting vector $\vec{\mathcal{S}} = \frac{1}{\mu_0}\vec{\mathcal{E}} \times \vec{\mathcal{B}}$, the Maxwell stress tensor $\overleftrightarrow{\mathbf{T}} = \varepsilon_0\mathcal{E}_m\mathcal{E}_n + \frac{1}{\mu_0}\mathcal{B}_m\mathcal{B}_n - u\delta_{mn}$.

9.3.4.1 Energy and momentum conservation

Using the space-time formalism the energy and momentum conservation laws can be summarized by,

$$f^{\mu} + \partial_{\nu}T^{\mu\nu} = 0 \qquad \text{and} \qquad T^{\mu\nu} = T^{\nu\mu} \ . \tag{9.125}$$

This can be seen by applying Maxwell's equations,

$$F^{\mu\nu}j_v + \tfrac{1}{\mu_0}\partial_{\nu}\left(F^{\mu}_{\ \alpha}F^{\alpha\nu} + \tfrac{1}{4}F_{\alpha\beta}F^{\alpha\beta}g^{\mu\nu}\right) = 0 \ . \tag{9.126}$$

In matrix notation we obtain,

$$\begin{pmatrix} 0 & -\frac{1}{c}\vec{\mathcal{E}} \\ \frac{1}{c}\vec{\mathcal{E}} & -(\epsilon_{mnk}\mathcal{B}_k) \end{pmatrix} + \begin{pmatrix} \frac{\partial}{c\partial t}u + \frac{1}{c}\nabla\cdot\vec{\mathcal{S}} \\ \varepsilon_0\mu_0\frac{\partial}{\partial t}\vec{\mathcal{S}} - \nabla(T_{mn}) \end{pmatrix} = 0 \ , \tag{9.127}$$

and therefore,

$$\begin{pmatrix} P/c & \mathbf{f} \end{pmatrix} + \begin{pmatrix} \frac{\partial}{c\partial t} & \nabla \end{pmatrix}\begin{pmatrix} u & \frac{1}{c}\vec{\mathcal{S}} \\ \frac{1}{c}\vec{\mathcal{S}} & -(T_{mn}) \end{pmatrix} = \begin{pmatrix} \frac{P}{c} + \frac{\partial}{c\partial t}u + \frac{1}{c}\nabla\cdot\vec{\mathcal{S}} \\ \mathbf{f} + \frac{1}{c}\frac{\partial}{c\partial t}\vec{\mathcal{S}} - \nabla(T_{mn}) \end{pmatrix}^{\mathsf{T}} \tag{9.128}$$

$$= \begin{pmatrix} -\frac{1}{c}\mathbf{j}\cdot\vec{\mathcal{E}} + \frac{\partial}{c\partial t}u + \frac{1}{c}\nabla\cdot\vec{\mathcal{S}} \\ \rho\vec{\mathcal{E}} + \mathbf{j}\times\vec{\mathcal{B}} + \varepsilon_0\mu_0\frac{\partial}{\partial t}\vec{\mathcal{S}} - \nabla(T_{mn}) \end{pmatrix}^{\mathsf{T}} = 0 \ .$$

9.3.4.2 Properties of the energy and momentum tensor

Note however, that in a dielectric medium, the matrix elements can be decomposed into separate contributions of the radiation field and the medium. Taken by parts the contributions do not necessarily satisfy the symmetry requirements [9].

[9] See the Abraham-Minkowski controversy.

Defining the angular momentum density of the shear via,

$$M^{\mu\nu g} = T^{\mu\nu}x^g - T^{\mu g}x^\nu \ . \tag{9.129}$$

Conservation of angular momentum means,

$$\partial_\mu M^{\mu\nu g} = 0 \ . \tag{9.130}$$

9.3.5 Solution of the covariant wave equation

Inserting into Maxwell's equations (9.108) the representation of the fields in terms of potentials (9.104), we calculate,

$$\mu_0 j^\mu = \partial_\mu F^{\mu\nu} = \partial_\mu(\partial^\mu A^\nu - \partial^\nu A^\mu) = \Box A^\nu + \partial^\nu \cancelto{0}{(\partial_\mu A^\mu)} \ . \tag{9.131}$$

The second term disappears in the Lorentz gauge (9.103). Then, the inhomogeneous wave equation is,

$$\boxed{\Box A^\mu = \mu_0 j^\mu} \ . \tag{9.132}$$

Analogously to the three-dimensional Green function (6.99) we can define a four-dimensional one,

$$\Box D(x) \equiv \delta^{(4)}(x) \tag{9.133}$$

with $x = r - r'$. With the representation of the Dirac function,

$$\delta^{(4)}(x) = \tfrac{1}{(2\pi)^4}\int d^4k e^{-\imath k\cdot x} \ , \tag{9.134}$$

where $k \cdot x = k^\mu x_\mu = \omega t - \mathbf{k}\cdot\mathbf{r}$, and the Fourier transform of the Green function,

$$D(x) = \tfrac{1}{(2\pi)^4}\int d^4k\tilde{D}(k)e^{-\imath k\cdot x} \ , \tag{9.135}$$

the equation (9.132) becomes,

$$\begin{aligned}\left[\frac{1}{c^2}\frac{\partial^2}{\partial t^2} - \nabla^2\right]\frac{1}{(2\pi)^4}\int d^4k\tilde{D}(k)e^{-\imath k\cdot x} &= \frac{1}{(2\pi)^4}\int d^4k\tilde{D}(k)\left(-\frac{\omega^2}{c^2} + \mathbf{k}^2\right)e^{-\imath k\cdot x} \\ &= \frac{1}{(2\pi)^4}\int d^4k e^{-\imath k\cdot x} = \delta^{(4)}(x) \ ,\end{aligned} \tag{9.136}$$

that is,

$$\tilde{D}(k) = -\frac{1}{k\cdot k} \ . \tag{9.137}$$

With this, the Green function becomes,

$$D(x) = \tfrac{-1}{(2\pi)^4}\int d^4k\frac{e^{-\imath k\cdot x}}{k\cdot k} \ . \tag{9.138}$$

The integral can be solved by contour integration [47], yielding,

$$D_{r,a}(r - r') = \tfrac{1}{2\pi}\theta(\pm ct \mp ct')\delta[(r - r')^2] \ , \tag{9.139}$$

where the index 'r' refers to *retarded* and 'a' to *advanced*. Finally the solution of inhomogeneous wave equation is,

$$\boxed{A^\mu(r) = A^\mu_{r,a}(r) + \mu_0 \int d^4r' D_{r,a}(r-r')j^\mu(r')} \ , \tag{9.140}$$

where $A^\mu_{r,a}(r)$ are the solutions of the homogeneous wave equation for an incoming, respectively, outgoing wave.

The radiation fields are defined by the difference of the incident and outgoing fields. Thus, the vector potential of the radiation is,

$$A^\mu_{rad}(r) = A^\mu_{out}(r) - A^\mu_{in}(r) = \mu_0 \int d^4r' D(r-r')j^\mu(r') \ , \tag{9.141}$$

with $D(x) \equiv D_r(x) - D_a(x)$.

We can generalize the parametrization of 4-current by,

$$j^\mu(r) = ec \int d\tau u^\mu(\tau)\delta^{(4)}[r - r'(\tau)] \ . \tag{9.142}$$

By inserting this current into (9.140) we obtain the Liénard-Wiechert potentials.

9.3.6 Exercises

9.3.6.1 Ex: Motion in constant fields

In the Newtonian world, electric fields accelerate particles on straight lines and magnetic fields make the particles move in circles. Here, we will re-analyze the Coulomb-Lorentz force in the relativistic framework. The force remains the same, but the momentum is now $\mathbf{p} = m\gamma\mathbf{u}$.
a. Consider a constant electric field $\vec{\mathcal{E}} = \mathcal{E}\hat{\mathbf{e}}_x$ without magnetic field.
b. Consider a constant magnetic field $\vec{\mathcal{B}} = \mathcal{B}\hat{\mathbf{e}}_z$ without electric field.

9.3.6.2 Ex: Electric and magnetic dipole moment of moving dipoles

The electric dipole moment $\mathbf{d}$ and the magnetic dipole moment $\vec{\mu}$ of a particle in its rest frame will appear in a lab frame through which the particle is moving with velocity $\mathbf{v}$ as,

$$\boxed{\mathbf{d}' = \mathbf{d} + \tfrac{1}{c^2}\mathbf{v}\times\vec{\mu} \quad \text{and} \quad \vec{\mu}' = \vec{\mu} - \tfrac{1}{2}\mathbf{v}\times\mathbf{d}} \ .$$

Verify this for a particle with a purely magnetic dipole moment via a Lorentz transform using by the following procedure:
a. Derive the Lorentz transform from a rest frame S, flying through the lab frame S' into arbitrary direction $\vec{\beta}$, back into the lab frame for (i) the charge-current density quadrivector, (ii) the time-position quadrivector, and (iii) a volume element using the generalized Lorentz boost (9.60).
b. Parametrize the electric and magnetic dipole moment by appropriate charge and current densities, e.g. assuming two equal charges dislocated in opposite directions of the z-axis, respectively, a circular current in the xy-plane.
c. Apply the Lorentz transform to the electric dipole moment by transforming all quantities of the defining formula. (It is convenient to choose $\beta_y = 0$.)

9.4 Lagrangian formulation of electrodynamics

9.4.1 Relation with quantum mechanics

In classical and relativistic mechanics we learn to deal with *masses* and in electrodynamics with *charges* and with fields and electromagnetic waves. We will show in Sec. 9.4.2.1 how electrodynamics can be integrated into the classical and relativistic mechanics by the prescription of *minimal coupling*,

$$\boxed{p^\mu \to p^\mu - qA^\mu} \ . \tag{9.143}$$

Revolutionary discoveries in the early twentieth century culminated in the development of quantum mechanics, where we learned to accept that the microscopic world works differently. On one hand, massive particles have undulating properties; they can diffract and interfere. On the other side, light has corpuscular properties; it consists of indivisible energy packets called *photons*. Fortunately, classical theories can be incorporated into quantum mechanics by canonical procedures called first and second quantization.

9.4.1.1 Treatment of massive particles in quantum mechanics

In quantum mechanics we learn [10] that matter propagates like a scalar wave (in contrast to electromagnetic waves, which are vectorial). Consequently, in quantum mechanics, massive particles are described by wavefunctions obeying wave equations. Slow particles obey the Schrödinger equation, whereas bosonic relativistic particles obey a wave equation called *Klein-Gordon equation* and fermions obey the *Dirac equation*. The Schrödinger and Klein-Gordon equations are obtained from a simple prescription for canonical quantization:

$$\boxed{p^\mu \to \imath\hbar\partial^\mu} \ . \tag{9.144}$$

Obtaining the Dirac equation is a bit more involved.

9.4.1.2 Quantization of the electromagnetic field

We also learn in quantum mechanics [11] that light consists of indivisible energy packets. This fact is taken into account, by dividing space into modes that can be filled with discrete numbers of photons. Each mode is treated as a harmonic oscillator. Quantum field theories explain, how we must quantize non-radiative electric and magnetic fields.

These topics will not be covered in this course.

9.4.2 Classical mechanics of a point particle in a field

For a system with m degrees of freedom specified by generalized coordinates $q_1, .., q_m$ and the generalized velocities $\dot{q}_1, .., \dot{q}_m$ the classical action is determined by the *Lagrangian* $\mathcal{L}(q_i, \dot{q}_i)$ via,

$$\mathcal{S}[q_i, \dot{q}_i] = \int dt\mathcal{L}(q_i, \dot{q}_i, t) \ . \tag{9.145}$$

[10] See script on *Quantum mechanics* (2023).
[11] See script on *Quantum mechanics* (2023).

Thus, the action is a functional of the generalized coordinates. According to Hamilton's *least action principle*, the dynamics of a classical system is described by equations that minimize the action, $\delta\mathcal{S} = 0$. These equations of motion can be expressed by the Lagrangian in the form of *Euler-Lagrange equations*,

$$\frac{d}{dt}\frac{\partial\mathcal{L}}{\partial\dot{q}_i} - \frac{\partial\mathcal{L}}{\partial q_i} = 0 \; . \tag{9.146}$$

The *canonical momentum* is given by equation,

$$p_i(q_i, \dot{q}_i, t) = \frac{\partial\mathcal{L}}{\partial\dot{q}_i} \; , \tag{9.147}$$

and the Hamiltonian is defined by the *Legendre transform*,

$$\mathcal{H}(q_i, p_i) = \dot{q}_i\frac{\partial\mathcal{L}}{\partial\dot{q}_i} - \mathcal{L} = p_i\dot{q}_i - \mathcal{L}(q_i, \dot{q}_i) \; . \tag{9.148}$$

using Einstein's summing convention. Comparing the differentials of the left with the one of the right-hand side of this equation,

$$\begin{aligned} \frac{\partial\mathcal{H}}{\partial q_i}dq_i + \frac{\partial\mathcal{H}}{\partial p_i}dp_i + \frac{\partial\mathcal{H}}{\partial t}dt = d\mathcal{H} \\ = \dot{q}_i dp_i + p_i d\dot{q}_i - \frac{\partial\mathcal{L}}{\partial q_i}dq_i - \frac{\partial\mathcal{L}}{\partial\dot{q}_i}d\dot{q}_i - \frac{\partial\mathcal{L}}{\partial t}dt \; , \end{aligned} \tag{9.149}$$

we obtain Hamilton's equations of motion,

$$\boxed{\dot{q}_i = \frac{\partial\mathcal{H}}{\partial p_i} \quad , \quad \dot{p}_i = -\frac{\partial\mathcal{H}}{\partial q_i} \quad , \quad \frac{\partial\mathcal{H}}{\partial t} = -\frac{\partial\mathcal{L}}{\partial t}} \; . \tag{9.150}$$

From these equations it follows, that if the Hamiltonian is independent of a particular coordinate q_i, the corresponding moment p_i is constant. For conservative forces, the Lagrangian and the Hamiltonian can be written as $\mathcal{L} = T - V$ and $\mathcal{H} = T + V$, with T the kinetic energy and V the potential energy [12].

9.4.2.1 Electrodynamic Lagrangian

So far we have focused on free particles or particles confined by scalar potentials. In what follows, we will address the influence of a magnetic field on a charged particle. Classically, the force on a charged particle in electric and magnetic fields is given by the Lorentz force law and the exerted work by Ohm's law:

$$\frac{dW}{dt} = e\mathbf{v} \times \vec{\mathcal{E}} \qquad \text{and} \qquad \mathbf{F} = q(\vec{\mathcal{E}} + \mathbf{v} \times \vec{\mathcal{B}}) \; , \tag{9.151}$$

where q denotes the charge and $\mathbf{v}$ the velocity. In this case, the generalized coordinates $q_i \equiv r_i \equiv (r_1, r_2, r_3)$ are precisely the Cartesian coordinates specifying the position, and $\dot{q}_i = \dot{r}_i = (\dot{r}_1, \dot{r}_2, \dot{r}_3)$ the velocity of the particles. These equations

[12] Thus, a particle chooses its trajectory in a way to minimize the conversion between kinetic and potential energy.

of motion are sufficient to describe the dynamics of a system. The force which depends on the velocity and is associated with the magnetic field is quite different from the conservative forces associated with scalar potentials. Let us now study, how the Lorentz force appears in the Lagrange formulation of classical mechanics.

With revised these foundations, we will return to the problem of the influence of an electromagnetic field on the dynamics of a charged particle. Since the Lorentz force depends on velocity, it can not simply be expressed as a gradient of some potential. However, the classical trajectory of the particle is still specific to the least action principle.

The electric and magnetic fields can be expressed in terms of a scalar and a vector potential as,

$$\vec{\mathcal{E}} = -\nabla\Phi - \partial_t \mathbf{A} \qquad \text{and} \qquad \vec{\mathcal{B}} = \nabla \times \mathbf{A} \ . \tag{9.152}$$

The Lorentz force is,

$$\mathbf{F} = q\left[-\nabla\Phi - \frac{\partial \mathbf{A}}{\partial t} + \mathbf{v} \times (\nabla \times \mathbf{A})\right] \ . \tag{9.153}$$

We now analyze the x-component,

$$\begin{aligned} F_x &= q\left[-\frac{\partial\Phi}{\partial x} - \frac{\partial A_x}{\partial t} + v_y\left(\frac{\partial A_y}{\partial x} - \frac{\partial A_x}{\partial y}\right) - v_z\left(\frac{\partial A_x}{\partial z} - \frac{\partial A_z}{\partial x}\right) + v_x\frac{\partial A_x}{\partial x} - v_x\frac{\partial A_x}{\partial x}\right] \\ &= q\left[-\frac{\partial\Phi}{\partial x} + \mathbf{v}\cdot\frac{\partial \mathbf{A}}{\partial x} - \frac{dA_x}{dt}\right] \ , \end{aligned} \tag{9.154}$$

where we used,

$$\frac{d}{dt} = \frac{\partial}{\partial t} + v_i\frac{\partial}{\partial x_i} \ . \tag{9.155}$$

Since the potentials do not depend on the velocity, we can also write,

$$F_x = q\left[-\frac{\partial\Phi}{\partial x} + \frac{\partial \mathbf{v}\cdot\mathbf{A}}{\partial x} - \frac{d}{dt}\frac{\partial \mathbf{v}\cdot\mathbf{A}}{\partial v_x}\right] = -\frac{\partial U}{\partial x} + \frac{d}{dt}\frac{\partial U}{\partial v_x} \ , \tag{9.156}$$

introducing the generalized potential,

$$U \equiv q\Phi - q\mathbf{A}\cdot\mathbf{v} \ . \tag{9.157}$$

The corresponding Lagrangian takes the form:

$$\boxed{\mathcal{L}(r_i, \dot{r}_i) = \tfrac{m}{2}\dot{\mathbf{r}}^2 - q\Phi + q\dot{\mathbf{r}}\cdot\mathbf{A} = \tfrac{m}{2}\dot{r}_i\dot{r}_i - q\Phi + q\dot{r}_iA_i} \ . \tag{9.158}$$

The important point is that the *canonical momentum*

$$\boxed{p_i = \frac{\partial\mathcal{L}}{\partial\dot{r}_i} = m\dot{r}_i + qA_i} \tag{9.159}$$

is no longer equal to velocity times the mass, $mv_i \neq p_i$, because there is an extra term!

Using the definition of the corresponding Hamiltonian,

$$\begin{aligned}\mathcal{H}(r_i, p_i) &= (m\dot{r}_i + qA_i)\dot{r}_i - \tfrac{m}{2}\dot{r}_i\dot{r}_i + q\Phi - q\sum_i \dot{r}_i A_i \\ &= \left(\tfrac{m}{2}\dot{r}_i + qA_i\right)\dot{r}_i + q\Phi = \tfrac{m}{2}\mathbf{v}^2 + q\Phi \ .\end{aligned} \tag{9.160}$$

Obviously, the Hamiltonian has just the familiar form of the sum of kinetic and potential energies. However, to obtain Hamilton's equations of motion, the Hamiltonian must be expressed only in terms of the coordinates and the canonical momenta, that is,

$$\boxed{\mathcal{H}(r_i, p_i) = \frac{1}{2m}(\mathbf{p} - q\mathbf{A})^2 + q\Phi = qv_j\frac{\partial A_j}{\partial r_i} + q\Phi} \ . \tag{9.161}$$

Let us now consider Hamilton's equations of motion,

$$\begin{aligned}\dot{r}_i &= \frac{\partial \mathcal{H}}{\partial p_i} = \frac{1}{m}(p_i - qA_i) \\ \dot{p}_i &= -\frac{\partial \mathcal{H}}{\partial r_i} = -\frac{1}{2m}\frac{\partial}{\partial r_i}(p_j - qA_j)^2 - q\frac{\partial \Phi}{\partial r_i} \ .\end{aligned} \tag{9.162}$$

The first equation reproduces the canonical momentum (9.158), while the second gives the Lorentz force. To understand how, we need to remember that *dp/dt is not the acceleration*: The term dependent on $\mathbf{A}$ also varies over time in a rather complicated way, since it is the field seen by the moving particle.

Example 105 (*Lorentz force from the Lagrangian*): Obviously, we can recover the Lorentz force from the Hamiltonian: Differentiating the canonical momentum (9.158),

$$\begin{aligned}m\ddot{r}_i &= -q\dot{A}_i + \dot{p}_i = -q\dot{A}_i - \frac{\partial \mathcal{H}}{\partial r_i} \\ &= -q\dot{A}_i - \frac{\partial}{\partial r_i}q\left(\sum_j v_j\frac{\partial A_j}{\partial r_i} - \frac{\partial \Phi}{\partial r_i}\right) = -q\dot{A}_i + q\nabla_i(\mathbf{A}\cdot\mathbf{v}) - q\nabla_i\Phi \ .\end{aligned}$$

that is,

$$\begin{aligned}m\ddot{\mathbf{r}} &= -q\nabla\Phi + q\mathbf{v}\times(\nabla\times\mathbf{A}) + q(\mathbf{v}\cdot\nabla)\mathbf{A} - q\frac{d\mathbf{A}}{dt} \\ &= -q\nabla\Phi + q\mathbf{v}\times(\nabla\times\mathbf{A}) - q\frac{\partial\mathbf{A}}{\partial t} = q\vec{\mathcal{E}} + q\mathbf{v}\times\vec{\mathcal{B}}\end{aligned}$$

using the rules (9.155) and $\mathbf{v}\times(\nabla\times\mathbf{A}) = \nabla(\mathbf{A}\cdot\mathbf{v}) - (\nabla\cdot\mathbf{v})\mathbf{A}$.

Using the Coulomb gauge $\nabla\cdot\mathbf{A} = 0$ the Coulomb-Lorentz force can be derived from the Lagrangian via the equation (9.158) or from the Hamiltonian via the second equation (9.162).

9.4.3 Generalization to relativistic mechanics

We now want to generalize the Lagrangian treatment of a particle to relativistic mechanics. Not all forces known in classical mechanics can be put into a covariant form. One example is the Newtonian gravitational force, understood as a force acting at a distance, which is incompatible with the theory of relativity. On the other side, electrodynamics is automatically Lorentz-invariant. Therefore, let us discuss the Lagrangian only for two examples: 1. a totally free particle and 2. a particle under the influence of electromagnetic forces.

Analogously to the classical case, we want to derive, from the principle of minimum action (9.145) Euler-Lagrange type equations (9.146). To put the action into a Lorentz-invariant form, we go to the particle's rest frame via $t = \gamma\tau$,

$$\mathcal{S}[r^\mu, u^\mu] = \int \gamma\mathcal{L}(q^\mu, u^\mu, \tau)d\tau \ . \tag{9.163}$$

We note, however, that we must now distinguish co- and contravariant indices to take account of non-Euclidean metrics. Since $\mathcal{S}$ is an invariant scalar, $\gamma\mathcal{L}$ must be an invariant scalar as well. The Euler-Lagrange equations are now,

$$\frac{d}{d\tau}\frac{\partial\mathcal{L}}{\partial u_\mu} - \frac{\partial\mathcal{L}}{\partial x_\mu} = 0 \ . \tag{9.164}$$

The ansatz for the Lagrangian,

$$\mathcal{L} \equiv \tfrac{m}{2}u_\mu u^\mu \tag{9.165}$$

inserted into the Euler-Lagrange equation gives,

$$\frac{d}{d\tau}mu^\mu - 0 = \frac{d}{d\tau}p^\mu = 0 \ , \tag{9.166}$$

which makes sense in the absence of external forces [13].

9.4.3.1 Lagrangian relativistic electrodynamics

We now consider a charged particle interacting with an external electromagnetic field [47]. In relativistic notation the Lorentz force and the Ohm's law (9.145) become [compare (9.117)],

$$\frac{mdu^\mu}{d\tau} = qF^{\mu\nu}u_\nu \ , \tag{9.167}$$

where m is the resting mass, τ the proper time in the particle's system, and $(u^\mu) = (\gamma c, \gamma\mathbf{u}) = (p^\mu/m)$ its 4-velocity. Following the classical model (9.157) we can make for the Lagrangian the covariant ansatz [37],

$$\boxed{\mathcal{L} = \mathcal{L}_{free} + \mathcal{L}_{int} = \tfrac{m}{2}u_\mu u^\mu + qu_\mu A^\mu} \ . \tag{9.168}$$

The canonical momenta are,

$$p_\mu = \frac{\partial\mathcal{L}}{\partial u^\mu} = mu_\mu + qA_\mu \ , \tag{9.169}$$

such that the Euler-Lagrange equations (9.164) result in,

$$\frac{d}{d\tau}(mu_\mu + qA_\mu) - \frac{\partial}{\partial x_\mu}(qu_\nu A^\nu) = 0 \ . \tag{9.170}$$

[13] We note, that any ansatz $\mathcal{L}(z) \equiv \mathcal{L}(u_\mu u^\mu)$ satisfying $\partial_z\mathcal{L} = \frac{m}{2}$ is possible. We will show this in Exc. 9.4.5.1.

That is,

$$K_\mu = \frac{d}{d\tau} m u_\mu = \frac{\partial}{\partial x_\mu}(q u_\nu A^\nu) - \frac{d}{d\tau}(q A_\mu) \ , \tag{9.171}$$

which is precisely the Minkowski type Lorentz force.

The total energy is,

$$E_{tot} = c p^0 = c(E + q\Phi) \ , \tag{9.172}$$

where E is the kinetic energy including the rest mass (9.88). We calculate,

$$m^2 u_\mu u^\mu = m^2 c^2 = (p_\mu - q A_\mu)(p^\mu - q A^\mu) = m^2 u_0 u^0 - (\mathbf{p} - q\mathbf{A})^2 = E^2/c^2 - (\mathbf{p} - q\mathbf{A})^2 \ . \tag{9.173}$$

That is,

$$E^2 = (\mathbf{p} - q\mathbf{A})^2 - m^2 c^2 \ . \tag{9.174}$$

In Exc. 9.4.5.3 we show an example for the application of the relativistic electrodynamic Lagrangian.

9.4.3.2 Charges and currents interacting with an electromagnetic field

In the case of continuous variables we use Lagrangian densities,

$$\mathcal{L} = \sum_i \mathcal{L}_i(q_i, \dot{q}_i) \longrightarrow \int \mathcal{L}(\phi_k, \partial^\alpha \phi_k) d^3x \ . \tag{9.175}$$

For example, the Lagrangian of the electromagnetic field is [38],

$$\mathcal{L} = T - V = \mathcal{L}_{field} + \mathcal{L}_{int} = -\tfrac{1}{4\mu_0} F^{\mu\nu} F_{\mu\nu} - A_\mu j^\mu \ , \tag{9.176}$$

but we will not deepen this here.

9.4.4 Symmetries and conservation laws

> *Symmetry* is a feature of a system conserving specific properties under some transformation.

For example, the geometry of a system does not change, when we apply a reflection and the interaction energy between two charges does not change when we switch their coordinates.

In the Lagrangian formalism we call a quantity (or generalized momentum) *conserved*, when the Lagrangian does not depend on the associated coordinate,

$$\mathcal{L} \neq \mathcal{L}(q_k) \qquad \Longrightarrow \qquad p_k \ \text{ is conserved} \ . \tag{9.177}$$

We can see this by the Euler-Lagrange equation,

$$\frac{dp_k}{dt} = \frac{d}{dt} \frac{\partial \mathcal{L}}{\partial \dot{q}_k} = \frac{\partial \mathcal{L}}{\partial q_k} = 0 \ . \tag{9.178}$$

Emmy Noether formulated the theorem, that a *symmetry transformation*, that is, a transformation that does not change the action,

$$t \to t + \delta t \qquad \text{and} \qquad \mathbf{q} \to \mathbf{q} + \delta\mathbf{q} \ , \tag{9.179}$$

conserves the following quantities:

$$\boxed{\left(\dot{\mathbf{q}} \cdot \frac{\partial \mathcal{L}}{\partial \dot{\mathbf{q}}} - \mathcal{L}\right) \delta t - \frac{\partial \mathcal{L}}{\partial \dot{\mathbf{q}}} \cdot \delta \mathbf{q}} \ . \tag{9.180}$$

For example, a *temporal translation*, $\delta t \neq 0$ without another transformed coordinate $\delta q_\alpha = 0$, $\forall \alpha$, leaves the *total energy*,

$$\dot{\mathbf{q}} \cdot \frac{\partial \mathcal{L}}{\partial \dot{\mathbf{q}}} - \mathcal{L} = \mathcal{H} \ , \tag{9.181}$$

(known by the Legendre transform) unchanged. The *spatial translation*, $\delta q_\alpha \neq 0$ but $\delta t = 0$, leave the *linear momentum*,

$$\frac{\partial \mathcal{L}}{\partial \dot{q}_\alpha} = p_\alpha \ , \tag{9.182}$$

unchanged. We note that in relativistic theory, these two conservation laws are related. *Spatial rotation* around an axis $\hat{\mathbf{e}}_n$, defined in Cartesian coordinates by,

$$\mathbf{r} \to \mathbf{r} + \delta\vec{\theta} = \mathbf{r} + \delta(\hat{\mathbf{e}}_n \times \mathbf{r}) \ , \tag{9.183}$$

with $\delta t \neq 0$, leaves the angular momentum,

$$\frac{\partial \mathcal{L}}{\partial \dot{\mathbf{q}}} \cdot \delta(\hat{\mathbf{e}}_n \times \mathbf{r}) = \mathbf{p} \cdot (\hat{\mathbf{e}}_n \times \mathbf{r}) = \hat{\mathbf{e}}_n \cdot (\mathbf{r} \times \mathbf{p}) = \hat{\mathbf{e}}_n \cdot \mathbf{L} = 0 \ , \tag{9.184}$$

unchanged.

symmetry class	symmetry	invariance	conserved quantity
Lorentz	homogeneity of time	translation in time	energy
	homogeneity of space	translation in space	linear momentum
	isotropy of space	rotation in space	angular momentum
discrete	T (isotropy of time)	time reversal	temporal parity
	P	coordinate inversion	spatial parity
	C	charge conjugation	charge parity
internal	U(1)	gauge transformation	electric charge

9.4.5 Exercises

9.4.5.1 Ex: Lagrangian relativistic of a free particle

Show that the Lagrangian $\mathcal{L}(z) = \mathcal{L}(u_\mu u^\mu)$ with $\mathcal{L}' = \frac{m}{2}$ satisfies the Euler-Lagrange equation.

9.4.5.2 Ex: Motion of charged particles in a magnetic field

A non-relativistic particle with mass m and charge q be in a static magnetic field,

$$\vec{\mathcal{B}}(\mathbf{r}) = \mathcal{B}_x(x,y,z)\hat{\mathbf{e}}_x + \mathcal{B}_y(x,y,z)\hat{\mathbf{e}}_y + \mathcal{B}_z(x,y,z)\hat{\mathbf{e}}_z \ .$$

Its Lagrange function is then,

$$\mathcal{L} = \frac{1}{2}m\mathbf{v}^2 + \frac{q}{c}\mathbf{v}\cdot\mathbf{A} \ ,$$

where $\mathbf{v}$ is the velocity of the particle and $\mathbf{A}$ the vector potential corresponding to the magnetic field $\vec{\mathcal{B}}$.
a. If $\mathbf{A} = A_x(x,y,z)\hat{\mathbf{e}}_x + A_y(x,y,z)\hat{\mathbf{e}}_y + A_z(x,y,z)\hat{\mathbf{e}}_z$ is given, what are the Cartesian components of $\vec{\mathcal{B}}$?
b. Using the formula $\frac{d}{dt}\frac{\partial L}{\partial \dot{q}} = \frac{\partial L}{\partial q}$ derive the equations of motion for the Cartesian components of $\mathbf{v}$.
c. What is the condition for $\mathcal{B}_x = \mathcal{B}_y = 0$ and $\mathcal{B}_z = \mathcal{B}_0$ to be constant?
d. Now, consider $A_x = A_y = 0$ and $A_y = \mathcal{B}_0 x$. What equations of motion for v_x, v_y, and v_z follow from this?
e. Calculate $v_x(t)$, $v_y(t)$, and $v_z(t)$. Contour conditions be given by $v_z(t=0) = v_0^{(\|)}$, $v_y(t=0) = 0$ and $v_x(t=0) = v_0^{(\perp)}$. Use the abbreviation $\omega_0 = \frac{q\mathcal{B}_0}{mc}$.
f. Calculate $x(t)$, $y(t)$, and $z(t)$ choosing $x(t=0) = y(t=0) = z(t=0) = 0$. What is the form of the trajectory that corresponds to this motion?
g. Suppose now that $A_x = A_y = 0$ and $A_y = \mathcal{B}(z)x$. What is the consequence of this for $\mathcal{B}_x$, $\mathcal{B}_y$, and $\mathcal{B}_z$? What are the corresponding equations of motion for v_x, v_y, and v_z ?
h. Now, let $\frac{\partial\mathcal{B}(z)}{\partial z} = \mathcal{B}'$ =constant. Discuss the motion equation for v_z, inserting as an approximation for $v_y(t)$ and $x(t)$ the solutions of parts (e) and (f). What, under this circumstance, is the consequence for $v_z(t)$?

9.4.5.3 Ex: Connection between kinetic and canonical momentum and the Abraham-Minkowski debate

The nonrelativistic Lagrangian that governs the interaction of a particle with electric and magnetic dipole moment with external electromagnetic fields can be written,

$$\mathcal{L} = \tfrac{m}{2}v^2 + \vec{\mathcal{E}}\cdot\mathbf{d} + \vec{\mathcal{B}}\cdot\vec{\mu} \ .$$

a. Based on the results of Exc. 9.3.6.2 calculate the kinetic and canonical momenta of a particle with flying at velocity $\mathbf{v}$ through a lab.
b. Now, average over a macroscopic number of particles introducing the polarization $\vec{\mathcal{P}} = \langle\sum_n \mathbf{d}_n\delta^3(\mathbf{r}-\vec{\mathcal{S}}_n)\rangle$ and the magnetization $\vec{\mathcal{M}} = \frac{1}{2}\langle\sum_n \vec{\mu}_n\delta^3(\mathbf{r}-\vec{\mathcal{S}}_n)\rangle$, and compare the kinetic and canonical momenta with the Abraham and Minkowski expressions for the linear momentum density.

9.5 Relativistic gravity

The starting point of Einstein's theory on *general relativity* is the famous *equivalence principle* stating that there is no difference in heavy mass and inert mass, that is, gravity and acceleration are fundamentally the same. Taking this axiom seriously, we must accept a series of astonishing corollaries, such as the fact that space-time is neither Euclidian, nor Minkowskian, but distorted by the presence of mass. Time and space coordinates are intertwined.

In the following, we briefly recapitulate Minkowskian metrics in Cartesian and spherical coordinates before introducing Schwarzschild metrics as a special case.

9.5.1 Metric and geodesic equation in curved space-time

Minkowskian metrics in Cartesian coordinates has been introduced in Sec. 9.1.1. In the following sections, we will briefly recapitulate it and extend it to spherical coordinates before generalizing the metrics to curved space-time.

9.5.1.1 Minkowski metrics

In Cartesian coordinates the line element and tetrad are given by,

$$\begin{aligned} & ds^2 = c^2t^2 - dx^2 - dy^2 - dz^2 \qquad (9.185)\\ & \mathbf{e}_t = \frac{1}{c}\partial_t \quad , \quad \mathbf{e}_x = \partial_x \quad , \quad \mathbf{e}_y = \partial_y \quad , \quad \mathbf{e}_z = \partial_z \\ & \mathbf{e}^t = cdt \quad , \quad \mathbf{e}^x = dx \quad , \quad \mathbf{e}^y = dy \quad , \quad \mathbf{e}^z = dz \ , \end{aligned}$$

and the metric tensor by,

$$g_{\mu\nu} = \frac{\partial x_\alpha}{\partial \xi^\mu}\frac{\partial x^\alpha}{\partial \xi^\nu} = \begin{pmatrix} 1 & 0 & 0 & 0 \\ 0 & -1 & 0 & 0 \\ 0 & 0 & -1 & 0 \\ 0 & 0 & 0 & -1 \end{pmatrix} . \qquad (9.186)$$

Note that the matrix representation of the metric is defined via,

$$\boxed{ds^2 = g^{\mu\nu} dx_\mu dx_\nu} . \qquad (9.187)$$

In spherical coordinates,

$$\begin{pmatrix} t \\ x \\ y \\ z \end{pmatrix} = \begin{pmatrix} t \\ r\sin\theta\cos\phi \\ r\sin\theta\sin\phi \\ r\cos\theta \end{pmatrix} , \qquad (9.188)$$

the line element and tetrad are given by,

$$\begin{aligned} & ds^2 = c^2t^2 - dr^2 - r^2 d\theta^2 - r^2\sin^2\theta d\phi^2 \qquad (9.189)\\ & \mathbf{e}_t = \frac{1}{c}\partial_t \quad , \quad \mathbf{e}_r = \partial_r \quad , \quad \mathbf{e}_\theta = \frac{1}{r}\partial_\theta \quad , \quad \mathbf{e}_\phi = \frac{1}{r\sin\theta}\partial_\phi \ , \end{aligned}$$

and the metric tensor,

$$g_{\mu\nu} = \frac{\partial x_\alpha}{\partial \xi^\mu}\frac{\partial x^\alpha}{\partial \xi^\nu} = \begin{pmatrix} 1 & 0 & 0 & 0 \\ 0 & -1 & 0 & 0 \\ 0 & 0 & -r^2 & 0 \\ 0 & 0 & 0 & -r^2\sin^2\theta \end{pmatrix} , \qquad (9.190)$$

with $\xi^\mu, \xi^\nu = t, r, \theta, \phi$ and $x_\alpha = t, x, y, z$. The Minkowski metrics is a generalization of Euclidian metric to four-dimensional space-time.

9.5.2 Schwarzschild metric

General relativity breaks with the concept of Euclidian space allowing for space-time to be distorted. The simplest example is the *Schwarzschild metric* which assumes a distortion of time and space as a function of the distance from a heavy mass. Schwarzschild's solution was the first exact solution of Einstein's field equations. It holds on the outside of non-charged non-rotating masses.

Metric and tetrad of Schwarzschild coordinates (t, r, θ, ϕ) are given by,

$$c^2 d\tau^2 = \left(1 - \tfrac{r_s}{r}\right) c^2 dt^2 - \left(1 - \tfrac{r_s}{r}\right)^{-1} dr^2 - r^2 d\theta^2 - r^2 \sin^2\theta d\phi^2 \tag{9.191}$$

$$\mathbf{e}_t = \frac{1}{c\sqrt{1 - r_s/r}}\partial_t \quad , \quad \mathbf{r} = \sqrt{1 - \frac{r_s}{r}}\partial_r \quad , \quad \mathbf{e}_\theta = \frac{1}{r}\partial_\theta \quad , \quad \mathbf{e}_r = \frac{1}{r\sin\theta}\partial_\phi ,$$

where,

$$r_s \equiv \frac{2\gamma_N M}{c^2} , \tag{9.192}$$

is called the *Schwarzschild radius*. The metric tensor in free (massless) space is,

$$g_{\mu\nu} = \frac{\partial x_\alpha}{\partial \xi^\mu}\frac{\partial x^\alpha}{\partial \xi^\nu} = \begin{pmatrix} 1 - \frac{r_s}{r} & 0 & 0 & 0 \\ 0 & -(1 - \frac{r_s}{r})^{-1} & 0 & 0 \\ 0 & 0 & -r^2 & 0 \\ 0 & 0 & 0 & -r^2\sin^2\theta \end{pmatrix} . \tag{9.193}$$

For $r \gg r_s$ this reduces to the Minkowski metric.

9.5.3 Christoffel symbols for relativistic space-time and geodesic equation

The Christoffel symbols are defined by,

$$\Gamma^\mu{}_{\alpha\beta} \equiv \frac{\partial \mathbf{e}_\alpha}{\partial x^\beta} \cdot \mathbf{e}^\mu = \frac{\partial^2 \xi^\gamma}{\partial x^\alpha \partial x^\beta}\frac{\partial x^\mu}{\partial \xi^\gamma} . \tag{9.194}$$

They yields for spherical coordinates,

$$\Gamma^a{}_{it} = \begin{pmatrix} 0 & 0 & 0 & 0 \\ 0 & 0 & 0 & 0 \\ 0 & 0 & 0 & 0 \\ 0 & 0 & 0 & 0 \end{pmatrix} \quad , \quad \Gamma^a{}_{ir} = \begin{pmatrix} 0 & 0 & -r & 0 \\ 0 & 0 & 0 & 0 \\ 0 & 0 & 0 & 0 \\ 0 & 0 & 0 & 0 \end{pmatrix} \tag{9.195}$$

$$\Gamma^a{}_{i\theta} = \begin{pmatrix} 0 & 0 & -r & 0 \\ 0 & 0 & 0 & 0 \\ 0 & 0 & 0 & 0 \\ 0 & 0 & 0 & 0 \end{pmatrix} \quad , \quad \Gamma^a{}_{i\phi} = \begin{pmatrix} 0 & 0 & 0 & 0 \\ 0 & 0 & 0 & 0 \\ 0 & 0 & 0 & 0 \\ 0 & 0 & 0 & 0 \end{pmatrix} .$$

In relativistic space-time the *geodesic equation* is a curve representing in some sense the shortest path between two points in a surface. The geodesic line is obtained by solving the differential equation,

$$\boxed{\frac{d^2x^\mu}{d\tau^2} + \Gamma^\mu{}_{\alpha\beta}\frac{dx^\alpha}{d\tau}\frac{dx^\beta}{d\tau} = 0}\,. \tag{9.196}$$

Define *Einstein tensor*, *Ricci tensor* (see 1.4.3).

9.5.4 Exercises

9.5.4.1 Ex: Space-time metric in spherical coordinates

Write down the space-time metric for Earth in spherical coordinates.

9.6 Further reading

J.D. Jackson, *Classical Electrodynamics* [ISBN]

D.J. Griffiths, *Introduction to Electrodynamics* [ISBN]

Chapter 10

Appendices to 'Electrodynamics'

10.1 Special topic: Goos-Hänchen shift with light and matter waves

Newton's corpuscular light model predicts a lateral shift of a light beam when totally reflected from an interface to an optically thin medium. Photons leaving the optically dense medium are reattracted to it by gravitation. The lateral distance covered during their ballistic flight corresponds to the shift, called *Goos-Hänchen shift* (GHS). It seems as if the light beam was reflected at a plane lying behind the boundary within the region of the evanescent wave (EW). Although the underlying model is incorrect (although De Broglie himself conjectured that the effect could point towards a finite photon mass), newer model based on the Maxwell theory also predict an energy flux within the EW forming within the thin medium. Many unsuccessful attempts have been undertaken to observe this flux, and it has still not been directly observed nowadays. The problem is that any probe brought into the EW undermines it and vanishes the GHS. Goos and Hänchen circumvented the problem by measuring only the lateral shift in the optically dense medium [40, 41, 15]. The agreement of their observations with Maxwell theory gives confidence in the existence of the flux.

10.1.1 Evanescent wave potentials

A light field reflected at an angle θ (= 52° for Landragin's dielectric prism) on a boundary to an optically thin medium is described by

$$\mathcal{E}(\mathbf{r}) = \mathcal{E}_0 e^{\imath qx-\kappa z} \ , \tag{10.1}$$

where $q = kn\sin\theta$ and $\kappa = k\sqrt{n^2\sin^2\theta - 1}$. Introducing the Rabi frequency

$$\Omega(\mathbf{r}) = \sqrt{\frac{\sigma_0\Gamma}{\hbar\omega}I(\mathbf{r})} = \sqrt{\frac{\epsilon_0 c^2\sigma_0\Gamma}{\hbar\omega}}\mathcal{E}_0 e^{-\kappa z} \ , \tag{10.2}$$

the interaction energy reads $\mathbf{d}\cdot\vec{\mathcal{E}} = \Omega(\mathbf{r})e^{\imath qx}$. The force $\mathbf{F} = -\nabla\mathbf{d}\cdot\vec{\mathcal{E}}$ is made of two contributions. Using the optical Bloch equations, we find the stationary solutions for the dipole and the dissipative forces [1]

$$\mathbf{F}_{dip} = -\frac{\hbar\Delta\Omega}{4\Delta^2 + 2\Omega(\mathbf{r})^2 + \Gamma^2}\nabla\Omega(\mathbf{r}) \ , \tag{10.3}$$
$$\mathbf{F}_{diss} = \frac{\hbar\Gamma\Omega^2}{4\Delta^2 + 2\Omega(\mathbf{r})^2 + \Gamma^2}\nabla\theta(\mathbf{r}) \ .$$

Treating the mechanical effects of light analogously to the Laguerre-Gaussian modes. For LGM the phase gradient is almost parallel with the Poynting vector except for higher order corrections for the axial component.

The dipole force can be derived from a conservative evanescent potential

$$V(z) = \frac{\Omega^2}{\Delta}e^{-2\kappa z} = \frac{\pi c^2\Gamma}{2\omega^3}\ I\ \left(\frac{1}{\Delta_{D1}} + \frac{2}{\Delta_{D2}}\right)e^{-2\kappa z} \ .$$

Apparently, radiation pressure accelerates the atoms not in the direction of the wavevector, but of the phase gradient [3]. Is this the same as the Poynting vector? This may lead to observable effects in evanescent waves. Hence, the observation of a transverse radiation pressure would already prove a Goos-Hänchen shift.

10.1.2 Energy flux in the evanescent wave

An incoming laser beam be expanded after phases

$$\mathcal{E}_i(x) = \mathcal{E}_{ip}\int f(\theta)e^{-\imath x k_{ix_0}\theta}d\theta \ . \tag{10.4}$$

The reflected beam then reads

$$\mathcal{E}_r(x) = \mathcal{E}_{ip}\int r(\theta)f(\theta)e^{-\imath x k_{ix_0}\theta}d\theta \ , \tag{10.5}$$

where $r(\theta) = \frac{a-\imath b}{a+\imath b}$ according to the Fresnel equations or $r = e^{i\varphi}$. We assume that we can linearize the phase $\varphi(\theta) = \varphi(\theta_0) + (\theta-\theta_0)\partial_\theta\varphi(\theta_0) \equiv \chi + \theta\partial_\theta\varphi(\theta_0)$. Then equation (10.5) can be written

$$\mathcal{E}_r(x) = \mathcal{E}_{ip}e^{-\imath\chi}\int f(\theta)e^{-\imath(x-\Delta x_{GH})k_{ix_0}\theta}d\theta = \mathcal{E}_i(x-\Delta x_{GH})e^{-\imath\chi} \ , \tag{10.6}$$

where $\Delta x_{GH} = \frac{2\cos\theta_0}{k_{ix_0}}\partial_\theta\varphi(\theta_0) = \frac{2}{k_i}\partial_\theta\varphi(\theta_0)$. The reflected laser beam is parallel shifted.

Calculations show [78, 55] that the energy flux penetrates the thin medium only where the transverse profile of the beam shows a gradient. In the regions of constant intensity the flux is inside the plane of incidence and parallel to the surface. Hence, the Goos-Hänchen shift is only observable with spatially inhomogeneous beams.

10.1.2.1 Expression for the shift

Let us now estimate the GHS for a prism $n_1 = 1.5$, the Rb D_2-line for which $\lambda = 2\pi/k = 780$ nm. The EW penetration depth ζ is given by $k\zeta = \sqrt{n_1^2\sin^2\theta - n_2^2}^{\,-1}$

$$\frac{\Delta_{GH}}{2\zeta} = \frac{n_1^2 n_2^2\sin\theta\cos^2\theta}{n_1^4\sin^2\theta + n_2^4\cos^2\theta - n_1^2 n_2^2} \ . \tag{10.7}$$

We assume that the angle of incidence is close to the critical angle $\theta = \theta_c + \xi = \arcsin n_1^{-1} + \xi$. Near the critical angle the GHS diverges as does the penetration depth. Hence, the GHS should be measured very close to the critical angle. The expansion in ξ yields

$$\frac{\Delta_{GH}}{2\zeta} = \frac{n_1}{n_2}\left(1 + \xi\frac{n_2^2 n_1^2 - n_2^4 - 2n_1^4}{n_2^3\sqrt{n_1^2 - n_2^2}}\right) . \tag{10.8}$$

The Goos-Hänchen shift is proportional to the penetration depth of the evanescent wave. It has been measured by [15].

10.1.2.2 Goos-Hänchen shift with resonant absorbers

Resonant absorbers have an impact on the evanescent wave and hence on the Goos-Hänchen shift as has been measured by [73]. Hence, we now consider the presence of an resonant gas with a small index of refraction, $n_2 = 1 + \bar{n}$, so that

$$\frac{k\Delta_{GH}}{2} = \frac{1}{\sqrt{n_1^2 \sin^2\theta - (1+\bar{n})^2}} \frac{n_1^2(1+\bar{n})^2 \sin\theta\cos^2\theta}{n_1^4 \sin^2\theta + (1+\bar{n})^4\cos^2\theta - n_1^2(1+\bar{n})^2} . \tag{10.9}$$

To first order in $\bar{n}$ and ξ

$$\Delta_{GH}(\bar{n},\xi) \approx \frac{A\bar{n}}{\sqrt{\xi}\,(B\xi - \bar{n})} + \Delta_{GH}(\bar{n} = 0, \xi) . \tag{10.10}$$

According to [65] (Eq. 4.6),

$$\begin{aligned} T &= -\frac{N|d\epsilon_1|^2}{\eta\varepsilon_0\hbar|\epsilon_1|^2}\int d\mathbf{v}W(\mathbf{v})\theta(v_z)\frac{1}{\Gamma + \eta k v_z - \imath(\Delta - \alpha k v_x)} \qquad (10.11)\\ &= -\frac{N|d|^2}{\eta\varepsilon_0\hbar}\left(\frac{3}{2\pi v_0^2}\right)^{3/2}\int_0^\infty dv_z e^{-3v_z^2/2v_0^2}\int_{-\infty}^\infty dv_y e^{-3v_y^2/2v_0^2}\int_{-\infty}^\infty dv_x e^{-3v_x^2/2v_0^2}\frac{1}{\Gamma - \imath\Delta}\\ &= -\frac{N|d|^2}{\eta\varepsilon_0\hbar}\frac{1}{\sqrt{2}}\frac{1}{\Gamma - \imath\Delta} . \end{aligned}$$

An effective refractive index variation may be define [65] (Eq. 3.16) with $\beta = i\eta$,

$$\delta n = -\beta T = \beta\frac{N|d|^2}{\sqrt{2}\eta\varepsilon_0\hbar}\frac{1}{\Gamma - \imath\Delta} = \imath\frac{N|d|^2}{\sqrt{2}\varepsilon_0\hbar}\frac{\Gamma + \imath\Delta}{\Gamma^2 + \Delta^2} . \tag{10.12}$$

The interesting question is, whether the energy flux in the evanescent wave is directly observable. The existence of an EW is not questionable. On the contrary it has become an important in quantum optics, where near-resonant EWs are used for *selective reflection spectroscopy*. In cold atom optics, far-off resonant EWs are used to repel ultracold atoms from surfaces. Does the energy flux related to the GHS leave any footprints in the atomic cloud (possibly a BEC)? Certainly, one has to stay at a detuning, where the flux in the evanescent wave satisfies $\mathfrak{Im}\,\mathbf{k} \perp \mathfrak{Re}\,\mathbf{k}$, so that there is no energy transfer. Think about phase shift of the de Broglie wave underneath a fixed envelope, analogy to geometric phases or the Aharonov-Bohm effect.

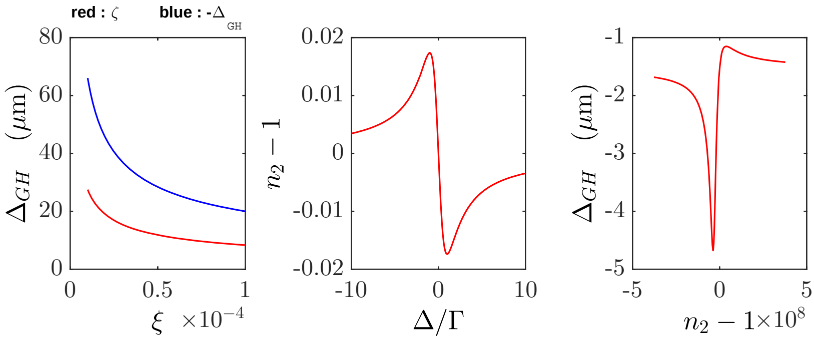

Figure 10.1: (code) Selective reflection Goos.

10.1.3 Imbert-Fedorov shift

A transverse shift should be expected for circularly polarized light or Laguerre-Gaussian modes. This shift called Imbert-Fedorov shift can be described with the flux method. The effect should be small, $\Delta x_{IF} \approx 0.1\ \Delta x_{GH}$. It has been observed with microwaves [28] and light [75].

For this case it is interesting that the wavevector $\mathbf{k}$ and the flux $\mathbf{S}$ are both parallel to the surface, but orthogonal on each other. The flux is perpendicular to the plane of incidence.

The symmetry breaking (upward or downward flux) is inherent in the circularly polarized laser beam [4, 35, 68]. Here the Poynting vector describes a helix about the optical axis.

For matter waves the index of refraction can be tuned via the particle energy, which is not possible with light. E.g. if $E = V_2 > V_1$, the critical angle for total reflection is $\alpha = 0$. Do we expect a Imbert-Fedorov shift for spinor condensates? Is the plane wave approximation good or should be use real BEC wavefronts?

The total reflection of Laguerre-Gaussian beams has also been studied [66].

10.1.4 Matter wave Goos-Hänchen shift at a potential step

The phase of a BEC could be a sensitive probe for the Goos-Hänchen shift. Here, it is important that the de Broglie wavelength be longer than the edge of the potential. Otherwise, the effect is trivial even in the classical particle picture.

Matter waves behave analogously to optical waves, except that the Schrödinger equation must be used. Consider the situation of a particle moving towards a potential step at an angle α as shown in Fig. 10.2. The energy of the particle is $E > V_2 > V_1$. The incidence region V_1 corresponds to the atom optically thick medium (the de Broglie wavelength is shorter, the propagation velocity fast, $\hbar k_1 = \sqrt{2m(E-V_1)}$. V_2 is the atom optically thin medium.

Consequently we expect a critical angle α_c beyond which the matter wave is totally reflected,

$$\sin\alpha_c = \sqrt{\frac{E-V_2}{E-V_1}}\ . \tag{10.13}$$

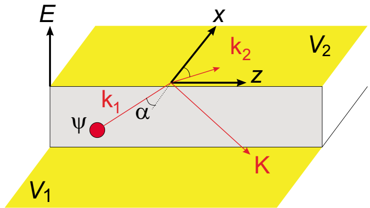

Figure 10.2: Matter wave refraction at a potential step.

For partial reflection, if the incident wave is described by [78] $\psi_0 = e^{\imath x k_{x1} + \imath y k_{y1}}$, the reflected and refracted wave are

$$\begin{aligned} \psi_1 &= \frac{\cos\alpha - \sqrt{\sin^2\alpha_c - \sin^2\alpha}}{\cos\alpha + \sqrt{\sin^2\alpha_c - \sin^2\alpha}} e^{-\imath x k_{x1} + \imath y k_{y1}} \\ \psi_2 &= \frac{2\cos\alpha}{\cos\alpha + \sqrt{\sin^2\alpha_c - \sin^2\alpha}} e^{-\imath x \sqrt{k_2^2 - k_{y1}^2} + \imath y k_{y1}} \ . \end{aligned} \tag{10.14}$$

For total reflection,

$$\begin{aligned} \psi_1 &= \exp\left(-\imath 2 \arctan\sqrt{\frac{\sin^2\alpha - \sin^2\alpha_c}{1 - \sin^2\alpha}}\right) e^{-\imath x k_{x1} + \imath y k_{y1}} \\ \psi_2 &= \frac{2\cos\alpha}{\cos\alpha + \imath\sqrt{\sin^2\alpha - \sin^2\alpha_c}} e^{-x\sqrt{k_{1y}^2 - k_2^2} + \imath y k_{y1}} \ . \end{aligned} \tag{10.15}$$

The matter wave Goos-Hänchen shift Δ_{GH} can be estimated by comparing the matter wave flux $\mathbf{J} = -i\frac{\hbar}{2m}(\psi^*\nabla\psi - \psi\nabla\psi^*)$ in the evanescent wave with the flux in a Δ_{GH} wide strip of the reflected beam. The result [78] is

$$\frac{\Delta_{GH}}{2} = \frac{\sin\alpha\cos^2\alpha}{k\cos^2\alpha_c\sqrt{\sin^2\alpha - \sin^2\alpha_c}} \ . \tag{10.16}$$

See [78, 45].

The difficult question is now what the matter wave analogue of the Imbert-Fedorov shift would be. It is known for relativistic electrons that momentum and velocity must not necessarily be collinear [29]. How about particles with a real angular orbital momentum, e.g. the reflection of vortices?

10.2 Special topic: The dilemma of Abraham and Minkowski

If Minkowski is correct, then as a photon enters an atomic cloud with $n > 1$, then the cloud receives a collective momentum in the direction opposite to the photon propagation [21]. 'Momentum conservation requires then that the medium also has a mechanical momentum. When a pulse of light enters the medium, the particles in the medium are accelerated by the leading edge of the pulse and decelerated by the trailing edge.' However, near resonance the refraction index is dispersive. I.e. for blue-detuning we should expect $n < 1$ and hence a collective momentum in the direction of photon propagation.

A picturesque interpretation would be, that the acceleration of the atoms by the leading or trailing edge of the light pulse is due to the dipole force (real part of susceptibility). For red (blue) detuning, the atoms are accelerated backwards (forwards) by the leading edge of the pulse and forwards (backwards) by the trailing edge. In case, that the cloud absorbs or diffracts photons, a net momentum should remain in the cloud: [56] "The propagation of an optical pulse through a transparent dielectric causes no transfer of momentum to the material, as a positive Lorentz force in the leading part of the pulse is exactly balanced by a negative Lorentz force in its trailing part. However, this balance is removed in the present problem because of the attenuation of the light by its interaction with the charge carriers. This causes the leading part of the pulse at a given time to be weaker than the trailing part and produces a net negative transfer of momentum to the bulk semiconductor."

Out side the medium, we know that the photon momentum is,

$$p_{out} = mc \ , \tag{10.17}$$

with $m = \hbar\omega/c^2$. Inside the medium, it is

$$p_{in} = m\frac{c}{\eta} = \frac{\hbar\omega}{\eta c} \ . \tag{10.18}$$

According to Minkowski, we must use $m = \hbar\omega/(c/\eta)^2$.

10.2.1 Calculation of the momentum of light in a dielectric medium

Let us consider [63] a plane light wave within a dielectric medium given by $\varepsilon = \eta^2\varepsilon_0$ and $\mu = \mu_0$,

$$\vec{\mathcal{E}}(\mathbf{r},t) = \hat{\mathbf{e}}_x\mathcal{E}_0\cos\omega\,(t - z/c) \qquad \text{and} \qquad \vec{\mathcal{H}}(\mathbf{r},t) = \hat{\mathbf{e}}_y\sqrt{\frac{\varepsilon}{\mu_0}}\mathcal{E}_0\cos\omega(t - z/c) \ , \tag{10.19}$$

The energy densities and the energy flows, called 'Poynting vector', are (taking the temporal average),

$$u = \frac{1}{2}(\vec{\mathcal{E}}\cdot\vec{\mathcal{D}} + \vec{\mathcal{B}}\cdot\vec{\mathcal{H}}) = \tfrac{1}{2}\varepsilon\mathcal{E}_0^2 \qquad \text{and} \qquad \mathbf{S} = \vec{\mathcal{E}}\times\vec{\mathcal{H}} = \tfrac{1}{2}\sqrt{\frac{\varepsilon}{\mu_0}}\mathcal{E}_0^2\hat{\mathbf{e}}_z = \frac{c}{\eta}u\hat{\mathbf{e}}_z \ . \tag{10.20}$$

Therefore, the intensity of a light field, $I = |\mathbf{S}|$, is increased by the dielectric. Rewriting this in terms of the average number of photons q in a volume V, we obtain for the energy,

$$\int ud^3r = \tfrac{1}{2}\varepsilon\mathcal{E}_0^2V = N\hbar\omega \ . \tag{10.21}$$

The energy flow of a field of light is equal to the momentum carried by the photons. For a single photon, we have,

$$\mathbf{p}_{Abr} \equiv \frac{1}{N}\frac{1}{c^2}\int\mathbf{S}d^3r = \frac{\hbar\mathbf{k}_0}{\eta} \ . \tag{10.22}$$

However, Minkowski's point of view was,

$$\mathbf{p}_{Min} = \frac{1}{N}\int dV\vec{\mathcal{D}}\times\vec{\mathcal{B}} = \eta\hbar\mathbf{k}_0 \ . \tag{10.23}$$

The recoil frequency is modified from $\hbar\omega_{rec} = \frac{\hbar^2k^2}{2m}$ to $\hbar\omega^{\eta}_{rec} = \eta^2\omega_{rec}$ [21].

10.2.2 Exercises

10.2.2.1 Ex: Einstein box Gedankenexperiment with a BEC

Estimate whether the Einstein box experiment is feasible with a BEC using EIT to cancel absorption?

10.3 Special topic: Advanced Gaussian optics

The most common mode is a Gaussian laser beam, which is the lowest order Hermite-Gaussian mode. But other modes are possible.

10.3.1 Laguerre-Gaussian beams

Since several years, attention has been drawn on an unusual feature of light: The fact that it carries angular momentum when it is in special modes called a *Laguerre-Gaussian mode* [87]. Furthermore, while it is well-known that the light polarization couples to the internal degrees of freedom of atoms, the light angular momentum has been predicted to couple to external degrees of freedom, i.e. light should be able to exert a torque to the atomic motion [2, 8, 3, 1, 4, 67]. The torque has been observed on macroscopic particles [87]. For a hot atomic gas, the Doppler-effect precludes the direct observation of torsional effect. Recently, phase-conjugation by Non-Degenerate Four-Wave Mixing (ND4WM) in a Magneto-Optical Trap (MOT) has been used to indirectly proof that the atoms acquired angular momentum from light [92]. Also, magneto-optical trap have been constructed based on laser beams [50, 90]. Those experiments exploited the doonat-shaped intensity distribution of the LG modes, but did not demonstrate the effect of the torque. And frequency shift [27]. Most traps for neutral atoms are based on light forces, for example the MOT works with radiation pressure. Deliberate misalignement of the optical beams within a plane can give rise to vortex forces and set up a racetrack for the atoms [96, 11].

Laguerre-Gaussian modes can be generated using a *Fresnel zone plate*.

10.3.1.1 Energy density in Laguerre-Gaussian modes

Besides plane and spherical waves, Gaussian beams and many other functions, the Laguerre-Gaussian modes (LGM) are a solution of Maxwell's equations, i.e. they satisfy $\nabla^2u + k^2u = 0$, where u is the scalar mode function of the beam [49]. The vector potential in the Lorentz gauge, $\Phi = -\frac{1}{\imath k}\nabla\cdot\mathbf{A}$, of those modes in the paraxial approximation [51] is given by [2],

$$\boxed{\begin{array}{rcl} \mathbf{A}_{nm}(\mathbf{r}) &=& \hat{\mathbf{e}}_x u_{nm}(\mathbf{r}) e^{-\imath kz} \\ u_{nm}(\mathbf{r}) &=& u_{00}(\mathbf{r}) \left(\frac{r\sqrt{2}}{w(z)}\right)^{|l|} L_p^{|l|}\left(\frac{2r^2}{w(z)^2}\right) e^{-\imath l\phi} e^{\imath(2p+|l|)\arctan\frac{z}{z_R}} \\ u_{00}(\mathbf{r}) &=& \frac{u_0}{\sqrt{z^2+z_R^2}} e^{-\frac{r^2}{w(z)^2}} e^{-\frac{\imath kr^2z}{2(z^2+z_R^2)}} e^{\imath\arctan\frac{z}{z_R}} \end{array}} , \tag{10.24}$$

where $l = n - m$ and $p = \min(n, m)$. In the following we will use the convenient cylindrical coordinate system defined in (1.43). Note that, for $l = p = 0$ we recover a Gaussian beam, as will be shown in Exc. 10.3.2.3.

10.3.1.2 Poynting vector in Laguerre-Gaussian modes

The energy flux is given by the Poynting vector $\vec{\mathcal{S}} = \mu_0^{-1}\vec{\mathcal{E}} \times \vec{\mathcal{B}} = c^2\mathbf{p}$. $|\vec{\mathcal{S}}|$ is the beam intensity. The energy density is $u = \frac{1}{2}(\varepsilon_0|\vec{\mathcal{E}}|^2 + \mu_0^{-1}|\vec{\mathcal{B}}|^2)$. The linear momentum and angular momentum densities and total momenta are defined as,

$$\begin{array}{rclcrcl} \mathbf{p} &=& \int \vec{\wp} d^3r & \text{with} & \vec{\wp} &=& \varepsilon_0\vec{\mathcal{E}} \times \vec{\mathcal{B}} \\ \mathbf{L} &=& \int \vec{\ell} d^3r & \text{with} & \vec{\ell} &=& \mathbf{r} \times \vec{\wp} \end{array} . \tag{10.25}$$

The cycle-average of the real part of the linear momentum density can in the paraxial approximation be traced back to the mode function u, respectively, the scalar potential Φ and the vector potential $\mathbf{A}$ using (6.78),

$$\begin{aligned} \langle\vec{\wp}\rangle &= \frac{\varepsilon_0}{2}(\vec{\mathcal{E}}^* \times \vec{\mathcal{B}} + \vec{\mathcal{E}} \times \vec{\mathcal{B}}^*) \\ &= \imath\omega\frac{\varepsilon_0}{2}(u^*\nabla u - u\nabla u^*) + \omega k\varepsilon_0|u|^2\hat{\mathbf{e}}_z + \omega\sigma\frac{\varepsilon_0}{2}\frac{\partial|u|^2}{\partial r}\hat{\mathbf{e}}_\phi . \end{aligned} \tag{10.26}$$

The components of the linear momentum density are [4],

$$\vec{\wp} = \varepsilon_0\omega k|u|^2\left[\hat{\mathbf{e}}_z + \frac{rz}{z^2+z_r^2}\hat{\mathbf{e}}_r + \left(\frac{l}{kr} - \frac{\sigma}{2|u|^2}\frac{\partial|u|^2}{k\partial r}\right)\hat{\mathbf{e}}_\phi\right] . \tag{10.27}$$

The Poynting vector is in general not parallel to the wavevector $\mathbf{k}$, but spirals about the optical axis.

10.3.1.3 Poynting vector in Hermite-Gaussian modes

This holds even for Hermite-Gaussian beams, as we will show in the following. We start from the energy density of a LGM in Eq. (10.24). For a Gaussian mode $l = p = 0$,

$$|u_{00}(\mathbf{r})| = \frac{u_0 e^{-r^2/w(z)^2}}{w(z)} . \tag{10.28}$$

we find, as will be shown in Exc. 10.3.2.3,

$$\vec{\wp} = \varepsilon_0\omega k|u|^2\left[\hat{\mathbf{e}}_z + \frac{rz}{z^2+z_r^2}\hat{\mathbf{e}}_r + \sigma\frac{rz_R}{z^2+z_R^2}\hat{\mathbf{e}}_\phi\right] . \tag{10.29}$$

i.e. the radial component vanishes for small beam divergence, the azimuthal component is on the order $w_0/z_R \approx 500$ times smaller.

Inserting the full expression of the energy density of a LGM, one finds one term containing σ and hence predicting spin-orbit coupling. It can be shown that it results in a dissipative force proportional to $l\sigma$ [1].

10.3.1.4 Mechanical forces exerted by Laguerre-Gaussian modes

The Laguerre-Gaussian modes are labeled by n and m, where $l = n - m$ and $p = \min(n, m)$, such that $2p + |l| = m + n$. We should recover the Gaussian field for $l = 0$. The electric field $\mathcal{E}_{lp}(\mathbf{r}) = \varepsilon_{lp}(\mathbf{r})e^{i\theta_{lp}(\mathbf{r})}$ is,

$$\varepsilon_{lp}(\mathbf{r}) = \varepsilon_{00}\sqrt{\frac{p!}{(|l|+p)!}}\ \frac{e^{-r^2/w(z)^2}}{\sqrt{1+z^2/z_R^2}}\ \left(\frac{r\sqrt{2}}{w(z)}\right)^{|l|}\ L_p^{|l|}\left(\tfrac{2r^2}{w(z)^2}\right)\ , \tag{10.30}$$

$$\theta_{lp}(\mathbf{r}) = \frac{kr^2z}{2\left(z^2+z_R^2\right)} + l\phi + (2p+l+1)\arctan\frac{z}{z_R} + kz\ .$$

With the Rabi frequency defined through,

$$\Omega_{lp}(\mathbf{r}) = \Omega_0\frac{w_0}{w(z)}\ e^{-r^2/w(z)^2}\ \left(\frac{r\sqrt{2}}{w(z)}\right)^{|n-m|}\ L_{\min(n,m)}^{|n-m|}\left(\tfrac{2r^2}{w(z)^2}\right)\ , \tag{10.31}$$

Using the optical Bloch equations, we find the stationary solutions for the dipole and the dissipative forces [1],

$$\mathbf{F}_{dip} = -2\hbar\Omega_{lp}(\mathbf{r})\ \frac{\Delta}{4\Delta^2+2\Omega_{lp}(\mathbf{r})^2+\Gamma^2}\nabla\Omega_{lp}(\mathbf{r})\ , \tag{10.32}$$

$$\mathbf{F}_{diss} = 2\hbar\Omega_{lp}^2(\mathbf{r})\ \frac{\Gamma}{4\Delta^2+2\Omega_{lp}(\mathbf{r})^2+\Gamma^2}\nabla\theta_{lp}(\mathbf{r})\ .$$

where the gradients are,

$$\nabla\Omega_{lp}(\mathbf{r}) = ... \tag{10.33}$$

and,

$$\nabla\theta_{lp}(\mathbf{r}) = -\nabla\left[-kz - l\phi - \frac{kr^2z}{2(z^2+z_R^2)} - (n+m+1)\tan^{-1}\frac{z}{z_R}\right] \tag{10.34}$$

$$= \left(k + \frac{kr^2}{2(z^2+z_R^2)}\left(1 - \frac{2z^2}{z^2+z_R^2}\right) + \frac{(n+m+1)z_R}{z^2+z_R^2}\right)\hat{\mathbf{e}}_z + \frac{krz}{z^2+z_R^2}\hat{\mathbf{e}}_r + \frac{l}{r}\hat{\mathbf{e}}_\phi\ .$$

Here we assume the velocity cold enough not to influence the detuning. Otherwise, we must substitute $\Delta \to \Delta - \mathbf{v}\nabla\theta$. At the waist $z = 0$ and for typical experimental conditions $r, k^{-1} \ll z_R$,

$$\nabla\theta_{lp}(\mathbf{r}) \approx k\hat{\mathbf{e}}_z + \frac{l}{r}\hat{\mathbf{e}}_\phi\ . \tag{10.35}$$

We can now write the azimuthal force and the torque in analogy to the radiation pressure,

$$\mathbf{F}_{az} = \hbar\frac{\mathbf{l}}{r}\ \frac{I}{\hbar\omega}\ \sigma(\Delta) \tag{10.36}$$

and,

$$\mathbf{T} = \hbar \frac{\mathbf{r} \times \mathbf{l}}{r} \frac{I}{\hbar\omega} \sigma(\Delta) \ . \tag{10.37}$$

If we further concentrate on the first Laguerre-Gaussian mode given by $l = 1$ and $p = 0$ or $n = 1$ and $m = 0$, and assume low saturation $\Omega \ll \Gamma$, we find the force,

$$\mathbf{F}_{diss} = -\hbar\Gamma \left[k\hat{\mathbf{e}}_z + \frac{\hat{\mathbf{e}}_\phi}{r} \right] e^{-2r^2/w_0^2} \frac{2r^2}{w_0^2} \frac{\Omega_0^2}{4\Delta^2 + \Gamma^2} \ . \tag{10.38}$$

It consists of a rotational torque and a component in $\mathbf{k}$ direction. For a normal Gaussian field, $l = 0$. The LG modes have a ring-shaped intensity distribution $I^{(Lag)}(x, y)$. Therefore, the rotational force depends on the distance from the axis and has a maximum at the radius $r = w_0/2$. The dipole force contribution may be neglected close to resonance, and higher-order contributions from the LG mode as well.

10.3.1.5 Laguerre-Gaussian standing wave

Many experiments are performed within the Rayleigh range, $z \ll z_R$, where,

$$\mathcal{E}_{pl}(r, \phi) = \mathcal{E}_0 f_{pl}(r) \ e^{-\imath l\phi} e^{\imath(\omega t - kz)} \ , \tag{10.39}$$
$$f_{pl}(r) = \frac{\Omega_{pl}(r)}{\Omega_0} = \frac{e^{-r_w^2/2}}{z_R} r_w^{|l|} \ L_p^{|l|}(r_w^2) \ .$$

where we introduced the normalized paraxial distance $r_w \equiv r\sqrt{2}/w_0$. When such a Laguerre-Gaussian beam is reflected form a mirror reflected from a mirror it changes the signs of $k \longrightarrow -k$ but not $l \to l$. We obtain a standing wave, made of ring-shaped potentials,

$$\left| f_{pl}(r) \ e^{-\imath l\phi} e^{\imath(\omega t - kz)} + f_{pl}(r) \ e^{-\imath l\phi} e^{\imath(\omega t + kz)} \right|^2 = 4f_{pl}^2(r) \cos^2 kz \ . \tag{10.40}$$

At $z = 0$ the potential reads

$$U_{pl} = \frac{\Omega^2}{4\Delta} = \frac{\sigma_0 \Gamma I(x, y)}{\hbar\omega 4\Delta} = \frac{\Omega_0^2}{4\Delta} 4f_{pl}^2(r) \ , \tag{10.41}$$

If in contrast the counterpropagating beam has an inverse angular momentum,

$$\left| f_{pl}(r) \ e^{-\imath l\phi} e^{i(\omega t - kz)} + f_{pl}(r) \ e^{\imath l\phi} e^{\imath(\omega t + kz)} \right|^2 = 4f_{pl}^2(r) \cos^2(kz - l\phi) \ , \tag{10.42}$$

the superposition of a Laguerre-Gaussian beam with a reflected beam gives an azimuthally periodic modulation like a circular $1D$ lattice, which is twisted along the $\hat{z}$-axis. However there is no axial confinement. The intensity resembles a knot of l worms winding about the $\hat{z}$-axis at constant distance like helices. Axial modulation has to be obtained by an additional plane wave [5].

Let us calculate the dipole force via $\mathbf{F} = -\nabla U$,

$$\frac{\partial f_{pl}^2(r)}{\partial x} = 2f_{pl}(r) \frac{\partial r}{\partial x} \frac{\partial}{\partial r} \frac{e^{-r_w^2/2}}{z_R} r_w^{|l|} \ L_p^{|l|}(r_w^2) \tag{10.43}$$
$$= f_{pl}(r)^2 \frac{8x}{w_0^2} \left[\frac{|l|}{2r_w^2} - \frac{1}{2} - \frac{L_{p-1}^{|l|+1}(r_w^2)}{L_p^{|l|}(r_w^2)} \right]$$

using $\frac{d}{dx} L_n^{(m)}(x) = -L_{n-1}^{(m+1)}(x)$.

10.3.1.6 Creation of Laguerre-Gaussian modes

The polarization of light couples to the internal degrees of freedom of the atoms. But special light modes, i.e. the higher-order Laguerre-Gaussian (LG) modes, may carry orbital angular momentum. This angular momentum couples to the external degrees of freedom of the atoms [2, 8, 3, 1], i.e. the light exerts a torque onto the atoms. This light force is, however, very weak and in a gas cell with hot atoms, the Doppler-effect smears out the motional effect. Nevertheless, the torque has been observed with macroscopic particles [87]. And in a Magneto-Optical Trap (MOT), phase-conjugation by nondegenerate four-wave mixing has been used to indirectly prove the transfer of angular momentum to the atoms [92]. Finally, MOTs using Laguerre-Gaussian laser beams been constructed, however without demonstrating the effect of the torque [50, 90].

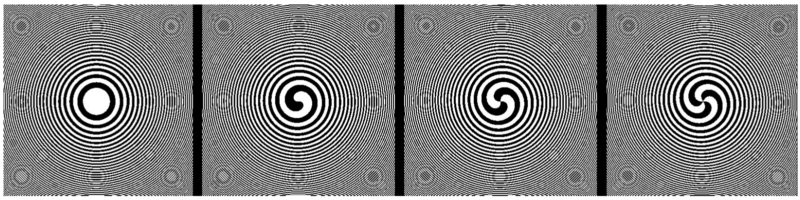

Figure 10.3: Masks for generating Laguerre-Gaussian beams.

The interference of such a mode with a plane wave v yields interference patterns proportional to,

$$u_{nm}(\mathbf{r})e^{-ikz} + v_{nm}(\mathbf{r})e^{-ikz} \propto \cos\left(-l\phi - \frac{kr^2 z}{2z_R^2} - (m+n+1)\arctan\frac{z}{z_R}\right) . \quad (10.44)$$

At some distance $z \neq 0$ and for $l \neq 0$ the patterns have Yin-Yang spiral shape. Inversely, like in holography, plane waves are *diffracted* at the spiral patterns in such a way that they generated a Laguerre-Gaussian mode. This is not an image. Images are also formed with undiffracted parts of the plane wave. The patterns form a fundamental focus at a distance f and subfoci at distances $f/2$, $f/3$, ... The fundamental beam is separated from the undiffracted and higher-order Fresnel modes by a short focal length lens placed in the fundamental focus. A spiral mask can be generated by setting $z = z_R$ in Eq. (10.44) and filling black the region where r and ϕ satisfy [44],

$$\cos\left(-l\phi - \frac{kr^2}{2z_R} - \pi(n+1/2)\right) > 0 . \quad (10.45)$$

A special case is defined by $l = 0$ which reproduces the *Fresnel zone plate*. The orbital momentum may be transferred to the atomic motion. Perhaps this also has an effect on the internal degrees of freedom: The higher-order orbital angular momentum may couple to higher multipole moments. At reflection on a mirror, the symmetry of the LG mode is inverted. Therefore, we can build a standing wave LG beam with no axial force (if the intensities are balanced and the waists matched) and twice the torque. LG modes can also be created from normal Gaussian modes with an arrangement of cylindrical lenses.

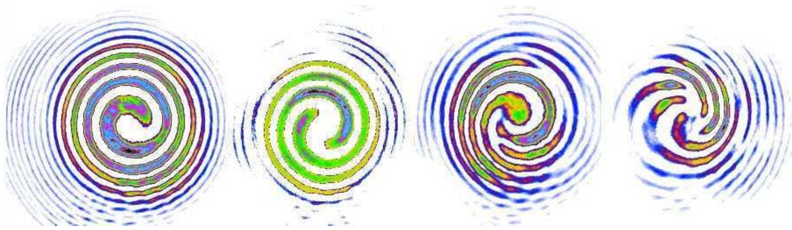

Figure 10.4: Laguerre-Gaussian beams with various charges.

10.3.1.7 Optical signatures

The interference of a Laguerre-Gaussian mode (LGM) with a phase-matched plane wave Gaussian beam yields interference patterns shown in the above figure. In the far-field, the laser beam forms a ring-shaped LGM. Higher-order topological charges are easily detected in the interference patterns through the occurrence of bifurcations or by the number of arms spiraling into the center.

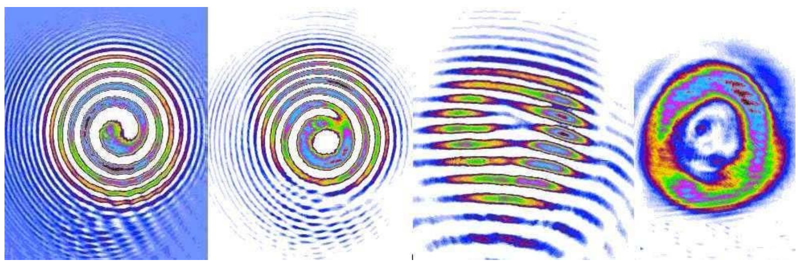

Figure 10.5: Bifurcations in a Laguerre-Gaussian beam.

10.3.2 Exercises

10.3.2.1 Ex: Gaussian and Laguerre-Gaussian beams

Convince yourself that the Laguerre-Gaussian beam parametrized in (10.24) corresponds to the Gaussian beam of (7.267).

10.3.2.2 Ex: Motion of atoms in Laguerre-Gaussian beams

Programs on the motion of atoms in Laguerre-Gaussian beams.

10.3.2.3 Ex: Linear momentum density for Hermite-Gaussian modes

Compare the linear momentum density for Hermite-Gaussian (7.267) and Laguerre-Gaussian (10.24) modes.

10.4 Special topic: Superconductivity

At low temperatures some metals completely give up electric resistance. This effect found by Kammerlingh-Onnes is called *superconductivity* and has been explained through Bose-Einstein condensation of electron pairs [25]. But before we outline this theory let us try a classical approach based on electrodynamics as proposed by Fritz and Heinz London.

10.4.1 London model of superconductivity and the Meissner effect

We learned in Sec. 3.3.2 that *Ohm's law* is explained within the Drude model by the fact that the accelerating Coulomb force of the electric field, $m\dot{\mathbf{v}} = q\vec{\mathcal{E}}$, is spoiled by collisions,

$$\mathbf{j} = \varsigma\vec{\mathcal{E}} . \tag{10.46}$$

Let us now suppose a perfect conductor, where collisions are absent. Then, if we want the current density $\mathbf{j} = \varrho\mathbf{v}$ to be constant,

$$0 = \dot{\mathbf{j}} = \varrho\dot{\mathbf{v}} = -\frac{q^2 n_e}{m}\vec{\mathcal{E}} , \tag{10.47}$$

where $\varrho = -en_e$ is the free electron charge density.

Let us now study the behavior of the magnetic field in a conductor with $\mu_0 = 0$. Maxwell's equations require,

$$\nabla\times\vec{\mathcal{E}} = -\dot{\vec{\mathcal{B}}} \qquad \text{and} \qquad \nabla\times\vec{\mathcal{B}} = \mu_0\mathbf{j} + \dot{\vec{\mathcal{D}}} . \tag{10.48}$$

Assuming $\dot{\vec{\mathcal{D}}} = 0$ the above equations can easily be solved, yielding,

$$\boxed{\nabla^2\dot{\vec{\mathcal{B}}} = \frac{\mu_0 n_e q^2}{m}\dot{\vec{\mathcal{B}}}} . \tag{10.49}$$

This equation describes the behavior of a magnetic field in and around a perfect conductor.

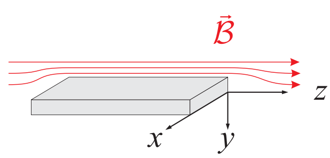

Figure 10.6: Scheme of the Meissner effect.

As we will see in Exc. 10.4.5.1, the solution of Eq. (10.49) predicts an expulsion of the magnetic field out of the conductor, as illustrated in Fig. 10.6. This effect is termed the *Meissner-Ochsenfeld effect*. That is, in the absence of resistivity, a conductor acts like a perfect diamagnetic (magnetic susceptibility $\chi_m = 1$). According to the Lenz rule, the electrons try to compensate any $\mathcal{B}$-field change by collectively rotating such as to counteract the change. The electrons rotate in such a way that the $\mathcal{B}$-field disappears inside the conductor, which leads to an amplification of the field near the surfaces. As a consequence, permanent magnets are repelled from superconducting surfaces.

The problem is that the discontinuity of the magnetic field at the periphery of the superconductor should violate the continuity equation. And in fact, it is experimentally observed, that the magnetic field is not completely expelled from thin superconducting films, because the magnetic field penetrates somewhat into the superconductor with the penetration depth λ_L. In order to understand this, it is necessary to replace the classical *Ohm's law* for the current density $\mathbf{j}$ and the electric field $\vec{\mathcal{E}}$, $\mathbf{j} = \varsigma\vec{\mathcal{E}}$, by the *London equation*.

The London brothers postulates that the magnetic field inside a superconductor would not only be constant, as predicted by Eq. (10.49) by vanish altogether,

$$\boxed{\nabla^2\vec{\mathcal{B}} = \frac{\mu_0 n_e q^2}{m}\vec{\mathcal{B}}} \ . \tag{10.50}$$

We will study consequences of this equation in Exc. 10.4.5.2.

10.4.1.1 Derivation of the London equation

The London equation can be derived in the framework of quantum mechanics, considering the superconducting state as a macroscopically extended quantum state described by the following wavefunction,

$$\psi(\mathbf{r}) = \psi_0 e^{\imath S(\mathbf{r})} \ , \tag{10.51}$$

where $S = S(\mathbf{r})$ is the phase of the macroscopic wavefunction. $\psi_0^2 = n_e$ corresponds to the density of the number of Cooper pairs in the superconductor. The implicit assumption of a homogeneous density of the Cooper pairs is reasonable, since the pairs are negatively charged and repel each other. Any imbalance of the density of pairs would therefore generate an electric field, which would be compensated immediately. The kinetic momentum operator in the presence of a magnetic field, $\mathbf{p} = -\imath\hbar\nabla - q\mathbf{A}$, where $\mathbf{A} = \mathbf{A}(\mathbf{r}, t)$ is the vector potential of the magnetic field, applied to the wavefunction ψ gives,

$$m\mathbf{v}\psi = \mathbf{p}\psi = (\hbar\nabla S - q\mathbf{A})\psi \ . \tag{10.52}$$

That is,

$$\mathbf{v} = \frac{\hbar}{m}\nabla S - \frac{q}{m}\mathbf{A} \ . \tag{10.53}$$

With $\mathbf{j} = qn_e\mathbf{v}$ follows immediately,

$$\boxed{\mathbf{j} = \frac{n_e q\hbar}{m}\nabla S - \frac{n_e q^2}{m}\mathbf{A}} \ . \tag{10.54}$$

This is the London equation.

There are two useful forms of this equation, sometimes referred to as the 1^{st} and the 2^{nd} London equation,

$$\partial_t\mathbf{j} = \frac{n_e q^2}{m}\vec{\mathcal{E}} \ , \tag{10.55}$$

and

$$\nabla \times \mathbf{j} = -\frac{n_e q^2}{m}\vec{\mathcal{B}} \,. \tag{10.56}$$

The phase S does not contribute to these two equations. It does not contribute to the first equation, because the phase is only dependent on the position and therefore constant in time, and it does not contribute to the second equation, because $\nabla \times \nabla S = 0$ [1]

10.4.2 BCS theory

Many-body effects like superconductivity are not explained by the free electron or the Bloch model. Superconductivity is characterized by two main features: The disappearance of electrical resistance in some metals at temperatures below roughly $T \simeq 10\,\text{K}$, and the expulsion of magnetic flux lines out of the metals, known as Meissner-Ochsenfeld effect.

According to Bardeen-Cooper-Schrieffer near the edge of the Fermi surface induced by weak attractive interactions strong correlations in momentum space may build up. Such interations can be mediated by local polarization traces, i.e. deformations of the lattice or phonons, imprinted by a moving electron into the metallic lattice and sensed by a second electron following at a reasonable distance [16, 22]. Thus Fermi gases are unstable with respect to formation of bound fermion pairs. However, fermion pairs are not bound in the ordinary sense, and the presence of a filled Fermi sea is essential. Rather, we have a many-body state. Hence, the interpretation as a Bose-condensate of Cooper pairs explains some characteristics like the existence of a delocalized macroscopic wavefunction and the superfluid-like behavior suppressing the electrical resistance. But it oversimplifies and does not account for the important role of fermionic statistics in the many-body state.

The requirements for Cooper pairing are 1. low temperature to rule out thermal phonons, 2. strong electron-lattice interaction, 3. many electrons just below E_F, 4. anti-parallel spins, and 5. antiparallel momentum of the electrons.

Below T_c the motions of the electrons and the ions in the lattice are highly correlated. Cooper pairs are weakly bound, in thermal equilibrium with unpaired electrons, and have a vanishing total momentum. The typical distance of the electrons in a pair is roughly 100 nm. Although the fraction of paired electrons is only 10^{-4}, their number within the volume occupied by a single pair is 10^6.

Cooper-pairs form through scattering processes. Since all states below the Fermi surface are occupied, the final momenta must be above k_F. In other words, the two electrons are excited from slightly below $E = E_F$ to slightly above $E + E_g/2 = E_F$, where they profit from the large amount of available empty states allowing for their high mobility and letting them transit into the strongly correlated pairing state. The pairs then have the binding energy E_g, because the increase in kinetic energy must

[1]Note that, although the phase does not contribute to the last two formulas, it should not be neglected! If the phase component were not included, it would mean that the current density without magnetic field would have to be zero. In reality, however, the phase gradient can also contribute to the current density, which therefore need not necessarily be zero, i.e. the current density is not zero, although no magnetic field is applied.

be overcompensated by the potential energy. Such processes smooth out the Fermi edge even at $T = 0$, as if the temperature really were at $T \simeq T_c$.

An energy gap forms which has just the width E_g. Its origin is understood as follows: If an electron could slightly change its energy, the pair correlation would immediately break up and the binding energy E_g liberated. But this energy cannot be dissipated. Since the binding energy for Cooper pairs is roughly $E_g \simeq 3k_BT_c$, a thermal noise source must at least provide the energy $3k_BT_c$, which is not possible if $T < T_c$. At higher temperatures, the pairing gap narrows and vanishes at $T = T_c$. The gap can be spectroscopically probed with IR radiation.

Higher $\mathcal{B}$ fields require lower critical temperatures. The critical temperature drops with rising mass of the ions, $T_c m^{1/2} = const$. This indicates that the vibration of the lattice ions is crucial for superconductivity.

Magnetic fields trying to penetrate superconducting wires perturb the superconductivity. This problem can be reduced in type II superconductors, where the size of the Cooper pairs are reduced and employing superconducting wires containing normal conducting channels.

The quantitative treatment starts with the two-body Schrödinger equation,

$$\left[-\frac{\hbar^2}{2m}(\nabla_1^2 + \nabla_2^2) + V(r_1 - r_2)\right]\Psi(r_1, r_2) = (E + 2E_F)\Psi(r_1, r_2) \ . \tag{10.57}$$

Here we assume singlet pairing s-wave collisions. Center-of-mass and relative coordinates are now separated, giving,

$$\left[-2\frac{\hbar^2}{2m}\nabla_r^2 + V(r)\right]\psi(r) = \left(E + 2E_F - \frac{\hbar^2K^2}{4m}\right)\Psi(r) \ . \tag{10.58}$$

Transforming into momentum space, assuming that the Fourier transform $V(p, p') = V^{-1}\int e^{-\imath(p-p')r}V(r)d^3r$ is only nonzero, $= V_0$, inside an energy interval smaller than the Debye frequency $\hbar\omega_D$ close to the Fermi surface, we finally arrive at the binding energy of the Cooper-pair,

$$E = -\frac{2\hbar\omega_D}{e^{2/V_o D(E_F)} - 1} \ , \tag{10.59}$$

where $D(E_F) \propto k_F$ is the density of states at the Fermi surface. Estimating $V(r) \approx \hbar^2/ma^2$ the Fourier transform goes like $V_0 \propto a$, so that $k_BT_{BCS} \propto -e^{-\pi/2k_F|a_s|}$.

A full quantum treatment reveals the presence of a gap. This gap can also be understood in the following way. In the normal state the energy spectrum is twofold degenerate. A state with a hole in the Fermi surface has the same energy as a state with an electron above the Fermi surface. Cooper-pairing couples those states, which leads to energy splitting and introduces a *pairing gap*,

$$|u_k|^2 = \frac{1}{2}\left[1 + \frac{\epsilon_k - E_F}{\sqrt{\Delta_0^2 + (\epsilon_k - E_F)^2}}\right] = 1 - |v_k|^2 \tag{10.60}$$

$$\Delta = -\sum_k u_k v_k \ .$$

The product $u_k v_k$ only contributes near the Fermi surface. We get a density of states,

$$D_s(E) = D_n \frac{|E - E_F|}{\sqrt{-\Delta_0^2 + (\epsilon_k - E_F)^2}} \ , \tag{10.61}$$

which has a gap. The states are redistributed toward the edges of the gap.

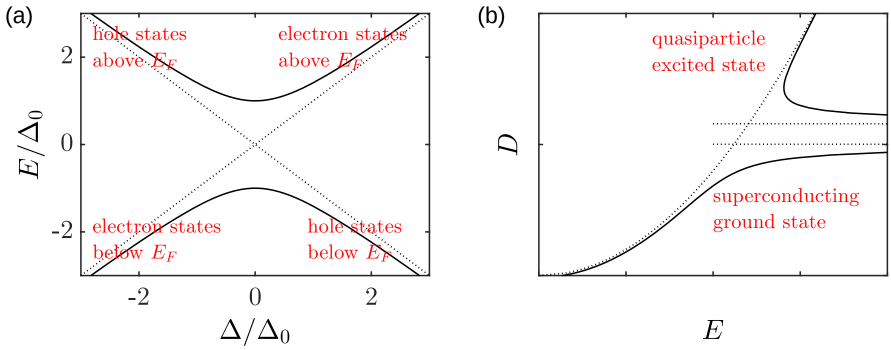

Figure 10.7: Pairing gap in the energy spectrum and the density of states.

10.4.3 Josephson junctions

Two superconductors that are joined by a nm thin isolating oxide layer build a *Josephson junction* (JJ) [48]. Cooper pairs may tunnel through the junction producing a current flow i_J. The basic JJ is described by,

$$i_J = I_c \sin \varphi \qquad \text{and} \qquad v = \frac{\Phi_0}{2\pi} \frac{d\varphi}{dt} \ , \tag{10.62}$$

where

$$\Phi_0 = \frac{h}{2e} \ . \tag{10.63}$$

I_c is the critical supercurrent of the junction, and v is the voltage at the JJ. φ is a dynamical variable describing the phase difference between the macroscopic wave functions on both sides of the junction. Note that for small φ we have $u \propto i$ similar to the situation in a magnetic coil. The *ac*-Josephson effect consists in applying a constant voltage. Then φ increases linearly in time and the Josephson-current oscillates at a given (microwave) frequency [36],

$$f_J = \frac{v}{\Phi_0} \ . \tag{10.64}$$

This allows a very precise measurement of h/e.

10.4.4 Synchronization of coupled Josephson junctions

The superconducting flux is quantized. A *superconducting quantum interference device* consist of two JJs connected in parallel. In that way the *supercurrent* is split and recombined.

10.4.4.1 Resistively shunted junctions

In a widely accepted model of nonideal *resistively shunted junctions* (RSJ) [74] the junction current consists of three components: A superconducting current $i_J = I_c \sin\varphi$, a resistive current $i_R = v/R$, and a capacitance current $\dot{v}C$ (see Fig. 10.8). From Kirchhoff's laws using (10.62),

$$C\frac{\Phi_0}{2\pi}\frac{d^2\varphi}{dt^2} + \frac{1}{R}\frac{\Phi_0}{2\pi}\frac{d\varphi}{dt} + I_c \sin\varphi = i \;, \tag{10.65}$$

if the resistance is assumed independent of the applied voltage. Located in front of the term $\dot{\varphi}$ the resistivity is inversely proportional to the dissipation. The reason for this is that dissipation occurs via *single-particle tunneling*. Note that the equation is identical to that of an overdamped rotator or of a phase-locked loop.

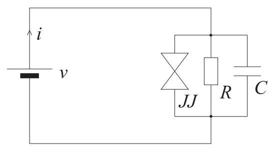

Figure 10.8: Resistively shunted Josephson junction.

Neglecting the resistance, the equation of motion can be derived from the Hamiltonian,

$$\hat{H} = \frac{p_\varphi^2}{2C\Phi_0/2\pi} - i\varphi - I_c\cos\varphi \;, \tag{10.66}$$

via $\dot{\varphi} = \frac{\partial H}{\partial p_\varphi}$ and $\dot{p}_\varphi = -\frac{\partial H}{\partial \varphi}$. The φ and p_φ are conjugate variables,

$$[\varphi, p_\varphi] = \imath \;. \tag{10.67}$$

Let us go to scaled variables via $\tilde{H} \equiv H/(C\Phi_0/2\pi)$, $\tilde{p_\varphi} \equiv p_\varphi/(C\Phi_0/2\pi)$, $K \equiv I_c/(C\Phi_0/2\pi)$, and $\lambda \equiv i/(C\Phi_0/2\pi)$,

$$\tilde{H} = \frac{\tilde{p}_\varphi^2}{2} - \lambda\varphi - K\cos\varphi \;, \tag{10.68}$$

In these units,

$$[\varphi, \tilde{p}_\varphi] = \imath\frac{e}{\hbar C} \;. \tag{10.69}$$

10.4.4.2 Response to *ac* driving sources

Let the applied voltage be $v(t) = V_0 + V_s\cos\omega_s t$. We may substitute the voltage in (10.62) and integrate,

$$\varphi = \varphi(0) + \frac{2\pi}{\Phi_0}V_0 t + \frac{2\pi}{\Phi_0}\frac{V_s}{\omega_s}\sin\omega_s t \;. \tag{10.70}$$

The resistive current is then,

$$i_R = \frac{V_0}{R} + \frac{V_s}{R}\cos\omega_s t \;, \tag{10.71}$$

and plugging (10.70) this into the Josephson current (10.62),

$$i_J = I_c \sin\left(\varphi(0) + \frac{2\pi}{\Phi_0}V_0 t + \frac{2\pi V_s}{\Phi_0\omega_s}\sin\omega_s t\right) \tag{10.72}$$
$$= I_c \sum_n (-1)^n J_n\left(\frac{2\pi V_s}{\Phi_0\omega_s}\right)\sin\left[(f_J - n\omega_s)t + \varphi(0)\right] ,$$

where we expanded the double sine into Bessel-functions. The time-averaged Josephson current disappears unless $f_J = n\omega_s$,

$$\bar{i}_J = I_c \sum_n (-1)^n J_n\left(\frac{2\pi V_s}{\Phi_0\omega_s}\right)\sin\left[\varphi(0)\right]\ \delta(f_J - n\omega_s) . \tag{10.73}$$

The averaged total current $\bar{i} = \bar{i}_R + \bar{i}_J$ as a function of the applied voltage v thus obtains a washboard-type characteristics,

$$\bar{i} = \frac{V_0}{R} + I_c \sum_n (-1)^n J_n\left(\frac{2\pi V_s}{\Phi_0\omega_s}\right)\sin\left[\varphi(0)\right]\ \delta(v - n\omega_s\Phi_0) . \tag{10.74}$$

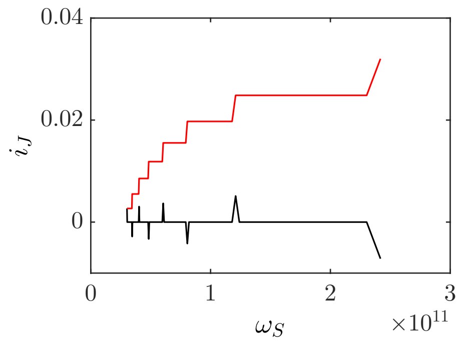

Figure 10.9: (code) Shapiro steps and their derivative.

The plateaus in the i-v characteristics are called *Shapiro steps*. They appear at voltages $n\hbar\omega_s/4\pi e$. In the case of arrays of m JJs, steps are also observed at voltages corresponding to rational fractions of frequencies $m\omega_j = n\omega_s$, provided the JJs are locked [23].

10.4.4.3 Locking

To study the locking phenomenon we simplify the JJ equation by neglecting dissipation, $C = 0$,

$$\frac{\Phi_0}{2\pi}\frac{d\varphi}{dt} = Ri + RI_c \sin\varphi . \tag{10.75}$$

This is the so-called *Adler equation*,

$$\frac{d\psi}{dt} = -\nu + \varepsilon\sin\psi , \tag{10.76}$$

whose formal solution is [74],

$$t = \int \frac{d\psi}{\varepsilon \sin \psi - \nu} \ . \tag{10.77}$$

The beat frequency is,

$$\Omega_\psi = 2\pi \left| \int \frac{d\psi}{\varepsilon\left(1 - \frac{\psi^2}{2}\right) - \nu} \right|^{-1} \ , \tag{10.78}$$

expanding around the maximum at $\psi = \pi/2$,

$$\Omega_\psi \simeq \pi\varepsilon \left| \int \frac{d\psi}{-\psi^2 - 2\frac{\nu}{\varepsilon} + 2} \right|^{-1} = \pi\sqrt{2\varepsilon}\sqrt{\varepsilon - \nu} \left| \int \frac{d\tilde{\psi}}{1 - \tilde{\psi}^2} \right|^{-1} \simeq \pi\sqrt{2\varepsilon}\sqrt{\nu - \varepsilon} \ . \tag{10.79}$$

This is due to a locking of the drive frequency and the frequency of the oscillators.

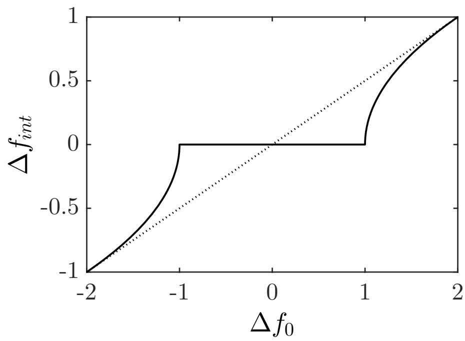

Figure 10.10: (code) Arnold tongue.

10.4.4.4 Devil's staircase

Locking can also happen between higher harmonics. To see this we chose an alternative treatment goes as follows. The equation of motion with a pure ac driving voltage without resistance is,

$$C\frac{\Phi_0}{2\pi}\frac{d^2\varphi}{dt^2} + I_c \sin\left(\varphi(0) + \frac{2\pi V_0}{\Phi_0}t + \frac{2\pi V_s}{\Phi_0\omega_s}\sin\omega_s t\right) = 0 \ . \tag{10.80}$$

It can be derived from the Hamiltonian,

$$\hat{H} = \frac{p_\varphi^2}{2C\Phi_0/2\pi} - I_c \cos\left(\varphi(0) + \frac{2\pi V_0}{\Phi_0}t + \frac{2\pi V_s}{\Phi_0\omega_s}\sin\omega_s t\right) \ . \tag{10.81}$$

Substituting $\tilde{H} \equiv H/(C\Phi_0/2\pi)$, $\tilde{p_\varphi} \equiv p_\varphi/(C\Phi_0/2\pi)$, $K \equiv I_c/(\omega_s C\Phi_0/2\pi)$, and $\lambda \equiv \imath/(\omega_s C\Phi_0/2\pi)$, ...

We now go to the annulus map describing the Josephson junction. The JJ map can be interpreted as a δ-kicked rotor. The dissipative map [102] predicts the occurrences of locking regions, known as Shapiro steps observed at all simple rational numbers m/n. They are equivalent to those of a *devil's staircase*.

10.4.4.5 Quantized JJ

The quantized energy levels of the JJ $\cos\psi$ potential result in a phase quantization. As a consequence, the energy exchange between an oscillating driving pump, ω_s, and the JJ, only occurs in multiples of ω_J.

To visualize quantum effects, one has to go to the quantum map $|\psi_{n+1}\rangle = \hat{U}\psi_n$.

10.4.5 Exercises

10.4.5.1 Ex: Perfect conductor

Calculate the magnetic field near a perfect conductor by solving equation (10.49).

10.4.5.2 Ex: Perfect conductor

Quantify the Meissner effect for a thin layer by solving equation (10.50).

10.4.5.3 Ex: Meissner-Ochsenfeld effect

Calculate the magnetic field inside a thin superconducting layer as a function of layer thickness and temperature.

10.5 Quantities and formulas in electromagnetism

10.5.1 Electromagnetic quantities

charge	Q	basic SI unit [C]
electric field (Coulomb law)	$\vec{\mathcal{E}}$	$d\vec{\mathcal{E}}(\mathbf{r}) = \frac{1}{4\pi\epsilon_0}\frac{dQ(\mathbf{r}-\mathbf{r}')}{\|\mathbf{r}-\mathbf{r}'\|^3}$
Coulomb law		$\vec{\mathcal{E}}(\mathbf{r}) = \frac{1}{4\pi\epsilon_0}\int_{\mathcal{V}}\frac{\rho(\mathbf{r}')(\mathbf{r}-\mathbf{r}')}{\|\mathbf{r}-\mathbf{r}'\|^3}d^3r'$
superposition principle		$\mathbf{F} = \mathbf{F}_1 + \mathbf{F}_2$
Coulomb force	$\mathbf{F}_C$	$\mathbf{F}_C = q\vec{\mathcal{E}}$
electric dipole moment	$\mathbf{p}$	$\mathbf{p} \equiv q\mathbf{r}$
electric torque	$\vec{\tau}$	$\tau = \mathbf{p}\times\vec{\mathcal{E}}$
potential energy of electric dipoles	U_e	$U_e = -\mathbf{p}\cdot\vec{\mathcal{E}}$
electric flux	Ψ_e	$\Psi_e \equiv \int_{\mathcal{S}}\vec{\mathcal{E}}\cdot d\mathbf{S}$
electric Gauß law		$\oint_{\mathcal{S}}\vec{\mathcal{E}}\cdot d\mathbf{S} = \frac{Q_{dentro}}{\epsilon_0} = \frac{1}{\epsilon_0}\int_{\mathcal{V}}\rho(\mathbf{r}')d^3r'$
gradient	∇	$\nabla \equiv \sum_k \hat{\mathbf{e}}_k\frac{\partial}{\partial x_k}$
potential	V	$V \equiv -\int_\gamma \vec{\mathcal{E}}\cdot d\mathbf{r}$
voltage	U	$U_{12} \equiv V_2 - V_1$
capacity	C	$C \equiv \frac{Q}{U}$
plate capacitor		$C = \frac{\epsilon_0 A}{d}$
resistance (Ohm's law)	R	$R \equiv \frac{U}{I}$
lei 1. de Kirchhoff		$\sum_k U_k = 0$ in every mesh
lei 2. de Kirchhoff		$\sum_k I_k = 0$ in every node
magnetic field (Biot-Savart law)	$\vec{\mathcal{B}}$	$d\vec{\mathcal{B}}(\mathbf{r}) = \frac{\mu_0}{4\pi}\int_{\mathcal{C}}\frac{Id\vec{\ell}\times(\mathbf{r}-\mathbf{r}')}{\|\mathbf{r}-\mathbf{r}'\|^3}$
Biot-Savart law		$\vec{\mathcal{B}}(\mathbf{r}) = \frac{\mu_0}{4\pi}\int_{\mathcal{V}}\frac{(\mathbf{r}-\mathbf{r}')\times\mathbf{j}(r')}{\|\mathbf{r}-\mathbf{r}'\|^3}d^3r'$
Lorentz force	$\mathbf{F}_L$	$\mathbf{F}_L = q\mathbf{v}\times\vec{\mathcal{B}}$
magnetic dipole moment	$\vec{\mu}$	$\vec{\mu} \equiv I\mathbf{A}$
magnetic torque	$\vec{\tau}$	$\vec{\tau} = \vec{\mu}\times\vec{\mathcal{B}}$
potential energy of magnetic dipoles	U_m	$U_m = -\vec{\mu}\cdot\vec{\mathcal{B}}$
magnetic flux	Ψ_m	$\Psi_m \equiv \int_{\mathcal{S}}\vec{\mathcal{B}}\cdot d\mathbf{S}$
magnetic Gauß law		$\oint_{\mathcal{S}}\vec{\mathcal{B}}\cdot d\mathbf{S} = 0$
Ampère's law		$\oint_{\mathcal{C}}\vec{\mathcal{B}}\cdot d\vec{\ell} = \mu_0 I_{dentro} = \mu_0\int_{\mathcal{S}} j(\mathbf{r}')d^2r'$
Faraday law		$U_{ind} = -\frac{d\Phi_m}{dt}$
inductance	L	$L \equiv -\frac{U_{ind}}{dI/dt}$
self-inductance of a coil		$L = \mu_0\frac{N^2\pi r^2}{\ell}$
Poynting vector	$\vec{\mathcal{S}}$	$\mathbf{S} \equiv \vec{\mathcal{E}}\times\vec{\mathcal{H}}$

electric displacement	$\vec{\mathcal{D}}$	$\vec{\mathcal{D}} = \varepsilon\vec{\mathcal{E}}$
polarization	$\vec{\mathcal{P}}$	$\vec{\mathcal{P}} = \vec{\mathcal{D}} - \varepsilon_0\vec{\mathcal{E}}$
magnetic excitation	$\vec{\mathcal{H}}$	$\vec{\mathcal{H}} = \mu^{-1}\vec{\mathcal{B}}$
magnetization	$\vec{\mathcal{M}}$	$\vec{\mathcal{M}} = \mu_0^{-1}\vec{\mathcal{B}} - \vec{\mathcal{H}}$

10.5.2 Formulas of special relativity

metric	Kronecker symbol	$(\delta_{\mu\nu})$
	Lévi-Civita symbol	$(\epsilon_{\mu\nu\omega\kappa})$
	Minkowski metric	$(\eta_{\mu\nu})$
	Lorentz transform	$(\Lambda_{\mu\nu})$
	position	$(r^\mu) \equiv \binom{ct}{\mathbf{r}}$
	displacement	$(\Delta r^\mu) \equiv \binom{c\Delta t}{\Delta\mathbf{r}}$
	space-time interval	$\Delta s^2 \equiv \Delta r_\mu \Delta r^\mu = c^2\Delta t^2 - \Delta\mathbf{r}^2$
	proper time	$\Delta\tau \equiv \sqrt{\frac{\Delta s^2}{c^2}}$ for 'time-like' intervals $\Delta s^2 > 0$
	proper distance	$\lvert\Delta\vec{S}\rvert \equiv \sqrt{-\Delta s^2}$ for 'space-like' intervals $\Delta s^2 < 0$
	gradient	$(\partial^\mu) \equiv \binom{c^{-1}\partial_t}{-\nabla}$
	d'Alembertian	$\Box \equiv \partial_\mu \partial^\mu = \frac{1}{c^2}\frac{\partial^2}{\partial t^2} - \nabla^2$
mechanics	proper velocity	$(u^\mu) \equiv (\frac{\partial r^\mu}{\partial\tau}) = \binom{\gamma_u c}{\gamma_u \mathbf{u}}$
	momentum	$(p^\mu) \equiv (\frac{\partial u^\mu}{\partial\tau}) = \binom{E/c}{\mathbf{p}}$
	rest mass	$mc^2 = p_\mu p^\mu = \frac{E^2}{c^2} - \mathbf{p}^2$
	wave vector	$(k^\mu) \equiv \binom{\omega/c}{\mathbf{k}}$
	force	$(K^\mu) \equiv \binom{\gamma P/c}{\gamma\mathbf{F}}$
e-dynamics	current density	$(j^\mu) \equiv (\varrho_0 U^\mu) = \binom{c\varrho}{\mathbf{j}}$ with $\partial_\mu j^\mu = 0$
	el.-mag. potential	$(A^\mu) \equiv \binom{c^{-1}\phi}{\mathbf{A}}$ with $F^{\mu\nu} = \partial^\mu A^\nu - \partial^\nu A^\mu$
	Stokes theorem	$F \int F_{\mu\nu} ds^{\mu\nu} = \int A_\mu dx^\mu$
	el.-mag. flux	$(S^\mu) \equiv \binom{cu}{\mathbf{S}}$
	el.-mag. field tensor	$(F_{\mu\nu}) \equiv \begin{pmatrix} 0 & -\frac{1}{c}\vec{\mathcal{E}} \\ \frac{1}{c}\vec{\mathcal{E}} & (-\epsilon_{mnk}\mathcal{B}_k) \end{pmatrix}$
	dual tensor	$(\mathcal{F}_{\mu\nu}) \equiv \frac{1}{2}\epsilon^{\mu\nu\alpha\beta}F_{\alpha\beta} = \begin{pmatrix} 0 & -\vec{\mathcal{B}} \\ \vec{\mathcal{B}} & (\frac{1}{c}\epsilon_{mnk}\mathcal{E}_k) \end{pmatrix}$
	Lorentz force density	$f^\mu = F^{\mu\nu} j_\nu$
	Lagrangian	$\frac{1}{2\mu_0}F_{\mu\nu}F^{\mu\nu} = \frac{1}{\mu_0}\mathcal{B}^2 - \varepsilon_0\mathcal{E}^2$ $\mathcal{F}_{\omega\kappa}F^{\omega\kappa} = \frac{1}{2}\epsilon_{\mu\nu\omega\kappa}F^{\mu\nu}F^{\omega\kappa} = -\frac{4}{c}\vec{\mathcal{B}}\cdot\vec{\mathcal{E}}$

10.5.3 CGS units

Often used in electrodynamics are *CGS units*, also called *Gaussian units*. In this script we will use exclusively *SI units* of the *Système International d'Unités*. To do the conversion between the unit systems, it is enough let,

$$\begin{aligned}
e &\to e_{CGS}\sqrt{4\pi\varepsilon_0} \quad , \quad \mathbf{j} \to \mathbf{j}_{CGS}\sqrt{4\pi\varepsilon_0} \\
\vec{\mathcal{E}} &\to \vec{\mathcal{E}}_{CGS}\sqrt{\tfrac{1}{4\pi\varepsilon_0}} \quad , \quad \vec{\mathcal{B}} \to \vec{\mathcal{B}}_{CGS}\sqrt{\tfrac{\mu_0}{4\pi}} \\
\vec{\mathcal{D}} &\to \vec{\mathcal{D}}_{CGS}\sqrt{\tfrac{\varepsilon_0}{4\pi}} \quad , \quad \vec{\mathcal{H}} \to \vec{\mathcal{H}}_{CGS}\sqrt{\tfrac{1}{4\pi\mu_0}} \\
\vec{\mathcal{P}} &\to \vec{\mathcal{P}}_{CGS}\sqrt{4\pi\varepsilon_0} \quad , \quad \vec{\mathcal{M}} \to \vec{\mathcal{M}}_{CGS}\sqrt{\tfrac{4\pi}{\mu_0}} \ .
\end{aligned} \tag{10.82}$$

Maxwell's equations in the irrational Gaussian system are,

$$\text{rot } \vec{\mathcal{H}} = \tfrac{1}{c}\partial_t\vec{\mathcal{D}} + \tfrac{4\pi}{c}\mathbf{j} \quad , \quad \text{div } \vec{\mathcal{D}} = 4\pi\varrho \ . \tag{10.83}$$

Moreover,

$$u = \tfrac{1}{8\pi}(\vec{\mathcal{E}}^2 + \vec{\mathcal{B}}^2) \quad , \quad \mathbf{S} = \tfrac{c}{4\pi}(\vec{\mathcal{E}} \times \vec{\mathcal{B}}) \ . \tag{10.84}$$

The material equations for dielectric media are,

$$\vec{\mathcal{D}} = \varepsilon\vec{\mathcal{E}} \quad , \quad \vec{\mathcal{P}} = \chi_\varepsilon\vec{\mathcal{E}} \quad , \quad \varepsilon = 1 + 4\pi\chi_\varepsilon \ , \tag{10.85}$$

and for dia- and paramagnetic media,

$$\vec{\mathcal{B}} = \mu\vec{\mathcal{H}} \quad , \quad \vec{\mathcal{M}} = \chi_\mu\vec{\mathcal{H}} \quad , \quad \mu = 1 + 4\pi\chi_\mu \ . \tag{10.86}$$

10.6 Rules of vector analysis

10.6.1 Basic rules

$$\begin{aligned}
&\text{(i)} && \mathbf{A}\cdot\mathbf{B} = \mathbf{B}\cdot\mathbf{A} \quad \text{but} \quad \mathbf{A}\cdot\nabla \neq \nabla\cdot\mathbf{A} \ , \\
&\text{(ii)} && \phi\mathbf{B} = \mathbf{B}\phi \quad \text{but} \quad \phi\nabla \neq \nabla\phi \ , \\
&\text{(iii)} && \mathbf{A}\times\mathbf{B} = -\mathbf{B}\times\mathbf{A} \quad \text{but} \quad \mathbf{A}\times\nabla \neq -\nabla\times\mathbf{A} \ , \\
&\text{(iv)} && \mathbf{A}\cdot(\mathbf{B}\times\mathbf{C}) = \mathbf{B}\cdot(\mathbf{C}\times\mathbf{A}) \ , \\
&\text{(v)} && \mathbf{A}\times(\mathbf{B}\times\mathbf{C}) = \mathbf{B}(\mathbf{A}\cdot\mathbf{C}) - \mathbf{C}(\mathbf{A}\cdot\mathbf{B}) \ , \\
&\text{(vi)} && \nabla f(\phi(\mathbf{r})) = \frac{\partial f}{\partial\phi}\nabla\phi(\mathbf{r}) \quad \text{chain rule} \ , \\
&\text{(vii)} && \nabla(\mathbf{A}\cdot\mathbf{B}) = \nabla(A\mathbf{B}) + \nabla(\mathbf{A}B) \quad \text{product rule for scalars and vectors} \ .
\end{aligned} \tag{10.87}$$

10.6.2 Deduced rules

$$
\begin{aligned}
&\text{(i)} && \nabla(\phi+\psi) = \nabla\phi + \nabla\psi \ , && (10.88)\\
&\text{(ii)} && \nabla(\phi\psi) = \phi\nabla\psi + \psi\nabla\phi \ , \\
&\text{(iii)} && \nabla\cdot(\mathbf{A}+\mathbf{B}) = \nabla\cdot\mathbf{A} + \nabla\cdot\mathbf{B} \ , \\
&\text{(iv)} && \nabla\times(\mathbf{A}+\mathbf{B}) = \nabla\times\mathbf{A} + \nabla\times\mathbf{B} \ , \\
&\text{(v)} && \nabla\cdot(\phi\mathbf{A}) = \phi(\nabla\cdot\mathbf{A}) + (\nabla\phi)\cdot\mathbf{A} \ , \\
&\text{(vi)} && \nabla\times(\phi\mathbf{A}) = \phi(\nabla\times\mathbf{A}) + (\nabla\phi)\times\mathbf{A} \ , \\
&\text{(vii)} && \nabla\cdot(\mathbf{A}\times\mathbf{B}) = (\nabla\times\mathbf{A})\cdot\mathbf{B} - \mathbf{A}\cdot(\nabla\times\mathbf{B}) \ , \\
&\text{(viii)} && \nabla\times(\mathbf{A}\times\mathbf{B}) = (\mathbf{B}\cdot\nabla)\mathbf{A} - (\mathbf{A}\cdot\nabla)\mathbf{B} + \mathbf{A}(\nabla\cdot\mathbf{B}) - \mathbf{B}(\nabla\cdot\mathbf{A}) \ , \\
&\text{(ix)} && \nabla(\mathbf{A}\cdot\mathbf{B}) = \mathbf{A}\times(\nabla\times\mathbf{B}) + \mathbf{B}\times(\nabla\times\mathbf{A}) + (\mathbf{A}\cdot\nabla)\mathbf{B} + (\mathbf{B}\cdot\nabla)\mathbf{A} \ , \\
&\text{(x)} && \nabla\times(\nabla\phi) = 0 = \nabla\cdot(\nabla\times\mathbf{A}) \ , \\
&\text{(xi)} && \nabla\times(\nabla\times\mathbf{A}) = \nabla(\nabla\cdot\mathbf{A}) - \triangle\mathbf{A} \ , \\
&\text{(xii)} && \nabla\cdot(\nabla\phi) = \triangle\phi \ , \\
&\text{(xiii)} && \mathbf{A}\cdot(\nabla\phi) = (\mathbf{A}\cdot\nabla)\phi \ , \\
&\text{(xiv)} && \mathbf{A}\times(\nabla\phi) = (\mathbf{A}\times\nabla)\phi \ , \\
&\text{(xv)} && \nabla\phi = \frac{d\phi}{dr}\nabla r \qquad \text{chain rule} \ , \\
&\text{(xvi)} && \nabla\phi(\psi) = \frac{d\phi(\psi)}{d\psi}\nabla\psi \ , \\
&\text{(xvii)} && \nabla\cdot\mathbf{A}(\psi) = \frac{d\mathbf{A}(\psi)}{d\psi}\cdot\nabla\psi \ , \\
&\text{(xviii)} && \nabla\times\mathbf{A}(\psi) = -\frac{d\mathbf{A}(\psi)}{d\psi}\times\nabla\psi \ .
\end{aligned}
$$

10.6.3 Integral rules

(i) $$\int_{\mathcal{V}} \nabla\phi dV = \int_{\mathcal{S}} \phi d\mathbf{S}, \tag{10.89}$$

(ii) $$\int_{\mathcal{V}} \nabla\cdot\vec{\mathcal{E}} dV = \oint_{\partial\mathcal{V}} \vec{\mathcal{E}}\cdot d\mathbf{S} \qquad \text{Gauß' rule} ,$$

(iii) $$\int_{\mathbf{A}} \nabla\times\vec{\mathcal{E}}\cdot d\mathbf{S} = \oint_{\partial\mathcal{C}} \vec{\mathcal{E}}\cdot d\mathbf{l} \qquad \text{Stokes' rule} ,$$

(iv) $$\int_{\mathcal{V}} \phi(\nabla\psi) dV = \int_{\partial\mathcal{V}} \phi\psi d\mathbf{S} - \int_{\mathcal{V}} (\nabla\phi)\psi dV \qquad \text{Green's rule} ,$$

(v) $$\int_{\mathcal{V}} \left[\phi(\triangle\psi) - (\triangle\phi)\psi\right] dV = \int_{\partial V} \left[\phi(\nabla\psi) - (\nabla\phi)\psi\right]\cdot d\mathbf{S}$$

(vi) $$\int_{\mathcal{V}} \phi(\triangle\psi) dV = \int_{\mathcal{V}} (\triangle\phi)\psi dV \tag{10.90}$$

where $\triangle$ is hermitian, when $\lim_{r\to\infty} r\phi(r) = 0 = \lim_{r\to\infty} r\psi(r)$,

(vii) $$\frac{d}{dt}\int_{a(t)}^{b(t)} f(x,t)dx = \int_{a(t)}^{b(t)} \frac{\partial f}{\partial\tau}(x,t)dx + \frac{db(t)}{dt} f(b,t)dx - \frac{da(t)}{dt} f(a,t)dx .$$

Notation,

$$\nabla\phi\cdot d\mathbf{S} = \nabla\phi\cdot\mathbf{n}\ dS = \frac{\partial\phi}{\partial\mathbf{n}}\ dS . \tag{10.91}$$

10.7 Rules for Laplace and Fourier transforms

10.7.1 Laplace transform

Formulas for the *Laplace transform*:

$$\begin{aligned}
&\text{(definition)} && (\mathcal{L}f)(p) = \int_0^\infty f(t)e^{-pt}dt && (10.92)\\
&\text{(inversion)} && \mathcal{L}^{-1}\mathcal{L}f = f \quad \text{where} \quad (\mathcal{L}^{-1}\mathcal{L}f)(t) = \int_{\varepsilon-\imath\omega}^{\varepsilon+\imath\omega} \mathcal{L}f(p)e^{pt}\frac{dp}{2\pi\imath}\\
&\text{(linearity)} && \mathcal{L}(af+bg) = a\mathcal{L}(f) + b\mathcal{L}(g)\\
&\text{(similarity)} && \mathcal{L}[f(at)] = a^{-1}\mathcal{L}f(a^{-1}p)\\
&\text{(translation)} && \mathcal{L}\mathcal{T}f = \mathcal{L}f\cdot e^{-pT} \quad \text{where} \quad \mathcal{T}f(t) = f(t-T)\\
& && \mathcal{L}\left(fe^{qt}\right) = \mathcal{T}\mathcal{L}f\\
&\text{(differentiation)} && \mathcal{L}\partial_t f = p\mathcal{L}f - f(0)\\
& && \mathcal{L}(-tf) = \partial_p\mathcal{L}f\\
&\text{(pulse response)} && \mathcal{L}\delta = 1 \quad \text{where} \quad \delta(t) = \mathcal{L}^{-1}1\\
&\text{(step response)} && \mathcal{L}\delta' = p^{-1}\\
&\text{(integration)} && \mathcal{L}\int_0^t dt\ f = p^{-1}\mathcal{L}f\\
& && \mathcal{L}(t^{-1}f) = \int_p^\infty dp\ \mathcal{L}f\\
&\text{(convolution)} && \mathcal{L}(f\star g) = \mathcal{L}f\cdot\mathcal{L}g\\
&\text{(periodic functions)} && \mathcal{L}(f=\mathcal{T}f) = \int_0^{-T} dt\ \frac{e^{-pt}f(t)}{1-e^{pT}}\\
&\text{(eigenfunctions)} && f\star e^{pt} = \mathcal{L}f\cdot e^{pt}\ .
\end{aligned}$$

10.7.2 Correlation

Formulas for the *correlation*:

$$\begin{aligned}
&\text{(definition)} && (f\diamond g)(t) = \int_{-\infty}^{\infty} f(\tau)g(t+\tau)d\tau && (10.93)\\
&\text{(non-commutativity)} && (f\diamond g)(t) = (g\diamond f)^s\\
&\text{(complex autocorrelation)} && |f\diamond g^*| \leq f\diamond g^*(0)\ .
\end{aligned}$$

10.7.3 Fourier transform

Formulas for the *Fourier transform*:

(definition) $$(\mathcal{F}f)(\omega) = \int_{-\infty}^{\infty} f(t)e^{-\imath\omega t}dt \tag{10.94}$$

(inversion) $$\mathcal{F}^{-1}\mathcal{F}f = f \quad \text{where} \quad (\mathcal{F}^{-1}\mathcal{F}f)(t) = \int_{-\infty}^{\infty} \mathcal{F}f(\omega)e^{\imath\omega t}d\omega$$

(linearity) $$\mathcal{F}(af+bg) = a\mathcal{F}(f) + b\mathcal{F}(g)$$

(similarity) $$?$$

(translation) $$\mathcal{F}\mathcal{T}f = \mathcal{F}f\cdot e^{-\imath\omega T} \quad \text{where} \quad \mathcal{T}f(t) = f(t-T)$$

$$\mathcal{F}\left(fe^{\imath\omega t}\right) = \mathcal{T}\mathcal{F}f$$

(differentiation) $$\mathcal{F}[tf(t)] = \imath\partial_\omega(Ff)(\omega)$$

$$\mathcal{F}[f'(t)] = \imath\omega(Ff)(\omega)$$

(pulse response) $$\mathcal{F}\delta = 1 \quad \text{where} \quad \delta(t) = \mathcal{F}^{-1}1$$

(step response) $$\mathcal{F}\delta' = ?$$

(duality) $$\mathcal{F}\mathcal{F}\ f = f^s \quad \text{where} \quad f^s(t) = f(-t)$$

$$\mathcal{F}\ f^* = (\mathcal{F}\ f)^{*s} \quad \text{where} \quad f^s(t) = f(-t)$$

(symmetry) $$f = f^s = f^* \quad \Leftrightarrow \quad \mathcal{F}\ f = (\mathcal{F}\ f)^s$$

$$f = -f^s = f^* \quad \Leftrightarrow \quad \mathcal{F}\ f = -(\mathcal{F}\ f)^*$$

$$f = f^* \quad \Leftrightarrow \quad \mathcal{F}\ f = (\mathcal{F}\ f)^{*s}$$

(convolution) $$\mathcal{F}(f\star g) = \mathcal{F}f\cdot\mathcal{F}g$$

$$\mathcal{F}(f\cdot g) = \mathcal{F}f\star\mathcal{F}g$$

(eigenfunctions) $$f\star e^{\imath\omega t} = \mathcal{F}f\cdot e^{\imath\omega t}\ .$$

10.7.3.1 Fast Fourier transform

The *discrete Fourier transform* is defined by,

$$\begin{aligned} H_n &= \sum_{k=0}^{N-1} e^{-2\pi\imath nk/N}h_k \\ &= \sum_{k=0}^{N-1} e^{-2\pi\imath nk/(N/2)}h_{2k} + e^{-2\pi\imath k/N}\sum_{k=0}^{N/2-1} e^{-2\pi\imath nk/(N/2)}h_{2k+1} \\ &= even + odd\ . \end{aligned} \tag{10.95}$$

The inverse transform is,

$$h_k = \frac{1}{N}\sum_{k=0}^{N-1} e^{2\pi\imath nk/N}H_n\ . \tag{10.96}$$

The sine transform of a real vector s_k is,

$$S_n = \frac{2}{N}\sum_{k=1}^{N-1} s_k\sin\pi nk/N\ . \tag{10.97}$$

In MATLAB the fast Fourier transform is defined by:

$$F(k+1) = \sum_{n=0}^{N-1} f(n+1)e^{-2\pi\imath/N\cdot kn} \ . \tag{10.98}$$

inversion:

$$f(n+1) = \frac{1}{N}\sum_{k=0}^{N-1} F(k+1)e^{2\pi\imath/N\cdot kn} \ . \tag{10.99}$$

symmetry,

$$f(n+1) = f^*(n+1) \tag{10.100}$$
$$\Longrightarrow K(k+1) = \sum_{n=0}^{N-1} f^*(n+1)e^{-2\pi\imath/N\cdot kn}e^{-2\pi\imath/N\cdot Nn} = F^*(N-k+1) \ .$$

and,

$$f(N-n) = f(n+1) = f^*(n+1) \tag{10.101}$$
$$\Longrightarrow F(k+1) = \sum_{n=0}^{N-1} f^*(N-n)e^{-2\pi\imath/N\cdot kn}$$
$$= \sum_{n=0}^{N-1} f^*(n'+1)e^{2\pi\imath/N\cdot kn'}e^{-2\pi\imath/N\cdot(N-1)} = F^*(k+1)e^{2\pi\imath/N} \ .$$

and,

$$-f(N-n) = f(n+1) = f^*(n+1) \tag{10.102}$$
$$\Longrightarrow F(k+1) = \sum_{n=0}^{N-1} -f^*(N-n)e^{-2\pi\imath/N\cdot kn}$$
$$= \sum_{n=0}^{N-1} -f^*(n'+1)e^{2\pi\imath/N\cdot kn'}e^{-2\pi\imath/N\cdot(N-1)} = -F^*(k+1)e^{2\pi\imath/N} \ .$$

Hence, we choose, $\mathcal{F}f(n+1) = F(k+1)e^{-\pi\imath/N}$.

10.7.3.2 Fourier expansion

The complex *Fourier expansion* is defined by,

$$\boxed{f_N(x) = \sum_{n=-N}^{N} c_n e^{\imath nx}} \ , \tag{10.103}$$

where

$$c_n \equiv \frac{1}{2\pi}\int_{2\pi} s(x)e^{-\imath nx}dx \ . \tag{10.104}$$

10.7.4 Convolution

Formulas for the *convolution*:

$$\text{(definition)} \qquad (f\star g)(t)=\int_{-\infty}^{\infty}f(\tau)g(t-\tau)d\tau \tag{10.105}$$

$$\begin{aligned}
&\text{(neutral element)} && f\star\delta^{(n)}=f^{(n)}\\
&\text{(distributivity)} && (f+g)\star h=f\star h+g\star h\\
& && af\star g=f\star ag\\
&\text{(commutativity)} && f\star g=g\star f\\
&\text{(associativity)} && (f\star g)\star h=f\star(g\star h)\\
&\text{(translational invariance)} && \mathcal{T}(f\star g)=\mathcal{T}f\star g=f\star\mathcal{T}\\
&\text{(differentiation)} && \partial_x(f\star g)=\partial_x f\star g=f\star\partial_x g\\
&\text{(integration)} && \int_x(f\star g)=\int_x f\int_x g\\
&\text{(complexity)} && f=f_r+\imath f_i\\
&\text{(Dirac function)} && \mathcal{T}f=f\star\mathcal{T}\delta\\
& && f(T)=f\cdot\mathcal{T}\delta\ .
\end{aligned}$$

Example 106 (*Convolution of two Lorentzians*): The convolution of two *Lorentzians*,

$$\mathcal{L}_a(x)\equiv\frac{a}{\pi}\frac{1}{x^2+a^2}\qquad\text{with}\qquad\int_{-\infty}^{\infty}\mathcal{L}_a(x)dx=1\ ,$$

is simply another Lorentzian with the linewidth $a+b$,

$$\boxed{(\mathcal{L}_a\star\mathcal{L}_b)(x)=\mathcal{L}_{a+b}(x)}\ .$$

In order to demonstrate this, we first we apply the method of partial fractions to the expression,

$$\frac{1}{y^2+a^2}\frac{1}{(x-y)^2+b^2}=\frac{A}{y^2+a^2}+\frac{B}{(x-y)^2+b^2}$$
$$\text{with}\quad A=\frac{2xy+(x^2-a^2+b^2)}{(x^2+a^2+b^2)^2-4a^2b^2}\quad,\quad B=\frac{-2x(y-x)+(x^2+a^2-b^2)}{(x^2+a^2+b^2)^2-4a^2b^2}\ .$$

Now, we calculate the convolution,

$$\begin{aligned}
(\mathcal{L}_a\star\mathcal{L}_b)(x)&=\frac{ab}{\pi^2}\int_{-\infty}^{\infty}\frac{1}{y^2+a^2}\frac{1}{(x-y)^2+b^2}dy\\
&=\frac{ab}{\pi^2}\frac{1}{(x^2+a^2+b^2)^2-4a^2b^2}\left(\int_{-\infty}^{\infty}\frac{2xy+(x^2-a^2+b^2)}{y^2+a^2}dy+\int_{-\infty}^{\infty}\frac{-2x(y-x)+(x^2+a^2-b^2)}{(x-y)^2+b^2}dy\right)\\
&=\frac{ab}{\pi^2}\frac{1}{(x^2+a^2+b^2)^2-4a^2b^2}\left((x^2-a^2+b^2)\int_{-\infty}^{\infty}\frac{1}{y^2+a^2}dy+(x^2+a^2-b^2)\int_{-\infty}^{\infty}\frac{1}{(x-y)^2+b^2}dy\right)\\
&=\frac{ab}{\pi^2}\frac{(x^2-a^2+b^2)\frac{\pi}{a}+(x^2+a^2-b^2)\frac{\pi}{b}}{(x^2+a^2+b^2)^2-4a^2b^2}=\frac{a+b}{\pi}\frac{1}{x^2+(a+b)^2}=\mathcal{L}_{a+b}(x)\ .
\end{aligned}$$

Example 107 (*Convolution of two Gaussians*): The convolution of two *Gaussians*,

$$\mathcal{G}_a(x) \equiv \sqrt{\frac{1}{\pi}\frac{1}{a}}e^{-x^2/a^2} \qquad \text{with} \qquad \int_{-\infty}^{\infty} \mathcal{G}_a(x)dx = 1 ,$$

is simply another Gaussian with the linewidth $\sqrt{a^2+b^2}$,

$$\boxed{(\mathcal{G}_a \star \mathcal{G}_b)(x) = \mathcal{G}_{\sqrt{a^2+b^2}}(x)} .$$

We demonstrate this by calculating,

$$\begin{aligned}
(\mathcal{G}_a \star \mathcal{G}_b)(x) &= \frac{1}{\pi ab}\int_{-\infty}^{\infty} e^{-y^2/a^2}e^{-(x-y)^2/b^2}dy = \frac{\sqrt{ab}}{\pi}\int_{-\infty}^{\infty} e^{-(a^{-2}+b^{-2})y^2+2b^{-2}xy-b^{-2}x^2}dy \\
&= \frac{1}{\pi ab\sqrt{(a^{-2}+b^{-2})}}\int_{-\infty}^{\infty} e^{-\tilde{y}^2+\frac{2x}{b^2\sqrt{a^{-2}+b^{-2}}}\tilde{y}-b^{-2}x^2}d\tilde{y} \\
&= \frac{1}{\pi\sqrt{a^2+b^2}}\int_{-\infty}^{\infty} e^{-\left(\tilde{y}-\frac{x}{\sqrt{b^4/a^2+b^2}}\right)^2-\frac{x^2}{a^2+b^2}}d\tilde{y} \\
&= \frac{1}{\pi\sqrt{a^2+b^2}}e^{-\frac{x^2}{a^2+b^2}}\int_{-\infty}^{\infty} e^{-\tilde{y}^2}d\tilde{y} = \frac{1}{\sqrt{\pi}\sqrt{a^2+b^2}}e^{-\frac{x^2}{a^2+b^2}} = \mathcal{G}_{\sqrt{a^2+b^2}}(x) .
\end{aligned}$$

10.7.5 Green's functions

If a differential operator $\mathcal{L}_x$ acting on a variable x admits a *Green's function* $\mathcal{G}$ such that,

$$\boxed{\mathcal{L}_x\mathcal{G}(x,x') = \delta(x-x')} , \tag{10.106}$$

The Green function can be used to solve any equation,

$$\mathcal{L}_x f(x) = \varrho(x) \tag{10.107}$$

by calculating,

$$f(x) = \int \mathcal{G}(x,x')\varrho)(x)dx . \tag{10.108}$$

10.7.5.1 List of Green functions

The following table provides a list of useful Green functions.

differential operator $\mathcal{L}$	Green function $\mathcal{G}$
∂_t^n	$\frac{t^{n-1}}{(n-1)!}\Theta(t)$
$\partial_t + \gamma$	$\Theta(t)e^{-\gamma t}$
$\triangle$	$-\frac{1}{4\pi r}$
$\nabla\cdot$	$-\frac{\mathbf{r}-\mathbf{r}'}{4\pi R^3}$
$\nabla\times$	$-\frac{(\mathbf{r}-\mathbf{r}')\times(\mathbf{r}-\mathbf{r}')}{4\pi R^3}$
$\Box$	$-\frac{1}{4\pi r}\delta(t \mp \frac{1}{c}r)$
$\triangle + k^2$	$-\frac{e^{\imath kr}}{4\pi r}$
$-\nabla\times\nabla\times + k^2$	see Sec. 7.3.1

Example 108 (*Green function for time derivation*): To solve the differential equation,

$$(\partial_t + \gamma)f(t) = c \; ,$$

we search the Green function for the equation,

$$(\partial_t + \gamma)\mathcal{G}(t,t') = \delta(t-t') \; .$$

From the above table, we get,

$$f(t) = \int_{-\infty}^{\infty} \mathcal{G}(t,t')\; c\; dt' = c\int_{-\infty}^{\infty} \Theta(t-t')e^{-\gamma(t-t')}dt' = \frac{c}{\gamma}e^{-\gamma t} \; .$$

10.8 Further reading

R. Grimm et al., *Optical dipole traps for neutral atoms* [DOI]

S. Varró et al., *Spontaneous emission of radiation by metallic electrons in the presence of electromagnetic fields of surface plasmon oscillations* [DOI]

B. Cabrera, *First Results from a Superconductive Detector for Moving Magnetic Monopoles* [DOI]

R. Bachelard et al., *Resonances in Mie scattering by an inhomogeneous atomic cloud* [DOI]

P.L. Saldanha et al., *Interaction between light and matter: a photon wave function approach* [DOI]

10.8.1 on the Abraham-Minkowski dilemma

G.K. Campbell et al., *Photon Recoil Momentum in Dispersive Media* [DOI]

S.M. Barnett, *Resolution of the Abraham-Minkowski Dilemma* [DOI]

I. Brevik et al., *Possibility of measuring the Abraham force using whispering gallery modes* [DOI]

M. Mansuripur, *Resolution of the Abraham-Minkowski controversy* [DOI]

P.W. Milonni et al., *Momentum of Light in a Dielectric Medium* [DOI]

J.C. Garrison et al., *Canonical and kinetic forms of the electromagnetic momentum in an ad hoc quantization scheme for a dispersive dielectric* [DOI]

N.I. Balazs, *The Energy-Momentum Tensor of the Electromagnetic Field inside Matter* [DOI]

U. Leonhardt, *Energy-momentum balance in quantum dielectrics* [DOI]

R. Loudon et al., *Radiation pressure and momentum transfer in dielectrics: The photon drag effect* [DOI]

G.P. Fisher et al., *The Electric Dipole Moment of a Moving Magnetic Dipole* [DOI]

Wen-Zhuo Zhang et al., *Testing the equivalence between the canonical and Minkowski momentum of light with ultracold atoms* [DOI]

Weilong She et al., *Observation of a Push Force on the End Face of a Nanometer Silica Filament Exerted by Outgoing Light* [DOI]

R.N.C. Pfeifer et al., *Colloquium: Momentum of an electromagnetic wave in dielectric media* [DOI]

C. Baxter et al., *Radiation pressure and the photon momentum in dielectrics* [DOI]

C. Baxter et al., *Canonical approach to photon pressure* [DOI]

F. Ravndal, *Symmetric and conserved energy-momentum tensors in moving media* [DOI]

E.A. Hinds et al., *Momentum Exchange between Light and a Single Atom: Abraham or Minkowski?* [DOI]

M.P. Haugan et al., *Spectroscopy of atoms and molecules in gases: Corrections to the Doppler-recoil shift* [DOI]

J.P. Gordon et al., *Radiation Forces and Momenta in Dielectric Media* [DOI]

F. Goos et al., *Ein neuer und fundamentaler Versuch zur Totalreflektion* [DOI]

Changbiao Wang et al., *Can the Abraham Light Momentum and Energy in a Medium Constitute a Lorentz Four-Vector?* [DOI]

P.L. Saldanha, *Division of the energy and of the momentum of electromagnetic waves in linear media into electromagnetic and material parts* [DOI]

P.L. Saldanha et al., *Hidden momentum and the Abraham-Minkowski debate* [DOI]

A.F. Gibson et al., *Photon drag in germanium* [DOI]

Li Zhang et al., *Experimental evidence for Abraham pressure of light* [DOI]

Bibliography

[1] L. Allen, M. Babiker, W. K. Lai, and V. E. Lembessis, *Atom dynamics in multiple laguerre-gaussian beams*, Phys. Rev. A **54** (1996), 4259, .

[2] L. Allen, M. W. Beijersbergen, R. J. C. Spreeuw, and J. P. Woerdman, *Orbital angular momentum of light and the transformation of laguerre-gaussian laser modes*, Phys. Rev. A **45** (1992), 8185, .

[3] L. Allen, V. E. Lembessis, and M. Babiker, *Spin-orbit coupling in free-space laguerre-gaussian light beams*, Phys. Rev. A **53** (1996), R2937, .

[4] L. Allen and M. J. Padgett, *The poynting vector in laguerre-gaussian beams and the interpretation of their angular momentum density*, Opt. Comm. **187** (2000), 67, .

[5] L. Amico, A. Osterloh, and F. Cataliotti, *Quantum many particle systems in ring-shaped optical lattices*, Phys. Rev. Lett. **95** (2005), 063201, DOI.

[6] F. T. Arecchi and R. Bonifacio, IEEE J. Quantum Electron. **1** (1965), 169.

[7] Koray Aydin, Irfan Bulu, and Ekmel Ozbay, *Focusing of electromagnetic waves by a left-handed metamaterial flat lens*, Opt. Exp. **13** (2005), 08753.

[8] M. Babiker, W. L. Power, and L. Allen, *Light-induced torque on moving atoms*, Phys. Rev. Lett. **73** (1994), 1239, .

[9] R. Bachelard, H. Bender, Ph. W. Courteille, N. Piovella, C. Stehle, C. Zimmermann, and S. Slama, *Role of mie scattering in the seeding of matter-wave superradiance*, Phys. Rev. A **86** (2012), 043605.

[10] R. Bachelard, Ph. W. Courteille, R. Kaiser, and N. Piovella, *Resonances in mie scattering by an inhomogeneous atomic cloud*, Europhys. Lett. **97** (2012), 14004.

[11] V. S. Bagnato, N. P. Bigelow, G. I. Surdutovich, and S. C. Zilio, *Dynamical stabilization: A new model for supermolasses*, J. Opt. Soc. Am. B **19** (1994), 1568.

[12] S. M. Barnett, *Resolution of the Abraham-Minkowski dilemma*, Phys. Rev. Lett. **104** (2010), 070401, .

[13] H. Bender, C. Stehle, S. Slama, R. Kaiser, N. Piovella, C. Zimmermann, and Ph.W. Courteille, *Observation of cooperative mie scattering from an ultracold atomic cloud*, Phys. Rev. A **82** (2011), 011404(R).

[14] M. Born, 1980, ISBN.

[15] F. Bretenaker, A. Le Floch, and L. Dutriaux, *Direct measurement of the optical Goos-Hänchen effect in lasers*, Phys. Rev. Lett. **68** (1992), 931, .

[16] W. Buckel, *Supraleitung, grundlagen und anwendungen*, 1977, ISBN.

[17] S. Y. Buhmann, *Dispersion forces ii*, Springer Tracts in Modern Physics 248, 287, Springer-Verlag Berlin Heidelberg, 2012, ISBNDOI.

[18] I. Bulu, H. Caglayan, and E. Ozbay, *Experimental demonstration of labyrinth-based left-handed metamaterials*, Opt. Exp. **13** (2005), 10238.

[19] P. N. Butcher and D. Cotter, Cambridge University Press, 1991, ISBN.

[20] B. Cabrera, *First results from a superconductive detector for moving magnetic monopoles*, Phys. Rev. Lett. **48** (1982), 1378.

[21] G. K. Campbell, A. E. Leanhardt, J. Mun, M. Boyd, E. W. Streed, W. Ketterle, and D. E. Pritchard, *Photon recoil momentum in dispersive media*, Phys. Rev. Lett. **94** (2005), 170403.

[22] Jr. Ch. P. Poole, H. A. Farach, and R. J. Creswick, *Superconductivity*, 2007, ISBN.

[23] Qijin Chen, J. Stajic, Shina Tan, and K. Levin, *Shapiro steps observed in a dc superconducting quantum interference device with multiple junctions in each arm*, Appl. Phys. Lett. **80** (2002), 1025, .

[24] Qiang Cheng and Tie Jun Cui, *High-power generation and transmission in a left-handed planar waveguide excited by an electric dipole*, Opt. Exp. **13** (2005), 10230.

[25] L. N. Cooper, *Bound electron pairs in a degenerate fermi-gas*, Phys. Rev. **104** (1956), 1189.

[26] Ph. W. Courteille, S. Bux, E. Lucioni, K. Lauber, T. Bienaimé, R. Kaiser, and N. Piovella, *Modification of radiation pressure due to cooperative scattering of light*, Euro. Phys. J. D **58** (2010), 69.

[27] J. Courtial, D. A. Robertson, K. Dholakia, L. Allen, and M. J. Padgett, *Rotational frequency shift of a light beam*, Phys. Rev. Lett. **81** (1998), 4828, .

[28] J. J. Cowan and B. Anicin, *Longitudinal and transversal displacements of a bounded microwave beam at total internal reflection*, J. Opt. Soc. Am. **67** (1977), 1307.

[29] O. Costa de Beauregard, *Translational internal spin effect with moving particles*, Phys. Rev. **134** (1964), .

[30] A B. Djurisic and E. H. Li, *Modeling the index of refraction of insulating solids with a modified lorentz oscillator model*, Appl. Opt. **37** (1998), 5291, DOI.

[31] J. Durnin, J. J. Miceli, and J. H. Eberly, *Diffraction-free beams*, Physical Review Letters **58** (1987), 1499.

[32] C. Fabre, R. G. DeVoe, and R. G. Brewer, *Ultrahigh-finesse optical cavities*, Opt. Lett. **6** (1986), 365.

[33] M. Fichet, F. Schuller, D. Bloch, and M. Ducloy, *van der waals interactions between excited-state atoms and dispersive dielectric surfaces*, Phys. Rev. A **51** (1995), 1553, DOI.

[34] DOIR. Bachelard and N. Piovella and Ph. W. Courteille, *Cooperative scattering and radiation pressure force in dense atomic clouds*, Phys. Rev. A **84** (2011), 013821.

[35] E. J. Galvez, P. R. Crawford, H. I. Sztul, M. J. Pysher, P. J. Haglin, and R. E. Williams, *Geometric phase associated with mode transformations in optical beams bearing orbital angular momentum*, Phys. Rev. Lett. **90** (2003), 203901, .

[36] I. Giaver, *Detection of the ac josephson effect*, Phys. Rev. Lett. **14** (1965), 904.

[37] H. Goldstein, *Klassische mechanik*, Akademische Verlagsgesellschaft Wiesbaden, 1983.

[38] H. Goldstein, C. P. Poole, and J. L. Safko, *Classical mechanics*, Addison Wesley, 2000, ISBN.

[39] J. W. Goodman, *Introduction to fourier optics*, McGraw-Hill physical and quantum electronics series, W. H. Freeman, 1996, ISBN.

[40] F. Goos and H. Hänchen, *Ein neuer und fundamentaler versuch zur totalreflektion*, Ann. Physik (Leipz.) **1** (1947), 333.

[41] F. Goos and H. Lindberg-Hänchen, *Neumessung des strahlversetzungeffectes bei totalreflexion*, Ann. Physik (Leipz.) **5** (1949), 251.

[42] D. J. Griffiths, *Introduction to electrodynamics*, Prentiss-Hall, 1989, ISBN.

[43] R. Grimm, M. Weidemüller, and Y. B. Ovchinnikov, *Optical dipole traps for neutral atoms*, Adv. At. Mol. Opt. Phys. **42** (2000), 95, .

[44] N. R. Heckenberg, R. McDuff, C. P. Smith, and A.G. White, *Generation of optical phase singularities by computer-generated holograms*, Opt. Lett. **17** (1992), 221.

[45] J. Herb, P. Meerwald, M. J. Moritz, and H. Friedrich, *Quantum-mechanical deflection function*, Phys. Rev. A **60** (1999), 853, .

[46] E. A. Hinds and St. M. Barnett, *Momentum exchange between light and a single atom: Abraham or minkowski?*, Phys. Rev. Lett. **102** (2009), 050403, DOI.

[47] J. D. Jackson, *Classical electrodynamics*, John Wiley and Sons, 1999, ISBN.

[48] B. D. Josephson, *Possible new effects in superconductive tunneling*, Phys. Lett. **1** (1962), 251.

[49] H. Kogelnik and X. Y. Li, *Laser beams and resonators*, Appl. Opt. **5** (1966), 1550, DOI.

[50] T. Kuga, Y. Torii, N. Shiokawa, T. Hirano, Y. Shimizu, and H. Sasada, *Novel optical trap of atoms with a doughnut beam*, Phys. Rev. Lett. **78** (1997), 4713, .

[51] M. Lax, W. H. Louisell, and W. B. McKnight, *From maxwell to paraxial wave optics*, Phys. Rev. A **11** (1975), 1365, .

[52] R. H. Lehmberg, *Radiation from an n-atom system. i. general formalism*, Phys. Rev. A **3** (1970), 883, DOI.

[53] U. Leonhardt, *Optical conformal mapping*, Science **312** (2006), 1777, .

[54] W. Lichten, *Precise wavelength measurements and optical phase shifts: I. general theory*, J. Opt. Soc. Am. A **2** (1985), 1869, .

[55] H. K. Lotsch, *Beam displacement at total reflection: The Goos-Hänchen effect*, Optik **2** (1970), 116.

[56] R. Loudon, S. M. Barnett, and C. Baxter, *Radiation pressure and momentum transfer in dielectrics: The photon drag effect*, Phys. Rev. A **71** (2005), 063802, .

[57] W. T. Lu and S. Sridhar, *Flat lens without optical axis: Theory of imaging*, Opt. Exp. **13** (2005), 10673.

[58] Chiyan Luo, S. G. Johnson, and J. D. Joannopoulos, *All-angle negative refraction in a three-dimensionally periodic photonic crystal*, Appl. Phys. Lett. **81** (2002), 2352, .

[59] Chiyan Luo, S. G. Johnson, J. D. Joannopoulos, and J. B. Pendry, *All-angle negative refraction without negative effective index*, Phys. Rev. B **65** (2002), 201104(R), .

[60] ———, *Negative refraction without negative index in metallic photonic crystals*, Opt. Exp. **11** (2003), 00746, .

[61] ———, *Subwavelength imaging in photonic crystals*, Phys. Rev. B **68** (2003), 045115, .

[62] D. McGloin and K. Dholakia, *Bessel beams: Diffraction in a new light*, Contemporary Physics **46** (2005), 15.

[63] P. W. Milonni and R. W. Boyd, *Momentum of light in a dielectric medium*, Adv. Opt. Phot. **2** (2010), 519, .

[64] A. Narayanaswamy and G. Chen, *Dyadic green's functions and electromagnetic local density of states*, J. Quant. Spectr. Rad. Transfer **111** (2009), 12, DOI.

[65] G. Nienhuis, F. Schuller M., and Ducloy, *Nonlinear selective reflection from an atomic vapor at arbitrary incidence angle*, Phys. Rev. A **38** (1988), 5197, .

[66] H. Okuda and H. Sasada, *Huge transverse deformation in nonspecular reflection of a light beam possessing orbital angular momentum near critical incidence*, Opt. Exp. **14** (2006), 8393, .

[67] A. T. OŃeil, I. MacVicar, L. Allen, and M. J. Padgett, *Intrinsic and extrinsic nature of the orbital angular momentum of a light beam*, Phys. Rev. Lett. **88** (2002), 053601, .

[68] M. Onoda, S. Murakami, and N. Nagaosa, *Hall effect of light*, Phys. Rev. Lett. **93** (2004), 083901, .

[69] G. Y. Panasyuk, J. C. Schotland, and V. A. Markel, *Short-distance expansion for the electromagnetic half-space green's tensor: general results and an application to radiative lifetime computations*, J. Phys. A: Math. Theor. **42** (2009), 275203, DOI.

[70] J. Pendry, *Playing tricks with light*, Science **285** (1999), 1687, .

[71] J. B. Pendry, *Negative refraction makes a perfect lens*, Phys. Rev. Lett. **85** (2000), 3966, .

[72] ———, *Negative refraction*, Cont. Phys. **45** (2004), 191, .

[73] E. Pfleghaar, A. Marseille, and A. Weis, *Quantitative investigation of the effect of resonant absorbers on the Goos-Hänchen shift*, Phys. Rev. Lett. **70** (1993), 2281, .

[74] A. Pikovsky, M. Rosenblum, and J. Kurths, *Synchronization: A universal concept in nonlinear sciences*, Cambridge, University press (2001).

[75] F. Pillon, H. Gilles, S. Girard, M. Laroche, R. Kaiser, and A. Gazibegovic, *Goos-Hänchen and Imbert-Fedorov shifts for leaky guided modes*, J. Opt. Soc. Am. B **22** (2005), 1290.

[76] J. Preskill, *Magnetic monopole*, Ann. Rev. Nucl. Part. **34** (1984), 461, .

[77] A. D. Rakic, A. B. Djurisic, J. M. Elazar, and M. L. Majewski, *Optical properties of metallic films for vertical-cavity optoelectronic devices*, Appl. Opt. **37** (1998), 5271, DOI.

[78] R. H. Renard, *Total reflection: A new evaluation of the Goos-Hänchen shift*, J. Opt. Soc. Am. **54** (1964), 1190.

[79] W. Rindler, *Relativity and electromagnetism: The force on a magnetic monopole*, Am. J. Phys. **57** (1989), 993, .

[80] S. M. Rytov, *Electromagnetic properties of a finely stratified medium*, Sov. Phys. JETP **2** (1954), 466, .

[81] A. Schilke, C. Zimmermann, Ph. W. Courteille, and W. Guerin, *Optical parametric oscillation with distributed feedback in cold atoms*, Nature Phot. **6** (2012), 101 letter.

[82] M. O. Scully, E. S. Fry, C. H. Raymond Ooi, and K. Wodkiewicz, *Directed spontaneous emission from an extended ensemble of n atoms: Timing is everything*, Phys. Rev. Lett. **96** (2006), 010501, DOI.

[83] M. O. Scully and A. A. Svidzinsky, *The super of superradiance*, Science **325** (2009), 1510, DOI.

[84] I. V. Shadrivov, A. A. Sukhorukov, and Y. S. Kivshar, *Complete band gaps in one-dimensional left-handed periodic structures*, Phys. Rev. Lett. **95** (2005), 193903.

[85] R. A. Shelby, D. R. Smith, and S. Schultz, *Experimental verification of a negative index of refraction*, Science **292** (2001), 77.

[86] A. E. Siegman, J. Opt. Soc. Am. A **2** (1985), 1793.

[87] N. B. Simpson, K. Dhokalian, L. Allan, and M. J. Padt, *Mechanical equivalence of spin and orbital angular momentum of light: An optical spanner*, Opt. Lett. **22** (1997), 52.

[88] S. Slama, C. von Cube, B. Deh, A. Ludewig, C. Zimmermann, and Ph. W. Courteille, *Phase-sensitive detection of bragg-scattering at 1d optical lattices*, Phys. Rev. Lett. **94** (2005), 193901.

[89] S. Slama, C. von Cube, M. Kohler, C. Zimmermann, and Ph. W. Courteille, *Multiple reflections and diffuse scattering in bragg scattering at optical lattices*, Phys. Rev. A **73** (2006), 023424.

[90] M. J. Snadden, A. S. Bell, R. B. M. Clarke, E. Riis, and D. H. McIntyre, *Doughnut mode magneto-optical trap*, J. Opt. Soc. Am. B **14** (1997), 544, .

[91] O. Svelto, *Self-focussing, self-trapping, and self-phase modulation of laser beams*, Progr. Opt. **12** (1974), 1, DOI.

[92] J. W. R. Tabosa and D. V. Petrov, *Optical pumping of orbital angular momentum of light in cold cesium atoms*, Phys. Rev. Lett. **83** (1999), 4967, .

[93] Zhixiang Tang, Runwu Peng, Dianyuan Fan, Shuangchun Wen, Hao Zhang, and Liejia Qian, *Absolute left-handed behaviors in a triangular elliptical-rod photonic crystal*, Opt Exp. **13** (2005), 09796.

[94] V. G. Veselago, *The electrodynamics of substances with simultaneously negative values of ε and μ*, Sov. Phys. Uspekhi **10** (2008), 509, .

[95] D. G. Voelz, *Computational fourier optics: A matlab tutorial*, SPIE Press monograph, SPIE Press, 2011, ISBN.

[96] T. Walker, D. Sesko, and C. Wieman, *Collective behaviour of optically trapped neutral atoms*, Phys. Rev. Lett. **64** (1990), 408, .

[97] Changbiao Wang, *Can the Abraham light momentum and energy medium constitute a Lorentz four-vector?*, J. Mod. Phys. **4** (2013), 1123, DOI.

[98] M. Weissbluth, *Atoms and molecules*, Students Edition Academic Press, San Diego, 1978, ISBN.

[99] Amnon Yariv, *Quantum electronics*, 1967, ISBN.

[100] M. Zamboni-Rached, L. A. Ambrosio, A. H. Dorrah, and M. Mojahedi, *Structuring light under different polarization states within micrometer domains: exact analysis from the maxwell equations*, Optics Express **25** (2017), 10051.

[101] M. Zamboni-Rached and E. Recami, *Subluminal wave bullets: Exact localized subluminal solutions to the wave equations*, Phys. Rev. A **77** (2008), 033824.

[102] O. V. Zhirov and D. L. Shepelyansky, *Quantum synchronization*, Eur. Phys. J. D **38** (2006), 375, .

Index